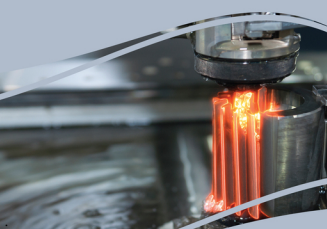


Premier Reference Source

# Non-Conventional Machining in Modern Manufacturing Systems

Copyright 2019. Engineering Science Reference. All rights reserved.  
May not be reproduced in any form without permission from the  
publisher, except fair uses permitted under U.S. or applicable  
copyright law.



EBSCO Publishing : eBook Collection  
(EBSCOhost) - printed on 2/14/2023 1:49 PM  
via

AN: 1880494 ; Kumar, K., Kumari, Nisha,  
Davim, J. Paulo.; Non-Conventional Machining  
in Modern Manufacturing Systems  
Account: ns335141



# Non-Conventional Machining in Modern Manufacturing Systems

Kaushik Kumar  
*Birla Institute of Technology, India*

Nisha Kumari  
*Birla Institute of Technology, India*

J. Paulo Davim  
*University of Aveiro, Portugal*

A volume in the Advances in Mechatronics and  
Mechanical Engineering (AMME) Book Series



Published in the United States of America by

IGI Global  
Engineering Science Reference (an imprint of IGI Global)  
701 E. Chocolate Avenue  
Hershey PA, USA 17033  
Tel: 717-533-8845  
Fax: 717-533-8661  
E-mail: [cust@igi-global.com](mailto:cust@igi-global.com)  
Web site: <http://www.igi-global.com>

Copyright © 2019 by IGI Global. All rights reserved. No part of this publication may be reproduced, stored or distributed in any form or by any means, electronic or mechanical, including photocopying, without written permission from the publisher. Product or company names used in this set are for identification purposes only. Inclusion of the names of the products or companies does not indicate a claim of ownership by IGI Global of the trademark or registered trademark.

Library of Congress Cataloging-in-Publication Data

Names: Kumar, K. (Kaushik), 1968- editor. | Kumari, Nisha, 1991- editor. |  
Davim, J. Paulo, editor.

Title: Non-conventional machining in modern manufacturing systems / Kaushik  
Kumar, Nisha Kumari, and J. Paulo Davim, editors.

Description: Hershey PA : Engineering Science Reference, an imprint of IGI  
Global, [2019] | Includes bibliographical references and index.

Identifiers: LCCN 2018002544 | ISBN 9781522561613 (hardcover) | ISBN  
9781522561620 (ebook)

Subjects: LCSH: Machining.

Classification: LCC TJ1185 .N578 2019 | DDC 671.3/5--dc23 LC record available at <https://lcn.loc.gov/2018002544>

This book is published in the IGI Global book series Advances in Mechatronics and Mechanical Engineering (AMME)  
(ISSN: 2328-8205; eISSN: 2328-823X)

British Cataloguing in Publication Data

A Cataloguing in Publication record for this book is available from the British Library.

All work contributed to this book is new, previously-unpublished material. The views expressed in this book are those of the authors, but not necessarily of the publisher.

For electronic access to this publication, please contact: [eresources@igi-global.com](mailto:eresources@igi-global.com).



# Advances in Mechatronics and Mechanical Engineering (AMME) Book Series

J. Paulo Davim  
University of Aveiro, Portugal

ISSN:2328-8205  
EISSN:2328-823X

## MISSION

With its aid in the creation of smartphones, cars, medical imaging devices, and manufacturing tools, the mechatronics engineering field is in high demand. Mechatronics aims to combine the principles of mechanical, computer, and electrical engineering together to bridge the gap of communication between the different disciplines.

The **Advances in Mechatronics and Mechanical Engineering (AMME) Book Series** provides innovative research and practical developments in the field of mechatronics and mechanical engineering. This series covers a wide variety of application areas in electrical engineering, mechanical engineering, computer and software engineering; essential for academics, practitioners, researchers, and industry leaders.

## COVERAGE

- Intelligent Sensing
- Design and Manufacture
- Medical robotics
- Vibration and acoustics
- Bioengineering Materials
- Manufacturing Methodologies
- Computer-Based Manufacturing
- Tribology and surface engineering
- Autonomous Systems
- Nanomaterials and nanomanufacturing

IGI Global is currently accepting manuscripts for publication within this series. To submit a proposal for a volume in this series, please contact our Acquisition Editors at [Acquisitions@igi-global.com](mailto:Acquisitions@igi-global.com) or visit: <http://www.igi-global.com/publish/>.

The Advances in Mechatronics and Mechanical Engineering (AMME) Book Series (ISSN 2328-8205) is published by IGI Global, 701 E. Chocolate Avenue, Hershey, PA 17033-1240, USA, [www.igi-global.com](http://www.igi-global.com). This series is composed of titles available for purchase individually; each title is edited to be contextually exclusive from any other title within the series. For pricing and ordering information please visit <http://www.igi-global.com/book-series/advances-mechatronics-mechanical-engineering/73808>. Postmaster: Send all address changes to above address. Copyright © 2019 IGI Global. All rights, including translation in other languages reserved by the publisher. No part of this series may be reproduced or used in any form or by any means – graphics, electronic, or mechanical, including photocopying, recording, taping, or information and retrieval systems – without written permission from the publisher, except for non commercial, educational use, including classroom teaching purposes. The views expressed in this series are those of the authors, but not necessarily of IGI Global.



## Titles in this Series

For a list of additional titles in this series, please visit: [www.igi-global.com/book-series](http://www.igi-global.com/book-series)

### *Stochastic Methods for Estimation and Problem Solving in Engineering*

Seifedine Kadry (Beirut Arab University, Lebanon)

Engineering Science Reference • copyright 2018 • 275pp • H/C (ISBN: 9781522550457) • US \$205.00 (our price)

### *Design and Optimization of Mechanical Engineering Products*

K. Kumar (Birla Institute of Technology, India) and J. Paulo Davim (University of Aveiro, Portugal)

Engineering Science Reference • copyright 2018 • 347pp • H/C (ISBN: 9781522534013) • US \$235.00 (our price)

### *Managerial Approaches Toward Queuing Systems and Simulations*

Salvador Hernandez-Gonzalez (Tecnológico Nacional de México en Celaya, Mexico) and Manuel Dario Hernandez Ripalda (Tecnológico Nacional de México en Celaya, Mexico)

Engineering Science Reference • copyright 2018 • 311pp • H/C (ISBN: 9781522552642) • US \$195.00 (our price)

### *Socio-Technical Decision Support in Air Navigation Systems Emerging Research and Opportunities*

Tetiana Shmelova (National Aviation University, Ukraine) Yuliya Sikirda (National Aviation University, Ukraine)

Nina Rizun (Gdansk University of Technology, Poland) Abdel-Badeeh M. Salem (Ain Shams University, Egypt) and Yury N. Kovalyov (National Aviation University, Ukraine)

Engineering Science Reference • copyright 2018 • 305pp • H/C (ISBN: 9781522531081) • US \$175.00 (our price)

### *Soft Computing Techniques and Applications in Mechanical Engineering*

Mangey Ram (Graphic Era University, India) and J. Paulo Davim (University of Aveiro, Portugal)

Engineering Science Reference • copyright 2018 • 336pp • H/C (ISBN: 9781522530350) • US \$215.00 (our price)

### *Advanced Numerical Simulations in Mechanical Engineering*

Ashwani Kumar (Government of Uttar Pradesh, India) Pravin P. Patil (Graphic Era University, India) and Yogesh Kr. Prajapati (National Institute of Technology Uttarakhand, India)

Engineering Science Reference • copyright 2018 • 242pp • H/C (ISBN: 9781522537229) • US \$165.00 (our price)

### *Numerical and Analytical Solutions for Solving Nonlinear Equations in Heat Transfer*

Davood Domiri Ganji (Babol Noshirvani University of Technology, Iran) and Roghayeh Abbasi Talarposhti (University of Mazandaran, Iran)

Engineering Science Reference • copyright 2018 • 275pp • H/C (ISBN: 9781522527138) • US \$195.00 (our price)



701 East Chocolate Avenue, Hershey, PA 17033, USA

Tel: 717-533-8845 x100 • Fax: 717-533-8661

E-Mail: [cust@igi-global.com](mailto:cust@igi-global.com) • [www.igi-global.com](http://www.igi-global.com)

# Table of Contents

<b>Preface</b> .....	xii
 <b>Chapter 1</b>	
Non-Conventional Technologies Selection: A Holistic Economic Assessment Applied to Micro-Manufacturing .....	1
<i>Paulo Peças, Universidade de Lisboa, Portugal</i>	
<i>Pedro Dias Pereira, Universidade de Lisboa, Portugal</i>	
<i>Inês Ribeiro, Universidade de Lisboa, Portugal</i>	
<i>Elsa Henriques, Universidade de Lisboa, Portugal</i>	
 <b>Chapter 2</b>	
An Insight on Current and Imminent Research Issues in EDM.....	33
<i>Azhar Equbal, National Institute of Foundry and Forge Technology, India</i>	
<i>Md. Israr Equbal, Aurora's Technological and Research Institute, India</i>	
<i>Md. Asif Equbal, Cambridge Institute of Technology, India</i>	
<i>Anoop Kumar Sood, National Institute of Foundry and Forge Technology, India</i>	
 <b>Chapter 3</b>	
Optimization of Process Parameters for Silicon Carbide Powder Mixed EDM .....	55
<i>Sasmeeta Tripathy, Siksha 'O' Anusandhan (Deemed University), India</i>	
<i>Deba Kumar Tripathy, IIT Kharagpur, India</i>	
 <b>Chapter 4</b>	
Optimization of Surface Roughness Parameters by Different Multi-Response Optimization Techniques During Electro-Discharge Machining of Titanium Alloy .....	82
<i>Anshuman Kumar Sahu, National Institute of Technology Rourkela, India</i>	
<i>Siba Sankar Mahapatra, National Institute of Technology Rourkela, India</i>	
 <b>Chapter 5</b>	
Evaluation of Electrical Discharge Machining Performance on Al (6351)–SiC–B4C Composite.....	109
<i>Uthayakumar M., Kalasalingam University, India</i>	
<i>Suresh Kumar S., Kalasalingam University, India</i>	
<i>Thirumalai Kumaran S., Kalasalingam University, India</i>	
<i>Parameswaran P., IGCAR, India</i>	

## **Chapter 6**

Recent Developments in Wire Electrical Discharge Machining ..... 125

*Nadeem Faisal, Birla Institute of Technology, India*

*Sumit Bhowmik, National Institute of Technology Silchar, India*

*Kaushik Kumar, Birla Institute of Technology, India*

## **Chapter 7**

Modeling and Optimization of Ultrasonic Machining Process Using a Novel Evolutionary

Algorithm..... 153

*Mantra Prasad Satpathy, KIIT (Deemed University), India*

*Bharat Chandra Routara, KIIT (Deemed University), India*

## **Chapter 8**

An Investigation Into Non-Conventional Machining of Metal Matrix Composites ..... 175

*Divya Zindani, National Institute of Technology Silchar, India*

*Kaushik Kumar, Birla Institute of Technology, India*

## **Chapter 9**

Photochemical Machining: A Less Explored Non-Conventional Machining Process..... 188

*Sandeep Sitaram Wangikar, Shri Vithal Education and Research Institute, India*

*Promod Kumar Patowari, National Institute of Technology Silchar, India*

*Rahul Dev Misra, National Institute of Technology Silchar, India*

*Nitin Dnyaneshwar Misal, Shri Vithal Education and Research Institute, India*

## **Chapter 10**

Performance and Surface Evaluation Characteristics on Cryogenic-Assisted Abrasive Water Jet

Machining of AISI D2 Steel ..... 202

*Yuvaraj N., Vel Tech Rangarajan Dr. Sagunthala R&D Institute of Science and Technology,  
India*

*Pradeep Kumar M., Anna University, India*

## **Chapter 11**

Finite Element Analysis of Tool Wear in Hot Machining Process: Hot Machining..... 232

*Asit Kumar Parida, Indian Institute of Technology, India*

## **Chapter 12**

FEM-ANN Sequential Modelling of Laser Transmission Welding for Prediction of Weld Pool

Dimensions ..... 249

*Bappa Acherjee, Birla Institute of Technology, India*

**Compilation of References** ..... 262

**About the Contributors** ..... 295

**Index**..... 301

# Detailed Table of Contents

<b>Preface</b> .....	xii
----------------------	-----

## **Chapter 1**

Non-Conventional Technologies Selection: A Holistic Economic Assessment Applied to Micro-Manufacturing .....	1
--	---

*Paulo Peças, Universidade de Lisboa, Portugal*

*Pedro Dias Pereira, Universidade de Lisboa, Portugal*

*Inês Ribeiro, Universidade de Lisboa, Portugal*

*Elsa Henriques, Universidade de Lisboa, Portugal*

Micro-engineering is nowadays a key industrial area with applications in a wide range of products and sectors. The need for a multiplicity of products fostered the development of several processes and combinations of processes in the world of micro-engineering. There are different feasible alternatives to produce the same kind of product. The manufacturing cost is usually the decision factor to select the best alternative among them. But cost is affected by dozens of factors and if not properly modelled causes controversy in so complex decisions. In this chapter, the application of process-based cost modelling is proposed as the engine to identify the best performance spaces for each alternative, using its potential for sensitive analysis of uncertain and/or critical parameters. To illustrate the approach, a case study is developed analyzing four alternatives for the production of a light diffuser with micro-features imbedded, involving micro-injection molding, hot-embossing, micromachining, and powder-injection molding.

## **Chapter 2**

An Insight on Current and Imminent Research Issues in EDM.....	33
--	----

*Azhar Equbal, National Institute of Foundry and Forge Technology, India*

*Md. Israr Equbal, Aurora's Technological and Research Institute, India*

*Md. Asif Equbal, Cambridge Institute of Technology, India*

*Anoop Kumar Sood, National Institute of Foundry and Forge Technology, India*

Electrical discharge machining (EDM) is an important unconventional manufacturing process which machines the workpieces by a series of recurring electrical discharges between tool and workpiece completely immersed in a dielectric. A power supply establishes an electric field between tool and workpiece while a proper gap is maintained between them by a servo controller. Electrostatic force causes electrons to get plucked out from tool and workpiece forming a channel called plasma having low dielectric strength which easily ionizes producing sparks responsible for machining the workpiece. When the power supply is withdrawn, the continuous flushing of dielectric removes the debris from machined cavity in workpiece. EDM is used in machining of dies, molds, parts of aerospace, automotive industry,

and surgical components. The study presents an insight on various research issues in EDM which would help the research community to establish their research objective to investigate. Based on current research trends and need of EDM study, the chapter also proposes some important future research issues.

### Chapter 3

Optimization of Process Parameters for Silicon Carbide Powder Mixed EDM ..... 55

*Sasmeeta Tripathy, Siksha 'O' Anusandhan (Deemed University), India*

*Deba Kumar Tripathy, IIT Kharagpur, India*

The present chapter deals with the investigations on the effect of process parameters like powder concentration (Cp), peak current (Ip), pulse-on-time (Ton), duty cycle (DC), and gap voltage (Vg) on output responses like material removal rate (MRR), tool wear rate (TWR), electrode wear ratio (EWR), surface roughness (SR), recast layer thickness (RLT), and micro-hardness (HVN) for PMEDM of H-11 hot work tool steel. Multi-objective optimization using grey relational analysis (GRA) has been implemented to identify the optimum set of input parameters to achieve maximum MRR and HVN with minimum TWR, EWR, SR, and RLT at the same time. Predicted results on verification with confirmation tests improve the preference values by 0.09468 with GRA. The recommended settings of process parameters is found to be Cp=6g/l, Ip=3Amp, Ton=100μs, DC=70%, and Vg=30V from GRA. The microstructures were examined with scanning electron microscope (SEM) to find the presence of surface deformities and identify alterations on the surface in comparison to the base material.

### Chapter 4

Optimization of Surface Roughness Parameters by Different Multi-Response Optimization Techniques During Electro-Discharge Machining of Titanium Alloy ..... 82

*Anshuman Kumar Sahu, National Institute of Technology Rourkela, India*

*Siba Sankar Mahapatra, National Institute of Technology Rourkela, India*

In this chapter, the EDM process is performed by taking titanium alloy as work piece and AlSiMg prepared by selective laser sintering (SLS) process as tool electrode along with copper and graphite. The EDM is performed by varying different process parameters like voltage (V), discharge current (Ip), duty cycle (τ), and pulse-on-time (Ton). The surface roughness parameters like Ra, Rt, and Rz are measured by the use of surface roughness measurement machine. To reduce the number of experiments, design of experiment (DOE) approach like Taguchi's L27 orthogonal array has been used. The surface properties of the EDM specimen are optimized by desirability function approach, TOPSIS and VIKOR method, and the best parametric setting is reported for the EDM process. All the optimization techniques convergence to the same optimal parametric setting. The type of tool is the most significant parameter followed by discharge current and voltage. Better surface finish of EDM specimen is produced with lower level of parametric setting along with the use of AlSiMg RP electrode during EDM.

### Chapter 5

Evaluation of Electrical Discharge Machining Performance on Al (6351)–SiC–B4C Composite..... 109

*Uthayakumar M., Kalasalingam University, India*

*Suresh Kumar S., Kalasalingam University, India*

*Thirumalai Kumaran S., Kalasalingam University, India*

*Parameswaran P., IGCAR, India*

Electrical discharge machining (EDM) process is a non-conventional machining process used for the material which are difficult to machine. In this research work, an attempt has been made to determine the

influence of Boron Carbide (B<sub>4</sub>C) particles on the machinability of the Al (6351) alloy reinforced with 5 wt. % Silicon Carbide (SiC) Metal Matrix Composite (MMC) through EDM. Influence of machining parameters such as pulse current (I), pulse on time (Ton), duty factor ( $\tau$ ), and gap voltage (V) on affecting the output performance characteristics namely Electrode Wear Ratio (EWR), Surface Roughness (SR) and Power Consumption (PC) which are studied. The result shows that the addition of B<sub>4</sub>C particles significantly affects the machinability of the composite, with a contribution of 1.6% on EWR, 3.5% on SR and 19.8% on PC. The crater, recast layer formation, and Heat Affected Zone (HAZ) in the machined surface of the composite are also reported in detail.

## Chapter 6

Recent Developments in Wire Electrical Discharge Machining ..... 125

*Nadeem Faisal, Birla Institute of Technology, India*

*Sumit Bhowmik, National Institute of Technology Silchar, India*

*Kaushik Kumar, Birla Institute of Technology, India*

The tremendous growth of manufacturing industries and desired need of accuracy and precision has put a great importance on non-traditional machining processes. Metal and non-metals having properties like high strength, toughness, and hardness is generally machined by non-conventional machining methods. One of earliest non-traditional machining that is still in use and being effectively utilized in industries is wire electrical discharge machine. This machining technique gives a tough line of competition to conventional machining process like milling, grinding, broaching, etc. Cutting intricate and delicate shapes with accuracy and precision gives this machining technique an edge over other conventional machining and non-conventional machining processes. This chapter provides an insight to various research and prominent work done in field of WEDM by various scientists, researchers, and academicians. The chapter also emphasizes various advantages and disadvantages of different modelling and optimization methods used. The chapter concludes with some recommendations about trends for future WEDM researchers.

## Chapter 7

Modeling and Optimization of Ultrasonic Machining Process Using a Novel Evolutionary Algorithm ..... 153

*Mantra Prasad Satpathy, KIIT (Deemed University), India*

*Bharat Chandra Routara, KIIT (Deemed University), India*

Ultrasonic machining (USM) is one of the non-conventional techniques for machining of hard and brittle materials like glass, ceramics, and ceramic matrix composites. The objective of the study includes the investigation of material removal rate (MRR), hole oversize (HOS), and circularity of holes (COH) during USM of soda lime glass and finding out the optimal parametric condition by an evolutionary algorithm. Taguchi philosophy was employed to carry out experiments using the process parameters such as power rating, abrasive slurry concentration, and static load. A novel optimization algorithm called imperialist competitive algorithm (ICA) was used to obtain maximum MRR and minimum HOS and COH. This algorithm is inspired by the imperialistic competition and has several advantages over other evolutionary algorithms like its simplicity, less computational time, and accuracy in predicting the results. The Technique for order of preference by similarity to ideal solution (TOPSIS) is utilized to convert these multiple performance characteristics to a single response. Moreover, the prediction outcomes of this TOPSIS integrated ICA methodology demonstrates excellent conformity with the experimental values and can be applied to solve complex problems.

## Chapter 8

An Investigation Into Non-Conventional Machining of Metal Matrix Composites ..... 175

*Divya Zindani, National Institute of Technology Silchar, India*

*Kaushik Kumar, Birla Institute of Technology, India*

One of the recently developing fields is that of non-traditional machining of particle reinforced metal matrix composites. The complexity associated with traditional machining of particle reinforced metal matrix composite is very high, and therefore, the researchers have begun to show more focus towards non-traditional machining. In the present work, the investigation has been carried out for non-traditional machining such as laser beam machining, electro-chemical machining, abrasive water jet machining, and electro-chemical discharge. Material removal rate, surface finish, and the mechanism of machining has been studied for each of the aforementioned processes. The main material removal mechanisms as has been identified are melting, mechanical erosion, vaporization, and chemical dissolution. The investigation reveals that the major reasons for the damage of the machined surface are the presence of reinforcement particles and thermal degradation.

## Chapter 9

Photochemical Machining: A Less Explored Non-Conventional Machining Process..... 188

*Sandeep Sitaram Wangikar, Shri Vithal Education and Research Institute, India*

*Promod Kumar Patowari, National Institute of Technology Silchar, India*

*Rahul Dev Misra, National Institute of Technology Silchar, India*

*Nitin Dnyaneshwar Misal, Shri Vithal Education and Research Institute, India*

The chapter focuses on the history and the development of photochemical machining in brief. The relevant studies related to photochemical machining and parametric effect are also discussed followed by gaps identified along with scope for the work and then the PCM process is explained in detail. The significant control parameters and their effect on the response measures are demonstrated with a fishbone diagram is explored. Further the detailed parametric effect on the response measures along with the scientific explanation of the effect is presented. The chapter is concluded with the two case studies (i.e., PCM of brass and Inconel 718).

## Chapter 10

Performance and Surface Evaluation Characteristics on Cryogenic-Assisted Abrasive Water Jet Machining of AISI D2 Steel ..... 202

*Yuvaraj N., Vel Tech Rangarajan Dr. Sagunthala R&D Institute of Science and Technology, India*

*Pradeep Kumar M., Anna University, India*

The chapter reports on the investigation of cryogenic-assisted abrasive water jet (CAAWJ) machining of AISI D2 steel with varying the jet impact angles and abrasive mesh sizes. The performance measurement is considered in this study such as depth of penetration and taper ratio. Also, the surface integrity characteristics are considered in the present study such as abrasive contamination, surface topography, XRD peaks, residual stress, and micro hardness. The CAAWJ machining process improves the performance measurement such as higher depth of penetration and lower taper ratio for the machining of D2 steel. Also, the CAAWJ cut surface consists of better surface integrity features over the AWJ cut surface. The phase

transformation effect of target material under cryogenic cooling helps to turn the mode of the material removal mechanism from ductile to brittle erosion process and yield a better performance. The results also indicate that the oblique jet impact angles have been produced better performance characteristics than the jet impact angle of 90° at room temperature.

## **Chapter 11**

Finite Element Analysis of Tool Wear in Hot Machining Process: Hot Machining .....	232
<i>Asit Kumar Parida, Indian Institute of Technology, India</i>	

Super alloys have been used widely in all sectors (e.g., automobile, aerospace, biomedical, etc.) for their properties like high hardness, high wear, and corrosion resistance. A central challenge is the significantly higher temperature and pressure on the cutting tool, hence rapid tool wear and bad surface finish. In the present study, a FEM analysis has been developed to calculate the effect of preheating temperature on the surface of the workpiece on tool wear on machining Inconel 718. Usui's tool wear model has been implemented in DEFORM software. In order to validate the results, an experimental investigation has been carried out with same cutting conditions. The evaluated results were also compared with the room temperature machining condition. It was observed that the heating temperature increased the tool life by reducing tool wear, tool temperature compared to room temperature machining condition. The predicted tool wear, tool temperature, and chip morphology have been compared with the experimental results and good correlation was found.

## **Chapter 12**

FEM-ANN Sequential Modelling of Laser Transmission Welding for Prediction of Weld Pool Dimensions .....	249
<i>Bappa Acherjee, Birla Institute of Technology, India</i>	

In this chapter, a sequential modeling approach has been applied for modeling of laser transmission welding process using finite element method (FEM) and artificial neural network (ANN) technique to predict the weld pool dimensions in a shorter time frame. The scripting language, APDL (ANSYS® Parametric Design Language), is used to develop the three-dimensional FE model. During preprocessing, all the major physical phenomena of laser transmission welding process are incorporated into the model physics. Based on the temperature field predicted by the model, the weld pool dimensions (i.e., weld width and weld penetration depth) are calculated. The weld dimensions predicted by the developed FE model are further used for training a neural network model. It is found from the results of test data sets that the developed ANN model can predict the outputs with significant accuracy and takes less prediction time, which in turn saves time, cost, and the efforts for performing experiments.

<b>Compilation of References .....</b>	<b>262</b>
<b>About the Contributors .....</b>	<b>295</b>
<b>Index.....</b>	<b>301</b>



## Preface

In the present era of revolution of the industrial environment “Industry 4.0” (I40) which represents the comprehensive transformation of the entire industrial production through the merging of Internet and information and communication technologies (ICT) incorporating smart technologies. So the customer satisfaction calls for optimal cost, time and quality. Aimed toward these three variables, companies continuously develop / improve practices and techniques to satisfy the consumer requirements and in turn increase their market share and profit. There are several critical factors affecting them adversely which are the main concerns for the management and usage of new practices eliminates hurdles or barriers.

Manufacturing sectors few decades ago completely relied on traditional machining processes like turning, grinding, shaping, drilling, milling, etc. for most of their work. But with development of new materials and newer/customized shapes for recent customized products have risen to certain constraints in usage of traditional machining processes. Extremely hard and brittle materials, workpiece in which length to diameter ratio is very high or workpiece with a very complicated shape are getting more and more difficult in machining using traditional processes so development of non-traditional or non-conventional machining (NCM) processes came into picture which is also known as advanced manufacturing process. NCM is used when the traditional manufacturing processes are not practical and economical. Non-Traditional manufacturing processes offer many advantages when compared to the traditional manufacturing processes including zero surface defects. The main aim of non-conventional machining is to provide efficient and cost-effective solutions to the materials using different state-of-the art. Many different types of non-traditional processes are discussed along with its applications and limitations.

The major characteristics of Traditional Machining is in the fact that material removal takes place due to application of cutting forces in form of macroscopic chip by shear deformation, hence it is customary that the cutting tool is harder than work piece at room temperature as well as under machining conditions. NCM processes, on the other hand, removes excess material by various techniques involving mechanical, thermal, electrical or chemical energy or combinations of these energies but do not use a sharp cutting tools as it needs to be used for conventional manufacturing processes. So on the basis of principle form of energy used; NCM can be classified as Mechanical, Electrical, Thermal and Chemical. Techniques utilising Mechanical form of Energy are AFM (Abrasive Flow Machining), AJM (Abrasive Jet Machining), HDM (Hydrodynamic Machining), LSG (Low Stress Grinding), RUM (Rotary Ultrasonic Machining), TAM (Thermally Assisted Machining), TFM (Total Form Machining), USM (Ultrasonic Machining), WJM (Water Jet Machining) etc. Some of the techniques utilizing Electrical energy are ECD (Electrochemical Deburring), ECDG (Electrochemical Discharge Grinding), ECG (Electrochemical Grinding), ECH (Electrochemical Honing), ECM (Electrochemical Machining), ECP (Electrochemical Polishing), ECS (Electrochemical Sharpening), ECT (Electrochemical Turning), ES

## **Preface**

(Electro-Stream), STEM (Shaped Tube Electrolytic Machining) etc. Similarly under Thermal energy EBM (Electron Beam Machining), EDG (Electrical Discharge Grinding), EDM (Electrical Discharge Machining), EDS (Electrical Discharge Sawing), EDWC (Electrical Discharge Wire Cutting), LBM (Laser Beam Machining), LBT (Laser Beam Torch), PBM (Plasma Beam Machining) etc. and with the aid of Chemical energy CHM (Chemical Machining), ELP (Electro-polish), PCM (Photochemical Machining), TCM (Thermo-chemical Machining), TEM (Thermal Energy Machining) etc. techniques are currently being utilized. More techniques involving more than one form of energy under Hybrid Techniques are also being developed and utilized.

The main objective of the book is concentrated on the usage and performance of NCM techniques and target audience are all Academics Students, Researchers and Industry Practitioners, Engineers, Research Scientists/ Academicians involved in Non Conventional Machining of Engineering products.

There are 12 chapters in the book. It starts with Chapter 1 which talks about Non-Conventional Technologies selection for Micro-engineering which is nowadays a key industrial area with applications to a wide range of products and sectors. The need for a multiplicity of products fostered the development of several processes and combinations of processes in the world of micro-engineering. There are different feasible alternatives to produce the same kind of product. The manufacturing cost is usually the decision factor to select the best alternative among them. In this chapter the application of process-based cost modelling is proposed as the engine to identify the best performance spaces for each alternative, using its potential for sensitive analysis of uncertain and/or critical parameters. To illustrate the approach a case study has been developed analyzing four alternatives for the production of a light diffuser with micro-features imbedded, involving micro-injection molding, hot-embossing, micromachining and powder-injection molding.

Electro-discharge machining (EDM) is the most common and most used NCM, and hence, in next four chapters, i.e. Chapter 2 – Chapter 5, different work and aspect of EDM have been illustrated.

Chapter 2 provides a review of the most important unconventional manufacturing process, i.e. Electrical discharge machining (EDM) currently being employed in a wide range of industries from aerospace to medical. The chapter presents an insight on various research issues in EDM which would help the research community to establish their research objective to investigate upon. Based on current research trends and need of EDM, study also proposes some important future research issues.

In Chapter 3 investigations on the effect of process parameters like powder concentration ( $C_p$ ), peak current ( $I_p$ ), pulse-on-time ( $T_{on}$ ), duty cycle (DC) and gap voltage ( $V_g$ ) on output responses like material removal rate (MRR), tool wear rate (TWR), electrode wear ratio (EWR), surface roughness (SR), recast layer thickness (RLT) and micro-hardness (HVN) for PMEDM of H-11 hot work tool steel was performed. Multi-objective optimization was performed to identify the optimum set of input parameters to achieve maximum MRR and HVN with minimum TWR, EWR, SR and RLT at the same time. The results were authenticated with the aid of Scanning Electron Microscope (SEM) to find the presence of surface deformities and identify alterations on the surface in comparison to the base material.

Chapter 4 utilizes EDM process for machining work piece of Titanium alloy with AlSiMg, prepared by selective laser sintering (SLS) process, as tool electrode along with copper and graphite. In this chapter also the optimal process parameters were identified by desirability function approach, TOPSIS and VIKOR method. It was found that all the optimization techniques converged to the same optimal parametric setting.

In Chapter 5, the last chapter dealing with EDM process deals with machining of Metal Matrix Composite. In this work, in order to determine the influence of Boron Carbide ( $B_4C$ ) particles on the machinability

of the Al (6351) alloy reinforced with 5 wt. % Silicon Carbide (SiC) Metal Matrix Composite (MMC) through EDM, detailed experimentation was performed. The result indicated that the addition of B4C particles significantly affects the machinability of the composite. The crater, recast layer formation and Heat Affected Zone (HAZ) in the machined surface of the composite have also been reported in detail.

Chapter 6 describes another technique i.e. Wire Electrical Discharge Machine (WEDM), the next most sort after technique by industries globally. This chapter provides an insight to various research and prominent work done in field of WEDM by various scientists, researchers, and academicians. Chapter also emphasizes various advantages and disadvantages of different modelling and optimization methods used. The chapter concludes with some recommendations about trends for future WEDM researchers.

Chapter 7 describes Ultrasonic machining (USM) being one of the non-conventional techniques for machining of hard, brittle and non conducting materials like glass, ceramics and ceramic matrix composites. The objective of the work was to investigate material removal rate (MRR), hole oversize (HOS) and circularity of holes (COH) during USM of soda lime glass and obtaining the optimal parametric condition by an evolutionary algorithm called imperialist competitive algorithm (ICA). This algorithm is inspired by the imperialistic competition and has several advantages over other evolutionary algorithms like its simplicity, less computational time and accuracy in predicting the results. Moreover, the prediction outcomes of this TOPSIS integrated ICA methodology demonstrates excellent conformity with the experimental values.

Chapter 8 talks about non-traditional machining of particle reinforced metal matrix composites. In this chapter the investigation has been carried out using Laser Beam Machining (LBM), Electro-Chemical Machining (ECM), Abrasive Water Jet Machining (AWJM) and Electro-Chemical Discharge (EDM). Material removal rate, surface finish and the mechanism of machining had been studied for each of the aforementioned processes. The main material removal mechanisms have been identified are melting, mechanical erosion, vaporization and chemical dissolution.

Chapter 9 takes up yet another NCM i.e. photochemical machining (PCM) which the researchers feel to be one of the least explored non-conventional machining process. The chapter, hence, introduces the reader to the background, steps and mechanism of the process. It then continues to brief control and response parameters along with various elements contributing significantly the outputs i.e. material removal rate and surface roughness. In this connection two supporting case studies on PCM of brass and Inconel 718 are discussed.

The next chapter, Chapter 10 reports the investigation of cryogenic assisted abrasive water jet (CAAWJ) machining of AISI D2 steel with varying the jet impact angles and abrasive mesh sizes. The inputs varied were depth of penetration and taper ratio. The surface integrity characteristics such as abrasive contamination, surface topography, XRD peaks, residual stress and micro hardness were evaluated. The researchers also indicated that phase transformation effect of target material under cryogenic cooling helped to turn the mode of the material removal mechanism from ductile to brittle erosion process and yielded a better performance. The results also illustrated that, the oblique jet impact angles have been produced better performance characteristics than the jet impact angle of 90° at room temperature.

Next two chapters, Chapter 11 and Chapter 12 deal with Finite Element Analysis of machining.

In Chapter 11 FEM analysis has been developed to calculate the effect of preheating temperature on the surface of the workpiece on tool wear on machining Inconel 718. The researcher has utilized Usui' tool wear model in DEFORM software. In order to validate the results, an experimental investigation has also been carried out with same cutting conditions. The evaluated results were found to be in good correlation with the FEM results.

## ***Preface***

Chapter 12, the last chapter of the book, uses finite element method (FEM) and artificial neural network (ANN) technique as a sequential modeling approach for modeling of laser transmission welding process. The scripting language, ANSYS APDL was used to develop the 3-dimensional FE model. Based on the temperature field predicted by the model, the weld pool dimensions i.e. weld width and weld penetration depth were calculated. The weld dimensions predicted by the developed FE model were further utilized for training a neural network model. It is found, from the results of test data sets, that the developed ANN model could predict the outputs with significant accuracy and took very less prediction time, which in turn saved the time, cost and the efforts for performing experiments.

First and foremost, the editors would like to thank God. It was His blessings that this work could be completed to our satisfaction. You have given the power to believe in passion, hard work and pursue dreams. The Editors could never have done this herculean task without the faith they have in you, the Almighty. They are thankful for this.

The editors would also like to thank all the chapter contributors, the reviewers, the editorial advisory board members, book development editor and the team of publisher IGI Global for their availability for work on this editorial project.

Throughout the process of editing this book, many individuals, from different walks of life, have taken time out to help. Last, but definitely not least, the editors would like to thank them all, their well wishers, for providing them encouragement. They would have probably given up without their support.

*Kaushik Kumar*

*Birla Institute of Technology, India*

*Nisha Kumari*

*Birla Institute of Technology, India*

*J. Paulo Davim*

*University of Aveiro, Portugal*

# Chapter 1

## Non-Conventional Technologies Selection: A Holistic Economic Assessment Applied to Micro-Manufacturing

**Paulo Peças**

*Universidade de Lisboa, Portugal*

**Pedro Dias Pereira**

*Universidade de Lisboa, Portugal*

**Inês Ribeiro**

*Universidade de Lisboa, Portugal*

**Elsa Henriques**

*Universidade de Lisboa, Portugal*

### ABSTRACT

*Micro-engineering is nowadays a key industrial area with applications in a wide range of products and sectors. The need for a multiplicity of products fostered the development of several processes and combinations of processes in the world of micro-engineering. There are different feasible alternatives to produce the same kind of product. The manufacturing cost is usually the decision factor to select the best alternative among them. But cost is affected by dozens of factors and if not properly modelled causes controversy in so complex decisions. In this chapter, the application of process-based cost modelling is proposed as the engine to identify the best performance spaces for each alternative, using its potential for sensitive analysis of uncertain and/or critical parameters. To illustrate the approach, a case study is developed analyzing four alternatives for the production of a light diffuser with micro-features imbedded, involving micro-injection molding, hot-embossing, micromachining, and powder-injection molding.*

DOI: 10.4018/978-1-5225-6161-3.ch001

## INTRODUCTION

### Brief Chapter Overview

Micro-engineering is nowadays a key industrial area with applications in a wide range of products and sectors. The need for a multiplicity of products fostered the development of several processes combining different technologies in the realm of micro-engineering, from the Micro-Electro-Mechanical Systems (MEMS) based technologies to the Energy Assisted and Mechanical Processes. Usually, the first step of technology selection is the physical processes capability to accomplish the desired micro-shape(s). The second step is the selection of the most adequate process (or combination of processes) usually based on the individual performance (e.g. using target costing for the economic performance) and/or on comparative analysis of alternatives (e.g. conventional vs. non-conventional technologies). In this chapter the application of process-based cost modelling (PBCM) is proposed to support an informed decision making during the second step mentioned, by integrating the technology relations of each alternative process with i) the cost factors and ii) the production scenario and context, allowing the identification of the best performance spaces for each alternative. A holistic economic assessment approach is used taking into account technological limitations, uncertainty on specific parameters and different industrial environments. The PBCM models are built up and the subsequent sensitivity analyses is structured assuring its adequacy to compare and understand the economical behavior of technologies that are already implemented in companies and the ones that are under development and/or giving the first steps, which is frequently the case of the non-conventional technologies. To illustrate the approach a case study is developed analyzing four alternatives for the production of a plastic light diffuser with micro-features imbedded, being used micro-injection molding and micro-hot embossing for the plastic part production and also micro-milling and powder-injection molding (PIM) for the mold production. Therefore, this chapter demonstrates the pertinence of using PBCM for technology selection in the realm of micro-engineering and gives also a contribution to the fields of micro-injection molding, micro-hot embossing and micro-milling by an holistic comparison of the economic performance of these processes.

### The Challenges of Economic Performance Assessment of Micro-Engineering Related Technologies

Micro-engineering was defined by Alting *et al.*, (2003) as the “development and manufacturing of products, whose functional features or at least one dimension are in order of  $\mu\text{m}$ , characterized by a high degree of integration of functionalities and components”. Due to society’s demands, micro-parts have been introduced in several types of products. The downsizing of electronic products and automobile parts and the rapid development of biotechnology and medical devices have transformed micro-engineering in a key technological area (Asad *et al.*, 2007; Masuzawa, 2000; Verdian, 2017). In parallel, manufacturing processes have been developed or adapted for miniaturization and there are nowadays extensive studies regarding different processes and materials (Anasane & Bhattacharyya, 2017; Rathod *et al.*, 2014; Wu *et al.*, 2017).

The impetus to develop new technologies or adapt the existing ones to the demanding micro-engineering applications fosters the development of several alternatives to manufacture micro-parts, micro-products and parts/products with micro-features. Micro-manufacturing technologies have been classified into three types (Brinksmeier *et al.*, 2001): i) the ones for Micro-Electro-Mechanical Systems (MEMS) comprising

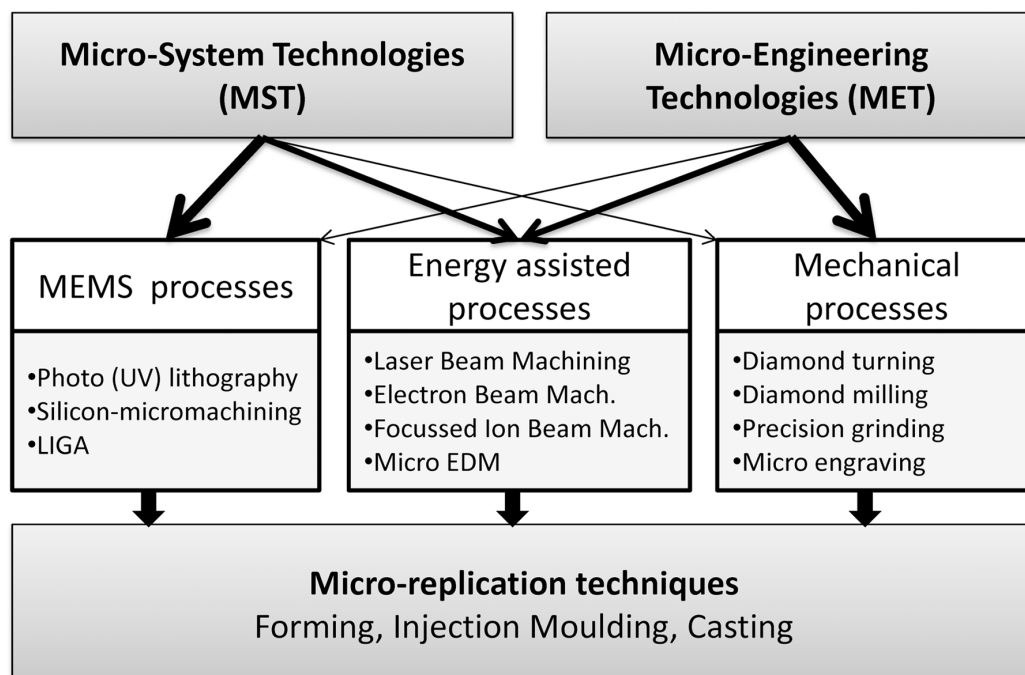
## Non-Conventional Technologies Selection

photo-lithography and silicon micro-machining, among others; ii) Energy-assisted processes, namely laser beam, electron-beam, focused ion beam and micro-electro discharge machining; iii) mechanical processes including diamond turning, and milling, precision grinding and engraving adapted to the micro scale. In addition, the micro-replication technologies often appear has a separated class, including micro-forming (including embossing), injection molding and casting (Figure 1).

Some of these alternatives are available as commercial technologies others are in the process of pre-industrialization or even in the phase of research results validation. Furthermore, replication alternatives contemplate the two usual manufacturing stages: the tool production and the replication process. Consequently, to compare the performance of competing manufacturing alternatives in the realm of micro-engineering is crucial to tackle two demanding challenges: 1) the lack of comprehensive knowledge and/or lack of significant industrial experience about the replication processes; 2) the inclusion of the tool manufacturing process selection (usually machining) on the performance of the micro product/part replication process. To overcome these challenges the comparative models should incorporate a holistic perspective of the manufacturing processes required to produce the parts and to allow sensitive analysis to assess the influence of uncertainty derived from lack knowledge about processes performance. The use of PBCM allows to deal with these challenges as explained in the next paragraphs and demonstrated throughout the chapter.

In general, the comparison among manufacturing alternatives, in a preliminary decision level, should be performed using intrinsic consequences and resulted properties of those alternatives (Kim, 1999). So, the several candidate alternatives are selected as the possible ones to potentially produce the product based on the product/part's requirements related with geometric accuracy, defects absence, etc.

*Figure 1. Classification of micro-manufacturing technologies  
(adapted from Brinksmeier et al. (2001))*



(intrinsic properties) and mechanical behavior, durability, color stability, etc. (resultant properties). On a second level of decision the emergent properties of the manufacturing alternatives must be compared. The economic performance is considered an emergent property since it is dependent not only upon characteristics of the product/part, but also on other broader domains including the context in which the product is produced and handled, and on the characteristics of the market (Kim, 1999). Therefore, the assessment of the economic performance must be carefully done to cover comprehensively the aspects that can affect the economic performance. In other words, it should include the aspects related with the replication manufacturing process as well as the ones related with the tooling design and manufacturing. In addition, sensitivity analysis of the several parameters for which there is a lack of established knowledge and/or production experience should be undertaken. The type of parameters to include in these sensitivity analysis can be technological related (cycle time, process variability, etc.), part related (dimensions, complexity, etc.) and industrial related (production volume, manufacturing environment, level of technology incorporation, etc.)

The PBCM are for sure a powerful tool to be used as a way to tackle the mentioned challenges (Folgado et al., 2010; Peças et al., 2010; Ribeiro et al., 2016). Taking advantage of its parametric nature the use of properly designed PBCM permits i) the inclusion of technological relations, for estimating time and resources consumed depending on the model inputs: process parameters and part parameters; ii) the consideration of different production contexts on model inputs: production volume, type of machine, etc.; iii) the analysis of the economic performance for different types of production: existent technologies, cost of resources, cost of equipment, etc. So, the PBCM allows a comprehensive sensitivity analysis to the several uncertain and/or unknown parameters and contexts.

Finally, this chapter focuses the important aspects on the development of PBCM to face the particular situation of micro-engineering. In particular, attention is given to the need to identify the critical parameters of the recent or under development alternatives (technologies). The use of best performance spaces is proposed and discussed as an answer for the limited knowledge or level of industrial experience. Additionally, for a holistic economic assessment, the inclusion of the tool manufacturing processes in the PBCM is foreseen as mandatory to assure a trustable and defensible economic comparison in the world of micro-engineering.

A case study is presented regarding the production of a light diffuser with micro-features made of Poly(methyl methacrylate) (PMMA) polymer. Four technological alternatives that use different combinations of tooling and replication processes are presented and compared. The alternatives use micro-injection molding and micro-hot embossing for the plastic part production and also micro-milling and PIM for the mold production.

## **PROCESS-BASED COST MODELS**

### **General Use and Particular Aspects Fostering Its Use on Micro-Engineering**

The PBCM models are built to estimate in an early design stage the cost of a product or component taking into consideration the several processes and characteristics of the required manufacturing or assembly system. This type of models has been applied by researchers within different scopes, always with the intent to compare alternatives – either in materials, processes or product architectures (Field et al. 2007;

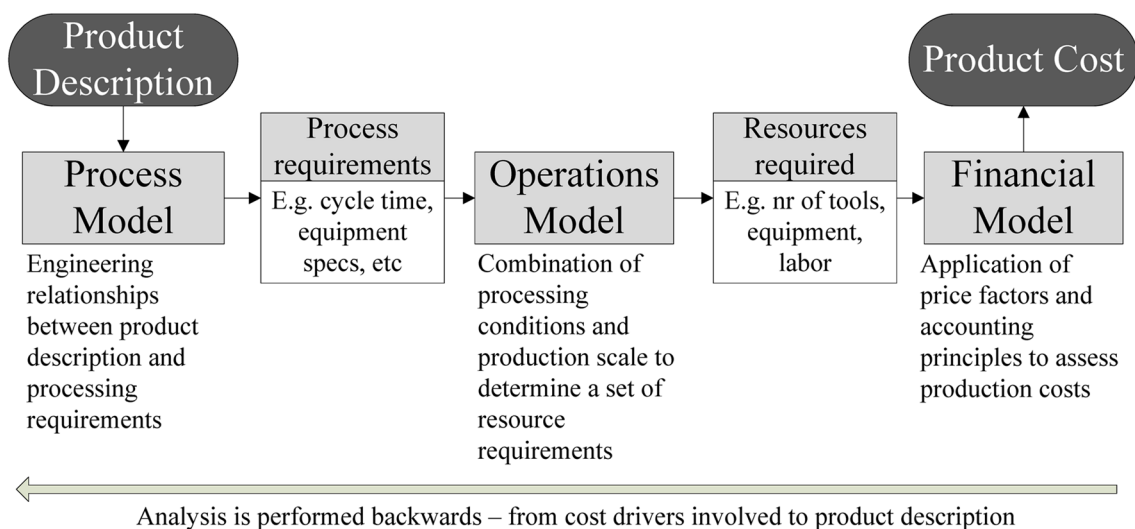


## Non-Conventional Technologies Selection

Fixson, 2005; Fuchs et al., 2008; Peças et al., 2013). The usual PBCM is constructed backwards: from the model's objective (cost) to the model required inputs (physical parameters that can be controlled) (Johnson & Kirchain, 2009). An illustration of the modelling phases and the content of each model can be seen in Figure 2. The Process Model involves identifying the relevant engineering relationships between physical parameters and cost-determinant attributes of a process (e.g., cycle time, equipment performance requirements). In the Operations Model these processing attributes are related to the manufacturing resources requirements (e.g., materials quantity, number of laborers, number of machines, and/or tools). The Financial Model translates these requirements to a specific cost by applying price factors and accounting principles to assess production costs.

Therefore, cost modeling through PBCM allows translating into a cost metric, in an early stage, the complex and interrelated consequences of design and/or process technology changes. It can be considered as a tool for strategic analysis of design, material and process choice since the referred translation is done in a way that is technologically defensible while retaining the transparency necessary to support that defense (Field et al., 2007). Beside this usefulness, PBCMs have proven to be particularly valuable as tools for improving communication and discussion of cost with diverse groups (Fuchs et al., 2008; Peças et al., 2009; Peças et al., 2013; Ribeiro et al., 2016), since they can be used as platforms for creating a working dialog about the most relevant factors that drive design and production costs. These two main virtues of the PBCM match flawlessly with the actual stage of development of micro-engineering related process and products: i) specific and robust cost related analysis must be performed in an early development stage of processes and technologies, and ii) an open discussion should be promoted under a normalized standardized communication framework. To fully exploit the potential of the use of PBCM in micro-engineering applications particular attention should be given to some aspects of PBCM development, which are following discussed and illustrated by a case study deployment in the next section.

Figure 2. Schematic of Process-based cost modeling



## **Process Model: The Importance of Scope Extension**

The aim of the process modeling when constructing a PBCM is to establish correlations between product description and processing requirements based on engineering relationships and physical parameters. The scope of traditional PBCM takes into consideration mainly the primary processes of product/component replication (Field et al., 2007; Fuchs et al., 2008). In the case of micro-engineering related analysis this scope should be also extended to the process(es) of tool(s) manufacturing and to other indirect manufacturing processes required to obtain the product/component (Peças et al., 2013; Ribeiro et al., 2013). In the realm of micro-engineering, product replication alternatives proliferate together with alternatives for tool manufacturing, being the latter usually composed by a manufacturing sequence of technologies (e.g., powder injection molding (PIM), laser cusing). It must be noted that some of these tools have a short lifetime and/or limited numbers of repetition cycles, and are often considered as disposable tools (e.g., silicon tools, PIM tools). In addition, the reduced dimension of parts demands for specific treatments/processing (e.g., cleaning, impingement), specific handling operations (e.g., transport, positioning) and/or specific mountings (e.g., setup of a set of parts), which can affect significantly the overall process performance and consequently the total production cost, despite they can be considered as indirect or auxiliary process/tasks.

In traditional PBCM there is a tendency to assume the tooling as a “black-box” item with a respective price (acquisition cost) and disregard its manufacturing process due to its low relevance in the overall process cost (percentage of production cost). The rationale is related with its steadiness with the production volume and with data and knowledge available related with many years of industrial practice. In the case of PBCM for micro-engineering applications the parameterization all the indirect processes is in general recommended, as well as all the tool manufacturing steps due i) to its novelty and/or lack of (low) industrial experience and ii) because in some cases the alternatives under analysis have relevant differences in the performance of these intermediate manufacturing steps. By assuming this level of extended scope, the potential of the PBCM under development is used allowing the sensitivity analysis on several influencing parameters and on production/technical scenarios where the behavior of the alternatives is not yet completely known.

Another important point of discussion is related with the inclusion or not of a life cycle perspective. In the traditional approach of PBCM the decision of using a life cycle perspective is defined usually by the need to assess the impact of the design/process alternatives in the use, disposal and end-of-life phases (EoL) of the product (Folgado et al., 2010; Ribeiro et al. 2013; Ribeiro et al., 2008). In the micro-engineering applications the manufacturing processes to include in the PBCM are recent and new materials, new uses of existent materials, new handling devices and disposable items proliferate, with recycling and recovering circuits are in most of the cases not yet established and/or standardized. Consequently, when these aspects exist and have a potential significant effect on the economic performance of the alternatives under analysis, their consideration and accounting is important since it might impose specific actions (so costs) to the firm using these materials and processes. In the absence of an established recycling and recovery praxis, a closed-circuit approach is recommended considering the necessary local operations/tasks to assure materials and devices recycling, recovery or disposal. This closed-circuit approach assures the impacts accounting without the need of the formal aspects of LCC disposal and EoL phases.

As regards the use phase, it must be noted that the costs of this phase incur in a different moment of the manufacturing costs. In general, even in traditional PBCM it is a hard task to compare alternatives based on cost when the costs are incurred in different moments and are perceived differently by the different stakeholder. In the cases that the impact of a micro-engineering component in a macro-engineering system is very low (due to its dimensions and mass), the inclusion of the use phase in PBCM for products/components of micro-engineering can be only considered when the product/component produced by the different alternatives has important impact in the different stakeholders.

The final remark regarding the scope of the process modeling is related with the different stakeholders of the PBCM, meaning the ones among whom the study and results of the PBCM will be discussed and used as a valuable support for informed decision-making. In the framework of micro-engineering applications, the PBCM can be used to select a technology or process to produce a product/component by a manufacturing company, but also on a more research-based perspective fostering a more universal comparison of process/technologies alternatives. In the present stage of micro-engineering technologies (MET, see Figure 1) PBCM can support the identification of application ranges of competing manufacturing alternatives and of critical parameters that are limiting the performance of a technology. These kinds of analyses will allow taking informed decisions about next research planning and stop and go decisions on the development of a certain technology. Therefore, depending on the aim of the study to be done, the scope of the PBCM must be clearly decided and specified in the beginning of modeling tasks.

### **Operations Model: The Importance of Model Flexibility**

The operations modeling aims to determine the full set of required resources, combining the processing conditions, operational parameters and production scale. The required resources depend upon how the technical process is physically implemented and how the actual operation of the physical plant is organized. The aimed scale of operation is also an important parameter in any cost model since several technical and operational decisions are predicted upon satisfying production targets (Field et al., 2007). For the particular case of PBCM development for micro-engineering applications most of the aspects related with plant organization and production stages are not fully defined. In fact they might be considered as analyzing parameters. The early development stage of the processes and technologies and the eventually absence of related industrial experience will cause the modeler of the operations model to introduce flexibility in the computing logics. In traditional PBCM, the modeling parameters like cycle time and parts per cycle are usually independent parameters (that of course can be changed due to the parameterized nature of PBCM). Nevertheless, when dealing with processes under development these parameters and their correlation with other parameters like material wastes, rejection rate, etc. might be not so well defined. Other aspects demanding for flexibility are related with equipment reliability and maintenance related requirements. If there is no industrial experience with the equipment these parameters cannot be introduced as a simple percentage of the production cost but be varied for a estimation range in order to assess its influence. A final remark is related with the danger of such a flexible model when it is used by an unexperienced user. The interdependence between parameters might create parameter settings that are not real if the model doesn't contain warnings about parameter levelling and limits. In this case the creation of several parameters options (fixed combinations) is recommended, keeping the flexibility as well as the model accuracy.

## **Financial Model: The Importance of Transparency and Correctness**

The process and operations models allow enumerating and computing the resources required to produce a product/component. The aim of the financial model is to convert resources requirements into their economic cost. In the case of variable cost items like energy, materials, consumables and labor, the cost can be easily achieved by multiplying the resource quantity by their price factors. The costs related with equipment, facilities and to other fixed cost items have to be calculated with more indirect allocation strategies. These allocation strategies depend on the financial model, firm strategy and study objective (Fixson, 2005; Fuchs et al., 2008; Johnson & Kirchain, 2009). As in any other cost modeling, a sound and reliable PBCM for micro-engineering applications must offer a full transparency to the analysis so that the alternatives can be properly and fairly compared. Since in the micro-engineering framework several processes are still under development or in the early stages of application, frequently the related market prices of equipment, components and consumables can be difficult to gather or to be considered as standard or definitive. In the cases the item is not available in the market, the most probable price ranges can be defined by data gathering through comparison, surveys or experts. Of course, these ways of price definition must be declared and similar to all the alternatives for the sake of equity. In addition, the analysis of several business scenarios might be useful, namely when the production level is low the use renting, sub-contracting or other types of outsourcing should be considered.

Another important aspect of the financial model is the output of results. The alternatives should be compared not only based on the product/component total cost, but also on the cost breakdown and the cost of each production phase. Whenever it is applicable, the breakeven cost between alternatives should be output by the financial model. In addition, the cost related results should be assessed not only for a specific parameter setting and for a specific most likely scenario, but also sensitivity analysis should be presented for different production scenarios (production volumes, equipment uptimes, etc.). In the framework of micro-engineering there are critical parameters for which the knowledge is usually limited (tool life, processing rate, rejects percentage, etc.), so sensitivity analysis is mandatory for these parameters.

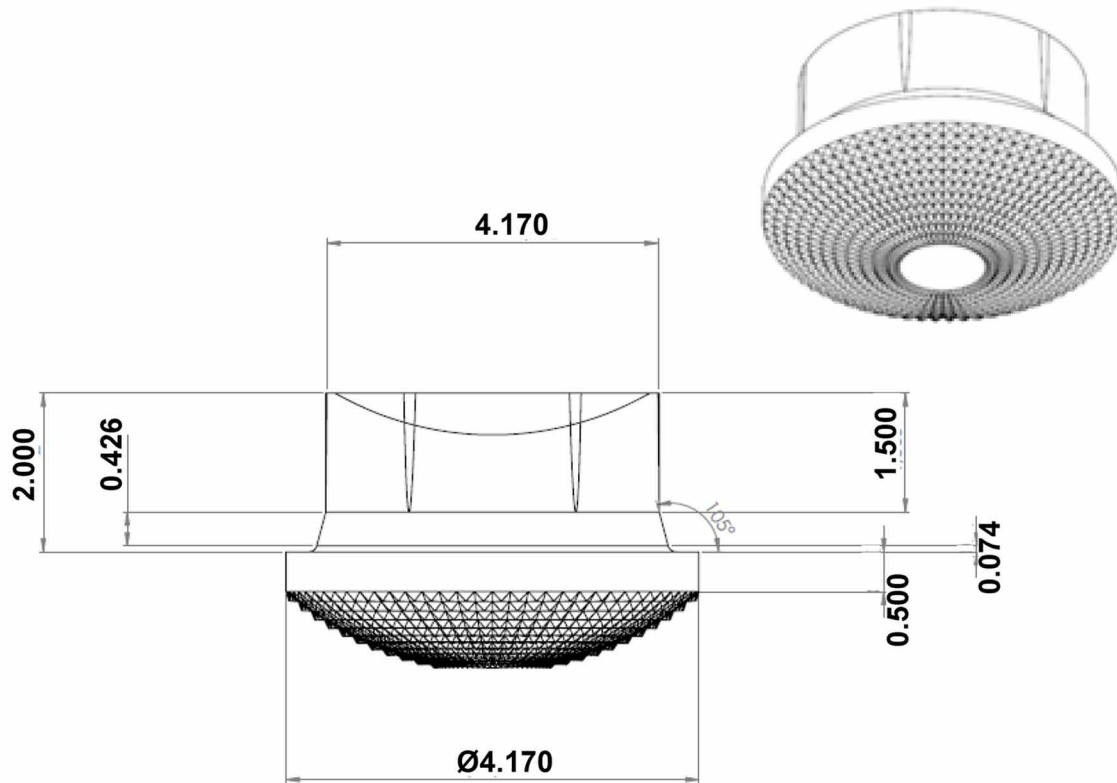
In summary, respecting the required scope, flexibility, transparency and correctness it is possible to produce important results with the developed PBCM allowing, in the realm of micro-engineering: i) the alternatives performance comparison (component cost) for specific production scenarios and most likely performance of critical parameters; ii) the best performance spaces for the alternatives in the range of variation of the critical parameters; iii) break even analysis between alternatives; iv) discussion among researchers, experts, technology developers and users about the future trends for technologies development/research; v) support the decision-making process of technology users on the technology selection.

## **CASE STUDY**

The selected case study illustrates the potential of the use of process-based cost modeling to assess comprehensively technologies and processes that are in an early stage of development and to validate most of the identified critical aspects related with micro-engineering alternatives comparison. The product or component to be produced is a light diffuser (Figure 3). This part is within the micro-engineering range not because of the overall part dimensions but due to the part micro-features that require machining/

## Non-Conventional Technologies Selection

Figure 3. Light diffuser (dimensions in mm)



forming. The part is made of PMMA polymer (Poly (methyl methacrylate)) and an annual production volume of 500,000 parts is expected for 8 years. The case study includes 4 manufacturing sequences to produce the same part. The 4 alternatives include 2 replication techniques (micro-injection molding and micro-hot embossing) and 3 tool production techniques (micro-machining, micro-hot embossing and PIM). Some of these tools can be considered as disposable tools (or containing disposable inserts) for the expected production volume while others assure all the parts production with only one tool, as following detailed.

There is some knowledge available regarding each of the techniques used individually being the novelty its integration in a process to obtain the part. The main aims of the consortium of firms and research institutes involved in this study were i) to identify the alternative that permits the low production costs and ii) to identify the critical parameters that can be tuned to reduce that cost in the industrialization phase. Additional insight is foreseen by the development of the PBCMs related with the application ranges of the 4 alternatives changing both the critical parameters of the technologies (e.g., tool life, material waste) and production related parameters (e.g., production volume, parts per cycle).

So, this case study is a good example of the myriad of possible combinations of processes and technologies in the micro-engineering realm. Before describing the case study alternatives, some remarks are given regarding the technologies and materials involved.

## TECHNOLOGIES AND MATERIALS

Polymers have been replacing other materials like metals, glasses and silicones since the middle of the last century due to their reduced cost, weight and increasing functionalities (Shah et al., 2008). Also in micro-scale they are widely chosen for their economic advantage in producing large batches of micro-parts through hotembossing, injection molding, reaction injection molding, injection compression molding and thermoforming. As some authors point out the first two options seem to be the most industrially viable processes to produce micro-parts (Gibozet et al., 2007; Sahli et al., 2009). Parts manufactured by these processes can have overall sizes of less than 1mm or have larger overall dimensions but with micro features incorporated of less than 200 $\mu$ m (Griffiths et al, 2007).

Micro-injection molding is a key technology in micro-fabrication due to its ability to produce complex part shapes in large volumes with short cycle times and potential for full-automation. It is a well-established technique for mass production of macroscopic polymeric parts and therefore, with vast know-how transferable for micro-parts production (Attia et al., 2009). In opposition, micro-hot embossing requires long cycle times (Velten et al., 2010) but allows for simpler plant setups and easier tooling modifications. Regarding part quality, several authors have analyzed the performance or optimized the process parameters (Liou & Chen, 2006; Sahli et al., 2009). Both processes are capable of accurate replication and dimensional control. Micro-hot embossing involves reduced process temperature (Heckele & Schomburg, 2004) and it is characterized by short flow distances from the molten semi-finished product into the cavities. Compared to micro-injection molding the flow distance and velocity are smaller, which results in a significantly lower shear stress of the polymer. This reduced shear stress during cavity filling brings about a lower residual stress of the final parts and therefore higher fatigue performance and lower fretting, crack initiation and propagation (Worgull, 2009).

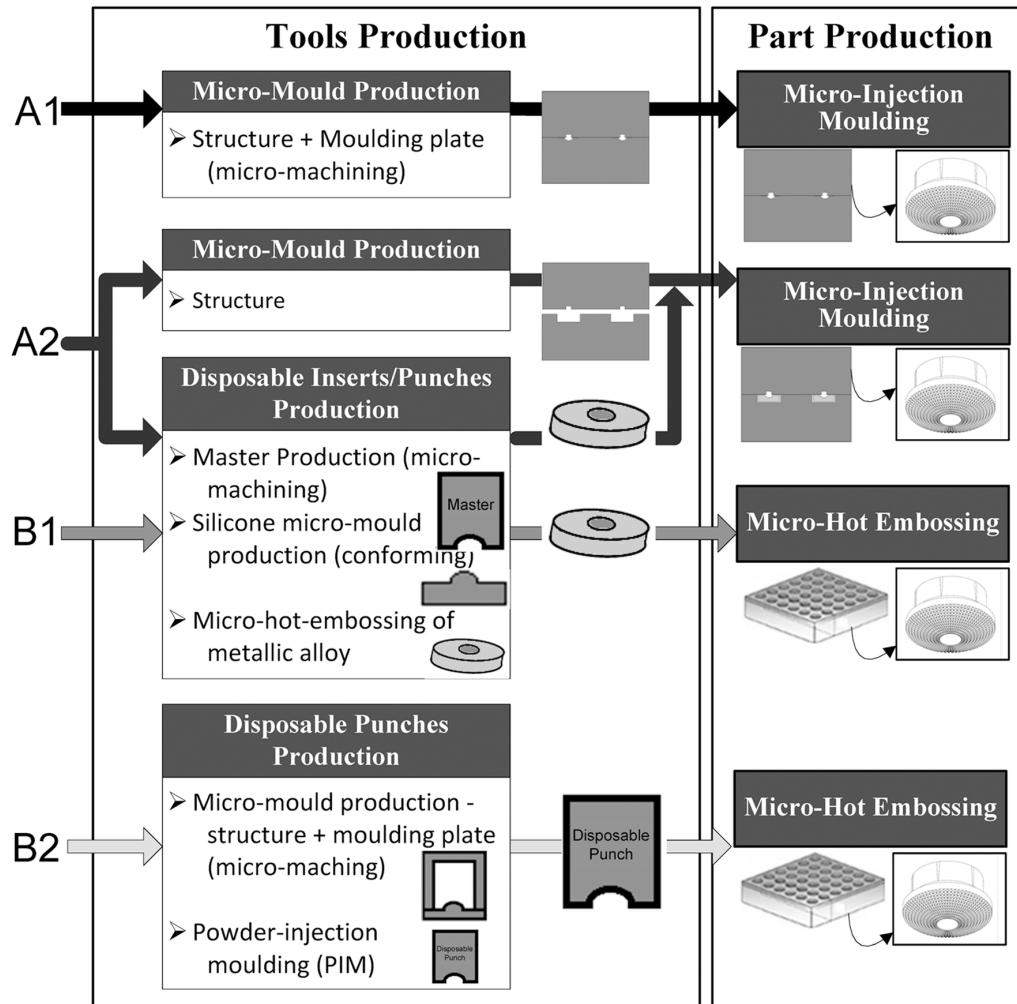
The limitations and industrial solutions of both processes have also been addressed in literature (Attia & Alcock, 2010; Heckele & Schomburg, 2004), although the analysis of these processes in an industrial scenario is still lacking. Some studies have approached part handling for improving the processes ability for industrialization (Cecil et al., 2007; Ouyang et al., 2008; Sanchez-Salmeron et al., 2005; Tracht et al., 2012), but they do not tackle the analysis of the economic costs.

Although different options are possible to produce the tools for the abovementioned replication technologies, usually micro-engineering technologies (namely micro-milling, micro-grinding, micro-electro discharge machining, electron-beam machining, among others) are applied. Papers found in literature analyze or develop separately these technologies (Afazov et al., 2013; Aurich et al., 2009; Pham et al., 2004), but no comprehensive analysis was found comparing technical and economical possibilities for both levels – tool production and part production.

### Technological Alternatives for Replication

Figure 4 illustrates the four technological alternatives considered in this study as most promising to produce the tooling and replicate the light diffuser. Together with coherent tooling technologies, two main replication alternatives are analyzed: micro-injection molding (Ai alternatives) and micro-hot embossing (Bi), as a more suitable option to extend the life of the stress sensitive light diffuser.

Figure 4. Technological alternatives for part replication. Ai alternatives – Part production with micro-injection molding; Bi alternatives– Part production with micro-hot embossing.



### Micro-Injection Molding: Ai

Micro-injection molding is the process of transferring a thermoplastic material in the form of granules into a heated barrel so that it becomes molten and soft. The material is then forced under pressure inside a mold cavity, where it is subjected to a holding pressure to compensate for material shrinkage. The material solidifies as the mold temperature is decreased below the glass transition temperature of the polymer. After the material solidifies into the mold shape, the part is ejected. The cycle restarts again for the next part. The micro-mold can be produced to have 8, 16, 32 or 64 cavities. The cycle time is constant but the resources and time required to obtain molds with more cavities is obviously higher.

In this case study, two tool production options (mold production) were analyzed (Figure 4). In alternative A1, a mold is entirely produced by micro-engineering technologies (milling, grinding and laser milling), including the molding surfaces with the negative shape of the part micro-features machined

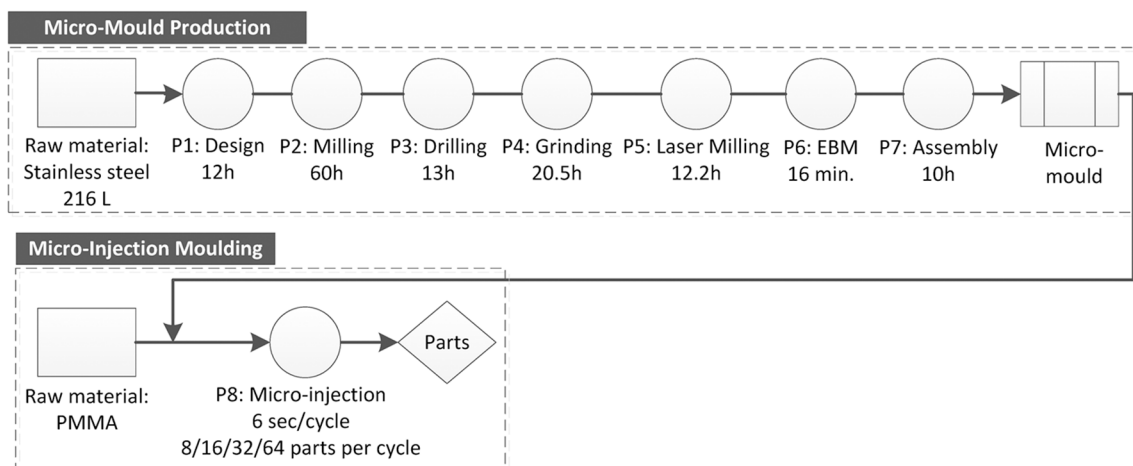
directly in the mold cavities/cores plates (Figure 5). In alternative A2 only the mold structure is produced by micro-engineering technologies (Figure 6). Cavity and core inserts are placed in the mold corresponding plates to shape the micro-features of the diffuser. These inserts are produced by micro-hot embossing of a metallic alloy (Steel 216L). For this, a metallic punch is machined with the negative shape of the micro-features of the part to conform a silicon mold to generate the inserts through micro-hot embossing. Once these inserts are placed in the mold structure, the part micro-features are shaped and replicated.

Alternative A2 requires more process steps and seems to be more complex. However, after having produced the metallic punch, it demands for a less effort in the replacement of mold inserts when they wear out. In fact, there is an erosion effect caused by the abrasive material that in such small micro features cause a significant geometrical change in the molding surfaces. So, in Alternative A2 once the inserts have wear symptoms, they can be easily replaced by new, as they are disposable inserts. In Alternative A1 when the molding surfaces get worn out, it is necessary to replace the cavity and core plates, meaning that the negative shape of the part micro-features needs to be machined from scratch. The resources and time required to obtain the Alternative A1 mold is expected to be higher than the ones required for the disposable inserts of Alternative A2.

### Micro-Hot Embossing: Bi

In the micro-hot embossing process a tool (tool insert), containing the negative micro-features of the part is pressed in an evacuated chamber into a thermoplastic plate, which has been heated above its softening temperature. The tool insert filled by the plastic material replicates the part microstructures in detail. Then the setup is cooled and the tool insert is withdrawn from the plastic. The embossing die and counter tool are not completely closed and a layer is produced, serving as a magazine for demolding and handling before the dicing process. The cycle restarts again for the next part. The micro-hot embossing die can be produced to have 75, 195 or 378 magazines. The number of magazines per die

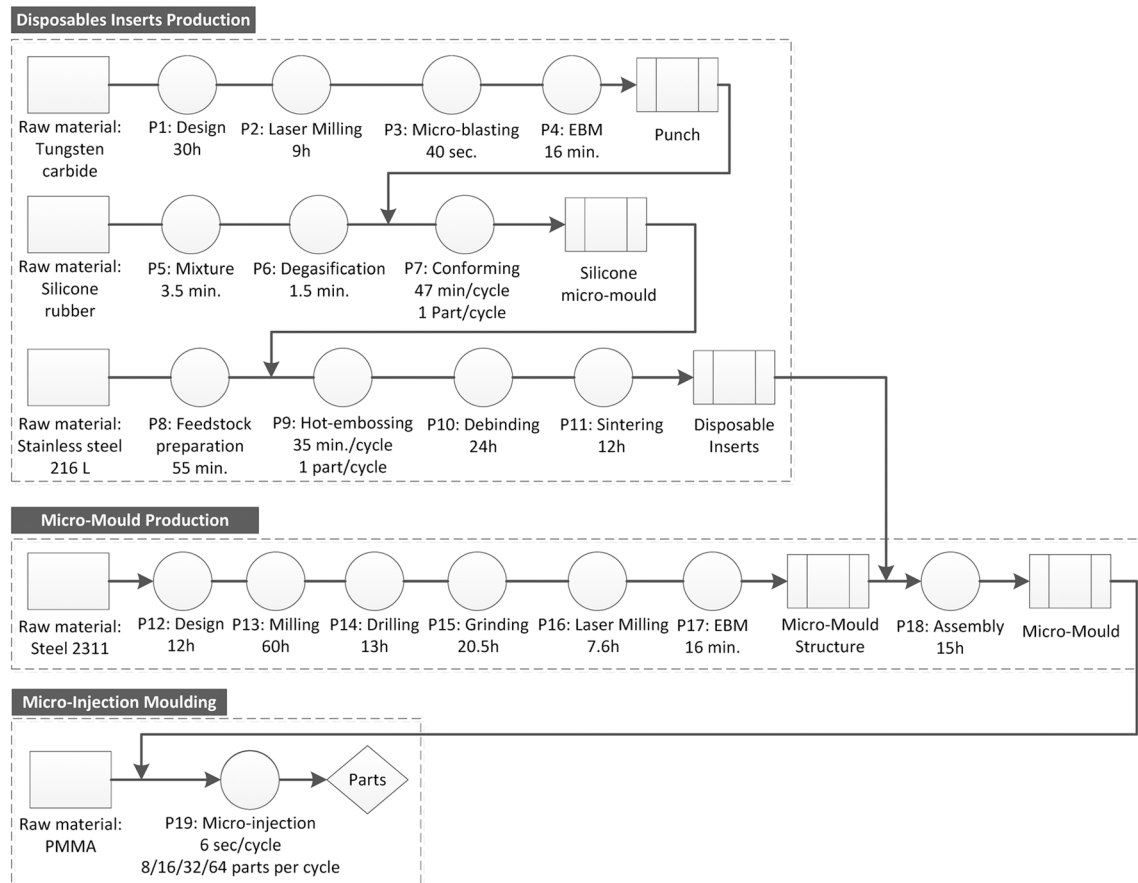
Figure 5. Process flow diagram of alternative A1





## Non-Conventional Technologies Selection

Figure 6. Process flow diagram of alternative A2

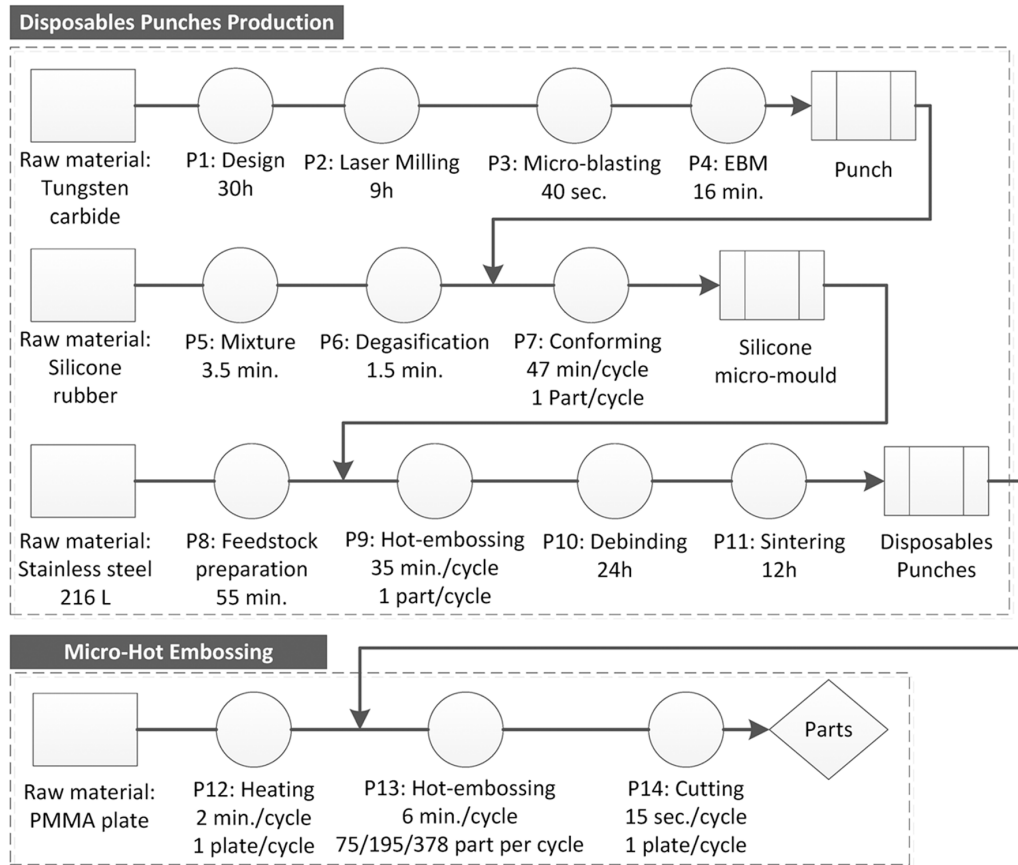


depends on the maximum working space of the hot-embossing machine, the size of each magazine and on the minimum distance required between magazines. The cycle time is constant but the resources and time required to obtain dies with more magazines is obviously higher.

The alternative tools considered for part replication by the micro-hot embossing process differ mainly on the processes to produce the tooling inserts containing the micro-features (Figure 4). In the alternative B1 (Figure 7) inserts are produced by micro-hot embossing of a metallic alloy (Steel 216L) - the same process of obtaining inserts in alternative A2. In alternative B2 (Figure 8) the disposable inserts are shaped by PIM process using a mold produced by micro-engineering technologies (milling, grinding, electron-beam machining, etc.).

The Process Model of the PBCM includes the description of the replication processes, tool manufacturing processes and indirect relevant processes of each alternative. Its extended scope assures that the cost modeling will produce robust and relevant results for the several stakeholders identified. The downstream phases of the light diffuser life cycle were not included, since the eventual different impacts of the alternatives in those phases were considered as no relevant by the stakeholders. Therefore a close circuit management of materials, devices and wastes was assumed as detailed in the next section.

Figure 7. Process flow diagram of alternative B1

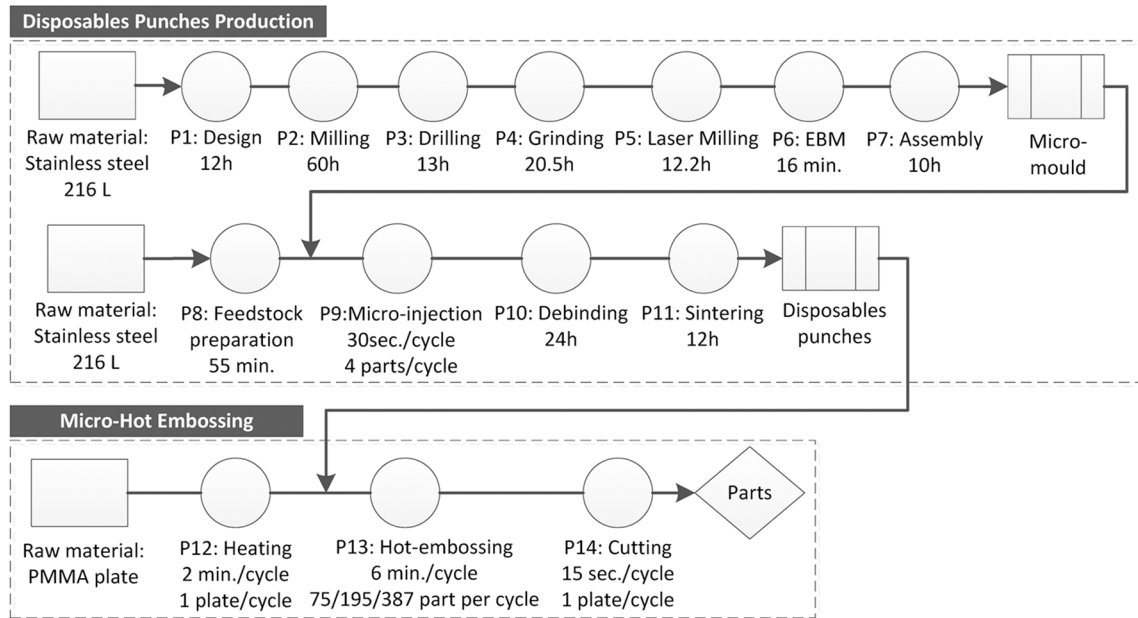


## Resource Requirements

The operations models were split into the two manufacturing sequences involved in each alternative: the tool production and the parts production (repetition process). The inputs required for each manufacturing sequence were broken down into four categories: parts and materials related, process related, operational, and financial. The parts and material related category includes information regarding the amount of material and components required per cycle allowing the estimation of the related resource consumption for an expected annual volume (Table 1). The consumption rates of the consumables are listed in Table 4 of the Appendix. The process related category includes information regarding cycle times, setup times and part per cycle that combined with the operational category inputs, like tool life, equipment uptime and power required (Table 3 of the Appendix) permits to compute the required production time and energy (Table 1). The primary financial information about equipment acquisition cost can be input in this phase as an equipment parameter (Table 3 of the Appendix) to be then processed by the financial model depending on the depreciation accounting strategy. Some equipment is industrially implemented while other is being used in an exploratory way by the companies, so there is not a clear “plant organization” with standard operational procedures. To keep all the alternatives balanced

## Non-Conventional Technologies Selection

Figure 8. Process flow diagram of alternative B2



in what concerns operational aspects an equipment uptime of 90% and one working shift (including one operator) were considered for the base-line analysis. The operations model flexibility is assured by the parameterization of all inputs categories. The automatic computing of material waste and tool life with cycle time and parts per cycle were introduced in the model for the sake of accuracy. In this way the model accuracy is assured keeping model flexibility.

The wasted materials were considered to be sent to recycling. The in-process wastes were considered to be re-used in the process therefore were not accounted as wastes. The materials requirements listed in Table 1 include the total materials quantity required to produce the molds, dies and parts.

The type of materials required to perform the tools differs in accordance with the technological processes but the quantities used are in general very low. The molds of alternatives Ai and of alternative B2 are the ones consuming more mass of material (steel). The alternative A1 is the one requiring lower tool production time, followed closely by alternative B2 that besides the injection mold also requires the production of disposal inserts (punches). Alternatives A2 and B1 are the ones requiring more time to produce the tools because of the time spent to produce the silicon master and then the required disposable inserts.

The life of the tools has an important role on the final performance of each alternative. Depending on the production volume several tools of the same type might be necessary because of the wear induced by the conformation process. For the base-line production volume of 500,000 light diffusers per year during 8 years, only the tungsten carbide punch (master) can support its corresponding number of life cycles, so for the remaining tools there is the need to produce two or more unities. As an example, for the alternative B1 it is necessary to produce 50 silicon molds and 10 inserts (disposable punches). It means that despite the very low volume and mass of most of the tools, their relatively low use life might cause the need for several times the unitary mass of material and of production time and resources.

*Table 1. Resource requirements for the expected annual production volume (500,000 parts per year) assuming an uptime of 90% of one shift working time; and for the following parts per cycle or number of cavities per shot/stroke in the replication process: A1 – 32, A2 – 32, B1 – 378, B2 – 378*

Tools Production		Alt. A1	Alt. A2	Alt. B1	Alt. B2
Material [kg]					
Master	Tungsten Carbide	-	0.07	0.07	-
Silicone Mold	V340/CA 45 Silicone Rubber	-	0.03	0.12	-
Insert B1	Stainless Steel 216L	-	0.03	0.41	-
	Polymeric binder M1 Atect	-	1.2E-5	1.5E-4	-
Mold	Steel 2311	18.4	18.4	-	4.6
Insert B2	Stainless Steel 216L	-	-	-	2.5
	Polymeric binder M1 Atect	-	-	-	0.25
Production Time [h]					
Master		-	39	39	-
Silicone Mold		-	1	3	-
Insert A2/B1		-	56	263	-
Injection Mold		128	128	-	124
Insert B2		-	-	-	38
Tool Life [cycles]					
Master		-	1,000,000	1,000,000	-
Silicone Mold		-	100	100	-
Insert A2/B1		-	300,000	50,000	-
Injection Mold		300,000	300,000	-	300,000
Insert B2		-	-	-	50,000
Parts Production		Alt. A1	Alt. A2	Alt. B1	Alt. B2
Material		PMMA			
Amount of Material [kg]		37.9	37.9	661.2	661.2
Percentage of waste [%]		0.08	0.08	94.3	94.3
Power of injection equipment [kW]		8.7	8.7	-	-
Power of hot-embossing equipment [kW]		-	-	30	30
Energy [kWh]		227	227	3307	3307
Cycle Time [sec]		6	6	300	300
Parts per cycle		32	32	378	378

The main differences between the two replication technologies for the part production are material waste, the required machine, the consumed power and cycle time. The joining effects of longer cycle times and high machine power of the alternatives Bi causes a significant higher energy consumption of these alternatives. In addition, the alternatives Bi has much higher material waste than alternative Ai because the micro-hot embossing process uses a PMMA plate to produce the part and around 94% of

## ***Non-Conventional Technologies Selection***

that plate is wasted in the replication process. Therefore the Bi alternatives show several disadvantages regarding resources consumption comparing with the alternatives that use micro-injection molding to produce the parts. The results for one variant of number of cavities per shot/stroke for each alternative and for the specific production volume per year are shown in Table 1.

In the next section the resource requirements translation into production costs is presented and discussed.

## **Cost Analysis**

The combination of the resources requirements with price factors and financial information is in the core of the financial module of the PBCM model. The cost computing for resources like materials, consumables, and energy is directly obtained by the product of the quantity consumed to the respective price factor listed in Table 4 of Appendix. As regards the accounting of the cost related with equipment used time, the acquisition cost of the equipment (Table 3 of Appendix) and an uptime of 90% for all equipment were considered to compute the cost per hour (assuming non-dedicated equipment). As regards the tooling cost, the PBCM model calculates the number of tools and inserts required for a demanded production volume, and this number is majored for the closest integer value (it means that a tool or insert that was used only part of his life was consider with no remaining life after production – each tool and insert are dedicated to a specific product/shape). Therefore the cost of the dedicated tools include the materials, consumables and other resources consumed and also the cost of using equipment for the time required.

The results obtained are presented in Table 2 for each alternative and for the specific production volume and are discussed in the following section. After that, the influence of tools options is analyzed, as well as the production volume and other process parameters whose value was estimated based on empirical and eventually biased discernments. This allows mapping the best alternative according to different contexts.

## **Cost Breakdown**

This section presents the cost breakdown structure of each alternative for a fixed production volume of 500,000 parts per year and fixed parameters of machine uptime (90% of the available time: 8hours/day, 5 days/week) and parts per cycle (Table 2). Some differences between replication alternatives can be immediately observed. First, the cost of the consumed material is much higher with the micro-hot embossing process (Bi alternatives) because of the higher material waste associated to the process when compared with micro-injection molding (alternatives Ai). The second main difference is in machine cost parcel, in which micro-hot embossing alternative presents again much higher costs. This is due to the higher cycle time when compared with micro-injection molding. This difference is also reflected in labor cost, energy and other costs (maintenance, process consumables) since all this cost factors are correlated with the production time. Regarding to tool cost, the differences depend on several factors that act simultaneously like the tool and inserts life vis-à-vis the production volume. For this specific production configuration, alternative B1 has the lowest tooling cost because it doesn't require any injection mold and the other alternatives requires several one for the production level specified.

Regarding the cost per part, reflecting the total cost of the 500,000 units, the alternative A1, micro-injection molding with a mold produced by micro-engineering technologies, is the best economical option for the referred base-line of operational and production parameters setting.

*Table 2. Cost Breakdown of alternative technologies for the expected annual production volume (500,000 parts per year assuming an uptime of 90% of one shift working time). Parts per cycle or number of cavities per shot/stroke in the replication process: A1 – 32, A2 – 32, B1 – 378, B2 – 378*

	Alternative A1		Alternative A2		Alternative B1		Alternative B2	
	€	%	€	%	€	%	€	%
Variable Costs								
Material	76	1.5	76	1.2	1322	14.0	1322	10.3
Labor	110	2.2	110	1.8	810	8.6	810	6.3
Energy	25	0.5	115	1.8	386	4.1	386	3.0
Fixed Costs								
Machine	484	9.8	484	7.7	4158	44.0	4158	32.4
Dedicated tools	4219	85.0	5414	86.7	2329	24.7	5705	44.5
Others	48	1.0	48	0.8	438	4.6	438	3.4
<b>Total Production [€]</b>	<b>4,962</b>	<b>100</b>	<b>6,247</b>	<b>100</b>	<b>9,443</b>	<b>100</b>	<b>12,819</b>	<b>100</b>
<b>Cost per part [€/part]</b>	<b>0.010</b>		<b>0.012</b>		<b>0.019</b>		<b>0.026</b>	

The costs breakdown reflecting the relative influence of each manufacturing phase or process in the total cost can also be presented to better understand the costs associated to each alternative and promote an effective analysis and discussion among the stakeholders (Figure 9). It is possible to observe the importance of the tooling and part manufacturing processes in the overall costs of the alternatives: the tooling weight on the overall cost is higher in injection molding alternatives, mainly because the cost of producing the light diffusers is significant lower than in the other alternatives (so the relative importance is higher). Nevertheless, in alternative A1 the entire injection mold must be replaced by the action of the PMMA (an abrasive material) after 300,000 injection cycles. The use of disposable inserts in alternative A2 reduces the cost with the injection mold (and its relative contribution to part cost) but the overall costs with tooling is higher because it is necessary to produce the inserts and the silicon mold (see Table 2). So, the lower influence of the tool production in total cost of alternative B2 is caused by much higher influence of the production cost of the light diffuser, being this alternative the one with higher cost for this production parameters setting. Despite the lower tooling cost in alternative B1 (and lower influence in total cost) this alternative also presents an high total cost because of the longer cycle time and material waste of the hot-embossing replication process.

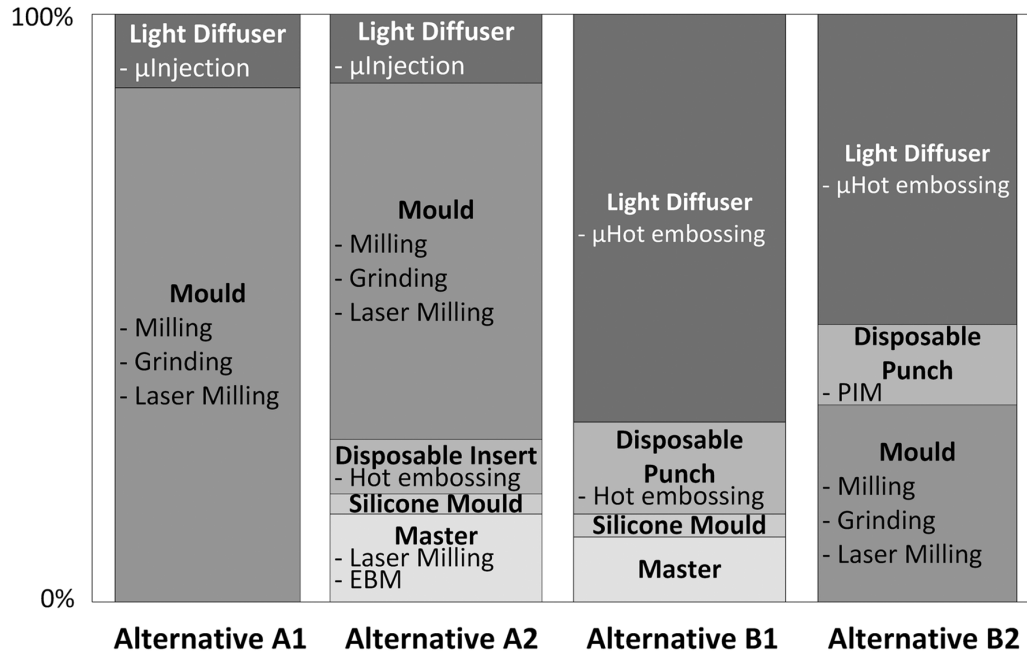
The discussion of the last paragraphs is only a parcel of the possible discussions and findings based on the cost breakdown in cost categories and in manufacturing phases for the expected industrial scenario. Further understanding and decision can be derived taking advantage of the developed PBCM in performing sensitivity analysis, as illustrated in the next section.

## Sensitivity Analysis

The parametric characteristic of the developed PBCM model allow for different sensitivity analysis to different process parameters. In this case study there are some parameters that can be considered critical i) by its clear influence in the total cost, ii) by the relevant interest to the stakeholders and ii) by the limit

## Non-Conventional Technologies Selection

Figure 9. Distribution of the manufacturing costs for an expected annual production volume of 500,000 parts. Parts per cycle (shot/stroke) in the replication process: A1 – 32, A2 – 32, B1 – 378, B2 – 378



knowledge about its influence and real values since some of the process are on the research or development stage. Consequently, the sensitivity analysis here presented will focus on the influence of i) parts per cycle and part geometry, ii) production volume and iii) tool life, respectively.

In the industrial context, part production volume is known as deeply affecting the technology selection. The available time and uptime of the production infrastructure, which might be different among the fixed resources involved, also influences the part cost. However, after performing tests with marginal changes on the uptime previously considered for all technological alternatives (90% of one shift working time) it was found that there is no change in the best alternative hierarchy for the different technological alternatives. So, the results of this analysis is neither presented nor discussed in this chapter.

A major impact in the part cost is caused by the tool design options, in particular in regard to the number of parts that the tool produces in each cycle (affecting production time in the replication process) and tool life (affecting the number of tool replacements required). This is true for both replication technologies, being the number of parts per cycle the result of the number of molding cavities in the case of replication by micro-injection, and of PMMA plate area in the micro-hot embossing case.

The following sensitivity analyzes, although later analyzed together, are first addressed to the replication alternatives in separate for better understanding of the processes behavior.

### Micro-Injection Molding replication Alternatives

For the alternatives based on micro-injection molding, a sensitivity analysis was performed to understand the influence of the annual production volume and of the number of mold cavities (that dictate the number of parts per injection shot/cycle) on the part final cost. The different number of cavities analyzed

(8/16/32/64) are within the range of the molding area for the equipment considered. The best economic alternatives regarding the mold and the associated costs are illustrated in Figure 10 and Figure 11.

If only micro-injection molding alternatives are considered for the replication of the light diffusers, the alternative A1 (mold made by micro-engineering technologies) with 8 molding cavities machined in integral cavity/core plates is the best one for very low production volumes. When the production volume increases, A1 remains the best alternative until around 20 million parts per year. However, the number of cavities per mold allowing the lower overall cost increases with the increasing of the production volume (after around 1 million parts per year the mold with 64 cavities is the best). Above 20 million parts per year, the best alternative is A2 with 64 molding cavities built by inserts attached to the cavity/core plates. This is due to the fact that this option, although representing a higher investment regarding the mold to produce the micro-inserts, represents lower costs to replace the molding cavities: the spare molding cavities are produced by a replication process (micro-hot embossing) while in alternative A1 new cavity and core plates have to be integrally machined starting from prismatic blocks of steel.

### Micro-Hot Embossing: Bi Alternatives

Figure 12 and Figure 13 illustrates the best technological alternatives, among the ones based on the light diffusers replication by micro-hot embossing, for different production volumes (alternatives Bi).

Figure 10. Best alternatives mapping considering replication processes based on micro-injection molding for low production volumes. A1 – Mold produced just by micro-engineering technologies; A2 - Mold produced by micro-engineering technologies and micro-inserts for the mold cavities through micro-hot embossing

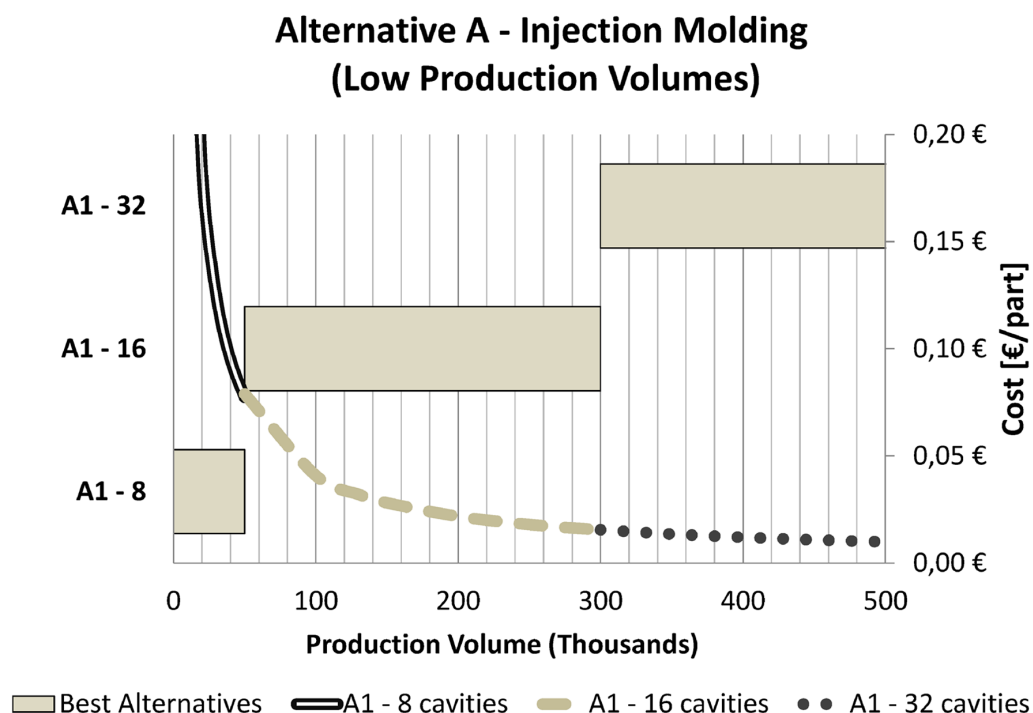
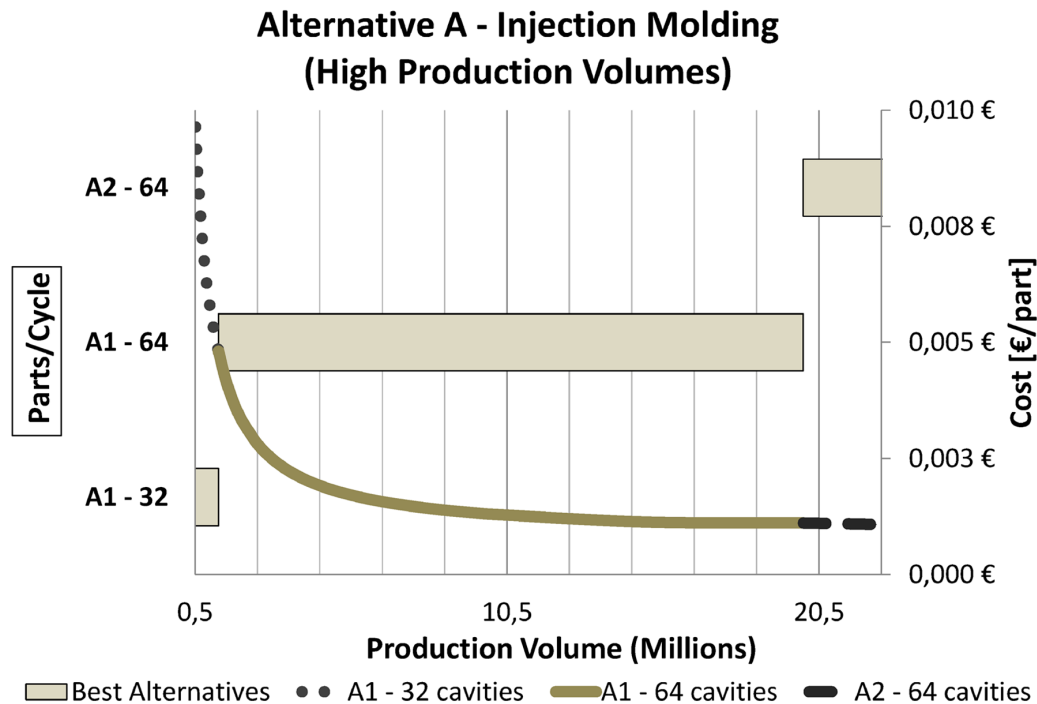




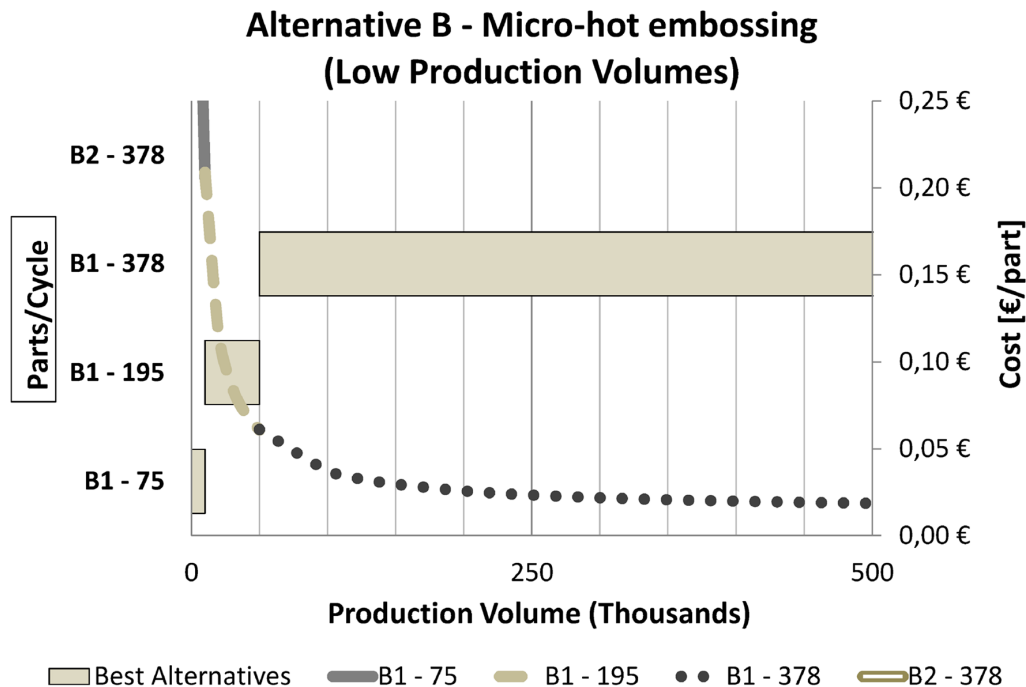
Figure 11. Best alternatives mapping considering replication processes based on micro-injection molding for high production volumes. A1 – Mold produced just by micro-engineering technologies; A2 - Mold produced by micro-engineering technologies and micro-inserts for the mold cavities through micro-hot embossing



Different amounts of parts produced per cycle were analyzed (75, 195 and 378 parts per stroke), within the working area and working forces of the equipment considered. The increasing of the number of parts produced per cycle requires larger PMMA plates and the number of inserts to be produced. For the hot embossing replication alternatives, B1 is the best economic alternative for production volumes below 10 million parts per year, holding changes in the number of parts production per cycle. Until this production level the best alternative benefits from the lower initial investment to produce the inserts through micro-hot embossing of metals. This explains the trend observed with the production volume: the increase of the number of parts produced per cycle in the mapping of best alternatives. For higher production volumes B2 becomes the best alternative using the PMMA plate with higher dimensions to accommodate more parts per stroke. When compared with B1 this option is more suitable for high production volumes because of the higher initial investment in the micro-mold, with the positive shape of the part micro-features, required to produce the inserts through PIM. Only when a certain level of inserts is required this initial higher investment is compensated by the lower variable costs of PIM of inserts (due essentially to a smaller cycle time, PIM variable costs are lower than micro-hot embossing ones).

An important cost driver in micro-hot embossing is the part material cost, associated to the high significant percentage of material waste in this replication process. The material waste is dependent on part geometry, as the location of the inserts to mold the PMMA plate obeys to specific rules regarding the spacing between parts. Parts with higher surface area lead to lower material waste. An analysis was

Figure 12. Best alternatives mapping considering only replication processes based on micro-hot embossing for low production volumes. B1 - inserts to replicate the diffuser produced by micro-hot embossing of metals; B2 - inserts produced by the PIM using a mold produced by micro-engineering technologies.

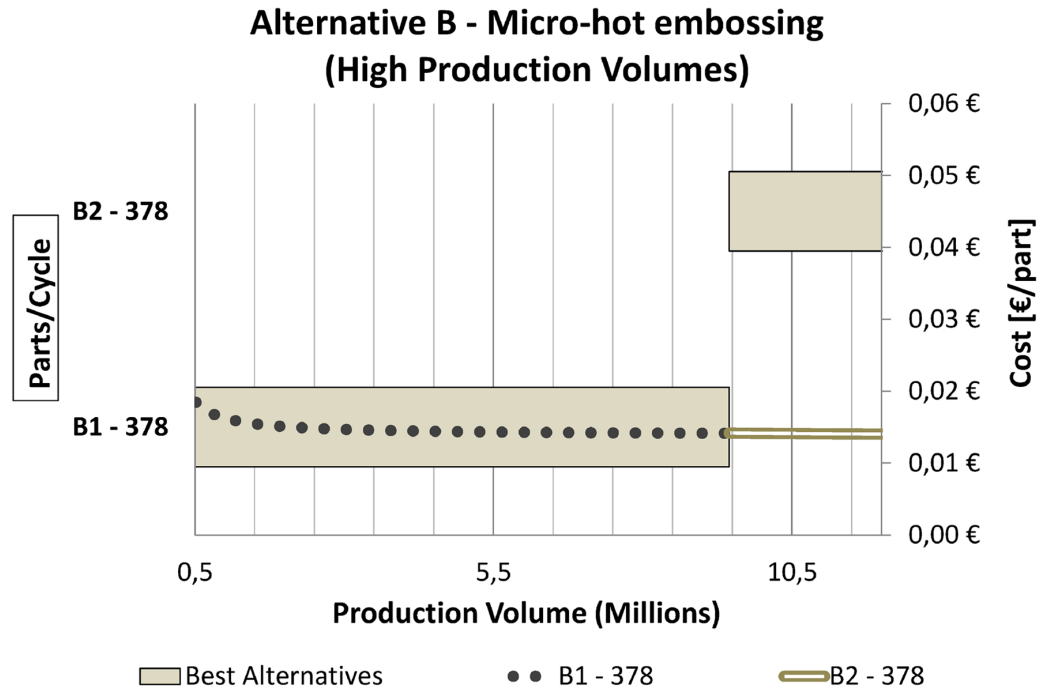


developed to understand how changes in part geometry influence the economical domain of the alternatives under study. As illustrated in Figure 14, although the increase of part area effectively causes a decrease of material waste, it is not significant enough to lower material waste below 94%. The high amount of material waste in this process is explained by the distance required between the punches, as illustrated in Figure 15: each punch, with a diameter of 4.2 mm, is placed in a holding device with a diameter of 9 mm, positioned with a distance of 10mm from each other.

### Micro-Injection Molding and Micro-Hot Embossing

Figure 15 Figure 16 illustrates the best alternatives comparing all the technological processes for production volumes below 500,000 parts per year. When comparing both replication alternatives the suitability of micro-hot embossing for lower production volumes and micro-injection molding for higher ones, in particular for production volumes above 130,000 parts/year, becomes clear. Again, the increase of the number of parts per cycle is a pattern for best alternatives with the increase of the production volume. However, when comparing both replication processes, the alternative B2, micro-hot embossing using inserts made by PIM, is never a best choice. Being the best alternative among the micro-hot embossing replication ones for higher production volumes, it is surpassed by the micro-injection molding for this range of volumes. The micro-injection molding alternative with inserts machined in the cavity/core plates of the mold (alternative A1) has its best domain above this production level and until a production

Figure 13. Best alternatives mapping considering only replication processes based on micro-hot embossing for high production volumes. B1 - inserts to replicate the diffuser produced by micro-hot embossing of metals; B2 - inserts produced by the PIM using a mold produced by micro-engineering technologies.



volume of 20 million, since its higher initial investment is compensated by lower variable costs in the replication phase. After 20 million the alternative A2 is the best as already explained (see Figure 10).

The tool life is a critical issue in processes that use dedicated tools. In particular, when evaluating and selecting manufacturing processes (prior to industrialization) making use of new technologies, the expected life of dedicated tools embodies a high uncertainty. In this case study, a significant uncertainty is related to the life of the inserts produced by hot embossing (used in alternatives B1 and A2). If abrasive materials, which is the case of PMMA, and high production volumes are envisaged, this uncertainty can bias the selection of the best option. To understand the influence of tool life in the mapping of the best alternatives, a sensitivity analysis was performed considering the tool life variation between  $\pm 50\%$  of the expected tool life of the inserts. Figure 17 illustrates the results.

No variation is observed in the mapping of best alternatives for the production volumes in which B1 is the best alternative (below 100 parts per year). When varying the tool life in B1 alternative and considering this extremely low production volumes per year, the inserts have a relative high life span (8 years of production) even if the tool life is decreased by 50%. Since in alternative A2 the production volumes domain, changes in tool life influences slightly the best alternative selection. The change in the threshold curve of A2 domain is explained by the fact that A1 tool life is well known and so it is kept fixed, unlike what happens to A2. The life decrease of the mold inserts produced by micro-hot embossing of A2 alternative leads to an increase of its annual cost as far as more replacements are required. In parallel, an increase of the inserts life leads to a decrease of tooling costs.

Figure 14. Sensitivity analysis to the percentage of material waste with variation of the part area considering the micro-hot embossing based alternative (B1). Part area variation: 0 – Surface area of the part in this case study, negative and positive variation in part area related to this value in the interval [-50%; 50%].

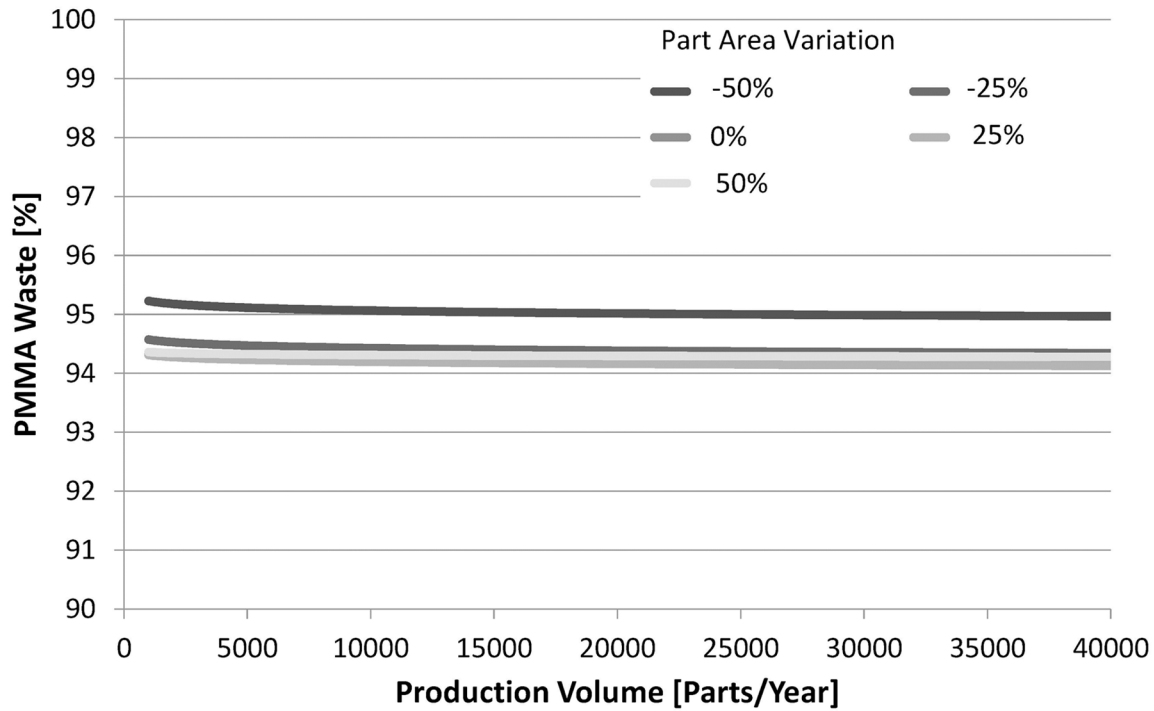
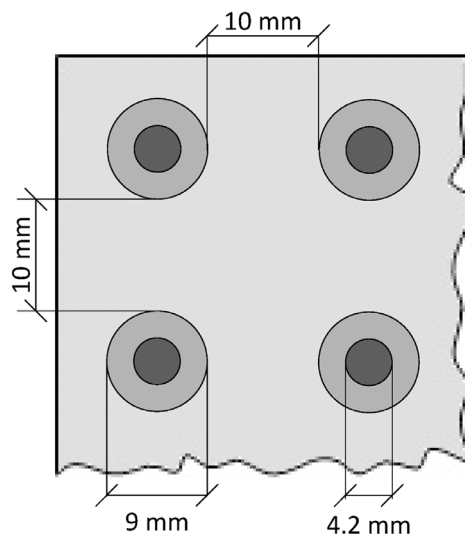


Figure 15. Partial section of the PMMA plate and position of the punches



### ***Non-Conventional Technologies Selection***

Figure 16. Best alternatives mapping considering both replication technologies (low production volumes). A1 – micro-injection molding with mold produced just by micro-engineering technologies, B1 – Micro-hot embossing using inserts to replicate the diffuser produced by micro-hot embossing.

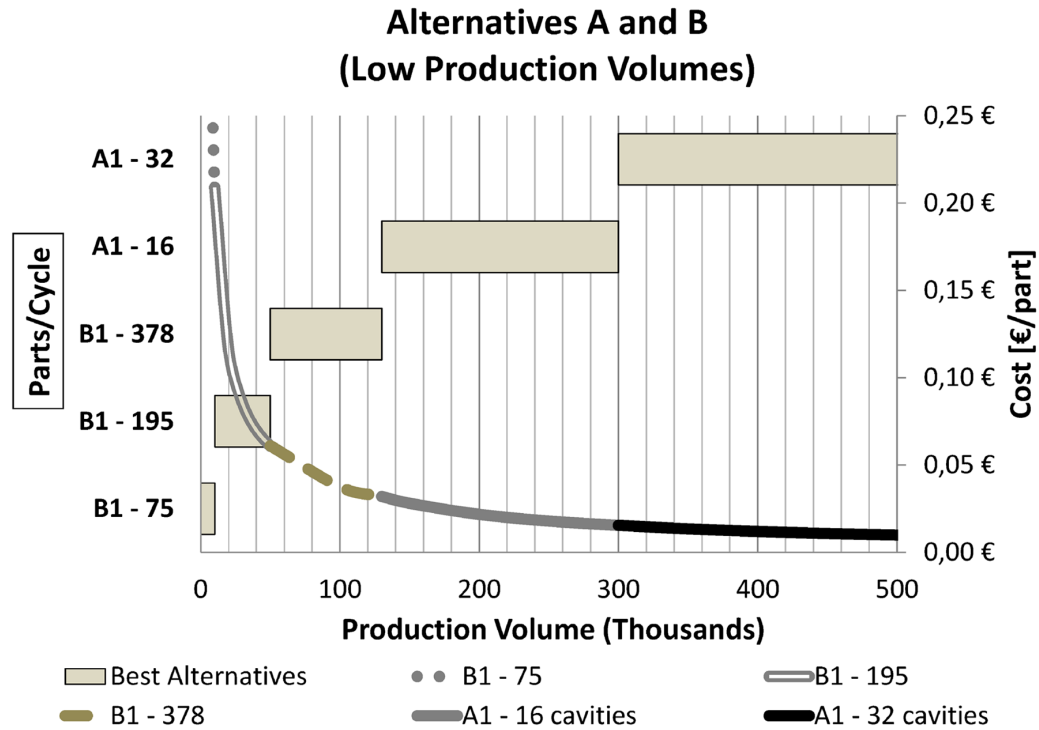
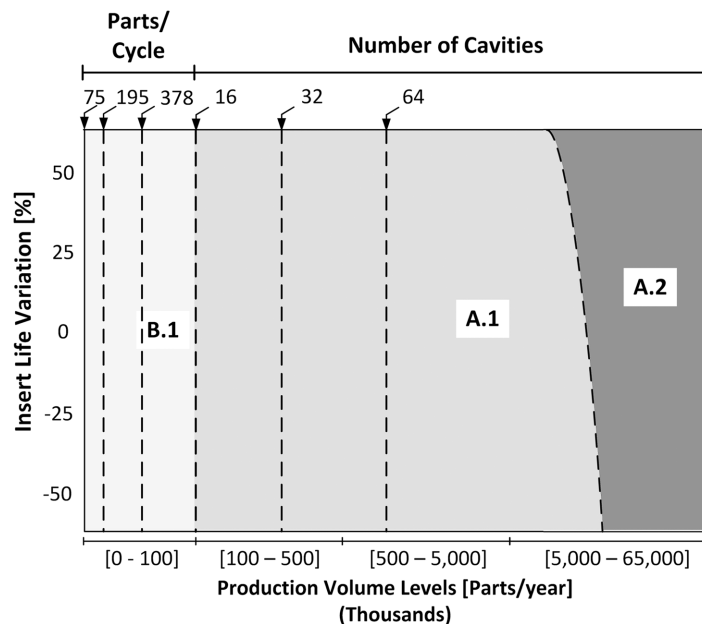


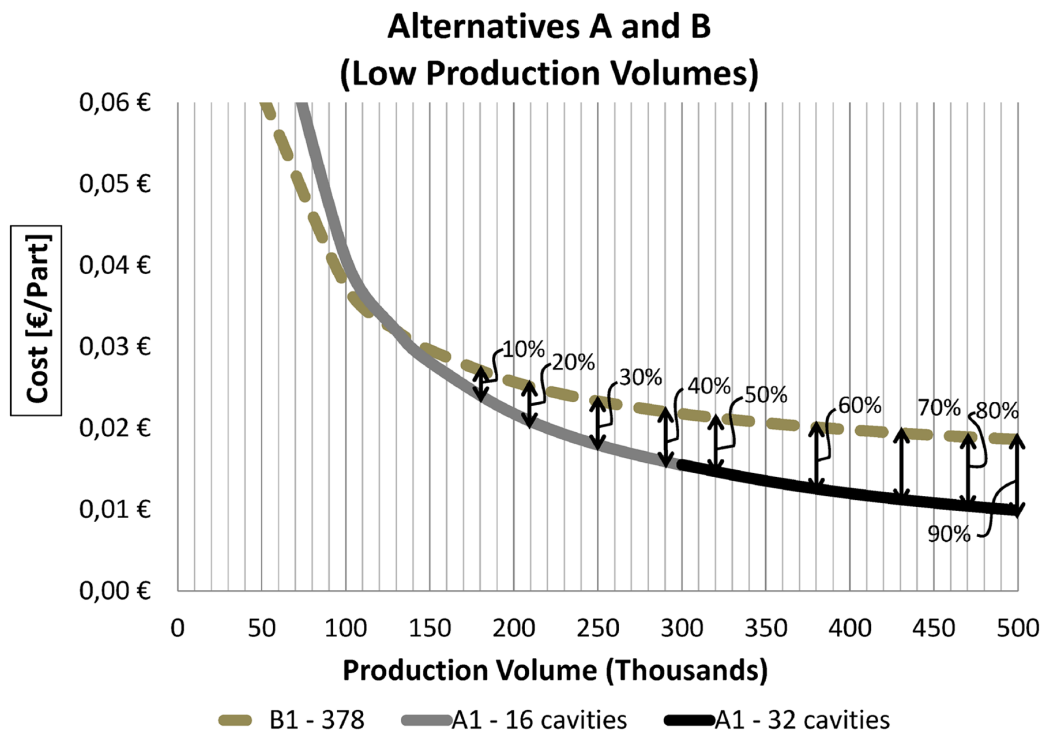
Figure 17. Mapping of best alternatives according to production volume and tool life variation [-50%; 50%]



In addition, these results show that an increase of the PMMA plate area, in the case of micro-hot embossing, and of the number of mold cavities, in micro-injection molding case, with the increasing of the production volume has economically a positive trend: the “best” parts per cycle increases with the production volume.

Finally, literature review on micro-manufacturing showed that several authors address the advantage of parts produced by micro-hot embossing when compared to micro-injection molding. Micro-hot embossing is a process with shorter flow distances and velocity. The consequence is that parts produced by this process present lower residual stresses than the micro-injection molded ones, which affects the part quality in particular as regards to fatigue resistance and crack initiation and propagation. So, independently of the production volume, clients are often willing to pay more for parts produced by micro-hot embossing. Due to some subjective nature of quality and its dependency on the product use, the choice depends on the willingness of the client to pay for the increased quality properties. The perceived differences were not taken into account in this study, but the analysis presented in Figure 18 allows to discuss this topic based on the PBCM model outputs. The analysis shows the cost difference between parts produced by micro-injection molding and micro-hot embossing alternatives for different production volumes. It demonstrates the increase of cost for the producer and therefore indirectly for the client, if micro-hot embossing technology is the preferred one for the diffusers production. For the annual production volume expected in this case study (500,000 diffusers per year during 8 years) the diffuser replicated by micro-hot embossing is 90% more expensive than the one replicated by micro-injection.

Figure 18. Evolution of the cost with the production volume in the case of diffusers replicated by micro-injection molding and by micro-hot embossing (alternatives A1 and B1)



## **CONCLUSION**

Micro-engineering has a long way to go through the industrialization phase. Several micro-technologies have been developed in the last decades and frequently the same product can be produced by different alternatives. Two of the most promising replication technologies are micro-injection molding and micro-hot embossing. In addition, different tooling solutions exist within the same replication process. So, appropriate selection methods must be used to deal with the complexity of comparing these (and new) technological alternatives. This chapter proposes a methodology for technology selection based on Process-Based Cost Models, prior to their industrialization, allowing sensitivity analysis to the parameters that most affecting the part cost, have a high uncertainty, and/or are susceptible of changing over time or with the industrial scenarios.

In the case study regarding the production of a light diffuser with micro-features, four technological alternatives were analyzed based on micro-injection molding and micro-hot embossing replication technologies. Within these processes, different tooling solutions were studied. Using the proposed methodology based on PBCM it was possible to map the conditions in which the alternatives analyzed perform economically better. Furthermore, it was possible to assess some significant parameters affecting the costs in each alternative. In fact, it was observed the importance of selecting not only the replication process, but also the tooling based on a comprehensive analysis. Different tool solutions appear as best alternatives depending on the production context. Moreover, in particular for high production volumes, tool life is determinant in tool selection. The life span of certain tool is determined by several factors, namely part material and process conditions. However, in new technological areas the influence of these conditions in the tool life is frequently ill-defined and the tool life might be quite uncertain. The sensitivity analysis showed that even earlier in the manufacturing process design when decisions are need is possible to gather the relevant information to map the alternatives and get more informed process decisions. At part production level, given the different process conditions of the alternatives, the final parts may present different quality attributes regarding fatigue and crack propagation. Therefore, the costs differences must be assessed between alternatives for different production volumes and compared with the clients' willingness to pay for the increased quality. Depending on the specific case, the decision making team needs to consider the capability and the domain of the alternative technologies together with the cost effectiveness of the manufacturing alternatives embracing both levels of part production – the part replication and the design and production of tooling.

## **REFERENCES**

- Afazov, S. M., Zdebski, D., Ratchev, S. M., Segal, J., & Liu, S. (2013). Effects of micro-milling conditions on the cutting forces and process stability. *Journal of Materials Processing Technology*, 213(5), 671–684. doi:10.1016/j.jmatprotec.2012.12.001
- Alting, L., Kimura, F., Hansen, H. N., & Bissacco, G. (2003). Micro Engineering. *CIRP Annals - Manufacturing Technology*, 52(2), 635–657. 10.1016/S0007-8506(07)60208-X
- Anasane, S. S., & Bhattacharyya, B. (2017). Experimental investigation into micromilling of microgrooves on titanium by electrochemical micromachining. *Journal of Manufacturing Processes*, 28, 285–294. doi:10.1016/j.jmapro.2017.06.016

- Asad, A. B. M. A., Masaki, T., Rahman, M., Lim, H. S., & Wong, Y. S. (2007). Tool-based micro-machining. *Journal of Materials Processing Technology*, 192–193, 204–211. doi:10.1016/j.jmatprotec.2007.04.038
- Attia, U. M., & Alcock, J. R. (2010). Integration of functionality into polymer-based microfluidic devices produced by high-volume micro-moulding techniques. *International Journal of Advanced Manufacturing Technology*, 48(9–12), 973–991. doi:10.1007/00170-009-2345-8
- Attia, U. M., Marson, S., & Alcock, J. R. (2009). Micro-injection moulding of polymer microfluidic devices. *Microfluidics and Nanofluidics*, 7(1), 1–28. doi:10.1007/10404-009-0421-x
- Aurich, J. C., Engmann, J., Schueler, G. M., & Haberland, R. (2009). Micro grinding tool for manufacture of complex structures in brittle materials. *CIRP Annals - Manufacturing Technology*, 58(1), 311–314. doi:10.1016/j.cirp.2009.03.049
- Brinksmeier, E., Riemer, O., & Stern, R. (2001). Machining of Precision Parts and Microstructures. In I. Inasaki (Ed.), *Initiatives of Precision Engineering at the Beginning of a Millennium* (pp. 3–11). Berlin: Springer. doi:10.1007/0-306-47000-4\_1
- Cecil, J., Powell, D., & Vasquez, D. (2007). Assembly and manipulation of micro devices-A state of the art survey. *Robotics and Computer-integrated Manufacturing*, 23(5), 580–588. doi:10.1016/j.rcim.2006.05.010
- Field, F., Kirchain, R., & Roth, R. (2007). Process cost modeling: Strategic engineering and economic evaluation of Materials technologies. *JOM*, 59(10), 21–32. doi:10.1007/11837-007-0126-0
- Fixson, S. K. (2005). Product architecture assessment: A tool to link product, process, and supply chain design decisions. *Journal of Operations Management*, 23(3–4), 345–369. doi:10.1016/j.jom.2004.08.006
- Folgado, R., Peças, P., & Henriques, E. (2010). Life cycle cost for technology selection: A Case study in the manufacturing of injection moulds. *International Journal of Production Economics*, 128, 368–378. doi:10.1016/j.ijpe.2010.07.036
- Fuchs, E. R. H., Field, F. R., Roth, R., & Kirchain, R. E. (2008). Strategic materials selection in the automobile body: Economic opportunities for polymer composite design. *Composites Science and Technology*, 68(9), 1989–2002. doi:10.1016/j.compscitech.2008.01.015
- Giboz, J., Copponnex, T., & Mélé, P. (2007). Microinjection molding of thermoplastic polymers: A review. *Journal of Micromechanics and Microengineering*, 17(6), R96–R109. doi:10.1088/0960-1317/17/6/R02
- Griffiths, C. A., Dimov, S. S., Brousseau, E. B., & Hoyle, R. T. (2007). The effects of tool surface quality in micro-injection moulding. *Journal of Materials Processing Technology*, 189(1–3), 418–427. doi:10.1016/j.jmatprotec.2007.02.022
- Heckele, M., & Schomburg, W. K. (2004). Review on micro molding of thermoplastic polymers. *Journal of Micromechanics and Microengineering*, 14(3), R1–R14. doi:10.1088/0960-1317/14/3/R01
- Johnson, M. D., & Kirchain, R. E. (2009). Quantifying the effects of product family decisions on material selection: A process-based costing approach. *International Journal of Production Economics*, 120(2), 653–668. doi:10.1016/j.ijpe.2009.04.014



## **Non-Conventional Technologies Selection**

- Kim, J. (1999). Making sense of emergence. *Philosophical Studies*, 95(1), 3–36. doi:10.1023/A:1004563122154
- Liou, A. C., & Chen, R. H. (2006). Injection molding of polymer micro- and sub-micron structures with high-aspect ratios. *International Journal of Advanced Manufacturing Technology*, 28(11–12), 1097–1103. doi:10.1007/00170-004-2455-2
- Masuzawa, T. (2000). State of the Art of Micromachining. *CIRP Annals - Manufacturing Technology*, 49(2), 473–488. doi:10.1016/S0007-8506(07)63451-9
- Ouyang, P. R., Tjiptoprodjo, R. C., Zhang, W. J., & Yang, G. S. (2008). Micro-motion devices technology: The state of arts review. *International Journal of Advanced Manufacturing Technology*, 38(5–6), 463–478. doi:10.1007/00170-007-1109-6
- Peças, P., Henriques, E., & Ribeiro, I. (2010). Integrated approach to product and process design based on life cycle engineering. In *Handbook of Research on Trends in Product Design and Development: Technological and Organizational Perspectives*. Academic Press. doi:10.4018/978-1-61520-617-9.ch021
- Peças, P., Ribeiro, I., Folgado, R., & Henriques, E. (2009). A Life Cycle Engineering model for technology selection: A case study on plastic injection moulds for low production volumes. *Journal of Cleaner Production*, 17(9), 846–856. doi:10.1016/j.jclepro.2009.01.001
- Peças, P., Ribeiro, I., Silva, A., & Henriques, E. (2013). Comprehensive approach for informed life cycle-based materials selection. *Materials & Design*, 43. doi:10.1016/j.matdes.2012.06.064
- Pham, D. T., Dimov, S. S., Bigot, S., Ivanov, A., & Popov, K. (2004). Micro-EDM - Recent developments and research issues. *Journal of Materials Processing Technology*, 149, 50–57. doi:10.1016/j.jmatprotec.2004.02.008
- Rathod, V., Doloi, B., & Bhattacharyya, B. (2014). Experimental investigations into machining accuracy and surface roughness of microgrooves fabricated by electrochemical micromachining. *Proceedings of the Institution of Mechanical Engineers. Part B, Journal of Engineering Manufacture*, 229(10), 1781–1802. doi:10.1177/0954405414539486
- Ribeiro, I., Kaufmann, J., Schmidt, A., Peças, P., Henriques, E., & Götze, U. (2016). Fostering selection of sustainable manufacturing technologies - A case study involving product design, supply chain and life cycle performance. *Journal of Cleaner Production*, 112, 3306–3319. doi:10.1016/j.jclepro.2015.10.043
- Ribeiro, I., Peças, P., & Henriques, E. (2013). Incorporating tool design into a comprehensive life cycle cost framework using the case of injection molding. *Journal of Cleaner Production*, 53, 297–309. doi:10.1016/j.jclepro.2013.04.025
- Ribeiro, I., Peças, P., Silva, A., & Henriques, E. (2008). Life cycle engineering methodology applied to material selection, a fender case study. *Journal of Cleaner Production*, 16(17), 1887–1899. doi:10.1016/j.jclepro.2008.01.002
- Sahli, M., Millot, C., Roques-Carmes, C., Khan Malek, C., Barriere, T., & Gelin, J. C. (2009). Quality assessment of polymer replication by hot embossing and micro-injection moulding processes using scanning mechanical microscopy. *Journal of Materials Processing Technology*, 209(18–19), 5851–5861. doi:10.1016/j.jmatprotec.2009.06.011

- Sanchez-Salmeron, A. J., Lopez-Tarazon, R., Guzman-Diana, R., & Ricolfe-Viala, C. (2005). Recent development in micro-handling systems for micro-manufacturing. *Journal of Materials Processing Technology*, 167(2-3), 499–507. doi:10.1016/j.jmatprotec.2005.06.027
- Shah, A. A., Hasan, F., Hameed, A., & Ahmed, S. (2008). Biological degradation of plastics: A comprehensive review. *Biotechnology Advances*, 26(3), 246–265. doi:10.1016/j.biotechadv.2007.12.005 PMID:18337047
- Tracht, K., Weikert, F., & Hanke, T. (2012). Suitability of the ISO 10303-207 standard for product modeling of line linked micro parts. In *Procedia CIRP* (Vol. 3, pp. 358–363). Academic Press. doi:10.1016/j.procir.2012.07.062
- Velten, T., Schuck, H., Haberer, W., & Bauerfeld, F. (2010). Investigations on reel-to-reel hot embossing. *International Journal of Advanced Manufacturing Technology*, 47(1–4), 73–80. doi:10.1007/00170-009-1975-1
- Verdian, M. M. (2017). *Comprehensive Materials Finishing*. Comprehensive Materials Finishing. doi:10.1016/B978-0-12-803581-8.09200-6
- Worgull, M. (2009). Hot embossing: theory and technology of microreplication. *Annals of Physics*, 54. 10.1016/B978-0-8155-1579-1.50001-X
- Wu, B., Wu, X., Lei, J., Xu, B., Ruan, S., & Zhong, J. (2017). Study on machining 3D micro mould cavities using reciprocating micro ECM with queued foil microelectrodes. *Journal of Materials Processing Technology*, 241, 120–128. doi:10.1016/j.jmatprotec.2016.11.011

## APPENDIX

*Table 3. Data collected in industrial field regarding process consumables*

Manufacturing Process	Designation	Flow Rate	Acquisition Costs	Alternatives/Processes (refer to Figure 5 to Figure 8)
Milling	Lubricant	0.2 L/h	17 €/L	A1 – P2 A2 – P13 B2 – P2
Drilling	Lubricant	0.1 L/h	7 €/L	A1 – P3 A2 – P14 B2 – P3
Grinding	Lubricant	0.014 L/h	30 €/L	A1 – P4 A2 – P15 B2 – P4
Laser Milling	Carbon Dioxide	15 ml/min	2.83 €/L	A1 – P5 A2 – P2, P16 B1 – P2 B2 – P5
EBM	Hydrogen	25.5 L/cycle	0.009 €/L	A1 – P6 A2 – P4, P17 B1 – P4 B2 – P6
	Oxygen	5.1 L/cycle	3.6 €/L	
Micro-blasting	MS 300 A	1 kg/h	37 €/kg	A2 – P3 B1 – P3
	MS 550 BT	1 kg/h	45 €/kg	
Debinding	Argon with 5% Hydrogen	0.012 m <sup>3</sup> /h	10 €/m <sup>3</sup>	A2 – P10, P11 B1 – P10, P11 B2 – P10, P11
Sintering				
Hot-embossing	Lubricant	0.04 L/h	5 €/L	A2 – P9 B1 – P9, P13 B2 – P13

*Table 4. Machine data collected in the industrial field. The energy consumption cost considered was 0.07 Euros/kWh.*

Manufacturing Process	Designation	Installed Power [kW]	Acquisition Cost [€]	Equipments Life [years]	Alternatives/ Processes (refer to Figure 5 to Figure 8)
Design	iMac	0.31	2,000	4	A1 - P1 A2 - P1, P12 B1 - P1 B2 - P1
Milling/Drilling	Sigma 5	30	170,000	8	A1 - P2, P3 A2 - P13, P14 B2 - P2, P3
Grinding	Okamoto	5	45,000	8	A1 - P4 A2 - P15 B2 - P4
Laser Milling	Deckel-Maho 40SI	21.6	245,000	8	A1 - P5 A2 - P2, P16 B1 - P2 B2 - P5
Micro-blasting	Peenmatic	0.145	20,000	8	A2 - P3 B1 - P3
EBM	Sodick Pikka Finish	0.055	200,000	8	A1 - P6 A2 - P4, P17 B1 - P4 B2 - P6
Injection Molding (Feedstock and PMMA)	BOY 22A	9	150,000	8	A1 - P8 A2 - P19 B2 - P9
Hot-embossing (Feedstock)	LLOYD LR 10k	16	50,000	8	A2 - P9 B1 - P9
Hot-embossing (PMMA)	Famolde Machine	30	250,000	8	B1 - P13 B2 - P13
Feedstock Preparation	Z-Blade	8	50,000	8	A2 - P8 B1 - P8 B2 - P8
Debinding and Sintering	Binder	36	40,000	8	A2 - P10, P11 B1 - P10, P11 B2 - P10, P11
Heating	Binder	6	10,000	8	B1 - P12 B2 - P12
Cutting	Cutting machine	4	3,000	8	B1 - P14 B2 - P14
Degasification	LT-212 vacuum pump/air compressor	5	800	8	A2 - P6 B1 - P6
Conforming	Muffle furnace	36	10,000	8	A2 - P7 B1 - P7

## Chapter 2

# An Insight on Current and Imminent Research Issues in EDM

**Azhar Equbal**

*National Institute of Foundry and Forge Technology, India*

**Md. Israr Equbal**

*Aurora's Technological and Research Institute, India*

**Md. Asif Equbal**

*Cambridge Institute of Technology, India*

**Anoop Kumar Sood**

*National Institute of Foundry and Forge Technology, India*

### ABSTRACT

*Electrical discharge machining (EDM) is an important unconventional manufacturing process which machines the workpieces by a series of recurring electrical discharges between tool and workpiece completely immersed in a dielectric. A power supply establishes an electric field between tool and workpiece while a proper gap is maintained between them by a servo controller. Electrostatic force causes electrons to get plucked out from tool and workpiece forming a channel called plasma having low dielectric strength which easily ionizes producing sparks responsible for machining the workpiece. When the power supply is withdrawn, the continuous flushing of dielectric removes the debris from machined cavity in workpiece. EDM is used in machining of dies, molds, parts of aerospace, automotive industry, and surgical components. The study presents an insight on various research issues in EDM which would help the research community to establish their research objective to investigate. Based on current research trends and need of EDM study, the chapter also proposes some important future research issues.*

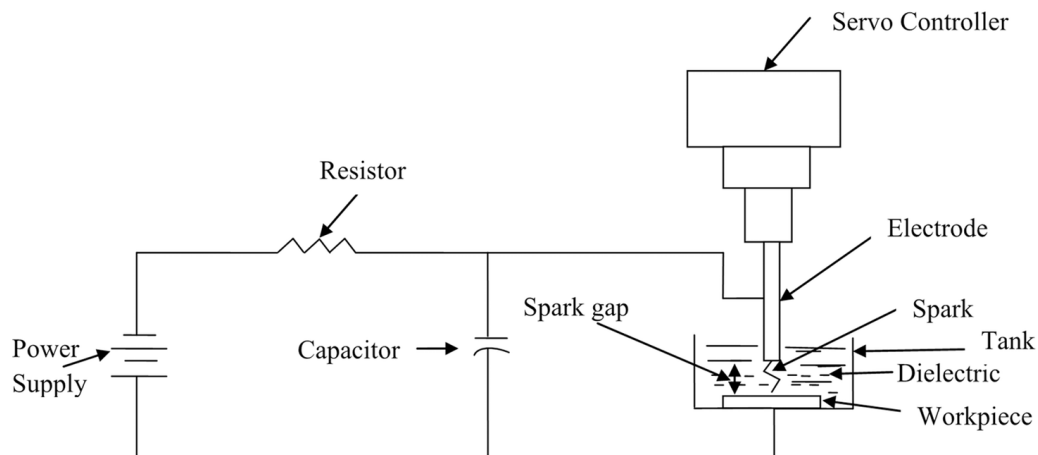
DOI: 10.4018/978-1-5225-6161-3.ch002

## 1. INTRODUCTION

Electrical discharge machining (EDM) is one of the most extensively used non-conventional material removal processes. EDM mainly consists of two major components: machine tool and a power supply (Figure 1). The machine tool holds a shaped electrode and a workpiece whereas power supply provides energy for performing the machining. The power supply uses a transformer to convert AC supply to DC supply through rectifier. Based on type of polarity namely straight polarity and reverse polarity either terminal of power supply is connected to electrode and workpiece.

Both the electrode and workpiece are completely submerged under dielectric. The commonly used dielectric are hydrocarbon oil, silicon based oil and de-ionized water. A servo controller is used to maintain a constant gap between the electrode and workpiece. Depending upon the voltage and the gap an electric field is established between the tool and workpiece (Yunxiao et al., 2018; Jha et al., 2011). As the electric field is established free electrons on the tool are subjected to electrostatic forces and electrons having less bonding energy are plucked out from the tool and accelerated towards the workpiece through the dielectric medium. As they gain more velocity while moving towards the workpiece, collisions occur between the electrons and dielectric molecules resulting in the ionization known as dielectric breakdown (Hamid, 2017; Ganguly, 2012). This cyclic process increases the concentration of electrons and ions at the gap creating a channel known as “plasma”. The electrical resistance of plasma is very less, therefore electrons with high energy move from negative terminal to positive terminal and highly energize ions will flow from positive to negative terminal. The kinetic energy of the electrons and ions on impact with the surface of the work and tool gets converted into thermal energy which increases the temperature of workpiece and tool resulting in erosion of material due to instant melting and vaporization of the respective material. The material is removed in form of debris. When the power supply is withdrawn, the plasma channel expands and collapsed generating pressure which flushes the debris out from machined surface (Ganguly, 2012). Simultaneous erosion of workpiece and tool increases gap between them and thus the electrode is lowered automatically by servo controller to maintain this gap and the process continues. One of the main advantages of this process is that there is no direct contact

*Figure 1. Schematic diagram of EDM*



between tool and workpiece and thus there is no forces in machining and even soft and delicate materials can be machined. EDM is widely used in machining of dies, moulds, parts of aerospace, automotive industry and surgical components. Important trends in EDM was marked in 1990 and since then numerous works have been established in EDM (Rajurkar, 1994). Irrespective of wide use of EDM, there is still a scope of improvement in line with latest developments in areas of science and technology. Based on this important research areas are identified and addressed in this chapter. Section 2 presents these research issues in detail and section 3 summarizes the study undertaken. An insight on few important future research issues is also presented in section 4.

## **2. VARIOUS RESEARCH ISSUED IN EDM**

For convenience of understanding various issues are presented separately in subsections:

### **2.1 Variants of EDM**

The basic principal of EDM relies on melting and erosion of materials but depending on utility common EDM variants are Die sinking EDM, Wire EDM and micro-EDM. Die sinking EDM is used for macro-EDM by removing larger amount of materials from workpiece. Based on the input energy a pulse discharge occurs in gap between the work piece and the electrode and the material is removed by melting and erosion of workpiece. Machined cavity is the mirror image of electrode shape used. They are used to produce deep and complex cavities under roughing and finishing operations (Amorim et al., 2014). Wire EDM uses same machining principal as die sinking EDM but metal wire is used as electrode. Wire electrode moves longitudinally during machining and are guided by two guide wires located separately above and beneath the workpiece. Common wire electrode is brass wire or coated steel wires but in case of thin wires tungsten or molybdenum wires are preferred. It is mainly used for making slits and cuts in the workpiece (Kapoor et al., 2010). Micro-EDM is helpful for precision engineering purposes as well as for machining in miniature workpiece that require material removal at micro level. It can produce micro-parts ranging from 50 $\mu$ m - 100 $\mu$ m and can easily drill micro holes or button holes (Mahendran et al., 2010). The working principal of is similar to other EDM processes but uses low voltage and current and thus material removed per spark is in the order of microns or nanometre. Micro-EDM produces excellent machined surface but the accuracy of machining is affected by the electrode wear. The wear of electrode becomes large for thin electrode or in the location of small curvature (Tsai et al., 2001). Integration of AEM (assisted electrode method) with inner-jet-liquid rotating electrode was investigated (Zhang et al., 2016). The angle between brass tube electrode and workpiece covered with copper assisted electrode was adjusted by fixing copper electrode and workpiece to a clamp. Dielectric was injected through brass electrode and the flushing pressure is controlled by relief valve. Improvement in process efficiency was observed. To improve the performance and save the machining energy high speed abrasive electrical discharge machining (AEDM-HS) was also investigated (Liu et al., 2015). Hollow cylindrical tool electrode containing diamond as abrasive was used which shows better result than conventional EDM.

In conventional EDM, due to high current the electrode gets locally melted and problem of arcing is often encountered and moreover discharge is uncontrollable (Mahendran et al., 2010). Pulsed DC power supply is a critical element for controlling the parameters and discharge (Wong et al., 2003). The common power supplies available are RC pulse generator, rotary impulse generator and transistor pulse

generator. RC pulse generator is based on charging and discharging of capacitor connected to power supply. In RC generator and impulse generator discharge energy is produced by charging of capacitor. The impedance of plasma channel is low which generates discharge current for short duration and is suitable for low material removal rate. They are suitable for wire EDM and micro-EDM (Mahendran et al., 2010). Transistor power systems are generally used in die sinking EDM in which discharge frequency can be controlled by on/off time of the transistor that control the charging pulse for capacitor. It produces high discharging current and high voltage increasing the material removal rate of system. They also have provision for automatic prevention of current flow when short circuit occurs. Transistor-type isopulse generator shows that material removal rate is two or three times higher than that of the traditional RC pulse generator (Han et al., 2007). To enhance efficiency and quality of wire EDM, auxiliary-pulse voltage supply was used which produces higher voltage for breaking the insulation between the electrode and the poly-silicon workpiece (Yu et al., 2011). Better machining efficiency and improvement in surface quality is recorded.

Dielectric fluid acts as an insulating medium between the electrode and workpiece. Once it ionizes with electrons and ions from electrode and workpiece it serves as conductor in the gap between electrode and workpiece and allows the machining. It also acts as a coolant to cool the electrode and workpiece and flushes away the debris formed during machining. The most commonly used dielectric is petroleum-based hydrocarbon oil and distilled water. Distilled water is cheap and is used for its good insulation, high thermal conductivity, low viscosity and high flowing rate. Distilled water as a dielectric can produce high material removal rate and low tool wear rate (Singh et al., 2011). However, water can cause rusting of work materials and also during machining it get dissociates into hydrogen and oxygen which is an explosive pair to deal with. To overcome the same use of deionized water is recommended. It has high resistivity, low viscosity, high cooling rate and high flowing rate and also is non-fire hazardous (Benedict, 1987). It was observed that EDM with deionized water reduces tool wear rate and improves surface finish (Chung et al., 2007, 2009). Hydrocarbon oils like kerosene are cheap, easily available and don't cause rusting. Hydrocarbon oils are however toxic, causes skin irritation on handling, release harmful vapours (CO and CH<sub>4</sub>) and has strong and unpleasant odour (Zhang et al., 2006). Their use in EDM is limited only to few cycles and after that it turns into waste and not only affects the environmental balance (by mixes with soil after disposal and affects its fertility) but also affect the economic impact because of its use for short run. To overcome the problems associated with water or hydrocarbon dielectrics, dry EDM using compressed air or gas is a current research area. In dry EDM process the electrode is either in the form of tube or pipe and the gas (dielectric) is supplied through the tube to the inter electrode gap (Skrabalaka et al., 2013). Researchers have reported that use of dry EDM significantly increases material removal rate (Tao et al., 2008; Choudhary et al., 2014). Different materials like graphite, silicon and aluminium in the form of tiny particles are mixed into the dielectric fluid causing earlier dielectric breakdown and hence improve machining efficiency. Dielectric performance is affected by powder material, particle size and its concentration. Use of silicon powder in kerosene as dielectric reduces surface roughness and decreases operating time (Pecas et al., 2003). Dielectric mixed with aluminium powder showed thinner recast layer and better surface finish than pure kerosene (Wu et al., 2005). Aluminium powder mixed in dielectric cause earlier breakdown of dielectric which increases material removal rate, decreases tool wear rate and improves surface finish (Singh et al., 2010).

Flushing of dielectric remove debris formed during machining increasing material removal rate and improving surface finish. Common flushing methods are jet flushing, through electrode pressure flushing, pressure flushing and pot flushing. Jet flushing is the simplest method in which a jet of dielectric



from nozzle is continuously circulated in dielectric tank to remove debris from in and around the crater (Masuzawa et al., 1992). Through electrode flushing uses a hole in electrode for continuous dielectric flushing. In pot flushing method a hole is drilled in workpiece to assist the flushing. Flushing of dielectric through the gap between electrode and workpiece minimizes heat and removes the debris formed. Researches shows that increase in flushing pressure increases the material removal rate and minimizes tool wear rate (Yan et al., 1999; Wang et al., 2000). Higher flushing pressure can otherwise cause poor surface quality (Munz et al., 2013).

## **2.2 Materials**

The materials in EDM are classified as workpiece material and electrode material.

### **2.2.1. Workpiece Material**

EDM is generally used for the machining of hard and brittle materials like steel, titanium and tungsten carbide. With the development, the demand for advance materials like super-alloys composites and ceramics increases (Prasad et al., 2014; Teicher et al., 2013; Gopalakannan et al., 2013). These materials are hard and difficult to get machined by traditional machining processes and EDM has evolved as a suitable method for machining of these materials. It is mainly used for semi-roughing and finishing operation apart from some application where it is also used for roughing operation. EDM of AISI D5 tool steel shows development of four different zones (Hascaly et al., 2004). The first or outermost zone consists of debris. The second layer is high carbon content brittle white layer and the layer beneath it is annealed and softer than the parent material. The fourth layer is of parent material itself. The white layer shows the presence of micro cracks which are radial in direction and present all around the crater. These micro cracks are identified as the initiation points for the failure of material (Lee et al., 2003). Composite materials reinforced with  $Al_2O_3$  and  $Si_3N_4$  particles are more susceptible to formation of surface micro-cracks during EDM (Peronczyk et al., 2011). EDM of Sialon and  $Al_2O_3$ -TiC shows development of intrinsic cracks and severe drop in flexural strength of ceramics (Lok et al., 1999). To avoid micro-cracks and produce uniform surface a low intensity of current is recommended (Younis et al., 2015). The high energy input during machining will change the chemical composition, metallographic structure, phase and geometric structure of material resulting in change in material properties (Peronczyk et al., 2011). Thermal action in EDM may cause micro-cracks, induces residual stresses and changes the micro-hardness of the sub-surface and surface layers and also results in carbon and hydrogen diffusion (Rajurkar et al., 2013). Use of ultra-high frequency for short pulse duration is recommended for low level of workpiece damage in EDM of aerospace parts (Aspiwall et al., 2008). For the case of INCOLONEL due to its high fracture toughness, work hardening behaviour and low conductivity traditional machining techniques are not suitable. These properties results in high cutting temperature which is associated with deformation and friction at the tool-chip and tool-workpiece interface (Ezugwu et al., 2003). EDM in magnesium nano alumina composites shows the generation of large amount of heat forming recast layer and causing structural change (Ponappa et al., 2010). Recast layer is formed by re-solidification of molten metal or debris on the surface of the workpiece and causes stresses resulting in material failure. It was propose that proper selection of machining parameter can minimizes the formation of recast layer (Rajurkar et al., 2013). EDM of reinforced metal matrix composites shows that in compared to normal EDM abrasive electrical discharge machining is more suitable for machining of these composites as machining

efficiency was higher and the process does not produce any recast layer around the crater (Liu et al., 2015). Machining of inclined holes in TBC (Thermal barrier coated) nickel super alloys namely IN718, NiCoAlY and 8YSZ was compared and it was observed that in comparison to IN718 and NiCoAlY, bond coating machined surface of 8YSZ ceramic show more fracture and pits (Zhang et al., 2016). With increase in inclination angle of hole to be machined the delaminating of coating, poor surface quality and stress concentration is also observed. EDM of Ti-6Al-4V shows the presence of carbon and oxygen on its surface and also it experiences the re-solidification of debris which were not completely flushed (Moses et al., 2015). Post EDM analysis of Ti-6Al-4V shows that EDM at high current deteriorate their properties (Harcuba et al., 2012).

### 2.2.2. Electrode Material

Various properties that determine the applicability of electrode materials in EDM are electrical conductivity, heat resistance, melting point, mechanical strength, wear and cost. Traditional electrode materials are brass, copper, tungsten, tungsten-carbide, zinc and graphite (Ezugwu et al., 2003). Most of these electrode materials experience problems such as severe wear, brittleness and low mechanical strength. To overcome these problems and to obtain better machining performance researches are focused on developing new electrode materials with better properties such as higher melting point and better electrical conductivity. Use of titanium carbide (TiC) in Cu-W (copper tungsten) electrode shows that sintering of Cu-W/TiC with nickel (Ni) will improve densification of electrode as nickel has good solubility in Cu and W (Li et al., 2001). Also, optimum concentration of TiC will improve tool wear, material removal rate and surface finish in EDM. In comparison to Cu electrode Cr/Cu based composite electrode will increase the material removal rate and reduces the crack formation (Tsai et al., 2003). During the machining chromium (Cr) in composite electrode will migrate to the work piece and increases its corrosion resistance. Cu-ZrB<sub>2</sub> composite electrodes for micro EDM showed better corrosion resistance and wear resistance in comparison with traditional electrodes when machined on the same experimental conditions (Yuangang et al., 2003). Zhang et al. showed that Cu-graphite, Cu-ZrB<sub>2</sub> and Cu-TiB<sub>2</sub> composite electrode gives high material removal rate and less tool wear rate (Zhang et al., 2001). Addition of tungsten in Cu will increase the melting point of composite and will remove more material for same volume of electrodes under similar machining conditions (Wei et al., 2013). In micro-EDM a thin tool electrode of diameter less than 10µm is required for machining which is difficult to fix in holder. To overcome this difficulty and to provide thicker electrode for easy handling a method is proposed in which electrode required for machining is electroplated with low melting point material (Tanabe et al., 2011). Electrode is then fixed in holder and plated layer can be removed with short electrical pulse. In their study tungsten wire (core electrode) is electroplated with zinc and during machining zinc gets removed by single or double pulse and then tungsten can be used for machining. They also suggested that after removal of zinc, coating can be repeated but for better efficiency of process improvement in method of centring of the core during plating is proposed. To improve the uniformity and stability of electrode a bunched electrode made by integration of small tubes is proposed by Gu and Zhao (Gu et al., 2011 and Zhao et al., 2010). In a tube electrode flushing takes place through the electrode and machined cavity is directly exposed to dielectric flushing which shows better flushing and hence material removal rate increases. EDM performance also depends on geometry and size of electrode. Four different geometries of electrode namely triangular, rectangular, square and circular were investigated (Sohaniet al., 2009). Based on machining results they propose that for higher material removal rate and lowest tool wear rate circular electrode is first choice.

The result is followed by triangular, rectangular and square cross section. Effect of electrode shape on EDM of Din 1.2379 steel was also studied (Matin et al., 2015). It was observed that triangular electrode provides highest MRR but shows maximum tool wear. Minimum tool wear was for the case of circular electrode. Effect of electrode diameter on micro-EDM shows that higher material removal rate and higher tool wear rate was observed when larger diameter of electrode was used for machining (Liu et al., 2016).

## **2.3 Automation**

In a CNC machining, complicated profile region is divided into sub-regions and accordingly the path for the movement of tool is generated by a CAD system. Likewise, implementation of intelligent CAD/CAM tool is required for reducing the tooling problem and manual intervention in EDM. For contouring EDM offsetting algorithm is used for generation of tool path (Mizugaki, 1996). First an offset surface is generated with parallel distance between the two surfaces equivalent to the radius of the ball-nosed cylindrical electrode. The tool path is then generated by designing tool path first on a plane and projecting it to the offset surface. Obtaining offset surface with full detail is however difficult. Tool path generation method for 4-axis contour EDM rough milling was proposed (Ding et al., 2004). The tool path is first generated in CAD/CAM system and cutter contact (CC) points between electrode and workpiece is calculated. The electrode in EDM is then adjusted by rotating it around the CC points. An algorithm to solve the problem of electrode path calculation starts by considering the electrode in its final position and increasing or decreasing degree of freedom (Gang et al., 2007). The electrode is moved to a defined distance in a mention degree of freedom and the value of rest of the degree of freedom is calculated. To find optimal combination of degrees of freedom an objective function evaluating the optimal combination of rotations is defined and minimized by optimization. In this method electrode geometry doesn't allow interference free path and electrode is modified which reduces its size. In order to obtain a smoother path An electrode design method and a feed path planning method called tangent tracking method was also developed (Liu et al., 2013). In their method the electrode is adjusted to the profile of cavity to be machined and electrode path is then searched by coinciding tangent vector of the electrode centre curve with the tangent vector of the flow channel in various steps. A smooth feed path is obtained which helps in reducing the number of electrodes and machining time.

Design of electrode is another important aspect of automation. Unlike the availability of CAD/CAM systems in mould design and specific commercial CAD/CAM systems customized for injection mould applications there are no intelligent CAD tools available for electrode design in EDM. A sharp corner uncut algorithm for the design of EDM electrodes was presented (Ding et al., 2000). Boundary of the regions in the mould that requires EDM are identified and projected on the XY plane (i.e., the plane that is perpendicular to the EDM direction). To ensure that projected boundary forms a close loop trimming and extension of the boundary curves was used. The close-loop boundary is then extruded along the Z direction to create a solid that defines the region that requires machining. Subtraction of the part geometry from the extruded solid then gives the solid model of the electrode. Knowledge based design of EDM electrodes for mould cavities pre-machined by high-speed milling (HSM) was also given (Mahaja et al., 2004). The STL file of the mould cavity machined with HSM was given as input the system and the file determines the region of the mould that cannot be milled and require machining by EDM. The area to be machined is then divided into different regions and using the rules these regions are recombined. From this method all possible electrode design can be then made and based on machining time and cost electrode design can be made. An integrated system for the design of the product and tool manufactur-

ing by DFM (design for manufacture) is proposed (Valentincic et al., 2007). The plane that divides the tool in two half is first defined by the system and then features are decided in each half of tool according to the product design. Appropriate machining of the feature can be done and if the complexity of the design requires special parts for machining then designer can update those configurations in system for easy manufacturing of tool. If the designer wants to change the design of tool itself then he can update the design requirements and DFM system will itself generates the required machining processes and machining parameters.

### **2.3 Process Parameter Optimization**

Performance measures of EDM process are material removal rate ( $MRR$ ), tool wear ratio ( $TWR$ ), surface roughness ( $SR$ ) and dimensional accuracy ( $DA$ ) of machined profile. These performance measures are directly linked with the various processing parameters of the process such as current, voltage, spark on and off time, flushing pressure and etc. Optimization of these parameters will improve the performance measures and increase the efficiency of the process. Numerous researchers focus on the optimization of process parameters either by closely examining the experimental procedure or by carrying out the simulation of the process. In this direction effect of process parameters on EDM of Al-SiC was studied using a mathematical model developed by response surface methodology (Habib, 2009). It was observed that increase in current ( $I$ ) and pulse on time ( $T_{on}$ ) increases  $MRR$ ,  $TWR$ ,  $SR$  and gap size. They also observe that with increase in percentage of SiC gap size decreases. With increase in  $I$  and  $T_{on}$  discharge increases which increases diameter of plasma channel and form large crater thereby increasing  $MRR$  but at the same time causing more tool wear and poor surface finish. EDM of Al-SiC nano-composite shows that  $MRR$  is mainly affected by  $I$  and  $T_{on}$ . With increase in current  $MRR$  increases but with increase in pulse on time  $MRR$  first increase then decreases (Gopalakannan et al., 2013). Increase in surface roughness was also observed with increase in current and pulse on time. For minimizing tool wear rate Singh et al. suggested use of higher pulse off time ( $T_{off}$ ) (Singh et al., 2013). At higher  $T_{off}$  enough time is available for re-establishment of dielectric strength and frequency of spark decreases. Increase in  $MRR$  and decrease in  $TWR$  is observed with increase of  $T_{on}$  (Kumar et al., 2014). At higher  $T_{on}$ , plasma channel spreads causing increase in diameter of plasma due to which heat transfer to the tool reduces whereas heat transfer to workpiece is increased causing decrease in  $TWR$  and increase in  $MRR$ . An EDM characteristic in deep-hole drilling of INCONEL 718 revealed that peak current, duty factor, and electrode rotation were the most influential factors in  $MRR$  whereas surface roughness is strongly affected by pulse-on time (Kuppan et al., 2008). A review on die-sinking propose that for achieving good dimensional accuracy in EDM the gap stability is very important (Garg et al., 2010). Dewangan et al. suggested that higher current and pulse on time have negative influence on the dimensional accuracy (Dewangan et al., 2015). Tool wear is unavoidable during EDM machining and surface roughness of workpiece increases with increase increased wear of electrodes (Kiyak & Cakir, 2007). Deposition of heigher carbon on tool surface decreases tool wear and therefore hydrocarbon-based dielectric is suggested in EDM (Marafona et al., 2000). It was experimentally verified that  $TWR$  is higher in the early stages of the process because of higher discharge energy used at the beginning of machining (Fred et al., 2007). Effect of process parameters on  $MRR$  of EN-31 tool steel in powered mixed EDM suggested that peak current and concentration of silicon powder in dielectric fluid maximizes the  $MRR$  (Kansal et al., 2005). Increase in concentration of the powder causes bridging effect between the electrode and workpiece which spreads the discharge thereby increases the  $MRR$ . Due to bridging effect several discharge trajectories are formed in a single

pulse creating multiple discharge spots which increases *MRR* and improves surface finish (Chaw et al., 2000). Influence of EDM parameters on *MRR* and surface roughness of an INCONEL 600 alloy were investigated with straight polarity and reverse polarity (Torres et al., 2015). They proposed that current is the most influential factor affecting the *MRR* in both polarities. However, they concluded that with straight polarity, the material removal rate is significantly higher. For surface roughness, it was observed that independent of polarity it increases with increase in current and pulse time. Effect of polarity on EDM tool steel was studied and it was recommended that use of straight polarity for getting higher *MRR*, lower *TWR* and better surface finish (Reza et al., 2010). In a straight polarity few electrons moved to tool but maximum electrons are migrated to workpiece as it is positive charge and attracts electron thus increasing *MRR*. Minimization of tool wear rate in straight polarity is also proposed by Lee et al (Lee et al., 2007). EDM of alloy steel shows higher *MRR* and larger *TWR* with increases in flushing pressure (Lonardo et. al, 1999). Large increase in flushing pressure can otherwise cause poor surface quality (Wang et al., 2000; Munz et al., 2013).

To analyse the effect of process parameters on wire-EDM and to provide the optimized parameter settings for responses Taguchi's design was proposed. Based on results of nonlinear regression model it was observed that for each response optimized process parameters are different. Multi-objective optimization using genetic algorithm proposed that optimized process parameter setting results in improved value of the responses (Mahapatra et al., 2006). Multi-objective optimization was also presented by using data envelopment analysis (DEA) approach (Sahu et al., 2013). It was observed that responses vary with change in processing conditions. To improve the machining efficiency optimized factors setting are proposed. For improving the machining efficiency of AISI D6 tool steel range of EDM parameters was also proposed (Barenji et al., 2016).

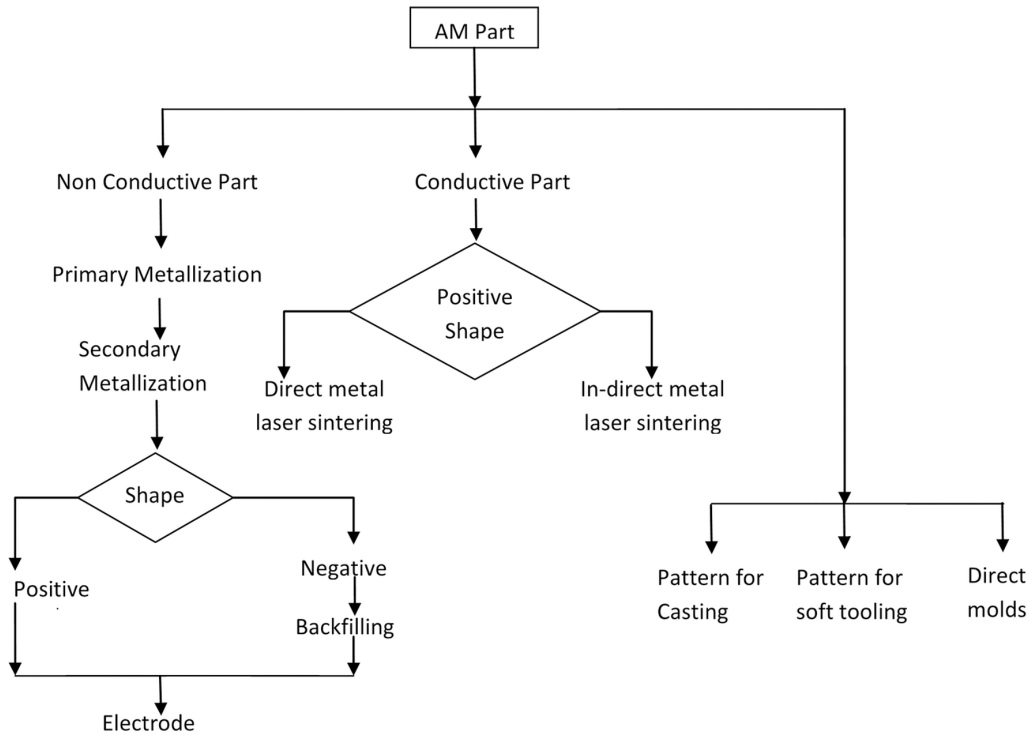
## **2.4 Rapid Electrode Manufacturing**

EDM represents higher cost in any manufacturing industries and out of total EDM cost more than 50% of cost is invested in electrode production. This cost increase with the complexity of cavity to be machined. A systematic system needs to be developed that can accelerate the electrode production rate so that the time and cost can be minimized and economic balance can be established. Rapid electrode fabrication is therefore an important area to investigate. Research trends shows integration of additive manufacturing (AM) with the existing manufacturing methods is a preferred practice in this direction (Zhang et al., 2003 and Liu et al., 2013). Integration of AM with EDM will be very promising in this respect. AM techniques can produce the electrodes in three different ways as shown in Fig. 2. One approach uses metal-based AM processes to directly manufacture EDM electrodes whereas the other approach use the AM process to generate a part which is then metalized with suitable technique to gain conductivity and satisfy the EDM requirement. It can be used as pattern for casting or can be used as a master pattern to produce more patterns. In some cases it can also directly produce moulds (Kechagias et al., 2008).

### **2.4.1. Electrodes of Conductive Material**

Present research in EDM electrode manufacturing using conductive materials focuses on expanding the available materials and increasing the performances of AM techniques. Selective laser sintering (SLS) is most extensively researched in this respect. SLS uses metal compounds and binder powders for manufacturing of metal parts. It can be either direct metal laser sintering (DMLS) or indirect metal laser sintering

Figure 2. Possible variations of EDM electrode manufacture using AM



(IMLS). IMLS uses a plastic binder material while DMLS uses a metal binder. In DMLS prototypes and production tools are produced from metal powder without the use of polymer binder. For EDM electrode production, DMLS uses metal powder system of Nickel, bronze and few percent of copper (Durr et al., 1999). Good machining rate was achieved but tool wear was high and surface roughness was very poor. Improvements in dimensional accuracy of electrode are suggested for better electrode performance and improved surface finish. Experimental investigation proposed that the electrode wear at the front edge was higher than the side wear due to the porosity of the DMLS electrodes (Meena et al., 2006). DMLS is used to produce four different electrodes namely solid copper electrode, copper electroplated electrode, an electroless copper plated electrode and an untreated DMLS electrode (Tay & Hyder, 2001). They suggested that DMLS electrode is suitable for both semi roughing and roughing condition when minimal material is to be removed and electroless copper electrode can be used for moderate material removal and better dimensional accuracy. Shell thickness of copper electroplated DMLS electrodes was also investigated (Dimla et al., 2004). Electroplating was used to produce a complex part and thickness of copper shell was then measured at different position. A big difference of shell thickness at different position was observed with outer faces having good copper deposition whereas the inner cavities have least deposition. They propose that electroplated DMLS electrodes were unsuitable for industrial use due to the uneven copper shell thickness.

Due to problematic expansion of metal powders during IMLS the research mainly concentrated on the development of new materials with advance material properties. Production of EDM electrodes using metal matrix composites (MMC) was investigated (Strucker et al., 1995, 1997, Cheng et al., 1996). A

powder mixture of  $ZrB_2$  and a polymer was used and simple cubed electrode was made by cold-pressing. For complex electrode SLS is used. For sintering the  $ZrB_2$  particles the electrode was then kept in temperature-controlled furnace and they are infiltrated with copper. EDM of tool steel was done using these electrodes. It was observed that *MRR* increases with increase in current but after a critical on time it slightly decreases. Increase in *MRR* with increasing the pulse off time and keeping the pulse on time constant was also observed. For tool wear they mentioned that it decreases with increase in pulse on time. Effect of sintered copper based EDM electrodes has shown that electrodes having 15% TiC have the highest relative density, lowest electrical resistivity and good EDM performance (Li et al., 2001). EDM electrode was produced using powder system of steel, polyester and phosphate using SLS/RAP-I system (Zhao et al., 2003). Post treatment was applied in three steps. First low temperature sintering was applied to decompose the polyester and then high temperature sintering was applied producing a rigid inorganic compound from phosphate- steel reaction. At last copper infiltration was applied to improve the electrode quality. Machining at different conditions shows that these electrodes were only suitable for finishing cuts in EDM. For rapid electrode production by SLS, copper-nickel and zirconium diboride was used (Tiago et al., 2014) and influence of SLS parameters and material content on the densification behaviour and porosity of the electrodes was investigated. They proposed that  $ZrB_2$ -CuNi electrodes presented a much superior performance than SLS copper powder electrodes but their performance was inferior to solid copper electrodes.

#### **2.4.2. Electrodes of Non-Conductive Material**

Electrode of non-conductive AM part is divided into two categories: positive metal coated parts (direct tooling) and negative metal coated parts (indirect tooling). The surface of non-conductive AM part is first cleaned and then it is subjected to primary metallization to induce conductivity in AM part. Once the conductivity is induced the part is subjected to secondary metallization to increase the thickness of metallic layer and to reinforce the final electrode properties. For positive AM part only the above three sub processes (Finishing, primary metallization and secondary metallization) is applied. In case of negative shape, apart from above three sub processes two extra steps of backfilling of metal shell cavity and mandrel removal is required. In this direction, EDM of copper plated stereolithography (SLA) electrode produce acceptable results during semi-finishing and finishing operations in EDM but for roughing operations electrodes are found unsuitable (Arthur et al., 1995). They concluded that metalized thickness of more than 180  $\mu m$  is to be used for general EDM applications. The failure of above electrode because of heat distribution was investigated by same researchers (Arthur et al., 1996, 1998). They stated that due to different linear expansion between plastic core and metalized layer shear stress occur between their interfaces leading to electrode failure. It was also observed that there is substantial drop in the electrical conductivity of copper between room temperature and operating temperature range of EDM. To improve process efficiency further investigation on its effect on heat generation was proposed. Dimensional accuracy of copper electroplated electrodes shows that accuracy of electroplated electrode is a function of three factors: the accuracy of RP model, accuracy of primary metallization and accuracy of copper shell thickness (Gillot et al., 2005) To avoid primary metallization they used a CNC machine copper part. It was found that because of lack of dimensional accuracy electroplated electrodes were not satisfactory for industrial use. Spraying metal on a positive or a negative SLA pattern shows inferior characteristics to electroplated and electroformed electrodes (Dickens et al., 1992). To improve the efficiency of electroplated electrode use copper pyrophosphate in place of acidic copper was proposed (Bocking et al.,

1997). Good pore closure properties were observed but shear due to high operating temperature stress between interfaces increases resulting in distortion of metallic shell. For electrode production integration of stereolithography (SLA) and electroforming has been studied (Yang et al., 1999). In their research part manufactured by stereolithography technique is plated with copper and then backed with low melting point alloy. The uniformity in plating is however not maintained in their study. During EDM burning of SLA part and solidification of backing materials occurs leading to deformation of electrode and larger deviations in dimensions of machined cavity was observed. Electroforming of rapid prototyping mandrels was also investigated (Allan et al., 2001). Their research drawn a conclusion that thin walled copper electroforms electrode backed with suitable filler materials are ideal for use as electro-discharge machining electrodes. However, these electrodes are only preferable for low current values ranging between 15 and 20 mA/cm<sup>2</sup>. Indirect tooling approach for producing EDM electrode was adapted (Yarlagadda et al., 1999). In their research stereolithography (SLA) pattern was fabricated and then silicon RTV and vacuum casting are used to produce flexible silicon cavities. This is followed by copper electroforming on the above cavities to produce a copper shell. The shells were then preheated and backfilled with zinc to give the necessary mechanical strength to the electrode. Distortions were observed due to incomplete filling of the backing material. It was proposed that copper electroforming of SLA electrode shows uneven shell thickness at different locations. Use of hybrid adaptive layer manufacturing concluded that though accurate parts can be manufactured but the produced tools may be inferior to their conventional counterparts in composition and tool life (Akula et al., 2006).

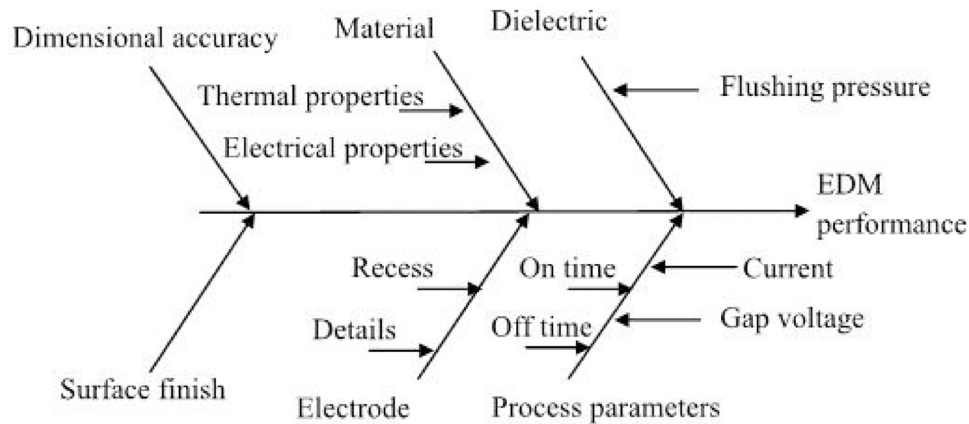
### **3. SUMMARY OF RESEARCH**

EDM is based on thermoelectric energy between the work piece and an electrode. A spark occurs in a small gap between the electrode and the work piece and removes the material from the work piece through melting and vaporising. The electrode and the work piece must be electrically conductive. During machining the part and the electrode are eroded simultaneously. EDM performance is mostly affected by the process parameters and thus their values must be set as per machining performance required. The electrode material used must have suitable properties to decrease the electrode wear rate and increase the material removal rate. The electrode material must have high mechanical strength and high melting point to reduce the tool wear. As the machined cavity solely depends on the shape of the electrode therefore dimensional accuracy of part produced depends on the dimensional accuracy and surface finish of the electrode. Figure 3 presents a fish bone diagram explaining the different factors affecting the performance of EDM process.

With the development the use of advanced materials like ceramics, composites and super alloys are increasing in automobile and aerospace industries and EDM has emerges as a suitable candidate for machining these materials. Die sinking EDM and wire EDM are the most commonly used EDM processes. Removal of material at macro and micro level is possible by different EDM variants. Recent researches are using newer EDM like high speed abrasive electrical discharge machining and integration of assisted electrode method with inner-jet-liquid rotating electrode which significantly improves process efficiency (Zhang et al., 2016 and Liu et al., 2015). Power supply in EDM is generally provided by using RC and RLC generator (Wong et al., 2003). These methods uses capacitor for storing electrical



*Figure 3. Fishbone diagram showing factors affecting EDM performance*



energy and discharge energy for machining is provided by charging and discharging of capacitor. The impedance of plasma channel is low which generates energy for short duration and is therefore suitable for low material removal rate. To overcome this, use of transistor assisted power system is preferred which produces high voltage and high discharge energy which increases the MRR of system (Han et al., 2007). For better machining efficiency research also reports the use of modified power supply such as auxiliary-pulse voltage supply which produces higher voltage for easy breaking of the insulation between the electrode and workpiece (Singh et al., 2011). Dielectric in EDM is required for cooling the tool and workpiece and also enables the flushing of debris formed during machining. Hydrocarbon based oils are commonly used but due to their limited life cycle and health hazards associated with them use of distilled water, deionised water, dry EDM and powder mixed EDM is preferred in present industries (Chung et al., 2007; Skrabalaka et al., 2013; Wu et al., 2005).

EDM requires very high input energy for machining and machining at such high energy changes material properties like chemical composition, micro structural change, change in phase and change in geometrical structures (Peronczyk, 2011). During machining solidification of molten metal or debris on the surface of the workpiece resulting in formation of recast layer which is hard and brittle leading to the formation of micro-cracks on the workpiece surfaces (Ezugwu et al., 2003; Ponappa et al., 2003). To overcome these difficulties machining at low current and low pulse time is proposed (Younis et al., 2015). Use of finish machining or precision grinding after EDM is also recommended for avoiding formation of recast layer and micro-cracks. Electrode material and its property also affect the EDM performance. Due to their good machinability and conductivity commonly used electrode materials are copper, brass, graphite and tungsten (Rajurkar et al., 2013). These electrodes are more suitable for machining of steels and other low melting point alloys but machining of advance materials requires very high energy input for machining and these electrodes are not suitable. Machining of advance materials requires electrodes with high melting point, high electrical conductivity, high wear resistance and high heat resistance. Use of composite electrodes like Cu/Cr, Cu-W/TiC which have distinct attractive properties like better electrical conductivity, high heat and wear resistance and high melting point are gaining much importance in current EDM practice (Li et al., 2012; Tsai et al., 2013; Zhang et al., 2011;

Tanabe et al., 2011; Zhao et al., 2010). It has shown in literatures that use of composite electrodes in EDM increases *MRR* and reduces *TWR*. Better surface finish and reduction in crack formation were also observed with the machining of composite electrodes (Tsai et al., 2003; Yuangang et al., 2009). For improving machining efficiency shape of electrode is also very important. Researchers have shown that use of circular cross section of electrode results in increased *MRR*, low *TWR*, better surface finish and low overcut (Sohani et al., 2009; Matin et al., 2015). Performance measures of EDM are highly affected by processing conditions thus optimized factors settings is required for optimum EDM performance. Optimization can be for single objective or multi-objectives as required and will help the practitioners to select the optimal parameters for machining (Habib et al., 2009, Kumar et al., 2014; Kuppan et al., 2008; Garg et al., 2010, Mahapatra et al., 2006). To reduce the tooling problems and to prevent the human interference in EDM implementation of CAD/CAM tool is preferred to make the EDM process automated (Ding et al., 2000 and 2004, Gang et al., 2007, Mahajan et al., 2004). For reduction of cost and time in EDM use of additive manufacturing (AM) techniques can accelerate the electrode production rate and can generate the complex profile of electrodes in very less time. AM techniques can also produce various electrodes in single cycle.

#### 4. FUTURE RESEARCH TRENDS

Many applications of EDM have been identified since EDM was proposed in 1943 and EDM has undergone rapid improvements in terms of capability, economic operation, speed and flexibility. Presently there are many new applications which are continually emerging which can discover the improvement of the process. Considering the history of EDM, need and perspective of modern manufacturing scenario few significant future trends in EDM are:

1. **Machining of Non-Conductive Materials:** EDM is a suitable technology for machining of conductive materials but high resistivity showed by non-conductive materials makes them impossible to be machined by EDM and it is therefore highly challenging to machining non-conductive materials through EDM. A novel technique named double electrodes synchronous servo electrical discharge grinding (DESSDYG) for non-conductive ceramics showed that machining of non-conductive material is possible using EDM (Xiaopeng et al., 2012). More alternate methods capable of satisfactorily machining non-conductive workpieces by EDM is a promising area of research.
2. **Electrode Shape in EDM:** Selection of electrode shape in EDM also affects machining performance. Circular cross section of electrode for higher *MRR* and lowest *TWR* was proposed (Sohani et al., 2009). Matin et al. however proposed use of triangular electrode for maximum *MRR* (Matin et al., 2015). Results are conflicting and demands proper justification. Well established research with proper reasoning is required in this direction.
3. **Integration of AM and EDM:** For reduction in cost and time in EDM rapid fabrication of EDM electrode is a prime concern. Research trends shows that application of AM techniques can assist in rapid fabrication of EDM electrodes the research is however only limited to SLA and SLS (Arthur et al., 1995, 1996, 1998, Dickens et al., 1992). FDM (fused deposition modelling) is another AM technique which uses ABS as its part material and literature show that ABS has excellent metalization possibility which can turn it into conductive and it can be used in EDM as an electrode. Immense possibility of FDM in EDM electrode production thus needs to be investigated.

4. **Automation in EDM:** EDM performances like *MRR*, *TWR* and surface integrity is primarily affected by discharge energy in terms of current and used for machining and thus monitoring of electric current and voltage in real EDM condition is required for proper control of process behaviour. Use of automated test system design to acquire suitable electric voltage and current is proposed (Mendes et al., 2004). Further investigation is not reported in literature and thus development of automated system for controlling EDM's behaviour is highly challenging and requires more investigation.

## REFERENCES

- Akula, S., & Karunakaran, K. P. (2006). Hybrid adaptive layer manufacturing: An Intelligent art of direct metal rapid tooling process. *Robotics and Computer-integrated Manufacturing*, 22(2), 113–123. doi:10.1016/j.rcim.2005.02.006
- Allan, E. W., Bocking, C., & Bennett, R. (2001). Electroforming of rapid prototyping mandrels for electro-discharge machining electrodes. *Journal of Materials Processing Technology*, 110(2), 186–196. doi:10.1016/S0924-0136(00)00878-5
- Amorim, F. L., & Weingaertner, W. L. (2007). The behaviour of graphite and copper electrodes on the finish die-sinking electrical discharge machining (EDM) of AISI P20 tool steel. *Journal of the Brazilian Society of Mechanical Sciences and Engineering*, 29(4), 366–371. doi:10.1590/S1678-58782007000400004
- Amorim, F. L., & Weingaertner, W. L. (2014). Die sinking electrical discharge machining of a high strength copper based alloy for injection molds. *Journal of the Brazilian Society of Mechanical Sciences and Engineering*, 26(2), 137–144.
- Arthur, A., & Dickens, P. M. (1998). Measurement of heat distribution in stereolithography electrodes during electro - discharge machining. *International Journal of Production Research*, 36(9), 2451–2461. doi:10.1080/002075498192625
- Arthur, A., & Dickens, P. M. (1995). Rapid prototyping of EDM electrode by stereolithography. Proceedings of International Symposium for Electromachining (ISEM X1), 17-20, 691-699.
- Arthur, A., Dickens, P. M., Cobb, R. C., & Bocking, C. E. (1996). Wear and failure mechanisms for SL EDM electrodes. In *SFFF Symposium*. University of Texas at Austin.
- Aspiwall, D. K., Soo, S. L., Berrisford, A. E., & Walder, G. (2008). Workpiece surface roughness and integrity after WEDM of Ti- 6Al-4V and Inconel 718 using minimum damage generator technology. *CIRP Annals - Manufacturing Technology*, 57(1), 187-190.
- Barenji, R. V., Pourasl, H. H., & Khojastehnezhad, V. M. (2016). Electrical discharge machining of the AISI D6 tool steel: Prediction and modelling of the material removal rate and tool wear ratio. *Precision Engineering*, 45, 435–444. doi:10.1016/j.precisioneng.2016.01.012
- Benedict, G. F. (1987). *Non-traditional manufacturing process*. CRC Press.
- Bocking, C.E., Bennett, G.R., Dover, S.J., Arthur, A., Cobb, R.C., & Dickens, P.M. (1997). Electrochemical routes for engineering tool production. *GEC Journal of Technology*, 14(2), 66.

Cheng, Y. M., Eubank, P. T., & Gadalla, A. M. (1996). Eubank, P.T. and Gadalla, A.M. Electrical Discharge Machining of ZrB<sub>2</sub>-Based Ceramics. *Materials and Manufacturing Processes*, 11(4), 565–574. doi:10.1080/10426919608947509

Choudhary, S. K., & Jadoun, R. S. (2014). Current research development in dry electric discharge machining. *International Journal of Emerging Technology and Advanced Engineering*, 4(8), 832–839.

Chow, H. M., Yan, B. H., Huang, F. Y., & Hung, J. C. (2000). Study of added powder in kerosene for the micro-slit machining of titanium alloy using electro-discharge machining. *Journal of Materials Processing Technology*, 101(1-3), 95–103. doi:10.1016/S0924-0136(99)00458-6

Chung, D. K., Kim, B. H., & Chu, C. N. (2007). Micro electrical discharge milling using deionized water as a dielectric fluid. *Journal of Micromechanics and Microengineering*, 17(5), 867–874. doi:10.1088/0960-1317/17/5/004

Chung, D. K., Shin, H. S., Kim, B. H., Park, M. S., & Chu, C. N. (2009). Shin, H.S. Kim, B.H. Park, M.S. and Chu, C.N. Surface finishing of micro-EDM holes using deionized water. *Journal of Micromechanics and Microengineering*, 19(4), 045025. doi:10.1088/0960-1317/19/4/045025

Czelusniak, T., Amorim, F. L., Lohrengel, A., & Higa, C. F. (2014). Development and application of copper–nickel zirconium diboride as EDM electrodes manufactured by selective laser sintering. *International Journal of Advance Manufacturing Technology*, 72, 905-917.

Dewangan, S., Gangopadhyay, S., & Biswas, C. K. (2015). Study of surface integrity and dimensional accuracy in EDM using Fuzzy TOPSIS and sensitivity analysis. *Measurement*, 63, 364–376. doi:10.1016/j.measurement.2014.11.025

Dickens, P. M., & Smith, P. J. (1992). Stereolithography tooling. *Proceedings of the first European conference on RP&M*, 309-317.

Dimla, D. E., Hopkinson, N., & Rothe, H. (2004). Investigation of complex rapid EDM electrodes for rapid tooling applications. *International Journal of Advance Manufacturing Technology*, 23, 249-255.

Ding, S., & Jiang, R. (2004). Tool path generation for 4-axis contour EDM rough machining. *International Journal of Machine Tools & Manufacture*, 44(14), 1493–1502. doi:10.1016/j.ijmachtools.2004.05.010

Ding, X. M., Fuh, J. Y. H., Lee, K. S., Zhang, Y. F., & Nee, A. Y. C. (2000). A computer-aided EDM electrode design system for mold manufacturing. *International Journal of Production Research*, 38(13), 3079–3092. doi:10.1080/00207540050117459

Durr, H., Pilz, R., & Eleser, N. S. (1999). Rapid tooling of EDM electrodes by means of selective laser sintering. *Computers in Industry*, 39(1), 35–45. doi:10.1016/S0166-3615(98)00123-7

Ezugwu, E. O. (2003). Key improvements in the machining of difficult-to-cut aero- space super alloys. *International Journal of Machine Tools and Manufacture*, 45, 1353-1367.

Gang, L.I., & Sheng, Z. W. (2007). A special CAD/CAM software for electro-discharge machining of shrouded turbine blisks. *Journal of Shanghai Jiaotong University*, 11(1), 74-78.

- Ganguly, S. (2012). A detailed review of the current research trends in electrical discharge machining (edm). *Proceedings of the National conference on trends and advances in mechanical engineering*, 657-669.
- Garg, R. K., Singh, K. K., Sachdeva, A., Sharma, V. S., Ojha, K., & Singh, S. (2010). Review of research work in sinking EDM and WEDM on metal matrix composite materials. *International Journal of Advance Manufacturing Technology*, 50, 611-624.
- Gillot, F., Mognol, P., & Furet, B. (2005). Dimensional accuracy studies of copper shells used for electro-discharge machining electrodes made with rapid prototyping and the electroforming process. *Journal of Materials Processing Technology*, 159(1), 33-39. doi:10.1016/j.jmatprotec.2003.11.009
- Gopalakannan, S., & Senthilvelan, T. (2013). Application of response surface method on machining of Al - SiC nano-composites. *Measurement*, 46(8), 2705-2715. doi:10.1016/j.measurement.2013.04.036
- Gopalakannan, S., & Senthilvelan, T. (2013). EDM of cast Al/SiC metal matrix nano composites by applying response surface method. *International Journal of Advanced Manufacturing Technology*, 67(1), 485-493. doi:10.1007/00170-012-4499-z
- Gowthaman, S., Balamurugan, K., Kumar, P. M., Ali, S. K. A., Kumar, K. L. M., & Ram Gopal, N. V. (2018). Electrical Discharge Machining studies on Monel- Super Alloy. *Procedia Manufacturing*, 20, 386-391. doi:10.1016/j.promfg.2018.02.056
- Gu, L., Le, L., Zhao, W., & Rajurkar, K. P. (2012). Electrical discharge machining of Ti6Al4V with bundled electrode. *International Journal of Machine Tools & Manufacture*, 53(1), 100-106. doi:10.1016/j.ijmachtools.2011.10.002
- Habib, S. S. (2009). Study of the parameters in electrical discharge machining through response surface methodology approach. *Applied Mathematical Modelling*, 33(12), 4397-4407. doi:10.1016/j.apm.2009.03.021
- Hamid, S., & Ramezanali, M. (2017). A comparative investigation on temperature distribution in electric discharge machining process through analytical, numerical and experimental methods. *International Journal of Machine Tools & Manufacture*, 114, 35-53. doi:10.1016/j.ijmachtools.2016.12.005
- Han, F., Chen, L., Yu, D., & Zhou, X. (2007). Basic study on pulse generator for micro-EDM. *International Journal of Advanced Manufacturing Technology*, 33(5), 474-479. doi:10.1007/00170-006-0483-9
- Harcuba, P. (2012). Surface treatment by electric discharge machining of Ti-6Al-4V alloy for potential application in orthopaedics. *Journal of the Mechanical Behavior of Biomedical Materials*, 7, 96-105. doi:10.1016/j.jmbbm.2011.07.001 PMID:22340689
- Hascaly, A., & Caydas, U. (2004). Experimental study of wire electrical discharge machining of AISI D5 tool Steel. *Journal of Materials Processing Technology*, 148(3), 362-367. doi:10.1016/j.jmatprotec.2004.02.048
- Jha, B., Ram, K., & Rao, M. (2011). An overview of technology and research in electrode design and manufacturing in sinking electrical discharge machining. *Journal of Engineering Science and Technology Review*, 4(2), 118-130.

- Kansal, H. K., Singh, S., & Kumar, P. (2005). Parametric optimization of powder mixed electrical discharge machining by response surface methodology. *Journal of Materials Processing Technology*, 169(3), 427–436. doi:10.1016/j.jmatprotec.2005.03.028
- Kapoor, J., Singh, S., & Khamba, J. S. (2010). Recent developments in wire electrodes for high performance WEDM. *Proceedings of the world congress on engineering*, 2, 1065–1068.
- Kechagias, J. (2008). EDM electrodes manufacture using rapid tooling: A review. *Journal of Materials Science*, 43, 2522–2535. doi:10.1007/10853-008-2453-0
- Kiyak, M., & Cakır, O. (2007). Examination of machining parameters on surface roughness in EDM of tool steel. *Journal of Materials Processing Technology*, 191(1-3), 141–144. doi:10.1016/j.jmatprotec.2007.03.008
- Kumar, R., Sahani, O.P., & Vashista, M. (2014). Effect of EDM process parameters on tool wear. *Journal of Basic and Applied Engineering Research*, 1(2), 53–56.
- Kuppan, P., Rajadurai, A., & Narayanan, S. (2008). Influence of EDM process parameters in deep hole drilling of Inconel 718. *International Journal of Advance Manufacturing Technology*, 38, 74–84.
- Lee, H. T., & Tai, T. Y. (2003). Relationship between EDM parameters and surface crack formation. *Journal of Materials Processing Technology*, 142(3), 676–683. doi:10.1016/S0924-0136(03)00688-5
- Lee, S. H., & Li, X. P. (2007). Study of the effect of machining parameters on the machining characteristics in electrical discharge machining of tungsten carbide. *Journal of Materials Processing Technology*, 115(3), 344–358. doi:10.1016/S0924-0136(01)00992-X
- Li, L. (2001). EDM performance of TiC/CU based sintered electrode. *Materials & Design*, 22, 669–678. doi:10.1016/S0261-3069(01)00010-3
- Li, L., Wong, Y. S., Fuh, J. Y. H., & Lu, L. (2001). Effect of TiC in copper Tungsten electrodes on EDM performance. *Journal of Materials Processing Technology*, 113(1-3), 563–567. doi:10.1016/S0924-0136(01)00622-7
- Liu, J. W., Wu, Y.-Z., & Yue, T.-M. (2015). High Speed Abrasive Electrical Discharge Machining of Particulate Reinforced Metal Matrix Composites. *International Journal of Precision Engineering and Manufacturing*, 16(7), 1399–1404. doi:10.1007/12541-015-0184-0
- Liu, L., Zhuang, Z., Liu, F., & Zhu, M. (2013). Additive manufacturing of steel-bronze bimetal by shaped metal deposition: Interface characteristics and tensile properties. *International Journal of Advanced Manufacturing Technology*, 69(9), 2131–2137. doi:10.1007/00170-013-5191-7
- Liu, Q., Zhang, Q., Zhu, G., Wang, K., Zhang, J., & Dong, C. (2016). Effect of electrode size on the performances of Micro EDM. *Materials and Manufacturing Processes*, 31(4), 391–396. doi:10.1080/10426914.2015.1059448
- Liu, X., Kang, X., Zhao, W., & Liang, W. (2013). Electrode feeding path searching for 5-axis EDM of integral shrouded blisks. *Procedia CIRP*, 6, 107–111. doi:10.1016/j.procir.2013.03.041

- Lok, Y. K., & Lee, T. C. (1999). Processing of advanced ceramics using the Wire-Cut EDM process. *Journal of Materials Processing Technology*, 63(1-3), 839–843. doi:10.1016/S0924-0136(96)02735-5
- Lonardo, P. M., & Bruzzone, A. A. (1999). Effect of flushing and electrode material on die sinking EDM. *Annals of the CIRP*, 48(1), 123–126. doi:10.1016/S0007-8506(07)63146-1
- Luciano, A. M., Fred, L. A., & Walter, L. W. (2014). Automated system for the measurement of spark current and electric voltage in wire EDM performance. *Journal of Brazilian Society of Science and Engineering*.
- Mahajan, K. R., Knoppers, G. E., Oosterling, J. A. J., & Luttervelt, C. A. (2004). Knowledge based design of EDM electrodes for mould cavities pre-machined by high-speed milling. *Journal of Materials Processing Technology*, 149(1-3), 71–76. doi:10.1016/j.jmatprotec.2004.02.007
- Mahapatra, S. S., & Patnaik, A. (2006). Optimization of wire electrical discharge machining (WEDM) process parameters using Taguchi method. *International Journal of Advance Manufacturing Technology*, 34, 911-925.
- Mahendran, S., Devarajan, R., Nagarajan, T., & Majdi, A. (2010). A Review of Micro-EDM. *Proceeding of international multi conference of engineers and computer scientist*, 2, 981-986.
- Marafona, J., & Wykes, C. (2000). A new method of optimising material removal rate using EDM with copper-tungsten electrodes. *International Journal of Machine Tools & Manufacture*, 40(2), 153–164. doi:10.1016/S0890-6955(99)00062-0
- Masuzawa, T., Cui, X., & Taniguchi, N. (1992). Improved jet flushing for EDM. *CIRP Annals - Manufacturing Technology*, 41(1), 239-242.
- Matin, R., Shabgard, M. R., & Barzegar, R. (2015). Effect of electrode shape configuration on tool steel (DIN1.2379) in Electrical Discharge Machining (EDM). *National Conference on Economics, Management and Accounting*.
- Meena, V. K., & Nagahanumaiah. (2006). Optimization of EDM machining parameters using DMLS electrode. *Rapid Prototyping Journal*, 12(4), 222–228. doi:10.1108/13552540610682732
- Mizugaki, Y. (1996). Contouring electrical discharge machining with on-machine measuring and dressing of a cylindrical graphite electrode. *Proceedings of the IEEE IECON, 22nd International conference on industrial electronics, control, and instrumentation*, 1514-1517. 10.1109/IECON.1996.570608
- Moses, M. D., & Jahan, M. P. (2015). Micro-EDM machinability of difficult-to-cut Ti-6Al-4V against soft brass. *International Journal of Advance Manufacturing Technology*, 81(5), 1345-1361.
- Munz, M., Risto, M., & Haas, R. (2013). Specifics of flushing in electrical discharge drilling. *Procedia CIRP*, 6, 83–88. doi:10.1016/j.procir.2013.03.024
- Pecas, P., & Henriques, E. (2003). Influence of silicon powder-mixed dielectric on conventional electrical discharge machining. *International Journal of Machine Tools & Manufacture*, 43(14), 1465–1471. doi:10.1016/S0890-6955(03)00169-X

Peronczyk, J. (2011). Selected problems of electrical discharge machining (edm) of metal composite materials applied in manufacturing of mechanical vehicles. *Journal of KONES Power Train and Transport*, 18(1), 429-442.

Ponappa, K., Aravindan, S., Rao, P. V., Ramkumar, J., & Gupta, M. (2010). The effect of process parameters on machining of magnesium nano alumina composites through EDM. *International Journal of Advance Manufacturing Technology*, 46, 1035-1042.

Prasad, A. V. S. R., Ramji, K., & Datta, G.L. (2014). An experimental study of wire EDM on Ti-6Al-4V alloy. *Procedia Materials Science*, 5, 2567-2576.

Rajurkar, K. P. (1994). Non-traditional Manufacturing Processes. In *Handbook of Design, Manufacturing and Automation*. Wiley.

Rajurkar, K. P., Sundaram, M. M., & Malshe, A. P. (2013). Review of electrochemical and electro discharge machining. *Procedia CIRP*, 6, 13–26. doi:10.1016/j.procir.2013.03.002

Reza, M. S., Azmir, M. A., Tomadi, S. H., Hassan, M. A., & Daud, R. (2010). Effects of polarity parameter on machining of tool steel workpiece using electrical discharge machining. *National conference in mechanical engineering research and postgraduate students*, 621-626.

Sahu, J., Mohanty, C. P., & Mahapatra, S. S. (2013). A DEA Approach for Optimization of Multiple Responses in Electrical Discharge Machining of AISI D2 Steel. *Procedia Engineering*, 51, 585–591. doi:10.1016/j.proeng.2013.01.083

Singh, H., & Singh, A. (2013). Effect of pulse on/pulse off on machining of steel using cryogenic treated copper electrode. *International Journal of Engineering Research and Development*, 5(12), 29-34.

Singh, P. (2010). Some experimental investigation on aluminum powder mixed EDM on machining performance of hastelloy steel. *International Journal of Advances in Engineering and Technology*, 1(2), 28–45.

Singh, S., & Bhardwaj, A. (2011). Review to EDM by Using Water and Powder-Mixed Dielectric Fluid. *Journal of Minerals & Materials Characterization & Engineering*, 10(2), 199–230. doi:10.4236/jmmce.2011.102014

Skrabalaka, G. (2013). Optimization of dry EDM milling process. *Procedia CIRP*, 6, 332–337. doi:10.1016/j.procir.2013.03.027

Sohani, M. S., Gaitonde, V. N., Siddeswarappa, B., & Deshpande, A. S. (2009). Investigations into the effect of tool shapes with size factor consideration in sink electrical discharge machining (EDM) process. *International Journal of Advance Manufacturing Technology*, 45, 1131-1145.

Stucker, B. E., Bradley, W.L., Eubank, P.T., Norasetthekul, S., & Bozkurt, B. (1997). Zirconium Diboride/Copper EDM electrodes from selective laser sintering. *Proceedings of the solid free form fabrication symposium*, 257-265.

Stucker, B. E., Bradley, W. L., Norasetthekul, S., & Eubank, P. T. (1995). The production of electrical discharge machining electrodes using SLS: Preliminary results. *Proceedings of the solid free form fabrication symposium*, 278-286.



- Tanabe, R., Ito, Y., Mohri, N., & Masuzawa, T. (2011). *Development of peeling tool for micro-EDM* (Vol. 60). CIRP Annals - Manufacturing Technology.
- Tao, J., Shih, A. J., & Ni, J. (2008). Experimental study of the dry and near dry electrical discharge milling processes. *Journal of Manufacturing Science and Engineering*, 130(1), 1–9. doi:10.1115/1.2784276
- Tay, F., & Haider, E. (2001). The potential of plating techniques in the development of rapid EDM tooling. *International Journal of Advance Manufacturing Technology*, 18, 892-896.
- Teicher, U., Müller, S., Münzner, J., & Nestler, A. (2013). Micro-EDM of carbon fibre-reinforced plastics. *Procedia CIRP*, 6, 320–325. doi:10.1016/j.procir.2013.03.092
- Torres, A., Luis, C. J., & Puertas, I. (2015). Analysis of the influence of EDM parameters on surface finish, material removal rate, and electrode wear of an INCONEL 600 alloy. *The International Journal of Advance Manufacturing Technology*, 80(1), 123-140.
- Tsai, H. C., Yan, B. H., & Huang, F. Y. (2003). EDM performance of Cr/Cu-based composite electrodes. *International Journal of Machine Tools & Manufacture*, 43(3), 245–252. doi:10.1016/S0890-6955(02)00238-9
- Tsai, Y. Y., Masuzawa, T., & Fujino, M. (2001). Investigations on electrode wear in micro EDM. *International symposium for electromachining XIII*, 2, 719-726.
- Valentincic, J., Brissaud, D., & Junkar, M. (2007). A novel approach to DFM in toolmaking: A case study. *International Journal of Computer Integrated Manufacturing*, 20(1), 28–38. doi:10.1080/09511920600667333
- Wang, C. C., & Yan, B. H. (2000). Blind-hole drilling of  $\text{Al}_2\text{O}_3/6061\text{Al}$  composite using rotary electro-discharge machining. *Journal of Materials Processing Technology*, 102(1-3), 90–102. doi:10.1016/S0924-0136(99)00423-9
- Wei, C., Zhao, L., Hu, D., & Ni, J. (2013). Electrical discharge machining of ceramic matrix composites with ceramic fiber reinforcements. *International Journal of Advanced Manufacturing Technology*, 64(1), 187–194. doi:10.100700170-012-3995-5
- Wong, Y. S., Rahman, M., Lim, H. S., Han, H., & Ravi, N. (2003). Investigation of micro-EDM material removal characteristics using single RC pulse discharges. *Journal of Materials Processing Technology*, 140(1-3), 303–307. doi:10.1016/S0924-0136(03)00771-4
- Wu, K. L., Yan, B. H., Huang, F. Y., & Chen, S. C. (2005). Improvement of surface finish on SKD steel using electro-discharge machining with aluminum and surfactant added dielectric. *International Journal of Machine Tools & Manufacture*, 45(10), 1195–1201. doi:10.1016/j.ijmachtools.2004.12.005
- Xiaopeng, L., Yonghong, L., & Renjie, J. (2012). A new method for electrical discharge machining of non-conductive engineering ceramics. *Proceedings of 2<sup>nd</sup> International conference on electronic and mechanical engineering and information technology*, 1266-1269.
- Yan, B. H., & Wang, C. C. (1999). The machining characteristics of  $\text{Al}_2\text{O}_3/6061\text{Al}$  composite using rotary electro-discharge machining with a tube electrode. *Journal of Materials Processing Technology*, 95(1-3), 222–231. doi:10.1016/S0924-0136(99)00322-2

- Yang, B., & Leu, M. C. (1999). Integration of rapid prototyping and electroforming for tooling application. *Annals of the CIRP*, 48(1), 119–123. doi:10.1016/S0007-8506(07)63145-X
- Yarlagadda, P. K. D. V., Christodoulou, P., & Subramanian, V. S. (1999). Feasibility studies on the production of electro-discharge machining electrodes with rapid prototyping and the electroforming process. *Journal of Materials Processing Technology*, 89-90, 231–237. doi:10.1016/S0924-0136(99)00072-2
- Younis, A.M., Gouda, M., Mahmoud, F., & Abd Allah, A.S. (2015). Effect of electrode material on electrical discharge machining of tool steel surface. *Ain Shams Engineering Journal*, 6(3), 977-986.
- Yu, P. H., Lin, Y.-X., Lee, H.-K., Mai, C.-C., & Yan, B.-H. (2011). Improvement of wire electrical discharge machining efficiency in machining polycrystalline silicon with auxiliary-pulse voltage supply. *International Journal of Advanced Manufacturing Technology*, 57(9-12), 991–1001. doi:10.1007/00170-011-3350-2
- Yuangang, W., Fuling, Z., & Jin, W. (2009). Wear-resist Electrodes for Micro-EDM. *Chinese Journal of Aeronautics*, 22(3), 339–342. doi:10.1016/S1000-9361(08)60108-9
- Yunxiao, H., Zhidong, L., Zhongli, C., Linglei, K., & Mingbo, Q. (2018). Mechanism study of the combined process of electrical discharge machining ablation and electrochemical machining in aerosol dielectric. *Journal of Materials Processing Technology*, 254, 221–222. doi:10.1016/j.jmatprotec.2017.11.025
- Zhang, G., Guo, Y., & Wang, L. (2016). Experimental study on the machining of inclined holes for thermal barrier-coated nickel super alloys by EDM. *Journal of Materials Engineering and Performance*, 25(10), 4574–4580. doi:10.1007/11665-016-2287-x
- Zhang, L. (2011). A Survey on Electrode Materials for Electrical Discharge Machining, Advances in Materials Manufacturing Science and Technology XIV. *Materials Science Forum*, 495, 697–698.
- Zhang, Q. H., Du, R., Zhang, J. H., & Zhang, Q. (2006). An investigation of ultrasonic-assisted electrical discharge machining in gas. *International Journal of Machine Tools & Manufacture*, 46(12-13), 1582–1588. doi:10.1016/j.ijmachtools.2005.09.023
- Zhang, Y. M., Chen, Y., Li, P., & Male, A. T. (2003). Weld deposition-based rapid prototyping: A preliminary study. *Journal of Materials Processing Technology*, 135(2), 347–357. doi:10.1016/S0924-0136(02)00867-1
- Zhao, J., Li, Y., Zhang, J., Yu, C., & Zhang, Y. (2003). Analysis of the wear characteristics of an EDM electrode made by selective laser sintering. *Journal of Materials Processing Technology*, 138(1-3), 475–478. doi:10.1016/S0924-0136(03)00122-5
- Zhao, J., Yang, M. K. G., & Yuan, X. M. (2010). Performance of bunched-electrode in EDM. *Key Engineering Materials*, 447-448, 282–286. doi:10.4028/www.scientific.net/KEM.447-448.282

# Chapter 3

## Optimization of Process Parameters for Silicon Carbide Powder Mixed EDM

**Sasmeeta Tripathy**

*Siksha 'O' Anusandhan (Deemed University), India*

**Deba Kumar Tripathy**

*IIT Kharagpur, India*

### ABSTRACT

*The present chapter deals with the investigations on the effect of process parameters like powder concentration ( $C_p$ ), peak current ( $I_p$ ), pulse-on-time ( $T_{on}$ ), duty cycle ( $DC$ ), and gap voltage ( $V_g$ ) on output responses like material removal rate ( $MRR$ ), tool wear rate ( $TWR$ ), electrode wear ratio ( $EWR$ ), surface roughness ( $SR$ ), recast layer thickness ( $RLT$ ), and micro-hardness ( $HVN$ ) for PMEDM of H-11 hot work tool steel. Multi-objective optimization using grey relational analysis ( $GRA$ ) has been implemented to identify the optimum set of input parameters to achieve maximum  $MRR$  and  $HVN$  with minimum  $TWR$ ,  $EWR$ ,  $SR$ , and  $RLT$  at the same time. Predicted results on verification with confirmation tests improve the preference values by 0.09468 with  $GRA$ . The recommended settings of process parameters is found to be  $C_p=6g/l$ ,  $I_p=3Amp$ ,  $T_{on}=100\mu s$ ,  $DC=70\%$ , and  $V_g=30V$  from  $GRA$ . The microstructures were examined with scanning electron microscope ( $SEM$ ) to find the presence of surface deformities and identify alterations on the surface in comparison to the base material.*

### INTRODUCTION

The modern manufacturing concept uses energy forms like light, sound, mechanical, chemical, electrons, ions etc. The technological advancement has led to the development of many new materials which have brilliant properties and find huge complexity to be machined using conventional methods. Non-traditional machining has grown up with the idea to machine these exotic materials. Electrical Discharge Machining ( $EDM$ ), one of the widely used non-conventional methods, is broadly employed for making tools, dies and other parts with higher accuracy. It has replaced drilling, milling, grinding and former traditional

DOI: 10.4018/978-1-5225-6161-3.ch003

machining operations (Ho & Newman, 2003). It has been globally established as a benchmark in manufacturing and has become a well established preferred machining method for industries all over the world for machining geometrically complex material components such as composites, super alloys, ceramics, heat treated tool steels, carbides, heat resistant steels etc. It has found application in the recent fields of sports, optics, medical and surgical instruments (Narasimhan et al., 2004). It is a sought after process to meet the growing demands for small sized and complicated components like multi-functional parts used for micro-electronics (Das et al., 2003). PMEDM finds wide application in surgical equipments, dental instruments and medical implants.

The influence of process parameters on SR during machining H-11 steel with copper tool using Al powder mixed dielectric was investigated. The SR improved and reverse polarity of the tool was identified to be desirable for achieving low SR (Singh et al., 2012). Response surface methodology with desirability approach has been implemented for modeling and optimization of process parameters during EDM of CK-45 die steel using  $Al_2O_3$  powder suspension into dielectric. The optimum set of process parameters maximized the MRR (Assarzadeh and Goreishi, 2013). Multi-objective optimization using Taguchi-based GRA on wire EDM was used (Singh et al., 2004). A simple model on Taguchi and Utility approach has been proposed for multi-characteristics optimization of the process parameters to achieve the optimum set during machining of H-11 die steel using Si powder and copper tool (Kansal et al., 2006). An optimum set of input parameters was proposed for rough and finish machining on EN-31, H-11 and HCHCr die steel using aluminium and graphite powders using different combinations of tool and dielectric (Bhattacharya et al., 2012). Multi-objective optimization of PMEDM using Taguchi, GRA and Principal Component Analysis (PCA) was used to control the process parameters (Datta et al., 2008). TOPSIS was used to optimize multiple responses while machining Al-CuTiB<sub>2</sub> to attain the best possible set of process parameters for machining (Senthil et al., 2014). Adding graphite powder to kerosene increased the MRR by 60% and decreased the TWR by 15% (Jeswani, 1981). Researchers have studied the effect of mixing different powders and additives to the dielectric and resulting surface modifications. Effect of adding silicon and aluminium powder to the dielectric has also been evaluated (Kansal et al., 2007, Batish et al., 2012, Wu et al., 2005).

From the available literature it is evident that several researchers have reported results using different powders mixed during EDM, but performance features of H-11 during PMEDM needs investigation. The quality of the machined component is identified by different output features such as MRR, TWR, SR, recast layer thickness, micro-hardness obtained on the machining surface etc. Thus, evaluating the importance of the process parameters relating to the output performance characteristics becomes essential. The problem of PMEDM can be considered as a multi-objective optimization problem. The objective of this study is to obtain a single optimal setting of various input parameters to achieve the best output performance. Multi-attribute decision making techniques like GRA have not yet been used to find the optimal setting during PMEDM of H-11. The present work is a stride in this direction. Taguchi design of experiments is used to conduct the experiments using  $L_{27}$  orthogonal array. An effort has been made to find an optimal set of process variables by using multi-objective optimization using GRA to maximize the MRR and minimize the TWR, EWR, SR, RLT and maximum HVN by adding silicon carbide powder to the dielectric in different concentrations. ANOVA has been used to create a relationship among the significant input parameters on the output responses. A comparative study for the EDM and PMEDM surface characteristics has been done using scanning electron microscope. The optimal parameter setting obtained from GRA can be used for quality improvement in industrial applications involving PMEDM.

## **MATERIALS AND METHODS**

The machines, materials and design of experiment technique used for the estimation of output responses are presented in this section. The procedure used for optimization has also been highlighted in this section.

### **EDM Machine Set-Up**

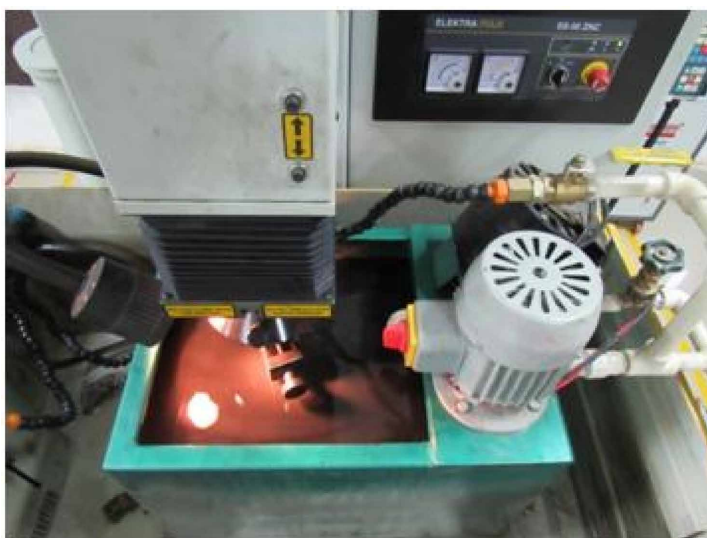
The electric discharge machine, model ELECTRONICA- ELECTRAPULS PS 50ZNC has been used for the experiments. Commercial grade EDM oil has been used as dielectric fluid. The current and voltage waveforms were recorded on a “Digital Storage Oscilloscope”. Figure 1 shows the machine used in the present study.

The machine had a working tank capacity of 300 litres for the circulation of dielectric fluid. The powder particles were required to be added in different concentrations for which changing the entire dielectric fluid and removing the powder particles from the circulating system would have been difficult. The existing circulation system might have choked due to the presence of powders and debris. To minimize the cost, avoid the wastage of dielectric and for effective use of powder particles, a separate machining tank has been designed with a capacity of 20 litres. It consists of a machining tank to perform the operation placed in the working tank of EDM. The machining tank was filled up with the dielectric fluid. A pump was installed to ensure proper distribution of powder in dielectric fluid. To avoid the powder from settling down, a stirring arrangement was installed. Each run was carried out for time duration of 15 minutes. The set up of the tank is shown in Figure 2.

*Figure 1. EDM machine used for the experiment*



Figure 2. PMEDM Set up



## Selection of Materials

The mechanical properties and composition of the work piece and tool material used for the present experiment has been discussed in this section.

## Work Piece Material

H-11 hot work tool steel is the workpiece material. This steel possesses very high strength, abrasion resistance, wear resistance, compressive strength, hardenability, toughness and it is not susceptible to hot cracking. The presence of chromium in the H-11 steel resists oxidization whereas molybdenum prevents corrosion in non-oxidizing environments. The mechanical properties of the H-11 steel are given in Table 1. Applications of H-11 is found in aircraft components, structural use, die casting dies,

Table 1. Mechanical properties of H-11 steel

Properties	H-11
Density	7.81g/cm <sup>3</sup>
Modulus of Elasticity	210 GPa
Poisson's Ratio	0.30
Yield Strength	1650 MPa
Ultimate Tensile Strength	1990 MPa
Specific gravity	7.8
Melting Temperature	1427°C
Thermal Conductivity	42.2 W/mK
Hardness	55 HRC

extrusion tooling, forging dies, piercing tools, hot work punches, tool holders, ejector pins etc. The properties cause a great challenge during machining by conventional methods. The chemical composition of this material as obtained by glow discharge-optical emission spectrometer is given in Table 2. Each surface of the work piece and tool were machined using CNC-milling machine to get smooth mirror-like surfaces. The electrodes were subjected to surface grinding for proper contact and alignment of surfaces during machining. The dimension of the work piece used for this EDM  $120 \times 60 \times 25$  mm operation was  $120 \times 60 \times 25$  mm.

## Tool Material

Electrolytic copper electrode (99.9%) has been used as the tool electrode material. A square tool of dimension  $20 \times 20 \times 60$  mm has been used to perform the machining operation. The mechanical properties of the tool material are given in Table 3. The work material was mounted on the T-slot table and positioned at the desired place and clamped. The electrode was clamped and its alignment was checked.

## Process Parameters

The process parameters chosen for the present research work are powder concentration ( $C_p$ ), peak current ( $I_p$ ), pulse on time ( $T_{on}$ ), duty cycle (DC) and gap voltage ( $V_g$ ) to study their effect on output parameters e.g. material removal rate (MRR), tool wear rate (TWR), electrode wear ratio (EWR), surface roughness (SR), recast layer thickness (RLT) and micro-hardness (HVN) based upon the significant effect on the EDM and PMEDM process and the extensive literature review presented. Methodology to assess the performance characteristics are discussed below:

## Material Removal Rate

High material removal rate is the most sought-after output response for any machining process which leads to increased productivity. After each machining operation, the work piece material was taken out and weighed to find out the weight loss. Weight of the work piece before and after the experiment was measured using an electronic balance with a least count of 0.001 gm. Time duration of each experimental

*Table 2. Chemical composition of H-11 steel*

Constituent	C	Si	Mn	P	S	Cr	Mo	Co	Cu	V	Fe
% Composition	0.39	1	0.5	0.03	0.02	4.75	1.1	0.01	0.01	0.5	Balance

*Table 3. Properties of tool electrode material*

Electrode Material	Density (g/cc)	Specific Heat (J/kg/K)	Thermal Conductivity (W/mK)	Electrode Resistivity ( $\mu$ -ohm)	Hardness BHN
Electrolytic Copper	8.9	386	388	1.69	48

run was recorded using a digital stop watch. From the weight loss obtained, the material removal rate was calculated for different experimental runs. MRR is calculated using the volume loss from the work piece material as cubic millimetre per minute (mm<sup>3</sup>/min). The MRR is expressed as:

$$\text{MRR} \left( \text{mm}^3 / \text{min} \right) = \frac{\text{Wear weight of the work piece}}{\dot{A} \times \text{time}} \quad (1)$$

$$\text{MRR} = (w_i - w_f) / \rho \times T$$

where  $w_i$  and  $w_f$  are initial and final weights of the work piece before and after the machining process,  $\rho$  is density of the work piece material and  $T$  is the machining time in minutes.

### **Tool Wear Rate**

The tool material for machining are selected basing upon the principle that the material should have low resistance to electricity and high melting point. The tool electrode was taken out and weighed after each machining operation to find out the weight loss. Weight of the tool before and after the experiment was measured to determine the tool wear rate. The TWR is expressed as:

$$\text{TWR} \left( \text{mm}^3 / \text{min} \right) = \frac{\text{Wear weight of the tool}}{\dot{A} \times \text{time}} \quad (2)$$

$$\text{TWR} = (t_i - t_f) / \rho \times T$$

where  $t_i$  and  $t_f$  are initial and final weights of the tool before and after the machining process,  $\rho$  is density of the tool and  $T$  is the machining time in minutes.

### **Electrode Wear Ratio**

The electrode wear ratio is dependent on the MRR and TWR. Lower EWR is desirable to enhance the productivity of the process. EWR can be defined as “the ratio of weight of the electrode wear to the weight of the work piece wear after machining” and is expressed as:

$$\text{EWR} (\%) = \frac{\text{Wear weight of the tool}}{\text{Wear weight of the work piece}} \times 100 \quad (3)$$

$$\text{EWR} = w_t / w_w \times 100$$



where  $w_t$  and  $w_w$  are the wear weights of the tool and work piece material measured after the machining operation is carried out in relation to the TWR and MRR.

## **Surface Roughness**

Larger is the vertical deviation, rougher is the surface. The surface roughness is measured basing upon various statistical descriptors out of which centre line average method is mostly used. SR is the arithmetic mean of the deviations from the mean line. The expression for  $R_a$  is given as:

$$R_a = \left( \frac{1}{L} \right) \int_0^L |y(x)| dx \quad (4)$$

Where,  $L$  is the sampling length,  $y$  is the profile curve sampled by the set of  $N$  points and  $x$  is the profile direction. The roughness of the surface was measured using a surface roughness tester (Talysurf, Rank Taylor Hobson, England, Model-Surtronic S-100 series).

## **Recast Layer Thickness**

During the machining process, a small amount of material gets re-solidified after being melted due to the refrigeration effect of the dielectric fluid. This layer is known as the recast layer. Material transfer also takes place from the powder suspended in the dielectric fluid and also from the electrode to the machined surface. Beyond this layer lies the heat affected zone and the base material. In order to find out the structural features present below the machined surface and the distribution of cracks in the recast layer, specimens were cut from the machined surface in a traverse direction and were then mounted for metallographic studies. The recast layer thickness was measured using a scanning electron microscope (FESEM, model: Supra 55, Zeiss, Germany) for all the experiments by taking three set of readings for a particular experiment and considering the average of the three values as the average recast layer thickness.

## **Micro-Hardness**

After the metallographic analysis, the samples were measured for hardness in a micro-hardness tester (LM 247AT of LECO) under a load of 10mgf. The purpose of obtaining the micro-hardness of the material before and after machining was to examine the change in hardness and its effect on the machining surface due to addition of the powder particles during machining. The micro-hardness was measured at three different locations and the average value was considered to be the micro-hardness of the machined specimen.

## **Design of Experiments**

Taguchi's Technique uses a philosophy and methodology to improve the quality of the process and minimizes the cost involved to carry out the process by optimizing the product design using statistical

concepts. Analysis of variance (ANOVA) helps to determine the statistically significant parameters affecting the responses. Predicted results obtained by Taguchi's technique were verified through confirmatory tests for validation and minimization of errors. Taguchi prescribes the use of orthogonal arrays (OA) for experiments. The design of experiments involves the assignment of important and influencing parameters to appropriate columns in the array with the use of linear graphs or triangular tables as suggested by Taguchi. The use of array in the design provides almost identical experimental runs. The most important stage in the DOE lies in the selection of control factors and their levels. The results are further analysed to establish the optimal condition for a product or process, estimation of the contribution of individual parameters affecting the response and to determine the optimum response under the best condition. The best condition may be determined by analysing the behaviour of minimum effects of each of the parameters which provides the trend of each parameter and its influence on the process. The ANOVA table suggests which parameters need to be controlled. Based upon the trial experiments and extensive literature survey, the significant machining parameters taken into consideration are concentration of powder ( $C_p$ ), peak current ( $I_p$ ), pulse on time ( $T_{on}$ ), duty cycle (DC) and gap voltage ( $V_g$ ) and their effect on the output responses has been investigated. Three set of experimental runs have been performed at each condition. The control factors were selected based upon the literature survey and some preliminary investigations.  $L_{27}$  Taguchi's orthogonal array was used for the experiments as shown in Table 4.

## Selection of Orthogonal Array and Parameter Assignment

Selection of orthogonal array depends on the number of controllable parameters, their interactions with each other and the number of levels to be selected. The number of controllable parameters with their levels considered in the present work is shown in Table 4. The minimum DOF required for the experiment are the sum of all the degrees of freedom of the factors. In the present experimental investigation, five three-level factors are considered for study. As per Taguchi's experimental design philosophy, a set of three levels assigned to each parameter has two degrees of freedom. Thus, total DOF of the experiment becomes 10. The OA to be used should have more than 10 DOF. Hence, an  $L_{27}$  OA was chosen which has 27 trials and 26 DOF as shown in Table 5. Twenty seven experiments each were conducted for three different powders mixed to the dielectric fluid using Taguchi's experimental design methodology, repeating each experiment three times. The designs, plots and analysis have been carried out with MINITAB 15 software.

Table 4. Selection of levels for the factors

Factors with Symbol and Units	Levels		
	Level 1	Level 2	Level 3
Concentration of silicon carbide powder ' $C_p$ ' (g/l)	0	3	6
Peak Current ' $I_p$ ' (Amp)	3	6	9
Pulse On Time ' $T_{on}$ ' ( $\mu$ s)	100	150	200
Duty Cycle 'DC' (%)	7	8	9
Gap Voltage ' $V_g$ ' (V)	30	40	50

Table 5. Taguchi's  $L_{27}$  standard Orthogonal Array

Column No.	1	2	3	4	5
Run	$C_p$	$I_p$	$T_{on}$	DC	$V_g$
1	1	1	1	1	1
2	1	1	1	1	2
3	1	1	1	1	3
4	1	2	2	2	1
5	1	2	2	2	2
6	1	2	2	2	3
7	1	3	3	3	1
8	1	3	3	3	2
9	1	3	3	3	3
10	2	1	2	3	1
11	2	1	2	3	2
12	2	1	2	3	3
13	2	2	3	1	1
14	2	2	3	1	2
15	2	2	3	1	3
16	2	3	1	2	1
17	2	3	1	2	2
18	2	3	1	2	3
19	3	1	3	2	1
20	3	1	3	2	2
21	3	1	3	2	3
22	3	2	1	3	1
23	3	2	1	3	2
24	3	2	1	3	3
25	3	3	2	1	1
26	3	3	2	1	2
27	3	3	2	1	3

## Analysis of Variance

Analysis of variance (ANOVA) was performed to determine the significant effect of process parameters on performance characteristics. The main effect plots for factors show the trend of the influence of factors towards the process. The importance of process variables with respect to output responses helps determine the optimum set of parameters using ANOVA from Minitab15 software. Various steps involved in the analysis are:

**Step 1:** Total of all results (T)

$$T = \sum_{i=1}^n \sum_{j=1}^R y_{ij} \quad (5)$$

where,  $y_{ij}$  is the value of the characteristic in the  $i^{\text{th}}$  trial and  $j^{\text{th}}$  repetition.

**Step 2:** Correction Factor (C.F)

$$C.F. = T^2/N, \text{ where } N \text{ is the total number of experiments i.e. } 3 \times 27=81. \quad (6)$$

**Step 3:** Total sum of squares ( $SS_T$ ):

$$SS_T = \sum_{i=1}^n \sum_{j=1}^R y_{ij}^2 - C.F \quad (7)$$

**Step 4:** Sum of squares of parameter A ( $SS_A$ )

$$SS_A = \left[ \frac{A(1)^2}{N_{A1}} + \frac{A(2)^2}{N_{A2}} + \frac{A(3)^2}{N_{A3}} \right] - C.F \quad (8)$$

Where,  $N_{A1}$ ,  $N_{A2}$  and  $N_{A3}$  are the number of experiments with parameter A at levels 1, 2 and 3, respectively. The sums of squares for all the factors are calculated similarly.

**Step 5:** Error sum of squares

$$SS_e = SS_T - (\text{Summation of sum of squares of all the parameters}) \quad (9)$$

where, e stands for the error.

**Step 6:** Degrees of freedom

$$\text{Total DOF} = (\text{total number of trials}-1) = (R \times n - 1) = 80 \quad (10)$$

$$\text{DOF of each parameters} = (\text{Number of levels of each parameter} - 1) = 2$$

The DOF for all parameters are calculated in the similar way.

**Step 7:** Mean square of variance (V)

$$V_A = \text{Variance due to parameter A} = \frac{SS_A}{f_A} \quad (11)$$

Variance for the other parameters is obtained in the similar manner.

**Step 8:** Percentage contribution (P)

$P_A$  = Percentage contribution of parameter A towards mean of the response

$$P_A = \left( \frac{SS_A}{SS_T} \right) \times 100 \quad (12)$$

Similarly, the percentage contribution of all other parameters is calculated.

**Step 9:** F-ratios

The F-ratio is defined as the ratio of variance due to a parameter and due to its error.

$$F_A = \frac{V_A}{V_e} \quad (13)$$

The F-ratio is calculated for all the parameters in the similar manner.

## **Multi-Objective Optimization**

Taguchi's experimental philosophy is focused on optimizing the process parameters in the perspective of a single quality criterion which does not give sufficient idea about the influence on other performance characteristics involved. The performance of the product is evaluated by various response parameters. Taguchi technique cannot solve a multi-response optimization problem. Hence, multi-objective optimization techniques are implemented where in the quality characteristics are optimized and the results for the best levels are obtained. Taguchi technique is often combined with multi-objective optimization techniques to switch a multi-decision making technique to a single objective optimization problem. The decision maker assigns different priority weights to the responses basing upon their relative importance.

## **Grey Relational Analysis (GRA)**

Grey Relational Technique was developed to resolve problems using complex inter-relationships amongst the multiple performance characteristics. Grey Relational Technique provides an approach to create an idea about the system which is indecisive, incomplete and not apparent (Tripathy & Tripathy, 2016).

Grey relational analysis uses normalized values of the results obtained from the experimental investigation. In grey relational analysis, the experimental values of the measured quality characteristics are normalized in a range from zero to one. This is known as grey relational generation. This is followed by the calculation of grey relational coefficient (GRC). The overall performance characteristic depends on the computation of the grey relational grade (GRG). Thus, a multiple response process optimization is transformed into a single objective problem. The highest grey relational grade will be evaluated as the optimal parametric combination. For grey relational generation, the MRR and HVN corresponding to “higher the better” criterion can be expressed as shown in equation 14 and 15:

$$x_i(k) = \frac{y_i(k) - \min \min y_i(k)}{\max y_i(k) - \min \min y_i(k)} \quad (14)$$

TWR, EWR, SR and RLT corresponding to “lower the better” criterion can be expressed as:

$$x_i(k) = \frac{\max \max y_i - y_i(k)}{\max y_i(k) - \min \min y_i(k)} \quad (15)$$

where  $x_i(k)$  is the value obtained for grey relational generation,  $\min y_i(k)$  is the smallest value of  $y_i(k)$  for the  $k^{\text{th}}$  response and  $\max y_i(k)$  is the largest value for the  $k^{\text{th}}$  response where  $k= 1,2,3,4$  for the various output responses considered in a sequence. The normalized data after the grey relational generation are then tabulated. The grey relational coefficient is computed to establish a relationship between the best data and the actual normalized data. The GRC is calculated as shown in equation 16:

$$\xi_i(k) = \frac{\Delta_{\min} + \psi \Delta_{\max}}{\Delta_{0i}(k) + \psi \Delta_{\max}} \quad (16)$$

where  $\Delta_{0i}(k) = |x_0(k) - x_i(k)|$ ,  $\psi$  is the distinguishing coefficient lying between  $0 \leq \psi \leq 1$ ,  $\Delta_{\min}$  is the minimum value of  $\Delta_{0i}$  and  $\Delta_{\max}$  is the maximum value of  $\Delta_{0i}$ . The values for  $\Delta_{0i}$  are then tabulated which is followed by the calculation table for grey relational coefficient. The Grey Relational Grade is then calculated and presented using equation 17:

$$\gamma_i = \frac{1}{n} \sum_{k=1}^n \xi_i(k) \quad (17)$$

where  $n$  is the number of output responses. The higher the value of GRG, the corresponding combination of parameters is closer to the optimal.

## **Confirmatory Experiment for Grey Relational Analysis**

After the estimation of optimal parameter setting, prediction and confirmation for the improvement of quality characteristic using the optimal setting is carried out. The estimated grey relational grade  $\hat{\gamma}$  using the optimal level of the design parameters is calculated as shown in equation (18):

$$\hat{\gamma} = \gamma_m + \sum_{i=1}^p (\gamma_i - \gamma_m) \quad (18)$$

where  $\gamma_m$  is the total mean GRG,  $\gamma_i$  is the mean GRG at the optimal level and  $p$  is the number of key design parameters affecting the performance characteristics. Thus, the predicted GRG is equivalent to the mean GRG and the summation of the difference between the mean GRG of each factor at optimum level and the total mean GRG. The confirmatory experiments were carried out at the optimal level predicted from the result. An assessment between the input parameters with the estimated parameters under optimal conditions has been presented which indicates good agreement. The experiments are satisfactory if the confirmation result falls within the range of predicted measures.

## **ANOVA for Grey Relational Analysis**

The results of factor responses have been calculated by using ‘higher-the-better’ expectation using MINITAB software and have been presented for each type of powder. The significance of the process parameters affecting the process can be observed from ANOVA tables for means. From the response tables, the average of each response characteristic from raw data for each level of input parameters may be determined. The table demonstrates the ranks based upon the delta statistics which compare the relative magnitude of effects. For each factor, the delta statistics may be obtained as the difference between the highest and the lowest value of average of each response. Ranks are assigned based upon the higher to lower delta values. The ranks thus indicate the relative importance of each input parameter to the response. The higher grey relational grades are considered as optimum.

## **RESULTS AND DISCUSSIONS**

Experimental results obtained by varying the chosen set of input parameters for the selected output responses have been presented in this section. The discussion of the obtained results and the variations in their behaviour has also been detailed in the present section.

### **Experimental Results**

Experiments were conducted using Taguchi’s  $L_{27}$  orthogonal array. The results are represented in Table 6.

Table 6.  $L_{27}$  experimental design with response variables

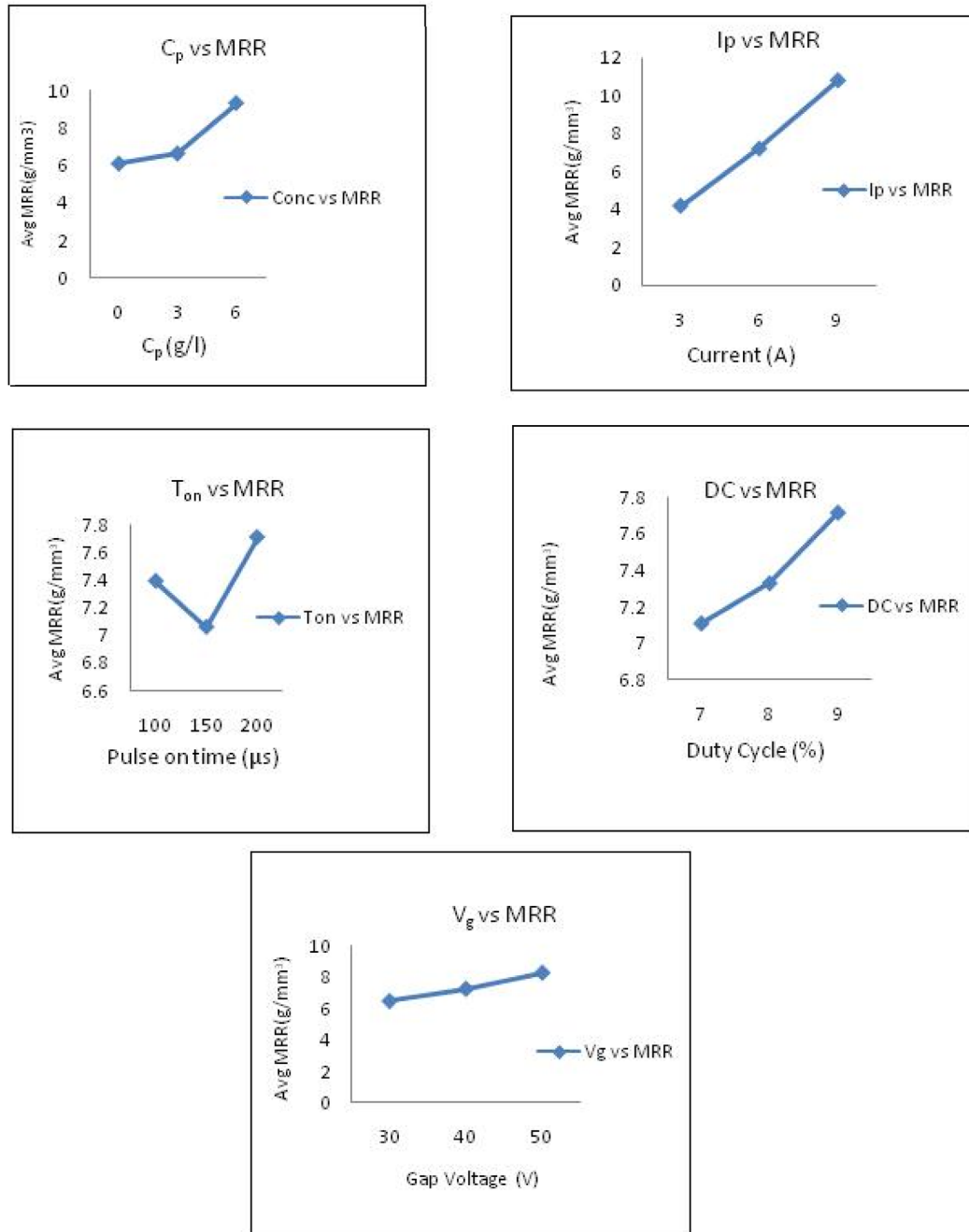
Run	$C_p$	$I_p$	$T_{on}$	DC	Vg	Avg MRR	Avg TWR	Avg EWR	Avg SR	Avg RLT	Avg HVN
1	0	3	100	7	30	2.564	0.0172	0.6718	3.8	13.8	784
2	0	3	100	7	40	2.649	0.0194	0.735	4.1	14.4	778
3	0	3	100	7	50	2.735	0.0224	0.8216	4.5	15.2	786
4	0	6	150	8	30	4.529	0.0277	0.6118	4.87	18.76	795
5	0	6	150	8	40	5.470	0.0307	0.5614	5.45	19.24	804
6	0	6	150	8	50	6.666	0.0367	0.5505	5.86	19.76	798
7	0	9	200	9	30	9.401	0.3895	4.1430	6.5	20.58	809
8	0	9	200	9	40	10.256	0.4868	4.7471	7.47	21.6	802
9	0	9	200	9	50	10.940	0.5243	4.7928	9.2	22.24	811
10	3	3	150	9	30	2.87	0.0123	0.429	2.48	22.6	833
11	3	3	150	9	40	3.54	0.0134	0.380	2.97	25.67	862
12	3	3	150	9	50	3.97	0.0152	0.383	3.42	25.31	841
13	3	6	200	7	30	4.42	0.0171	0.387	4.16	28.86	884
14	3	6	200	7	40	6.638	0.0186	0.2813	4.37	26.74	898
15	3	6	200	7	50	8.54	0.0192	0.224	4.82	29.2	876
16	3	9	100	8	30	9.26	0.0235	0.254	5.74	31.19	905
17	3	9	100	8	40	9.82	0.0261	0.266	6.41	34.42	929
18	3	9	100	8	50	11.04	0.0291	0.2639	6.72	37.64	976
19	6	3	200	8	30	5.56	0.0349	0.628	1.64	24.36	845
20	6	3	200	8	40	6.41	0.0378	0.5897	1.92	26.63	878
21	6	3	200	8	50	7.23	0.0398	0.5506	2.23	27.59	859
22	6	6	100	9	30	8.37	0.0448	0.5363	2.62	29.21	893
23	6	6	100	9	40	8.858	0.0463	0.523	2.94	32.49	904
24	6	6	100	9	50	11.23	0.0496	0.441	3.36	35.93	916
25	6	9	150	7	30	11.86	0.0586	0.494	3.82	36.2	941
26	6	9	150	7	40	12.07	0.0753	0.624	4.48	37.56	966
27	6	9	150	7	50	12.54	0.0880	0.7018	5.24	38.92	952

## Material Removal Rate

The machining efficiency of the process can be characterised by the material removal rate. The main aim behind machining should be more amount of material removal with less tool wear and improved surface properties. When no powder is added to the dielectric, it has been observed that the MRR increases with increase in current and pulse on time. From the experimental results it has been found that, when no powder is added to the dielectric and the current and pulse on time increase, MRR increases. This is because with the increase in electrical power, additional thermal energy is generated in the discharge channel. Addition of powder particles to the dielectric fluid causes decrease in insulating strength of the dielectric



Figure 3. Variation of MRR with input parameters



fluid and the inter-electrode gap increases causing an easy removal of debris. The accumulation of large amount of powder particles at higher concentrations may cause machining instabilities which increases the ratio of arc and short circuit pulses thus decreasing the MRR. The experimental observations of MRR show that when 3g/l of SiC powder is added, the MRR increases with the increase in current. With an

increase in the concentration of powder to 6g/l, the MRR further increases. It is observed that with the increase in concentration of SiC powder increases the MRR improving the surface quality for H-11 die steel. The MRR tends to increase with the increase in current for any value of other factors. Maximum MRR is obtained at high current. MRR is also influenced by powder concentration and pulse on time.

## **Tool Wear Rate**

The concept of machining should involve more amount of material removal accompanied by less tool wear. The tool material for machining is selected based on the principle that the material should have low resistance to electricity and high melting point. Due to the increased thermal energy, the TWR also increases. Due to the bridging effect, faster sparking occurs resulting in faster erosion from the workpiece and tool surface. This easy short circuit improves the machining rate of the process. Adding 3g/l of SiC powder decreases the TWR in comparison to the machining without addition of powder. Further increase in  $C_p$  to 6g/l, decreases the TWR and improves the surface properties. This is because the widening of the plasma channel produces stable and uniform sparks. Thus shallow craters are formed on the workpiece surface with improved surface quality.

## **Electrode Wear Ratio**

The tendency of a perfect tool should be the capability of removing maximum material from the workpiece and it should also have the ability to resist self erosion. The EWR increases with the increase in  $I_p$  and  $T_{on}$  during the machining using no powder condition. With the addition of powder, the EWR decreases which is the result of less tool wear with more material removal from the workpiece.

## **Surface Roughness**

The texture of the surface created by electro-discharge machining is directly associated with the magnitude of the crater formed and the distribution of recast layer on the surface. The experimental investigation shows that the roughness of the surface varies within a range of 3.8 $\mu$ m to 9.2 $\mu$ m when no powder is added to the dielectric fluid. It can also be observed that with the rise in pulse current, the roughness of the surface also increases as the large dispersive energy cause violent sparks and impulsive forces which consequently form larger craters causing increase in SR. While flushing, the cooling takes place and a quantity of molten material is not entirely flushed away and re-solidifies on the surface increasing the SR. On the addition of SiC powder to the dielectric fluid, the surface quality improves as the SR diminishes. When 3g/l of SiC powder is added, the roughness values are reduced to a range of 2.48 $\mu$ m to 6.72 $\mu$ m. On increasing the concentration of powder to 6g/l, the roughness additionally gets reduced to a range of 1.64 $\mu$ m to 5.24 $\mu$ m. It is seen that when  $T_{on}$  is increasing, there is a decrease in pulse intensity and increase in plasma channel which creates smoother surfaces as compared to low  $T_{on}$  and higher pulse current combinations. The SR was considered as the arithmetic mean of roughness obtained for the examined surface using a contact type surface roughness tester. It can be explained that the roughness of the machined surface during EDM is caused due to the evaporation, melting and re-solidification of the molten material and the prevailing temperature conditions which affects the material beneath the recast layer and the heat affected zone. The variation found in the layer beneath the heat affected zone

is caused due to the properties of the recast layer, crack propagation to the underlying layers and surface modification. This disparity occurs due to the melting phenomenon and the concentration of the powder particles. It can be seen that adding foreign particles in proper size and quantities reduce the SR during machining. Addition of more amount of powder will cause difficulty in stirring and will settle down in the tank and do not contribute in improvement of the surface properties.

## **Recast Layer Thickness**

After performing the machining process and conducting the confirmatory tests, samples were prepared for detailed microscopic examination and necessary investigations were carried out. The erosion of the work piece material depends on the effects of heat concentration. Instant rise in temperature during machining causes material removal along with the change in surface properties of the surrounding material due to the formation of discharge pits with concave and convex edges. The material on the surface gets re-solidified after being melted due to the refrigeration effect of the dielectric fluid. This re-solidification and re-deposition of the molten material leads to the formation of recast layer which is also known as white layer and is brittle in nature. The recast layer is the effect of material migration from the tool, the breakdown of hydro-carbon from the dielectric and the powder suspended in the dielectric fluid. The properties of these layers are not desirable for engineering applications as they decrease the fatigue strength of the material under repeated cycle of loading. Reduction of extent of recast layer formation and improvement of surface properties form an important aspect in the field of research concerning to EDM. Beyond the recast layer lies the heat affected zone (HAZ) and the base material. The micro-structural characteristics and the metallurgical behaviour of the recast layer are very different from the base material. The quality of the machined surface is usually interpreted in terms of size of craters, cracks, shape and size of the recast deposits and surface roughness of the machined specimen. When the machining operation was carried out in the presence of silicon carbide powder mixed to the dielectric fluid, it has been observed that the surface properties show improvement as the surface roughness reduces in comparison to machining performed in the absence of powder particles. The cracks formed are smaller in size compared to that obtained while machining without powder particles. Carbon and copper rich regions are seen and much exposed recast layer are observed. The surface topography shows improvement over that produced without addition of powder. Since the material removal depends on the heat concentration, some removal takes place instantly on attaining the desired temperature and the surrounding material known as the altered material zone shows some metallographic changes occurred as an effect to the machining process. With the change in the process parameters, the white layer thickness also varied. Beneath this layer is the heat affected zone and unaffected zone. When the powder particles were added in a concentration of 3g/l, the material removal rate varied in a range of 2.87 to 11.04mm<sup>3</sup>/min whereas the tool wear rate varied from 0.012 to 0.029mm<sup>3</sup>/min. On addition of 6g/l of powder the material removal rate increased from 5.56 to 12.54mm<sup>3</sup>/min for a corresponding tool wear rate of 0.03 to 0.08 mm<sup>3</sup>/min. This shows that both the material removal rate and tool wear rate increase and with the change in concentration of powder more amount of material is removed from both tool and work piece surfaces. More amount of material removed creates more uneven surfaces as observed from the surface micrographs which result in the formation of thicker recast layers. Also the values of  $I_p$  regulate the SR and the thickness of recast layer.

## Micro-Hardness

After the SEM analysis, the surfaces were put to micro-hardness testing for the examination of the change in hardness at the micron level and its effect on the machining surface to investigate the change in hardness on the recast layer. The micro-hardness was measured at three different locations and the average value was considered to be the micro-hardness of the machined specimen. The micro-hardness of the base material was also measured before the machining was carried out to identify the change in micro-hardness as an effect to the machining operation. The micro-hardness of the base material was found to be 621 HVN. SiC powders being abrasive in nature, remove more amount of material and the debris remain on the machined surface causing re-solidification resulting in the formation of thicker recast layers. This is because increase in peak current increases the pulse energy which causes rapid melting and evaporation and when flushing conditions are poor, the re-solidification occurs during the pulse-off-time. At low pulse-on-time, short pulses cause less vaporization of the work material, whereas the plasma channel gets expanded during longer pulse-on-time causing less energy density on the work piece which is insufficient to vaporize the material resulting in increased RLT.

## Grey Relational Analysis

Grey relational analysis has been implemented to the experimental results obtained by addition of silicon carbide powder to the dielectric fluid in different concentrations. The normalized values are obtained for grey relational generation and have been presented in Table 7.

The values for  $\Delta_{0i}$  are then tabulated in Table 8. which is followed by the calculation table for grey relational coefficient as shown in Table 9.

The overall performance characteristic depends on the computation of the grey relational grade (GRG). From the values obtained for grey relational coefficient as shown in Table 9, the grey relational grade is computed and presented in Table 10.

It can be observed that experimental run #18 exhibits the best multiple performance characteristics having the highest GRG, hence it is the optimal setting followed by #26 and #25. It is possible to separate the effect of each parameter at different levels in case of orthogonal experimental design. The mean GRG for each level of input parameter can be determined by estimating the averages of GRG for the particular level setting from the obtained experimental results. For all the levels, the mean GRG can be computed in the similar manner as shown in Table 11. Total mean GRG is the average of all the GRG obtained in Table 10. The total mean GRG is calculated to be 0.6541.

## Confirmatory Experiment for Grey Relational Analysis

After the estimation of optimal parameter setting, prediction and confirmation for the improvement of quality characteristic using the optimal setting is carried out. The estimated grey relational grade  $\hat{\gamma}$  using the optimal level of the design parameters is calculated as shown in equation (19):

$$\hat{\gamma} = \gamma_m + \sum_{i=1}^p (\gamma - \gamma_m) \quad (19)$$

*Table 7. Grey Relational Generation for each performance characteristic*

Run	MRR	TWR	EWR	SR	RLT	HVN
Ideal Sequence	1	1	1	1	1	1
1	0	0.9904	0.90199	0.7142	1	0.0303
2	0.0085	0.98613	0.88815	0.6746	0.9761	0
3	0.01714	0.98028	0.869	0.6216	0.9442	0.0404
4	0.19697	0.96992	0.9151	0.5727	0.8025	0.0858
5	0.2913	0.96406	0.92615	0.496	0.7834	0.1313
6	0.41119	0.95234	0.9285	0.4417	0.7627	0.101
7	0.68535	0.26328	0.1422	0.3571	0.73	0.1565
8	0.77105	0.07324	0.0100	0.2288	0.689	0.1212
9	0.83962	0	0	0	0.664	0.1666
10	0.03067	1	0.955	0.8888	0.6496	0.2777
11	0.09784	0.99785	0.9659	0.824	0.5274	0.4242
12	0.14094	0.99434	0.96519	0.7645	0.5417	0.3181
13	0.18605	0.99063	0.96432	0.6666	0.4004	0.5353
14	0.4084	0.9877	0.98745	0.6388	0.4848	0.606
15	0.59904	0.9865	1	0.5793	0.3869	0.4949
16	0.67121	0.97813	0.99343	0.4576	0.3077	0.6414
17	0.72735	0.97305	0.9908	0.369	0.1791	0.7626
18	0.84964	0.96719	0.9912	0.328	0.0509	1
19	0.30032	0.95586	0.9115	1	0.5796	0.3383
20	0.38553	0.9502	0.9199	0.9629	0.4892	0.505
21	0.46772	0.9463	0.9285	0.9219	0.451	0.4090
22	0.58198	0.9365	0.9316	0.87037	0.3865	0.5808
23	0.63091	0.93359	0.9345	0.828	0.2559	0.6363
24	0.86869	0.92715	0.9525	0.7724	0.119	0.6969
25	0.93184	0.9096	0.9409	0.711	0.108	0.8232
26	0.95289	0.877	0.91245	0.6243	0.054	0.9494
27	1	0.85215	0.8954	0.523	0	0.8787

The confirmatory experiments were carried out at the optimal level predicted from the result. Table 12 presents an assessment between the input parameters with the estimated parameters under optimal conditions which indicate good agreement.

From the Table 12, it can be observed that the MRR is increased from 2.564 to 6.5mm<sup>3</sup>/min and the TWR correspondingly increases from a value of 0.0172 to 0.028mm<sup>3</sup>/min. The EWR decreases from 0.6718 to 0.4307% and SR gets reduced from 3.8 to 1.4µm respectively. The RLT increases from a value of 13.8 to 17.5µm. The micro-hardness increased from 784 to 895. Also the results from the confirmation test show good agreement with the predicted values. An improvement of 0.09468 is noted in GRG after validation.

*Table 8. Estimation of  $\Delta_{oi}$  for each performance characteristic*

Run	MRR	TWR	EWR	SR	RLT	HVN
Ideal Sequence	1	1	1	1	1	1
1	1	0.0095	0.098	0.2857	0	0.9696
2	0.991	0.0138	0.1118	0.3253	0.0238	1
3	0.9828	0.0197	0.1308	0.3783	0.0557	0.9595
4	0.803	0.03	0.0848	0.4272	0.1974	0.9141
5	0.7087	0.0359	0.0738	0.5039	0.2165	0.8686
6	0.5888	0.0476	0.0714	0.5582	0.2372	0.898
7	0.3146	0.7367	0.8577	0.6428	0.2699	0.8434
8	0.2289	0.9267	0.9899	0.7711	0.31051	0.8787
9	0.1603	1	1	1	0.3359	0.8333
10	0.9693	0	0.0448	0.1111	0.3503	0.7222
11	0.9021	0.0021	0.0341	0.1759	0.4725	0.5757
12	0.8590	0.0056	0.0348	0.2354	0.4582	0.6818
13	0.8139	0.0093	0.0356	0.3333	0.5995	0.4646
14	0.591	0.0123	0.0125	0.3611	0.5151	0.3939
15	0.4009	0.0134	0	0.4206	0.613	0.505
16	0.3287	0.0218	0.0065	0.5423	0.6922	0.3585
17	0.2726	0.0269	0.0091	0.6309	0.82	0.2373
18	0.1503	0.0328	0.0087	0.6719	0.949	0
19	0.6996	0.0441	0.0884	0	0.4203	0.6616
20	0.6144	0.0498	0.08	0.037	0.5107	0.4949
21	0.5322	0.0537	0.0714	0.078	0.5489	0.5909
22	0.418	0.0634	0.0683	0.129	0.6134	0.4191
23	0.369	0.0664	0.0654	0.1719	0.744	0.3636
24	0.1313	0.0728	0.0474	0.2275	0.88	0.30303
25	0.0681	0.09	0.059	0.288	0.891	0.1767
26	0.0471	0.123	0.0875	0.3756	0.945	0.0505
27	0	0.1478	0.1045	0.476	1	0.1212

## ANOVA for Grey Relational Analysis

ANOVA is a statistical decision making tool used for detecting any differences in the average performance of the group of items tested. The significant effect of process variables on the performance characteristics can be determined by using ANOVA. The results of factor responses are calculated by using 'higher-the-better' expectation using MINITAB software. ANOVA result presented in Table 13 indicates that  $C_p$ ,  $I_p$ ,  $T_{on}$  and DC are parameters which have significant contribution towards improvement in GRG while the role of  $V_g$  is insignificant.

# Optimization of Process Parameters for Silicon Carbide Powder Mixed EDM

Table 9. Estimation of Grey Relational Coefficient for each performance characteristic with ( $\psi=0.5$ )

Run	MRR	TWR	EWR	SR	RLT	HVN
Ideal Sequence	1	1	1	1	1	1
1	0.3333	0.9812	0.8361	0.6363	1	0.3402
2	0.3352	0.973	0.8172	0.6057	0.9544	0.3333
3	0.3371	0.962	0.7926	0.5692	0.8997	0.3425
4	0.3837	0.9432	0.8548	0.5392	0.7168	0.3535
5	0.4136	0.9329	0.8713	0.498	0.6977	0.3653
6	0.4592	0.9129	0.8749	0.472	0.6781	0.3574
7	0.6137	0.4042	0.3682	0.4375	0.6494	0.372
8	0.6859	0.3504	0.3355	0.3933	0.6168	0.3626
9	0.7571	0.3333	0.3333	0.3333	0.598	0.375
10	0.3402	1	0.9176	0.8181	0.588	0.409
11	0.3565	0.9957	0.936	0.7397	0.5141	0.4647
12	0.3679	0.9887	0.9349	0.6798	0.5218	0.423
13	0.3805	0.9815	0.9333	0.6	0.4547	0.5183
14	0.458	0.9759	0.9755	0.5806	0.4925	0.5593
15	0.5549	0.9737	1	0.5431	0.4492	0.4974
16	0.603	0.958	0.987	0.4796	0.4193	0.5823
17	0.647	0.9488	0.9819	0.4421	0.3785	0.67808
18	0.7688	0.9384	0.9828	0.4266	0.345	1
19	0.4167	0.918	0.8497	1	0.543	0.4304
20	0.4486	0.9094	0.862	0.931	0.494	0.5025
21	0.4843	0.9029	0.8749	0.8649	0.476	0.4583
22	0.5446	0.8873	0.8797	0.7941	0.449	0.5439
23	0.5753	0.8827	0.8842	0.744	0.4019	0.5789
24	0.7919	0.8728	0.9132	0.6872	0.362	0.6226
25	0.88	0.8468	0.8943	0.6342	0.3592	0.7388
26	0.9138	0.8025	0.8509	0.5709	0.3458	0.9082
27	1	0.7717	0.827	0.5121	0.3333	0.8048

The graphical representation of the main effect plot for s/n ratio to identify the influence of machining parameters at various levels on the grey relational grade is represented in Figure 4. The significance of the process parameters affecting the process can be observed from ANOVA tables for means represented in Table 5.8. From the response table shown in Table 14, the average of each response characteristic from raw data for each level of input parameters may be determined. The higher grey relational grades are considered as optimum, therefore, considering the grades as “higher-the-better” type of quality characteristic, the tendency of deviation of the response curves reveal that “the third level of parameters of  $C_p$ , first level of  $I_p$ , first level of  $T_{on}$ , first level of DC and first level of  $V_g$ ” offer maximum grades and are considered to be the optimum set of process parameters.

# Optimization of Process Parameters for Silicon Carbide Powder Mixed EDM

Table 10. Estimation of Grey Relational Grade with rank order

Experiment No.	Grey Relational Grade	Order
1	0.6878	8
2	0.6698	16
3	0.6505	20
4	0.6319	22
5	0.6298	23
6	0.6258	24
7	0.4742	25
8	0.4574	26
9	0.455	27
10	0.6788	11
11	0.6678	18
12	0.6527	19
13	0.6447	21
14	0.6736	14
15	0.6697	17
16	0.6716	15
17	0.6794	10
18	0.7436	1
19	0.6931	6
20	0.6913	7
21	0.677	13
22	0.6831	9
23	0.6778	12
24	0.7083	4
25	0.7255	3
26	0.732	2
27	0.7082	5

Table 11. Estimation of mean Grey Relational Grade

Factors	Grey Relational Grade			
	Level 1	Level 2	Level 3	Delta
C <sub>p</sub>	0.5869	0.6758	0.6996	0.1127
I <sub>p</sub>	0.6743	0.6605	0.6274	0.0469
T <sub>on</sub>	0.6858	0.6725	0.6040	0.0854
DC	0.6847	0.6715	0.6061	0.0786
V <sub>g</sub>	0.65458	0.6532	0.65457	0.0013
Total Mean Grey Relational Grade = 0.6541				



## Optimization of Process Parameters for Silicon Carbide Powder Mixed EDM

Table 12. Results of confirmatory experiment

Initial factor Setting		Optimal Condition	
		Predicted	Experimental
Level	$C_{p1} I_{p1} T_{on1} DC_1 V_{g1}$	$C_{p3} I_{p1} T_{on1} DC_1 V_{g1}$	$C_{p3} I_{p1} T_{on1} DC_1 V_{g1}$
Concentration of SiC powder (g/l)	0		6
Peak Current (Amp)	3		3
Pulse On Time ( $\mu$ s)	100		100
Duty Cycle (%)	7		7
Gap Voltage (Volts)	30		30
MRR ( $\text{mm}^3/\text{min}$ )	2.564		6.5
TWR( $\text{mm}^3/\text{min}$ )	0.0172		0.028
EWR (%)	0.6718		0.4307
SR ( $\mu$ m)	3.8		1.4
RLT( $\mu$ m)	13.8		17.5
HVN	784		895
GRG	0.69680	0.78258	0.79148
Improvement in GRG=0.09468			

Table 13. ANOVA Table for Means of GRG

Source	DF	Seq SS	Adj SS	Adj MS	F	P	P (%)
$C_p$	2	0.06348	0.06348	0.03174	86.5	0.000	43.38
$I_p$	2	0.01045	0.01045	0.00522	14.24	0.000	7.14
$T_{on}$	2	0.03465	0.03465	0.01732	47.21	0.000	23.68
DC	2	0.03184	0.03184	0.01592	43.39	0.000	21.76
$V_g$	2	0.00001	0.00001	0.000005	0.01	0.986	0.006
Residual Error	16	0.00587	0.00587	0.00036			
Total	26	0.146314					
S= 0.01916	R-Sq= 96%	R-Sq(adj)= 93.5%					

From the optimal setting it can be assumed that as the abrasive powder concentration increases, the bridging effect causes more amount of material removal resulting in better MRR. Thus the optimal powder concentration is 6g/l for silicon carbide powder mixed dielectric.

## Microstructure Analysis

The surface texture depends on the distribution of recast layer. The mechanism of melting and mixing of powder in proper concentrations vary the surface properties of the material resulting in its modification.

Figure 4. Main effect plot for S/N ratio of GRG

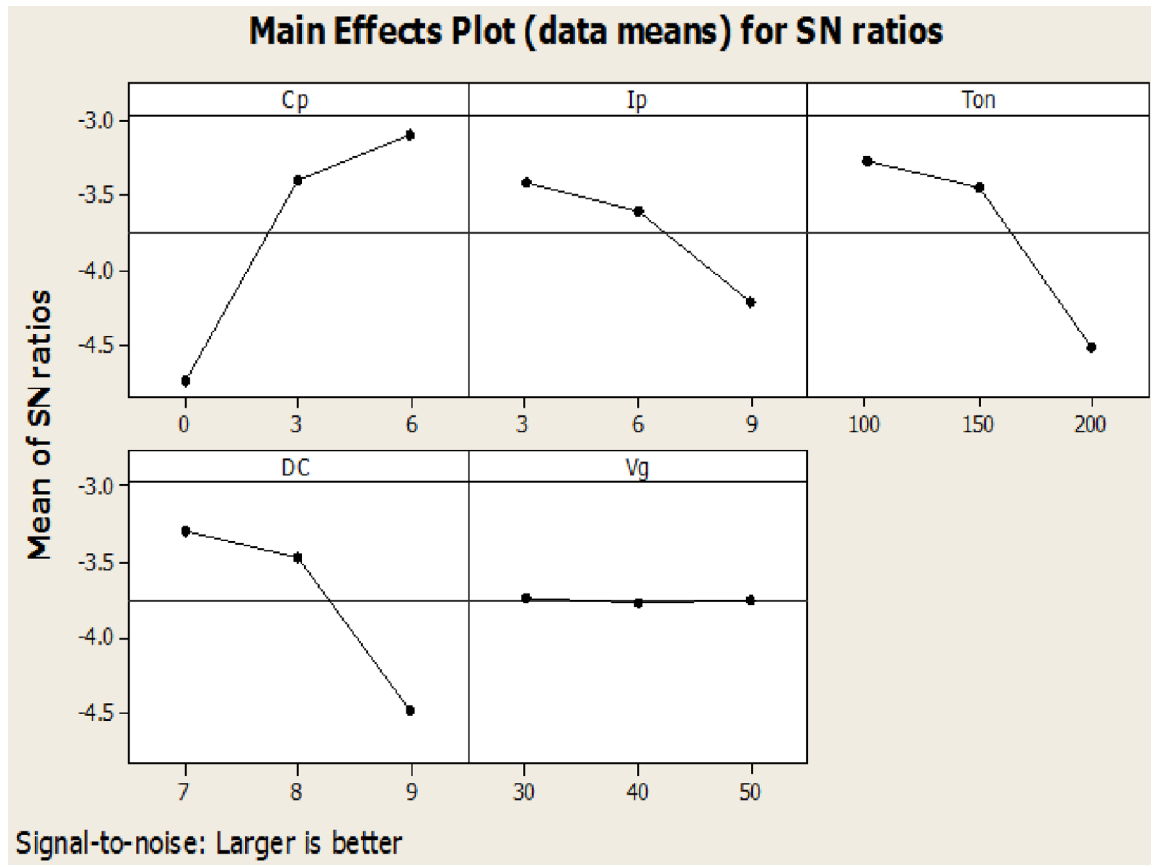
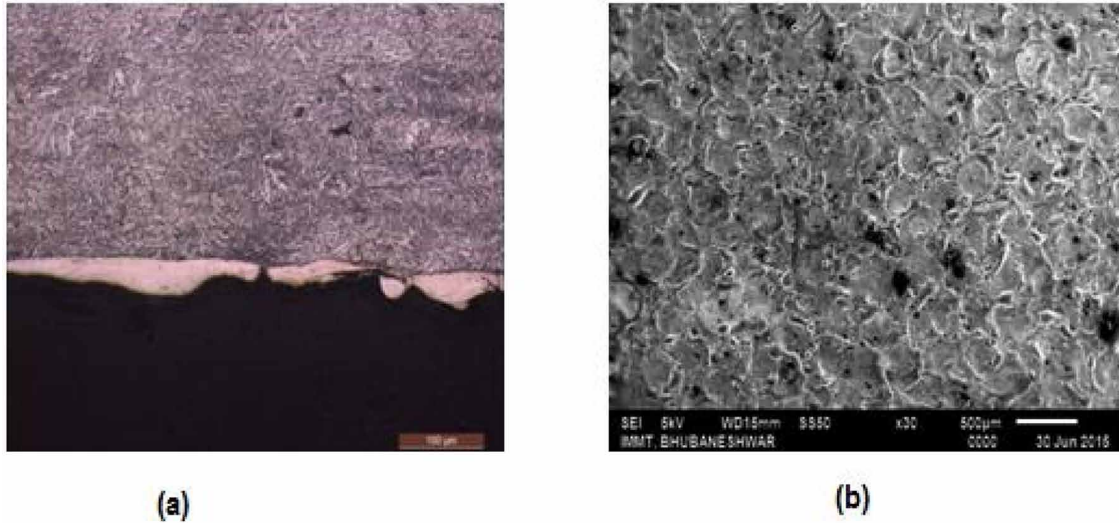


Table 14. Response Table for Means of GRG

Level	C <sub>p</sub>	I <sub>p</sub>	T <sub>on</sub>	DC	V <sub>g</sub>
1	0.5869	0.6743	0.6858	0.6847	0.65458
2	0.6758	0.6605	0.6894	0.6715	0.6532
3	0.6996	0.6274	0.6040	0.6061	0.65457
Delta	0.1127	0.0469	0.0854	0.0786	0.0013
Rank	1	4	2	3	5

The presence of foreign particles if added in appropriate quantities reduces the SR of the machined parts. SEM analysis of machined surface for the optimal setting is shown in Figure 5a and 5b at a magnification of 100 $\mu$ m. Addition of powder to the dielectric improves the surface properties by reducing the micro-cracks formed on the surface of the machined specimen. Proper selection of powder in appropriate concentration for suspension to the dielectric fluid thus reduces the RLT and crack formation leading to better surface properties.

Figure 5. SEM of surfaces and sub-surfaces for the machining with SiC powder mixed dielectric  
a) Optical microscopy image of recast layer, b) SEM micrograph of recast layer



## CONCLUSION

The present investigation aims to determine the optimal setting for the process variables to increase the MRR and HVN and minimize the TWR, EWR, SR and RLT simultaneously for H-11 hot work tool steel by adding silicon carbide powder to the dielectric fluid. Taguchi's technique has been used to conduct the experiments by altering  $C_p$ ,  $I_p$ ,  $T_{on}$ , DC and  $V_g$ . Multi-objective optimization has been performed using Grey Relational Analysis to identify the optimum set of input parameters that improve the process performance. The findings from the present work are as follows:

1. With the increase in powder concentration, the surface texture showed tremendous improvement due to increased material removal rate, reduced surface roughness, recast layer thickness, improved micro-hardness and superior surface quality with less micro-crack.
2. The multi-objective optimization results show that  $C_p$  of 6g/l,  $I_p$  of 3A,  $T_{on}$  of 100  $\mu$ s, DC of 70% and  $V_g$  of 30 V i.e.  $C_{p3}I_{p1}T_{on1}DC_1V_{g1}$  is the optimal setting using TOPSIS. The optimal setting obtained can develop the performance of the quality characteristics under consideration.
3. Confirmatory test shows improvement of 0.09468 in the preferred values for the optimum set using TOPSIS as compared to the initial setting, which is satisfactory.
4. The significant machining parameters affecting the process characteristics at 95% confidence interval were determined using ANOVA. The adjusted  $R^2$  value was found to be 96% which means that 96% of the response variables fit the linear model.
5. The model is appropriate for use to identify the most suitable set of input parameters for the required performance characteristics. The outcome of the present research work will be a substantial aid to the industries concerned with use of materials processed through PMEDM.
6. Adding powder particles to the dielectric widens the gap, improves the flushing and makes the process stable. However, powders should be added in appropriate concentrations as they tend to settle down in the tank and cause difficulty in stirring.

## REFERENCES

- Assarzadeh, S., & Ghoreishi, M. (2013). A dual response surface-desirability approach to process modeling and optimization of  $\text{Al}_2\text{O}_3$  powder-mixed electric discharge machining (PMEDM) parameters. *International Journal of Advanced Manufacturing Technology*, 64(9-12), 1459–1477. doi:10.100700170-012-4115-2
- Batish, A., Bhattacharya, A., Singla, V. K., & Singh, G. (2012). Study of Material Transfer Mechanism in Die steels using powder mixed Electrical Discharge Machining. *Materials and Manufacturing Processes*, 27(4), 449–456. doi:10.1080/10426914.2011.585498
- Bhattacharya, A., Batish, A., Singh, G., & Singla, V. K. (2012). Optimal parameter settings for rough and finish machining of die-steels in powder-mixed EDM. *International Journal of Advanced Manufacturing Technology*, 61(5-8), 537–548. doi:10.100700170-011-3716-5
- Das, S., Klotz, M., & Klocke, F. (2003). EDM simulation: Finite element-based calculation of deformation, microstructure and residual stresses. *Journal of Materials Processing Technology*, 142(2), 434–451. doi:10.1016/S0924-0136(03)00624-1
- Datta, S., Bandyopadhyay, A., & Pal, P. K. (2008). Solving multi-criteria optimization problem in submerged arc welding consuming a mixture of fresh flux and fused slag. *International Journal of Advanced Manufacturing Technology*, 35(9-10), 935–942. doi:10.100700170-006-0776-z
- Ho, K. H., & Newman, S. T. (2003). State of the art electrical discharge machining (EDM). *International Journal of Machine Tools & Manufacture*, 43(13), 1287–1300. doi:10.1016/S0890-6955(03)00162-7
- Jayakumar, N., Yu, Z., & Kamlakar, R. P. (2004). Tool wear compensation and path generation in micro and macro EDM. *Transactions of NAMRI/SME*, 32, 1-8.
- Jeswani, M. L. (1981). Effects of the addition of graphite powder to kerosene used as dielectric fluid in electrical discharge machining. *Wear*, 70(2), 133–139. doi:10.1016/0043-1648(81)90148-4
- Kansal, H. K., Singh, S., & Kumar, P. (2006). Performance parameters optimization (multi-characteristics) of powder mixed electric discharge machining (PMEDM) through Taguchi's method and utility concept. *Indian Journal of Engineering and Materials Sciences*, 13, 209–216.
- Kansal, H. K., Singh, S., & Kumar, P. (2007). Effect of Silicon powder mixed EDM on machining rate of AISID2 die steel. *Journal of Manufacturing Processes*, 9(1), 13–22. doi:10.1016/S1526-6125(07)70104-4
- Senthil, P., Vinodh, S., & Singh, A. K. (2014). Parametric optimisation of EDM on Al-Cu/TiB2 in-situ metal matrix composites using TOPSIS method. *International Journal of Machining and Machinability of Materials*, 16(1), 80–94. doi:10.1504/IJMMM.2014.063922
- Singh, B., Singh, P., Tejpal, G., & Singh, G. (2012). An experimental study of surface roughness of H-11 in EDM process using copper tool electrode. *International Journal of Advances in Engineering and Technology*, 3(4), 30–33.
- Singh, N. P., Raghukandan, K., & Pai, B. C. (2004). Optimization by Grey relational analysis of EDM parameters on machining Al–10% SiCP composites. *Journal of Materials Processing Technology*, 155–156.

### **Optimization of Process Parameters for Silicon Carbide Powder Mixed EDM**

Tripathy, S., & Tripathy, D. K. (2017). Grey Relational Analysis and its application on surface properties during EDM and Powder Mixed EDM. *Journal of Engineering Science and Technology*, 12(9), 2374–2392.

Tripathy, S., & Tripathy, D. K. (2017). Multi-response optimization of machining process parameters for powder mixed electro- discharge machining using grey relational analysis and topsis. *Machining Science and Technology*, 21(3), 362–384. doi:10.1080/10910344.2017.1283957

Tripathy, S., & Tripathy, D. K. (2017). Surface Characterization and Multi-response optimization of EDM process parameters using powder mixed dielectric. *Materials Today: Proceedings*, 4(2), 2058–2067. doi:10.1016/j.matpr.2017.02.051

Wu, K. L., Yan, B. H., Huang, F. Y., & Chen, S. C. (2005). Improvement of surface finish on SKD steel using electro-discharge machining with aluminium and surfactant added dielectric. *International Journal of Machine Tools & Manufacture*, 45(10), 1195–1201. doi:10.1016/j.ijmachtools.2004.12.005

## Chapter 4

# Optimization of Surface Roughness Parameters by Different Multi-Response Optimization Techniques During Electro-Discharge Machining of Titanium Alloy

**Anshuman Kumar Sahu**

*National Institute of Technology Rourkela, India*

**Siba Sankar Mahapatra**

*National Institute of Technology Rourkela, India*

### ABSTRACT

*In this chapter, the EDM process is performed by taking titanium alloy as work piece and AlSiMg prepared by selective laser sintering (SLS) process as tool electrode along with copper and graphite. The EDM is performed by varying different process parameters like voltage (V), discharge current ( $I_p$ ), duty cycle ( $\tau$ ), and pulse-on-time ( $T_{on}$ ). The surface roughness parameters like  $R_a$ ,  $R_t$ , and  $R_z$  are measured by the use of surface roughness measurement machine. To reduce the number of experiments, design of experiment (DOE) approach like Taguchi's L27 orthogonal array has been used. The surface properties of the EDM specimen are optimized by desirability function approach, TOPSIS and VIKOR method, and the best parametric setting is reported for the EDM process. All the optimization techniques convergence to the same optimal parametric setting. The type of tool is the most significant parameter followed by discharge current and voltage. Better surface finish of EDM specimen is produced with lower level of parametric setting along with the use of AlSiMg RP electrode during EDM.*

DOI: 10.4018/978-1-5225-6161-3.ch004

## **INTRODUCTION**

Now-a-days, Electro-discharge machining (EDM) is a widely used non-conventional machining process due to its applications to produce complex, intrinsic cavity with excellent surface finish components, which can be used in automobile, chemical, aerospace, biomedical, tool and die industries. In EDM process, both work piece and tool electrode are submerge inside a dielectric fluid. During machining, a spark channel is generate in between the electrode and work piece gap with generation of very high temperature of around 10000°C. This high temperature is sufficient to melt and vaporizes tiny amount of material from the work piece surface that leads to the material removal from the work piece surface. The use of EDM process is required to machine difficult to machine materials, which required accurate dimensions and excellent surface finish to meet its requirement in industries. Titanium and its alloys are used in biomedical industries like tooth implants and biomedical instrumentation and aerospace due to its properties like high strength to weight ratio, high corrosion and erosion resistance and good strength in wide range of temperature variation. To meet its requirement in industries, the parts produced must be excellent surface (Sahu, Mohanty, & Sahoo, 2017). To study the surface properties of the machined surfaces three characteristics are taken for analysis like average roughness (Ra), maximum height of the profile (Rt) and average height of the profile (Rz). To achieve excellent surface finish the performance of three different tool electrodes are studied. Here AlSiMg tool electrode prepared via selective laser sintering (SLS) process along with conventional copper and graphite electrodes are used. The SLS process is an additive manufacturing (AM) technique used the powder fused based techniques. Here, the laser fuses powder layers and produced three-dimensional components layer by layer. This SLS process also able to produce complex intrinsic tool electrode with less time (Durr, Pilz, & Eleser, 1999). Therefore, the performance of the SLS tool electrodes is studied as compare to copper and graphite electrode with consideration to the surface characteristics of the EDM machined surfaces.

## **BACKGROUND**

Pradhan et al. have analyzed the average surface roughness of the EDMed surface by neural network models during EDM of AISI D2 steel work piece material (Pradhan, Das, & Biswas, 2009). Similarly, the surface properties like Ra, Rt and Rz are measured. The best optimal parametric setting is found out by using optimization techniques like VIKOR based Harmony search algorithm and desirability function approach to get excellent surface finish during electrical discharge coating and electrical discharge machining of AISI 1040 stainless steel and Nitinol respectively (Sahu, Mahapatra, & Chatterjee, 2017; Sahu, Chatterjee, Nayak, & Mahapatra, 2017). SLS process is use to prepare EDM electrode and the surface characteristics performance of the machined surface is studied during EDM process by taking Nitinol as work piece material (Sahu, Chatterjee, Nayak, & Mahapatra, 2017). Arthur et al. have used epoxy with silver paint and copper coating electrode prepared by rapid prototype process during machining of hardened tool steel to study the EDM performance of the electrodes. The thin-coated SL tool were rupture during machining where coating thickness is less than 180µm. However, electrode can used for semi-roughing or for finishing operations (Arthur et al., 2007). Different researchers have used SLS process to prepared EDM tool electrodes of different composition like bronze-nickel with copper phosphite, steel, phosphate and polyester as binder (Durr, Pilz, & Eleser, 1999; Zhao, Li, Zhang, Yu, & Zhang, 2003). Similarly, some other rapid tooling process are adopted to prepare EDM electrodes

like abrading of SiC and corundum to prepare graphite electrode and copper and graphite electrodes by electroforming process and abrading process respectively (Tang, Hong, Zhou, & Lu, 2005; Ding, Lan, Hong, & Wu, 2004). From the previous works of the researchers, it was found that rapid tooling (RT) technology is a fast and effective technique to produce mold and RT has high prospective for decrease in time and cost.

During EDM process, surface finish of the machined Titanium alloy specimens are the important criteria in present scenario to be utilize in the industries. The surface attributes are the analyzed and studied to meet the demands of the excellent surface finish product in recent scenario. The optimization tools have an important role in succeeding the above stated objectives. Therefore, multi-objective optimization is the important areas of research during EDM process. In past few years, different multi-objective optimization techniques were used in different machining process. Sahu et al. have used Taguchi based GRA method to optimize the responses during EDM of Titanium alloy and 316L stainless steel (Sahu, Mohanty, & Sahoo, 2017). Similarly, desirability function approach and VIKOR based Harmony search algorithm were used to optimize the surface roughness parameters during EDM and EDC of Nitinol and 1040 stainless steel work piece material. The studies were focused on to decrease the surface characteristics (Sahu, Mahapatra, & Chatterjee, 2017; Sahu, Chatterjee, Nayak, & Mahapatra, 2017). TOPSIS and GRA methods were utilized to optimize the responses like MRR, TWR, electrode wear ratio and average surface roughness in powder mixed EDM of H-11 die steel (Tripathy, & Tripathy, 2016). Fuzzy TOPSIS and sensitivity analysis are used to analyze surface properties and dimensional accuracy in the EDM of AISI P20 tool steel (Dewangan, Gangopadhyay, & Biswas, 2015). Response surface based desirability approach used to optimize the responses MRR and average surface roughness during  $Al_2O_3$  powder mixed EDM (Assarzadeh, & Ghoreishi, 2013). GRA, MRSN, WSN and VIKOR methods are used to optimize the wire electrical discharge machining process (Gauri & Chakraborty, 2010). TOPSIS method is used to optimize the responses like cutting velocity, material removal rate and kerf width during gear cutting of Inconel 718 material by wire electrical discharge machining (Mohapatra, & Sahoo, 2018).

Some of the other machining process of where multi-response optimization techniques are used to optimize the machining processes are as follows. TOPSIS method is used to optimize the multi-response during cryogenic drilling of Ti6Al4V alloy (Ahmed & Kumar, 2016). Similarly, the same TOPSIS method is used to find out the optimal process parameter during turning of pure titanium by considering the output responses like cutting force, average surface roughness, tool tip temperature and MRR (Khan, & Maity, 2017). Desirability function analysis and Utility concept and Taguchi based Desirability function analysis are used for the optimum parametric selection in machining of EN25 steel and glass-fibre-reinforced plastic (Singaravel, & Selvaraj, 2016; Sait, Aravindan, & Haq, 2009).

## RESEARCH GAP

From previous literature, it is found that many works have been done in the field of EDM by the use of SLS tool electrodes. However, until now, very few literatures have been found to study the performance of different types of tool electrodes during EDM process. In EDM process, responses like material removal rate, tool wear rate, and average surface roughness are studied. However, very few literatures explains the optimization of surface characteristics and effect of process parameters on the surface characteristics of the EDM machined surfaces.



## **MAIN FOCUS OF THE CHAPTER**

The EDM process is used to machine difficult to machine materials, which required accurate dimensions and excellent surface finish to meet its requirement in industries. In this work, EDM performance of AlSiMg electrode prepared by SLS process along with conventional copper and graphite electrodes are study during the machining of Titanium alloy (Ti6Al4V). Titanium alloy is used in aerospace, automobile, biomedical and chemical industries due to its high strength and corrosion resistance in wide range of temperature variations. For the use of the machined specimens in chemical, aerospace, automobile, the surface finish produced must be of excellent quality. To investigate the surface properties of the machined surface during EDM, the different surfaces roughness characteristics consider are average roughness (Ra), maximum height of the profile (Rt) and average height of the profile (Rz). During machining, different EDM process parameters like voltage (V), discharge current (Ip), duty cycle ( $\tau$ ) and pulse on time (Ton) are varied along with different types of tool electrodes i.e. AlSiMg RP electrode, copper and graphite electrodes. To reduce the number of experiments, a 5-factor, 3-level design of experiment (DOE) methodology like Taguchi's  $L_{27}$  orthogonal array is used. Therefore, within 27 experimental run, the performance of the tool electrodes are analyzed along with the effect of the EDM parameters towards the surface properties. In this present work, three surface characteristics are considered to evaluate the surface characteristics of the EDM machined surface three optimization techniques used are DFA (desirability function approach), TOPSIS (Technique for Order of Preference by Similarity to Ideal Solution) and VIKOR (Vlse Kriterijumska Optimizacija I Komopromisno Resenje) method and the best parametric setting is reported for the EDM process. Here three optimization techniques as stated above are used to get the optimal parametric setting and their performance are compared.

## **METHODOLOGY**

### **Desirability Function Approach**

The desirability function approach is a widely used technique to solve multi-objective optimization problems. The elementary conception of desirability is to transform multi-objective optimization problem into single objective. Here each response variable  $y_i$  is converted into individual desirability value  $d_i$ , which value ranges between 0 to 1. If the characteristic of the output response is unacceptable, then desirability value is 0 and for optimal acceptable characteristic the desirability value is 1. After that composite or overall desirability is then calculated from the individual desirability. The higher value of overall desirability indicates the optimum parametric setting (Sahu, Chatterjee, Nayak, & Mahapatra, 2017; Assarzadeh, & Ghoreishi, 2012; Singaravel, & Selvaraj, 2016). The following steps are followed to calculate the individual desirability index ( $d_i$ ) and overall desirability index ( $d_o$ ).

1. Calculate the individual desirability index ( $d_i$ ).
  - a. Nominal is the best.

$$d_i = \begin{cases} \left( \frac{y_i - y_{\min}}{T - y_{\min}} \right)^s, & y_{\min} \leq y_i \leq T, s \geq 0 \\ \left( \frac{y_i - y_{\min}}{T - y_{\min}} \right)^s, & T \leq y_i \leq y_{\max}, s \geq 0 \\ 0 & \end{cases} \quad (1)$$

b. Larger is the better.

$$d_i = \begin{cases} 0, & y_i \leq y_{\min} \\ \left( \frac{y_i - y_{\min}}{y_{\max} - y_{\min}} \right)^r, & y_{\min} \leq y_i \leq y_{\max}, r \geq 0 \\ 1, & y_i \geq y_{\max} \end{cases} \quad (2)$$

c. Smaller is the better.

$$d_i = \begin{cases} 1, & y_i \leq y_{\min} \\ \left( \frac{y_i - y_{\max}}{y_{\min} - y_{\max}} \right)^r, & y_{\min} \leq y_i \leq y_{\max}, r \geq 0 \\ 0, & y_i \geq y_{\max} \end{cases} \quad (3)$$

where  $y_i$  = observed value from the experiment.

$y_{\max}$  = maximum observed value

$y_{\min}$  = minimum observed value

T = Target value

2. Calculate the composite or overall desirability.

$$d_o = \left( d_1^{w_1} \times d_2^{w_2} \times \dots \times d_i^{w_i} \right)^{1/w} \quad (4)$$

Where  $w_1 + w_2 + \dots + w_i = w$

## TOPSIS (Technique for Order Preference Through Similarity to Ideal Solution) Method

TOPSIS method is established for the measurement of the degree of closeness of the ideal solution from the most suitable alternatives. The principle of this method is to select the criteria which is nearest from the positive best solution and farthest from the negative best solution and the finest solution is having most relative closeness towards the ideal solution. The steps involve in TOPSIS are expressed as follows (Tripathy, & Thripathy; 2016, Ahmed, & Kumar, 2016; Khan, & Maity; 2017).

1. Find out the decision matrix having  $m$  number of attributes and  $n$  numbers of alternatives as follows in Eqn. (5).

$$D_m = \begin{bmatrix} x_{11} & x_{12} & x_{13} & \cdots & \cdots & x_{1m} \\ x_{21} & x_{22} & x_{23} & \cdots & \cdots & x_{2m} \\ x_{31} & x_{32} & x_{33} & \cdots & \cdots & x_{3m} \\ \vdots & \vdots & \vdots & \ddots & \ddots & \vdots \\ \vdots & \vdots & \vdots & \ddots & \ddots & \vdots \\ x_{n1} & x_{n2} & x_{n3} & \cdots & \cdots & x_{nm} \end{bmatrix} \quad (5)$$

2. Calculate the normalized decision matrix ( $r_{ij}$ ) as follows.

$$r_{ij} = \frac{X_{ij}}{\sqrt{\sum_{i=1}^n X_{ij}^2}}, i = 1, 2, \dots, n, j = 1, 2, \dots, m. \quad (6)$$

where,  $i$ = number of experimental runs,  $j$ = number of output responses,  $r_{ij}$  = normalized value of the  $i^{\text{th}}$  experimental run with respect to  $j^{\text{th}}$  output responses.

3. The weighted normalized value matrix ( $v_{ij}$ ) is calculated by multiplication of the normalized value into the weighted value as in the following equation.

$$v_{ij} = w_j \times r_{ij} \quad (7)$$

where,  $i = 1, 2, \dots, n, j = 1, 2, \dots, m$  and  $\sum w_j = 1$

4. For each experiment calculate the ideal experimental run that are the best ( $S^+$ ) and the worst ( $S^-$ ) experimental run performance as follows.

$$S^+ = \left[ \max(S_{ij}) \mid j \in J \right] \text{ or } \left[ \min(S_{ij}) \mid j \in J' \right], i = 1, 2, \dots, n, \quad (8)$$

$$S^- = \left[ \min(S_{ij}) \mid j \in J \right] \text{ or } \left[ \max(S_{ij}) \mid j \in J' \right], i = 1, 2, \dots, n \quad (9)$$

5. The performance of the responses are measured by the best experimental run distance ( $D_{ij}^+$ ) from the  $S^+$  values and the worst experimental run distance ( $D_{ij}^-$ ) from the  $S^-$  values as represented in the following equation.

$$D_{ij}^+ = \sqrt{\sum_{i=1}^m (v_{ij} - S_j^+)^2}, \quad (10)$$

$$D_{ij}^- = \sqrt{\sum_{i=1}^m (v_{ij} - S_j^-)^2}$$

where

$$i = 1, 2, \dots, n \quad (11)$$

6. The closeness coefficient ( $C_i$ ) for each experimental run are calculated by the following equation.

$$C_i = \frac{D_i^-}{D_i^- + D_i^+}, i = 1, 2, \dots, n; 0 \leq C_i \leq 1. \quad (12)$$

The best experimental parameters are chosen from the basis of high value of closeness coefficient, which is nearer to the ideal solution.

## VIKOR (Vise Kriterijumska Optimizacija I Komopromisno Resenje) Method

The VIKOR method is an optimization process used to optimize the process parameters to increase the desire output by minimizing the undesired parameters. To convert the multi-responses into single response VIKOR method has been used. The procedure of the VIKOR method is as follows (Sahu, Mahapatra, & Chatterjee, 2017; Gauri, & Chakraborty, 2010).

1. Calculate the scaled ( $Y_{ij}$ ) value of the responses.

$$Y_{ij} = \frac{y_{ij} - y_j^{\min}}{y_j^{\max} - y_j^{\min}} \quad (13)$$

### Optimization of Surface Roughness Parameters

$y_{ij}$  = response at  $i^{\text{th}}$  trial,  $j^{\text{th}}$  response variable.

$y_j^{\min}$  and  $y_j^{\max}$  are the minimum and maximum response variables.

2. Calculate the ideal ( $A^*$ ) and negative ideal ( $A^-$ ) solution.

$$A^* = \{\max Y_{ij}, i=1, 2, \dots, n\} = \{Y_1^*, Y_2^*, \dots\} \quad (14)$$

$$A^- = \{\min Y_{ij}, i=1, 2, \dots, n\} = \{Y_1^-, Y_2^-, \dots\} \quad (15)$$

3. Calculate the Utility ( $S_i$ ) and Regret ( $R_i$ ) measures for each experimental run.

$$S_i = \sum_{j=1}^n \frac{w_j (Y_j^* - Y_{ij})}{(Y_j^* - Y_j^-)} \quad (16)$$

$$R_i = \max_j \frac{w_j (Y_j^* - Y_{ij})}{(Y_j^* - Y_j^-)} \quad (17)$$

$w_j$  = weightage such that  $\sum w_j = 1$

4. Calculate the VIKOR index of the  $i^{\text{th}}$  experimental trial.

$$Q_i = \nu \left( \frac{S_i - S^*}{S^- - S^*} \right) + (1 - \nu) \left( \frac{R_i - R^*}{R^- - R^*} \right) \quad (18)$$

$i = 1, 2, 3, \dots, n,$

$S^* = \min S_i, \quad S^- = \max S_i, \quad R^* = \min R_i, \quad R^- = \max R_i.$

$\nu$  = weight of the maximum group utility, which is usually taken as 0.5.

## MATERIALS AND METHOD

In this work, electrical discharge machining of Titanium alloy (Ti6Al4V) is performed by taking AlSiMg electrode prepared by SLS process, copper and graphite tool electrodes, Commercial EDM 30 oil is taken

as dielectric fluid. The chemical composition of Titanium alloy in weight percentage of the elemental component is given in Table 1.

To study the influence of different types of tools like AlSiMg RP electrode, copper and graphite electrodes on the surface properties of the machined surfaces, the EDM process parameters like voltage (V), discharge current ( $I_p$ ), duty cycle ( $\tau$ ) and pulse on time ( $T_{on}$ ) are varied during the EDM process. The values of these process parameters with different levels are listed in Table 2. To reduce the number of experiments, a 3-level, 5-factor design of experiment (DOE) methodology like Taguchi's  $L_{27}$  orthogonal array is used. The EDM of Titanium alloy by taking different tool electrodes has been performed in a die sinking EDM (ELECTRA EMS 5535) [Figure 1]. To meet the required applications in the field

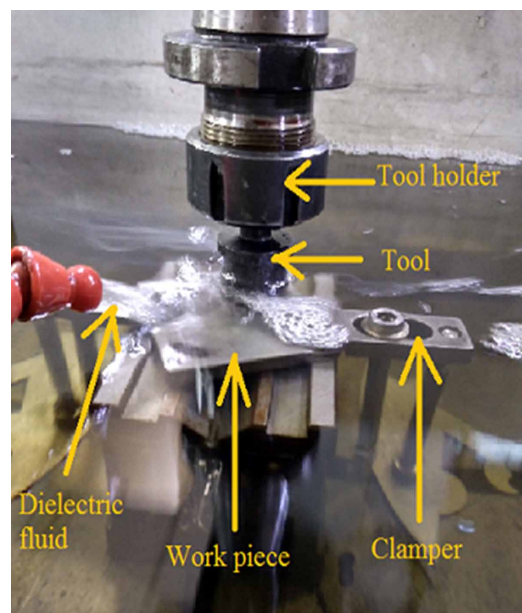
Table 1. Chemical composition of Titanium alloy

Composition	C	Fe	Al	O	N	V	H	Ti
wt. %	0.018	0.22	6.08	0.18	0.05	4.02	0.1	Balance

Table 2. Machining parameters with their levels

Parameters	Unit	Level 1	Level 2	Level 3
A-Open circuit voltage (V)	V	20	25	30
B-Discharge current ( $I_p$ )	A	10	15	20
C-Duty cycle ( $\tau$ )	%	67	75	83
D-Pulse-on-time ( $T_{on}$ )	$\mu s$	100	200	300
E- Tool material	-	AlSiMg RP Tool	Copper	Graphite

Figure 1. Electrical discharge machining process



### Optimization of Surface Roughness Parameters

of chemical, automobile, aerospace, biomedical, die and mold making industries, the EDM specimen must be prepared with high accuracy and excellent surface finish. The surface roughness parameters like average roughness (Ra), maximum height of the profile (Rt) and average height of the profile (Rz) are measured by the use of surface roughness measurement machine (Taylor-Hobson-PNEUNO-Suetronic 3+) (Sahu, Mahapatra, & Chatterjee, 2017; Pradhan, Das, & Biswas, 2009). The output surface characteristics values (Ra, Rt, Rz) for all the experiments along with the input parameters are listed in Table 3. Here, the surface roughness values are measured for three times and the average value for each EDM machined specimens is considered for further study. The surface roughness values are optimized by desirability function approach, TOPSIS and VIKOR and best optimal setting is obtained to get better surface finish of the machined specimens.

Table 3. Taguchi's  $L_{27}$  orthogonal array and output response of surface roughness parameters

Sl. No.	A	B	C	D	E	Ra ( $\mu\text{m}$ )	Rt ( $\mu\text{m}$ )	Rz ( $\mu\text{m}$ )
1	1	1	1	1	1	6.4	36.3	19.3
2	1	1	1	1	2	6.7	45.7	21.3
3	1	1	1	1	3	8.2	54.3	35.7
4	1	2	2	2	1	7.2	43.7	24.7
5	1	2	2	2	2	7	48.3	27.0
6	1	2	2	2	3	8.3	59.7	34.7
7	1	3	3	3	1	7.8	53.0	31.7
8	1	3	3	3	2	8.3	61.3	40.3
9	1	3	3	3	3	9.2	71.3	43.3
10	2	1	2	3	1	7.2	45.0	31.7
11	2	1	2	3	2	7.3	48.0	32.7
12	2	1	2	3	3	8.2	59.7	38.0
13	2	2	3	1	1	7.1	45.7	31.0
14	2	2	3	1	2	7.4	51.3	34.7
15	2	2	3	1	3	9.4	61.7	41.3
16	2	3	1	2	1	7.3	47.7	31.3
17	2	3	1	2	2	8.4	58.3	36.7
18	2	3	1	2	3	9	68.3	41.0
19	3	1	3	2	1	7.2	45.7	33.0
20	3	1	3	2	2	7.4	57.7	37.0
21	3	1	3	2	3	9.5	70.7	46.0
22	3	2	1	3	1	7.4	51.3	31.0
23	3	2	1	3	2	7.8	56.7	37.0
24	3	2	1	3	3	9.6	78.7	46.0
25	3	3	2	1	1	8.1	60.0	38.3
26	3	3	2	1	2	8.4	67.7	43.7
27	3	3	2	1	3	9.8	75.3	48.7

Average roughness (Ra) is the arithmetic mean of the absolute values of the contour heights along the estimated length. The average roughness (Ra) is estimated by the formula as given in Eqn. (1).

$$\text{Average roughness, } Ra = \frac{1}{L} \int y(x) dx = \frac{\sum_{i=1}^{i=n} y_i}{n} \quad (19)$$

Maximum height of the profile (Rt) is the perpendicular distance between the uppermost and lowermost points of the contour within the estimated length. The Rt is calculated as in Eqn. (2).

$$\text{Maximum height of the profile, } Rt = \text{Max}(y_i) \quad (20)$$

Average height of the profile (Rz) is the mean of the consecutive values of maximum height of the profile (Rt) calculated over the estimated length as mentioned in Eqn. (3).

$$\text{Average height of the profile, } Rz = \frac{\sum_{i=1}^n R_{ti}}{n} \quad (21)$$

where L is the sampler length, y is the profile curve, x is the profile direction,  $y_i$  is the height of the profile. The surface roughness values are measured within L=0.8mm having cut off length Lc=0.4mm and N=2.

## RESULT AND DISCUSSION

The experiment of EDM is performed by taking Titanium alloy work piece and the surface roughness parameters were measured as described in section 3. The surface roughness parameters like Ra, Rt, Rz are measured for three numbers of times and the average value is tabulated in Table 3.

### Effect of Parameters on Surface Characteristics

The main effect plot for average roughness (Ra), and interaction plot are presented in Figure 2-3. From the figure it is found that with increase in EDM parameters like voltage (V), discharge current (Ip), duty cycle ( $\tau$ ) and pulse on time (Ton) the average surface roughness (Ra) of the machined surface increased. This is due to the regeneration of more energy during sparking, which leads to more crater depth with increased average surface roughness (Ra). The surface of specimen machined with RP electrode is better with respect to average surface roughness (Ra) followed by surface machined with copper and graphite electrode. The analysis of variance (ANOVA) and main effect plots are found out by using MINITAB 16. The ANOVA for average surface roughness (Ra) is presented in Table 4 with  $R^2$  of 96.7%. Here tool type, voltage and discharge current are found to be the most significant parameters.

Similarly, the main effect plot and interaction plot for maximum height of the profile (Rt) are presented in Figure 4-5. From the figure it is found that with increase in the parameters like voltage (V), discharge



## Optimization of Surface Roughness Parameters

Figure 2. Main effect plot for average roughness ( $R_a$ )

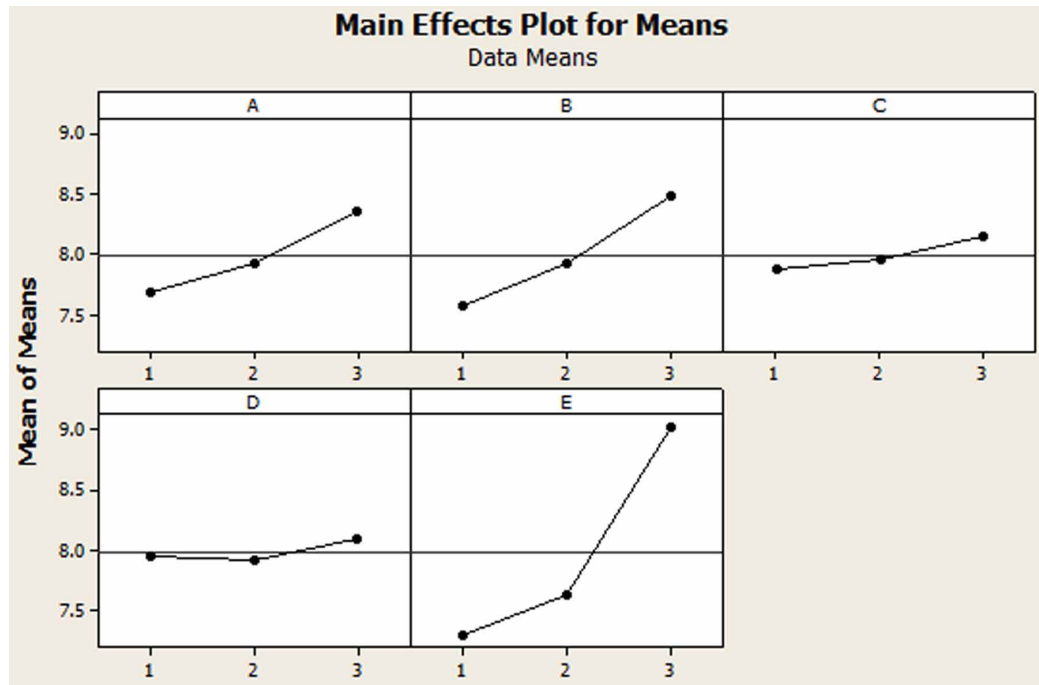


Figure 3. Interaction effect plot for average roughness ( $R_a$ )

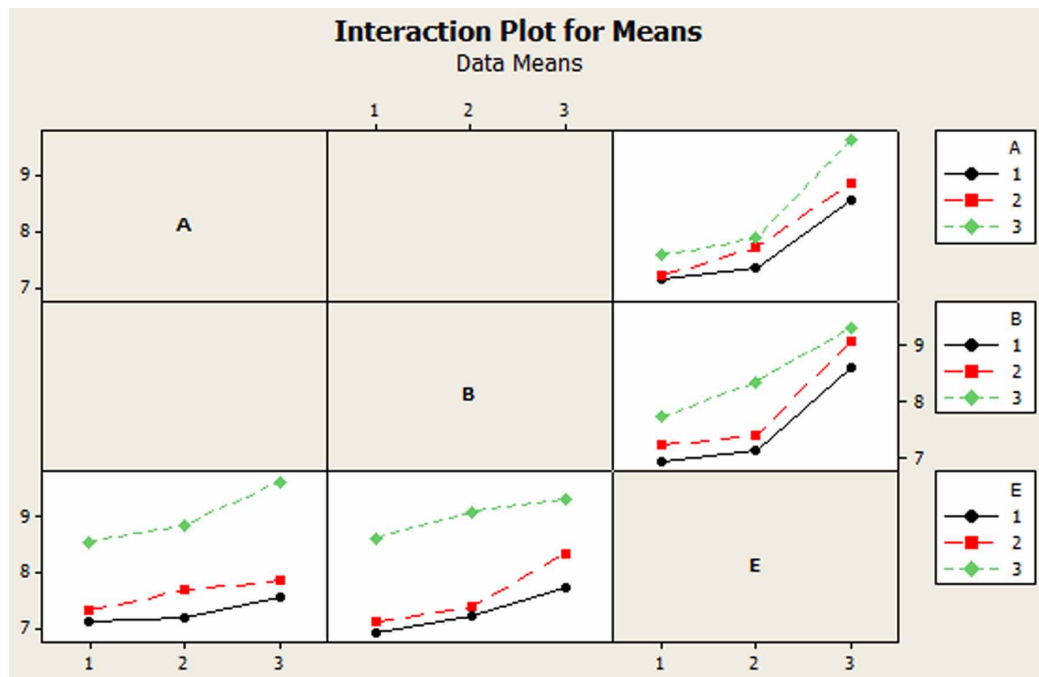
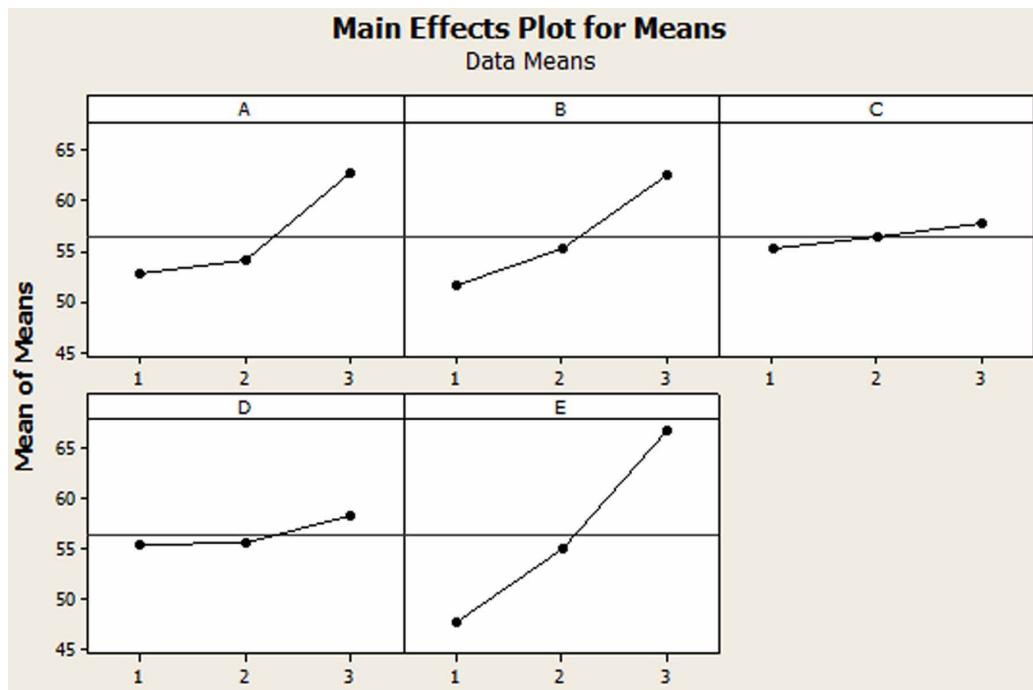


Table 4. ANOVA for the surface characteristics

Source	DF	Average roughness (Ra)			Maximum height of profile (Rt)			Average height of the profile (Rz)		
		SS	P	%Cont.	Seq SS	P	%Cont	Seq SS	P	%Cont
A	2	2.1207	0.005*	9.16	532.67	0.000*	17.99	380.03	0.000*	27.44
B	2	3.8096	0.001*	16.45	572.06	0.000*	19.32	224.56	0.000*	16.32
C	2	0.3696	0.205	1.60	24.75	0.296	0.84	84.54	0.004*	6.10
D	2	0.1474	0.492	0.64	50.13	0.114	1.69	27.12	0.068	1.96
E	2	15.0185	0.000*	64.86	1657.09	0.000*	55.96	598.38	0.000*	43.20
A*E	4	0.4681	0.371	2.02	30.84	0.513	1.04	16.87	0.385	1.22
B*E	4	0.4593	0.379	1.98	24.10	0.617	0.81	25.25	0.226	1.82
Error	8	0.7607		3.29	69.47		2.35	28.36		1.94
Total	26	23.1541		100	2961.11		100	1385.11		100
R <sup>2</sup>		96.7%			97.7%			98%		

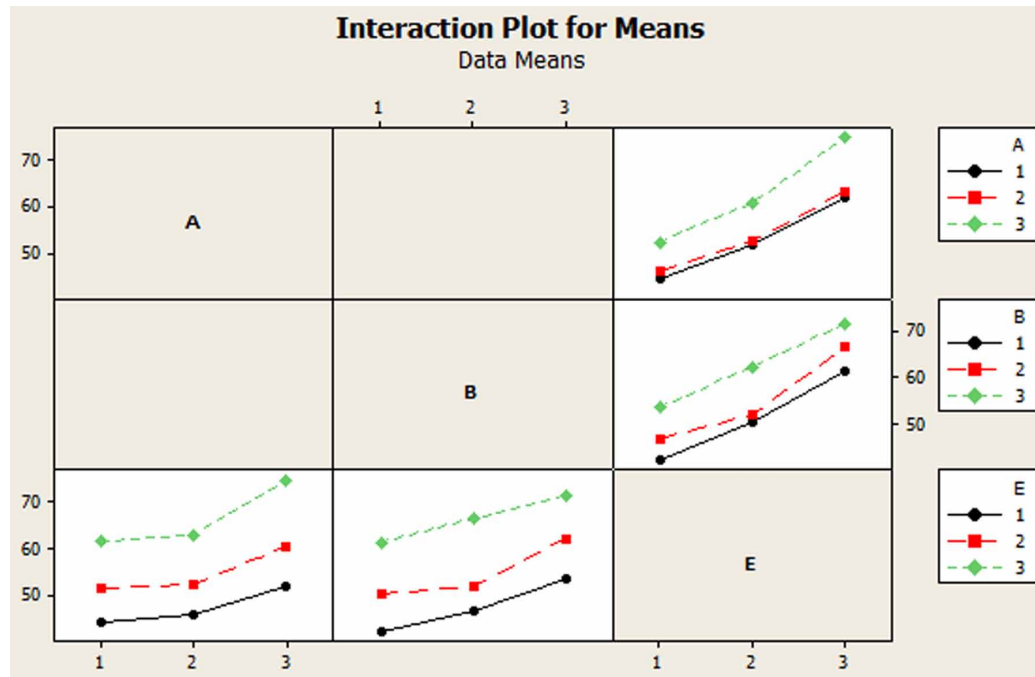
\*Significant parameters at 95% confidence interval

Figure 4. Main effect plot for maximum height of the profile (Rt)



current ( $I_p$ ), duty cycle ( $\tau$ ) and pulse on time ( $T_{on}$ ), the  $R_t$  value of the machined surface increased. This is due to the generation of more energy during sparking, which leads to more crater depth with increased  $R_t$ . The surface of specimen machined with RP electrode is better with respect to  $R_t$  followed by surface machined with copper and graphite electrode. The ANOVA for the  $R_t$  value is presented in Table 4 with  $R^2$  of 97.7%. Here tool type is the most significant parameter followed by discharge current and voltage.

Figure 5. Interaction plot for maximum height of the profile ( $R_t$ )



Likewise, the similar trend is found for average height of the profile ( $R_z$ ). Here also with increase in the process parameters the  $R_z$  value increased as shown in Figure 6-7. The  $R_z$  value of specimen machined with RP electrode is better with respect to surface machined with copper and graphite electrode. The ANOVA for the  $R_z$  value is presented in Table 4 with  $R^2$  of 98%. Here tool type is the most significant parameter followed by voltage, discharge current and duty cycle.

### Optimization by Desirability Function Approach

By following the steps of the Desirability function approach as explain in section 2.1[Eqns. 1-4] the individual desirability index ( $d_i$ ) and overall desirability index ( $d_o$ ) are calculated and tabulated in Table 5. Here the all three responses are surface properties. Therefore, equal weightage (i.e. 0.333) is given to calculate the overall desirability index ( $d_o$ ). For all the surface properties lower is better criteria is consider to evaluate the individual desirability index ( $d_i$ ). The ANOVA for overall desirability index ( $d_o$ ) is presented in Table 6 with  $R^2=98.4\%$  and the main effect plot and interaction plot for overall desirability index ( $d_o$ ) are shown in Figure 8 and 9 respectively. The overall desirability value consider as higher is the better. Therefore, lower parametric level of the EDM parameters given optimum surface characteristics with help of AlSiMg RP tool electrode. From the main effect plot (Figure 8) and the level average table (Table 7), the optimum parametric setting by the desirability function approach are found to be  $V=20V$ ,  $I_p=10A$ ,  $\tau=67\%$ ,  $T_{on}=200\mu s$  and tool=AlSiMg RP tool.

Figure 6. Main effect plot for average height of the profile ( $R_z$ )

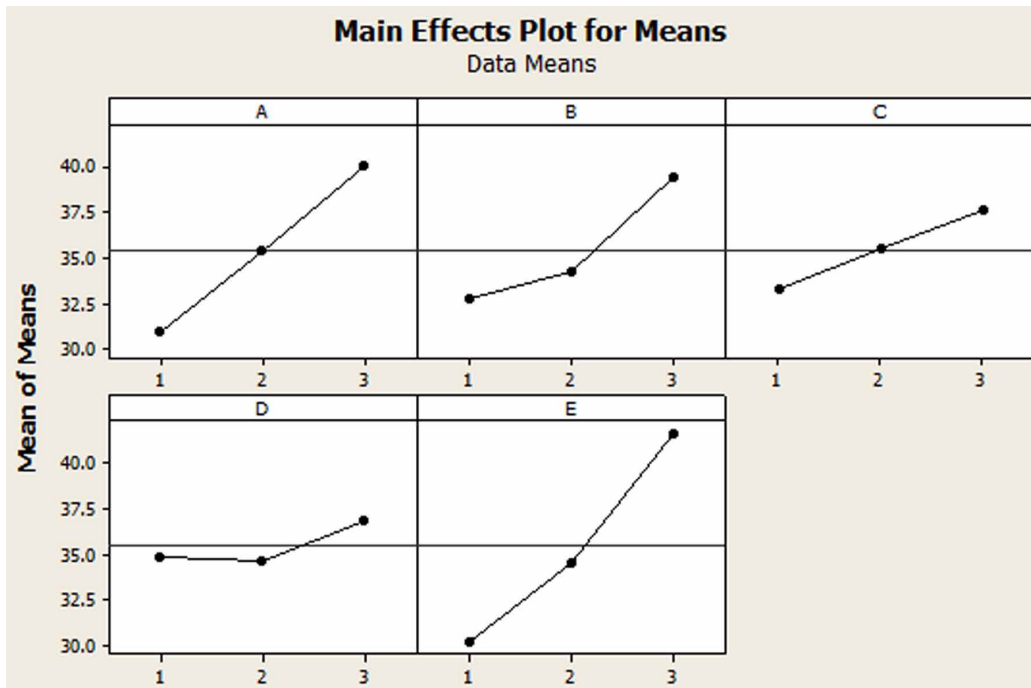
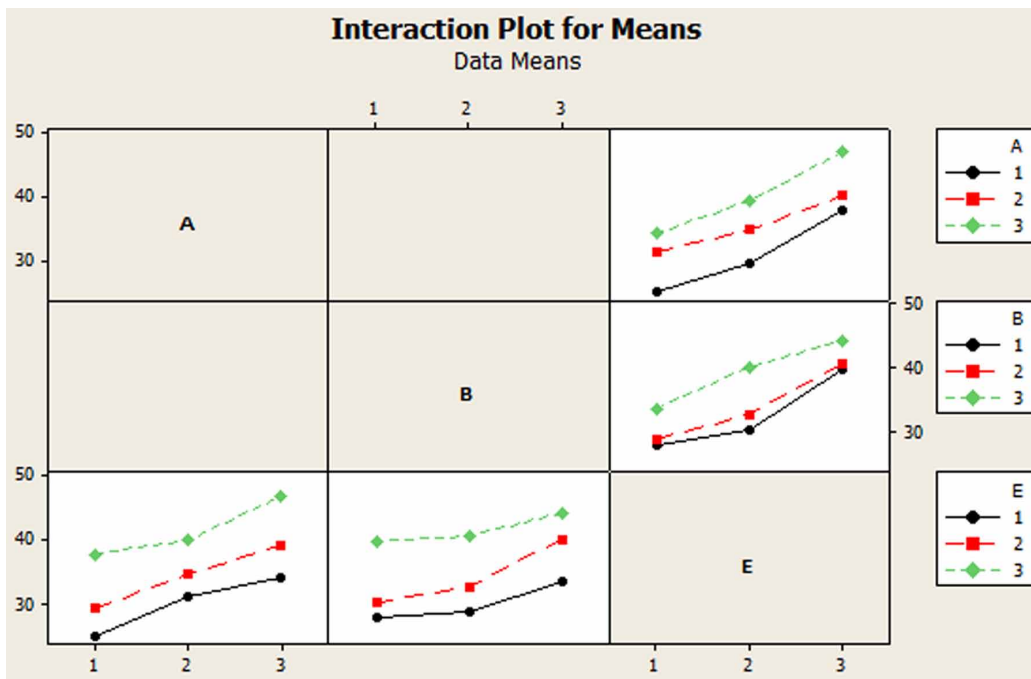


Figure 7. Interaction plot for average height of the profile ( $R_z$ )



## Optimization of Surface Roughness Parameters

Table 5. Individual desirability index ( $d_i$ ) and overall desirability index ( $d_o$ )

Sl. No.	$d_i(Ra)$	$d_i(Rt)$	$d_i(Rz)$	$d_o$
1	1	1	1	1
2	0.9118	0.7783	0.9320	0.8713
3	0.4706	0.5755	0.4422	0.4929
4	0.7647	0.8255	0.8163	0.8017
5	0.8235	0.7170	0.7381	0.7582
6	0.4412	0.4481	0.4762	0.4549
7	0.5882	0.6061	0.5782	0.5908
8	0.4412	0.4104	0.2857	0.3726
9	0.1765	0.1745	0.1837	0.1782
10	0.7647	0.7948	0.5782	0.7057
11	0.7353	0.7241	0.5442	0.6617
12	0.4706	0.4481	0.3639	0.4250
13	0.7941	0.7783	0.6020	0.7193
14	0.7059	0.6462	0.4762	0.6011
15	0.1176	0.4009	0.2517	0.2281
16	0.7353	0.7311	0.5918	0.6827
17	0.4118	0.4811	0.4082	0.4324
18	0.2353	0.2453	0.2619	0.2473
19	0.7647	0.7783	0.5340	0.6824
20	0.7059	0.4953	0.3980	0.5182
21	0.0882	0.1887	0.0918	0.1152
22	0.7059	0.6462	0.6020	0.6500
23	0.5882	0.51887	0.3980	0.4952
24	0.0588	0	0.0918	0
25	0.5	0.4410	0.3537	0.4273
26	0.4118	0.2594	0.1701	0.2629
27	0	0.0802	0	0

Table 6. ANOVA for overall desirability index ( $d_o$ )

Source	DF	Seq SS	Adj SS	Adj MS	F	P	%Cont
A	2	0.32185	0.32185	0.160927	45.66	0.000*	18.40
B	2	0.29880	0.29880	0.149400	42.39	0.000*	17.09
C	2	0.04191	0.04191	0.020954	5.94	0.026*	2.40
D	2	0.02441	0.02441	0.012206	3.46	0.083	1.40
E	2	0.98649	0.98649	0.493246	139.94	0.000*	56.41
A*E	4	0.02125	0.02125	0.005312	1.51	0.288	1.22
B*E	4	0.02599	0.02599	0.006497	1.84	0.214	1.49
Error	8	0.02820	0.02820	0.003525			1.59
Total	26	1.74890					100

\*Significant parameters at 95% confidence interval

Figure 8. Main effect plot for overall desirability index (do)

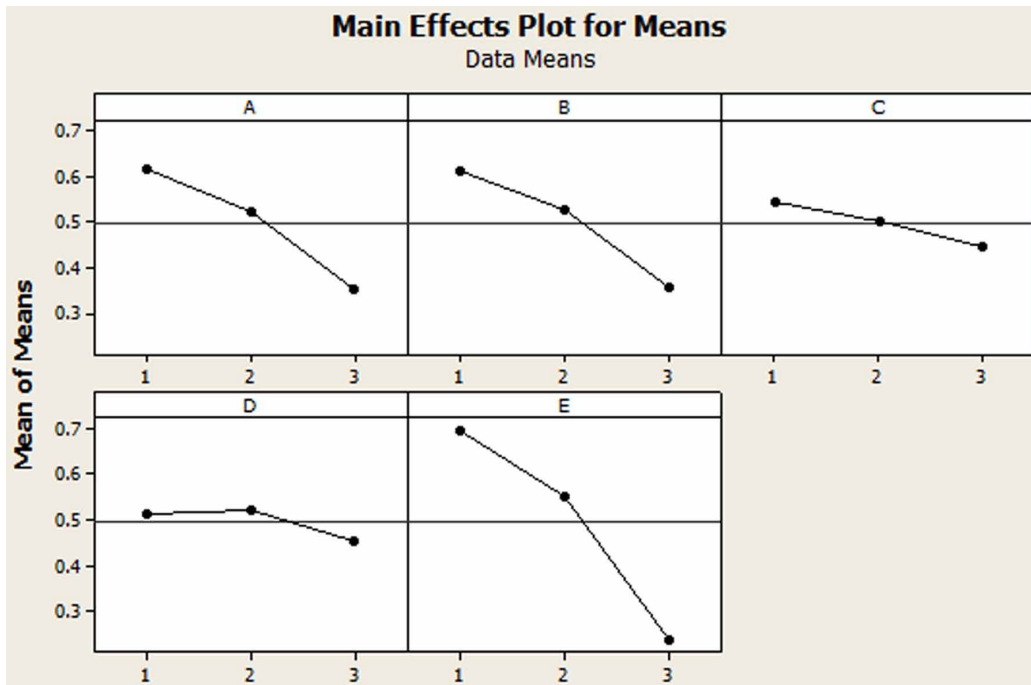


Figure 9. Interaction plot for overall desirability index (do)

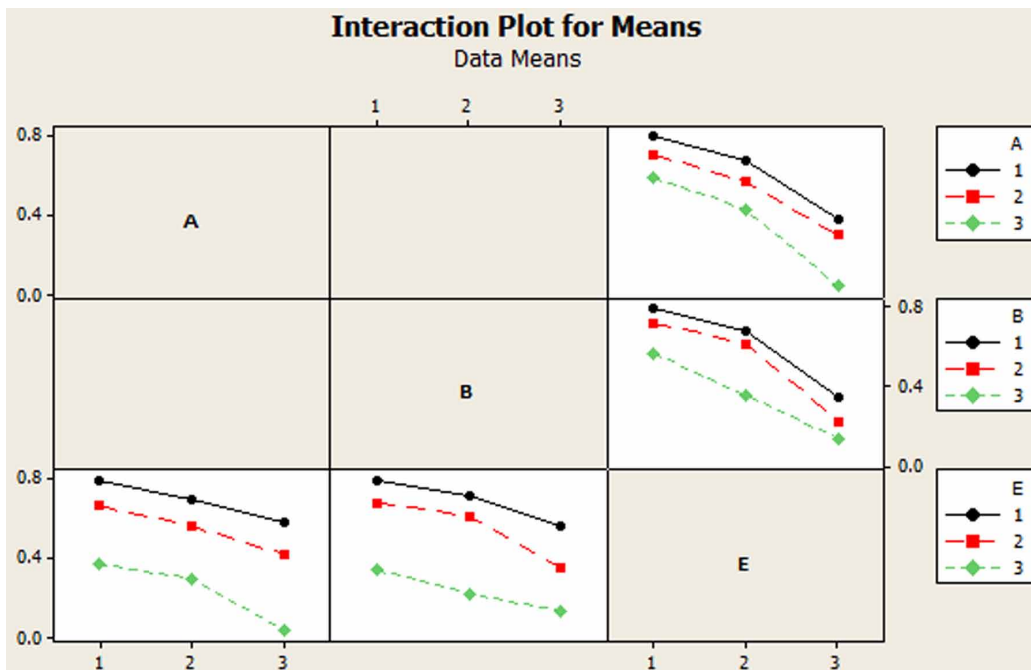


Table 7. Response Table for means of overall desirability index (do)

Level	A	B	C	D	E
1	0.6134*	0.6080*	0.5413*	0.5114	0.6955*
2	0.5226	0.5232	0.4997	0.5214*	0.5526
3	0.3501	0.3549	0.4451	0.4532	0.2379
Delta	0.2633	0.2531	0.0962	0.0682	0.4576
Rank	2	3	4	5	1

\*Optimal parametric setting

## Optimization by TOPSIS Method

By following the steps of the TOPSIS as explain in section 2.2 [Eqns. 5-12], the normalized decision matrix ( $r_{ij}$ ), weighted normalized decision matrix ( $v_{ij}$ ), best experimental run distance ( $D_{ij}^+$ ), worst experimental run distance ( $D_{ij}^-$ ) and the multi criteria performance index i.e. the closeness coefficient ( $C_i$ ) are calculated and tabulated in Table 8. Here the all three responses are surface properties. Therefore, equal weightage (i.e. 0.333) is given to calculate the weighted normalized value matrix ( $v_{ij}$ ). The ANOVA for the closeness coefficient ( $C_i$ ) is presented in Table 9 with  $R^2=98.5\%$ . The main effect plot and interaction plot for the closeness coefficient ( $C_i$ ) are shown in Figure 10 and 11 respectively. The

Figure 10. Main effect plot for closeness coefficient ( $C_i$ )

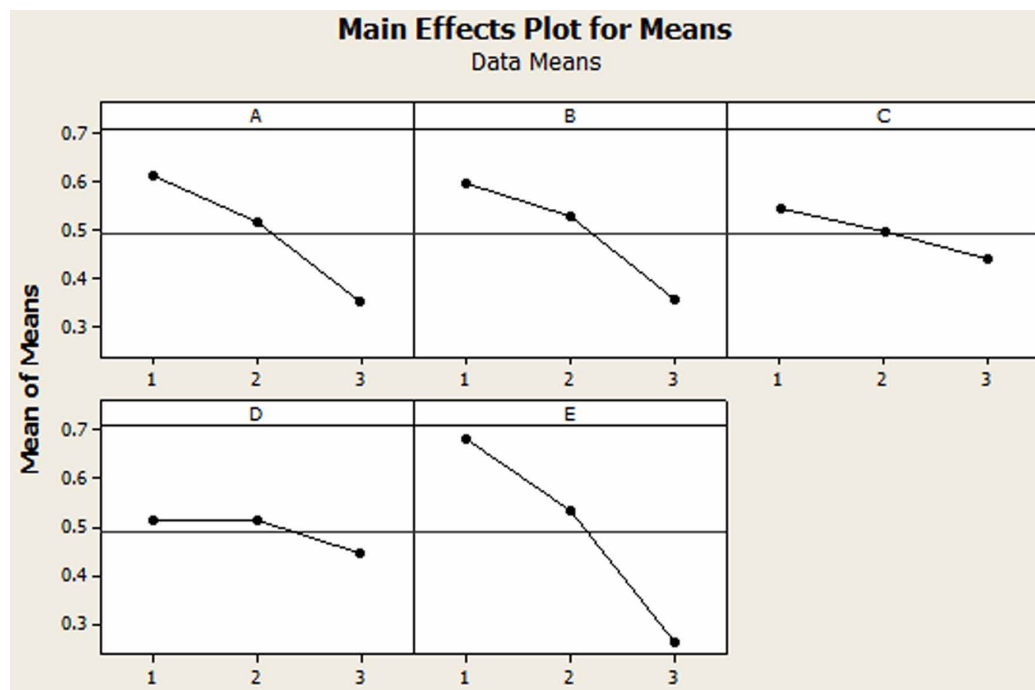


Table 8. Normalized decision matrix ( $r_{ij}$ ), weighted normalized decision matrix ( $v_{ij}$ ), best experimental run distance ( $D_{ij}^+$ ), worst experimental run distance ( $D_{ij}^-$ ) and the closeness coefficient ( $C_i$ )

Sl. No.	$r_{ij}$ (Ra)	$r_{ij}$ (Rt)	$r_{ij}$ (Rz)	$v_{ij}$ (Ra)	$v_{ij}$ (Rt)	$v_{ij}$ (Rz)	$D_{ij}^+$	$D_{ij}^-$	$C_i$
1	0.1532	0.1218	0.1027	0.0511	0.0406	0.0342	0	0.0755	1
2	0.1604	0.1533	0.1133	0.0535	0.0511	0.0378	0.0113	0.0658	0.8530
3	0.1963	0.1821	0.1900	0.0654	0.0607	0.0633	0.0382	0.0379	0.4984
4	0.1724	0.1466	0.1314	0.0575	0.0489	0.0438	0.0142	0.0614	0.8125
5	0.1676	0.1620	0.1437	0.0559	0.0540	0.0479	0.0197	0.0560	0.7394
6	0.1987	0.2002	0.1847	0.0662	0.0667	0.0616	0.0408	0.0348	0.4606
7	0.1867	0.1778	0.1687	0.0622	0.0593	0.0562	0.0309	0.0446	0.5904
8	0.1987	0.2056	0.2145	0.0662	0.0685	0.0715	0.0490	0.0273	0.3577
9	0.2203	0.2392	0.2304	0.0734	0.0797	0.0768	0.0620	0.0135	0.1792
10	0.1724	0.1509	0.1687	0.0575	0.0503	0.0562	0.0249	0.0525	0.6786
11	0.1748	0.1610	0.1740	0.0583	0.0537	0.0580	0.0281	0.0488	0.6349
12	0.1963	0.2002	0.2022	0.0654	0.0667	0.0674	0.0446	0.0312	0.4116
13	0.1700	0.1533	0.1650	0.0567	0.0511	0.0550	0.0239	0.0530	0.6891
14	0.1772	0.1721	0.1847	0.0591	0.0574	0.0616	0.0330	0.0438	0.5703
15	0.2250	0.2070	0.2198	0.0750	0.0690	0.0733	0.0539	0.0233	0.3021
16	0.1748	0.1600	0.1666	0.0583	0.0533	0.0555	0.0258	0.0505	0.6617
17	0.2011	0.1956	0.1953	0.0670	0.0652	0.0651	0.0426	0.0331	0.4377
18	0.2155	0.2291	0.2182	0.0718	0.0764	0.0727	0.0565	0.0190	0.2520
19	0.1724	0.1533	0.1756	0.0575	0.0511	0.0585	0.0272	0.0507	0.6504
20	0.1772	0.1935	0.1969	0.0591	0.0645	0.0656	0.0403	0.0367	0.4770
21	0.2274	0.2371	0.2448	0.0758	0.0790	0.0816	0.0658	0.0104	0.1367
22	0.1772	0.1721	0.1650	0.0591	0.0574	0.0550	0.0279	0.0479	0.6322
23	0.1867	0.1902	0.1969	0.0622	0.0634	0.0656	0.0404	0.0359	0.4708
24	0.2298	0.2640	0.2448	0.0766	0.0880	0.0816	0.0717	0.0050	0.0658
25	0.1939	0.2013	0.2038	0.0646	0.0671	0.0679	0.0450	0.0310	0.4081
26	0.2011	0.2271	0.2326	0.0670	0.0757	0.0775	0.0580	0.0188	0.2452
27	0.2346	0.2526	0.2592	0.0782	0.0842	0.0864	0.0732	0.0038	0.0494

closeness coefficient ( $C_i$ ) value is consider as higher is the better. Therefore, lower parametric level of the EDM parameters given optimum surface characteristics with help of AlSiMg RP tool electrode. From the main effect plot (Figure 10) and level average table (Table 10), the optimum parametric setting by the TOPSIS method are found to be V=20V, Ip=10A,  $\tau$ =67%, Ton=200 $\mu$ s and tool=AlSiMg RP tool.



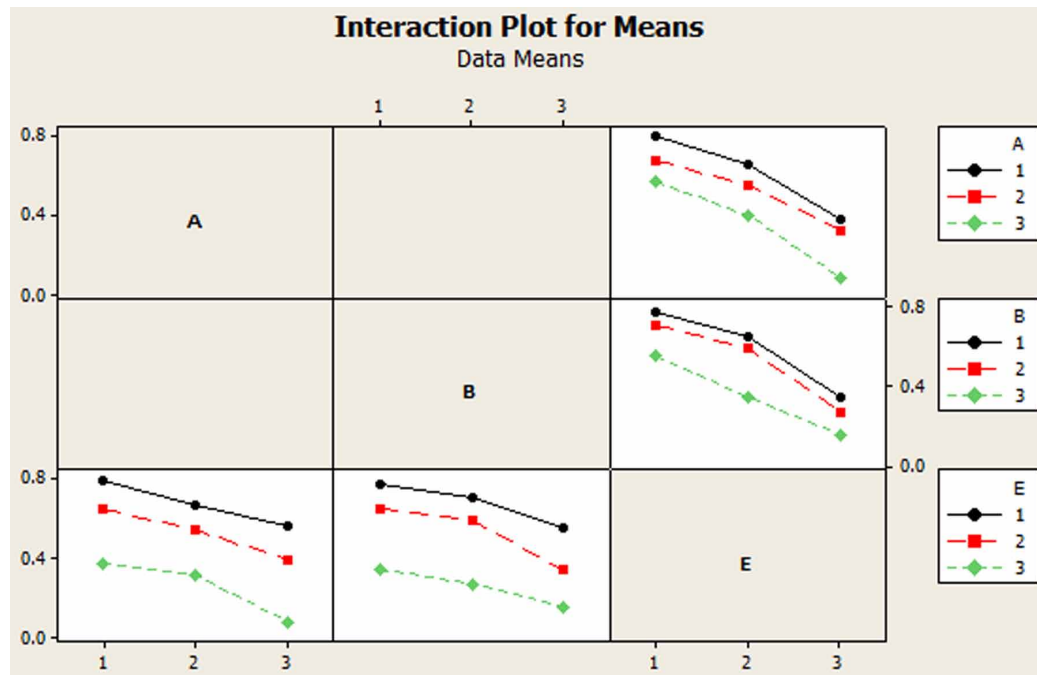
## Optimization of Surface Roughness Parameters

Table 9. ANOVA for closeness coefficient ( $C_i$ )

Source	DF	Seq SS	Adj SS	Adj MS	F	P	%Cont
A	2	0.31611	0.31611	0.158057	55.73	0.000*	20.69
B	2	0.27617	0.27617	0.138083	48.69	0.000*	18.07
C	2	0.04695	0.04695	0.023474	8.28	0.011*	3.72
D	2	0.02674	0.02674	0.013370	4.71	0.044*	1.75
E	2	0.81055	0.81055	0.405274	142.91	0.000*	53.04
A*E	4	0.01241	0.01241	0.003102	1.09	0.422	0.81
B*E	4	0.01653	0.01653	0.004133	1.46	0.301	1.08
Error	8	0.02269	0.02269	0.002836			0.84
Total	26	1.52814					100

\*Significant parameters at 95% confidence interval

Figure 11. Interaction plot for closeness coefficient ( $C_i$ )



## Optimization by VIKOR Method

By following the steps of the VIKOR method as explain in section 2.3 [Eqns. 13-18], the scaled responses ( $Y_{ij}$ ), utility measures ( $S_i$ ) and regret measures ( $R_i$ ) and multi criteria performance index i.e. the VIKOR index ( $Q_i$ ) are calculated and tabulated in Table 11. Here the all three responses are surface properties. Therefore, equal weightage (i.e. 0.333) is given to calculate the utility ( $S_i$ ) measures and

Table 10. Response table for means of closeness coefficient ( $C_i$ )

Level	A	B	C	D	E
1	0.6101*	0.5934*	0.5413*	0.5128	0.6803*
2	0.5153	0.5270	0.4934	0.5142 *	0.5318
3	0.3484	0.3535	0.4392	0.4468	0.2618
Delta	0.2618	0.2399	0.1021	0.0674	0.4186
Rank	2	3	4	5	1

\*Optimal parametric setting

Table 11. Scaled responses ( $Y_{ij}$ ), utility measures ( $S_i$ ), regret measures ( $R_i$ ) and the VIKOR index ( $Q_i$ )

Sl. No.	Yij(Ra)	Yij(Rt)	Yij(Rz)	Si	Ri	Qi
1	1	1	1	0	0	0
2	0.9118	0.7783	0.9320	0.1260	0.0740	0.1756
3	0.4706	0.5755	0.4422	0.5039	0.1859	0.5378
4	0.7647	0.8255	0.8163	0.1978	0.0784	0.2193
5	0.8235	0.7170	0.7381	0.2405	0.0943	0.2650
6	0.4412	0.4481	0.4762	0.5448	0.1863	0.5593
7	0.5882	0.6061	0.5782	0.4091	0.1406	0.4211
8	0.4412	0.4104	0.2857	0.6209	0.2381	0.6761
9	0.1765	0.1745	0.1837	0.8218	0.2752	0.8349
10	0.7647	0.7948	0.5782	0.2874	0.14059	0.3585
11	0.7353	0.7241	0.54422	0.3321	0.1519	0.3985
12	0.4706	0.4481	0.3639	0.5725	0.2120	0.6121
13	0.7941	0.7783	0.6020	0.2752	0.1326	0.3403
14	0.7059	0.6462	0.4762	0.3906	0.1746	0.4626
15	0.1176	0.4009	0.2517	0.74324	0.2941	0.8230
16	0.7353	0.7311	0.5918	0.3139	0.1361	0.3653
17	0.4118	0.4811	0.4082	0.5663	0.1973	0.5869
18	0.2353	0.2453	0.2619	0.7525	0.2549	0.7689
19	0.7647	0.7783	0.5340	0.3077	0.1553	0.3910
20	0.7059	0.4953	0.3980	0.4670	0.2007	0.5409
21	0.0882	0.1887	0.0918	0.8771	0.3039	0.9065
22	0.7059	0.6462	0.6020	0.3486	0.1327	0.3781
23	0.5882	0.5189	0.3980	0.4983	0.2007	0.5570
24	0.0588	0	0.0918	0.9498	0.3333	0.9879
25	0.5	0.4410	0.3537	0.5684	0.2154	0.6151
26	0.4118	0.2594	0.1701	0.7196	0.2766	0.7846
27	0	0.0802	0	0.9733	0.3333	1.0000

## Optimization of Surface Roughness Parameters

regret ( $R_i$ ) measures. The ANOVA for the VIKOR index ( $Q_i$ ) is presented in Table 12 with  $R^2=98\%$ . The main effect plot and interaction plot for the VIKOR index ( $Q_i$ ) are shown in Figure 12 and 13 respectively. The VIKOR index ( $Q_i$ ) value is consider as lower is the better. Therefore, lower parametric level of the EDM parameters given optimum surface characteristics with help of AlSiMg RP tool electrode. From the main effect plot (Figure 12) and level average table (Table 13), the optimum parametric

Table 12. ANOVA for VIKOR index ( $Q_i$ )

Source	DF	Seq SS	Adj SS	Adj MS	F	P	% Cont
A	2	0.34276	0.34276	0.171378	41.82	0.000*	20.74
B	2	0.26406	0.26406	0.132029	32.22	0.000*	15.98
C	2	0.06027	0.06027	0.030134	7.35	0.015*	3.65
D	2	0.02369	0.02369	0.011846	2.89	0.114	1.43
E	2	0.89091	0.89091	0.445457	108.71	0.000*	53.90
A*E	4	0.01251	0.01251	0.003126	0.76	0.578	0.76
B*E	4	0.02584	0.02584	0.006460	1.58	0.270	1.56
Error	8	0.03278	0.03278	0.004098			1.98
Total	26	1.65282					100

\*Significant parameters at 95% confidence interval

Figure 12. Main effect plot for VIKOR index ( $Q_i$ )

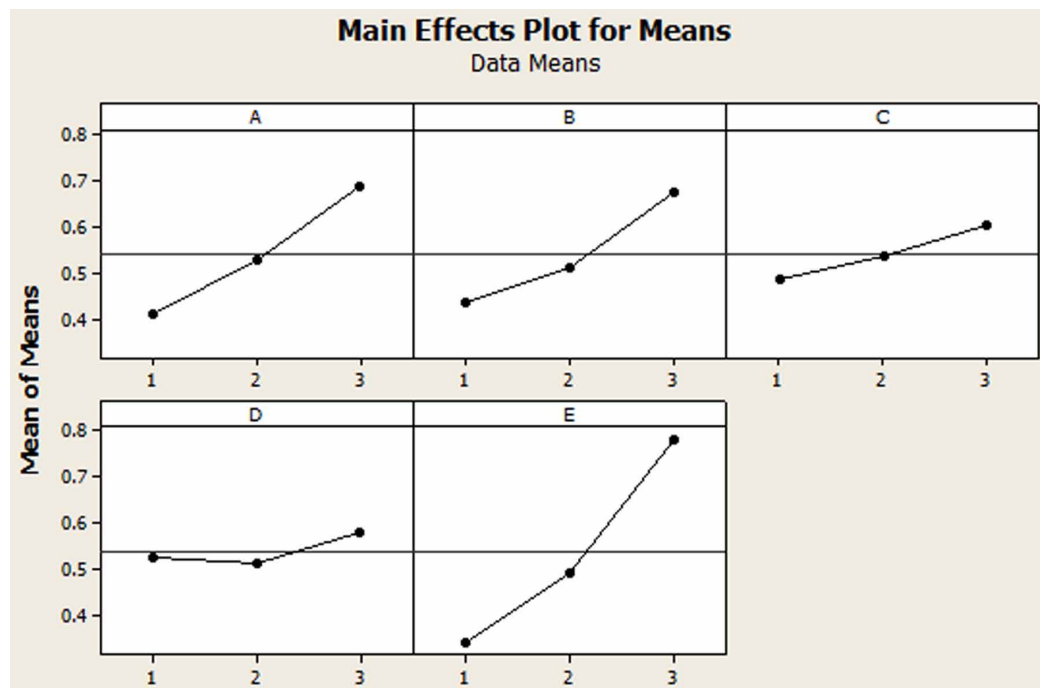


Figure 13. Interaction plot for VIKOR index ( $Q_i$ )

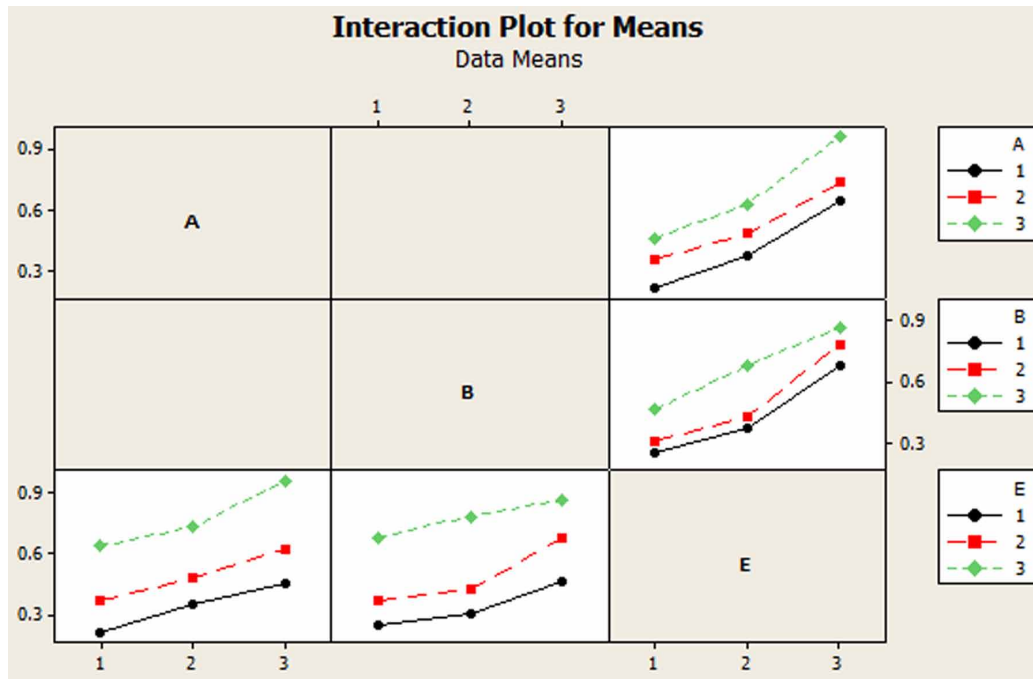


Table 13. Response table for means of VIKOR index ( $Q_i$ )

Level	A	B	C	D	E
1	0.4099*	0.4357*	0.4842*	0.5266	0.3432*
2	0.5240	0.5103	0.5347	0.5115*	0.4941
3	0.6846	0.6726	0.5996	0.5805	0.7812
Delta	0.2747	0.2369	0.1154	0.0690	0.4380
Rank	2	3	4	5	1

\*Optimal parametric setting

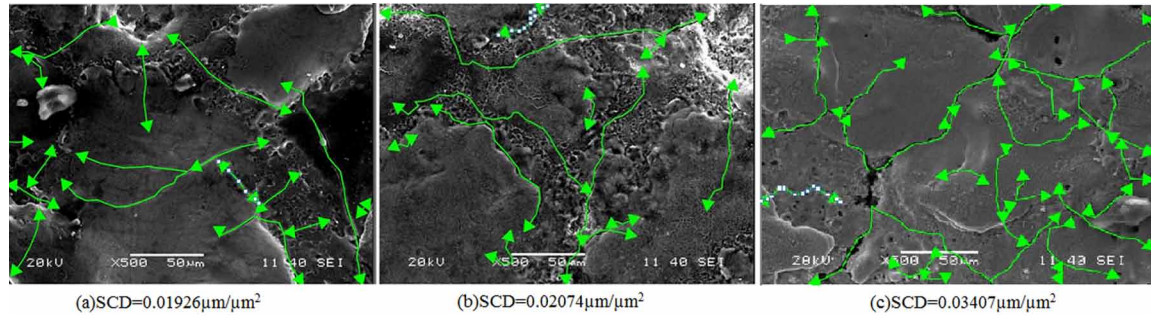
setting by the TOPSIS method are found to be  $V=20V$ ,  $I_p=10A$ ,  $\tau=67\%$ ,  $T_{on}=200\mu s$  and tool=AlSiMg RP tool.

## Surface Crack Density

The surface cracks are form due to the thermal stresses produce during the generation of very high temperature during the electrical sparking process. The surface cracks are also effect the performance of the machined parts during its applications. Therefore, surface cracks on the EDM machined surface must be as small as possible. The surface crack density (SCD) of the machined surfaces by the use of different tool electrodes are shown in Figure 14. It is found that, SCD of the machined surface produced

## Optimization of Surface Roughness Parameters

Figure 14. SCD produced on machined surfaces by different tool electrodes (a) AlSiMg RP, (b) Copper and (c) Graphite tool electrodes



by AlSiMg RP tool electrode is less as compare to copper and graphite tool electrodes. The SCD of machined surfaces by AlSiMg RP, copper and graphite tool electrodes are  $0.01926 \mu\text{m}/\mu\text{m}^2$ ,  $0.02074 \mu\text{m}/\mu\text{m}^2$  and  $0.03407 \mu\text{m}/\mu\text{m}^2$  respectively.

## CONCLUSION

The present work aims to improve the surface quality of the electrical discharge machining Titanium alloy (Ti6Al4V) work piece material. Taguchi's  $L_{27}$  orthogonal array is used to conduct the experiment. Three different types of tool electrodes like AlSiMg RP tool, copper and graphite tool electrodes are used during experiment by daring the EDM process parameters like voltage (V), discharge current ( $I_p$ ), duty cycle ( $\tau$ ) and pulse-on-time ( $T_{on}$ ). The surfaces roughness characteristics like average roughness ( $R_a$ ), maximum height of the profile ( $R_t$ ) and average height of the profile ( $R_z$ ) of the EDM machined surfaces are studied and the best parametric setting to get optimal surface finish is found out by using the multi-response optimization techniques like desirability function approach, TOPSIS and VIKOR method. The following conclusion can be drawn from the above experimental work.

1. Better surface properties can be achieve with lower values of the parametric setting, that are  $V=20V$ ,  $I_p=10A$ ,  $\tau=67\%$ ,  $T_{on}=200\mu s$  with the use of AlSiMg RP tool electrode.
2. With increase in the EDM parameters like voltage, discharge current and duty cycle the surface roughness values are increased with increase in the discharge energy, which produces more crater depth that increases surface roughness values. However, with increase in pulse-on-time the surface roughness values are first increase and then decrease. This is due to the increase in pulse-on-time the discharge energy increased that increase the crater depth, but after certain time the crater depth with increase in pulse-on-time the more crater depth is not formed with decreased in the surface roughness values.
3. Here three optimization techniques desirability function approach, TOPSIS method and VIKOR method are used to get the optimum parametric setting and by all the optimization techniques, same optimal parametric setting is found. However, desirability function approach required less calculation as compare to the other two techniques. So, by the use of desirability function approach less time is required to get the optimum parametric setting.

4. The ANOVA for individual surface characteristics (Ra, Rt, Rz) as well as for overall desirability index (do), The ANOVA for individual surface characteristics (Ra, Rt, Rz) as well as for overall desirability index (do), closeness coefficient ( $C_i$ ) and VIKOR index ( $Q_i$ ) are obtained. It is found that type of tool, discharge current and voltage are the most significant parameters, which influence the surface characteristics of the EDM machined Titanium alloy components.

## FUTURE RESEARCH DIRECTIONS

The present work describe the optimization of surface roughness parameters like average roughness (Ra), maximum height of the profile (Rt) and average height of the profile (Rz) during electro-discharge machining of Titanium alloy. Here, three different multi response optimizations techniques (desirability function approach, TOPSIS and VIKOR method) are used to get best parametric setting. Though, there are huge scopes in the field of electro-discharge machining process by using different types of tool electrodes prepared via additive manufacturing process with different composition of metallic powders. The output responses like surface crack density of machined surfaces, white layer thickness and material characteristics of the machined surface to be analyze. Different types of multi-response optimization techniques can be used to get the optimum parametric condition.

## REFERENCES

- Ahmed, L. S., & Kumar, M. P. (2016). Multiresponse optimization of cryogenic drilling on Ti-6Al-4V alloy using topsis method. *Journal of Mechanical Science and Technology*, 30(4), 1835–1841. doi:10.1007/12206-016-0340-1
- Arthur, A., Dickens, P. M., & Cobb, R. C. (1996). Using rapid prototyping to produce electrical discharge machining electrodes. *Rapid Prototyping Journal*, 2(1), 4–12. doi:10.1108/13552549610109036
- Assarzadeh, S., & Ghoreishi, M. (2013). A dual response surface-desirability approach to process modeling and optimization of Al 2 O 3 powder-mixed electrical discharge machining (PMEDM) parameters. *International Journal of Advanced Manufacturing Technology*, 64(9-12), 1459–1477. doi:10.1007/00170-012-4115-2
- Dewangan, S., Gangopadhyay, S., & Biswas, C. K. (2015). Study of surface integrity and dimensional accuracy in EDM using Fuzzy TOPSIS and sensitivity analysis. *Measurement*, 63, 364–376. doi:10.1016/j.measurement.2014.11.025
- Ding, Y., Lan, H., Hong, J., & Wu, D. (2004). An integrated manufacturing system for rapid tooling based on rapid prototyping. *Robotics and Computer-integrated Manufacturing*, 20(4), 281–288. doi:10.1016/j.rcim.2003.10.010
- Dürr, H., Pilz, R., & Eleser, N. S. (1999). Rapid tooling of EDM electrodes by means of selective laser sintering. *Computers in Industry*, 39(1), 35–45. doi:10.1016/S0166-3615(98)00123-7

- Gauri, S. K., & Chakraborty, S. (2010). A study on the performance of some multi-response optimisation methods for WEDM processes. *International Journal of Advanced Manufacturing Technology*, 49(1-4), 155–166. doi:10.100700170-009-2391-2
- Khan, A., & Maity, K. (2017). Application of MCDM-based TOPSIS method for the selection of optimal process parameter in turning of pure titanium. *Benchmarking: An International Journal*, 24(7), 2009–2021. doi:10.1108/BIJ-01-2016-0004
- Mohapatra, K., & Sahoo, S. (2018). A multi objective optimization of gear cutting in WEDM of Inconel 718 using TOPSIS method. *Decision Science Letters*, 7(2), 157–170. doi:10.5267/j.dsl.2017.6.002
- Pradhan, M. K., Das, R., & Biswas, C. K. (2009). Comparisons of neural network models on surface roughness in electrical discharge machining. *Proceedings of the Institution of Mechanical Engineers. Part B, Journal of Engineering Manufacture*, 223(7), 801–808. doi:10.1243/09544054JEM1367
- Sahu, A. K., Chatterjee, S., Nayak, P. K., & Mahapatra, S. S. (2018, March). Study on effect of tool electrodes on surface finish during electrical discharge machining of Nitinol. *IOP Conference Series. Materials Science and Engineering*, 338(1), 012033. doi:10.1088/1757-899X/338/1/012033
- Sahu, A. K., Mahapatra, S. S., & Chatterjee, S. (2017). Optimization of electro-discharge coating process using harmony search. In *International Conference on Materials, Manufacturing and Modelling (ICMMM)*. VIT University.
- Sahu, A. K., Mohanty, P. P., & Sahoo, S. K. (2017). *Electro discharge machining of Ti-alloy (Ti6Al4V) and 316L Stainless Steel and Optimization of process parameters by Grey relational analysis (GRA) method. In Advances in 3D Printing & Additive Manufacturing Technologies* (pp. 65–78). Singapore: Springer.
- Sait, A. N., Aravindan, S., & Haq, A. N. (2009). Optimisation of machining parameters of glass-fibre-reinforced plastic (GFRP) pipes by desirability function analysis using Taguchi technique. *International Journal of Advanced Manufacturing Technology*, 43(5-6), 581–589. doi:10.100700170-008-1731-y
- Singaravel, B., & Selvaraj, T. (2016). Application of desirability function analysis and utility concept for selection of optimum cutting parameters in turning operation. *Journal of Advanced Manufacturing Systems*, 15(01), 1–11. doi:10.1142/S0219686716500013
- Tang, Y., Hong, J., Zhou, H., & Lu, B. (2005). A new technique for the fabrication of graphite EDM electrodes. *Journal of Materials Processing Technology*, 166(2), 199–204. doi:10.1016/j.jmatprotec.2004.08.019
- Tripathy, S., & Tripathy, D. K. (2016). Multi-attribute optimization of machining process parameters in powder mixed electro-discharge machining using TOPSIS and grey relational analysis. *Engineering Science and Technology, an International Journal*, 19(1), 62–70.
- Zhao, J., Li, Y., Zhang, J., Yu, C., & Zhang, Y. (2003). Analysis of the wear characteristics of an EDM electrode made by selective laser sintering. *Journal of Materials Processing Technology*, 138(1-3), 475–478. doi:10.1016/S0924-0136(03)00122-5

## **KEY TERMS AND DEFINITIONS**

**Average Height of the Profile (Rz):** Average height of the profile (Rz) is the mean of the consecutive values of maximum height of the profile (Rt) calculated over the estimated length.

**Average Roughness (Ra):** The Average roughness (Ra) is the arithmetic mean of the absolute values of the profile heights along the estimated length.

**Electro-Discharge Machining (EDM):** Electro-discharge machining is a thermo-electrical material removal process by the succession of electrical sparks.

**Maximum Height of the Profile (Rt):** Maximum height of the profile (Rt) is the vertical distance between the highest and lowest points of the profile within the estimated length.

**Selective Laser Sintering (SLS):** Selective laser sintering process is an additive manufacturing (AM) technique used the powder fused based techniques to produce three dimensional components.



# Chapter 5

## Evaluation of Electrical Discharge Machining Performance on Al (6351)– SiC–B<sub>4</sub>C Composite

**Uthayakumar M.**

*Kalasalingam University, India*

**Suresh Kumar S.**

*Kalasalingam University, India*

**Thirumalai Kumaran S.**

*Kalasalingam University, India*

**Parameswaran P.**

*IGCAR, India*

### ABSTRACT

*Electrical discharge machining (EDM) process is a non-conventional machining process used for the material which are difficult to machine. In this research work, an attempt has been made to determine the influence of Boron Carbide (B<sub>4</sub>C) particles on the machinability of the Al (6351) alloy reinforced with 5 wt. % Silicon Carbide (SiC) Metal Matrix Composite (MMC) through EDM. Influence of machining parameters such as pulse current (I), pulse on time (Ton), duty factor (τ), and gap voltage (V) on affecting the output performance characteristics namely Electrode Wear Ratio (EWR), Surface Roughness (SR) and Power Consumption (PC) which are studied. The result shows that the addition of B<sub>4</sub>C particles significantly affects the machinability of the composite, with a contribution of 1.6% on EWR, 3.5% on SR and 19.8% on PC. The crater, recast layer formation, and Heat Affected Zone (HAZ) in the machined surface of the composite are also reported in detail.*

DOI: 10.4018/978-1-5225-6161-3.ch005

## INTRODUCTION

The metal matrix composites are having superior properties such as low density, high strength, light weight, lower thermal coefficient of expansion and good wear resistance. These materials are used in the various fields like aerospace, structural and automotive Industries (Ho & Newman, 2003). The recent research activity in MMC and its applications have been moved towards aluminum and aluminum alloy-based MMCs (Lindroos & Talvitie, 1995). The Aluminum metal matrix composites have wide application in the field of automotive engineering such as cylinder liner, piston and drive shaft and also in aerospace structure (Garg et al., 2010). The suitable fabrication method for MMCs is stir casting process since; this route is less expensive and appropriate to mass production (Kalaiselvan et al., 2011). However, aluminum metal matrix composites are hindered by high tool wear and poor machinability from the traditional machining process (Müller & Monaghan, 2000). Thus the non-conventional machining process like EDM is employed successfully to machine aluminum metal matrix composites (Taha, 2001). EDM is suitable to machine a composite material irrespective of their chemical and physical properties, but only applicable for electrically good conductor (Gopala Krishna & Prasad, 2009). Selection of EDM machining parameter is a difficult task, in order to improve the machining responses to achieve the requirements. The major response characteristics of electrical discharge machining process are surface roughness, electrode wear ratio and power consumption. In order to minimize product and process costs, the tool wear rate should be minimized with less effort. The optimal selection of input parameter is required to minimize the tool wear rate and maximize the material removal rate which in turn reduces the electrode wear ratio (Caroline et al., 2000). Rahman et al., (2010) have identified the influence of each input parameters with an aim to increase the metal removal while machining titanium alloy through EDM and concluded that the significant parameters are current and spark duration. Singh et al. (2012) have done machining on D3 tool steel by using die-sinking EDM with either copper or brass electrodes in kerosene dielectric. They found that a copper produced MRR at three times more than that when using an equivalent brass electrode. The on-time contributed to higher MRR significantly, but off-time had a less drastic change in MRR. Sultan et al. (2014) have reported the results of EDM on EN353 steel workpiece using copper tube electrode. Box-Behnken design was used for an experimental planning and they presented the results that MRR to be dependent not only on both peak current and on-time, but also off-time. Nur Seril et al., (2016) had attempted to predict material removal rate of different material using die sinking EDM process. The developed MRR model includes the EDM cumulative electrical charge for each cycle and melting temperature of workpiece material; it predicts two orders of magnitude closer to experimental data compared to a published model that is based on melting temperature and peak current alone.

The quality of the product is determined by the surface roughness measured on the machined region. Torres et al., (2014) have studied the performance of electrical discharge machining process on hard to machine alloys. They have done modeling to predict the surface finish, electrode wear and material removal rate with the variation of machining parameters. The experimental results show that the most influential factor in MRR and Ra is the current intensity and in the case of electrode wear is the pulse time. Karthikeyan et al., (1999) have done an analysis on the silicon carbide reinforced aluminum metal matrix composite, so as to predict the surface roughness by developing the mathematical model. Ahamed et al., (2009) have studied the EDM performance on the aluminum metal matrix composites to increase the metal removal, minimize the surface roughness and finally found that prolonged spark energy is required to remove the reinforced hard ceramic particle from the matrix. Patel et al., (2009) have investi-

gated the EDM performance on alumina-based composite and developed a mathematical model through the response surface methodology to predict the consequence of each parameter on surface roughness. The power consumption during machining of the composite material is also an important factor which plays major role in calculating the production cost. However, no literatures are reported with power consumption as an output response in EDM process and hence this study is proposed.

In this work, an evaluation of performance characteristics of electrical discharge machining has been planned on the Al (6351)-SiC-B<sub>4</sub>C composite. The significance of cutting parameter and its contribution on affecting the machining characteristics is identified through the Analysis of Variance (ANOVA). The surface characteristic of the prepared composites was also examined through Scanning Electron Microscope (SEM).

## EXPERIMENTAL METHODS

### Fabrication and Testing of Composites

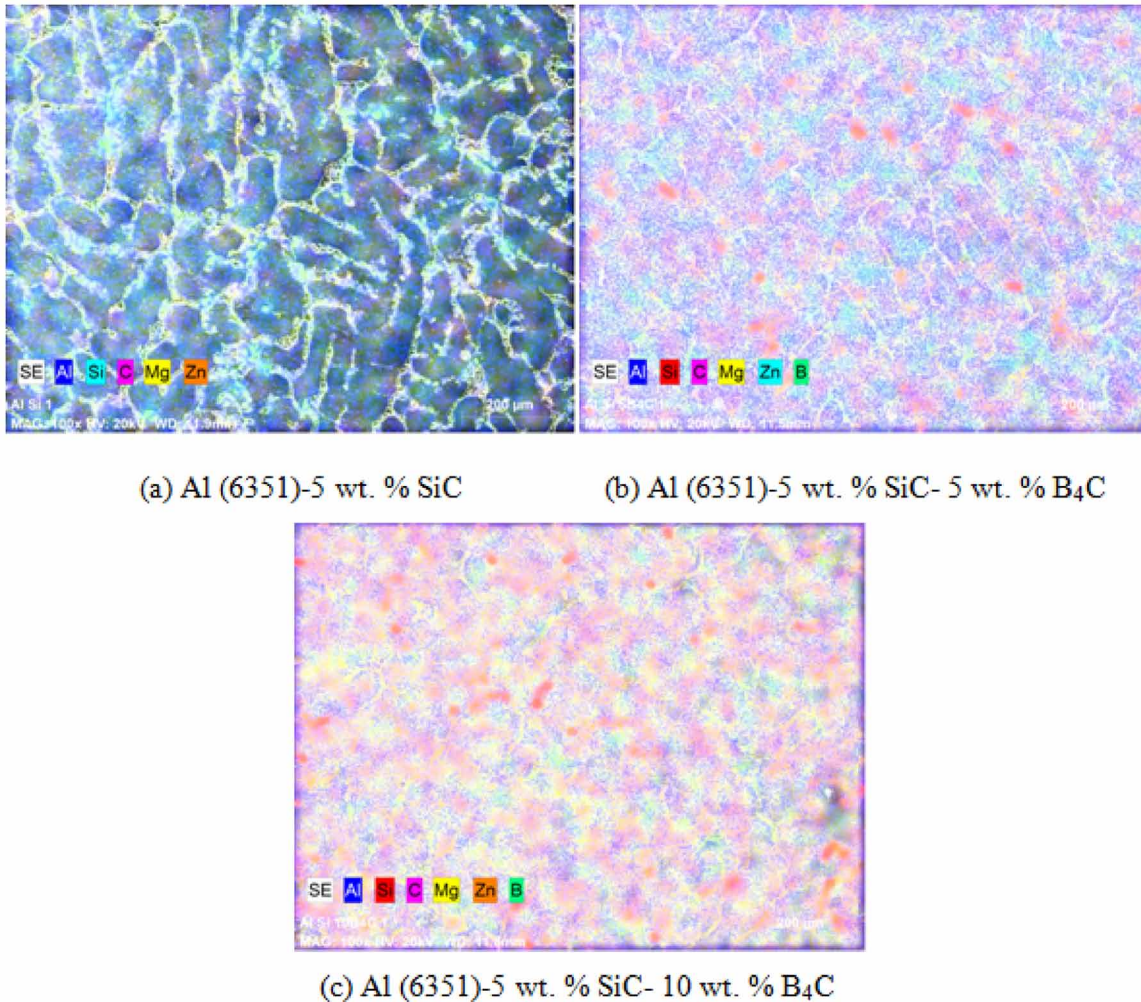
The prepared composite material consists of Al (6351) alloy as a matrix with the reinforcement of SiC of 5 weight % and the varying B<sub>4</sub>C weight % of (0%, 5%, and 10%) which are fabricated through the stir casting route. The SiC has good mechanical properties like low density, high hardness and it can highly withstand its properties at an elevated temperatures. B<sub>4</sub>C is also a hard ceramic particle which has neutron absorbing characteristics (Shorowordi, Haseeb, & Celis, 2006). The produced composite is suitable for nuclear applications as reactor control rod.

The Al 6351 cast rod is kept in the crucible and preheated in the furnace. The reinforcements are preheated to a higher temperature around 1000°C to 1200°C in order to oxidize their surfaces [Thirumalai Kumaran & Uthayakumar, 2014]. The particle size of the SiC is 60-75 µm and the B<sub>4</sub>C is 140-155 µm. The cast rod is heated above the liquidus temperature of 720°C and melted completely. This melt is cooled below to its liquidus temperature to maintain the cast in the semisolid stage (Suresh Kumar et al., 2014). The motorized stirring is employed while adding the preheated particles to the molten metal at speed of 500 rpm for a time period of 5-10 minutes to get uniform dispersion. The melt is maintained in the temperature range of 700°C ± 20°C while transferring to the mould of 100 mm diameter and 50 mm thickness. The specimens are prepared as per ASTM B557M-10 and the tensile and yield strength is reported in Table 1. The porosity is calculated based on the theoretical and experimental density. The uniform dispersion of particles in the aluminum phase is observed through microscopic image and is presented in Figure 1.

*Table 1. Properties of the composites*

Composites	Yield strength (N/mm <sup>2</sup> )	Tensile strength (N/mm <sup>2</sup> )	Theoretical Density (kg/m <sup>3</sup> )	Experimental Density (kg/m <sup>3</sup> )	Porosity (%)	Hardness (HB)
Al-5% SiC	81.37	105.62	2725	2621	3.81	66.81
Al-5% B <sub>4</sub> C -5% SiC	98.75	120.32	2715	2594	4.46	71.58
Al-10% B <sub>4</sub> C -5% SiC	107.43	132.48	2705	2616	3.29	76.78

*Figure 1. Microstructure of the composites*



## METHODOLOGY

The prepared composite specimen are subjected to machining through EDM powered with servo stabilizer unit (3 phase). A copper rod used as an electrode is connected with the positive polarity and workpiece is connected with negative polarity to carry out the experimental work. A 2 mm of machining depth is fixed for all the experiments. The details of the experimental work are shown in Table 2.

The experiments are done with varying input parameters namely, the pulse current, gap voltage, pulse on time and duty factor with an aim to decreases the responses such as electrode wear ratio, surface roughness and power consumption.

$$\text{Electrode wear ratio} = \frac{\text{Tool wear rate}}{\text{rate of metal removal}} \quad (1)$$

*Table 2. The details of Experimental work*

Considerations	Specification details
Machine	Electrical Discharge Machine (Make: M/s Electronica, Pune, India)
Dielectric medium	Electrol EDM oil
Dielectric flushing pressure	1.5 kg/cm <sup>2</sup>
Electrode	Copper rod (dia – 16 mm & length - 70 mm)
Process parameters	Pulse current (I) = 5-15A; Gap voltage (V) = 40-50V Pulse on time (T <sub>on</sub> ) = 50-100µs; Duty factor (τ) = 4-8,
Power harmonic analyzer	3φ/1φ True Root Mean Square (RMS) power clamp AC current-2000 A, AC voltage 600 V
Surface roughness measuring device	Mitutoyo - Surftest SJ-301

$$\text{Material Removal Rate} = \frac{\text{Amount of workpiece material removed}}{\text{Machining time}} \quad (2)$$

$$\text{Material removal rate} = \frac{\text{Amount of workpiece material removed}}{\text{Machining time}} \quad (3)$$

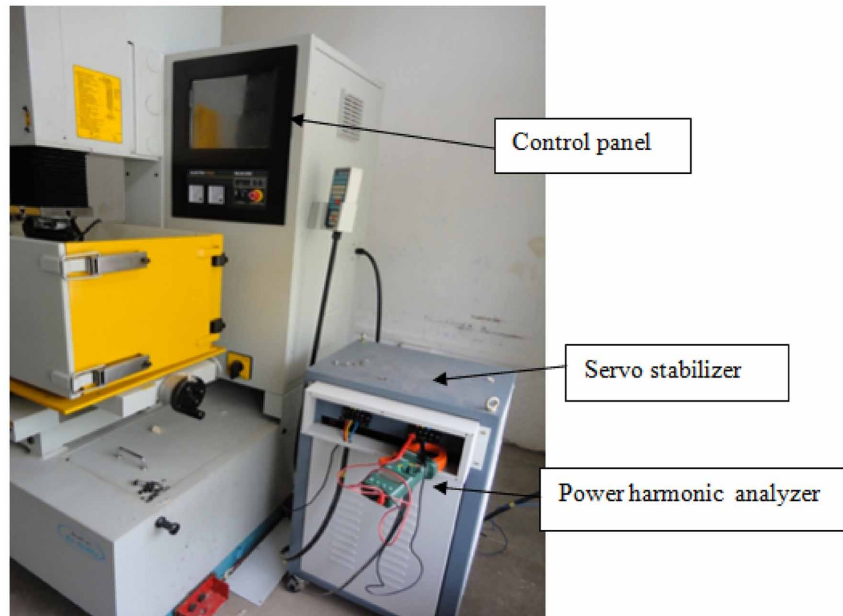
Electrode wear ratio (equation 1) can be defined as the ratio between the tool wear rate (equation 2) to the material removal rate (equation 3). The weight loss occurred in both tool and workpiece material during machining can be determined by weighing them before and after machining. Shimatzu weighing balance (AUX120), a high precision balance with an accuracy of 0.0001g is used to measure the weight.

The surface roughness on the electrical discharge machined surface is measured by a roughness measuring profile meter with the transverse speed of 0.25mm/s and the transverse length of 4mm.

The power harmonic analyzer measures the power consumption for the machining process by using the two probes inserted in the 3 phase EDM stabilizer at its corresponding terminals. This equipment directly read the power consumed for the given input during the machining and displays the value with the power factor. The measured power factor for all the experiments are ranges between 0.8 and 0.95. The typical EDM facility with power measurement setup is shown in Figure 2.

The number of experimental run is chosen based on degrees of freedom of each parameter and its levels. In this work, five factors which are set to three levels each. Hence, the total degree of freedom is 10. For the selection of design matrix, the total number of experiments should be greater than calculated degree of freedom. Thus, L27 orthogonal array is chosen to perform the experimental work and the interaction effect between the input parameter is eliminated (Narender Singh, Raghukandan, Rathinasabapathi, & Pai, 2004). The selected orthogonal array with the experimental result of all the three composites is shown in Table 3.

*Figure 2. Experimental setup*



## **RESULTS AND DISCUSSION**

### **Effect of Machining Parameters on Electrode Wear Ratio**

The amount of material eroded from the electrode, workpiece get increases with increase in the pulse current applied between two electrodes. Because, it discharges the electric energy in the spark gap and also melts and vaporizes material from the workpiece. The pulse current also increases the diffusion of spark energy which causes larger tool wear rate compared to the material removal rate. This will result in the increase of the electrode wear ratio. The electrode wear ratio is also found to be increased with the B<sub>4</sub>C content as a result of the occurrence of hard B<sub>4</sub>C particles on the matrix causes larger wear in the tool which is witnessed from Figure 3(a).

Figure 3(b) shows that electrode wear ratio decreases with increment in pulse duration. As spark duration increases, the carbon layer formed from decomposition of dielectric fluid during machining is adhered to the tip of the tool which may reduce the tool wear (Lin et al., 2012). However, the metal removal rate is increased with pulse duration which in turn reduces the electrode wear ratio. On the other hand, discharge of spark energy for a prolonged period, increases the discharge diameter and lowers the density of spark energy and hence the erosion of the tool is reduced (Sidhu, Batish, & Kumar, 2013).

The duty factor is in positive relation to the pulse duration at constant pulse current. When the duty factor gets increased, the spark density is also increased and results with an increase in the metal removal and reduces the electrode wear ratio. Figure 3(c) shows the decrease in the EWR with increase in the duty factor at constant pulse current. At higher current, a significant reduction of EWR is noticed. This may be due to the sudden increase of discharge energy into the spark gap.



## Evaluation of Electrical Discharge Machining Performance on Al (6351)–SiC–B<sub>4</sub>C Composite

Table 3. Experimental Result

Ex. No	Input parameters				Al-5% SiC			Al-5% B <sub>4</sub> C -5% SiC			Al-10% B <sub>4</sub> C -5% SiC		
	I (A)	T <sub>on</sub> (μs)	τ	V (Volts)	EWR (%)	SR (μm)	PC (kW)	EWR (%)	SR (μm)	PC (kW)	EWR (%)	SR (μm)	PC (kW)
1	5	50	4	40	0.511	4.95	1.13	1.319	6.31	1.21	0.239	5.49	2.66
2	5	50	6	45	0.538	5.45	2.22	1.145	4.88	2.14	0.248	4.54	2.13
3	5	50	8	50	0.767	6.73	2.47	1.585	4.86	1.98	0.294	6.48	2.3
4	5	75	4	45	0.520	5.54	2.06	1.09	6.19	3.58	0.460	5.83	2.7
5	5	75	6	50	0.365	5.93	2.19	1.081	7.78	2.66	0.506	5.88	2.8
6	5	75	8	40	0.411	10.75	2.04	0.623	6.05	2.56	0.404	6.19	2.18
7	5	100	4	50	0.374	6.96	2.53	0.797	5.07	4.18	0.239	5.34	2.56
8	5	100	6	40	0.411	6.13	3.19	0.238	6.75	3.28	0.138	6.38	2.55
9	5	100	8	45	0.110	8.13	4.21	0.238	9.77	2.78	0.193	6.61	1.72
10	10	50	4	40	1.077	6.46	2.52	1.630	6.98	2.68	2.583	8.21	1.66
11	10	50	6	45	1.780	7.94	3.43	1.960	7.06	3.71	2.445	7.79	2.12
12	10	50	8	50	1.469	8.24	3.13	2.006	7.38	2.19	2.206	6.91	2.14
13	10	75	4	45	1.670	7.18	3.01	1.282	7.34	3.23	1.893	7.93	1.98
14	10	75	6	50	1.122	7.69	3.2	1.649	7.85	2.75	1.710	9.11	2.04
15	10	75	8	40	1.487	8.53	3.18	0.797	8.54	1.72	1.737	7.83	2.01
16	10	100	4	50	0.812	8.97	3.52	1.52	7.88	2.56	1.130	7.69	1.85
17	10	100	6	40	0.821	9.31	3.37	1.2	7.59	1.37	0.883	9.52	1.87
18	10	100	8	45	1.068	9.88	3.71	0.357	7.82	1.6	0.947	8.31	1.63
19	15	50	4	40	3.139	6.98	2.67	2.739	8.9	2.57	3.181	8.48	1.75
20	15	50	6	45	2.573	9.05	2.32	2.482	8.66	1.79	2.997	8.56	1.64
21	15	50	8	50	2.108	9.38	2.03	2.5	8.91	1.64	2.629	8.81	1.35
22	15	75	4	45	2.154	9.66	1.64	2.024	10.19	1.91	2.500	10.03	1.47
23	15	75	6	50	2.427	11.29	1.88	2.381	9.13	1.47	2.169	9.27	1.49
24	15	75	8	40	1.624	7.75	1.57	0.623	9.07	1.78	2.206	9.74	1.4
25	15	100	4	50	2.145	10.74	1.87	2.482	9.55	2.11	1.939	8.95	1.36
26	15	100	6	40	1.241	8.92	3.24	1.291	9.87	1.32	1.845	12.82	1.12
27	15	100	8	45	1.542	11.17	1.68	1.182	10.38	1.33	1.820	13.33	0.85

A gradual increase in EWR is identified with voltage for lower percentage of B<sub>4</sub>C particle reinforced in the composite. When B<sub>4</sub>C content increases, wear ratio is also increased. However when the voltage increases, there is no significant increase in EWR for the 10 wt. % B<sub>4</sub>C reinforced composite (Figure 3(d)).

The influence of B<sub>4</sub>C particles on the matrix in order to affect the electrode wear ratio is calculated through ANOVA and presented in Table 4. It is found that the influence of B<sub>4</sub>C particle is around 1.6% and has a statistical and physical significance on affecting the electrode wear ratio at 95% confidence interval. The performance of Al- 5 wt. % SiC is found to be good to produce minimized electrode wear ratio.

Figure 3. Effect of machining parameters on EWR

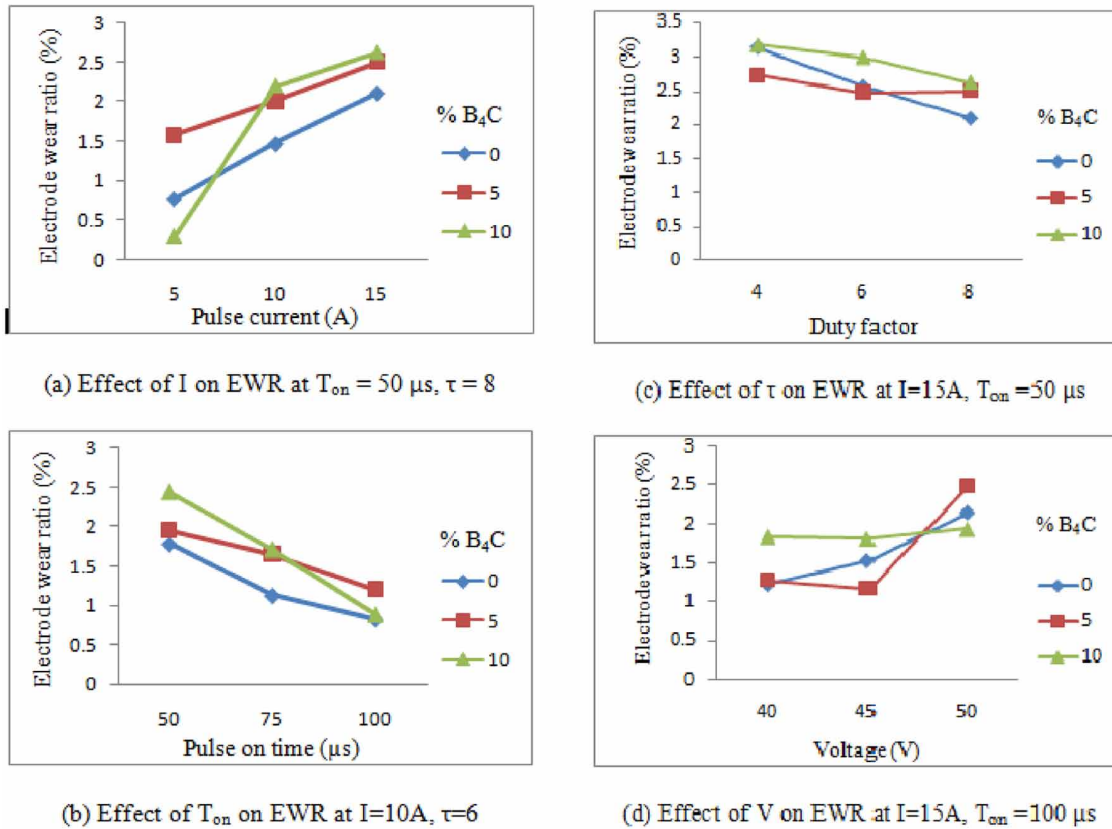


Table 4. ANOVA for EWR

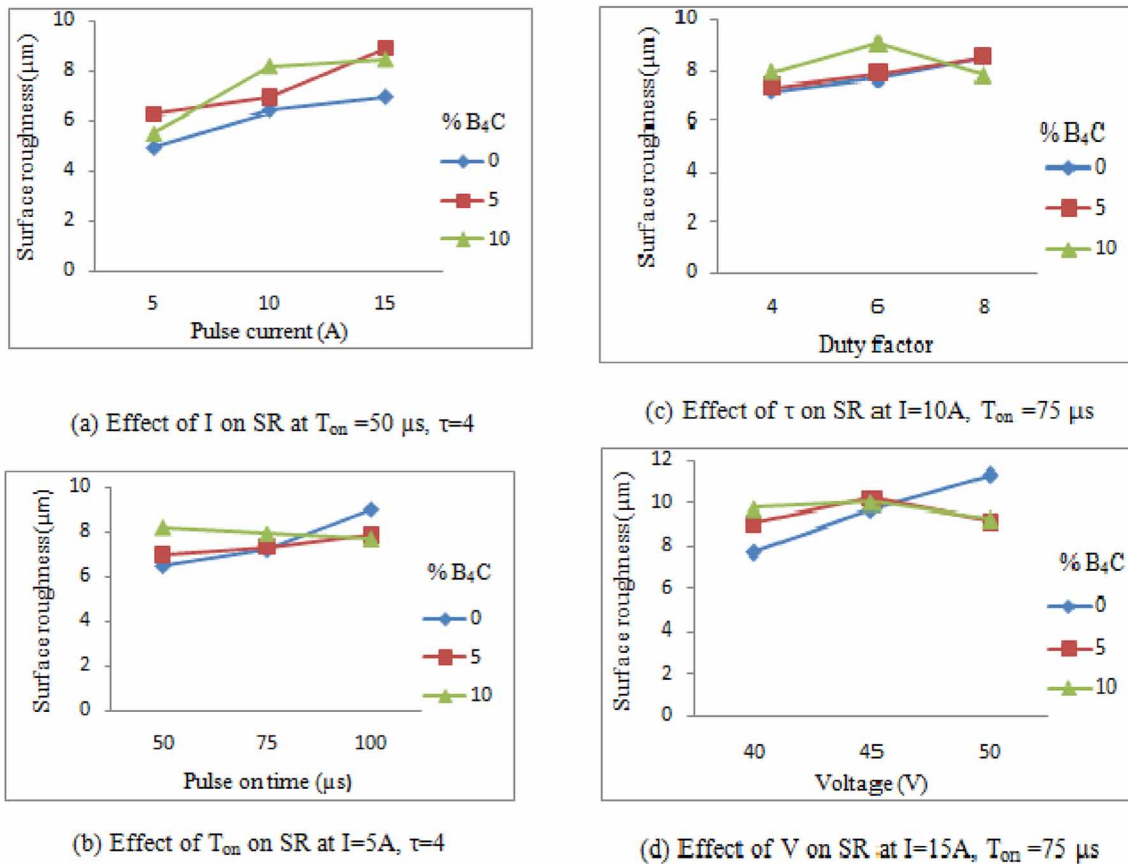
Parameters	Degrees of freedom	Sum of squares	Mean square	Contribution (%)	F value
Pulse current (I)	2	0.22057	0.11028	75.78	212.11
Pulse on time (T <sub>on</sub> )	2	0.02058	0.01029	7.07	19.795
Duty factor (τ)	2	0.01905	0.00953	6.55	18.326
Gap voltage (V)	2	0.01792	0.00896	6.16	17.233
B <sub>4</sub> C	2	0.00463	0.00232	1.59	4.4560
Error	16	0.00832	0.00051	2.86	
Total	26	0.29109			

## Effect of Machining Parameters on SR

Figure 4(a) shows the increase in SR with an increase in pulse current. When pulse current between the electrode increases, the discharge energy also increased gradually which produce bombarding forces in more quanta on the material (Kao, Tsao, & Hsu, 2010). The longer duration of spark discharge produces larger and wider craters on the composites with increased roughness. Hard ceramic particles present in the composites are not so easy to machine by the spark energy since it has a strong bonding with the matrix.



Figure 4. Effect of machining parameters on SR



The surface roughness is increased with the pulse duration at constant pulse current and duty factor. As pulse duration increases, more quantum of heat energy is produced through electric spark which forms cluster of craters on the machined surfaces which causes to poor finish (Gopalakannan, & Senthilvelan, 2013). In addition to this, longer the melt expulsion increases the roughness. A gradual increase in roughness value with an increase in the pulse on time is noticed in Figure. 4(b). However, a constant surface finish is observed at higher percentage of B<sub>4</sub>C particles.

From Figure 4(c), significant increase in surface roughness is noticed when the duty factor increases. At constant pulse current and pulse duration, roughness value is increased which is due to the reduced pulse off time. The melted material gets solidified on the machined surface and increases the roughness, which is due to the insufficient time elapsed for flushing (Mohammadreza et al., 2013).

A slow increase in the surface roughness is noticed with the voltage applied between electrodes. This is because of the increase in the spark energy which increases the material removal rate leading to rise in the SR. However, the presence of ceramic particle reduces the material removal rate and does not give sufficient energy to melt and vaporize the ceramic particles. Hence, decrease in SR is achieved when voltage increases beyond 45 V. In addition to this, the surface roughness is increased with an increase in the B<sub>4</sub>C particles at lower voltage, which is evident from the Figure 4(d).

Through ANOVA, the contribution of B<sub>4</sub>C particle on affecting the surface roughness on the machined composite is found to be 3.5%. All the parameters have statistical and physical significance on affecting the surface roughness which is shown in Table 5. The performance of Al- 5 wt. % SiC -5 wt. % B<sub>4</sub>C is found to be good to produce minimized surface roughness.

### Effect of Machining Parameters on PC

At constant pulse duration and duty factor, the PC is reduced with increased pulse current. At higher duty factor, the machining is done with higher efficiency and hence reduces the power required to melt the materials. The power consumption is reduced with the increase in B<sub>4</sub>C content in the composites which is witnessed from the Figure 5(a).

Power required to machine the material is increased as the T<sub>on</sub> increases at the constant pulse current and duty factor. Prolonged discharge of spark energy increases the electrical load and reduces the spark density thus increases the power consumption to melt the material (Suresh Kumar et al., 2014). Presence of ceramic particles in the composite material also increases the PC needed for the metal removal which is shown in Figure 5(b).

Figure 5(c) shows the variation of power consumption with the duty factor. At higher current, power consumed for the machining of the material is reduced continuously when the  $\tau$  value increases. Thus when the pulse off time reduces, the time provided for flushing away the melted material gets decreased and the power consumption also decreased gradually. While machining the composite, a ceramic reinforcement which is bound with the matrix gets pulled out at higher pulse current which results in poor finish.

A gradual increase in the power consumption is noticed with increase in gap voltage at higher pulse on time. Figure 5(d) shows that the increase in the B<sub>4</sub>C content reduces the power consumption for the machining. Longer pulse time removes the hard particles at minimized power input and reduced electrical load. However, slight decrease in power consumption at higher voltage and higher pulse duration is observed for the Al-SiC composite.

Through ANOVA, the contribution of B<sub>4</sub>C particles on affecting the power consumption on the machined composite is found to be 19.8% which is presented in Table 6. The performance of Al- 5 wt. % SiC -10 wt. % B<sub>4</sub>C is found to be good to consume less power.

*Table 5. ANOVA for SR*

Parameters	Degrees of freedom	Sum of squares	Mean square	Contribution (%)	F value
Pulse current (I)	2	0.19055	0.09527	70.09	644.652
Pulse on time (T <sub>on</sub> )	2	0.04393	0.02196	16.16	148.651
Duty factor ( $\tau$ )	2	0.02329	0.01165	8.57	78.805
Gap voltage (V)	2	0.00210	0.00105	0.77	7.109
B <sub>4</sub> C	2	0.00961	0.00480	3.53	32.51
Error	16	0.00236	0.00015	0.86	
Total	26	0.27186			

Figure 5. Effect of machining parameters on PC

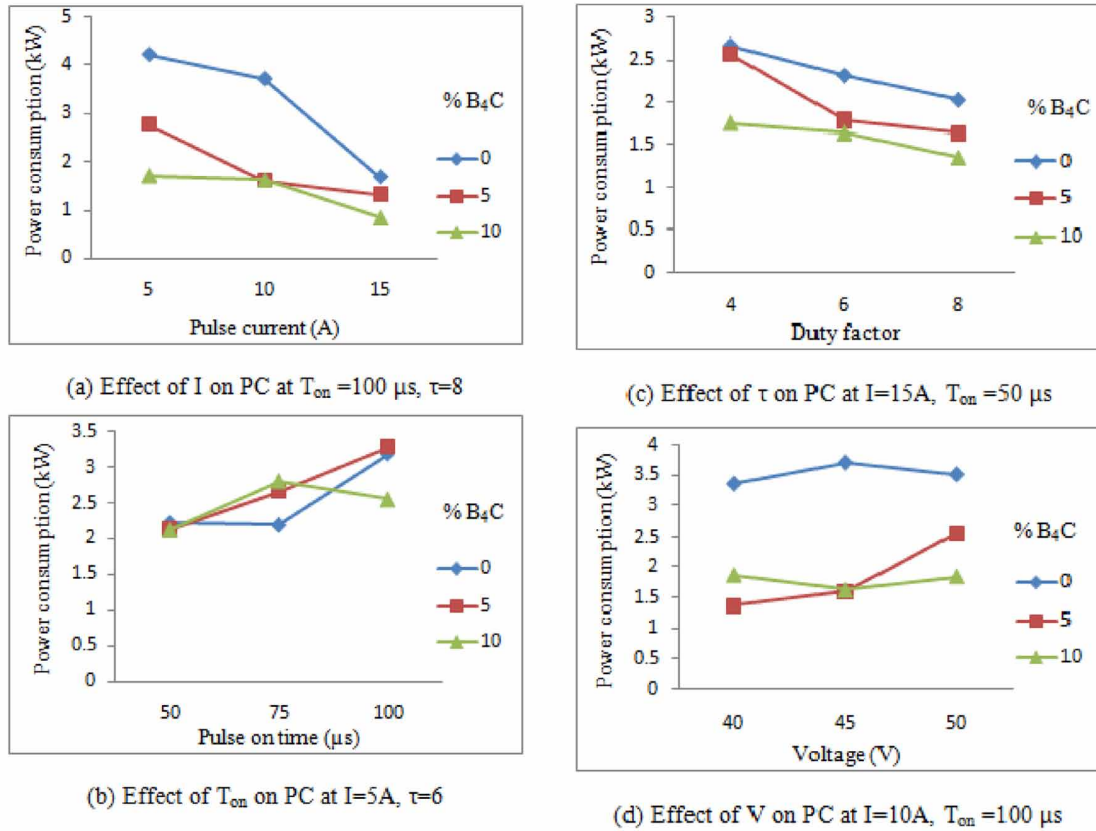


Table 6. ANOVA for PC

Parameters	Degrees of freedom	Sum of squares	Mean square	Contribution (%)	F value
Pulse current (I)	2	0.07095	0.03547	49.13	54.8254
Pulse on time (T <sub>on</sub> )	2	0.00813	0.00406	5.63	6.27959
Duty factor (τ)	2	0.00040	0.00020	0.28	0.31348
Gap voltage (V)	2	0.02598	0.01299	17.99	20.0817
B <sub>4</sub> C	2	0.02858	0.01429	19.80	22.0906
Error	16	0.01035	0.00065	7.17	
Total	26	0.14441			

## Machined Surface Analysis

The machined surface of the composite is transversely sectioned for the metallurgical examinations. At minimum current, the amount of heat energy formed in the spark gap is low. The sub surfaces of the composite and the surroundings observe partial amount of heat generated from the electrode gap. Hence, minimum heat energy is spent to melt and vaporize the material. The higher discharge current produces

enormous amount of heat energy between the electrodes and creates more bombarding forces on the material surface. This will result in the rejection of molten material and lead to forming poor surface finish on the machined areas.

When the pulse on time increases at constant duty factor, the plasma flushing efficiency gets reduced because of the time being spent for flushing out the molten material reduces. Hence, it keeps the molten material partially on the puddle area which re-solidifies and forms recast layer. Further, increase in the pulse duration generates higher heat energy to the sub surface of the materials.

The presence of ceramic particles reduces the efficiency of material removal and also the reinforcements do not melt while machining. This is a viscous operation which leads to the formation of white or recast layer. It is also noted that the reinforcements are deposited nearby this white layer with the matrix at higher discharge energy (Senthilkumar, & Uday, 2011). The machined surface are having waviness, white layer deposition and bubbles formation due to the collapse of the plasma during pause time on the molten metal and crater in the machined area of the different composite machined at same condition is presented in the Figure 6 (a-c).

The B<sub>4</sub>C particles present in the composite material affects the surface finish. When the B<sub>4</sub>C content in the matrix increases, the average crater diameter in the machined area for the same machining condition is also increased which leads to the increase in the surface roughness. In addition to this, it also increases the depth of heat affected zone in the composite.

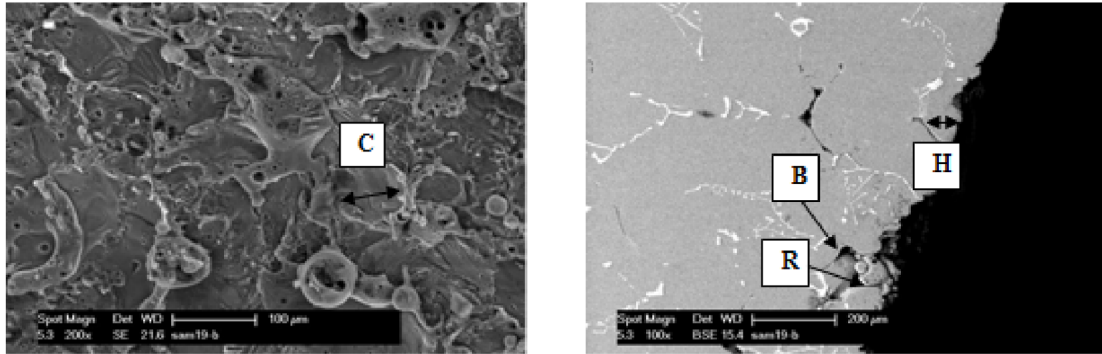
## CONCLUSION

The Al (6351)-5 wt. % SiC composite with varying weight percent of B<sub>4</sub>C particles (0%, 5%, 10%) is fabricated successfully by using the stir casting process and the following observations are made through EDM:

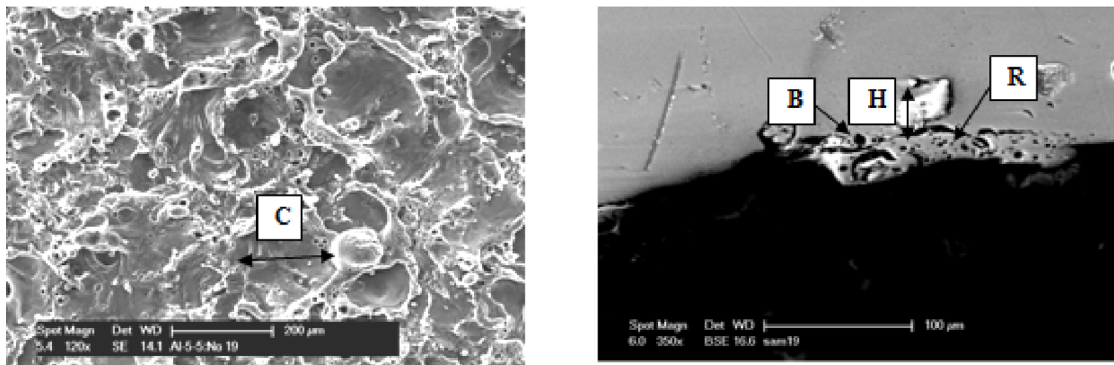
- Spark energy discharge between electrodes increases with pulse current which leads to higher tool wear and electrode wear ratio. However, duty factor and pulse duration have a negative influence on EWR.
- As the pulse current and pulse on time increases, a visible increase in surface roughness is observed. However, voltage does not contribute more on affecting it.
- Power consumption for the machining of composite material decreases with increase in pulse current and duty factor. However, pulse on time shows negative influence on it.
- Through ANOVA, it is found that the inclusion of B<sub>4</sub>C particles in the composite significantly affects the electrode wear ratio by 1.6%, surface roughness by 3.5% and the power consumption by 19.8%.
- The experimental analysis shows that Al-5 wt. % SiC composite produces minimized electrode wear ratio than hybrid composites. However, inclusion of 5 wt. % of B<sub>4</sub>C on the composite can produce better surface finish and 10 wt. % of B<sub>4</sub>C on the composite minimizes the power consumption.
- Higher pulse current produces more amounts of heat energy and bombarding forces which results in poor surface finish in the machined area. Higher pulse duration at constant duty factor, reduces the plasma flushing efficiency and forms a recast layer on machined areas.

## Evaluation of Electrical Discharge Machining Performance on Al (6351)–SiC–B<sub>4</sub>C Composite

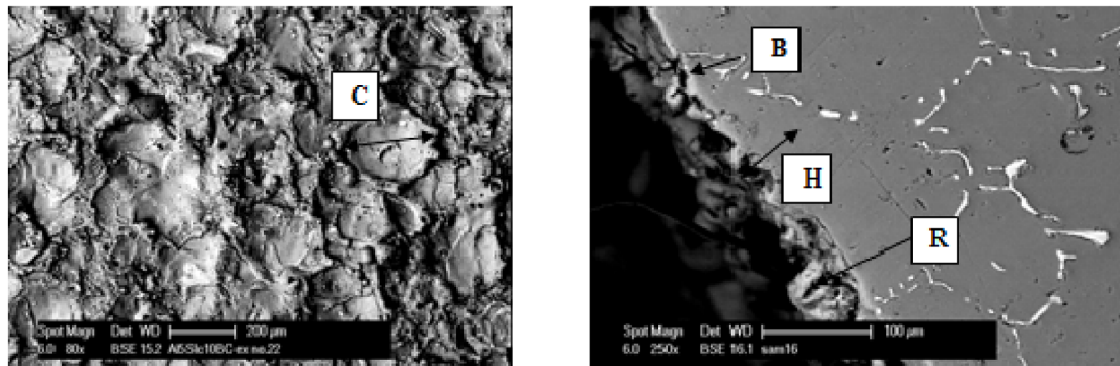
Figure 6. Formation of recast layer, bubbles, HAZ and crater



(a) Al-5 wt. % SiC composite



(b) Al- 5 wt. % SiC – 5 wt. % B<sub>4</sub>C composite



(c) Al- 5 wt. % SiC – 10 wt. % B<sub>4</sub>C composite

(R- Recast layer, B-Bubbles, H-Depth of heat affected zone and C-Crater diameter)

## ACKNOWLEDGMENT

The authors express their thanks to DAE-BRNS, Mumbai, for providing the financial support to carry out this work vide project no. 2012/34/39/BRNS. The authors also thank the Centre for Advanced Machining, Kalasalingam University, Krishnankoil, Tamil Nadu, India, for the support to carry out this work.

## REFERENCES

- Ahamed, A. R., Asokan, P., & Aravindan, S. (2009). EDM of hybrid Al-SiCp-B<sub>4</sub>Cp and Al-SiC<sub>p</sub>-glass<sub>p</sub> MMCs. *International Journal of Advanced Manufacturing Technology*, 44(5-6), 520–528. doi:10.100700170-008-1839-0
- Caroline, J. E. (2000). Machining of an aluminum/SiC composite using diamond inserts. *Journal of Materials Processing Technology*, 102(1-3), 25–29. doi:10.1016/S0924-0136(00)00425-8
- Garg, R. K., Singh, K. K., Sachdeva, A., Sharma, V. S., Ojha, K., & Singh, S. (2010). Review of research work in sinking EDM and WEDM on metal matrix composite materials. *International Journal of Advanced Manufacturing Technology*, 50(5-8), 611–624. doi:10.100700170-010-2534-5
- Gopala Krishna, A., & Prasad, D. V. S. S. V. (2009). Empirical modeling and optimization of wire electrical discharge machining. *International Journal of Advanced Manufacturing Technology*, 43(9-10), 914–925. doi:10.100700170-008-1769-x
- Gopalakannan, S., & Senthilvelan, T. (2013). A Parametric Study of Electrical Discharge Machining Process Parameters on Machining of Cast Al/B<sub>4</sub>C Metal Matrix Nanocomposite. *Proceedings of the Institution of Mechanical Engineers. Part B, Journal of Engineering Manufacture*, 227(7), 993–1004. doi:10.1177/0954405413479505
- Ho, K. H., & Newman, S. T. (2003). State of Art Electrical Discharge Machining (EDM). *International Journal of Machine Tools & Manufacture*, 43(13), 1287–1300. doi:10.1016/S0890-6955(03)00162-7
- Izwan, N. S. L. B., Feng, Z., Patel, J. B., & Hung, W. N. (2016). Prediction of Material Removal Rate in Die-sinking Electrical Discharge Machining. *Procedia Manufacturing*, 5, 658–668. doi:10.1016/j.promfg.2016.08.054
- Kalaiselvan, K., Muruganand, N., & Siva, P. (2011). Production and characterization of AA6061-B<sub>4</sub>C stir cast composite. *Materials & Design*, 32(7), 4004–4009. doi:10.1016/j.matdes.2011.03.018
- Kao, Y. C., Tsao, S. S., & Hsu, Y. (2010). Optimization of the EDM parameters on machining Ti-6Al-4V with multiple quality characteristics. *International Journal of Advanced Manufacturing Technology*, 47(1-4), 395–402. doi:10.100700170-009-2208-3
- Karthikeyan, R., Lakshmi Narayanan, P. R., & Naagarazan, R. S. (1999). Mathematical modeling for electric discharge machining of aluminum–silicon carbide particulate composites. *Journal of Materials Processing Technology*, 87(1-3), 59–63. doi:10.1016/S0924-0136(98)00332-X

- Lin, G., Lei, L., & Zhao, W. (2012). Electrical discharge machining of Ti6Al4V with a bundled electrode. *International Journal of Machine Tools & Manufacture*, 53(1), 100–106. doi:10.1016/j.ijmachtools.2011.10.002
- Lindroos, V. K., & Talvitie, M. J. (1995). Recent advances in metal matrix composites. *Journal of Materials Processing Technology*, 53(1-2), 273–284. doi:10.1016/0924-0136(95)01985-N
- Müller, F., & Monaghan, J. (2000). Non-conventional machining of particle reinforced metal matrix composite. *International Journal of Machine Tools & Manufacture*, 40(9), 1351–1366. doi:10.1016/S0890-6955(99)00121-2
- Narender Singh, P., Raghukandan, K., Rathinasabapathi, M., & Pai, B. C. (2004). Electric discharge machining of Al–10%SiCP as-cast metal matrix composites. *Journal of Materials Processing Technology*, 155–156, 1653–1657. doi:10.1016/j.jmatprotec.2004.04.321
- Patel, K. M., Pulak, M., Pandey, & Venkateswara Rao, P. (2009). Determination of an optimum parametric combination using a surface roughness prediction model for EDM of Al<sub>2</sub>O<sub>3</sub>/SiCw/TiC ceramic composite. *Journal of Materials and Manufacturing Process*, 24, 675–682.
- Rahman, M. M., Md. Khan, A. R., Kadirgama, K., Noor, M. M., & Baskar, R. A. (2010). Modeling of material removal on machining of Ti-6Al-4V through EDM copper tungsten electrode and positive polarity. *International Journal of Mechanical and Materials Engineering*, 3, 135–140.
- Senthilkumar, V., & Uday Omprakash, B. (2011). Effect of titanium carbide particles addition in the aluminum composite on EDM process parameters. *Journal of Manufacturing Processes*, 13(1), 60–66. doi:10.1016/j.jmapro.2010.10.005
- Shabgard, M., Ahmadi, R., Seyedzavvar, M., & Samad, N. B. O. (2013). Mathematical and Numerical modeling of the Effect of Input-parameters on the Flushing Efficiency of Plasma Channel in EDM process. *International Journal of Machine Tools & Manufacture*, 65, 79–87. doi:10.1016/j.ijmachtools.2012.10.004
- Shorowordi, K. M., Haseeb, A., & Celis, J. P. (2006). Tribo-surface characteristic B<sub>4</sub>C and Al-SiC composites worn under different contact pressures. *Wear*, 261(5-6), 634–641. doi:10.1016/j.wear.2006.01.023
- Sidhu, S. S., Batish, A., & Kumar, S. (2013). Fabrication and electrical discharge machining of metal-matrix composites: A review. *Journal of Reinforced Plastics and Composites*, 32(17), 1310–1320. doi:10.1177/0731684413489366
- Singh, H., & Singh, A. (2012). Effect of pulse on / pulse off time on machining of AISI D3 die steel using copper and brass electrode in EDM. *Journal of Engineering and Science*, 1(9), 19–22.
- Sultan, T., Kumar, A., & Gupta, R. D. (2014). Material removal rate, electrode wear rate, and surface roughness evaluation in die sinking EDM with hollow tool through response surface methodology. *Journal of Manufacturing Engineering*, 259, 1–16.
- Suresh Kumar, S., Uthayakumar, M., Thirumalai Kumaran, S., & Parameswaran, P. (2014). Electrical Discharge Machining of Al (6351)–SiC–B<sub>4</sub>C Hybrid Composite. *Materials and Manufacturing Processes*, 29(11-12), 1395–1400. doi:10.1080/10426914.2014.952024

Suresh Kumar, S., Uthayakumar, M., Thirumalai Kumaran, S., Parameswaran, P., & Mohandas, E. (2014). Electrical Discharge Machining of Al (6351)-5% SiC-10% B<sub>4</sub>C hybrid composite: A Grey Relational approach. *Modelling and Simulation in Engineering*, 2014, 7. doi:10.1155/2014/426718

Taha, M. A. (2001). Practicalization of cast metal matrix composites. *Materials & Design*, 22(6), 431–441. doi:10.1016/S0261-3069(00)00077-7

Thirumalai Kumaran, S., & Uthayakumar, M. (2014). Investigation on the machining studies of AA6351-SiC-B<sub>4</sub>C hybrid metal matrix composites. *International Journal of Machining and Machinability of Materials*, 15(3/4), 174–185. doi:10.1504/IJMMM.2014.060548

Torres, A., Puertas, I., & Luis, C. J. (2015). Modelling of surface finish, electrode wear and material removal rate in electrical discharge machining of hard-to-machine alloys. *Precision Engineering*, 40, 33–45. doi:10.1016/j.precisioneng.2014.10.001



# Chapter 6

## Recent Developments in Wire Electrical Discharge Machining

**Nadeem Faisal**

*Birla Institute of Technology, India*

**Sumit Bhowmik**

*National Institute of Technology Silchar, India*

**Kaushik Kumar**

*Birla Institute of Technology, India*

### ABSTRACT

*The tremendous growth of manufacturing industries and desired need of accuracy and precision has put a great importance on non-traditional machining processes. Metal and non-metals having properties like high strength, toughness, and hardness is generally machined by non-conventional machining methods. One of earliest non-traditional machining that is still in use and being effectively utilized in industries is wire electrical discharge machine. This machining technique gives a tough line of competition to conventional machining process like milling, grinding, broaching, etc. Cutting intricate and delicate shapes with accuracy and precision gives this machining technique an edge over other conventional machining and non-conventional machining processes. This chapter provides an insight to various research and prominent work done in field of WEDM by various scientists, researchers, and academicians. The chapter also emphasizes various advantages and disadvantages of different modelling and optimization methods used. The chapter concludes with some recommendations about trends for future WEDM researchers.*

### INTRODUCTION

One of the most widely and commonly used and popular non-traditional material removal procedure which is currently used often to manufacture components with complex shapes having great accuracy and precision is WEDM or better abbreviated as Wire Electrical Discharge Machining. Basically, it is deliberated as an extension of EDM (Electrical Discharge Machining) procedure which utilizes an electrode for starting the sparking process. Though, Wire-EDM uses a wire which acts as an electrode (as in

DOI: 10.4018/978-1-5225-6161-3.ch006

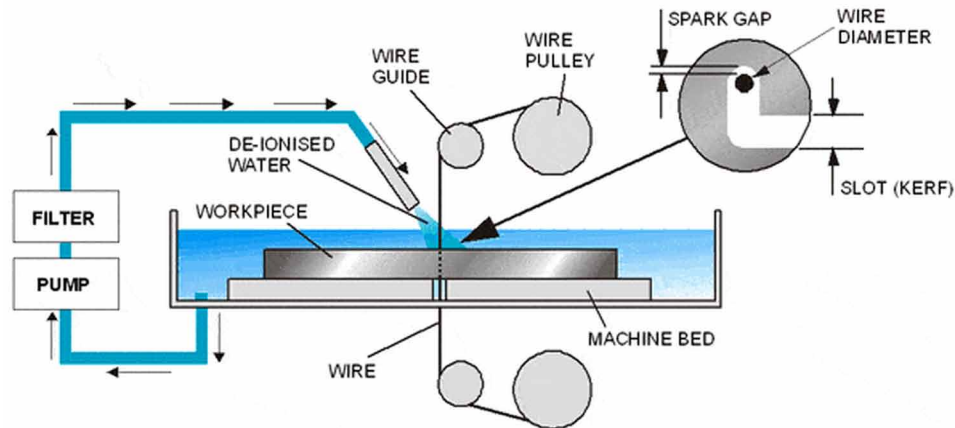
EDM) which is continuously traveling and is generally made up of thin brass, tungsten or copper, and is having a small diameter of 0.05-0.3 mm, and is quite competent of getting small corner radii. Part and the wire are submerged in dielectric (electrically non-conducting) fluid which additionally flushes away debris and acts as a coolant (Kuriakose and Shunmugam, 2004). Wire motion is regulated numerically to accomplish coveted 3-dimensional shape and high precision of work-piece (Mahapatra and Patnaik, 2006). With the help of a mechanical tensioning device, the wire is kept in tension, diminishing chances of creating inaccurate parts. Amid wire electrical discharge machining procedure, the material is eroded before wire and no immediate contact is there between workpiece and the wire, removing mechanical stresses amid machining. Likewise, the WEDM procedure can machine heat treated steels and high strength and temperature resistive (HSTR) materials.

WEDM were firstly used within industrial and manufacturing enterprises in the late 1960s. Advancement of the procedure was a consequence of looking for a system to supplant machined electrode utilized as a part of EDM. In the year 1974, D.H. Dulebohn connected optical line follower system to naturally govern the shape of section chosen to be machined by wire electrical discharge machining procedure (Jameson, 2001). By the year 1975, its acceptance was quickly increasing, as procedure and its capacities were well comprehended by companies and industries (Jameson, 2001). Just before the end of the 1970s, at a time when computer numerical control (CNC) system was brought into wire electrical discharge machining which achieved a noteworthy development of machining procedure. Subsequently, expansive capacities of WEDM procedure were widely used for any through-gap-opening machining inferable from wire, that needs to get through the part to be machined. Basic uses of wire electrical discharge machining incorporate extrusion tools and die, fixtures and gauges, models, airship and medical parts, and fabrication of stamping, grinding wheel form tools. This procedure has been generally utilized as a part of aviation, nuclear and car ventures, to machine exact, irregular and complex shapes in different hard to-machine electrically conductive materials (Jain, 2005; CunShan, 2012; Benedict, 1987). As of late, WEDM practice is additionally being utilized to machine a wide range of micro and miniaturized scale parts in sintered materials, alloys, cemented carbides, metals, ceramic and silicon (Mukherjee et al. 2012). These qualities make wire electrical discharge machining a procedure that has stayed as a competitive and economical machining choice satisfying requiring machining necessities forced by short product development cycles and growing expense [Ho et al., 2004; Jameson, 2001].

## **WIRE EDM PROCESS**

Wire Electrical Discharge Machining uses a continuously traveling/moving conductive wire (the most commonly used is brass). With the help of power supply rapid electric pulses are generated which creates a discharge between the work piece and the electrode (the wire is the electrode in Wire EDM process) (Figure 1). This discharge between the work piece and the electrode causes the melting and vaporization of the of a piece of the material from the work piece. In wire EDM, the conductive materials are machined with a series of electrical discharges (sparks) that are produced between an accurately positioned moving wire (the electrode) and the work piece. High-frequency pulses of alternating or direct current is discharged from the wire to the work piece with a very small spark gap through an insulating dielectric fluid (water). The heat of each electrical spark, estimated at around 15,000° to 21,000° Fahrenheit, erodes away a tiny bit of material that is vaporized and melted from the work piece. (Some of the wire material is also eroded away). These particles (chips) are flushed away from the cut with a stream

Figure 1. Wire EDM process



of de-ionized water through the top and bottom flushing nozzles. Any electrically conductive material can be machined regardless of the hardness of the material. The position of the wire with respect to the work piece is controlled in the x and y planes usually by CNC. Though on some machines the wire can be tilted to create tapered parts. The advantage of this Wire EDM is that zero mechanical stresses are created in the work piece because the wire does not make contact with it.

## RECENT DEVELOPMENTS IN WIRE EDM

A lot of research is being done in a most recent couple of years in wire EDM is, to increment metal removal rate, surface finish, tool life, and to limit time consumed for the procedure and so forth a portion of current advancements is discussed here.

## DEVELOPMENTS IN MACHINING COMPONENTS

### Wire Type

At the point when wire EDM was first presented, fundamental issues were wire material since the wire material ought to have many properties. Key physical properties that EDM wires must incorporate are, *Conductivity*, a high and good conductivity rating is imperative in light of the fact that, at any rate hypothetically, it implies wire may convey additional current, that compares to a ‘hotter’ spark and improved cutting rate.

*Tensile Strength*, that shows the capacity of wire to endure wire strain and tension, forced at wire amid cutting, keeping in mind end goal to mark a vertically straight cut. Also, significant properties are *Elongation*, which portrays in what way wire “gives” or gets plastically deforms before breaking. Another such property is, *Melting Point*, one will favor that wire electrode is fairly impervious to be melted too rapidly by electric sparks. Properties such as *Straightness*: which may favor the wire to remain straight.

Lastly, *Flush ability*, or in other words better flush-capacity, the quicker wire will cut and the possibility of wire breakage will diminish. *Cleanliness*, Wire can be “filthy”, because of pollution through residual metal powder available from drawing procedure, paraffin or drawing lubricant included to the wire by a few companies preceding to spooling. (Roger, 2007).

## **DIFFERENT WIRE MATERIALS**

### **Zinc Coatings**

Increased zinc level in wire electrode will improve execution of WEDM yet it is a problem to expand the level of zinc in wire o greater than 40%, because of wire drawing issues. Making alterations in wire grain structure could build wire excessively fragile for additionally preparing to fine diameters required for wire electrical discharge machining (Albert, 1997). To bypass it, zinc is mixed to the surface of the wire. Moreover, the zinc-coated wire could experience a secondary heat treatment procedure in an oxygen environment. This creates a very thin layer of oxide on the zinc surface, thus enables the wire to slide through wire guide and shields gentler zinc from chipping. This kind of coated wires offers the largest amount of efficiency by quicker cutting speed.

### **Brass Wires**

Different endeavors were made in recent times to enhance wire electrodes. Copper, that was in general practical usage at the beginning, were supplanted by brass. Different compounds composing of enhanced mechanical quality under traction are endeavored to enhance performance attributes of wire. It was found that the inclusion of (zinc + copper = brass) enhances cutting speed and execution when contrasted with copper in a few conducts. Amid cutting procedure, zinc in metal wire bubbles off, even vaporizes, that assists in cooling of wire and convey extra functional energy to work zone (Kern, 2007). Additionally, few zinc particles which were not sifted through of dielectric fluid will stay in the gap between electrode and work piece to help ionization of gap and cutting procedure. In a few conditions, huge brass deposit could stay on work piece after the cut that ends up being hard to expel. Since, it isn't possible and even convenient to cold draw wire having high zinc level in an overabundance of 40 percent, that prompted advancement of coated wires (Aoyama, 1999).

### **Coated Wire Electrodes [Brass/Copper Core]**

In the United States, earliest patent on Zinc coated wires (US Patent 1896613-1933) coordinated to change in nature of Zinc coated wires. In US Patent No. 14,927-1979, they unveiled, the wire electrode coated using an alloy or a metal bearing low vaporization temperature, for example, zinc, lead, antimony, cadmium, bismuth, tin, and alloys henceforth, securing center of wire contrary to thermal shock ensuing from rate of electrical discharge and which allows to increments frequency of electrical discharge deprived of risking cracking wire. US Patent No. 4,968,867-90 uncovers a wire electrode for WEDM, that incorporates a core wire enduring moderately higher thermal conductivity, low coating layer framed by a low-boiling point material (e.g., zinc) and an outermost layer of a metal possessing higher mechanical quality. Core wire is made from silver, copper, aluminum, or alloys. Some impacts, for example,

## ***Recent Developments in Wire Electrical Discharge Machining***

Vibration removal impact, thermal exchange effects and protection from breakage were watched which at last increments machining speed. Electrical Discharge Machining wire having a core made up of copper and a considerably nonstop coating of permeable epsilon phase brass, that said porous coating had been penetrated with graphite particles (US Patent No. 20070295695). High zinc level of epsilon stage coatings was discovered to coordinate execution of beta stage coatings. Along these lines, epsilon stage coating furnishes cutting execution at same level with beta or gamma stage coating, though at same time enduring a lower cost to make either beta or gamma stage.

### **Coated Wire Electrodes [Steel Core]**

For accomplishing great rigidity and strength, coating is done on steel wires. For better machining execution electrical discharge machining electrodes need to consume a decent electrical conductance, that empowers higher machining current to course over electrode and it needs to possess higher mechanical strength for increased traction force over machining zone. So as to acquire advantages wire electrode having firstly coating of copper on steel wire and after that plating a coating of lead, zinc, cadmium, tin, bismuth antimony, or compounds thereof were produced (US Patent 4287404-1981). Patents like Korean Patent No. 10-1985-0009194 reveals a wire electrode used for EDM, which incorporates a steel core coated along with copper or different parts [20], and copper-zinc alloy layer having CuZn10~CuZn50 composition coated on steel center. It is additionally acknowledged through earlier workmanship, for example by U.S. Patent No. 4,686,153-87, coating a copper clad steel wire with zinc and from that point to heat zinc coated wire to create interdiffusion among zinc and copper to along these lines change over zinc layer to a copper-zinc alloy. Also to bring to notice, U.S. Patent No. 4,686,153-87 portrays requirement of a beta phase alloy layer for electrical discharge machining. Copper and zinc have a percentage of zinc of around 45% by weight with percentage of zinc diminishing radially internally through external surface. Patent attested favored alloy material is a beta stage in the coating. Also to note, U.S. Patent No. 5,762,726-98 perceived high zinc content stages in the copper-zinc system, particularly gamma stage, will be extra attractive for EDM wire electrodes, yet powerlessness to adapt to the brittleness of these stages restricted business practicality of assembling such wire. U.S. Patent No. 4,998,552-91 uncovers a wire electrode for a travelling wire electrical discharge machining method, which incorporates a core built of steel, and a lower layer built up of homogeneous copper (Cu of 100%) and an upper brass layer with zinc of half by weight (about 50%). Core which is built of steel is encompassed by copper or copper alloy to frame a multi-layer structure, in this manner possessing a moderately huge mechanical strength. It is seen because of electric discharge, a force inverse to machining course is made on machining areas of wire electrode. Likewise, electromagnetic and electrostatic forces are made on wire electrode. Because of every one of these forces and because of vibrations of wire, real position of wire is unique in relation to programmed position. This outcome in exactness and accuracy issues. Deviation from customized and programmed outline at corners has as an outcome that round corners are acquired rather than coveted sharp corners. This prompted improvement of plain W(tungsten) or Mo (Molybdenum)- wires because of high elasticity and tensile strength (>1900 MPa). Inferable from downside of being costly and poor flush ability new kind of wire including a high quality perlite steel wire possessing carbon content greater than 0.06% and wire being a coating of copper free Zinc or Zinc alloy coating were developed. These outcomes in enhanced exactness and precision with increased mechanical load. High machining speed and enhanced surface finish were additionally acquired (US patent No.6875943-2005).

## **Diffusion Annealed Wires**

As Zinc coating had turned out to be a definitive coating aimed at improved execution. Zinc has a lower melting point and prerequisite of wires of higher zinc volume coating and higher melting point drove toward advancement of diffusion annealed wires. Moreover, it was revealed in US patent No.4935594-90, external layers of coated wire had richer zinc alloy. The encased wire is thereafter strengthened at such temperature till the point that alloy stretches out from outer surface to the core. Wire so delivered has a structural composition on its external coating having substantially more noteworthy protection regarding erosive wear compared to common eroding electrode. The alternative endeavor was made to enhance mechanical quality of electrodes although keeping up their advantages, for example, heat shield impact, removal of shot circuits. Generation rates were additionally increased with this development (US Patent No. 5196665-90). On numerous wire EDM operation, surface finish of part being created is of basic significance, it is in this way wanted to enhance speed of cutting without corrupting surface finish accomplished by cutting procedure. Also, it was revealed in U.S. Patent No.5, 945,010-97, that coating involved is copper-zinc alloy or coating is containing a nickel-zinc alloy. The core might include brass, copper clad steel, or other appropriate material. Coating 2nd metal can comprise of a metal chosen from a collection comprising of magnesium, aluminum, and zinc, by utilizing low temperature diffusion anneals. Subsequent EDM wire cuts speedier and preferable surface finish over traditional EDM wire electrodes or is fit for creating a prevalent finish at modest metal removal rates. The additional preferred standpoint of innovation is high zinc content in coating contrasted with earlier inventions of EDM wire that brings about an altogether volumetric heat of sublimation for coating and in this way make wire flush more productively although having enough diligence to endure EDM erosion process.

## **TECHNOLOGICAL AND PROCESS ENHANCEMENT**

### **Dry and Near Dry Wire Cut**

There exists a technique in wire EDM that is led to a gas atmosphere deprived of utilizing dielectric fluid, and the above approach is termed dry-WEDM. As of late, a novel technique has been presented in WEDM which is named Near-Dry Wire-Cut. In the above-named technique liquid, di-electric fluid is supplanted by base amount of liquid along with gas mixture (Boopathi, 2012).

Furudate and Kunieda (2001) directed examinations in dry WEDM (Wire Electrical Discharge Machining). It was discovered that in dry-WEDM, vibration of wire electrode is insignificant because of unimportantly little process response force. Furthermore, smaller gap distance and no corrosion for work piece amid machining are additional benefits of dry EDM. Such attributes can enhance precision and surface nature of work piece amid complete process of cutting. The fundamental downsides are bringing down material removal rate contrasted with traditional WEDM and streaks will probably be produced in the said strategy. Downsides could be settled by incrementing wire winding speed and diminishing genuine profundity of cut. These outcomes were in concurrence through different reports. For instance, Wang, et al. (2006); Wang, et al. (2008) examined finishing cut with Dry-WEDM and it was discovered, dry-WEDM have some preferred standpoint, for example, bring downs surface roughness, better straightness, and short gap length and primary hindrance of this technique was poorer material removal rate

in contrast to traditional method. In a contrast to this examination Abdulkareem et al. (2011) explored impacts of machining parameters on surface roughness in dry and wet WEDM, it was discovered, wet wire electrical discharge machining provides better surface roughness contrasted with dry wire electrical discharge machining, though to bring to notice, in this investigation normal machining had been considered (not finishing procedure).

Besides, Wang et al. (2006) contemplated High-speed wire electrical discharge machining (HS-WEDM) in Gas and emulsion fluid and test comes about have demonstrated that WEDM in environment offers a lot of points of interest, for example, better straightness accuracy and higher material removal rate. Other essential investigations work on dry WEDM are, for example, (Wang et al. (2004); Lu et al. (2012); Wang, et al. (2008); Furudate and Kunieda (2001); Wang et al. (2009); Wang et al. (2012).

### **Ultrasonic Vibrations**

Initiation of ultrasonic vibrations is a unique technique to enhance machining execution of hard to machine materials. It may cause a simple debris removal and in addition improvement of molten metal discharge because of making of huge pressure change amongst work piece and electrode. Henceforth, ultrasonic vibrations could be chiefly used for finishing procedures. Praneetpong et al. (2010) examined impacts on collective ultrasonic vibrations on machining attributes of Si<sub>3</sub>N<sub>4</sub>. They establish that ultrasonic vibrations must be connected afterward transition time is passed though vast amplitude values don't generally add to extensive MRR. In any case, surface roughness was expanded subsequently after introduction of ultrasonic vibration. Mohammadi et al. (2013) offered another technique for vibration transferal to wire in ultrasonic helped wire electrical discharge turning. From observation, they watched an optimum output power of ultrasonic transducer underneath that impact is irrelevant or if more it will short circuit and wire breakage can happen. Noteworthy diminishment in sliding friction was watched which was because of immediate changes in a vector of force, at last, adding to high MRR. Also to notice is the point that in roughing situation ultrasonic vibration impact was observed to be more noteworthy. Guo et al. (2014) contemplated machining component of wire EDM alongside ultrasonic vibration and found joined innovation of wire EDM and ultrasonic vibration encourages type of numerous channel discharge and increase use ratio of energy which prompts a change in surface roughness and cutting rate. Higher frequency vibration of wire enhances discharge concentration and decreases likelihood of wire rupture.

### **Machining of Composite Materials**

Composite material is produced using at least 2 constituent materials with essentially extraordinary chemical or physical properties which when joined, deliver a material having attributes unique in relation to singular components. Here procedure parameter and in addition machining capacity of composite materials, for example, ceramic semiconductors carbon materials has been contemplated with an orientation to wire electrical discharge machining and electrical discharge machining. Lavwers et.al (2004) introduced a very detailed examination of material removal mechanism of nearly financially accessible electrical conductive ceramic materials over investigation of debris and surface/subsurface quality. ZrO<sub>2</sub>-based, Si<sub>3</sub>N<sub>4</sub>-based and Al<sub>2</sub>O<sub>3</sub>-based ceramic materials by addition of electrical conductive stages for e.g., TiCN and TiN were examined. From observation, it was discovered that other than ordinary EDM material removal system like evaporation/melting spalling, another mechanism, for example, oxidation

and decay of base material could happen. Though latter particularly happens inside EDM of Si<sub>3</sub>N<sub>4</sub>-Tin utilizing deionized water. Additionally, spalling impact was glad to be unequivocally linked of formation breaks which were not perceived in machining of ZrO<sub>2</sub>-Tin that has high fracture toughness, contrasted with others.

Researchers like S. Lopez et.al (2001) introduced attributes of ceramic based semiconductor/oxide metal/nanocomposites and tried. likelihood of handing their composition over a request to give machinability by EDM. On observation their team found that by adding a metal and semiconductor to a superior ceramic, a composite which consolidates great electrical conductivity of both metal and semiconductor, with higher Mechanical properties of matrix could be delivered metal place a twofold part (a) through mechanical perspective great metal/ceramic interface gives composite fantastic mechanical properties. (b) by electrical perspective, Nickel gives machinability by electrical discharge machining to tests with adequate lower resistivity. Also, researchers like Hanaoka et. al (2013) contemplated discharge conduct of Si<sub>3</sub>N<sub>4</sub> ceramic/carbon nanostructure composite and EDM was completed utilizing capturing electrode methodology that helped in acquiring a superior hole edge shape when contrasted with normal or common technique and protecting Si<sub>3</sub>N<sub>4</sub> ceramics and Si<sub>3</sub>N<sub>4</sub>/CNT and Si<sub>3</sub>N<sub>4</sub>/GNP. Nanocomposites could be machined through this strategy. In any case, properties of electrode wear ration and surface roughness were superior in conductive materials yet MRR were discovered better in insulating materials.

## **Powder Mixed WEDM Using FEM**

Kansala et. al. (2008) suggested a basic and effectively sensible model for an axisymmetric 2-dimensional model for Powder Mixed EDM (PMEDM) utilizing FEM (Finite Element Method). Model utilizes numerous essential highlights, for example, temperature sensitive material attributes, size and shape of heat source (Gaussian heat flux distribution), % dissemination of heat amongst tool, dielectric fluid, material discharge effectiveness, pulse on/off time, work piece, and phase change etc., and so forth to see thermal conduct and material removal mechanism in Powder Mixed EDM (PMEDM) process. Model shows initially figure temperature diffusing in work piece material utilizing ANSYS programming and after that material removal rate (MRR) was quite predictable by temperature profiles. Impact of different process parameters on temperature flows alongside radius and depth of work piece had been contemplated. At long last, validation was finished by relating hypothetical MRR with test MRR got from a recently composed trial setup (Kansala et al. (2008); Kumar A., (2012)).

## **PROCESS RESPONSES**

### **MRR and CS**

Loads of research attempted to boost material removal rate and cutting speed by various methodologies. Since these elements could increment, monetary advantages in WEDM significantly. Relatively both these variables (cutting speed and material removal rate) decide similar marvels, that is machining rate.

Researchers like Rajurkar and Wang (1993) examined wire rupture phenomenon through a thermal model and trial examination. They discovered that material removal rate in wire electrical discharge machining increments at first with diminishing pulse off time. Notwithstanding, at a shorter pulse off time, gap turn out to be unstable which prompts a diminishment in machining rate. Also researchers



like, Singh and Garg (2009) displayed impacts of process parameters on material removal rate in wire electrical discharge machining, and it was discovered that, pulse on time and peak current increment material removal rate additionally increment however by expansion of servo voltage and pulse off time, MRR diminishes. The above mentioned outcomes were in concurrence with the one detailed by Po-Huai et al. (2011). Also, Poro's and Zaborski. (2009) examined effects of wire and work piece material on WEDM effectiveness, they discovered that high value of thermal conduction, and particularly heat capacity of machined material would cause diminishing of proficiency of wire electrical discharge machining. Besides, they also established that the specific heat capacity and thermal conductivity ended up being most noteworthy aspects in work piece that may decide MRR and volume of heat influenced zone. In another notable work (Mahapatra and Patnaik, 2006a) an endeavor was made to decide imperative machining constraints for execution measures like MRR, kerf width, thermal conductivity in wire electrical discharge machining procedure. Parameters like pulse duration, and dielectric flow rate, discharge current, and their relations had been found to assume a noteworthy part in harsh cutting processes for maximizing MRR. Shah, et al. (2011) examined impact of work piece thickness on MRR, it was normal that this parameter was a critical one though as per this exploration work piece thickness isn't a huge factor for MRR. Konda et al. (1999) arranged different potential variables influencing WEDM performance methods in 5 noteworthy categories. Where  $W$  and  $W_a$  are weights of work piece material before categories to be specific, diverse properties of work piece material and subsequently to machining (g), respectively. Dielectric fluid, machine characteristics,  $T$  is machining time (sec), adjustable machine and  $p$  is thickness of work piece material. Cutting speed likewise processes by partitioning cutting length by equivalent cutting time. Based on hypothesis increasing peak current could build energy of each discharge, delivering more extensive and more profound craters which causes to have higher MRR. Likewise incrementing pulse on time may increment term of each discharge which may expand MRR. Loads of studies affirm these speculations, for example, Tosun, et al. (2004) exhibited an examination on advancement and impact of machining parameters on material removal rate and kerf. In the said work, level of significance of machining parameters on material removal rate was established by utilizing ANOVA. Also, it was discovered, pulse duration and open circuit voltage were exceptionally successful constraints though wire speed and moreover dielectric flushing pressure was less viable element. As indicated by this examination open circuit voltage for monitoring material removal rate was around 6 times more vital than secondary factor (pulse duration). Furthermore, they applied design of experiments (DOE) procedure to optimize and investigate conceivable impacts of factors amid process design and development, and approved trial comes about utilizing noise to signal (S/N) ratio examination. There are vital investigations that work on MRR, for example, (Kozak et al., 1994; Spedding et al., 1997a; Kung and Chiang, 2008; Parashar et al. 2012)

## **Surface Roughness**

Heaps of investigation attempted to limit surface roughness by various methodologies. Based upon hypothesis surface roughness altogether influenced by peak current, pulse on time, surface roughness and cutting speed take an altogether opposite relationship. In light of the work done by Sarkar et al. (2008) examination surface roughness decrease as cutting rate increments. As indicated by various researcher's pulse on time is a huge factor which influences surface roughness. Apart from that, as pulse on time expands, surface roughness builds in light of "double sparking". In alternate words double sparking and localized sparking turn out to be more incessant as pulse on time increments. Double sparking yields

poor surface finish. The said outcomes are in concurrence with those revealed by Sarkar et al. (2005); Kanlayasiri and Boonmung (2007a, 2007b) and Kumar et al. (2012). Sarkar (2005) affirms that pulse on time is utmost imperative parameters which impacts on surface roughness trailed by peak current for zinc coated wire. Researchers like Kanlayasiri and Boonmung (2007a, 2007b) established that peak current and pulse on time have noteworthy impact on surface roughness and as the said variables increment surface roughness ends up noticeably being large. Also, Kumar et al. (2012) likewise affirms that bigger peak current and pulse on time would reason to double sparking that increases surface roughness values. Moreover, Tosun, et al. (2003) researched impacts of cutting attributes on size of erosion craters (depth and diameter) on wire electrode. Examination of wire electrode gaps is vital for comprehension of kerf size, wire rupture, surface roughness, of workpiece. Bigger size of gaps on wire increment danger of wire rupture and furthermore cause in poor work piece surface quality and poor machining accuracy. It was discovered that increasing open circuit voltage, pulse duration and wire speed increments crater size, while increasing dielectric flushing pressure diminishes crater size. Researchers like Rao et al. (2011) had expressed their efforts to optimize surface roughness and from investigation it was discovered that, constraints like pulse on time and peak current are generally critical. Servo voltage and Wire tension are noteworthy and flushing pressure, pulse off time and wire speed are lesser huge variables which influences surface roughness.

These outcomes are in concurrence with Kumar, et al., (2012) and Vamsi et al. (2010) and examination. Also, Haşçalık, A. and, Çaydas, U., (2004), examine impacts of various constraints on surface roughness. It uncovers that SR (surface roughness) expanded when pulse duration and open circuit voltage was incremented. It creates the impression that surface roughness principally relies upon these constraints, dielectric fluid weight and wire speed not appearing to have quite a bit of impact.

Recent investigations from Mahapatra and Patnaik (2006b) considered impacts of 6 factor incorporating, wire tension, discharge current, pulse frequency, wire speed, pulse duration, dielectric flow rate on SR surface roughness and MRR and it was discovered that parameters like pulse duration, discharge current, dielectric flow rate and their interaction play a critical part in surface roughness and MRR. Tosun et al. (2004). researched impact of open circuit voltage, dielectric flushing pressure, wire speed and pulse duration, on wire electrical discharge machining work piece surface roughness. It was discovered incrementing open circuit voltage, pulse length, and wire speed increments with surface roughness, though incrementing dielectric liquid weight diminishes surface roughness.

Other notable work on surface roughness to name a few are, (Spedding 1997b, Yan et al. 2004, Aspinwall, et al. 2008, Han, et al. 2007a, 2007b; Liao et al. 2004; Nishikawa and Kunieda 2009; Bamberg, and Rakwal, 2008).

## **Kerf Width and Sparking Gap**

Sparking gap and kerf width researches similar phenomena as talked about earlier above, and it is a measure of material which is wasted amid machining. It may decide dimensional accuracy of concluding part and inner corner radius of item in wire electrical discharge machining procedures are additionally restricted by the said factor (Parashar .et.al, 2010).

Sparking gap value is generally decided by the following equation:

$$\text{Sparking gap (mm)} = (\text{average of kerf width} - \text{diameter of wire}) / (2) \quad (1)$$

Some contention reports about peak current, dielectric flushing pressure and pulse off time duration for their impact on kerf width. Researchers like Parashar et.al 2010 examine impacts of WEDM parameters on kerf width whereas machining stainless steel, it was discovered that dielectric flushing pressure and pulse on time are utmost noteworthy elements, while pulse off time, wire feed, and gap voltage, are a less huge factor on kerf width. Similarly, Tosun, et al. (2004) introduced an examination on level of importance of machining parameters on kerf width by utilizing ANOVA. From that, it was discovered that pulse duration and open circuit voltage were very compelling constraints while dielectric flushing and wire speed pressure are less viable elements. As indicated by this exploration open circuit voltage for monitoring kerf width was around 3 times more essential than secondary positioning variable (pulse duration). Similarly, Swain et al. (2012) likewise examined kerf width and it was discovered, simply gap voltage is a huge factor that influences kerf width, whereas pulse off time, and also pulse on time are unimportant.

### **Wire Wear Ratio**

Many examines attempted to limit wire wear ratio by various methodologies. Since this aspect can diminish wire crack extensively.

Wire wear ratio (WWR) esteem regularly acquired by accompanying equation:

$$WWR = WWL / IWW \quad (2)$$

Where WWL is a weight loss of wire subsequent to machining and IWW is initial wire weight. Researchers like Tosun and Cogun (2003) researched impacts of various wire EDM constraints on wire wear ratio and they discovered tentatively that on incrementing open circuit voltage and pulse duration increments wire wear ratio though increasing dielectric liquid weight and wire speed diminishes it. What's more, it was discovered that high WWR is all. If there should be an occurrence of orthogonal corners, answer for this issue is really straightforward that is over travel method movement technique, however, things get confused when cutting is wanted alongside a curve. (Sinha, 2010)

Moreover, researchers like Puri and Bhattacharyya (2003) examined the impact of various WEDM constraints on wire lag amid trim cut and rough cut process. It was discovered that pulse off time, pulse peak current and pulse on time amid rough cutting; and wire tension, pulse peak voltage, servo start gap set voltage, amid trim cutting are noteworthy components. Other vital investigations that work on WEDM inaccuracies are (Huang 2004; Hsue, 1999; Yan et al. 2007; Zhang et al. 2012)

### **Wire Lag and Wire EDM Inaccuracy**

Wire electrical discharge machining is exceptionally valuable whenever complex geometry with tight resilience requires being created. In such condition, geometrical mistakes are totally unsuitable. Few researchers endeavored to limit wire lag in light of fact that geometrical incorrectness caused because of this phenomenon, though still there is absence of data to this reality. New research about wire lag could help for development of exactness in shape cutting with wire EDM.

Wires lag typically measure utilizing Profile Projector by determining projection image work piece (from Lopez et al., 2012). Nonetheless, Kuriakose and Shunmugam, (2004) examined impacts of vari-

ous constraints on surface attributes of Ti6Al4V. It is watched that more uniform surface qualities could be acquired through coated wire electrode. Besides, it was discovered that pulse off time is an utmost delicate constraint which impacts development of layer comprising of a combination of oxides. Having a lesser value off pulse of time, an impressive lessening in creation of oxides could be acquired.

Moreover, it was uncovered that constraints, for example, wire tension, pulse on time, dielectric flushing pressures, pulse off time, and wire speed are distinguished as essential process constraints of wire electrical discharge machining process, as of metallurgical perspective. Puri and Bhattacharyya (2003) has considered impact of process parameters on development and attributes of recast layer and in duration of recast layer it was discovered that pulse on time and peak discharge current to be driving components in deciding normal recast layer thickness and wire diameter along with peak discharge current did not show a critical impact by and large recast layer thickness.

Researchers like Puri and Bhattacharyya (2005) in their paper, an endeavor have been made to show white layer depth through response surface methodology (RSM) in a wire electrical discharge machining procedure involving a rough cut after a trim cut. They discovered that white layer depth increments with incrementing pulse on time amid primary cut and it diminish with incrementing pulse on time amid trim cutting. Furthermore, with incrementing cutting speed in trim cutting, white layer depth initially decreases and after that begins increasing. Also, Hassan et al. (2009) concentrated of surface respectability of AISI 4140 steel in WEDM and it could be reasoned that pulse on duration has a real impact in characterizing WEDM surface when contrasted with peak current.

## **Surface Integrity**

To enhance surface integrity of WEDM procedure, factors like white layer thickness, surface crack and surface roughness ought to be deliberated. High quality surface roughness will be able to join by high MRR and high R values. These repentances weak strength, wear resistance, and corrosion of outcomes was in concurrence with other researchers like Ramakrishnan and Karunamoorthy (2003)

## **PROCESS MODELLING, SIMULATION AND MULTI OPTIMIZATION**

### **Response Surface Methodology**

RSM or better abbreviated as Response Surface Methodology is a gathering of scientific and measurable method helpful for displaying and examination of issues in which responses of interest is impacted by a few factors and goal is to optimize the responses. Such trademark makes RSM valuable method for demonstrating and improvement of wire EDM. In RSM strategy if response is very much displayed by a linear function of non-dependent factors, at that point approximating capacity is the First-order mode.

In an event when there is curvature in the system, at that point a polynomial of higher degree ought to be utilized, for example, second order model.

In such a model,  $i$  is linear coefficient,  $\beta$  is regression coefficient,  $j$  is quadratic coefficient, and  $k$  is no. of considered and optimized parameters in investigation, and  $e$  is the random error. ANOVA or Analysis of Variance is considered with a specific end goal to evaluate appropriateness of regression model (Montgomery, 2009; Noordin et al. 2004). In this technique impacts of noise, factors are being considered. Likewise, statistical optimization model could conquer confinement of classical techniques

to acquire optimum procedure conditions. The primary detriment of this strategy is gotten an optimum value which can be a local optimum incentive. Besides, this technique is very costly in light of fact that a lot of examination should be finished. For example, if 8 factors are considered two to control 8 trial should be finished in full factorial plan (=256), regardless of whether we utilize half factorial outline quantity of analyses, wind up plainly 128 which is still high.

Many researchers endeavored to display this procedure utilizing Taguchi technique and RSM approach. Like Kumar et al. (2012); Puri and Bhattacharyya, (2005); Hewidy, et al. (2005); Kung and Chiang, (2008); Sarkar (2008); Ghodsiyeh et al. (2012a, 2012b, 2012c), and Datta and Mahapatra (2010) that used RSM combined with Gray-Taguchi technique.

### **Orthogonal Array**

This kind of Taguchi technique is exceptionally valuable intended for understanding and modeling WEDM procedure. This Taguchi technique takes into consideration examination of a wide range of parameters without carrying high numbers of experimentation. This trademark makes Orthogonal Array valuable method for demonstrating of wire EDM because of huge no. of parameters in this procedure. Fundamental hindrance of this strategy is that outcomes acquired are just relative and don't precisely demonstrate what parameter has a most noteworthy impact on execution trademark esteem. Additionally, since orthogonal clusters don't test every single variable combination, can't demonstrate hugeness of various factor connection which is quite essential in WEDM. Many researchers endeavored to demonstrate this procedure utilizing this technique like Tosun et al. (2004); Rao, et al. (2011), Bhattacharyya (2003); Kuriakose and Shunmugam (2004); Anand (2010); Huang et al. 1999; Puri et al. (2009), Vamsi et al. (2010), Parashar et al. (2010), Kuruvila, and Ravindra, (2011), Satishkumar et al. (2011).

### **Non-Traditional Optimization Algorithms**

During the mid 1960s, different scientific methods were created duplicating distinctive wonders of nature. The state of mind of engineers is that they could study, learn in and know from nature. Engineers take characteristic principles, for example, an artificial neural network, investigation of neurons is included, and in a genetic algorithm, laws of genetics were changed to be utilized as an optimization tool. Such calculations are exceptionally helpful for advancement of procedure that includes loads of parameters like WEDM. Many a times outcome proposed by these calculations can't be accomplished in all actuality; because of nonappearance of optimal parameter combination in a machine which may be primary disadvantage of this strategy (Mahapatra and Patnaik, 2006a). The justification behind utilization of these calculations is capacity of these calculations to locate global ideal parameters though conventional enhancement systems regularly have a tendency to be caught at a local optimum. (Mahapatra, and Patnaik, 2006c). A few researchers attempted to enhance wire electrical discharge machining by this strategy like Kuruvila and Ravindra, (2011); Mahapatra and Patnaik (2006c); Kuriakose and Shunmugam (2005), Jeyapaul et al. (2006), Debabrata et al. (2007).

Researchers like Mukherjee et al., (2012) thought about execution of various optimization algorithms on optimizing WEDM process. In the research 6 non-conventional optimizing algorithms are being compared, including; ant colony optimization, particle swarm optimization, genetic algorithm, sheep flock algorithm, artificial bee colony and biogeography-based optimization for single and multi-objective enhancement of wire electrical discharge machining process. It was discovered that albeit all

these 6 calculations had high potential in accomplishing ideal parameter settings, yet bio-geography-based calculation outflanks others as for optimization performances, quick convergence and dispersion of optimal solutions from their mean.

There are researchers which have utilized a customary method for demonstrating wire electrical discharge machining like Tarng et al. (1995) that used feed-forward neural system to show and simulated annealing (SA) algorithm is thereafter connected to the neural network for solving ideal cutting parameters issue. An additional one is Lin et al. (2000) which utilized Taguchi technique along with fuzzy logic for optimization and modeling. Also, Huang and Liao (2003) contemplated Wire Electrical Discharge Machining in light of Grey Relational and Statistical Analyses. Moreover, Kuriakose et al. (2003) utilized information mining methodology and C4.5 algorithms to demonstrate the procedure. Besides, Yuan et al. (2009) utilized Incorporating earlier model into Gaussian procedures regression for WEDM process modeling. Likewise, Çaydas et al. (2009) utilized neuro-fuzzy interference system (ANFIS) to show the procedure. Other than that Chen (2007) used a neural network integrated system Simulated annealing approach for improving WEDM.

## **MONITORING AND CONTROL SYSTEM**

The use of adaptive control systems for wire electrical discharge machining is fundamental for checking and control of procedure. The said area explores propelled observing and control systems comprising wire breakage, fuzzy, and self-tuning adaptive control systems utilized as a part of WEDM procedure.

### **Fuzzy Control System**

Relative controllers are generally being utilized as a part of servo feed control system to screen and assess gap condition amid WEDM procedure. Though execution of controllers was restricted by machining conditions, that significantly fluctuate with constraints settings. Researchers like Kinoshita et al. (1976) researched impacts of wire winding speed, wire feed rate, wire tension and electrical parameters on gap conditions amid wire electrical discharge machining. Accordingly, numerous customary control algorithms in view of explicit scientific and statistical models are being created for WEDM or EDM operations (Pandit, and Wittig, 1984; Rajurkar and Wang, 1990; Garbajs, 1985; Watanabe et al., 1990; Huang et al., 1986). A few researchers (Liao and Woo, 1997); Yan and Liao, 1995) have additionally built up a pulse segregation system giving a method for dissecting and observing pulse trains under different wire electrical discharge machining conditions quantitatively. Despite fact that such sorts of control systems could be connected to an extensive variety of machining conditions, it can't react to gap condition while there is a surprising unsettling influence (Yan and Laio, 1998).

As of late, fuzzy control system is being connected to wire electrical discharge machining procedure to accomplish ideal and exceptionally productive machining. A few researchers guaranteed that fuzzy logic control system executes a control procedure, that catches expert's information or administrator's involvement in keeping up coveted machining operation (Boccadoro, and Dauw 1995). What's more, fuzzy logic controller doesn't need any complete numerical models adjusting to dynamic behavior of wire electrical discharge machining operation (Yan et al. 1999). A few researchers (Liao and Woo, 1998) proposed sparking frequency observing and adaptive control systems in light of fuzzy logic control and altering procedures, which can be connected to an extensive variety of machining conditions. Liao and

Woo (2000) likewise outlined a fuzzy controller having an online pulse monitoring system including discharging noise and segregating ignition delay time of each pulse. EDM pulses could be characterized into open, spark, arc, off or short, that are reliant on ignition delay time, and affect MRR, SR, electrode wear and precision of part (Cogun, 1990, Bruyn and Pekelharing, 1982).

## **Wire Inaccuracy Adaptive Control System**

The event of wire breakage amid wire electrical discharge machining is a standout amongst utmost unwanted machining attributes significantly influencing machining accuracy and execution together with nature of part delivered. Many endeavors had made to build up an adaptive control system giving an online recognizable proof of any irregular machining condition and a control system keeping wire from breaking devoid of compromising different WEDM execution measures. The following area reports about through a gathering of distributed work including adaptive control of wire breakage, wire vibration and wire lag.

## **Wire Breakage**

A varied assortment of control techniques keeping wire from breaking is based on information of qualities of wire breakage. Researcher like Kinoshita et al. (1982) watched quick ascent in pulse frequency of gap voltage, that proceeds for around 5– 40 ms before the wire breaks. They built up an observing and control system which switches off pulse generator and servo system keeping wire from breaking however it influences machining effectiveness. A few researchers (Shoda et al. 1992; Kunieda 1990) additionally recommended that concentration of electrical discharge at one point of wire, that effects an expansion in limited temperature bringing about breaking of wire. Though, adaptive control system focusing on discovery of sparking location and decrease of discharge energy were created deprived of making any contemplations to MRR. The breakage of wire has likewise been connected to rise in a number of short circuit pulses going on for more than 30 ms until point that wire broke (Tanimura et al. 1977).

Different researchers (Rajurkar et al. 1991) contended that wire breakage is connected to sudden increment in sparking frequency. It was additionally discovered that their proposed monitoring and control system in light of online examination of sparking frequency and real-time regulation of pulse off-time influences MRR. Liao et al. (1997) helped issue by relating MRR to machining parameters and utilizing another computer supported pulse separation system in view of pulse train investigation to enhance machining speed. While Yan and Liao (1996) connected a self-learning fuzzy control procedure to control sparking frequency as well as to keep up a high MRR by altering progressively off time pulse under a consistent feed rate machining condition.

The breaking of wire is additionally because of exorbitant thermal load creating ridiculous heat on wire electrode. The greater part of thermal energy created amid WEDM procedure is exchanged to wire while rest is lost to flushing liquid or radiation (Rajurkar et al., 1991). However, when instantaneous energy rate surpasses a specific limit contingent upon thermal properties of wire material, wire will break. A few researchers (Jennes et al., 1984; Obara et al., 1995; Dekeyser et al., 1985) explored impact of different machining parameters on thermal load of wire and built up a thermal model recreating WEDM procedure. Notwithstanding sparking characteristics or temperature distribution, mechanical strength of wire additionally significantly affects event of wire breakage. Luo (1999) asserted that wire material yielding and crack add to wire breakage, while an expansion in temperature aggravates failure procedure.

## **Wire Lag and Wire Vibration**

Fundamental elements adding to geometrical error of Wire Electrical Discharge Machined part are different procedure forces following up on wire making it leave for programmed path. The said forces incorporate mechanical forces delivered by pressure from gas bubbles shaped by plasma of erosion mechanism, axial forces connected to straighten wire, hydraulic forces actuated by flushing, electrostatic forces following up on wire and electro-dynamic forces intrinsic to spark generation (Dauw and Beltrami, 1994; Kinsohita et al., 1984).

Subsequently, static redirection as a lag impact of wire is basically considered keeping in mind end goal to produce a precise cutting apparatus. A few researchers (Puri and Bhattacharyya, 2003; Huang and Liao 1997) played out a parametric report on geometrical incorrectness of part caused by wire lag and endeavored to demonstrate WEDM process numerically. While Beltrami and Dauw (1996) observed and controlled wire position online by methods for an optical sensor with a control algorithm empowering for all intents and purposes any shape to be cut at a generally high cutting speed. Various geometric device movement pay strategies, which increment machining gap and avoid checking or wire breakages when cutting areas with high curvatures, for example, corners with little radii have likewise been created (Wang and Ravani, 2003 Dekeyser and Snoeys, 1989; Lin et al. 2001) built up a control technique in light of fuzzy logic to enhance machining precision and aggregated sparking at corner parts without influencing cutting feed rates.

Moreover, dynamic conduct of wire amid WEDM is likewise controlled to abstain from cutting inaccuracies. There are a couple of discourses on design and advancement of monitoring and control system for remunerating conduct of wire vibration (Enache and Opran 1993; Dauw et al, 1989) likewise announced that vibration of wire can be generously diminished when wire and wire guides are totally submerged in working tank loaded with deionized water. A few researchers (Mohri et al. 1998) derived a scientific model investigating transient response of wire vibration in view of force following up on apparatus wire in a solitary discharge process. Various researchers (Rajurkar and Wang 1997, Snoeys et al. 1983) evaluated innovative work of different propelled monitoring and control systems utilized as a part of EDM and WEDM forms.

## **Self-Tuning Adaptive Control System**

As of late, WEDM work has been investigated to control systems acclimating to variety in power density necessary for machining a work piece through differing thickness. A few researchers (Kinoshita et al., 1982; Tanimura et al., 1977) discovered that an adjustment in work piece thickness amid machining prompts an increase in wire thermal thickness and an inevitable breaking of wire. Researchers like Rajurkar et al. [1994, 1997] suggested an adaptive control system having an input model which screens and have charge of sparking frequency as indicated by online recognized work piece height. Different researchers (Huang et al., 1986) built up a system which includes an unequivocal scientific model demanding various tests and measurable systems. Yan et al. (1996) utilized neural networks for evaluating work piece height and fuzzy control logic to stifle wire breakage when a work piece having variable stature is machined.

Use of a learning-based control system to control unfavorable WEDM conditions have likewise been tested. Snoeys et al. (1998) offered an information-centered system, that involves 3 modules, specifically work readiness, operator assistance or fault diagnosis, and process control empowering control



and monitoring of WEDM procedure. Work preparation module decides optimum machining parameter settings, whereas administrator help and fault diagnostics databases exhort administrators and analyze machining mistakes. Hence, abilities of these modules increment measure of self-governance provided to WEDM machine. Huang and Liao (2000) had likewise demonstrated significance of administrator help and fault diagnostics methods for WEDM procedure. They recommended a model artificial neural system centered system for maintenance schedule timetable and fault diagnosis of WEDM. Researchers like Dekeyser et al. (1988) built up a thermal model coordinated with a specialist system for anticipating and monitoring thermal over-burden experienced on wire. In spite of fact that model expands level of machine independence, it needs a lot of calculation, that backs off preparing speed and undermines online control execution.

## **FUTURE RESEARCH DIRECTION**

(WEDM) is a thermal machining process capable of precisely machining parts having complex shapes and forms, particularly for parts which are exceptionally hard to be machined through customary machining forms. It had been generally connected for machining and also micro-machining of parts having complex shapes and changing hardness needing prominent precision and tight dimensional resiliences. Optimization and improvement of WEDM procedure constraints is basic in light of fact that WEDM is a costly and broadly utilized process. A definitive objective of WEDM procedure is to accomplish a precise and proficient machining process. A few researchers had contemplated techniques to enhance surface quality and increment material removal rate of WEDM procedure. In any case, issue of choosing cutting parameters in WEDM procedure isn't completely explained, despite the fact that most up and coming CNC-WEDM machines are easily accessible. However, there is absence of data around various WEDM wire kinds. Henceforth additional research ought to be done for looking at changed wire types on various responses. Moreover, there isn't sufficient data about WEDM errors and inaccuracies. More research can enhance exactness amid WEDM machining uncommonly in contour cutting. What's more, it appears that there is absence of data about dry and near dry-WEDM. In addition, utilizing optimization algorithms could build up optimization procedure essentially though simply genetic algorithm broadly utilized for advancement of this procedure up to now and utilizing other calculation may upgrade optimization. The WEDM procedure must be continually enhanced to keep up as a competitive and practical machining operation in cutting-edge manufacturing ventures. At last, it appears that more research can upgrade abilities of WEDM process essentially to enhance machining profitability, precision and proficiency.

## **CONCLUSION**

WEDM is now already a well-recognized non-conventional material removal process equipped with meeting machining requirements demanded by metal cutting industries. It has been usually used for machining and micro-machining of parts with intricate shapes and varying hardness requiring accuracy, exactness, precision and tight dimensional resilience. Nonetheless, the downside of this procedure is moderately low machining speed, when contrasted with other non-conventional machining procedures, for example, laser-cutting procedure, to a great extent because of its thermal machining method. What's

more, development of more up to date and new exotic materials has tested viability and dependency of WEDM procedure later on in manufacturing condition. Subsequently, improvements need to be continuously made to current WEDM qualities with a specific end goal to expand machining ability and increment machining profitability and effectiveness.

A definitive objective of the WEDM procedure is to accomplish a precise and effective machining operation without negotiating machining performance. In spite of fact that researchers trust that WEDM procedure because of its capacity to proficiently machine parts with hard-to-machine materials and geometries has its own particular application zone unmatched by other manufacturing processes. To remain rivalry to other non-conventional manufacturing processes, wire EDM must utilize reliable strategies and algorithms with continuous outcomes.

## ACKNOWLEDGMENT

The authors sincerely acknowledge the comments and suggestions of the reviewers that have been instrumental for improving and upgrading the paper in its final form.

## REFERENCES

- Abdulkareem, S., Khan, A., & Zain, Z. M. (2011). Experimental Investigation of Machining Parameters on Surface Roughness in Dry & Wet Wire-Electrical Discharge Machining. *Advanced Materials Research*, 264-265, 831–836. doi:10.4028/www.scientific.net/AMR.264-265.831
- Albert, M. (1997). *Reaching New Heights with Wire EDM*. Modern Machine Shop.
- Anand, K. N. (1996). Development of process technology in wire-cut operation for improving machining quality. *Total Quality Management*, 7(1), 11–28. doi:10.1080/09544129650035016
- Aoyama, S. (1999). High-performance Coated Wire Electrodes for High-Speed Cutting & Accurate Machining. *Hitachi Cable Review No.18*.
- Aspinwall, D.K., Soo, S.L., Berrisford, A.E., & Walder, G. (2008). Work piece surface roughness & integrity after WEDM of Ti–6Al–4V & Inconel 718 using minimum damage generator technology. *CIRP Annals – Manufacturing Technology*, 57, 187–190.
- Bamberg, E., & Rakwal, D. (2008). Experimental investigation of wire electrical discharge machining of gallium-doped germanium. *Journal of Materials Processing Technology*, 197(1-3), 419–427. doi:10.1016/j.jmatprotec.2007.06.038
- Beltrami, I., & Dauw, D. (1996). A simplified post process for wire cut EDM. *Journal of Materials Processing Technology*, 58(4), 385–389. doi:10.1016/0924-0136(95)02212-0
- Benedict, G. F. (1987). *Electrical discharge machining (EDM)*. In *Non-Traditional Manufacturing Processes* (pp. 231–232). New York: Marcel Dekker, Inc.
- Boccardo, M., & Dauw, D. F. (1995). About application of fuzzy controllers in high-performance die-sinking EDM machines. *Annals CIRP*, 44(1), 147–150. doi:10.1016/S0007-8506(07)62294-X

- Boopathi, S. (2012). Experimental Comparative Study of Near-Dry Wire-Cut Electrical Discharge Machining (WEDM). *European Journal of Scientific Research*, 75(4), 472–481.
- Bruyn, H. E., & Pekelharing, A. J. (1982). Has delay time influence on EDM-process? *Annals CIRP*, 31(1), 103–106. doi:10.1016/S0007-8506(07)63277-6
- Çaydas, U., Haşçalık, A., & Ekici, S. (2009). An adaptive neuro-fuzzy inference system (ANFIS) model for wire-EDM. *Expert Systems with Applications*, 36(3), 6135–6139. doi:10.1016/j.eswa.2008.07.019
- Chen, H. C., Lin, J. C., Yang, Y. K., & Tsai, C. H. (2007). Optimization of wire electrical discharge machining for pure tungsten using a neural network integrated simulated annealing approach. *Expert Systems with Applications*, 37(10), 7147–7153. doi:10.1016/j.eswa.2010.04.020
- Cogun, C. (1990). A technique & its applications for evaluation of material removal contributions of pulses in electrical discharge machining. *International Journal of Machine Tools & Manufacture*, 30(1), 19–31. doi:10.1016/0890-6955(90)90038-K
- Datta, S., & Mahapatra, S. S. (2010). Modeling, simulation & parametric optimization of Wire-EDM process using response surface methodology coupled with Grey-Taguchi technique. *International Journal of Engineering Science and Technology*, 2(5), 162–183. doi:10.4314/ijest.v2i5.60144
- Dauw, D. F., & Beltrami, I. (1994). High-precision wire-EDM by online wire positioning control. *Annals CIRP*, 43(1), 193–197. doi:10.1016/S0007-8506(07)62194-5
- Dauw, D. F., Sthitoul, H., & Tricarico, C. (1989). Wire analysis & control for precision EDM cutting. *Annals CIRP*, 38(1), 191–194. doi:10.1016/S0007-8506(07)62682-1
- Debabrata, M., Pal, S.K. & Partha, S. (2007). Modeling of electrical discharge machining process using back propagation neural network & multi-objective optimization using non-dominating sorting genetic algorithm-II. *Journal of Materials Processing Technology*, 186(1-30), 154-162.
- Dekeyser, W., Snoeys, R., & Jennes, M. (1985). A thermal model to investigate wire rupture phenomenon for improving performance in EDM wire cutting. *Journal of Manufacturing Systems*, 4(2), 179–190. doi:10.1016/0278-6125(85)90024-X
- Dekeyser, W., Snoeys, R., & Jennes, M. (1988). Expert system for wire cutting EDM based on pulse classification & thermal modelling. *Robotics and Computer-integrated Manufacturing*, 4(1–2), 219–224. doi:10.1016/0736-5845(88)90080-4
- Dekeyser, W. L., & Snoeys, R. (1989). Geometric Accuracy of Wire EDM. *Proceedings of Ninth International Symposium for Electro-Machining (ISM-9)*.
- Enache, S., & Opran, C. (1993). Dynamic stability of technological machining system in EDM. *Annals CIRP*, 42(1), 209–214. doi:10.1016/S0007-8506(07)62427-5
- Furudate, C., & Kunieda, M. (2001). Fundamental study on dry-WEDM. *Journal of Japan Society for Precision Engineering*, 67(7), 1180–1184. doi:10.2493/jjspe.67.1180
- Garbajs, V., & Peklenik, J. (1985). Statistical model for an adaptive control of EDM-process. *Annals CIRP*, 34(1), 499–502. doi:10.1016/S0007-8506(07)61820-4

Ghodsiyeh, D., Golshan, A., Hosseiniyehzad, N., Hashemzadeh, M., & Ghodsiyeh, S. (2012). Optimizing Finishing process in WEDMing of Titanium Alloy (Ti6Al4V) by Zinc Coated Brass Wire based on Response Surface Methodology. *Indian Journal of Science and Technology*, 5(10), 3365–3377.

Ghodsiyeh, D., Lahiji, M. A., Ghanbari, M., Shirdar, M. R., & Golshan, A. (2012). Optimizing Material Removal Rate (MRR) in WEDMing Titanium alloy (Ti6Al4V) using Taguchi method. *Research Journal of Applied Sciences, Engineering and Technology*, 4(17), 3154–3161.

Ghodsiyeh, D., Lahiji, M. A., Ghanbari, M., Shirdar, M. R., & Shirdar, M. R. (2012). Optimizing Rough Cut in WED- Ming Titanium Alloy (Ti6Al4V) by Brass Wire Using Taguchi Method. *Journal of Basic and Applied Scientific Research*, 2(8), 7488–7496.

Guo, E. (2014). Surface integrity evolution from main cut to finish trim cut in W-EDM of shape memory alloy. *Procedia CIRP*, 13, 137–142. doi:10.1016/j.procir.2014.04.024

Han, F., Jiang, J., & Yu, D. (2007a). Influence of discharge current on machined surfaces by thermo-analysis in finish cut of WEDM. *International Journal of Machine Tools & Manufacture*, 47(7–8), 1187–1196. doi:10.1016/j.ijmachtools.2006.08.024

Han, F., Jiang, J., & Yu, D. (2007b). Influence of machining parameters on surface roughness in finish cut of WEDM. *International Journal of Advanced Manufacturing Technology*, 34(5–6), 538–546. doi:10.1007/00170-006-0629-9

Han, F., Zhang, J., & Soichiro, I. (2007). Corner error simulation of rough cutting in wire EDM. *Precision Engineering*, 31(4), 331–336. doi:10.1016/j.precisioneng.2007.01.005

Hanaoka, D., Fukuzawa, Y., Ramirez, C., Minrazo, P., Osend, M. J., & Belmonte, M. (2013). EDM machining of ceramic/ carbon nanostructure composites. *Procedia CIRP*, 6, 95–100. doi:10.1016/j.procir.2013.03.033

Hasçalık, A., & Çaydas, U. (2004). Experimental study of wire electrical discharge machining of AISID5 tool steel. *Journal of Materials Processing Technology*, 148(3), 362–367. doi:10.1016/j.jmatprotec.2004.02.048

Hassan, M. A., Mehat, N. S., Sharif, S., Daud, R., Tomadi, S. H., & Reza, M. S. (2009). Study of Surface Integrity of AISI 4140 Steel in Wire Electrical Discharge Machining. *Proceedings of International Multi Conference of Engineers & Computer Scientists, II*, 1–6.

Hewidy, M. S., El-Taweel, T. A., & El-Safty, M. F. (2005). Modelling machining parameters of wire electrical discharge machining of Inconel 601 using RSM. *Journal of Materials Processing Technology*, 169(2), 328–336. doi:10.1016/j.jmatprotec.2005.04.078

Ho, K. H., Newman, S. T., Rahimifard, S., & Allen, R. D. (2004). State of art in wire electrical discharge machining (WEDM). *International Journal of Machine Tools & Manufacture*, 44(12–13), 1247–1259. doi:10.1016/j.ijmachtools.2004.04.017

Hsue, W. J., Liao, Y. S., & Lu, S. S. (1999). Fundamental geometry analysis of wire electrical discharge machining in corner cutting. *International Journal of Machine Tools & Manufacture*, 39(4), 651–667. doi:10.1016/S0890-6955(98)00046-7

- Huang, J. T., & Liao, Y. S. (1997). A Study of Finish Cutting Operation Number & Machining Parameters Setting in Wire Electrical Discharge Machining. *Proceedings of International Conference on Precision Machining (ICPE'97)*.
- Huang, J. T., & Liao, Y. S. (2000). A wire-EDM maintenance & fault-diagnosis expert system integrated with an artificial neural network. *International Journal of Production Research*, 38(5), 1071–1082. doi:10.1080/002075400189022
- Huang, J. T., & Liao, Y. S. (2003). Optimization of machining parameters of Wire-EDM based on Grey relational & statistical analyses. *International Journal of Production Research*, 41(8), 1707–1720. doi:10.1080/1352816031000074973
- Huang, J. T., Liao, Y. S., & Hsue, W. J. (1999). Dedurationination of finish-cutting operation number & machining parameters setting in wire electrical discharge machining. *Journal of Materials Processing Technology*, 87(1-3), 69–81. doi:10.1016/S0924-0136(98)00334-3
- Huang, Y. H., Zhao, G. G., Zhang, Z. R., & Yau, C. Y. (1986). The identification & its means of servo feed adaptive control system in WEDM. *Annals CIRP*, 35(1), 121–123. doi:10.1016/S0007-8506(07)61852-6
- Jain, V.K. (2005). *Advanced Machining Processes*. Allied Publishers Pvt. Limited.
- Jameson, E. C. (2001). Description & development of electrical discharge machining (EDM). *Electrical Discharge Machining, Society of Manufacturing Engineers, 2001*, 16.
- Jennes, M., Dekeyser, W., & Snoeys, R. (1984). Comparison of various approaches to model thermal load on EDM-wire electrode. *Annals CIRP*, 33(1), 93–98. doi:10.1016/S0007-8506(07)61387-0
- Jeyapaul, R., Shahabudeen, P., & Krishnaiah, K. (2006). Simultaneous optimization of multi-response problems in Taguchi method using genetic algorithm. *International Journal of Advanced Manufacturing Technology*, 3(9-10), 870–878. doi:10.100700170-005-0095-9
- Kanlayasiri, K., & Boonmung, S. (2007a). An investigation on effects of wire-EDM machining parameters on surface roughness of newly developed DC53 die steel. *Journal of Materials Processing Technology*, 187-188, 26–29. doi:10.1016/j.jmatprotec.2006.11.220
- Kanlayasiri, K., & Boonmung, S. (2007b). Effects of wire- EDM machining variables on surface roughness of newly developed DC 53 die steel: Design of experiments & regression model. *Journal of Materials Processing Technology*, 192–193, 459–464. doi:10.1016/j.jmatprotec.2007.04.085
- Kansala, H. K., Singh, S., & Kumar, P. (2008). Numerical simulation of Powder Mixed Electric Discharge Machining (PMEDM) using finite element method. *Mathematical and Computer Modelling*, 47(11-12), 1217–1237. doi:10.1016/j.mcm.2007.05.016
- Kern, R. (2007). Techtips. *EDM Today Magazine*, Kinoshita, N., Fukui, M., & Gamo, G. (1982). Control of wire-EDM preventing electrode from breaking, *Annals. CIRP*, 31(1), 111–114.
- Kinoshita, N., Fukui, M., Shichida, H., Gamo, G., & Sata, T. (1976). Study on E.D.M. with wire electrode; gap phenomena. *Annals CIRP*, 25, 141–145.

- Kinsohita, N., Fukui, M., & Kimura, Y. (1984). Study on Wire-EDM: In process measurement of mechanical behaviour of electrode-wire. *Annals. CIRP*, 33(1), 89–92. doi:10.1016/S0007-8506(07)61386-9
- Konda, R., Rajurkar, K. P., Bishu, R. R., Guha, A., & Parson, M. (1999). Design of experiments to study & optimize process performance. *International Journal of Quality & Reliability Management*, 16(1), 56–71. doi:10.1108/02656719910226914
- Korean Patent No. 10-1985-0009194
- Kozak, J., Rajurkar, K. P., & Wang, S. Z. (1994). Material removal in WEDM of PCD blanks. *Journal of Engineering for Industry*, 116(3), 363–369. doi:10.1115/1.2901953
- Kumar, A. (2012). Modelling of Micro Wire Electro Discharge Machining (WEDM). In *Aerospeed Material*. NIT Rourkela.
- Kumar, A., Kumar, V., & Kumar, J. (2012). Prediction of surface roughness in wire electric discharge machining (WEDM) process base on response surface methodology. *IACSIT International Journal of Engineering and Technology*, 2(4), 708–719.
- Kung, K. Y., & Chiang, K. T. (2008). Modeling & Analysis of Machinability Evaluation in Wire Electrical Discharge Machining (WEDM) Process of Aluminum Oxide-Based Ceramic. *Materials and Manufacturing Processes*, 23(3), 241–250. doi:10.1080/10426910701860616
- Kunieda, M., Kojima, H., & Kinoshita, N. (1990). On-line detection of EDM spark location by multiple connection of branched electric wires. *Annals. CIRP*, 39(1), 171–174. doi:10.1016/S0007-8506(07)61028-2
- Kuriakose, S., Mohan, K., & Shunmugam, M. S. (2003). Data mining applied to wire-EDM process. *Journal of Materials Processing Technology*, 142(1), 182–189. doi:10.1016/S0924-0136(03)00596-X
- Kuriakose, S., & Shunmugam, M. S. (2004). Characteristics of wire-electro discharge machined Ti6Al4V surface. *Materials Letters*, 58(17-18), 2231–2237. doi:10.1016/j.matlet.2004.01.037
- Kuriakose, S., & Shunmugam, M. S. (2004). Characteristics of wire-electro discharge machined Ti6Al4V surface. *Materials Letters*, 58(17-18), 2231–2237. doi:10.1016/j.matlet.2004.01.037
- Kuriakose, S., & Shunmugam, M. S. (2005). Multi-objective optimization of wire electro discharge machining process by Non-Dominated Sorting Genetic Algorithm. *Journal of Materials Processing Technology*, 170(1-2), 133–141. doi:10.1016/j.jmatprotec.2005.04.105
- Kuruvila, N., & Ravindra, H. V. (2011). Parametric Influence & Optimization of Wire EDM of Hot Die Steel. *Machining Science & Technology. International Journal (Toronto, Ont.)*, 15(1), 47–75.
- Lavwers, B., Kruth, J. P., Liu, W., Eeraerts, W., Schacht, B., & Bleys, P. (2004). Investigation of MRR mechanism in EDM of composite ceramic material. *Journal of Materials Processing Technology*, 149(1-3), 347–352. doi:10.1016/j.jmatprotec.2004.02.013
- Liao, Y. S., Chu, Y. Y., & Yan, M. T. (1997). Study of wire breaking process & monitoring of WEDM. *International Journal of Machine Tools & Manufacture*, 37(4), 555–567. doi:10.1016/S0890-6955(95)00049-6

- Liao, Y. S., Huang, J. T., & Chen, Y. H. (2004). A study to achieve a fine surface finish in Wire-EDM. *Journal of Materials Processing Technology*, 149(1-3), 165–171. doi:10.1016/j.jmatprotec.2003.10.034
- Liao, Y. S., & Woo, J. C. (1997). The effects of machining settings on behaviour of pulse trains in WEDM process. *Journal of Materials Processing Technology*, 71(3), 433–439. doi:10.1016/S0924-0136(97)82076-6
- Liao, Y. S., & Woo, J. C. (1998). A New Fuzzy Control System for Adaptive Control of WEDM Process. *Proceedings of Twelfth International Symposium for Electro-Machining (ISEM-12)*.
- Liao, Y. S., & Woo, J. C. (2000). Design of a fuzzy control system for adaptive control of WEDM process. *International Journal of Machine Tools & Manufacture*, 40(15), 2293–2307. doi:10.1016/S0890-6955(00)00036-5
- Lin, C. T., Chung, I. F., & Huang, S. Y. (2001). Improvement of machining accuracy by fuzzy logic at corner parts of wire-EDM. *Fuzzy Sets and Systems*, 122(3), 499–511. doi:10.1016/S0165-0114(00)00034-8
- Lin, J. L., Wang, K. S., Yan, B. H., & Tarng, Y. S. (2000). Optimization of electrical discharge machining process based on Taguchi method with fuzzy logics. *Journal of Materials Processing Technology*, 102(1-3), 48–55. doi:10.1016/S0924-0136(00)00438-6
- Lopez J.G., Verleysen P., & Degrieck, J. (2012). Effect of fatigue damage on static & dynamic tensile behavior of electro-discharge machined Ti-6Al-4V. *Journal of Fatigue & Fracture & Engineering Materials & Structures*, 35(12), 1120–1132.
- Lu, Y., Wang, T., Wang, C., & Wang, C. (2012). Empirical Modeling of High-speed WEDM Finishing in Gas. *Advanced Materials Research*, 486, 503–508. doi:10.4028/www.scientific.net/AMR.486.503
- Luo, Y.F. (1999). Rupture failure & mechanical strength of electrode wire used in wire EDM. *J. Mater. Process. Technology*, 94(2–3), 208–215.
- Mahapatra, S. S., & Patnaik, A. (2006). Optimization of Wire Electrical Discharge Machining (WEDM) process parameters using genetic algorithm. *Indian Journal of Engineering and Materials Sciences*, 13, 494–502.
- Mahapatra, S. S., & Patnaik, A. (2006a). Optimization of wire electrical discharge machining (WEDM) process parameters using Taguchi method. *International Journal of Advanced Manufacturing Technology*, 34(9-10), 911–925. doi:10.1007/00170-006-0672-6
- Mahapatra, S. S., & Patnaik, A. (2006b). Parametric Optimization of Wire Electrical Discharge Machining (WEDM) Process using Taguchi Method. *Journal of Brazilian Society of Mechanical Sciences & Engineering*, 8(4), 422–429. doi:10.1590/S1678-58782006000400006
- Mahapatra, S. S., & Patnaik, A. (2006c). Optimization of Wire Electrical Discharge Machining (WEDM) process parameters using genetic algorithm. *Indian Journal of Engineering and Materials Sciences*, 13, 494–502.
- Mohammadi, A., Tehrani, A. F., & Abdullah, A. (2013). Introducing a new technique in wire electric discharge turning & evaluating ultrasonic vibration on MRR. *Procedia CIRP*, 6, 583–588. doi:10.1016/j.procir.2013.03.005

- Mohri, N., Yamada, H., Furutani, K., Narikiyo, T., & Magara, T. (1998). System identification of wire electrical discharge machining. *Ann. CIRP*, 47(1), 173–176. doi:10.1016/S0007-8506(07)62811-X
- Montgomery, D. C. (2009). *Design & Analysis of Experiments* (7th ed.). John Wiley & Sons (Asia) Pte Ltd.
- Mukherjee, R., Chakraborty, S., & Samanta, S. (2012). Selection of wire electrical discharge machining process parameters using non-traditional optimization algorithms. *Applied Soft Computing*, 12(8), 2506–2516. doi:10.1016/j.asoc.2012.03.053
- Nishikawa, M., & Kunieda, M. (2009). Prediction of wire-EDMed surface shape by in-process measurement of wire electrode behavior. *Journal of Japan Society for Precision Engineering*, 75(9), 1078–1082. doi:10.2493/jjspe.75.1078
- Noordin, M. Y., Venkatesh, V. C., Sharif, S., Elting, S., & Abdullah, A. (2004). Application of response surface methodology in describing performance of coated carbide tools when turning AISI 1045 steel. *Journal of Materials Processing Technology*, 145(1), 46–58. doi:10.1016/S0924-0136(03)00861-6
- Obara, H., Iwata, Y., & Ohsumi, T. (1995). An Attempt to Detect Wire Temperature Distribution During Wire EDM. *Proceedings of Eleventh International symposium for Electro-Machining (ISEM-11)*.
- Pandit, S. M., & Wittig, W. H. (1984). A data-dependent systems approach to optimal microcomputer control illustrated by EDM. *Journal of Engineering for Industry*, 106(2), 137–142. doi:10.1115/1.3185924
- Parashar V., Rehman, A., Bhagoria, J.L.(2012). Performance Measurement & Data Analysis of Material Removal Rate for Wire Cut Electro Discharge Machining Process. *Applied Mechanics & Materials*, 110-116, 1683-1690.
- Parashar, V., Rehman, A., Bhagoria, J. L., & Puri, Y. M. (2010). Kerfs width analysis for wire cut electro discharge machining of SS 304L using design of experiments. *Indian Journal of Science and Technology*, 3(4), 369–373.
- Poro's, D., & Zaborski, S. (2009). Semi-empirical model of efficiency of wire electrical discharge machining of hard-to- machine materials. *Journal of Materials Processing Technology*, 209(3), 1247–1253. doi:10.1016/j.jmatprotec.2008.03.046
- Praneetpong, C., Fakuzawa, Y., Nagasawa, S., & Yamashita, K. (2010). Effect of Edm Combined Ultrasonic Vibration on machining properties of Si3N4. *Materials Transactions*, 51(11), 2113–2120. doi:10.2320/matertrans.M2010194
- Puri, A. B., & Bhattacharyya, B. (2003). An analysis & optimization of geometrical inaccuracy due to wire lag phenomenon in WEDM. *International Journal of Machine Tools & Manufacture*, 43(2), 151–159. doi:10.1016/S0890-6955(02)00158-X
- Puri, A. B., & Bhattacharyya, B. (2005). Modeling & analysis of white layer depth in a wire-cut EDM process through response surface methodology. *International Journal of Advanced Manufacturing Technology*, 25(67), 301–307. doi:10.1007/00170-003-2045-8
- Rajurkar, K. P., & Wang, W. M. (1993). Thermal modeling & on-line monitoring of wire-EDM. *Journal of Materials Processing Technology*, 38(1-2), 417–430. doi:10.1016/0924-0136(93)90214-Q



- Rajurkar, K. P., & Wang, W. M. (1997). Improvement of EDM performance with advanced monitoring & control systems. *Journal of Manufacturing Science and Engineering*, 119(4B), 770–775. doi:10.1115/1.2836823
- Rajurkar, K. P., Wang, W. M., & Lindsay, R. P. (1990). Real-time stochastic model & control of EDM. *Annals CIRP*, 39(1), 187–190. doi:10.1016/S0007-8506(07)61032-4
- Rajurkar, K. P., Wang, W. M., & Lindsay, R. P. (1991). On-line monitor & control for wire breakage in WEDM. *Annals CIRP*, 40(1), 219–222. doi:10.1016/S0007-8506(07)61972-6
- Rajurkar, K. P., Wang, W. M., & McGeough, J. A. (1994). WEDM identification & adaptive control for variable-height components. *Annals CIRP*, 43(1), 199–202. doi:10.1016/S0007-8506(07)62195-7
- Rajurkar, K. P., Wang, W. M., & Zhao, W. S. (1997). WEDM-adaptive control with a multiple input model for identification of work-piece height. *Annals CIRP*, 46(1), 147–150. doi:10.1016/S0007-8506(07)60795-1
- Ramakrishnan, R., & Karunamoorthy, L. (2006). Multi response optimization of wire EDM operations using robust design of experiments. *International Journal of Advanced Manufacturing Technology*, 29(1-2), 105–112. doi:10.1007/00170-004-2496-6
- Rao, P. S., Ramji, K., & Satyanarayana, B. (2011). Effect of WEDM Conditions on Surface Roughness: A Parametric Optimization Using Taguchi Method. *International Journal of Advanced Engineering Sciences & Technologies*, 6, 41 – 48.
- Sarkar, S., Mitra, S., & Bhattacharyya, B. (2005). Parametric analysis & optimization of wire electrical discharge machining of  $\gamma$ -titanium aluminide alloy. *Journal of Materials Processing Technology*, 159(3), 286–294. doi:10.1016/j.jmatprotec.2004.10.009
- Sarkar, S., Sekh, M., Mitra, S., & Bhattacharyya, B. (2008). Modeling & optimization of wire electrical discharge machining of  $\gamma$ -TiAl in trim cutting operation. *Journal of Materials Processing Technology*, 205(1-3), 376–387. doi:10.1016/j.jmatprotec.2007.11.194
- Satishkumar, D., Kanthababu, M., Vajjiravelu, V., Anburaj, R., Thirumalai Sundarrajan, N., & Arul, H. (2011). Investigation of wire electrical discharge machining characteristics of Al6063/SiCp composites. *International Journal of Advanced Manufacturing Technology*, 56(9-12), 975–986. doi:10.1007/00170-011-3242-5
- Scott, D., Boyina, S., & Rajurkar, K. P. (1991). Analysis & optimization of parameter alloy in wire electrical discharge machining. *International Journal of Production Research*, 29(11), 2189–2207. doi:10.1080/00207549108948078
- Shah, A., Mufti, A. N., Rakwal, D., & Bamberg, E. (2011). Material Removal Rate, Kerf, & Surface Roughness of Tungsten Carbide Machined with Wire Electrical Discharge Machining. *Journal of Materials Engineering and Performance*, 20(1), 71–76. doi:10.1007/11665-010-9644-y
- Shoda, K., Kaneko, Y., Nishimura, H., Kunieda, M., & Fan, M. X. (1992). Adaptive Control of WEDM with On-line Detection of Spark Locations. *Proceeding of Tenth International Symposium for Electro-Machining (ISEM-10)*.

Singh, H., & Garg, R. (2009). Effects of process parameters on material removal rate in WEDM. *Journal of Achievements in Materials & Manufacturing Engineering*, 32, 70–74.

Sinha, S. K. (2010). Effects of Wire Lag in Wire Electrical Discharge Machining. *International Journal of Engineering Science and Technology*, 2(11), 6622–6625.

Snoeys, R., Dauw, D. F., & Kruth, J. P. (1983). Survey of EDM adaptive control in electro discharge machining. *Journal of Manufacturing Systems*, 2(2), 147–164. doi:10.1016/S0278-6125(83)80028-4

Snoeys, R., Dekeyser, W., & Tricarico, C. (1998). Knowledge-based system for wire EDM. *Annals CIRP*, 37(1), 197–202. doi:10.1016/S0007-8506(07)61617-5

Spedding, T. A., & Wang, Z. Q. (1997a). Study on modeling of wire EDM process. *Journal of Materials Processing Technology*, 69(1-3), 18–28. doi:10.1016/S0924-0136(96)00033-7

Spedding, T. A., & Wang, Z. Q. (1997b). Parametric optimization & surface characterization of wire electrical discharge machining process. *Precision Engineering*, 20(1), 5–15. doi:10.1016/S0141-6359(97)00003-2

Swain, A.K., Ray, S., & Mandal, N.K., (2012). Study on Kerf Width in Wire-EDM based on Taguchi Method. *Applied Mechanics & Materials*, 110-116, 1808-1816.

Tanimura, T., Heuvelman, C. J., & Vennstra, P. C. (1977). The properties of servo gap sensor with wire spark-erosion machining. *Annals CIRP*, 26(1), 59–63.

Tarng, Y. S., Ma, S. C., & Chung, L. K. (1995). Dedurationination of optimal cutting parameters in wire electrical discharge machining. *International Journal of Machine Tools & Manufacture*, 35(12), 1693–170. doi:10.1016/0890-6955(95)00019-T

Tosun, N., & Cogun, C. (2003). An investigation on wire wear in WEDM. *Journal of Materials Processing Technology*, 134(3), 273–278. doi:10.1016/S0924-0136(02)01045-2

Tosun, N., Cogun, C., & Inan, A. (2003). The Effect of Cutting Parameters on Workpiece Surface Roughness in Wire EDM. *Machining Science & Technology. International Journal (Toronto, Ont.)*, 7(2), 209–219.

Tosun, N., Cogunb, C., & Tosun, G. (2004). A study on kerf & material removal rate in wire electrical discharge machining based on Taguchi method. *Journal of Materials Processing Technology*, 152(3), 316–322. doi:10.1016/j.jmatprotec.2004.04.373

US Patent No. 14,927-1979

US Patent No. 1896613-1933

US Patent No. 20070295695 US Patent No. 4,686,153-87

US Patent No. 4287404-1981

US patent No. 4935594-90

US Patent No. 4,968,867-90

US Patent No. 4,998,552-91

## **Recent Developments in Wire Electrical Discharge Machining**

US Patent No. 5196665-90

US Patent No. 5,762,726-98

US Patent No. 5,945,010-97

US Patent No. 6875943-2005

Vamsi, K. P., Surendra, B. B., Madar, V. P., & Swapna, M. (2010). Optimizing Surface Finish in WEDM Using Taguchi Parameter Design Method. *Journal of the Brazilian Society of Mechanical Sciences and Engineering*, 32(2), 107–113.

Wang, C. C., Chowm, H. M., Yang, L. D., & Te Lu, C. (2009). Recast layer removal after electrical discharge machining via Taguchi analysis: A feasibility study. *Journal of Materials Processing Technology*, 209(8), 4134–4140. doi:10.1016/j.jmatprotec.2008.10.012

Wang, J., & Ravani, B. (2003). Computer aided contouring operation for travelling wire electric discharge machining (EDM). *Computer Aided Design*, 35(10), 925–934. doi:10.1016/S0010-4485(02)00207-5

Wang, T., & Kunieda, M. (2004). Dry WEDM for Finish Cut. *Key Engineering Materials*, 259-260, 562–566. doi:10.4028/www.scientific.net/KEM.259-260.562

Wang, T., Lu, Y. M., Hao, S. S., Xie, S. Q., Xu, X. C., & Wang, Y. (2009). Dry WEDM in Improving HS-WEDMed Surface Quality. *Key Engineering Materials*, 392-394, 624–628. doi:10.4028/www.scientific.net/KEM.392-394.624

Wang, T., Xie, S. Q., Xu, X. C., Chen, Q., Lu, X. C., & Zhou, S. H. (2012). Application of Uniform Design in Experiments of WEDM in Gas. *Advanced Materials Research*, 426, 11–14. doi:10.4028/www.scientific.net/AMR.426.11

Wang, T., Zhang, X., & Zhao, X. (2006). Study on Finishing Cut with Dry WEDM. *Materials Science Forum*, 532-533, 273–276. doi:10.4028/www.scientific.net/MSF.532-533.273

Wang, T., Zhang, X., & Zhao, X. (2008). Study on Dry WEDMed Surface Quality of Mould Steel. *Key Engineering Materials*, 375-376, 416–420. doi:10.4028/www.scientific.net/KEM.375-376.416

Watanabe, H., Sato, T., Suzuki, I., & Kinoshita, N. (1990). WEDM monitoring with a statistical pulse-classification method, *Annals. CIRP*, 39(1), 175–178. doi:10.1016/S0007-8506(07)61029-4

Xu, C. S. (2012). Working Principle & Performance of Wire Electrical Discharge Machining. *Advanced Materials Research*, 507, 180–183. doi:10.4028/www.scientific.net/AMR.507.180

Yan, M. T., & Huang, P. H. (2004). Accuracy improvement of wire-EDM by real-time wire tension control. *International Journal of Machine Tools & Manufacture*, 44(7-8), 807–814. doi:10.1016/j.ijmachtools.2004.01.019

Yan, M. T., & Laio, Y. S. (1998). Adaptive control of WEDM process using fuzzy control strategy. *Journal of Manufacturing Systems*, 17(4), 263–274. doi:10.1016/S0278-6125(98)80074-5

- Yan, M. T., Li, H. P., & Liang, J. F. (1999). The application of fuzzy control strategy in servo feed control of wire electrical discharge machining. *International Journal of Advanced Manufacturing Technology*, 15(11), 780–784. doi:10.1007/001700050131
- Yan, M. T., & Liao, Y. S. (1995). Adaptive Control of WEDM Process Using Fuzzy Control Strategy. *Proceedings of Eleventh International Symposium for Electro-Machining (ISEM-11)*.
- Yan, M. T., & Liao, Y. S. (1996). A self-learning fuzzy controller for wire rupture prevention in WEDM. *International Journal of Advanced Manufacturing Technology*, 11(4), 267–275. doi:10.1007/BF01351284
- Yan, M. T., & Liao, Y. S. (1996). Monitoring & self-learning fuzzy control for wire rupture prevention in wire electrical discharge machining. *International Journal of Machine Tools & Manufacture*, 36(3), 339–353. doi:10.1016/0890-6955(95)00050-X
- Yan, M. T., Liao, Y. S., & Chang, C. C. (2001). On-line estimation of work-piece height using neural networks & hierarchical adaptive control of WEDM. *International Journal of Advanced Manufacturing Technology*, 18(12), 884–891. doi:10.1007/PL00003956
- Yu, P.-H., Lee, H.-K., Lin, Y.-X., Qin, S.-J., Yan, B.-H., & Huang, F.-Y. (2011). Machining Characteristics of Polycrystalline Silicon by Wire Electrical Discharge Machining. *Materials and Manufacturing Processes*, 26(12), 1443–1450. doi:10.1080/10426914.2010.544808
- Yuan, J., Liu, C. L., Liu, X., Wang, K., & Yu, T. (2009). Incorporating prior model into Gaussian processes regression for WEDM process modeling. *Expert Systems with Applications*, 36(4), 8084–8092. doi:10.1016/j.eswa.2008.10.048
- Zhang, X. Y., Wang, D., & Li, X. J. (2012). Comparison study for finished accuracy of WEDM process. *Advanced Materials Research*, 479-481, 476–480. doi:10.4028/www.scientific.net/AMR.479-481.476

## Chapter 7

# Modeling and Optimization of Ultrasonic Machining Process Using a Novel Evolutionary Algorithm

**Mantra Prasad Satpathy**  
*KIIT (Deemed University), India*

**Bharat Chandra Routara**  
*KIIT (Deemed University), India*

### ABSTRACT

*Ultrasonic machining (USM) is one of the non-conventional techniques for machining of hard and brittle materials like glass, ceramics, and ceramic matrix composites. The objective of the study includes the investigation of material removal rate (MRR), hole oversize (HOS), and circularity of holes (COH) during USM of soda lime glass and finding out the optimal parametric condition by an evolutionary algorithm. Taguchi philosophy was employed to carry out experiments using the process parameters such as power rating, abrasive slurry concentration, and static load. A novel optimization algorithm called imperialist competitive algorithm (ICA) was used to obtain maximum MRR and minimum HOS and COH. This algorithm is inspired by the imperialistic competition and has several advantages over other evolutionary algorithms like its simplicity, less computational time, and accuracy in predicting the results. The Technique for order of preference by similarity to ideal solution (TOPSIS) is utilized to convert these multiple performance characteristics to a single response. Moreover, the prediction outcomes of this TOPSIS integrated ICA methodology demonstrates excellent conformity with the experimental values and can be applied to solve complex problems.*

DOI: 10.4018/978-1-5225-6161-3.ch007

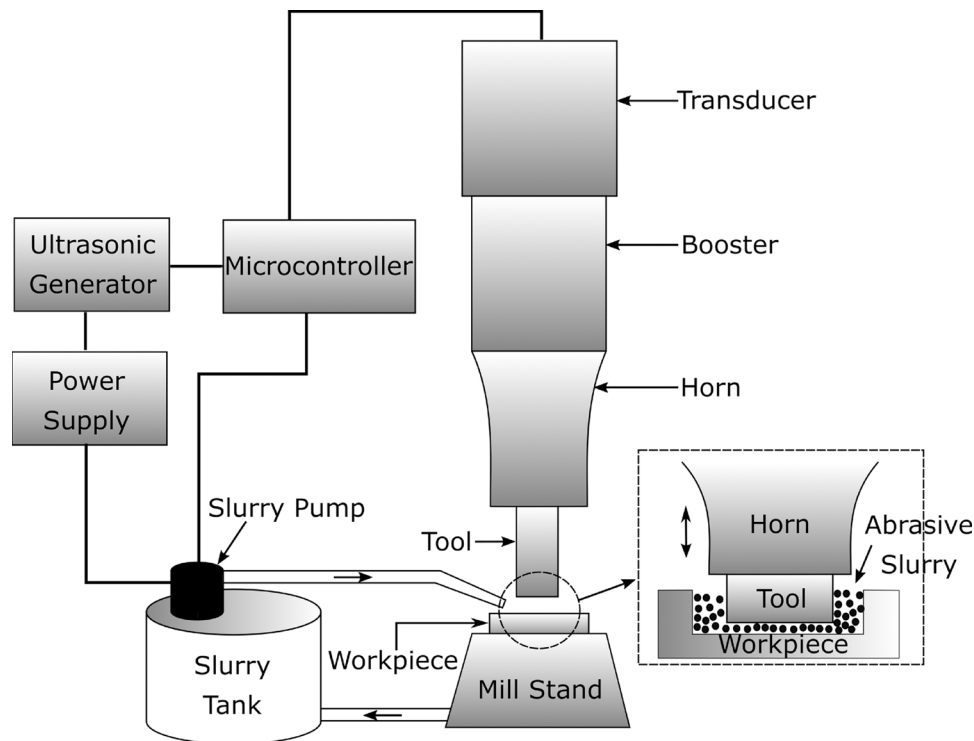
## INTRODUCTION

The technological advancement and introduction of newer materials in the manufacturing field put a challenging task in front of researchers. Mostly, these new materials have high strength, hardness and toughness properties and that make them difficult to machine by conventional techniques. Furthermore, whenever there is a need for complex and intricate shaped products, non-conventional manufacturing techniques are really suitable. Removal of unwanted material from the workpiece is one of the usual practice in all the manufacturing industries. Conventional machining processes like turning, drilling, milling, etc. show poor results as the workpiece is harder than the tool material. Thus, it is necessary to replace and to supplement the existing process with the novel machining concepts. Ultrasonic machining (USM) is one of the non-conventional mechanical material removal processes which uses high-frequency ultrasonic vibration. The other types of non-conventional mechanical machining processes are electric discharge machining (EDM), wire electric discharge machining (WEDM), electric chemical machining (ECM) and abrasive jet machining (AJM). The applications of EDM, WEDM and ECM processes are only limited to the electrically conductive materials. But USM is a widely used and versatile technique in the semiconductor industries for machining of both conducting and non-conducting materials with great accuracy. Thus, the hard and brittle materials which have low ductility properties and high hardness above 40 HRC like glass, ceramics, nickel and titanium alloys, etc. can be easily machined. However, the major hindrance to this process is the low material removal rate.

USM process works at a typical operating frequency of 20-40 kHz. This high-frequency electrical energy is produced by the ultrasonic generator. The piezoelectric or magnetostrictive transducer converts this high-frequency electrical energy to the mechanical vibration with some amplitude. But, this amplitude of vibration is not sufficient for machining purpose. Thus, a booster is generally used to amplify this amplitude. The ultrasonic energy transferred to the abrasive particles by a horn/tool. This tool is vibrated in a specific direction which is usually perpendicular to the workpiece surface. The abrasive slurry flows on the workpiece surface and underneath of the tool tip. The repetitive hammering of the tool tip on the abrasive particles of the slurry lead to the brittle fracture of the workpiece and the formation of a cavity precisely similar to the shape of the tool. Gradually, the tool is advanced in the direction of vibration until a through hole is produced. Figure 1 illustrates the schematic diagram of ultrasonic machining process on the brittle material. The beautifulness of the whole process is that there are no metallurgical and chemical composition changes during machining.

The right combination of input parameters is essential to obtain the best performance measure in the machining process. Typically, a slight change in the process parameters significantly affects the quality of the USM process. Thus, various statistical methods are employed during the experiments in order to identify the significant control parameters. In recent years, Taguchi philosophy grabs the attention of many researchers for minimizing the number of tests in a controlled way without compromising the quality of productivity. Another advantage of this philosophy is the variability of performance value around the target results by keeping the experimental cost at a minimum. Moreover, the technique for order of preference by similarity to ideal solution (TOPSIS) is one of the multi-criteria decision making (MCDM) methods used to convert multiple performance characteristics to a single response. As all the traditional optimization techniques trapped in the local optimum values and unable to solve complex problems, there is a need of metaheuristic techniques which can solve these problems with much accuracy and less time consumption. A lot of these metaheuristic techniques are applied in the manufacturing field to solve complex problems. However, it is not mandatory that if one technique gives the best result

*Figure 1. Schematic representation of USM setup*



for a particular problem, then that technique will be applied to other issues. Thus, it is a critical task for the researchers to apply the right technique for a specific problem. Imperialist Competitive Algorithm (ICA) is one of the socially based metaheuristic technique used to solve the current USM problem. It has several advantages over other evolutionary algorithms such as faster rate of convergence and less number of tuning parameters.

## **BACKGROUND OF USM PROCESS**

The USM was first patented by an American Engineer L. Balamuth in 1945 (Farrer, 1948). Many researchers have been working in this field since 60-70 years to develop this process considerably. The information regarding the industrial use of USM was published by the technical press in 1951 (Markov, 1966). The material removal rate (MRR) in USM process mainly depends on the workpiece, tool materials and machining parameters. Khairy (1990) demonstrated that the material removal of brittle materials like glass was due to the brittle fracture during USM. However, non-brittle materials exhibit plastic deformation for material removal. Meanwhile, it was observed that MRR decreased for the tougher materials like ceramics as comparable to the brittle materials (Henrik Dam, Quist, & Schreiber, 1995). With support to this, Komaraiah & Reddy (1993) presented the linear decreasing nature of MRR with the increase in material hardness and fracture toughness. The machining rate was also decreased with the increase in hardness of the brittle materials during USM (Komaraiah, Manan, Reddy, & Victor, 1988). The composites can be machined in USM provided it should be hardened. Majeed, Vijayaraghavan,

Malhotra, & Krishnamoorthy (2008) conducted USM experiments on  $\text{Al}_2\text{O}_3/\text{LaPO}_4$  composites. The results revealed that the machining rate was improved up to a certain value of hardness of workpiece. They also proposed a hollow tool to get better results. Kumar & Khamba (2009) also performed extensive experiments in USM by taking various controllable parameters and studied their effects on MRR and tool wear rate (TWR). They detected that high fracture toughness materials took a long machining time and it results in more TWR. On the other hand, the hard and brittle took less time as compared to the toughened materials, and it causes less TWR. Unlike workpiece material properties, the tool materials also play a vital role in USM process. Komaraiah & Reddy (1993b) reported that the MRR increased with the increase in tool hardness. Tungsten tool showed a superior result than the mild steel tool. It was also noticed that the tool made by high carbon steel performed better than other tools during machining of glass in USM (Kumar, Khamba, & Mohapatra, 2008). As the amplitude of vibration is an important parameter in USM, several authors also tried to design various types of horns and tools which can enhance the transfer of ultrasonic energy in the machining site (Amin, Ahmed, & Youssef, 1993; H Dam, Jensen, & Quist, 1993; Satyanarayana & Reddy, 1984).

Meanwhile, the MRR also depends on the machining parameters. Lee & Chan (1997) carried out an experiment considering the various abrasive grit sizes and vibration amplitude values. The large abrasive grits with a low amount of vibration amplitude exhibited a low MRR due to inadequate circulation of the abrasive slurry. Kainth, Nandy, & Singh (1979) explored the relationship between MRR and static load during the USM process. It was uncovered that this relationship was linear in the presence of non-uniform abrasive particles. Another USM experiment by Singh & Khamba (2008) also revealed the relationship between MRR and other input parameters (power, concentration of slurry, type of tool, type of slurry and abrasive size). Dvivedi & Kumar (2007) applied Taguchi philosophy to study the effects of various process parameters like abrasive grit size, workpiece material, power and slurry concentration on surface roughness (SR) during USM process. Singh & Khamba (2007) also used the similar process parameters to reduce their effect on SR using Taguchi technique. The whole process was modeled using Buckingham's  $\pi$ - theorem. Jadoun, Kumar, & Mishra (2009) also identified the optimal combination of process parameters in USM process and studied these effects on oversize, circularity of holes and conicity responses. Kumar & Khamba (2010) also employed Taguchi's L18 orthogonal array to investigate the impact of tool material, grit size and power on MRR. An empirical model was also developed between MRR and input parameters using dimensional analysis method. Gauri, Chakravorty, & Chakravorty (2011) conducted experiments using different control parameters and the multiple correlated responses like MRR, SR and TWR were optimized using weighted principal component analysis (WPCA), PCA based TOPSIS and PCA based grey analysis. However, WPCA outperformed than other methods due to its simplicity in the calculation. Venkata Rao, Pawar, & Davim(2009)utilized a metaheuristic technique called simulated annealing (SA) for optimization of process parameters in USM. The SA method conferred more accurate result than genetic algorithm (GA). Again, Rao, Pawar, & Davim(2010)applied various evolutionary algorithms such as harmony search (HS), artificial bee colony (ABC) and particle swarm optimization (PSO) to optimize the process parameters. The best result of MRR was noticed in these three methods while comparing with GA. Singh & Gill, (2009) modeled MRR in USM of porcelain ceramics using fuzzy logic. Venkata Rao & Kalyankar (2013) demonstrated that the teaching and learning based optimization (TLBO) in USM process exhibited the best optimal combination with that of ABC, PSO, GA and SA. Imperialist competitive algorithm (ICA) is one of the social based metaheuristic methods introduced by Atashpaz-Gargari & Lucas (2007) in the year 2007. Yazdipour & Ghaderi (2014) optimized the weld bead geometry in gas tungsten arc welding (GTAW) using ICA. The results showed that the



ICA converged to the global optimum value at a faster rate than genetic algorithm (GA). Mozafari, Abdi, & Ayob (2012) implemented ICA for optimization of the intermediate epoxy layer in between the two dissimilar sheets. The excellent capabilities of ICA demonstrated a better result while compared with GA and finite element method. Ghaderi, Aghakhani, Eslampanah, & Ghaderi (2015) performed experiments in submerged arc welding (SAW) process and optimized the deposition rate. They got the best solution by ICA, and it was validated through confirmatory tests. Atashpaz-Gargari & Lucas (2007a) applied ICA for designing proportional-integral-derivative (PID) controller. They concluded that the ICA conveyed a higher convergence rate to reach the best solution as compared to GA and analytical solutions. The ICA showed not only its applications in the manufacturing field but also it can be used in solving flow shop problems. Karimi, Zandieh, & Najafi (2011) used ICA to minimize the completion time in hybrid flexible flow shop problem. These computational results were compared with the random key genetic algorithm (RKGA) to show the predominance of ICA.

## **RESEARCH AND DEVELOPMENT ISSUES IN USM**

The previous literature demonstrates a substantial amount of work has already been accomplished by the various researchers in the USM field. Issues related to single and multiple response optimization problems were also solved by the introduction of metaheuristic techniques. But, the common problem of these techniques is the adjustment of many tuning parameters, and they are achieved near-optimal or sub-optimal results. In the present study, the USM experiment has been carried out on the soda lime glass by using Taguchi design of experiment and the effects of various input parameters on MRR, hole oversize (HOS) and circularity of holes (COH) has been investigated. Apart from solving the single objective problem, the multiple responses are combined to a single response called multi-response signal-to-noise (MRSN) by TOPSIS methodology. Furthermore, for getting excellent results, the whole process is modeled using regression analysis, and subsequently, ICA is applied to obtain maximum MRSN value. This novel algorithm has the immense potential not only to solve this USM problem but also to solve multi-dimensional complex manufacturing problems.

## **PROCESS PARAMETERS IN USM**

There are numerous numbers of controllable factors in USM process for the effective machining. These factors can be combined into following categories

1. Machine-related parameters
2. Workpiece material type
3. Tool material and its geometry
4. Abrasive slurry properties

### **Machine Related Parameters**

These parameters can be set on the USM setup

- Vibration amplitude
- Frequency of vibration
- Static load

### **Workpiece Material Type**

The machining rate of USM depend on the following characteristics of workpiece

- Brittle or ductile material
- Hardness and fracture toughness
- Thickness

### **Tool Material and Its Geometry**

The TWR is also an essential aspect of USM, and the tool properties include

- Brittle or ductile material
- Hardness and toughness
- Geometry
- Finishing

### **Abrasive Slurry Properties**

The material removal in USM depends on the adequate circulation of abrasive slurry in the machining site, and this includes

- Abrasive type
- Grit size of abrasive
- Concentration
- Feeding pressure
- Flow rate
- Type of feeding

## **EVALUATION OF PERFORMANCE MEASURES IN USM**

The production capability and its associated quality depends on the performance measures of any manufacturing process. USM involves the following performance characteristics

1. Material removal rate (MRR)
2. Tool wear rate (TWR)
3. Surface roughness (SR)
4. Hole oversize (HOS)
5. Circularity of holes (COH)

### **Material Removal Rate (MRR)**

MRR can be calculated by the weight difference of the sample before and after the experiment in USM process. It is expressed as volume material removal rate per machining time, i.e., mm<sup>3</sup>/min. The formula used for calculating MRR is

$$MRR = \frac{W_1 - W_2}{\rho \times t} \quad (1)$$

where  $W_1$  = Weight of the sample before the experiment,  $W_2$  = Weight of the sample after the experiment,  $\rho$  = Density of the workpiece and  $t$  = Time of machining

### **Tool Wear Rate (TWR)**

TWR can be calculated exactly as the MRR. Thus, the weight of the tool before and after experiment should be known to calculate TWR. The formula for finding out TWR is given below

$$TWR = \frac{TW_1 - TW_2}{\rho_t \times t} \quad (2)$$

where  $TW_1$  = Weight of the tool before the experiment,  $TW_2$  = Weight of the tool after the experiment,  $\rho_t$  = Density of the tool and  $t$  = Time of machining

### **Surface Roughness (SR)**

The surface finish is closely associated with the machining rate in USM. It depends on the factors such as abrasive grit size, tool face, vibration amplitude, and workpiece material properties. It is observed that larger the grit size, coarser is the surface finish. The amplitude of vibration has less effect on the surface roughness. But, if the amplitude of vibration raised then deeper craters are produced due to the high amount of pressing of individual abrasive particles. Usually, the average surface readings are taken during the experiments.

### **Hole Oversize (HOS)**

The increment in the size of the hole produced with respect to the size of the tool is known as hole oversize. In this study, the diameter of the cutting tool is 2mm, and three different diameters of the machined hole were measured at various places on its entry side. The HOS is estimated from the difference between the average diameter to the cutting tool diameter.

## Circularity of Holes (COH)

The circularity of hole refers to the errors present in the geometrical shape of the drilled holes. For this, diameters at different places can be measured, and COH is calculated by finding the difference between highest and lowest diameters of the drilled hole.

## OPTIMIZATION METHODOLOGY USED IN USM

### TOPSIS Methodology

This methodology is typically used in multi-response optimization problems. The solution obtained from this methodology is closest to the ideal alternative and farthest from the negative ideal alternative. The TOPSIS method consists of the following steps.

**Step 1:** The evaluation matrix was created with  $m$  alternatives and  $n$  criteria, intersecting each alternative and criteria as  $(X_{i,j})$ , therefore the matrix becomes  $(X_{i,j})_{m \times n}$

**Step 2:** The matrix  $(X_{i,j})_{m \times n}$  is normalized to form the matrix  $R = (r_{i,j})_{m \times n}$  using the normalization technique

$$(r_{i,j})_{m \times n} = \frac{X_{i,j}}{\sqrt{\sum_{i=1}^m X_{i,j}^2}}, i = 1, 2, 3, \dots, m, j = 1, 2, 3, \dots, n \quad (3)$$

**Step 3:** The weighted normalized values of the decision matrix is calculated by using the formulae:

$$T = (t_{i,j})_{m \times n} = (W_j r_{i,j})_{m \times n}, i = 1, 2, 3, \dots, m, j = 1, 2, 3, \dots, n \quad (4)$$

where  $(W_j)$  is the weight of the  $j^{th}$  criterion set by the decision maker so that  $\sum_{j=1}^n W_j = 1$

**Step 4:** The best alternative ( $A_B$ ) and the worst alternative ( $A_W$ ) is identified as

$$A_B = \left\{ \left( \max (W | i = 1, 2, 3, \dots, m | j \in j -) \right), \left( \min (W | i = 1, 2, 3, \dots, m | j \in j +) \right) \right\} \quad (5)$$

$$A_W = \left\{ \left( \min (W | i = 1, 2, 3, \dots, m | j \in j -) \right), \left( \max (W | i = 1, 2, 3, \dots, m | j \in j +) \right) \right\} \quad (6)$$

where  $j+ = (j=1, 2, \dots, nl \ j)$  associated with the criteria having maximization impact and  $j- = (j=1, 2, \dots, nl \ j)$  associated with the criteria having minimization impact.

**Step 5:** The Euclidean distance for each solution is calculated from the best and the worst alternative.

$$d_{iw} = \sqrt{\sum_{j=1}^n (t_{ij} - t_{wj})^2}, i = 1, 2, 3, \dots, m \quad (7)$$

$$d_{ib} = \sqrt{\sum_{j=1}^n (t_{ij} - t_{bj})^2}, i = 1, 2, 3, \dots, m \quad (8)$$

where,  $d_{iw}$  and  $d_{ib}$  are the distances from the target alternative  $i$  to the worst and the best conditions respectively.

**Step 6:** The Relative Closeness Coefficient (RCC) or  $(S_{iw})$  to the ideal solution is finally calculated by the following formulae:

$$S_{iw} = \frac{d_{iw}}{d_{iw} + d_{ib}}, 0 \leq S_{iw} \leq 1, i = 1, 2, 3, \dots, m \quad (9)$$

$S_{iw} = 1$ , if and only if the alternative solution is the best solution

$S_{iw} = 0$ , if and only if the alternative has the worst condition

### **Imperialist Competitive Algorithm (ICA)**

The proposed algorithm is one of the novel evolutionary optimization methods which is inspired by the socio-political mechanism of the countries. This algorithm includes countries which may play as imperialist or colony. The strongest country (based on the value of cost function) becomes the imperialist and others are treated as the colonies. The power of the imperialist country and the colonies create a powerful empire. The imperialist competition among the empires is the basis of this algorithm. At last, this competition converges towards a situation, where only one empire will present. ICA involves the following steps:

#### **Step 1: Generating initial empires**

This algorithm starts with the initial population (countries) like the chromosomes in GA. All the countries are divided into 2 categories (i) imperialists ( $N_{imp}$ ) and (ii) colonies ( $N_{col}$ ). The colonies are distributed among the imperialist according to their power. For this distribution of colonies, the normalized power of an imperialist has to be determined, and it is given by

$$w_n = \frac{NC_n}{\sum_{i=1}^{N_{imp}} NC_i} \quad (10)$$

where  $NC_n$  is the normalized cost of an imperialist. Initially, the number of colonies possessed by an empire is

$$NCol_n = round(w_n \times N_{col}) \quad (11)$$

where  $NCol_n$  is the initial number of colonies of  $n^{th}$  empire. Figure 2 demonstrates the initial population of each empire. In this figure, the size of the star symbol denotes the number of colonies that an empire possesses.

### Step 2: Assimilating policy

The colonies are developed by its corresponding imperialist countries. This fact is accomplished by moving all the colonies towards an imperialist.

### Step 3: Exchanging positions of imperialist and colony

A colony may reach the position of an imperialist with a less cost than the imperialist. In this case, the position of the colony and the relevant imperialist exchange their positions. The algorithm then continues with the newly made imperialist. Figure3 demonstrates the positions of colonies and imperialist before and after the exchange.

Figure 2. Initial population of empires and colonies

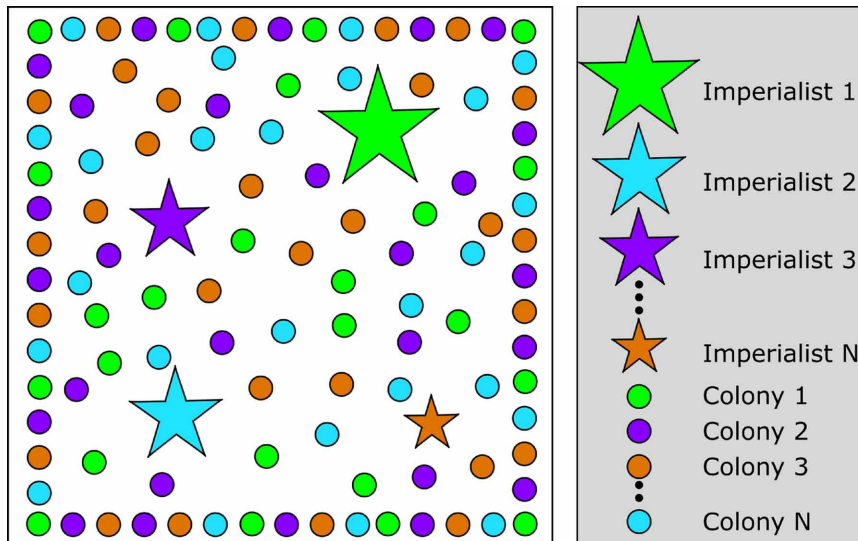
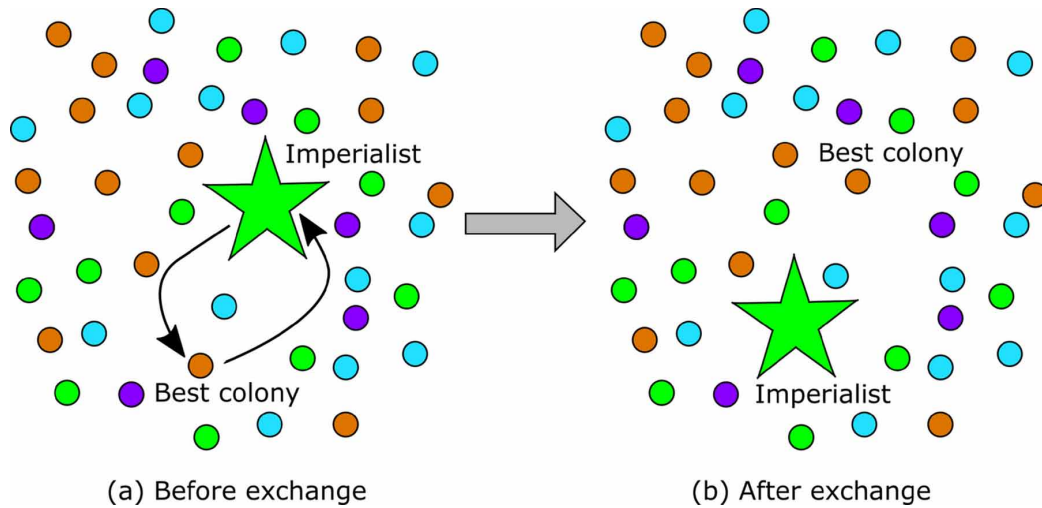


*Figure 3. Exchanging positions of imperialist and colony*



**Step 4: Total power of an empire**

Total power of an empire is evaluated by taking the total power of imperialist country and the power of colonies of an empire. Thus, the total cost will be

$$TC_n = C(\text{Imperialist}_n) + \lambda \times \text{mean}\{C(\text{Colonies of empires})\} \quad (12)$$

where  $TC_n$  is the total cost of  $n^{\text{th}}$  empire and  $\lambda$  is a positive integer less than 1.

**Step 5: Imperialistic competition**

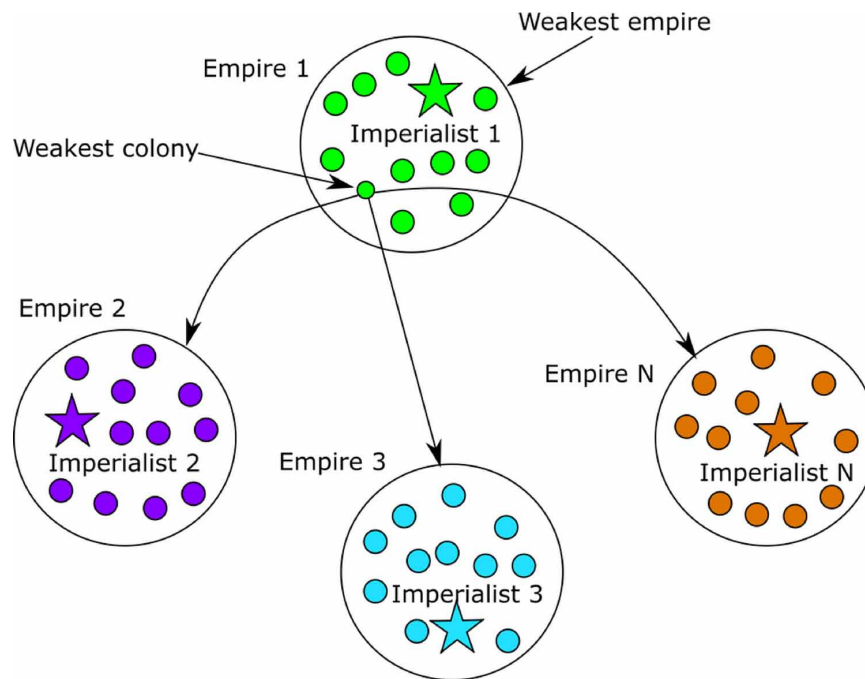
This is the most important phase of ICA in which all empires try to possess and control the colonies of other empires. Gradually, the weaker empire losses its power to the strongest one. This process is started by selecting the weakest colony of the weakest empire and assigning to the proper empire through competition. Figure4 illustrates the imperialistic competition mechanism. The probability of possession by each empire is

$$W_{w_n} = \left| \frac{NTC_n}{\sum_{i=1}^{N_{imp}} NTC_i} \right| \quad (13)$$

where  $NTC_n$  is the normalized total cost of  $n^{\text{th}}$  empire.

**Step 6: Eliminating powerless empires**

*Figure 4. Imperialistic competition mechanism*



Powerless empires will lose their colonies, and these are distributed among other empires.

#### **Step 7: Convergence**

The competition is continued until one empire exists in the search domain. The stopping criteria for this algorithm may be the maximum number of iterations or negligible improvement in the fitness function.

## **EXPERIMENTATION USING USM**

### **Work Material**

Soda lime glass/ soda-lime-silica glass of 20 mm × 20 mm × 2 mm is used as work material in the present investigation. It is one of the commonly used glasses for windowpanes, containers and some fancy items. It is usually prepared by melting the raw materials like sodium carbonate, lime, dolomite, silicon dioxide, aluminum oxide, and small quantities of sodium sulfate or sodium chloride at a temperature of 1675 °C. The properties of soda lime glass are furnished in Table 1.

### **Tool Material**

As the tool is an essential part of USM process, its wear rate affects the productivity. Thus, the tools should be made up of relatively ductile materials to lower the rate of wear. The typical tool materials



*Table 1. Workpiece material properties*

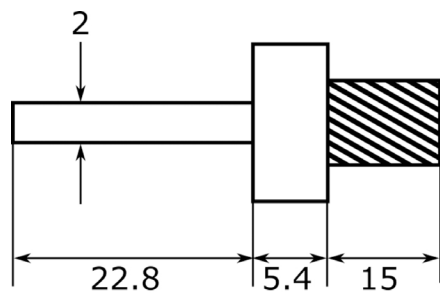
Properties	Values
Density (g/cm <sup>3</sup> )	2.44
Modulus of elasticity (Pa)	7.2E10
Poisson's ratio	0.22
Specific gravity	2.53
Thermal conductivity (Wm <sup>-1</sup> K <sup>-1</sup> )	1.1

like stainless steel, brass, and mild steel can be used. Depending upon the type and properties of abrasives, workpiece to TWR varies from 1:1 to 100:1. The present study includes tool steel (D2) as the tooling material. It has excellent wear resistance and toughness properties due to the presence of high chromium content. The different properties of tool material are presented in Table 2. The diameter of the cutting tool is 2 mm and length of 43.2 mm. The tool tip and tool holder comprises a single piece, and external threading has done on the tool holder to fit into the horn. No brazing operation has performed during the preparation of cutting tool. The schematic diagram of the cutting tool with its dimension is illustrated in Figure 5.

*Table 2. Tool material properties*

Properties	Values
Density (kg/m <sup>3</sup> )	7.7E3
Modulus of elasticity (Pa)	210E9
Poisson's ratio	0.3
Specific heat (J/kg*K)	461
Thermal conductivity (W/m*K)	20

*Figure 5. Schematic diagram of cutting tool*



(All dimensions are in mm)

## Experimental Setup

All the experiments have been performed in Sonic-Mill®, 500 W Ultrasonic machine with a constant frequency of 20 kHz. A highly efficient lead zirconate titanate electrostrictive element is used inside the transducer which has an energy conversion rate of 96%. Due to the excellent acoustical properties, titanium is considered as horn material. The abrasive slurry contains the boron carbide ( $B_4C$ ) powder of different grain sizes with water. This slurry is supplied to the machining site with various concentrations. Figure 6 represents a tabletop model of USM.

The concentration, power and static load have been considered as the process variables. The values of these process variables with their units are listed in Table 3. The weight of each sample before and after experiments have been measured accurately with the help of a high precision digital balance meter AFCOSET® (ER-180A). The maximum loading capacity of this instrument is 180 gm. The hole oversize (HOS) and circularity of holes (COH) have been determined precisely with the help of an OLYMPUS® (BX53M) microscope. According to the Taguchi's L9 orthogonal array, nine specimens (without interaction) have been machined in USM. A full-factorial design requires typically  $3^3 = 27$  experiments to study the effects of these three factors on responses, whereas Taguchi's design approach reduces it to only 9 runs, providing an excellent benefit with respect to experimental time and cost. Meanwhile, the constant machining time of 20 sec has taken for each sample. Table 4 presents the design table (all factors are in coded form) with the responses.

*Figure 6. Tabletop model of Sonic Mill*

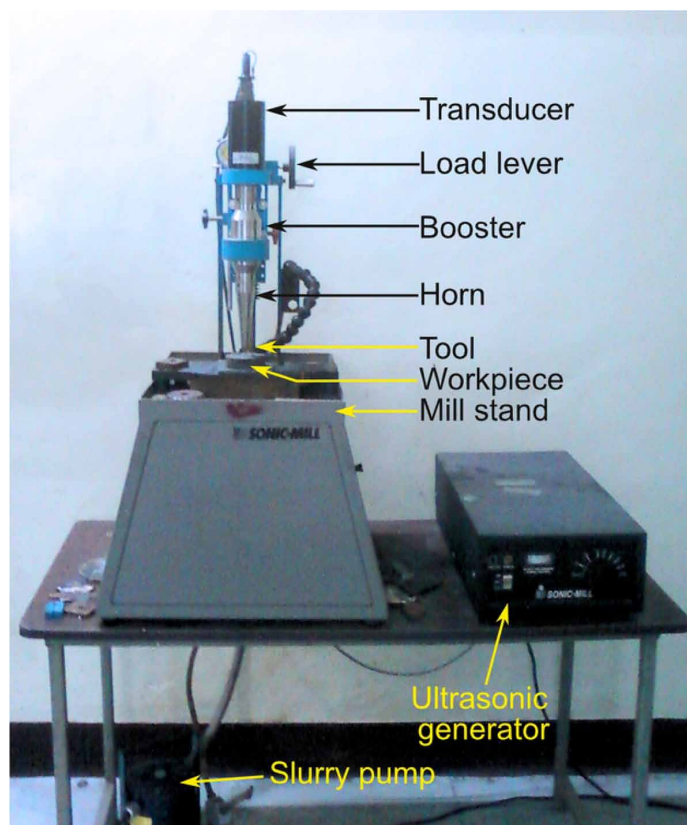


*Table 3. Process variables and their levels*

Parameters	Unit	Notation	Factor levels		
			1	2	3
Concentration	gm/m <sup>3</sup>	C	2%	3%	4%
Power	Watt	P	70	80	90
Static load	gm	F	500	700	900

*Table 4. Experimental design with responses*

Job no	Input parameters			Responses			RCC	MRSN (dB)
	Concentration(C)	Power(P)	Static load(F)	MRR (mm <sup>3</sup> /sec)	HOS (mm)	COH (mm)		
1	1	1	1	0.41	0.66	0.10	0.67	-3.35
2	1	2	2	0.71	1.20	0.40	0.52	-5.67
3	1	3	3	0.11	0.70	0.20	0.39	-8.17
4	2	1	2	0.69	1.10	0.20	0.72	-2.74
5	2	2	3	0.12	0.73	0.10	0.47	-6.40
6	2	3	1	0.16	0.83	0.30	0.26	-11.47
7	3	1	3	0.17	1.03	0.30	0.22	-12.96
8	3	2	1	0.22	0.83	0.10	0.51	-5.70
9	3	3	2	0.19	0.90	0.20	0.39	-8.07

## ANALYSIS OF OUTPUT RESULTS USING EXPERIMENTAL DESIGN

### Influence of Process Parameters on MRR

During the USM process, the effects of various machining factors on the MRR is displayed in Figure 7. It confers that MRR increases up to an optimal value of static load but, it decreases further with the increase of static load. Because there is a reduction in the abrasive particle size at higher static load resulting lower MRR. Likewise, when the other parameters like concentration of the abrasive slurry and power increases, MRR decreases. This is expected because an increase in the concentration of abrasives causing an insufficient slurry circulation in the machining zone. Moreover, at high power, the abrasive particles loose its cutting phenomena due to its reduction in size. However, it is better for abrasive wear declination and increment in tool life.

### Influence of Process Parameters on HOS

During the USM process, a considerable less amount of heat is developed. Thus, it is not responsible for the development of residual stress or damaged layer due to thermal effect. Influence on HOS is shown in Figure 8. It is highest at the entry side and gradually decreases towards the exit side. Meantime, the abrasive grain size and its concentration have a significant effect on the dimensional accuracy like HOS.

Figure 7. Control parameters effect on MRR

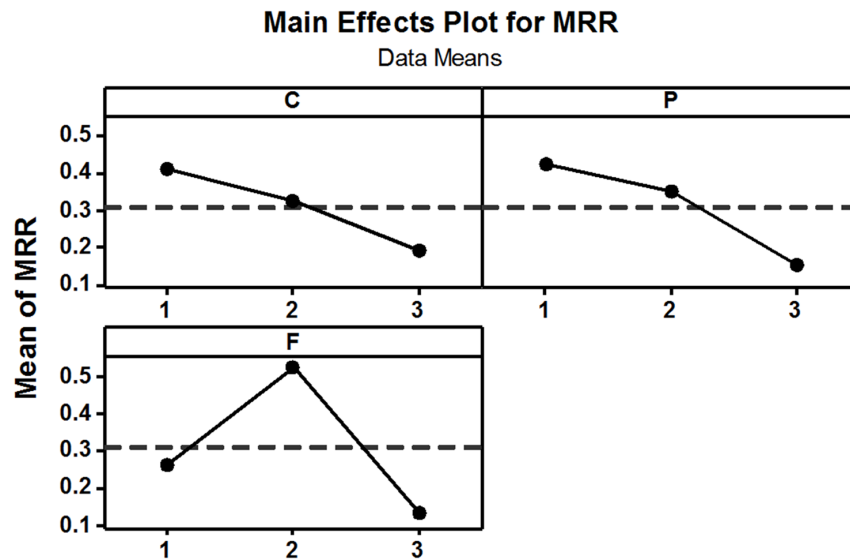
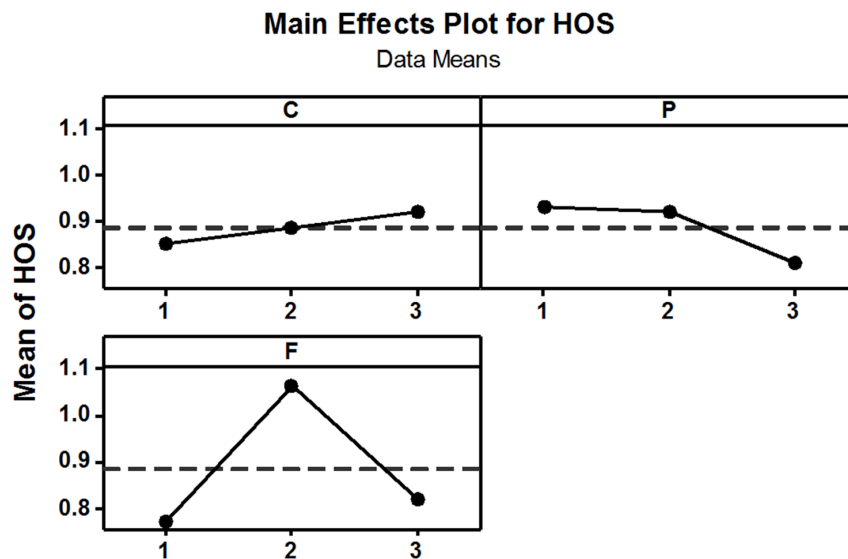


Figure 8. Control parameters effect on HOS



A decrease in concentration of abrasive in the slurry improves the surface finish and decrease in the size of the machined hole. It is quite obvious from the figure that the HOS is inversely proportional to the power. It is because of the fragmentation of abrasive particles at higher power. Likewise, the HOS increases with the increase in static load and it is undesirable. But, it decreases with the further increase in static load due to suppression of lateral vibration.

### Influence of Process Parameters on COH

The production accuracy in USM process depends on the form accuracy (COH). It denotes the accuracy of the machining process. Figure 9 depicts the relationship of COH with the process parameters. It gradually decreases with the increase in the concentration of abrasive slurry medium. There is a less deviation in the dimensional measurement at the entry side of the hole due to the high density of fine abrasive particles. Meanwhile, the COH is directly proportional to the power. When the static load increases, the COH increases in the same manner as HOS and then it decreases gradually. The surface roughness improves with the rise in static load which reduces the size of the abrasive particles. Thus, the COH is minimized at high static load.

### Influence of Process Parameters on MRSN

The acquired MRR, HOS and COH for all the 9 experimental runs along with their S/N ratios are illustrated in Table 4. This analysis is performed using MINITAB 16 software. Meantime, the capability and accuracy of USM process depend on these three responses. Thus, higher MRR with lower HOS and COH is desired. In order to achieve these values, three separate optimal conditions will be evolved. However, a single optimal combination can be achieved by compromising the desired values of responses. TOPSIS methodology is applied in this study to convert these multiple responses to a single response, i.e., relative closeness coefficient (RCC), and the related S/N ratio is calculated on the Higher-the-better criterion. Figure 10 displays the main effects plot for S/N ratio, and it can be easily comprehended that the factor combination of C1P2F2 gives the highest MRSN value. The Table 5 demonstrates that static load (F) has the most influence on MRSN followed by power (P) and concentration (C).

Figure 9. Control parameters effect on COH

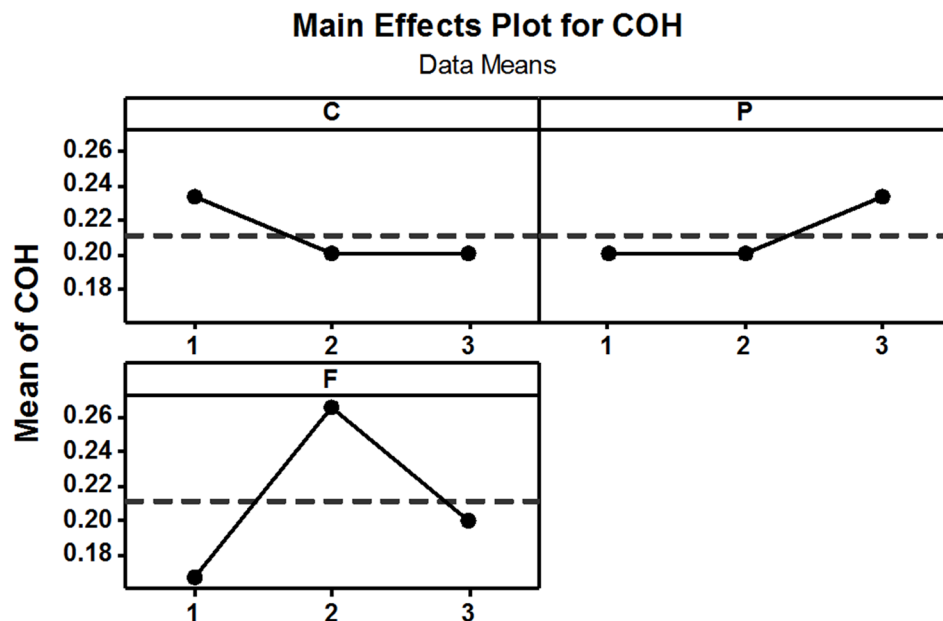


Figure 10. Control parameters effect on MRSN

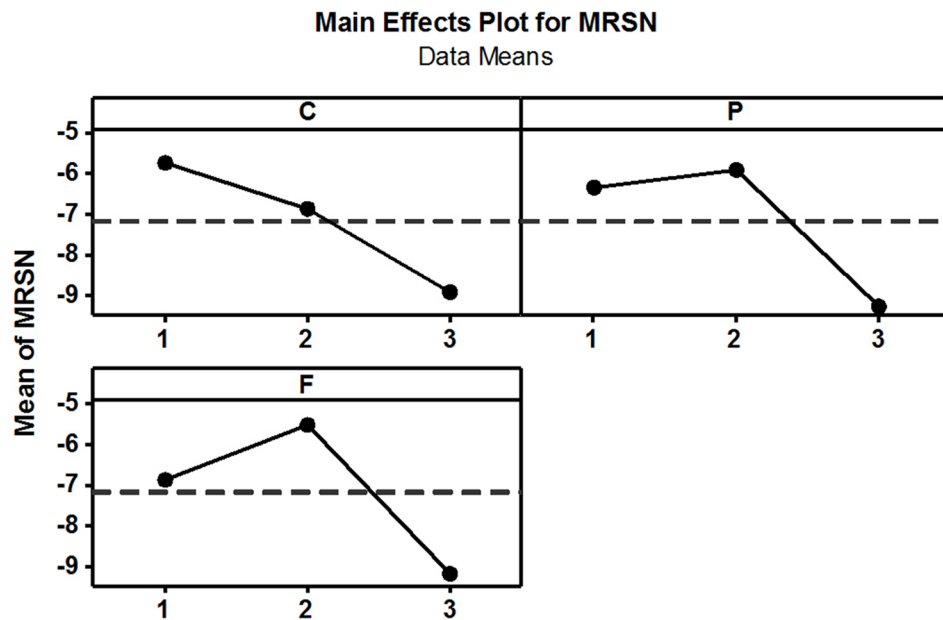


Table 5. Response table for S/N ratio of MRSN

Level	C	P	F
1	-5.733	-6.355	-6.844
2	-6.875	-5.927	-5.499
3	-8.916	-9.243	-9.181
Delta	3.183	3.316	3.682
Rank	3	2	1

## OPTIMIZATION OF USM PROCESS USING ICA

Regression analysis is a statistical technique utilized to develop the relationships among input and output variables. It includes many modeling techniques and in the present analysis, the quadratic model has been used. The regression equation for MRSN is presented in Eq. (14).

$$MRSN = -1.76 + 1.00 \times C - 13.38 \times P + 11.73 \times F - 0.44 \times C^2 + 0.37 \times P^2 - 0.46 \times F^2 + 4.09 \times C \times P - 4.49 \times C \times F \quad (14)$$

The higher value of MRSN, better is the machining performance. Thus, the objective of the current problem is to maximize the MRSN. The equation developed from regression (Eq. (14)) is incorporated with ICA as a cost function. The algorithmic parameters are tuned in several iterations, and finally, the optimum parameter condition is reached. The settings are furnished in Table 6.

*Table 6. Algorithm parameters settings for ICA*

Tuning Parameters	Values
Number of total countries	100
Number of imperialists	8
Number of decades	50
Revolution rate	0.3
Assimilating coefficient	0.8
Assimilating angle	0.5

Results demonstrate that at the C1P3F1 optimum parametric combination, maximum MRSN of -1.13 dB is observed. Moreover, the optimized results from Taguchi philosophy and ICA are compared (Table 7). Figure 11 illustrates a graph of mean cost of all imperialists and the number of iterations. From this figure, it can be inferred that the objective function is converged at the 24<sup>th</sup> iteration. Furthermore, the confirmatory test has also been performed to validate the results of ICA. A 2.58% error is noticed while comparing the results.

## CONCLUDING REMARKS

In the present work, multi-response optimization problem has been solved by TOPSIS based ICA technique. This technique is capable of producing high MRR with less HOS and COH. It is observed that the ICA technique takes less computational time as compared to other non-conventional optimization techniques. While examining the ICA result with the experimental result, the error is within the acceptable limit. The consequent optimal parametric combination in USM process provides a better idea to the process engineers in achieving high machining rate. Thus, the process engineers can now adopt this technique to get best combinations of input parameters in USM problems, and there is no need to depend on the manufacturer's handbook.

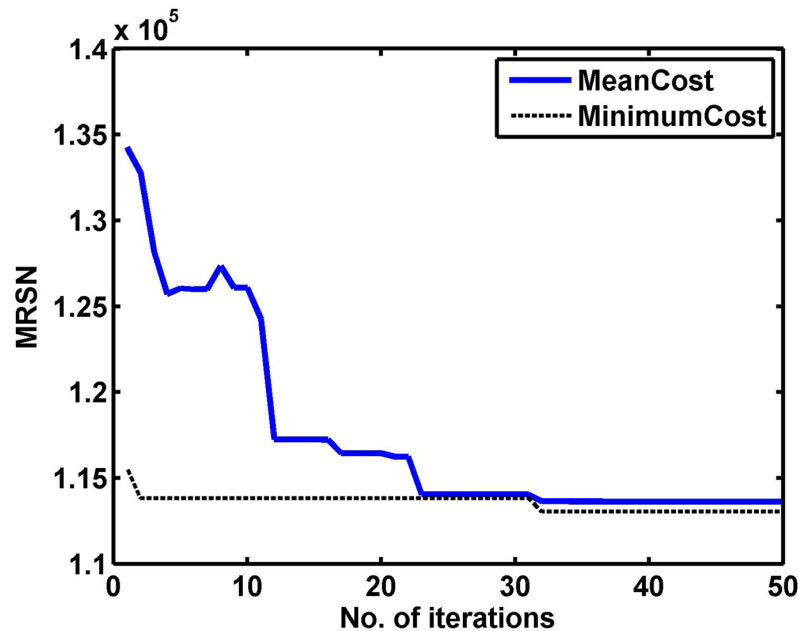
## FUTURE RESEARCH DIRECTIONS

USM process may be hybridized with electrochemical reaction for better machining performance. Ultrasonic tool and abrasive particles may be suspended in an alkaline electrolyte medium to machine hard

*Table 7. Comparison of results*

Methods	Optimal parametric combination			MRSN (dB)
	C	P	F	
Taguchi philosophy	1	2	2	-5.67
ICA	1	3	1	-1.13
Experimental	1	3	1	-1.16

Figure 11. Mean and minimum erosion rate versus iterations



materials such as monel, titan, etc. The effect of pre-heated abrasive slurry and cryogenically treated tool on the outputs in USM process may be analyzed. The effect of the rotational ultrasonic tool with various coatings for machining of the brittle material may be regarded as a new horizon of analysis in USM process.

## REFERENCES

- Amin, S. G., Ahmed, M. H. M., & Youssef, H. A. (1993). Optimum design charts of acoustic horns for ultrasonic machining. *Proceedings of the International Conference on AMPT*, 93, 139–147.
- Atashpaz-Gargari, E., & Lucas, C. (2007a). Designing an optimal PID controller using Colonial Competitive Algorithm. *Proceedings of the First Iranian Joint Congress on Fuzzy and Intelligent Systems*.
- Atashpaz-Gargari, E., & Lucas, C. (2007b). Imperialist competitive algorithm: an algorithm for optimization inspired by imperialistic competition. In *Evolutionary computation, 2007. CEC 2007. IEEE Congress on* (pp. 4661–4667). IEEE. 10.1109/CEC.2007.4425083
- Dam, H., Jensen, S., & Quist, P. (1993). Surface characterization of ultrasonic machined ceramics with diamond impregnated sonotrode. *Machining of Advanced Materials*, 125–133.
- Dam, H., Quist, P., & Schreiber, M. P. (1995). Productivity, surface quality and tolerances in ultrasonic machining of ceramics. *Journal of Materials Processing Technology*, 51(1-4), 358–368. doi:10.1016/0924-0136(94)01587-Q



- Dvivedi, A., & Kumar, P. (2007). Surface quality evaluation in ultrasonic drilling through the Taguchi technique. *International Journal of Advanced Manufacturing Technology*, 34(1-2), 131–140. doi:10.100700170-006-0586-3
- Farrer, J. O. (1948). *Improvements in or relating to cutting, grinding, polishing, cleaning, honing, or the like*. UK Patent (602801).
- Gauri, S. K., Chakravorty, R., & Chakraborty, S. (2011). Optimization of correlated multiple responses of ultrasonic machining (USM) process. *International Journal of Advanced Manufacturing Technology*, 53(9-12), 1115–1127. doi:10.100700170-010-2905-y
- Ghaderi, M. R., Aghakhani, M., Eslampanah, A., & Ghaderi, K. (2015). The application of imperialist competitive algorithm for optimization of deposition rate in submerged arc welding process using TiO<sub>2</sub> nano particle. *Journal of Mechanical Science and Technology*, 29(1), 357–364. doi:10.100712206-014-1242-8
- Jadoun, R. S., Kumar, P., & Mishra, B. K. (2009). Taguchi's optimization of process parameters for production accuracy in ultrasonic drilling of engineering ceramics. *Production Engineering*, 3(3), 243–253. doi:10.100711740-009-0164-2
- Kainth, G. S., Nandy, A., & Singh, K. (1979). On the mechanics of material removal in ultrasonic machining. *International Journal of Machine Tool Design and Research*, 19(1), 33–41. doi:10.1016/0020-7357(79)90019-2
- Karimi, N., Zandieh, M., & Najafi, A. A. (2011). Group scheduling in flexible flow shops: A hybridised approach of imperialist competitive algorithm and electromagnetic-like mechanism. *International Journal of Production Research*, 49(16), 4965–4977. doi:10.1080/00207543.2010.481644
- Khairy, A. B. E. (1990). Assessment of some dynamic parameters for the ultrasonic machining process. *Wear*, 137(2), 187–198. doi:10.1016/0043-1648(90)90135-W
- Komaraiah, M., Manan, M. A., Reddy, P. N., & Victor, S. (1988). Investigation of surface roughness and accuracy in ultrasonic machining. *Precision Engineering*, 10(2), 59–65. doi:10.1016/0141-6359(88)90001-3
- Komaraiah, M., & Reddy, P. N. (1993a). A study on the influence of workpiece properties in ultrasonic machining. *International Journal of Machine Tools & Manufacture*, 33(3), 495–505. doi:10.1016/0890-6955(93)90055-Y
- Komaraiah, M., & Reddy, P. N. (1993b). Relative performance of tool materials in ultrasonic machining. *Wear*, 161(1-2), 1–10. doi:10.1016/0043-1648(93)90446-S
- Kumar, J., & Khamba, J. S. (2009). An investigation into the effect of work material properties, tool geometry and abrasive properties on performance indices of ultrasonic machining. *International Journal of Machining and Machinability of Materials*, 5(2-3), 347–366. doi:10.1504/IJMMM.2009.023399
- Kumar, J., & Khamba, J. S. (2010). Modeling the material removal rate in ultrasonic machining of titanium using dimensional analysis. *International Journal of Advanced Manufacturing Technology*, 48(1-4), 103–119. doi:10.100700170-009-2287-1

- Kumar, J., Khamba, J. S., & Mohapatra, S. K. (2008). An investigation into the machining characteristics of titanium using ultrasonic machining. *International Journal of Machining and Machinability of Materials*, 3(1-2), 143–161. doi:10.1504/IJMMM.2008.017631
- Lee, T. C., & Chan, C. W. (1997). Mechanism of the ultrasonic machining of ceramic composites. *Journal of Materials Processing Technology*, 71(2), 195–201. doi:10.1016/S0924-0136(97)00068-X
- Majeed, M. A., Vijayaraghavan, L., Malhotra, S. K., & Krishnamoorthy, R. (2008). AE monitoring of ultrasonic machining of Al<sub>2</sub>O<sub>3</sub>/LaPO<sub>4</sub> composites. *Journal of Materials Processing Technology*, 207(1-3), 321–329. doi:10.1016/j.jmatprotec.2008.06.039
- Markov, A. I. (1966). *Ultrasonic machining of intractable materials*. London: Iliffe Books Ltd.
- Mozafari, H., Abdi, B., & Ayob, A. (2012). Optimization of adhesive-bonded fiber glass strip using imperialist competitive algorithm. *Procedia Technology*, 1, 194–198. doi:10.1016/j.protcy.2012.02.036
- Rao, R. V., & Kalyankar, V. D. (2013). Parameter optimization of modern machining processes using teaching–learning-based optimization algorithm. *Engineering Applications of Artificial Intelligence*, 26(1), 524–531. doi:10.1016/j.engappai.2012.06.007
- Rao, R. V., Pawar, P. J., & Davim, J. P. (2010). Parameter optimization of ultrasonic machining process using nontraditional optimization algorithms. *Materials and Manufacturing Processes*, 25(10), 1120–1130. doi:10.1080/10426914.2010.489788
- Satyanarayana, A., & Reddy, B. G. K. (1984). Design of velocity transformers for ultrasonic machining. *Electrical India*, 24(14), 11–20.
- Singh, J., & Gill, S. S. (2009). Fuzzy modeling and simulation of ultrasonic drilling of porcelain ceramic with hollow stainless steel tools. *Materials and Manufacturing Processes*, 24(4), 468–475. doi:10.1080/10426910802714407
- Singh, R., & Khamba, J. S. (2007). Taguchi technique for modeling material removal rate in ultrasonic machining of titanium. *Materials Science and Engineering A*, 460, 365–369. doi:10.1016/j.msea.2007.01.093
- Singh, R., & Khamba, J. S. (2008). Mathematical modelling of surface roughness in ultrasonic machining of titanium using Buckingham-II approach: A review. *International Journal of Abrasive Technology*, 2(1), 3–24. doi:10.1504/IJAT.2009.021635
- Venkata Rao, R., Pawar, P. J., & Davim, J. P. (2009). Optimisation of process parameters of mechanical type advanced machining processes using a simulated annealing algorithm. *International Journal of Materials & Product Technology*, 37(1-2), 83–101.
- Yazdipour, A., & Ghaderi, M. R. (2014). Optimization of weld bead geometry in gtaw of cp titanium using imperialist competitive algorithm. *International Journal of Advanced Manufacturing Technology*, 72(5-8), 619–625. doi:10.100700170-014-5682-1

# Chapter 8

## An Investigation Into Non-Conventional Machining of Metal Matrix Composites

**Divya Zindani**

*National Institute of Technology Silchar, India*

**Kaushik Kumar**

*Birla Institute of Technology, India*

### ABSTRACT

*One of the recently developing fields is that of non-traditional machining of particle reinforced metal matrix composites. The complexity associated with traditional machining of particle reinforced metal matrix composite is very high, and therefore, the researchers have begun to show more focus towards non-traditional machining. In the present work, the investigation has been carried out for non-traditional machining such as laser beam machining, electro-chemical machining, abrasive water jet machining, and electro-chemical discharge. Material removal rate, surface finish, and the mechanism of machining has been studied for each of the aforementioned processes. The main material removal mechanisms as has been identified are melting, mechanical erosion, vaporization, and chemical dissolution. The investigation reveals that the major reasons for the damage of the machined surface are the presence of reinforcement particles and thermal degradation.*

### INTRODUCTION

It is through the employment of machining processes that the final shape of the product is achieved through the removal of unwanted material from the main workpiece (Pramanik et al., 2009). The mechanism of material removal in case of traditional machining process involves the removal in the form of chips owing to the plastic deformation resulting because of the force being exerted by the sharp cutting tools (Pramanik et al., 2013). The tool life in machining of metal matrix composites (MMCs) is shortened because of the abrasive nature of the reinforcements (Pramanik et al., 2006). The surface finish is also worse due to the tool-particle-machined surface interactions. The aforementioned limitations put hindrance to the

DOI: 10.4018/978-1-5225-6161-3.ch008

use of MMCs (Pramanik et al., 2007). It becomes impossible for the conventional machining processes to machine MMCs with high percentage of reinforcing particles. Therefore, certain non conventional machining processes such as laser-beam, abrasive water jet, electro-discharge and electro-chemical have been developed for machining of such materials (Hihara et al., 2000). The last few decades have seen dominance of studies on traditional machining methods of MMCs over the non-traditional machining process such as electro-discharge machining (EDM), laser-beam, electro-chemical (ECM), abrasive water jet machining (AWJM) and photo-chemical machining (PCM). EDM process is one of the widely explored non-traditional machining process for particle reinforced metal matrix composites (PRMMCs) while PCM is the least explored of all. Thus it is obvious that a greater understanding is still required on machining of MMCs using non-traditional machining. A clear understanding of the different non-traditional methods used for machining of MMCs will aid in exploring the potential advantages of non-traditional methods over the traditional ones which then can then be applied in practical field. The present work therefore is an attempt to investigate the less explored non-traditional methods with focus on the mechanism of material removal, material removal rate, surface finish and the machining speed. The above parameters considered for the study will aid in assessing the recent developments, efficiency and the performance of the non-traditional methods. A better understanding on the mechanism of material removal rate leads to a proper visualization of the specific method and also the associated problems relating to the methods are revealed. The efficiency of machining process is reflected in its cutting speed which delineates the fact that how quickly the material removal takes place. The performance of a machining process is revealed by the level of surface finish and dimensional accuracy achieved. The performance of a machining process is considered worst if it gives rise to poor surface finish or poor dimensional accuracy. In the backdrop of the above discussion, the present work provides a brief overview of the non-traditional machining of MMCs by considering contributions from past researchers.

The rest of the chapter has been organized into: Laser beam machining, abrasive water jet machining, electro-chemical machining and electrochemical spark machining. The subsections in each of these sections describes in detail the material removal mechanism, major output response parameter and surface finish and dimensional accuracy for each of the aforementioned process. the chapter finally ends with the concluding remarks consisting of future directions.

## **LASER BEAM MACHINING**

Laser beam machining (LBM) is considered to be one of the most employed non-traditional machining processes. It is one of the thermal energy based advanced machining processes. The workpiece material is melted and vaporized using laser beam (Dubey et al., 2008). The LBM process is suitable for producing geometrically complex shapes and small holes. The thermal and the optical properties of a material determine the effectiveness of the LBM process. For higher performance of LBM, a material is required to possess low thermal conductivity and diffusivity. Mechanical properties such as brittleness and hardness are insignificant properties responsible for the LBM effectiveness (Müller and Monaghan 2000). Laser beam is the main source of heat energy that is transferred through irradiation. The absence of cutting forces, material damage due to mechanical forces and tool wear makes LBM a suitable machining process for MMCs. LBM can be used for a number of machining operations on a single machine such as cutting, drilling, welding and grooving (Pham et al., 2007). The most common type of lasers used for machining are CO<sub>2</sub> and Nd:YAG lasers (Dubey et al., 2008). CO<sub>2</sub> lasers are generally used for

machining of composites with matrix of very high thermal conductivity and are characterized with low absorption factor (Dahotre et al., 1989; Kagawa et al., 1989; Hong et al., 1997). Number of reports on LBM of MMCs is very scarce.

## **Mechanism of Machining**

The mechanism of LBM machining involves the following main stages: (i) melting, vaporization and chemical degradation, (ii) removal of transformed material and (iii) cooling. First, laser beam is focused on the workpiece surface and the transfer of thermal energy from the laser beam to the workpiece surface takes place. The thermal energy from the laser is absorbed by the workpiece surface transforming the parent material into a pool of molten material, vaporizing it and changing its chemical state. The transformed material is removed (Dubey et al., 2008) using a jet of pressurized inert gas which also is used for prevention of oxidation (Hong et al., 1997). The remaining material that hasn't been removed cools down and solidifies, forming the machined surface. For machining of MMCs, generally the diameter of laser beam used is higher than that of the reinforcement size (Di Pietro and Yao, 1995). Striation pattern are often observed on the machined surface which may be attributed to the fact that the high-pressure jet forces the melted material bottom causing downward flow of the molten material. Another issue is that of dross attachment at the bottom of machined surface. These complex issues are dependent on the machining conditions and therefore needs to be minimized (Müller and Monaghan 2000). Generation of heat-affected sub-surface layers is another drawback of LBM. The intense heat in the laser beam melts the sub-surface layer of the parent material and brings changes to the microstructure of the matrix used in the fabrication of PRMMCs. The melting process accelerates the chemical reaction amongst the constituting phases of the MMCs. For instance, needle like phases are produced because of the chemical reaction between Al and SiC particles which is then followed by solid state diffusion (Hong et al., 1997; Dahotre et al., 1989). The reaction can however be controlled by controlling the laser energy input (Dahotre et al., 1989). Three distinct zones were observed on laser cutting of SiC reinforced MMCs (Yue et al., 1996): (i) unaffected base material, (ii) melted matrix material that re-solidifies in this zone. This resulted in the formation of fine regular aluminium alloy wherein the silicon particles were absent. The SiC particles are distinguishable from matrix material in this zone as they do not dissolve and (iii) the melted SiC particles are dissolved in the already melted matrix material. The formation of  $Al_4C_3$  in the zone has been revealed (Hu and Baker, 1997; Hong et al., 1997). The three zones reflect on the higher thermal loading associated with the laser beam.

## **Cutting Speed**

One of the input parameters for LBM is cutting speed. Higher the cutting speed, lower is the associated depth of cut. The higher cutting speed for a given laser beam power is indicative of lesser amount of energy available for material removal in the cutting zone and thus the main reason behind lower depth of cut and kerf width. Further, a higher cutting speed results into rough surface finish which can be attributed to the unsteady motion of the molten layer. The striations are also prominent with the increasing cutting speed. The Al MMCs with high volume of SiC were laser cut with smooth surface finish and narrow heat affected zone. This was made possible using moderate speed of cuttings and employing argon shielding gas (Hong et al., 1997).

## **Surface Finish**

Typical patterns have been observed on laser machined surfaces owing to the intermittent flow of molten material (Di Pietro and Yao, 1995). The patterns observed are usually straight lines at slight angle and are dependent on the cutting parameters chosen for LBM machining (Müller and Monaghan 2000). There is an increasing trend of surface roughness with the increased feed rate and cutting speed and decreased power output (Lau et al, 1994). On observing the surface topography of Al alloy matrix without any reinforcements, a smooth surface finish was revealed at the entrance of the laser. However an increased surface roughness has been observed around the middle cut height. This was attributed to the fact that the aluminium alloy at upper part of the surface was removed as a result of vaporization while on the other hand the lower part of the material was melted by laser. The melted lower part was swept downwards owing to the high pressure of the shielding gas jet. In the SiC reinforced aluminium MMCs, the vaporizing process was revealed to be deterred during the LBM machining process. Higher viscosity of the melt produced a smoother striation surface (Müller and Monaghan 2000).

The literature reported on LBM machining of MMCs is scarce and is indicative of the limited research carried out in this domain (Dahotre et al., 1989; Di Pietro and Yao, 1995; Hong et al., 1997; Müller and Monaghan 2000). The reports are sufficient to reveal that the reinforcements melt on confrontation with the laser beam and thereby changing the microstructure of MMC substantially. The surface roughness is higher with the higher cutting speed owing to the unsteady motion of the molten layer or due to the intermittent blockage of the laser beam by the reinforcing particles. The main challenge associated with the LBM methodology is that of optimization of heat input.

## **ABRASIVE WATER JET MACHINING**

The material removal in abrasive water jet machining takes place through high velocity pressurized jet, water and abrasive slurry. The material is removed from the parent material by erosion (Shanmugam et al., 2002). AWJ machining has the potentiality to machine almost every available material but the research community has focused their attention for AWJ of difficult-to-machine and thermally sensitive materials (Ramulu, and Arola, 1993; Kovacevic et al., 1997). The abrasive water jet can be employed for turning, drilling and milling (Hashish, 1995). The main advantage associated with AWJ machining process is the absence of high temperature and hence the thermally affected zone (Müller and Monaghan 2000). Cutting instead of deformation wear promotes material removal in AWJ machining process (Müller and Monaghan 2000). High feed rates are achievable with the AWJ process and hence have the capability to fast machine the MMCs. Further, the process has the capability to cut materials in all the possible directions (Hashish, 1995). One of the major disadvantages with the AWJ process is its inability to fabricate workpiece with higher geometrical accuracy.

## **Mechanism of Machining**

The material removal process occurs with the impact of small abrasive particles onto the workpiece surface. Mostly 80-mesh abrasive grains have been recommended for use by the scientific community (Savrun and Taya, 1988; Shanmugam et al., 2002). The material removal process in MMCs depends to a great extent on the relative size of abrasive grains with respect to the size of reinforcing particles. The

diameter of nozzle employed for the high velocity pressurized jet of water is generally lesser than 1 mm. individual abrasive particles are responsible for small amount of material removal and therefore their combined effect removes significant amount of material. However, during the cutting process some of the abrasive grains may get embedded into the matrix phase (Savrun and Taya, 1988).

The mechanism of machining can be explained by considering three different cases: (i) the size of reinforcing particles is smaller than that of the abrasive grains, (ii) the size of reinforcing particles as well as the abrasive grains are almost similar and (iii) the reinforcing particles are much bigger than the size of the abrasive particles used. In the first case the material removal process entails the removal of number of reinforcing particles. The chances of fracture are higher in such a case and also that of pulling out of the reinforcing particles (Müller and Monaghan 2000). In case (ii) it becomes difficult to remove the reinforcing particle at a time. The abrasive particles in this case pressurize the reinforcing particles into and over the surface resulting into ploughing and indentation. In the third scenario the abrasive particles remove both the matrix as well as some portion of the reinforcing particles resulting into smooth surface finish (Hamatani and Ramulu, 1990). The rate of removal of reinforcing particles is smaller in comparison to that of the matrix material. Researchers have observed localized micro-melting in certain areas of the matrix as a result of high velocity jet (Savrun and Taya, 1988).

## **Cutting Speed**

Cutting speed is one of the major input parameters for the AWJ machining process. With the increased cutting speed the time to remove material per unit area also decreases. Lower depth of cut is obtained with the higher speed of cutting. Further, there is increase in surface roughness and striations with the increased cutting speed (Savrun and Taya, 1988).

## **Surface Finish**

Rough surface finish with the usage of AWJ process has been generally reported by the research community (Hashish, 1995; Capello et al., 1996; Müller and Monaghan 2000). However, the damage to the subsurface is minimal. No changes at micro-structural levels have been reported by the research community. The abrasive particles at times get embedded into the parent material and therefore full grooves appear on the machined surface (Savrun and Taya, 1988). With lower cutting speeds smoother surface finish is achievable. On the other hand the surface roughness increases with the increased abrasive particle size. Presence of striations has been reported while machining of thicker MMCs. Better surface finish have been reported with the increased flow rate of abrasive particles at high speed of cutting and with low abrasive flow rate at low cutting speed. The aforementioned fact signifies that optimal number of abrasive particles is required to participate at a time in the material removal process resulting into smoother surface finish. The number of abrasive particles increases with the flow rate and decreases with the cutting speed. However, at low cutting speed and increased flow rate, the machining process becomes inefficient because of overcrowding abrasive particles resulting into poor surface finish. This signifies that the surface roughness increases with the decreased flow rate and increased cutting speed and lower cutting speed in tandem with lower abrasive flow rate.

Single pass slot has been produced in SiC/6061-T6 MMC specimens using AWJ machining process (Hamatani and Ramulu, 1990) with constant rate of water supply and garnet abrasives. Cutting speed and size of the abrasive particles were found to be determining factors for the kerf taper ratio. Kerf taper

ration was observed to be smaller in case of lower speed of cutting. With the reduction in abrasive particles size the kerf ratio approaches to unity at critical speed. Beyond critical speed, kerf ratio increases beyond unity. For any precision process, there should be no degree of taper. The critical speed at which the slot is produced with no taper is dependent on the abrasive particle size (Hamatani and Ramulu, 1990), the critical speed increasing with the size of the abrasive particles. However, the bottom width reduces with the increasing volume percentage of reinforcing particles while no changes have been reported for the top width (Hashish, 1995).

The main attractions for the AWJ machining processes are the absence of thermally affected zone and higher speed of cutting. Very few reports have been published on investigation of AWJ machining processes. Following can be concluded from the investigations carried out (Savrun and Taya, 1988; Hamatani and Ramulu, 1990; Hashish, 1995; Müller and Monaghan 2000): the material removal mechanism involves abrasive shearing of the matrix phase, the ratio of sizes of abrasive particles to that of the reinforcing particles determines the mechanism of material removal, formation of striations while machining of thicker MMCs.

## **ELECTROCHEMICAL MACHINING**

Electrochemical dissolution of the workpiece material forms the principle behind material removal in electrochemical machining (ECM) (Kozak, 1998). The workpiece forms anode and tool is the cathode, both being separated by an electrolytic medium. Passage of electric current through the electrolytic solution marks the beginning of ECM process. Melting of the anodic workpiece takes place leading to material removal and the negative mirror of tool shape is produced on the workpiece. The electrolytic media is generally a concentrated salt solution. Pumping the electrolytic solution at high pressure aids in removal of reaction products and controlling the heat generated (Bhattacharyya, 2004). The anodic behaviour in a given electrolyte is the major determinant factor of ECM machining performance (Sorkhel, S. K., & Bhattacharyya, 1994). The miniature parts with complex shapes are suitably and efficiently fabricated by the ECM process irrespective of the workpiece hardness (De Silva, 2000; Ebeid et al., 2004). Burr and stress free surfaces, longer life of the cathodic tool etc., are some of the main advantages associated with the ECM process (De Silva, 2000, Senthilkumar et al., 2009).

### **Mechanism of Machining**

Machining of SiC/Al MMCs was done using copper as the cathodic tool and NaCl as electrolytic solution. Literatures have been published reporting the use of different electrolytic solution and cathodic tool for machining of MMCs. Calomel as cathode and aqueous sodium nitrate solution as electrolytic solution has been employed for machining of MMCs (Hihara and Panquites, 2003). Tolerances of the order of 0.05 mm have been achieved by maintaining current density greater than 1 A/cm<sup>2</sup> and small distance of around 0.5 mm between the cathodic tool and the anodic workpiece.

### **Material Removal Rate**

Increased feed, electrolytic flow rate and concentration and applied voltage enhance the material removal rate during the ECM process. Machining current in the gap between cathode and anode increases with



the increasing voltage and electrolytic concentration. The current density is also increased with the feed as the inter-electrode gap reduces. Mobility of metal ions is speeded up with the higher electrolytic flow rate and therefore the increased material removal rate is achieved (Senthilkumar et al., 2009).

Establishing the relationship between material removal rate and the various input parameters is key to enhance the ECM machining performance. Response surface methodology has been applied by Senthilkumar et al. (Senthilkumar et al., 2009) in establishing relationship between various material removal rate and various process parameters such as electrolytic flow rate (l/min) electrolytic concentration (g/l), feed rate (mm/min) and applied voltage (V). The findings reveal that at a given feed rate, the material removal rate increases with the voltage. The material removal rate also shows an increasing trend with the feed rate, applied voltage remaining constant. Increased voltage results into increased machining current at the inter-electrode gap resulting into higher material removal rate. Rapid dissolution of the anodic surface occurs with the higher feed rates owing to the reduction of the inter-electrode gap which increases the current density (Sen and Shan, 2005)

A higher electrolytic flow rate and its concentration have also been reported to increase the material removal rate (Sen and Shan, 2005). At higher electrolytic concentration, there is an increase in the number of ions in the inter-electrode gap resulting into increased material removal rate. The movement of ions also increases at increased electrolytic flow rate aiding in removal of hydrogen bubbles and speeding up the chemical reaction. Thus material removal rate also increases with the increased electrolytic flow rate (Rajurkar and Hewidy, 1988; da Silva Neto, 2006).

## **Surface Finish**

Various parameters such as electrolytic flow rate and its concentration, tool feed rate and applied voltage have a significant effect on the surface roughness. The change in dissolution valency of the anodic surface during the process of machining is one of the main reasons for the production of macro-defects onto the machined surface (Senthilkumar et al., 2009).

The surface roughness is higher for lower feed rate and voltage, the reason for which may be attributed to non-uniform and unsteady dissolution of the anodic metal (Osman and Abdel-Rahman, 1999). Uneven microstructure are obvious in etch pits resulting with low current density (Senthilkumar et al., 2009). The rate of metal ion deposition at anode increases with the increased voltage. The increased voltage results into increased density of current at the inter-electrode gap and therefore accelerating the rate of metallic ion deposition. However, as the concentration of metallic ion exceeds beyond a certain limit, precipitation of thin salt film incepts. The morphology of the dissolved material is affected by the thin salt film. The surface defects can however be suppressed with the usage of limiting current that may occur at high voltage. Therefore, at higher voltage better surface finish is achievable (Sen and Shan, 2005).

The electrolytic concentration and its flow rate are also important factors affecting the surface roughness. The surface roughness decreases until the electrolytic flow and its concentration increases and reaches their critical value. Beyond this the surface roughness increases. The low electrolytic flow rate associate with itself negligible turbulence. The low turbulence slows the motion of diffused material generating streak on the surface of material undergoing machining. Poor surface finish is produced with shortage of ions with lower concentration of electrolytic solution (Coughanowr and Dissaux, 1986). The increased electrolytic concentration results in higher current density which leads to increased pitting tendency. Smooth surface can however be achieved from the overlapping pits (Konig et al., 1978).

The surface roughness shows a downward trend with the increase in voltage at a constant electrolytic flow rate. Higher voltage results in excessive heating at the localized areas of the machining material and thereby resulting in poor surface finish (Senthilkumar et al., 2009). With the increasing flow rate, the surface finish shows an increasing trend which then begins to decrease beyond a certain limit of flow rate. This may be attributed to the increasing turbulence with increasing electrolytic flow rate, avoiding flow streak on the surface (Chetty and Radhakrishnan, 1981). However, there is non-uniformity in removal of material with further increase in flow resulting into poor surface finish.

## **ELECTRO-CHEMICAL SPARK MACHINING**

Electrochemical spark machining is yet another hybrid framework that encompasses the characteristics of electrochemical machining (ECM) and electrical discharge machining (EDM) (Liu et al., 2013). The hybrid framework has the potential ability to machine non-conductive materials such as ceramics and glass. The capabilities of the process are yet to be explored for the industrial applications (Wüthrich and Fascio, 2005). A pulsed or DC voltage is applied between the anode and the cathode, separated a few centimeters apart and dipped in a suitable electrolytic solution. Surface area of cathode is much lesser than that of anodic surface (Wüthrich and Fascio, 2005). The voltage reaching its critical value marks the beginning of the process. Formation of gas bubbles take place when the voltage goes beyond its critical value. These gas bubbles then coalesce to form a gas film that isolates the cathodic tool from the electrolytic solution. The electric field in the gas film becomes very high generating electrical discharges (Wüthrich and Fascio, 2005) across the bubbles. The material removal takes place through the mechanism of chemical erosion and electrical discharges (Fascio et al., 1999). The workpiece material is kept at a fixed distance from the anode and then brought closer to the cathodic surface, resulting in material removal in region where sparking occurs (Abrate and Walton, 1992).

### **Mechanism of Machining**

The material removal mechanism is complex entailing physical and chemical actions. The commonly used electrolytic solutions are sodium hydroxide (NaOH) and sodium nitrate ( $\text{NaNO}_3$ ). In case of machining MMCs cathode is the tool and workpiece material forms the anode. Flow of current across the machining gap take place as a result of pulsed voltage applied between the electrodes. Flowing current results in dissolution of anodic surface. The simultaneous occurrence of electro-chemical reactions increase the electrical resistance and voltage across the machining gap because of hydrogen bubble formation at the cathodic surface. Sparks are generated when the voltage applied reaches its critical value. The material removal then also takes place through the spark erosion process. The nature of the anodic surface or the workpiece material and the amount of gas evolved generally defines the machining performance of the ECDM process (Liu et al., 2013).

During the MMCs machining with ECDM process, higher current densities have been revealed around the matrix-particle interface. The removal of reinforcing particles and matrix material is accelerated as a result of higher interface current density. The ECM phase dissolves the metal around the reinforcement and also activates the sparking required for EDM in large spark gap (Liu et al., 2013). Removal of debris formed as a result of machining is facilitated by the larger spark gap. The nature of reinforcements doesn't have any effect on the critical voltage required to initiate the spark. The formation of gas bubbles at the

cathode surface however depends on the concentration of the electrolytic solution, its temperature and on the cathode geometry. The formation of gas bubbles is promoted by maintaining anode-to-cathode ratio over 100 (Liu et al., 2013).

## **Material Removal Rate**

Material removal rate has been reported to decrease with the increasing percentage of reinforcing material. The fact may be attributed to the higher percentage of matrix protection by the reinforcing particles. The material removal rate shows an increasing trend with the pulse duration until a certain critical limit is reached, but it then decreases with further increase in pulse duration beyond the critical value. The initial increased energy input is the major reason for the initial increase in material removal rate with the increasing pulse duration. However, with the increasing pulse duration the machined debris gets trapped within the spark gap resulting in clogging and hence declined material removal rate. The phenomenon of clogging is prominent wherein the size of the reinforcing particles is higher than that of the discharge gap. The instability in the machining process increases with the significant increase in number of trapped particles.

The machining current generally increases the material removal rate. With the increased current the ECD phase gets accelerated because of increasing gap which ultimately results in efficient flushing of the machined debris. The efficient flushing of debris results in improved machining stability. However, the material removal rate decreases with increase in gap beyond its optimum value. The material removal rate also increases with the increasing applied voltage. Further, like the machining current, there is an optimum electrolytic concentration until which the material removal rate is enhanced. At lower electrolytic concentration, the bubble formation is lower at the cathode surface. The impact of ECD phase is enhanced with the electrolytic concentration but it has an adverse effect on the EDE phase.

## **Surface Finish**

The surface roughness shows a decreasing trend with the increasing duration of pulse but then with increasing pulse duration the surface finish increases but at a lower rate. The ECD phase is increased with the increasing pulse duration. The material removal rate is mainly by ECM when the pulse duration is shorter. Increase in machining current results in increasing surface roughness. This may be attributed to the formation of larger crater as a result of higher pulse energy. At higher electrolytic concentration the dominant phase is that of ECD.

## **CONCLUSION**

Advancements and developments in machining of particle reinforced MMCs are still in its nascent stage and the progress made is gradual in the recent years. The complexity of the machining processes is increased with the presence of reinforcements and the material removal mechanism is totally different from that for the routine materials. Deficiencies are existent in understanding the mechanism of machining of reinforced composite materials. The changed composition of the material because of excessive heating is the major drawback of the laser beam machining. Attachment of dross and formation of striations are some of the other common problems in this case. In case of abrasive water jet machining,

the size of the abrasive particles defines the surface finish of the machined surface. The least explored non-conventional machining processes for particle reinforced MMCs are electro chemical and electro-chemical spark machining. The melting of matrix material around the reinforcement is the prominent limitation in case of electrochemical machining. Electro-chemical spark machining on the other hand is quite fast in comparison to the electrochemical machining owing to the combined ECM and EDM phases. The present work reveals that in-depth investigation in unconventional machining may result in enhanced precision in machining of MMCs.

A discussion on other non-traditional processes that haven't been explored yet such as ultrasonic machining etc. may be a possible scope for those working in the domain of non-traditional machining of PRMMCs.

## ACKNOWLEDGMENT

The authors sincerely acknowledge the comments and suggestions of the reviewers that have been instrumental for improving and upgrading the paper in its final form.

## REFERENCES

- Abrate, S., & Walton, D. (1992). Machining of composite materials. Part II: Non-traditional methods. *Composites Manufacturing*, 3(2), 85–94. doi:10.1016/0956-7143(92)90120-J
- Bhattacharyya, B., Munda, J., & Malapati, M. (2004). Advancement in electrochemical micro-machining. *International Journal of Machine Tools & Manufacture*, 44(15), 1577–1589. doi:10.1016/j.ijmach-tools.2004.06.006
- Capello, E., Polini, W., & Semeraro, Q. (1996). Abrasive water jet cutting of MMC: Analysis of the quality of the generated surfaces. In *ESDA Engineering Systems Design and Analysis Conference: presented at the Third Biennial Joint Conference on Engineering Systems Design and Analysis* (pp. 63-68). Academic Press.
- Chetty, O. K., & Radhakrishnan, V. (1981). A study on the influence of grain size in electrochemical machining. *International Journal of Machine Tool Design and Research*, 21(1), 57–69. doi:10.1016/0020-7357(81)90014-7
- Coughanowr, C. A., Dissaux, B. A., Muller, R. H., & Tobias, C. W. (1986). Electrochemical machining of refractory materials. *Journal of Applied Electrochemistry*, 16(3), 345–356. doi:10.1007/BF01008844
- da Silva Neto, J. C., Da Silva, E. M., & Da Silva, M. B. (2006). Intervening variables in electrochemical machining. *Journal of Materials Processing Technology*, 179(1-3), 92–96. doi:10.1016/j.jmatprotec.2006.03.105
- Dahotre, N. B., McCay, T. D., & McCay, M. H. (1989). Laser processing of a SiC/Al-alloy metal matrix composite. *Journal of Applied Physics*, 65(12), 5072–5077. doi:10.1063/1.343183

- De Silva, A. K. M., Altena, H. S. J., & McGeough, J. A. (2000). Precision ECM by process characteristic modelling. *CIRP Annals-Manufacturing Technology*, 49(1), 151–155. doi:10.1016/S0007-8506(07)62917-5
- Di Pietro, P., & Yao, Y. L. (1995). A new technique to characterize and predict laser cut striations. *International Journal of Machine Tools & Manufacture*, 35(7), 993–1002. doi:10.1016/0890-6955(94)00063-P
- Dubey, A. K., & Yadava, V. (2008). Laser beam machining—a review. *International Journal of Machine Tools & Manufacture*, 48(6), 609–628. doi:10.1016/j.ijmachtools.2007.10.017
- Ebeid, S. J., Hewidy, M. S., El-Taweel, T. A., & Youssef, A. H. (2004). Towards higher accuracy for ECM hybridized with low-frequency vibrations using the response surface methodology. *Journal of Materials Processing Technology*, 149(1-3), 432–438. doi:10.1016/j.jmatprotec.2003.10.046
- Fascio, V., Wuthrich, R., Viquerat, D., & Langen, H. (1999). 3D microstructuring of glass using electrochemical discharge machining (ECDM). In *Micromechatronics and Human Science, 1999. MHS'99. Proceedings of 1999 International Symposium on* (pp. 179–183). IEEE.
- Hamatani, G., & Ramulu, M. (1990). Machinability of high temperature composites by abrasive waterjet. *Journal of Engineering Materials and Technology*, 112(4), 381–386. doi:10.1115/1.2903346
- Hashish, M. (1995). Waterjet machining of advanced composites. *Material and Manufacturing Process*, 10(6), 1129–1152. doi:10.1080/10426919508935098
- Hihara, L. H., & Panquites, I. V. P. (2000). *U.S. Patent No. 6,110,351*. Washington, DC: U.S. Patent and Trademark Office.
- Hong, L., Vilar, R. M., & Youming, W. (1997). Laser beam processing of a SiC particulate reinforced 6061 aluminium metal matrix composite. *Journal of Materials Science*, 32(20), 5545–5550. doi:10.1023/A:1018668322943
- Hu, C., & Baker, T. N. (1997). A new aluminium silicon carbide formed in laser processing. *Journal of Materials Science*, 32(19), 5047–5051. doi:10.1023/A:1018653030270
- Kagawa, Y., Utsunomiya, S., & Kogo, Y. (1989). Laser cutting of CVD-SiC fibre/A6061 composite. *Journal of Materials Science Letters*, 8(6), 681–683. doi:10.1007/BF01730441
- Konig, W., Aachen, T. H., & Lindenlauf, P. (1978). Surface generation in electrochemical machining. *Annals of the CIRP*, 27(1), 97–100.
- Kovacevic, R., Hashish, M., Mohan, R., Ramulu, M., Kim, T. J., & Geskin, E. S. (1997). State of the art of research and development in abrasive waterjet machining. *Journal of Manufacturing Science and Engineering*, 119(4B), 776–785. doi:10.1115/1.2836824
- Kozak, J. (1998). Mathematical models for computer simulation of electrochemical machining processes. *Journal of Materials Processing Technology*, 76(1-3), 170–175. doi:10.1016/S0924-0136(97)00333-6
- Lau, W. S., Yue, T. M., & Wang, M. (1994). Ultrasonic-aided laser drilling of aluminium-based metal matrix composites. *CIRP Annals-Manufacturing Technology*, 43(1), 177–180. doi:10.1016/S0007-8506(07)62190-8

- Liu, J. W., Yue, T. M., & Guo, Z. N. (2013). Grinding-aided electrochemical discharge machining of particulate reinforced metal matrix composites. *International Journal of Advanced Manufacturing Technology*, 68(9-12), 2349–2357. doi:10.100700170-013-4846-8
- Müller, F., & Monaghan, J. (2000). Non-conventional machining of particle reinforced metal matrix composite. *International Journal of Machine Tools & Manufacture*, 40(9), 1351–1366. doi:10.1016/S0890-6955(99)00121-2
- Osman, H. M., & Abdel-Rahman, M. (1993). Integrity of surfaces produced by electrochemical machining. *Journal of Materials Processing Technology*, 37(1-4), 667–677. doi:10.1016/0924-0136(93)90126-Q
- Pham, D. T., Dimov, S. S., & Petkov, P. V. (2007). Laser milling of ceramic components. *International Journal of Machine Tools & Manufacture*, 47(3-4), 618–626. doi:10.1016/j.ijmachtools.2006.05.002
- Pramanik, A., Islam, M. N., Basak, A., & Littlefair, G. (2013). Machining and tool wear mechanisms during machining titanium alloys. *Advanced Materials Research*, 651, 338–343. doi:10.4028/www.scientific.net/AMR.651.338
- Pramanik, A., Neo, K. S., Rahman, M., Li, X. P., Sawa, M., & Maeda, Y. (2009). Ultraprecision turning of electroless nickel: Effects of crystal orientation and origin of diamond tools. *International Journal of Advanced Manufacturing Technology*, 43(7-8), 681–689. doi:10.100700170-008-1748-2
- Pramanik, A., Zhang, L. C., & Arsecularatne, J. A. (2006). Prediction of cutting forces in machining of metal matrix composites. *International Journal of Machine Tools & Manufacture*, 46(14), 1795–1803. doi:10.1016/j.ijmachtools.2005.11.012
- Pramanik, A., Zhang, L. C., & Arsecularatne, J. A. (2007). An FEM investigation into the behavior of metal matrix composites: Tool–particle interaction during orthogonal cutting. *International Journal of Machine Tools & Manufacture*, 47(10), 1497–1506. doi:10.1016/j.ijmachtools.2006.12.004
- Rajurkar, K. P., & Hewidy, M. S. (1988). Effect of grain size on ECM performance. *Journal of Mechanical Working Technology*, 17, 315–324.
- Ramulu, M., & Arola, D. (1993). Water jet and abrasive water jet cutting of unidirectional graphite/epoxy composite. *Composites*, 24(4), 299–308. doi:10.1016/0010-4361(93)90040-F
- Savrun, E., & Taya, M. (1988). Surface characterization of SiC whisker/2124 aluminium and Al<sub>2</sub>O<sub>3</sub> composites machined by abrasive water jet. *Journal of Materials Science*, 23(4), 1453–1458. doi:10.1007/BF01154616
- Sen, M., & Shan, H. S. (2005). Analysis of hole quality characteristics in the electro jet drilling process. *International Journal of Machine Tools & Manufacture*, 45(15), 1706–1716. doi:10.1016/j.ijmachtools.2005.03.005
- Senthilkumar, C., Ganesan, G., & Karthikeyan, R. (2009). Study of electrochemical machining characteristics of Al/SiC p composites. *International Journal of Advanced Manufacturing Technology*, 43(3-4), 256–263. doi:10.100700170-008-1704-1

***An Investigation Into Non-Conventional Machining of Metal Matrix Composites***

Shanmugam, D. K., Chen, F. L., Siores, E., & Brandt, M. (2002). Comparative study of jetting machining technologies over laser machining technology for cutting composite materials. *Composite Structures*, 57(1-4), 289–296. doi:10.1016/S0263-8223(02)00096-X

Sorkhel, S. K., & Bhattacharyya, B. (1994). Parametric control for optimal quality of the workpiece surface in ECM. *Journal of Materials Processing Technology*, 40(3-4), 271–286. doi:10.1016/0924-0136(94)90455-3

Wüthrich, R., & Fascio, V. (2005). Machining of non-conducting materials using electrochemical discharge phenomenon—an overview. *International Journal of Machine Tools & Manufacture*, 45(9), 1095–1108. doi:10.1016/j.ijmachtools.2004.11.011

Yue, T. M., & Lau, W. S. (1996). Pulsed Nd: YAG laser cutting of Al/Li/SiC metal matrix composites. *Materials and Manufacturing Processes*, 11(1), 17–29. doi:10.1080/10426919608947458

## Chapter 9

# Photochemical Machining: A Less Explored Non-Conventional Machining Process

**Sandeep Sitaram Wangikar**

*Shri Vithal Education and Research Institute, India*

**Promod Kumar Patowari**

*National Institute of Technology Silchar, India*

**Rahul Dev Misra**

*National Institute of Technology Silchar, India*

**Nitin Dnyaneshwar Misal**

*Shri Vithal Education and Research Institute, India*

### ABSTRACT

*The chapter focuses on the history and the development of photochemical machining in brief. The relevant studies related to photochemical machining and parametric effect are also discussed followed by gaps identified along with scope for the work and then the PCM process is explained in detail. The significant control parameters and their effect on the response measures are demonstrated with a fishbone diagram is explored. Further the detailed parametric effect on the response measures along with the scientific explanation of the effect is presented. The chapter is concluded with the two case studies (i.e., PCM of brass and Inconel 718).*

### INTRODUCTION

The stringent dimensional requirements with high surface finish and complex shapes are cannot be accomplished by the conventional machining processes. The hard materials are also constraints for the conventional machining methods. Furthermore, the augment in temperature and residual stresses generated in the work piece because of the conventional machining processes may possibly not be tolerable for various applications. Therefore, Now a day's, non-conventional machining processes are frequently

DOI: 10.4018/978-1-5225-6161-3.ch009



## Photochemical Machining

used for the manufacturing of a wide variety of parts. The non-conventional machining processes include Electrical Discharge Machining (EDM), Laser machining, Electrochemical Machining (ECM), Abrasive jet machining, Photochemical Machining (PCM), etc. The comparatively less studied non-conventional machining process is Photochemical etching (Figure 1) (Gamage and DeSiva, 2015). The PCM process is based on the amalgamation of photoresist imaging and chemical etching (Allen, 2004). Photochemical machining process is a precision contouring of metal into any shape, size or form without using of physical force, by a controlled chemical reaction. Material is etched by microscopic electrochemical cell action, as occurs in chemical dissolution or corrosion of a metal.

In photochemical machining, the difficult thin 2D flat metal components are produced which are free from stress and burr with low cost and less delivery time apart from other advantages. As this process is sovereign of intricacy of the machining, this process becomes an efficient, fast, cost competitive technique of producing components of metal with intricate designs unrivaled by any another conventional metal forming process. An additional benefit of the process is the possibility for etching a broad range of materials i.e. metals, alloys, glasses, ceramics, etc. However, the metals and alloys like copper, magnesium, zinc, aluminium, steels, nickel, monel, kovar, etc. are easily etched using PCM. Because of the assortment of materials used in the PCM process, the PCM is playing a dominant role in the precision parts manufacturing in different areas such as automotive, electronics, aerospace, optics, medical, jewellery, etc. Typical applications are the productions of integrated circuit lead frames, television shadow masks, mobile telephone gaskets, decoration on watch parts, suspension head assemblies, and jewellery (Yadev and Teli, 2014).

This chapter presents the parametric effect issues of the less explored photochemical machining process. The background focusing on the brief history and the selective literature review is discussed after this section. Further, the PCM process details along with the parameters for experimentation are presented in the succeeding section. Then, the influence of the process parameters on performance measures of the PCM is discussed. The surface topography of the photochemically machined sample specimens is also conferred using scanning electron microscopy (SEM) to reveal the process parameters influence. The scope for future work in this perspective for PCM is briefed following the summary of the chapter.

Figure 1. PCM - Less explored Non conventional machining process (Gamage and DeSiva, 2015)



\*For a more accurate representation see the electronic version.

## BACKGROUND

Photochemical Machining (PCM) process has originated from the knowledge of the acid attack on metals. The traces of this technology has been noted in the Greek and Egyptians ancient history as long ago as 2500 BC. The earliest reference to PCM process portrays an etchant made from the common salt, vinegar and charcoal acting through a hand scribed mask of linseed oil paint. The attractive patterns were also etched on the swords using a scribed wax as resist. The first photo etching was mentioned in 1826 but the first patent was assigned to William Fox Talbot in 1852, describing a photoetching process for etching copper with ferric chloride (Allen, 2004). But this process is explored very little by researchers in the latest past. Some of the recent trends of study are discussed as follows.

The simulation study related to etching has been reported by few researchers. The two dimensional simulation model for etching has been developed and the experimental analysis of the process parameters on micro geometry has been investigated by Bruzzone and Reverberi (2010). Furthermore, a single crystal silicon has been tested for three dimensional anisotropic wet etching employing a simulation model. A 3 dimensional simulation model has been developed by Lee and Won (2007) for the anisotropic wet etching of single-crystal silicon and reported that the developed simulation model promises for the thorough analysis of multifaceted three dimensional MEMS structures.

The micro-textures on carbon steel surfaces were fabricated using PCM and parametric study has been carried out by Zhang and Meng (2012). The surface textures have been produced on sheets of Monel 400 using PCM by Patil and Sadaiah (2015) and the effect of spinning speed on film of photoresist, and the effect of temperature and time of etching on the etched pattern have been studied.

The chemical machining of copper has been performed by Cakir (2005) using two different etchant as ferric chloride and cupric chloride and reported that the higher etching rate has been observed for ferric chloride etchant and the better surface quality has been produced with cupric chloride etchant. Further, Cakir et al. (2008) studied the chemical machining of aluminium for analyzing the influence of etching time and etchant temperature on the surface finish and rate of etching. The regeneration process for cupric chloride was also investigated by Cakir et al. (2006). The photochemical machining of inconel 600 using ferric chloride etchant has been carried out by Wagh et al. (2014) and discussed the parametric effect on the response measures. The influence sodium hydroxide concentration at constant temperature on the morphology of alumina nanotubes and nanowires has been investigated by Sadeghpour-Motlagh (2014). The PCM on OFHC copper has been carried out by Chaudhari et al. (2016) with ferric chloride etchant to observe parametric effect on undercut, surface roughness, and etch factor followed by optimization using Gray rational analysis. The optimization of process parameters for undercut and material removal rate was performed by using artificial neural network and Grey rational analysis (Saraf and Sadaiah 2013, Misal and Sadaiah 2013). Saraf and Sadaiah (2017) studied influence of magnetic field on an etch rate of SS316L. Further, they developed a novel 3D photochemical method for stent manufacturing. The effect of rolling direction on the PCM of Monel 400 has been studied by Patil and sadaiah (2016,2017). The PCM study for inconel 718 alloy has been performed by Misal and Sadaiah (2017) and reported the influence of grain size and selected parameters on the surface roughness through a surface topography study. The process parameter's optimization for PCM of inconel 600, brass, german silver, SS316, and SS316L steel have been carried out for the prophecy of material removal rate (MRR), surface roughness and undercut using response surface method and gray rational method. The control parameters have been considered as concentration, temperature, and time (Wagh and Dolas 2016, Wangikar et al.2017, 2018). The different manufacturing alternatives for fabrication of microchannel heat recovery unit has

## Photochemical Machining

been discussed by Gao et al. (2016) and reported that photochemical machining has been employed as a patterning process for producing channels. The microchannels also have been fabricated using photochemical machining by Wangikar et al. (2017, 2018) and Das et al. (2017).

From the above literature, it can be noted that the photochemical machining study for different materials have been reported by different researchers. However, the overall effect of various parameters on the performance of PCM for different materials has not been summarized. Also, the scientific explanation of the parametric effect and mechanism of material removal has not been outlined. In this chapter, a brief introduction about the photochemical machining along with the process parameters are discussed. The detailed parametric effect and the scientific explanation for the same for two different materials as brass and inconel 718 is discussed which reveals the causes for the material removal rate and the surface roughness. The study is supported with the surface topography study for the brass and inconel 718.

## PCM Process

Photochemical machining is one of the chemical machining processes in which the photographic and chemical etching techniques are employed. It utilizes chemical etching through a photoresists' stencil as the method of removal of material over the selected areas of the specimen. The technology is fairly modern and got recognized as a manufacturing process about many years before. Figure 2 shows the flow diagram of the PCM process which presents the main steps of photochemical machining applied to a metal plate viz. Photoresist Coating, etchants and scribing templates which have been summarized below:

The first step comprises the production of the photo-tool which is nothing but producing a required shape on a photographic film. The photo tool is a negative film of the image to be produced. The accuracy of the photochemically machined specimen principally depends upon the accuracy of Photo tool. The photo tools are generated by direct printing of the image from CAD drawing. The accuracy of the

Figure 2. PCM flow diagram

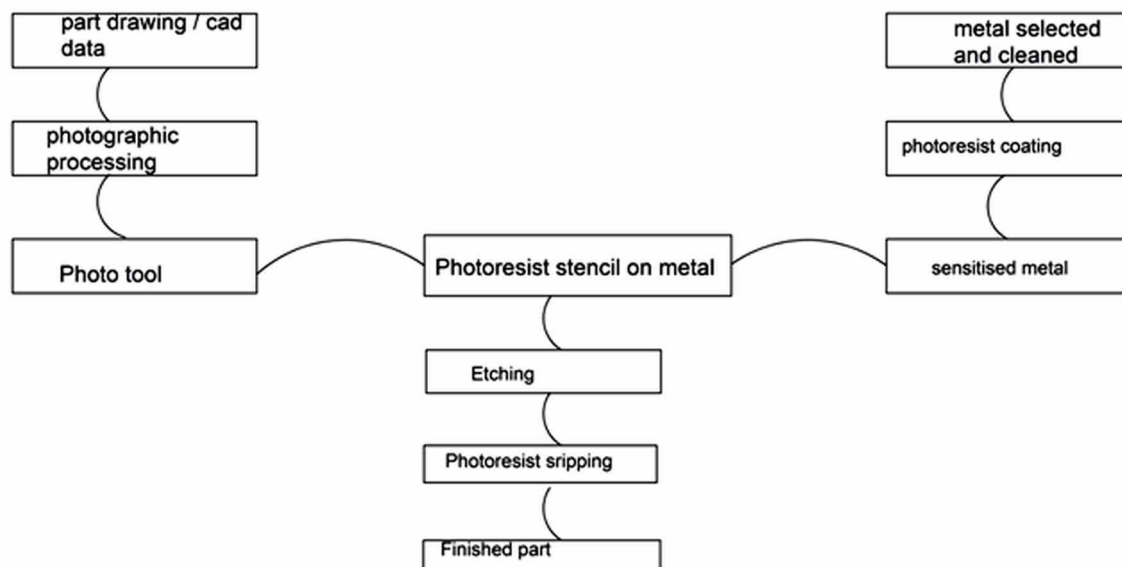


Photo tool is decided by the dpi (dots per inch) specification of the printer. The cartridge replacement and toner refilling also play a significant role in print quality. The photo tools are to be selected based on the edge deviation and overall quality. The sheet metals are cleaned chemically using solutions like acetone and coating of a photoresist film which is sensitive to light is applied. The photoresist will adhere to the surface of the specimen and acts as a stencil resist (protective layer) shielding the specimen surface throughout etching. Generally, the photoresist is available in liquid form and for application purpose, the specimen is required to be dipped in to the photoresist followed by drying. The photo-tools are employed in accurately registered pairs like one on the top, another at the bottom, and the material to be etched is sandwiched in between these two photo tools. This arrangement of photo-tool permits the both side etching of the material, which reduces the undercutting of photoresist and in turn produces straighter sidewalls on the specimen. The metal coated with the photoresist is afterward placed under the photo tool and exposed to an ultraviolet light source in an vacuum. This process transfers the image accurately onto the resist and becomes a replica of the desirable geometry after developing. Immersion or spraying then develop the exposed image. Each photoresist has its developing solution, like water, hydrocarbons, an alkaline solution, and other solvents. The exposed specimen is further washed to remove the unexposed photoresist on the areas of the specimen which is to be etched chemically. The imaged specimen passes through the solution (etchant) etch spray or dip where dissolution of the selected material of the specimen takes place. There are different etchants available for the various materials. The choice of the right etchant depends upon quality, cost, rate of material removal, and depth of etch.

## **PROCESS PARAMETERS**

The process parameters include control parameters (Input parameters) which will have effect on the process and the response parameters (output parameters). Some parameters kept constant during experimentation which are called as Fixed parameters.

**Control Parameters:** The performance of PCM has been influenced by many parameters and setting of these parameters strappingly depend on operator's experience and the parameters. So the primary task is to choose the input parameters. On the basis of review of literature, operators experience and from some pilot experiments, input parameter are generally selected. These input parameters are also called as control parameters. During experimentations, the control parameters are varied in a range in order to study their influence on performance measures. The control parameters have been given below:

- Temperature of etchant
- Concentration of etchant
- Etching time

In addition to these main control parameters, the photoresist thickness, ultraviolet light intensity, photo tool characteristics, etc. may also have the effect on the performance of PCM. Also, the different types of etchants and the addition of acids in etchant also have effect on the performance measures of PCM.

## Photochemical Machining

- **Response Parameters:** The parameters which have effect of selected control parameters are the responses or output parameters of the experimentation. The response parameters will be selected on the basis of their significance related to work or application. The performance of any photochemical machining process is stated by the following factors:
- **Material Removal Rate (Etch Rate):** The etching rate or rate of material removal depends on the chemical and metallurgical uniformity of the specimen and the homogeneity of the solution temperature. Normally, the castings have the largest grain sizes which show the roughest surface along with the lowest rate of machining. The rate of machining rate together with the best surface quality is generally given by rolled metal sheets. The etching rates are lower for hard metals and higher for the softer metals.
- **Surface Finish:** In PCM, the machining phase is observed for both the cases i.e. at the individual surface of the grains as well as at the grain boundaries. The fine grain size and a homogenous metallurgical structure are thus, necessary for fine surface quality of homogeneous appearance. The photochemically machined surfaces do not have a regular lay pattern. Based on the grain size and orientation, heat treatment, and previously induced stresses, each material has a fundamental surface finish which results from PCM for a certain period of time. While surface imperfections will not be eradicated by PCM, any prior surface indiscretion, dents, waviness, or scratches will be somewhat altered and reproduced in machined surface. Generally, slow etching will produce a surface finish similar to the original one.
- **Undercut:** During the etching process, the removal of material takes place depth wise in the unexposed portion as well as in the inward direction under the photoresist. The distance etched under the photoresist is called as undercut and the distance etched in the exposed portion is termed as depth of cut. After etching a bigger slot than that of requirement is produced due to the undercut. There is a requirement of consideration of undercut before etching for getting accurate dimension.
- **Etch Factor:** The etch factor is the ratio of undercut to the depth of etch. This ratio should be considered when scribing the mask using templates in chemical etching.
- **Edge Deviation:** The nonconformity of the edge of the machined component is referred as Edge Deviation (ED). It refers to the straightness of the edge produced while machining. The edge deviation plays a vital role in fabrication of micro parts like microchannels, heat sinks, etc. where the accuracy of the fabricated geometry is having significant effect on the performance of the part/device.
- **Etchants:** The different etchants are used in PCM for different materials. These etchants includes ferric chloride, cupric chloride, sodium hydroxide, and addition of acids for better performance like hydrochloric acid, nitric acid, hydrofluoric acid, etc. Ferric chloride ( $\text{FeCl}_3$ ) is a universal etchant and generally used for materials like steels, aluminum and its alloys, copper and its alloys, nickel, etc. It is cheap, providing a high etch rate and is reliable.

## Mechanism of Etching

The removal of material takes place by chemical etching in which the three main stages can be identified as follows:

1. Molecules or Ions from an solution of etchant diffused towards the exposed area on the specimen surface through boundary layer.

2. Soluble and gaseous by-products formed during the chemical reaction between etchant and the exposed specimen surface
3. A by-product from the surface of the work piece gets diffused through the boundary layer into the etchant solution.

## Parametric Effect

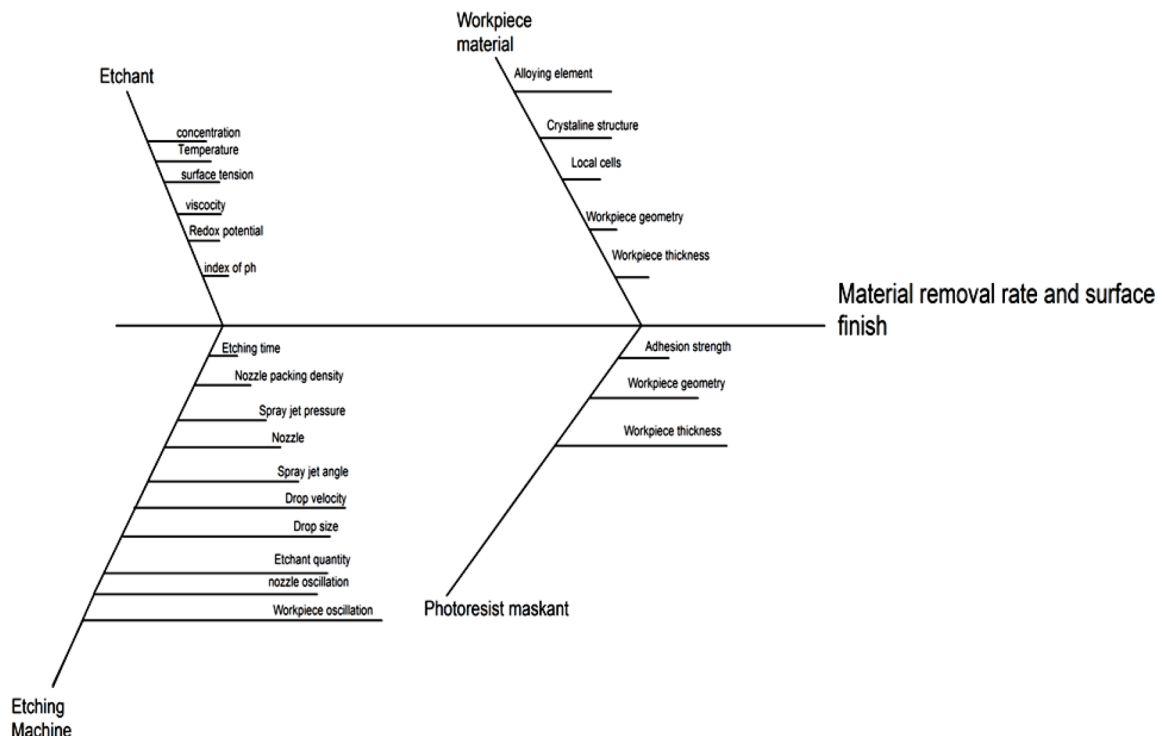
There are various control parameters having the effect on the performance of photochemical machining. The different response parameters for PCM are discussed above. But, the performance of PCM is principally governed by the two parameters viz. material removal rate and surface roughness. These two parameters have also been reported by various researchers.

It is observed from Figure 3 that there are four main elements that have prominent effect on the material removal rate and surface roughness in PCM.

## Workpiece Material

The workpiece material may be a metal, an alloy, ceramics or glasses. The composition of the elements present in the material, their nature (crystalline or amorphous) have a significant effect on material removal rate and surface roughness. The geometry of the part to be produced is also an important consideration. There is also influence of the specimen thickness and shape.

Figure 3. Fishbone diagram for material removal rate and surface roughness



## **Photoresist Maskant**

There are different (four types) photoresists like positive and negative and further wet and dry. The wet photoresist can be applied by dipping or by spin coating. The application method of photoresist decides the resist thickness in micron on the specimen and its uniformity. In this case also the workpiece shape, thickness and the geometry to be machined have influence on the performance. The different types of photoresists are available having different adhesion strength. Therefore photoresist application is primarily govern the PCM performance.

## **Etching Machine**

The etching may be carried out in etching machine for or in a beaker depending upon the quantity of specimens to be produced. The etching machine generally gives the spray etching facility which enhances the performance of the PCM process. The some important parameters in etching machine are etching time, nozzle packing density, spray jet pressure, nozzle type, spray jet angle, drop velocity, drop size, etchant quantity, nozzle oscillation, workpiece oscillation, etc.

## **Etchant**

The dissolution of material takes place in the solution which is called as etchant. There are different etchants used for etching of different materials. Therefore etchant selection is also important in order to achieve better etching rate. The etchant concentration, temperature and etching time play a vital role in PCM process and governs the material removal rate and surface roughness in a significant manner. In addition to that the redox potential, index of Ph, surface tension and viscosity are also effective parameters in for etchant.

From the above study of parameters and their effect on PCM performance, it can be noted that the workpiece material, photoresist and its application method and the way of etching (in beaker-for study purpose or using etching machine) once decided using the literature and some pilot experiments (if required) can further be considered as fixed parameters for the PCM experimentation. In case of etchant, the etchant selected based on the material can also be treated as the fixed parameter. Thus, the concentration of etchant, etchant temperature and the etching time may be considered as the variables for the PCM process. Further, the ranges for these can be decided based on the past study and pilot experimentations. The influence of concentration, temperature and etching time on material removal rate and surface roughness along with the detailed mechanism is explained below.

## **Effect of Concentration**

Concentration of etchant is one of the prominent factor having effect on the performance of the PCM. The number of molecules present in the etchant solution is decided by the concentration of the solution. The chemical reaction occurs when the molecules collides on the surface of the specimen. For lesser etchant concentration, less number of molecules will collide on the surface of surface of the specimen, which leads to less diffusion at the surface and in turn less etching means less material removal and good surface finish. With increase in concentration, the molecules in the etchant will increases. Hence, higher the number of molecules of reactant (reagents) present per unit volume in the etchant, there are

greater chances for reactive collisions to occur. As more molecules present in the etchant, more reactive collisions will occur at the specimen surface. This will results in enhanced diffusion and thus better etching means higher material removal rate but produces an uneven surface and hence poor surface finish. This is justified by the Fick's first law of diffusivity. The concentration gradient is directly proportional to the diffusion flux. The equation on the basis of which relation between diffusive flux and etchant concentration is given as:

$$J = -D \frac{dC}{dx} \quad (1)$$

where C: gradient of concentration, D: coefficient of diffusion, and J: diffusion flux.

From Eq. 1, it is clear that the concentration of etchant acts as a driving force.

The increase in concentration up to certain limit has significant effect on the material removal rate and surface roughness. The material removal rate and surface roughness will decrease with increase in concentration. The main reason behind this is the effect of viscosity. The etchant solution becomes more viscous which reduces flow ability and the movement of the formed product and fresh etchant goes on decreasing.

### Effect of Temperature

The chemical reactions occurs when the molecules (reagents) will collide with one another in a energetic way. The movement of molecules is governed by temperature as the temperature is a means of the kinetic energy present in molecules. The molecules will react only when they have a sufficient quantity of energy for a reaction. The molecular energy intensity will increase with the rise in the temperature of etchant which causes enhanced collisions between particles results in a better reaction rate. Normally, with an increase in temperature, etching rate increases. As the temperature increases, there is increase in the molecular energy level which leads to reactive collisions of the molecules on the specimen surface which results in better diffusion. Thus, a higher quantity of material will be removed from the surface leads to a rough surface. This results in better MRR and higher Ra with increase in temperature. The surface roughness as well as the etch rate is directly proportional to the diffusion coefficient (D). Stokes-Einstein's equation for the diffusion coefficient is as given:

$$D = \frac{kT}{6r\pi\mu} \quad (1)$$

where  $\mu$  is the viscosity of etchant,  $r$  is the radius of etchants particle;  $T$  is a temperature of etchant and  $k$  is Boltzman constant. Also the viscosity of the etchant changes with temperature

### Effect of Etching Time

If the molecules in the etchant will collide on the specimen surface for lesser time, then lesser diffusion will occur. This results in lower material dissolution in the etchant solution which in turn gives lower MRR but good surface finish (i.e. lesser Ra). The collision of molecules on the surface of specimen for

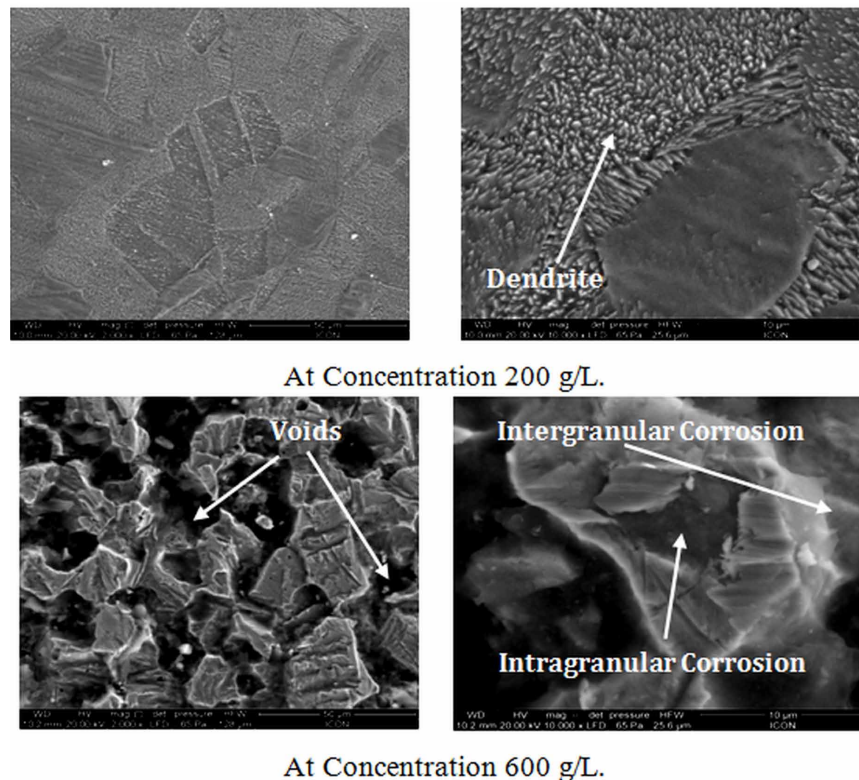


the longer time will improve the diffusion and material removal rate. But the surface obtained may be uneven due to collisions for a higher time leads to higher Ra. This gives an incessant increase in material removal rate and surface roughness with time.

### Case Study 1: Photochemical Machining of Brass

The photochemical machining of brass has been reported by Wangikar et al. (2017). The effect of the process parameters on the material removal rate and surface roughness are discussed with the help of scanning electron microscopy (SEM) images. The effect of concentration on the material removal rate and surface roughness has been explained with the help of SEM. At lower concentration, due to less molecules attack on the surface of the specimen, lesser material removal rate with a better surface roughness has been reported. The diffusion starts at grain boundaries characterized by inter-granular corrosion and further diffusion grows within the grain i.e. trans-granular corrosion. The dendrite structure has been reported for brass. The more molecules will attack on the surface for an etchant with higher concentration results in enhanced material removal rate with a rougher surface. This is depicted in Figure 4 for photochemical machining of brass with 200 g/L and 600 g/L concentration. The void formation due to combined intergranular and transgranular corrosion at higher concentration is reported and demonstrated in Figure 4. The increase in material removal rate and surface roughness with increase in temperature and etching time have also been reported.

*Figure 4. SEM images of Photochemically machined brass specimens at different concentrations (Wangikar et al. 2017)*



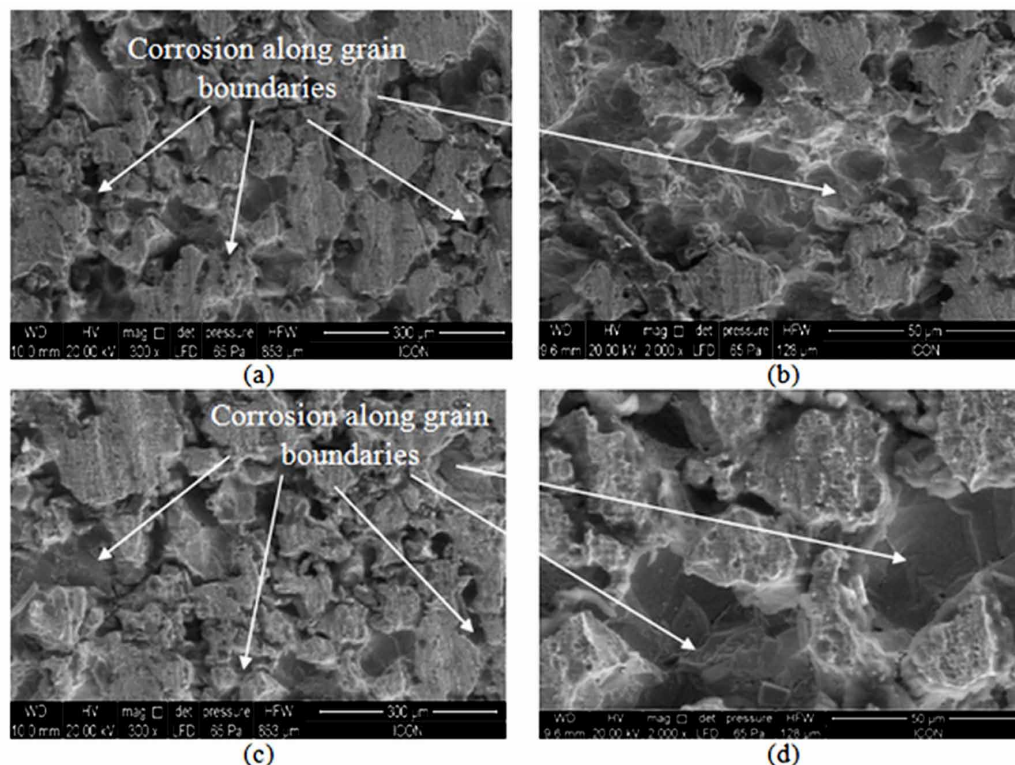
## Case Study 2: Photochemical Machining of Inconel 718

The PCM study of Inconel 718 has been reported by Misal et. al. (Misal et al. 2017). The effect of process parameters and the grain size on material removal rate and surface roughness has been reported. The effect of grain sizes at different temperatures have been investigated and reported that the smaller grain size results in higher material rate and surface roughness as compared to larger grain sizes. The influence of temperature on the surface topography is revealed using the SEM images as shown in figure 5. The etching progresses through intergranular corrosion as shown in figure 5 (a) and with higher magnification 5 (b). With an increase in temperature up to 65 °C, the etching rate increases as an effect of enhanced reaction rate. This is due to increased kinetic energy and improved collisions at the grain boundaries which results in enhanced corrosion at grain boundaries as shown in figure 5 (c), and also formation of voids have been reported (as presented in the magnified view- figure 5 (d)). Hence, increase in material removal rate and surface roughness with increase in temperature has been reported.

## SCOPE FOR FUTURE WORK

The photochemical machining process is one of the least explored non-conventional machining process and it has applications in various areas and capability to produce parts with complex shapes and geom-

*Figure 5. SEM images of photochemically machined Inconel 718 at different temperatures (a, b)- at 45 °C and (c, d) - at 65 °C (Misal et al. 2017)*



etries. In this regard, in view of the above mentioned discussion on various aspects of PCM, the scope for future work can be possible with respect to the following aspects.

- Parametric optimization for PCM of different materials and prediction of the optimum ranges of process parameters
- Comparative PCM study of different alloys (e.g. Copper alloys, Aluminium alloys, etc.)
- Effect of photoresist thickness on the PCM performance
- UV exposure effect on the PCM characteristics
- Regeneration of etchant
- Fabrication of nano particles from the dissolved metal in etchant and their characterization
- 3D PCM investigation and fabrication of micro parts using 3D PCM

## CONCLUSION

In this chapter, the least explored non conventional machining process viz. photochemical machining is discussed along with a thorough discussion on the various related aspects of the process. The PCM process is introduced in the first part of the chapter along with the detail stages in it. The history of PCM, background for the PCM process and the recent trends in the PCM are discussed. The different control parameters and performance parameters are discussed and the material removal rate and surface roughness are focused as the most significant performance parameters. The various factors contributing to material removal rate and surface roughness are briefed. The influence of the most important parameters i.e. concentration of etchant, temperature and etching time on the material removal rate and surface roughness is elaborated in detail with the mechanism. To support this, two case studies on PCM of brass and Inconel 718 has been reported in which the parametric effect is explained using SEM. The guidelines for further work in PCM are given which are focusing on the demanding areas for work in PCM.

## REFERENCES

- Allen, D. M. (2004). Photochemical machining: From ‘manufacturing’s best kept secret’ to a \$6 billion per annum, rapid manufacturing process. *CIRP Annals-Manufacturing Technology*, 53(2), 559–572. doi:10.1016/S0007-8506(07)60029-8
- Bruzzone, A. A. G., & Reverberi, A. P. (2010). An experimental evaluation of an etching simulation model for photochemical machining. *CIRP Annals*, 59(1), 255–258. doi:10.1016/j.cirp.2010.03.070
- Cakir, O. (2006). Copper etching with cupric chloride and regeneration of waste etchant. *Journal of Materials Processing Technology*, 175(1-3), 63-68.
- Çakır, O. (2008). Chemical etching of aluminium. *Journal of Materials Processing Technology*, 199(1-3), 337–340. doi:10.1016/j.jmatprotec.2007.08.012
- Çakır, O., Temel, H., & Kiyak, M. (2005). Chemical etching of Cu-ETP copper. *Journal of Materials Processing Technology*, 162, 275–279. doi:10.1016/j.jmatprotec.2005.02.035

- Chaudhari, K., Patil, A., Kolekar, M., & Patil, A. (2016). Photochemical machining. *International Journal on Recent and Innovation Trends in Computing and Communication*, 4(4), 132–136.
- Das, S. S., Tilekar, S. D., Wangikar, S. S., & Patowari, P. K. (2017). Numerical and experimental study of passive fluids mixing in micro-channels of different configurations. *Microsystem Technologies*, 23(12), 5977–5988. doi:10.100700542-017-3482-x
- Gamage, J. R., & DeSilva, A. K. M. (2015). Assessment of research needs for sustainability of unconventional machining processes. *Procedia CIRP*, 26, 385–390. doi:10.1016/j.procir.2014.07.096
- Gao, Q., Lizarazo-Adarme, J., Paul, B. K., & Haapala, K. R. (2016). An economic and environmental assessment model for microchannel device manufacturing: Part 2–Application. *Journal of Cleaner Production*, 120, 146–156. doi:10.1016/j.jclepro.2015.04.141
- Lee, J. G., & Won, T. (2007). Three-dimensional numerical simulation for anisotropic wet chemical etching process. *Molecular Simulation*, 33(7), 593–597. doi:10.1080/08927020601067508
- Misal, N. D., & Sadaiah, M. (2013). Comparison of Design of Experiments and Gray Rational Analysis of Photochemical Machining. *International Journal of Innovations in Engineering and Technology*, 3, 121–126.
- Misal, N. D., & Sadaiah, M. (2017). Investigation on Surface Roughness of Inconel 718 in Photochemical Machining. *Advances in Materials Science and Engineering*.
- Misal, N. D., Saraf, A. R., & Sadaiah, M. (2017). Experimental investigation of surface topography in photochemical machining of Inconel 718. *Materials and Manufacturing Processes*, 32(15), 1756–1763. doi:10.1080/10426914.2017.1317786
- Mudigonda, S., & Patil, D. H. (2015, June). Some investigations on surface texturing on monel 400 using photochemical machining. In *ASME 2015 International Manufacturing Science and Engineering Conference* (pp. V001T02A045-V001T02A045). American Society of Mechanical Engineers. 10.1115/MSEC2015-9294
- Patil, D. H., & Mudigonda, S. (2016). The effect of the rolling direction, temperature, and etching time on the photochemical machining of monel 400 microchannels. *Advances in Materials Science and Engineering*.
- Patil, D. H., & Mudigonda, S. (2017). Investigation on effect of grain orientation in photochemical machining of Monel 400. *Materials and Manufacturing Processes*, 32(16), 1831–1837. doi:10.1080/10426914.2017.1291953
- Sadeghpour-Motlagh, M., Mokhtari-Zonouzi, K., Aghajani, H., & Kakroudi, M. G. (2014). Effects of etching time and NaOH concentration on the production of alumina nanowires using porous anodic alumina template. *Journal of Materials Engineering and Performance*, 23(6), 2007–2014. doi:10.100711665-014-1011-y
- Saraf, A. R., & Sadaiah, M. (2013). Application of artificial intelligence for the prediction of undercut in photochemical machining. *International Journal of Mechatronics and Manufacturing Systems*, 6(2), 183–194. doi:10.1504/IJMMS.2013.053829

- Saraf, A. R., & Sadaiah, M. (2017). Magnetic field-assisted photochemical machining (MFAPCM) of SS316L. *Materials and Manufacturing Processes*, 32(3), 327–332. doi:10.1080/10426914.2016.1198014
- Saraf, A. R., & Sadaiah, M. (2017). Photochemical machining of a novel cardiovascular stent. *Materials and Manufacturing Processes*, 32(15), 1740–1746. doi:10.1080/10426914.2016.1198025
- Wagh, D. V., & Dolas, D. R. (2016). Multi Response Optimization of Process Parameters in PCM of Inconel 600 Using Desirability Function Approach of RSM. *International Journal of Engine Research*, 5(2), 127–130.
- Wagh, D. V., Dolas, D. R., & Dhagate, M. D. (2014). Experimental investigation of photochemical machining on Inconel 600 using ferric chloride. *International Journal of Engineering Research & Technology*, 4(2), 289–293.
- Wangikar, S. S., Patowari, P. K., & Misra, R. D. (2016, December). Parametric Optimization for Photochemical Machining of Copper Using Grey Relational Method. In *Techno-Societal 2016, International Conference on Advanced Technologies for Societal Applications* (pp. 933-943). Springer.
- Wangikar, S. S., Patowari, P. K., & Misra, R. D. (2017). Effect of process parameters and optimization for photochemical machining of brass and German silver. *Materials and Manufacturing Processes*, 32(15), 1747–1755. doi:10.1080/10426914.2016.1244848
- Wangikar, S.S., Patowari, P.K., & Misra, R.D. (2018). Parametric Optimization for Photochemical Machining of Copper using Overall Evaluation Criteria. *Materials Today Proceedings*. doi:10.1016/j.matpr.2017.12.046 (accepted for publication)
- Wangikar, S. S., Patowari, P. K., & Misra, R. D. (n.d.). Numerical and experimental investigations on the performance of a serpentine microchannel with semicircular obstacles. *Microsystem Technologies*, 1-14.
- Yadav, R. P., & Teli, S. N. (2014). A Review of issues in photochemical machining. *International Journal of Modern Engineering Research*, 4(7), 49–53.
- Zhang, J., & Meng, Y. (2012). A study of surface texturing of carbon steel by photochemical machining. *Journal of Materials Processing Technology*, 212(10), 2133–2140. doi:10.1016/j.jmatprotec.2012.05.018

# Chapter 10

## Performance and Surface Evaluation Characteristics on Cryogenic-Assisted Abrasive Water Jet Machining of AISI D2 Steel

**Yuvaraj N.**

*Vel Tech Rangarajan Dr. Sagunthala R&D Institute of Science and Technology, India*

**Pradeep Kumar M.**

*Anna University, India*

### ABSTRACT

*The chapter reports on the investigation of cryogenic-assisted abrasive water jet (CAAWJ) machining of AISI D2 steel with varying the jet impact angles and abrasive mesh sizes. The performance measurement is considered in this study such as depth of penetration and taper ratio. Also, the surface integrity characteristics are considered in the present study such as abrasive contamination, surface topography, XRD peaks, residual stress, and micro hardness. The CAAWJ machining process improves the performance measurement such as higher depth of penetration and lower taper ratio for the machining of D2 steel. Also, the CAAWJ cut surface consists of better surface integrity features over the AWJ cut surface. The phase transformation effect of target material under cryogenic cooling helps to turn the mode of the material removal mechanism from ductile to brittle erosion process and yield a better performance. The results also indicate that the oblique jet impact angles have been produced better performance characteristics than the jet impact angle of 90° at room temperature.*

DOI: 10.4018/978-1-5225-6161-3.ch010

## **INTRODUCTION**

Water jet machining process is a mechanical based unconventional machining technique, mainly employed for machining of hard materials. It is one of the successful machining processes, as it offers a lower cutting zone temperature with no thermal stress, and ability to employ lower cutting forces over the target material etc., (Folkes, 2009). In water jet machining process, injection type abrasive water jet machine (AWJ) is a typical machine tool used in modern machine workshops. This ensures, quality of the cutting edge obtained during this machining process as much superior to the other machining processes. In AWJ machining, material removal takes places through cutting and deformation erosion process, in which higher kinetic energy of water jet mixes with an abrasive particles focused in the direction of surface of the target material.

## **BACKGROUND**

Despite several benefits seen, AWJ has some limitations such as generation of a higher volume of secondary wastages, lower cutting efficiency, nozzle wear, striation formation, abrasive contamination, etc (Kuleki, 2002), causing a low depth of penetration, poor taper cut ratio and loss of surface integrity. As a result, the use of AWJ is limited in manufacturing industries. A few researchers have developed techniques which include nozzle oscillation, changing jet impact angle and abrasive mesh size, etc (Aich et al., 2013). These techniques were developed for restrict the defects seen on the AWJ machined surface such as abrasive contamination, wear tracks, striation formation and taper formation. However, the significant results are not yet obtained by researchers and scientists while machining hard materials.

A wide variety of materials can be machined by AWJ, only very few of them have reported comprehensive details of the cutting performance and surface integrity characteristics. However, a few hard materials were less machined by AWJ such as die steels, tool steels, Inconel, etc. Some results observed on the AWJ machined die and tool steels are summarized below.

Asif et al. (2011) have investigated the AWJ cutting of 4340 tool steel and Aluminium 2219. The thicknesses of the work material were 20 mm and 40 mm. They reported reduction in the roughness of the cutting wear zone through decrease in the traverse speed arising from sufficient contact time between the target material and abrasives. This consequence happened owing to the large number of abrasive particles employed in the cutting action. The result also indicated that the traverse rate and target material thickness as the most influencing factors for tool steel materials. Ankush and Lalwani (2013) reported the investigation of AWJ machined H13 die steel with a thickness of 12 mm and better surface finish obtained under a lower traverse rate along with a higher stand-off distance and with water jet pressure employed in the cutting process. Traverse rate as the significant parameter for the AWJ machining of die steel has been indicated. Zhao and Guo (2014) investigated the AWJ machined surface features in cold work mold steel, 6061 aluminium alloy, high strength low alloy steel and AISI 304 stainless steel. They reported the ductility of the material causing severe wear traces caused on the target material surfaces during the machining process.

Deepak et al. (2015) made a study of the jet penetration and taper angle in cutting of D2 steel by an AWJ with a thickness of 8 mm. The cutting experiments were carried out through variations in the water jet pressures. Depth of penetration was seen increasing with increase in water jet pressure. Lower water jet pressure did not produce any through cut in the work material. Moreover, they found an increase in

water jet pressure with a decrease in taper cut. Hlavac et al. (2015) investigated the taper angle in various grades of AWJ machined steel with a thickness of 30 mm. They found the variations in taper cut, and curvatures in the entry of kerf wall cut surface formed by the ductility of the steel leading to the deformation induced by the ductile work materials during the cutting process.

Later, Yuvaraj and Pradeep Kumar (2017a) investigated the surface evaluation studies on AWJ machined AISI D2 steel cut surfaces. They reported the production of a better surface profile through use of an oblique jet impact angle by the maintenance of the abrasive particles kinetic energy through a reduction of particle disintegration in the cutting zone. Researchers have developed different thermal enhancement techniques for jet cutting operations. The modified techniques are plasma assisted abrasive water jet (Patel & Tandon, 2015), cryogenic abrasive jet machining (Getu, Spelt, & Papini, 2008, 2011; Gradeen, Spelt, & Papini, 2012), cryogenic abrasive water jet with the replacement of conventional abrasives (Tsunemoto, Kazuhiro, & Katsuo, 2000; Bach, Hassel, Biskup, Hinte, & Schenk, 2010).

## **MAIN FOCUS OF THE CHAPTER**

The main focus of the chapter deals with cryogenics assisted machining process. Recently, investigations were made on the machining operations with the assistance of low temperature liquids like cryogenics. Cryogenic assisted machining is a safe environmental alternative approach for increasing the machining performance by enhancing the target material properties at low temperature liquids (Flynn, 2005; Reitz & Pendray, 2001). Different types of cryogenics such as liquid oxygen, hydrogen, nitrogen, helium, and CO<sub>2</sub> are available in a liquid state. Among the cryogenic liquids, liquid nitrogen (LN<sub>2</sub>) is the most beneficial substance which has no harmful effects, easy to dispose of the environment after machining, is non-corrosive, and non-inflammable. It was widely used by the previous researchers in different machining processes for improving machining performance and surface integrity which was improved through controllable phase changes in the target material at low temperature (Kaynak, Lu, & Jawahir, 2014). A few reports are available on the investigation of abrasive jet cutting operations with the use of cryogenics. These are briefly discussed below.

Uhlar et al. (2013) have investigated the AWJ cutting of cryogenic treatment of steels namely 1.4307, 1.4404 and 1.4845. They have analysed the cutting of non-corroding steels cut surfaces with a thickness of 30 mm samples treated with application of LN<sub>2</sub>. The result indicated the influence of cryogenic treatment becoming uncertainty as the influence of material structure and properties are opposite in that way. It happens due to the modifications of the micro (increase in surface roughness) and macro (increase in declination angle) conditions of the cryogenically treated cut surfaces over the cutting process at room temperature. Muju and Pathak (1988) developed the abrasive jet with an assistance of the LN<sub>2</sub> for cutting glass. Machining operations were carried out using cryogenic at room temperature. The results indicated the presence of a higher depth of cut at the cryogenic temperature machining of glass. Urbanovich et al. (1992) found increase in the erosion rate of the steel by about 1.7 times through cryogenic cooling over the room temperature.

Getu et al. (2008) studied the impact of cryogenic LN<sub>2</sub> on polymer materials using the abrasive jet micro-machining process. The result showed cryogenic cooling producing an improvement in the functional performance, while particle contamination was lower in the machined surfaces. They also found that the particle embedding was greatly reduced in the machined surfaces. Later, Getu et al. (2011)



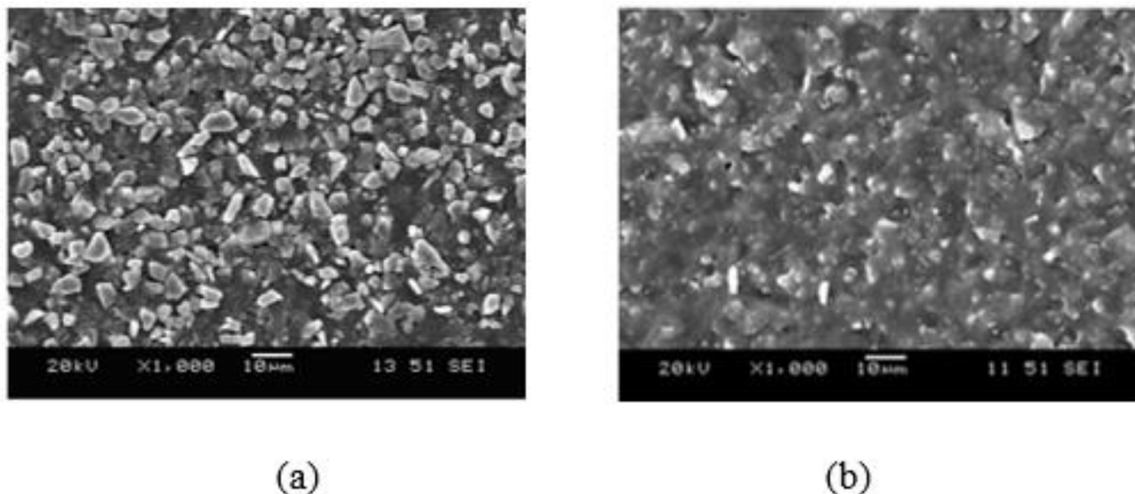
## Performance and Surface Evaluation Characteristics

examined the assistance of  $\text{LN}_2$  in abrasive jet machining of PDMS with various models. The models such as finite element and analytical models were used for optimizing the micro machined features.

There are also reports of reduction in the particle embedment in the cryogenic assisted abrasive jet machined surfaces is referred to by Gradeen et al. (2012), who studied the jet machining with the assistance of cryogenics at different temperatures. These are shown in Figure 1. The jet impact angle of  $90^\circ$  erosion rate at cryogenic temperature ( $-178^\circ\text{C}$ ) was approximately 15 times larger than for the other temperatures. Tsunemoto et al. (2000), report ice jet cutting process as similar to an abrasive jet machining, removing selective soft materials. Demonstration of ice jet machining was also done by Bach et al. (2010), who developed the cryogenic ice jet cutting setup for cutting and cleaning of AlMgSi1 with a thickness of 3 mm. In this study, ice particles were used as abrasive materials rather the conventional abrasives. Ice jet machining maintains the formation of microchipping action on the target material surface due to the supply of cryogenic liquid. Kim et al. (2009) have studied the feasibility of cryogenic jet cutting system for cutting steel of 10 mm thickness, with a reduction in secondary wastages, and particle contamination has been generated by the existing AWJ process. Conditions proposed earlier by researchers helped the improvement in the surface cleaning technology and the cutting performance without compromising on the features of surface quality. However, Yuvaraj and Pradeep Kumar (2016) did experimental work in AWJ machining of AA5083-H32 with cryogenic  $\text{LN}_2$  for improvements in cut surface quality features. The results indicated, better surface integrity obtained in the machined surfaces under cryogenic assisted machining at room temperature rather than the machining process. The results were confirmed by various characterization techniques such as SEM, surface topography, XRD profile, residual stress and microhardness.

Based on earlier reports, researchers have used cryogenics in AWJ with different methods including machining of aluminium alloy using cryogenic liquids in AWJ (Yuvaraj & Pradeep Kumar, 2016). However, no attempt has been made by earlier researchers in the area of cryogenic assisted abrasive water jet (CAAWJ) machining of die and tool steels. Hence, this chapter aims to investigate the CAAWJ machining of AISI D2 steel and establishment of the results on cutting performance and surface characteristics under AWJ and CAAWJ.

Figure 1. SEM images of machined PDMS at (a)  $-82^\circ\text{C}$  and (b)  $-178^\circ\text{C}$  (Gradeen et al., 2012)



## MATERIALS AND MEASUREMENTS

### Test Setup Procedure

Investigations were carried out on the OMAX MAXIEM injection type abrasive water jet machine (Model:1515). The maximum discharge of water employed was 3.2 l/min. This machine has a special provision for changeover attachment of jet impact angle with variations from 0 to 45 deg. Figure 2 shows the trapezoidal shape of AISI D2 steel which was considered for this study with dimensions of 200 x 150 x 80 mm. The cryogenic assisted machining arrangement is shown in Figure 3. It consists of a portable air compressor with a maximum pressure of 8 bar, TA55 cryogenic container (max.litres: 55), drier, pressure regulator, pneumatic hose, blow-off valve, flexible hose and nozzle. In this experimental study, liquid nitrogen was chosen among the various cryogenic liquids, considering its easy to disposal

Figure 2. Trapezoidal shaped work material

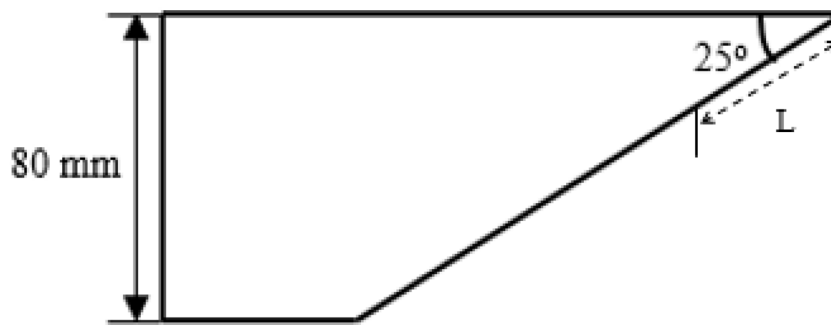
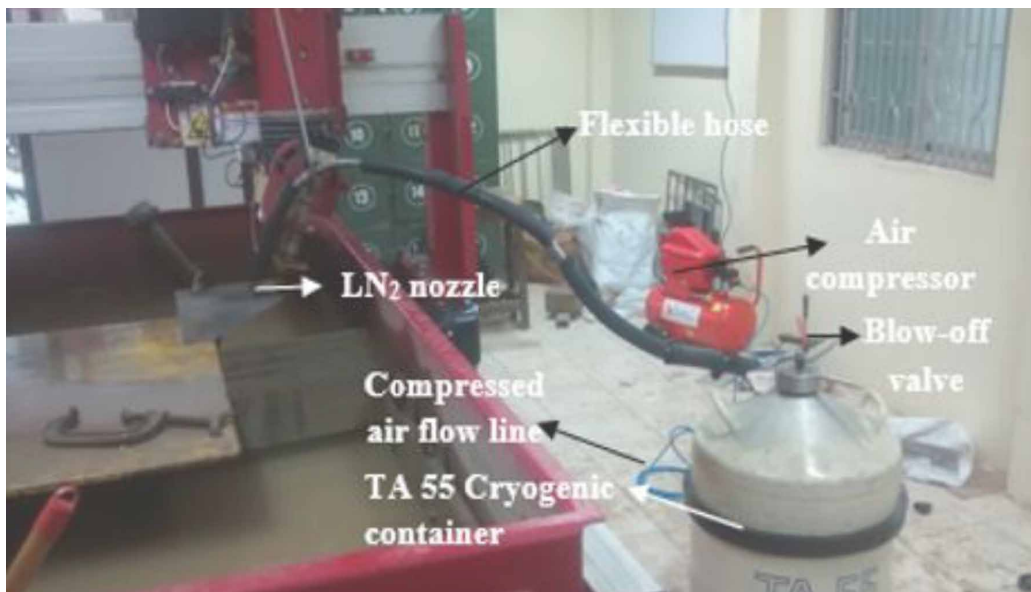


Figure 3. Experimental setup for CAAWJ cutting



## Performance and Surface Evaluation Characteristics

in the environment, its nontoxic feature and controllable phase changes in the target material (Shokrani, Dhokia, Munoz-Escalona, & Newman, 2013). This low temperature liquid was supplied to the machining zone by a stainless steel tube under a pressure of 5 bar. The flow pressure and rate were controlled by a blow-off valve. The LN<sub>2</sub> jet nozzle was positioned beside the abrasive water jet focusing nozzle with its center axis inclined from that of the nozzle.

## Machining Parameters

Water jet pressure, abrasive particle size, and jet impact angle were considered as variable cutting parameters, with variations in each variable cutting parameters vary from low to high level. Based on the factors and their levels, the design of experiment L<sub>27</sub> was chosen. Table 1 shows the machining process conditions.

The observations considered in this study such as depth of penetration, kerf taper ratio, abrasive contamination, surface morphology, topography with 3D roughness features, surface analysis with XRD peaks, surface residual stress and hardness.

## Performance Measurement

In the study, the following performance measurements are considered.

The depth of penetration (DOP) is measured by the length of jet penetration and angle of the modified work material. It is obtained by using the following Eqn. (1)

$$\text{DOP} = L * \sin\theta \quad (1)$$

where, L – jet penetration, mm;  $\theta$  – modified angle, deg.

Kerf taper ratio (KTR) is measured by the ratio between the upper and lower kerf width values. Tool maker's microscope was used to measure the kerf width values with a least count of 5 $\mu$ .

Table 1. Machining Conditions

Machining Parameters	Values
Water pressure	175, 200, 225 MPa
Jet impact angle	70°, 80°, 90°
Type of abrasive	Garnet
Abrasive particle size	80, 100, 120 (#)
Abrasive mass flow rate	0.450 kg/min
Traverse speed	12 mm/min
Stand-off distance	3 mm
LN <sub>2</sub> jet pressure	5 bar
LN <sub>2</sub> jet angle	60°
Focussing nozzle diameter	0.76 mm
Orifice diameter	0.25 mm

$$\text{KTR} = \text{Upper kerf width/Lower kerf width} \quad (2)$$

## **Surface Evaluation Characteristics**

Among the 27 experiments conducted for the performance measurement, the surface evaluation characteristics were analyzed for the AWJ and CAAWJ machined AISI D2 steel surfaces with significant cutting conditions.

Hitachi Model S-3400N Scanning electron microscopy (SEM) was employed for the examination of AWJ and CAAWJ kerf wall cut surfaces. SEM image was taken with a magnification of 100x and acceleration voltage of 15kV. Optical emission spectroscopy (Foundry Master-Pro, Oxford, Germany) was used for obtaining the required quantity of garnet particle contamination in the machined AISI D2 steel surfaces. This is shown in Figure 4. This test was conducted according to the standard procedure of ASTM E 1086. Figure 5 shows the percentage of weight of the chemical elements present in the AISI D2 steel as received condition.

3D surface topography was employed for the measurement of various roughness parameters under various machined surfaces by AWJ and CAAWJ. It was obtained through the use of non-contact type instrument (Taylor Hobson CCI) with a focusing length of 325  $\mu\text{m}$  and a magnification of 10x.

Optical microscopy was used for observing the microstructure of the AWJ and CAAWJ surfaces. The machined surfaces were submerged in the Vilella's etchant for less than 2 min. The etchant consists of 100 ml of ethanol, 5 ml of hydrochloric acid, and 1 gram of picric acid.

X ray diffractometer was employed for examining the crystal structure of the target material with a scanning speed of 0.04 deg/min. It helped the demonstration of residual stress on the surfaces under AWJ and CAAWJ. Vickers hardness tester (Wolpert Wilson) was used for the measurement of microhardness at 2 mm, 4 mm and 6 mm from the top kerf wall cutting region. Hardness measurement was carried out with a dwell time of 10s and load of 0.1 kg was employed.

*Figure 4. OES analysis of the AISI D2 Steel as received condition*

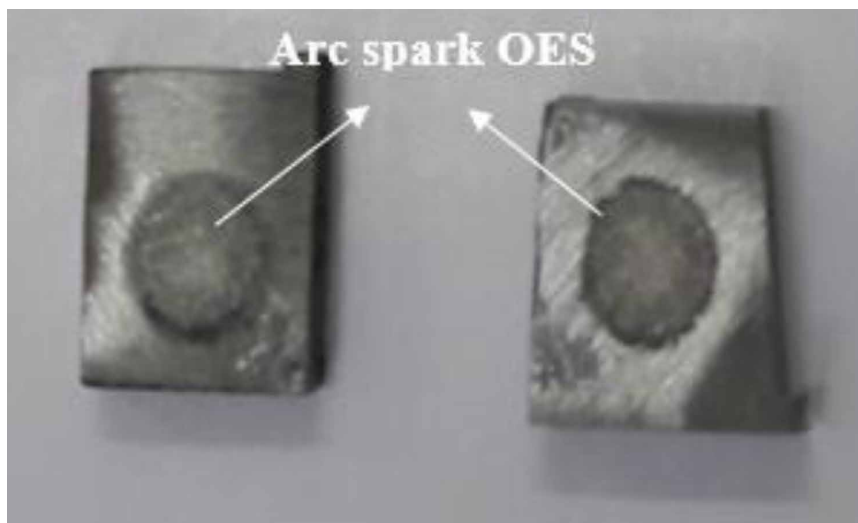
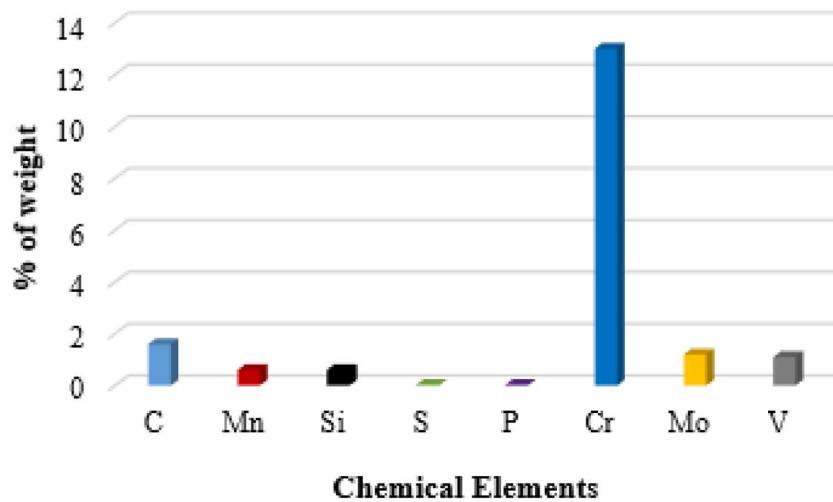


Figure 5. Composition of chemical elements in the AISI D2 Steel as received condition

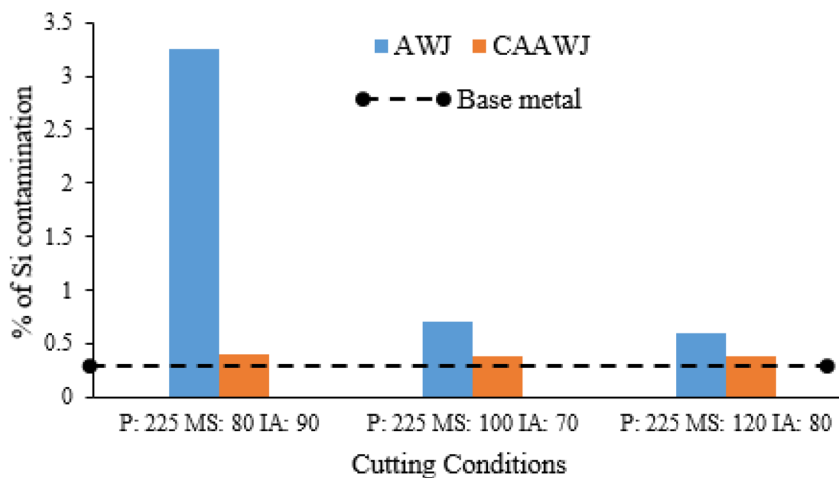


## RESULTS AND DISCUSSION

### Influence of Machining Parameters on the Abrasive Contamination

The elemental compositions of D2 steel cut surfaces under both the cutting conditions are shown in Figure 6.  $\text{Al}_2\text{O}_3$ ,  $\text{SiO}_2$ ,  $\text{TiO}_2$ ,  $\text{Fe}_2\text{O}_3$ ,  $\text{MgO}$ , and  $\text{CaO}$  form the composition of the garnet abrasive. Consequently, Si (silicon) and O elements were produced by disintegrating  $\text{SiO}_2$  during the cutting process. This explains the embedding of Si in the machined surface. This embedded particle is referred to as “abrasive particle contamination”, as silicon is the only element that makes a distinction between the

Figure 6. Influence of Machining Parameters on the Abrasive Contamination in the machined surfaces of AISI D2 Steel



chemical element composition between D2 steel and the garnet abrasives. The results, indicate the presence of silicon particles present in the AWJ and CAAWJ machined surfaces. This is shown in Table 2. It confirms the presence of a lower percentage of silicon particles in D2 cut surface compared to and over the cutting conditions. The occurrence of lower contamination was due to the fact CAAWJ process allows the kerf wall cut surface an increase in hardness and changes in the erosion process produced contamination of a small degree. The changes in the hardness and erosion process cause restrictions in the abrasives embedding in the machined surfaces. In addition, a lower contamination occurred in the AWJ cutting process as a result of the production of threshold kinetic energy by the combined effect of the jet impact angle of 70°, and the abrasive mesh size of #100 which machined the die steel with a reduction in abrasive embedment in the surfaces. The level of the contamination is lower than the jet impact angle of 90°. However, the contamination of abrasive seen was lower in both the AWJ kerf wall cut surfaces. This result was the indication of a better cut surface quality obtained through CAAWJ over the other machining techniques, which produce severe contaminated machined surfaces (Choi, Nam, & Lee, 2008). This was due to the difficulties in the various applications producing a higher contamination on the surface (Patel, 2004). Table 2 shows a reduction in contamination in the CAAWJ cutting process reduced by 36.66 - 54.54% compared to the AWJ process.

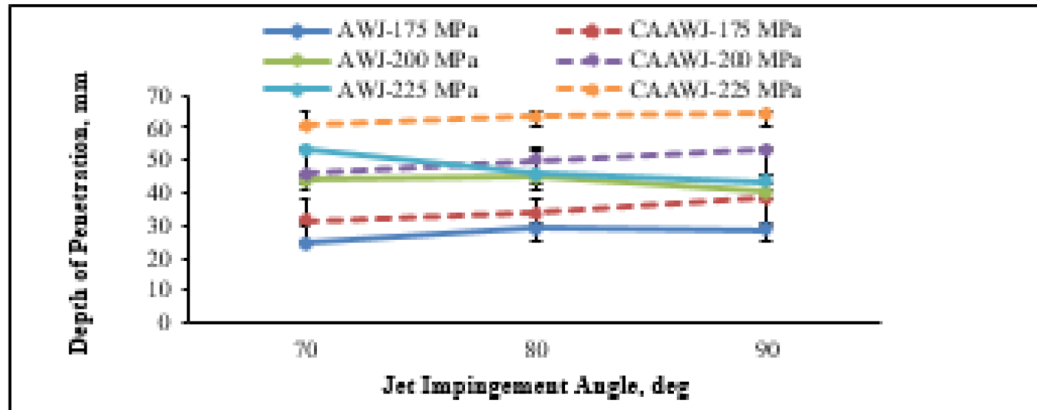
### Effects of the Process Parameters on the Depth of Penetration

Figure 7 shows the effect of  $LN_2$  on the DOP with various combinations of abrasive mesh sizes and jet impact angles. An increase in the DOP with an increase in jet pressure along with various mesh sizes of abrasives is seen. The results show the achievement of the maximum DOP under the CAAWJ cutting process when the combination of water jet pressure of 225 MPa, and jet impact angle of 90° with an abrasive mesh size of #80 was employed. This result obtained was due to the change in the mode of the material removal mechanism from ductile to brittle fracture in the cutting zone. This change of mechanism also caused a reduction in the particle embedding, disintegration, and deflection during the cutting process. These changes in the cutting process helped an increase in the DOP and the maximum DOP is found to be 64.40 mm. CAAWJ with all experimental conditions showed a higher DOP in the range of 1.43 - 35.93% over the cutting process at room temperature. The result was a result of the velocity of abrasives maintained in the cutting process when the ductile-to-brittle erosion process occurred at the cutting zone. This is because the ductile-to-brittle erosion process allows the breaking down of lower energy on the target material which helps retention of the cutting energy of the abrasives while the penetration depth was increased. The  $LN_2$  cooling in the machining zone permits removal of material

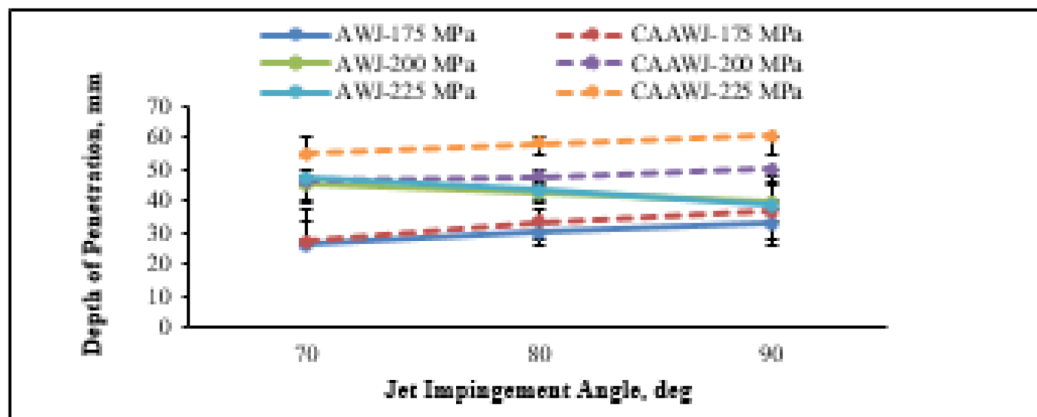
Table 2. Percentage of Si particles in the cutting of AISI D2 Steel kerf wall cut surfaces

S.No	Cutting Conditions	% of Si particles		% of Reduction Over AWJ
		AWJ	CAAWJ	
1.	P: 225 MPa MS: #80, IA: 90°	0.88	0.4	54.54
2.	P: 225 MPa MS: #100, IA: 70°	0.71	0.39	45.07
3.	P: 225 MPa MS: #100, IA: 80°	0.6	0.38	36.66
4.	Base metal (as received condition)	0.31		

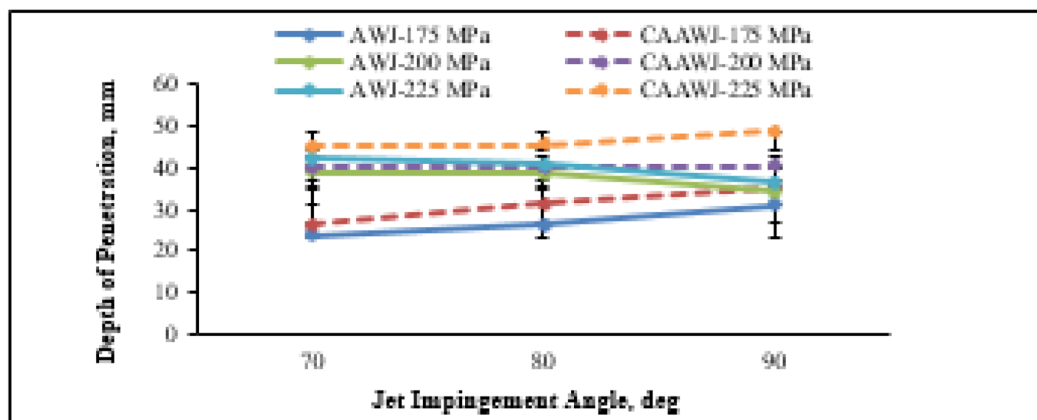
Figure 7. Variations of the depth of penetration under AWJ and CAAWJ conditions (a) #80 (b) #100 (c) #120



(a)



(b)



(c)

over a fine erosion debris, and yield a higher penetration effect. This result arising out of the reduction in the ductile fracture in the cutting zone through use of a low temperature liquid.

An abrasive mesh size of #80 and jet impact angle of 70° with a water jet pressure of 225 MPa was seen offering a higher DOP under AWJ and the value is found to be 53.67 mm. This result could be achieved by effective maintenance of the velocity of the abrasives, while the DOP was increased. The combination of a lower jet impact angle with coarse abrasive particles (#80) can contribute to a reduction in the cutting force of the abrasives over the jet impact angle of 90° was used. However, it has sufficient jet energy for disintegrating the target material and subsequently causing a rise in the penetration depth (Yuvaraj & Pradeep Kumar, 2017b). The abrasive particle retained its size and shape during the operation yielding a larger penetration effect while increasing the thickness of the target material as account of this.

### **Effects of the Process Parameters on the Kerf Taper Ratio**

The effect of LN<sub>2</sub> cooling on the KTR with different combinations of abrasive mesh sizes and jet impact angles, which depend on the three different water jet pressures is shown in Figure 8. Figure 8(a-c) shows increase in KTR with an increase in the water jet pressure for various levels of the jet impact angles and the abrasive mesh sizes in the CAAWJ process. A lower KTR could be attained with a higher level of water jet pressure of 225 MPa with a jet impact angle of 90° and abrasive mesh size of #80. This occurred due to the cutting energy of abrasives retained throughout the cutting operation; this happens due to the effect of the significant reduction in ductile fracture, thereby allowing a smaller quantity of fractured abrasive particles and particle embedding under the CAAWJ cutting process. This caused a retention in the energy of the abrasive particles at the bottom cut regions, and a smaller taper profile. There was a significant reduction of striation in the lower cutting region of the cut surface in the CAAWJ process, as shown in Figure 9(b).

The result also indicated that the oblique jet impact angles with water jet pressure of 200 MPa and 225 MPa in the AWJ cutting process offered a smaller KTR. This was a corollary of the uniform distribution of abrasive particles eroding the target material. Meanwhile, the lower water jet pressure had a positive influence on the top and bottom kerf widths from the capable CAAWJ, which offered a smaller deviation at the entry and exit of the cut surface in the target material, due to the LN<sub>2</sub> cooling jet being more effective. The conclusion was that, the effect of LN<sub>2</sub> jet cooling reduces the KTR by 1.72 - 28.40% in the CAAWJ cutting process. Striations were also formed in the lower cutting region of the cut surface in the AWJ process (Figure 9a). These were attributed to the availability of a smaller kinetic energy in the lower cutting region by the fragmented abrasive particles.

### **Evaluation of AWJ and CAAWJ Machined Surface Morphology**

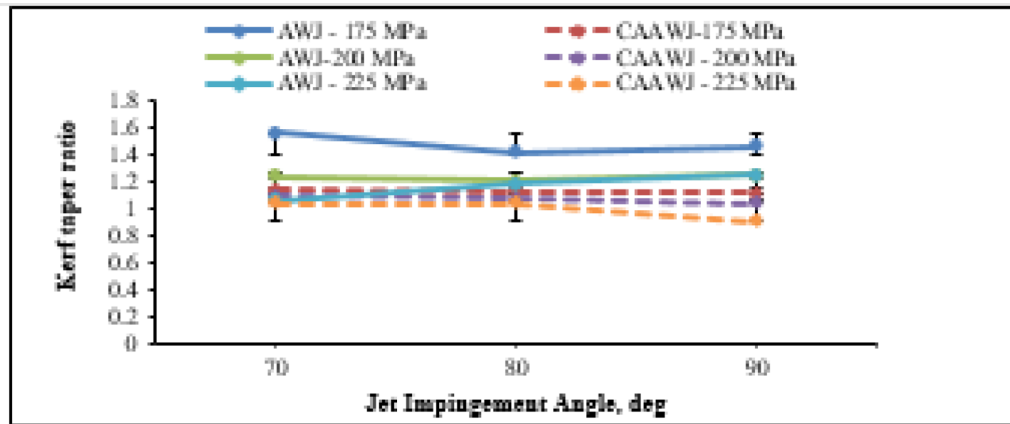
The micrographs were taken at the top kerf wall cut surfaces and bottom kerf wall cut surfaces is shown in Figure 10. Usually, the top cut surface is considered as a contaminated zone such as wear tracks, pits, and particle embedding.

In all cutting conditions, the CAAWJ process causes absence of wear tracks and abrasive contaminations in the kerf wall surfaces, due to the application of LN<sub>2</sub> jet in the cutting zone. As a result, increase in hardness and reduction of ductility of the work material in the cutting zone helps the production of a satisfactory machined surface under various levels of cutting process parameters. This CAAWJ cutting process allows jet erosion with ductile to brittle transition phase, which causes restrict the development

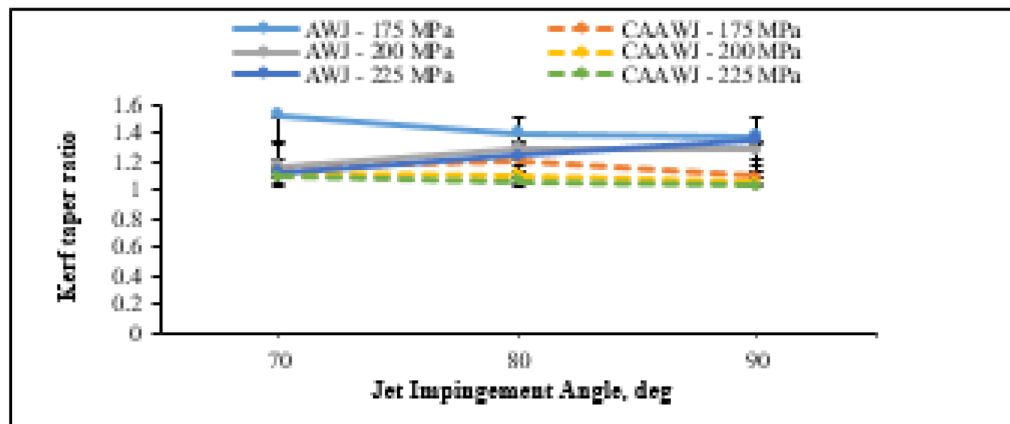


## Performance and Surface Evaluation Characteristics

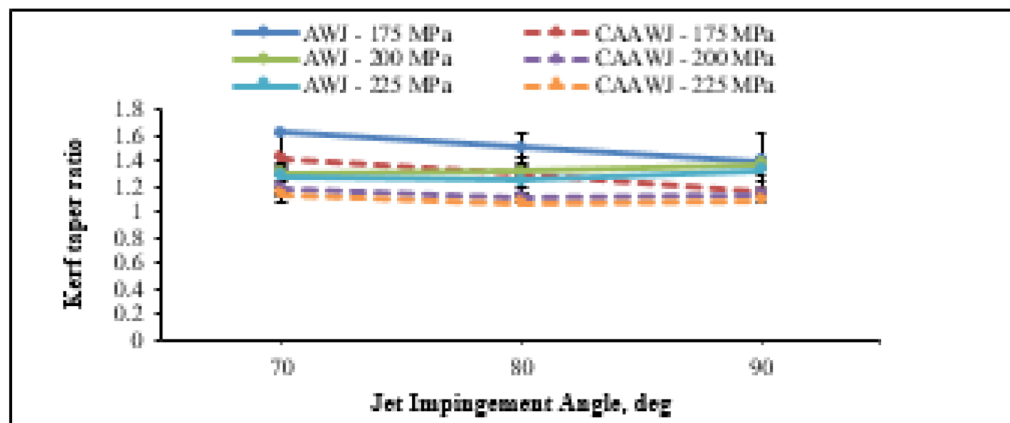
Figure 8. Variations of the kerf taper ratio under AWJ and CAAWJ conditions (a) #80 (b) #100 (c) #120



(a)

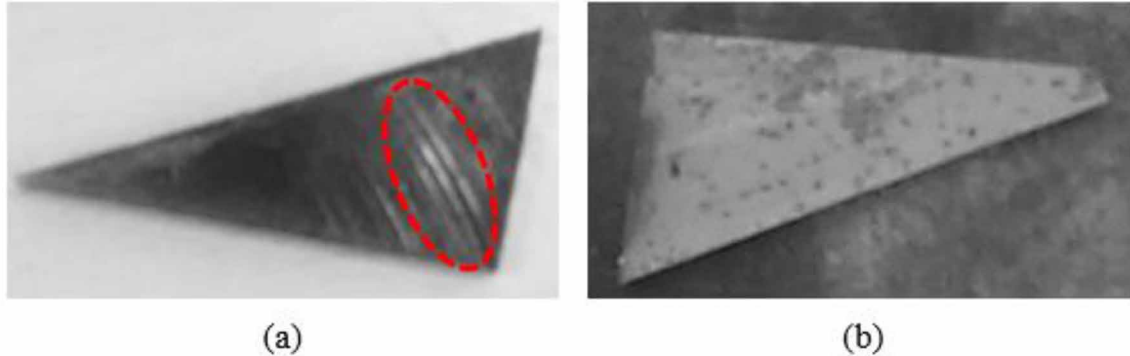


(b)



(c)

Figure 9. Photographs of the machined AISI D2 steel (a) AWJ kerf wall cut surface (b) CAAWJ kerf wall cut surface



of ploughing in the machined surface. The occurrence was due to the reduction in abrasive embedding and fractured abrasives in the kerf wall cut surface by reduction in the impact strength in the cutting zone through the assistance of  $\text{LN}_2$ . These results were confirmed along with the earlier results (Zhao & Guo, 2014), the smooth cutting surface was more easily obtained on hard materials than soft materials. This result was due to the ductility and higher hardness of the target material.

The micrographs of the top kerf wall cut surfaces in Figure 10 indicate the total absence of any contamination in the cut surfaces under CAAWJ machining process. In the AWJ process, a significant amount of abrasive embedment was found in the mesh size of abrasives #80 and #100 with jet impact angle  $90^\circ$  was used (Figure 10b and 10d). This particle embedment had affect on the surface morphology of the kerf wall cut surface produced by the AWJ cutting process (Boud, Murray, Loo, Clare, & Kinnell, 2014). A small pit could be observed on the surface, arising as a result of the initial bombardment of the jet over the entry of the target material. This kind of action induced the plastic flow of the material. This is encircled in Figure 10(b).

A jet impact angle of  $70^\circ$  with an abrasive mesh size of #100 produced a kerf wall cut surface of better quality compared to the jet impact angle of  $90^\circ$  in the AWJ cutting condition. Figure 10(c), shows an embedment of small fractured abrasives in the kerf wall cut surface. The occurrence of this result is, the offers of a smaller disintegration of abrasive grains with the jet impact angle of  $70^\circ$ , producing a sufficient kinetic energy during the cutting process. The result is a reduction in abrasive contamination, and wear tracks. However, the cutting conditions of the jet impact angle of  $90^\circ$  with an abrasive mesh size of #80 destruction energy of a larger magnitude. This combination caused fractured abrasive particles with a higher particle disintegration getting severely embedded in the kerf wall surface by a higher impulse of abrasive particles, as shown in Figure 10(d). A kerf wall cut surface was intensely ploughed by the shearing action of a single coarse grain in the abrasive mesh size #80. This arises as a result of the presence of a higher impulse in the abrasive particles. A separate wear track was therefore observed on the kerf wall cut surface, as shown in Figure 10(d). In connection with this, a shallower and longer wear track was found with embedded abrasives. The results confirmed the production of a substantial deformation effect by the AWJ cutting conditions, succeeded by a ductile fracture. A smaller contamination was seen in the cut surfaces (Figure 10e - 10f) while the employment of abrasive mesh size of #120. In CAAWJ process, free of abrasive contamination was observed in the cut surfaces under different jet impact angles.

Performance and Surface Evaluation Characteristics

Figure 10. SEM images on AWJ and CAAWJ machined AISI D2 Steel

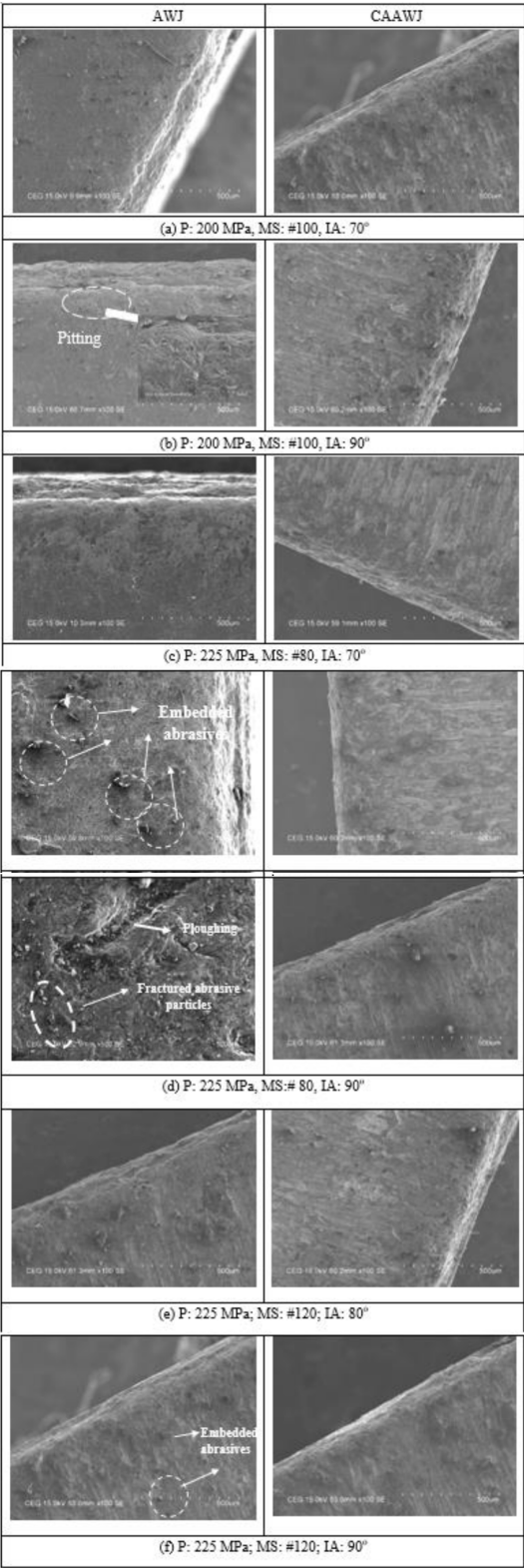
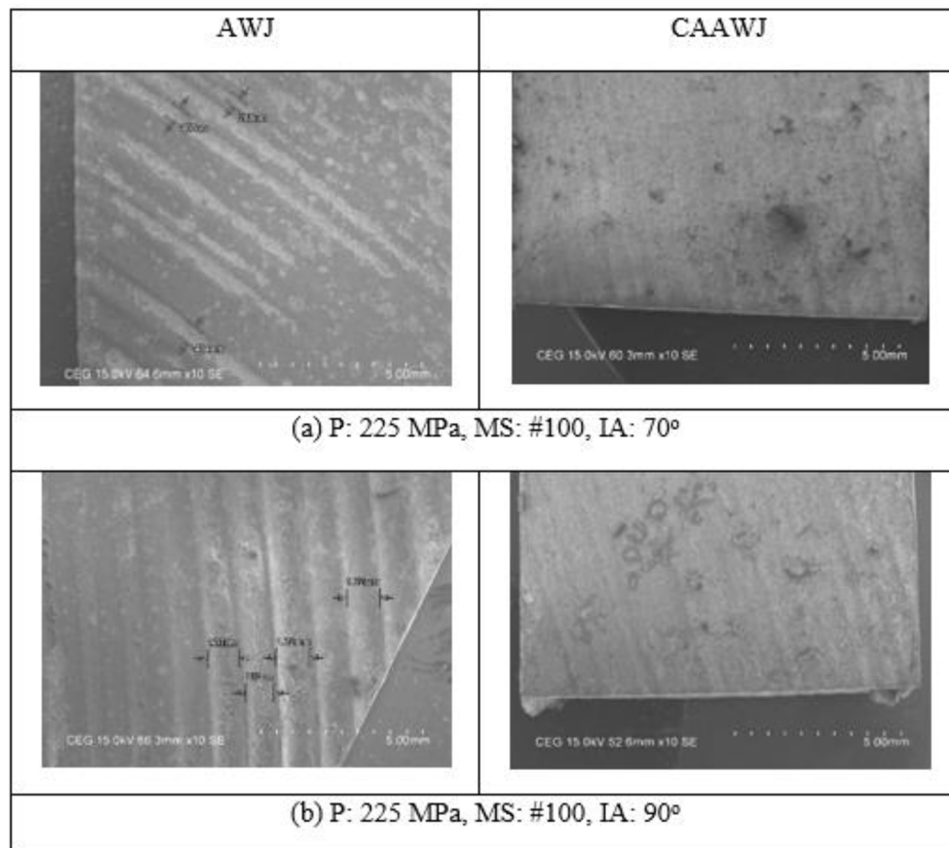


Figure 11 shows striation in bottom cutting zone surfaces in the form of a trough and peak. It can be produced in the bottom surface region through the effect of jet deflection by distribution of lower kinetic energy abrasives. This is shown in Figure 11(a). Occurrence of this result was due to a reduction in abrasives kinetic energy while increasing the thickness of the D2 material. These results were observed by earlier researchers (Hlavac, 2009; Orbanic & Junkar, 2008), who reported striation as a common phenomenon existing in the bottom cut surface under the jet impact angle of  $90^\circ$  as shown in Figure 11(b). This is because the jet impact angle of  $90^\circ$  produced high impulse of abrasive particles that allowed more fractured abrasives under ductile mode of erosion process. This result induced jet deflection while increasing the thickness of target material. However, reduction in striations was possible under CAAWJ cutting conditions with various jet impact angles. As a result of the retention of the abrasive particles energy in the lower region and leave the kerf wall cut surface with significant reduction of trough and peaks. This consequence occurs due to the reduction of the impact strength in the cutting zone using less amount of particles kinetic energy with a significant reduction in fractured abrasives. And, this cutting action helped bringing down the formation of trough and peaks in the bottom kerf wall surfaces through a large number of sufficient kinetic energy of particles used in the erosive action. This also be mitigated the jet deflection in the lower cutting regions. This result is contrast to the mixed action of abrasives involved in the cutting regions at room temperature for the production of a severe striation on

Figure 11. Formation of Striation in the various cut surfaces

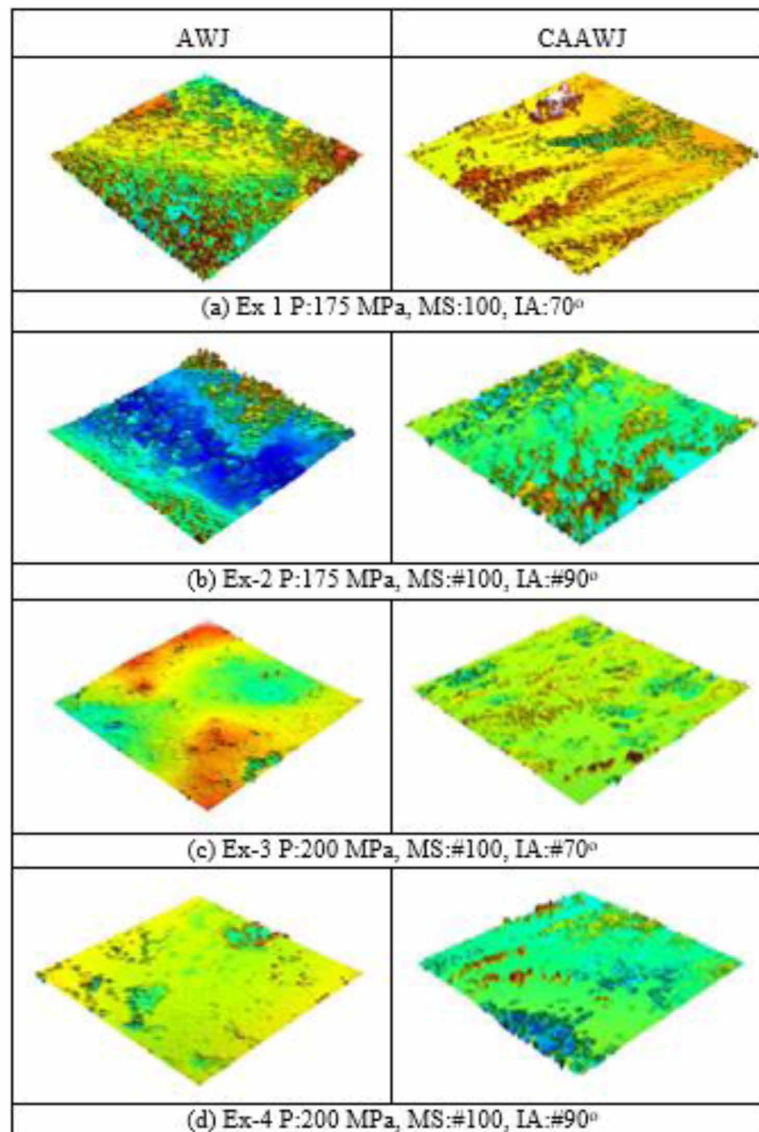


the bottom surface regions. The experimental results reveal the CAAWJ and the jet impact angle as the factors with the largest influence for improving the surface quality in the cut surfaces.

### AWJ and CAAWJ Machined Surface Topography Examination

Figure 12 shows the cut surfaces of 3D surface topography, revealing the peaks and valleys in different experimental cutting conditions. In the surface topography studies on AWJ and CAAWJ, the AWJ cut surface profiles were investigated. These have been reported by Yuvaraj and Pradeep Kumar (2017a) with various jet impact angles. This results were taken for a comparative study with CAAWJ cut surfaces.

*Figure 12. Surface topography of cut surfaces in AISI D2 Steel*

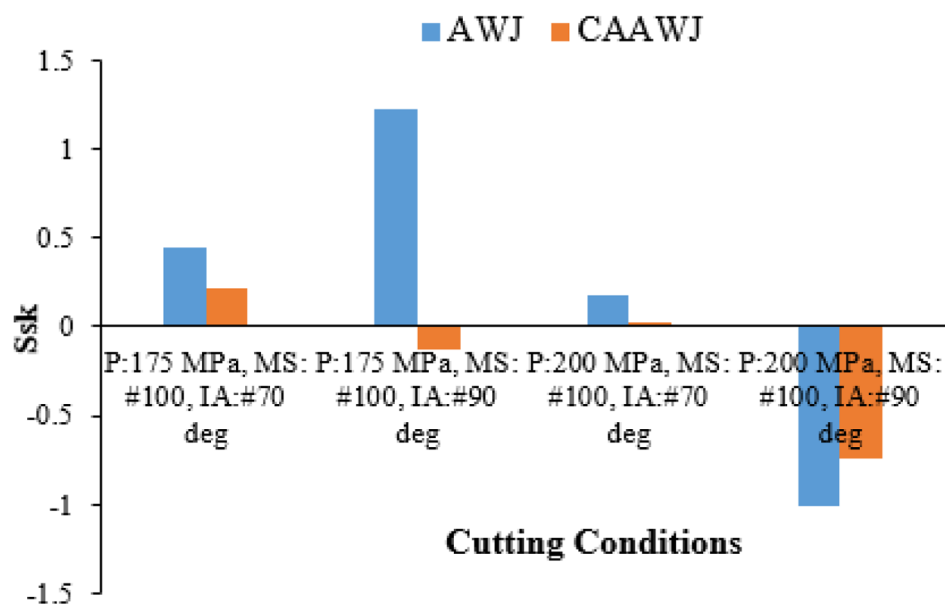


All the experiments carried out on machined surfaces characterized the presence of peaks and valleys in the 3D surface texture. Of all the cutting conditions, the CAAWJ process offered a lower projection of peaks and valleys with a smaller randomized formation noticed on the machined surfaces. In the case of the AWJ process, peaks and valleys were randomly observed on the surface topography especially the cut surface with a mesh size of #80 and impact angle of 90° showing a more randomized projection of peaks and valleys. The random feature of the profile was due to the critical energy of the jet, as they are known for a larger collision of abrasive particles, after generating deep and incomplete traces on the impinging surface. Further, the 3D surface parameter values are established from the respective cut surface profiles, and the discussion relating to them is given below.

In addition, various 3D roughness parameters were analyzed with various machining conditions under AWJ and CAAWJ processes. The 3D roughness parameters considered in this study were Ssk, Sp, Sv, Sku, Sz and Sa. These parameters are known for their significant influences on the functionality of the machined components especially in sliding contact and coating applications.

Figure 13 shows the variations in the Skewness (Ssk) values on different cut surfaces of CAAWJ and AWJ. The experimental results, show the offer of a lower Ssk value for the cutting of D2 steel by the CAAWJ process. This lower value indicates symmetry pattern of the surface heights being better than the others, arising from the jet impact angle of 70° with a different water jet pressures contributing to the uniform distribution of the jet over the target material, and enabling the achievement of a symmetrical pattern in the target material surface. This arose as a result of kinetic energy of the abrasives retained with sufficient kinetic energy while increasing the depth of penetration under the CAAWJ process. Changes in the erosion mechanism in the cutting zone by LN<sub>2</sub> jet explain the occurrence of this jet. This was confirmed by the skewness value which was nearer to zero (Ssk~0). Various patterns of surface heights were observed in the CAAWJ cut surfaces, confirmed by the Ssk>0 and Ssk<0.

Figure 13. Skewness value of AISI D2 Steel cut surfaces with various conditions



### Performance and Surface Evaluation Characteristics

In the CAAWJ process, the maximum value of Ssk was observed as the combined effect of water jet pressure 175 MPa and mesh size #100 with a jet impact angle 70° was employed. The maximum value indicates a majority of peaks seen on the surface, as confirmed by the maximum peak (Sp) values, shown in Table 3. However, it was lower than the AWJ machined surface. This arises due to the process parameters combination yielding a smaller abrasive particles energy through the mixing and acceleration process. Hence, energy is available for machining die steel is rather small. This level of energy helps removing the material through ductile to brittle erosion mechanism by the application of LN<sub>2</sub> jet. The production of Ssk values explains the changeover erosion mechanism.

Similarly, a few CAAWJ cut surfaces show Ssk value as less than zero (Table 3), indicating a majority of the work material as confined to the nearby peaks for the machined surface. However, the production of severe valleys was observed on the kerf wall cut surfaces by an AWJ, confirmed through a maximum of deeper values (Sp). The Sp values are shown in Table 3. Despite the formation of severe valleys by the jet impact angle of 90° with room temperature, the changeover erosion mechanism at low temperature caused restriction on the strong impact of abrasive particles on the surface, allowing reduction in severe peaks and deeper valleys for the cut surface. Maintenance of energy density of the jet was seen under CAAWJ process. The conclusion drawn from the results is that Ssk > 0 and Ssk < 0 get reduced through the employment of LN<sub>2</sub> in the cutting zone. This hardened cutting zone restricts the formation of severe peaks and valleys produced by the abrasive particles during the operations. The consequence of this result, was the maintenance of the velocity of the abrasives throughout the cutting depth, leading to the production of better surface finish in the lower cutting regions.

Of all experimental conditions, cryogenics play a vital role in the Ssk value. Similarly, the jet impact angle is seen playing a key role in the Ssk under AWJ machining process. Isotropic surface structure was formed in both cases. Indicating a uniform distribution of peaks and valleys with small projection of peaks (Figure 12a) or the absence of extreme peaks and deeper valleys on the surface, as graphically represented in Figure 12(c). Despite the formation of anisotropic structures on the AWJ cut surfaces, the use of LN<sub>2</sub> jet and oblique jet impact angle maintain the consistency on the surface structure as isotropic. These results are consistent with those of previous findings (Yuvaraj & Pradeep Kumar, 2017a).

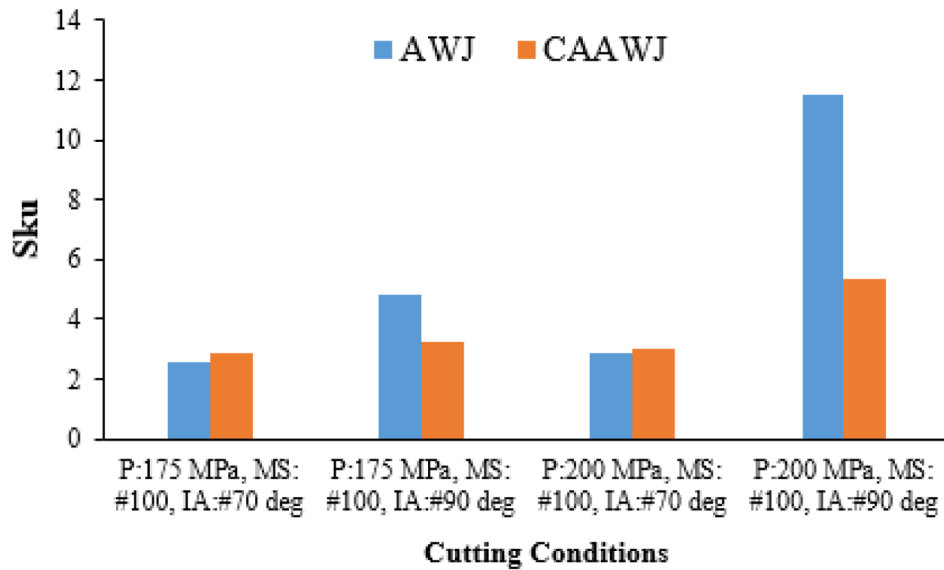
Sku is a kurtosis parameter value. The variation in the values for each machining condition are seen in Figure 14. These variations indicate the presence or absence of extreme peaks/valleys on the machined surface (Krolczyk, Krolczyk, Maruda, Legutko, & Tomaszewski, 2016). The CAAWJ cut surfaces are seen having lower Sku values than the AWJ cut surfaces. Hence, these Sku values are closer to 3, indicating the distribution of peaks and valleys in Figure 12(c), which are normal in the machined surface

Table 3. Maximum peak and deep valley values

S.No	Machining Conditions	Sp		% of Reduction Over AWJ	Sv		% of Reduction Over AWJ
		AWJ	CAAWJ		AWJ	CAAWJ	
1.	P: 175 MPa MS: #100, IA: 70°	19.7	6.17	68.68	17.5	9.4	46.29
2.	P: 175 MPa MS: #100, IA: 90°	33.3	21.9	34.23	25	15.3	38.80
3.	P: 200 MPa MS: #100, IA: 70°	11.05	10.3	6.79	8.3	7.35	11.45
4.	P: 200 MPa MS: #100, IA: 90°	24	10	58.33	18.8	14.1	25.00



Figure 14. Kurtosis value of AISI D2 Steel cut surfaces



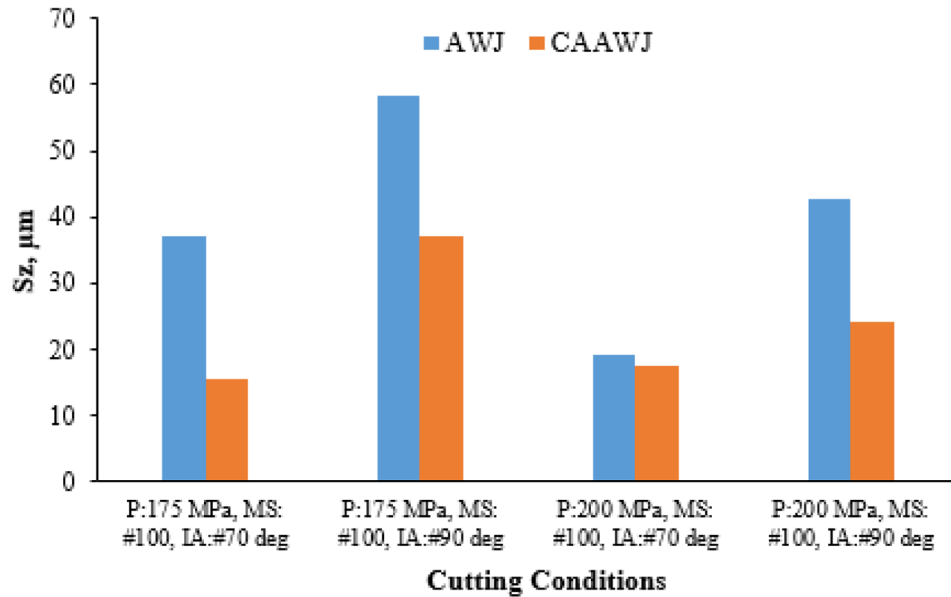
structure. Peaks and valleys of this kind are distributed with fine irregularities in the cut surface. These results can be produced by using  $\text{LN}_2$  in the cutting process, which allows lower  $S_{ku}$  values.

Among the cutting settings, a water jet pressure of 200 MPa and jet impact angle of  $90^\circ$  indicates a high  $S_{ku}$  value under the AWJ process. It means that the surface texture contains extreme count of peaks and valleys, as confirmed by the  $S_{ku}$  value that is greater than 3. It indicates the inordinate projection of peaks with deeper valleys present particularly on the kerf wall cut surface texture (Figure 12d), as confirmed by the  $S_{ku}$  value that is greater than 3. This feature is a consequence of the jet impact angle of  $90^\circ$  with higher hydraulic jet pressure providing a wavy distribution of abrasive particles arising out of a drop in the velocity of the abrasive particles, which produced inordinate peaks in the AWJ cut surface. Also, a few deeper valleys were formed as a result of the critical energy of certain coarse abrasives in the jet, when a jet impact angle  $90^\circ$  was employed. This consequence is reduced through the CAAWJ process, as it maintains the cutting energy of abrasive particles through the reduction of deflection and particle embedding in the cut surface. Also, inordinate peaks and valleys were absent in the AWJ machined D2 steel surface as seen in Figure 12(c). Hence, this  $S_{ku}$  value was maintained as 3 over the other AWJ cutting conditions.

The maximum height ( $S_z$ ) in the roughness profile values in different machined surfaces under CAAWJ and AWJ conditions is shown in Figure 15. The results show a lower  $S_z$  values at CAAWJ cut surfaces than the AWJ conditions. The production of lower values in CAAWJ cut surfaces permits a smaller sensitiveness to the contact applications such as sliding contact, coating, etc. This is because the production of a lower height value improves the surface quality, and functionality of the component through the reduction of friction/ crack being involved in the mating applications. However, the jet impact angle of  $90^\circ$  with water jet pressure of 175 MPa produced higher value among the other CAAWJ conditions. As a result of the combined effect of process parameter settings which offer more fractured abrasives through the cutting head and cutting zone by the employment of jet impact angle  $90^\circ$ . The reduction in impact energy of the target material by the  $\text{LN}_2$  jet compensates the energy produced by the AWJ with jet impact



*Figure 15. Maximum height in the profile of the machined surfaces*

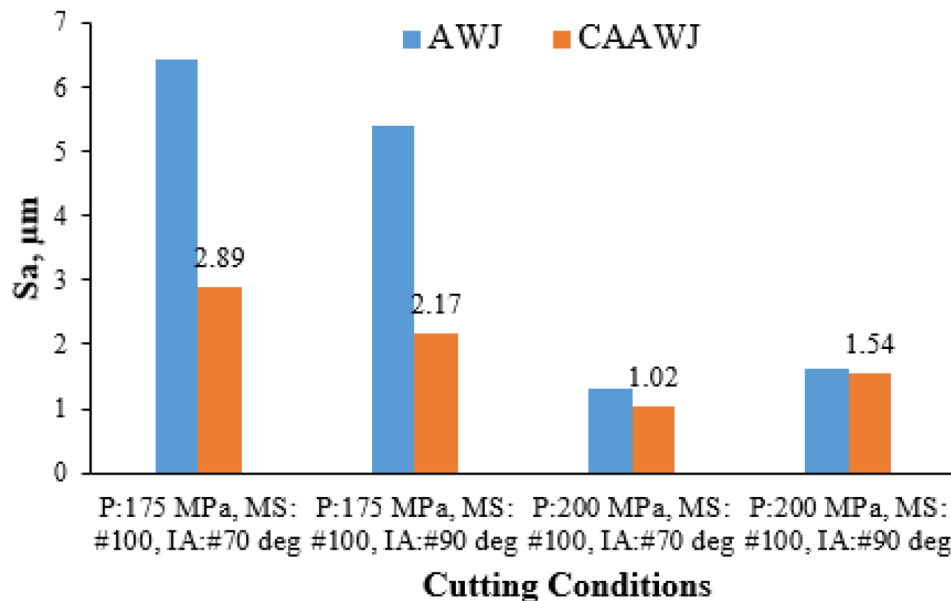


angle of 90° employed and producing a surface with reduction in the extreme peak height. The lower value of CAAWJ process produced a uniform surface profile with severe reduction in the extreme peak height in the cut surface by the action of fine erosion mechanism, which had a significant influence on the cutting zone. In contrast, extreme peak height was noticed in the AWJ machined surfaces, which is happened through the non-uniform distribution of abrasives with an employment of jet impact angle of 90° was used. Then, it allows the cut surface with an extreme projection peak heights.

The variation in the arithmetic mean height ( $S_a$ ) of the roughness profiles during the cutting of the die steel under AWJ and CAAWJ cutting is shown in Figure 16. Of the different cutting conditions,  $\text{LN}_2$  jet cooling was more significant. This was due to  $\text{LN}_2$  jet cooling, which increased the hardness of the cutting zone, producing a better surface finish through the occurrence of brittle erosion in the cutting process. A comparison of the various levels of cutting conditions showed a lower  $S_a$  value of 1.02  $\mu\text{m}$  in the CAAWJ process. Among the  $S_a$  variations in different cutting conditions, a lower  $S_a$  value was found under CAAWJ cutting condition, similar to the results of  $S_q$  and  $S_z$ . This result arose out of the effect of the jet impact angle of 70° and a water jet pressure of 200 MPa. This combination offered a sufficient threshold energy to each abrasive in the mesh size of #100, and produced a uniform roughness pattern on the cut surface. This result was due to the occurrence of brittle erosion at the cutting zone by the  $\text{LN}_2$  jet. This is confirmed by the lower value of  $S_a$ .

The results demonstrate the  $\text{LN}_2$  jet with jet impact angle and the water jet pressure as parameters making a substantial contribution to the surface quality of machined D2 steel. A lower  $S_a$  value was also found in jet impact angle of 90° used. This was a consequence of the ductile to brittle transformation effect, which subsequently allowed the cutting head with disintegration of particles at a jet impact angle of 90° employed. Eventhough the fractured abrasives in the mesh size of #100 gets a lesser kinetic

Figure 16. Arithmetic mean height value of the machined surfaces



energy to cut the material, the conclusion was the production of a better finish on the cut surface. The occurrence of this results in the impact energy of the target material getting dropped by the application of the  $\text{LN}_2$  jet compared to the room temperature. This reduction in an impact energy of the target material compensates the lower velocity of the abrasives involved in the machining process.

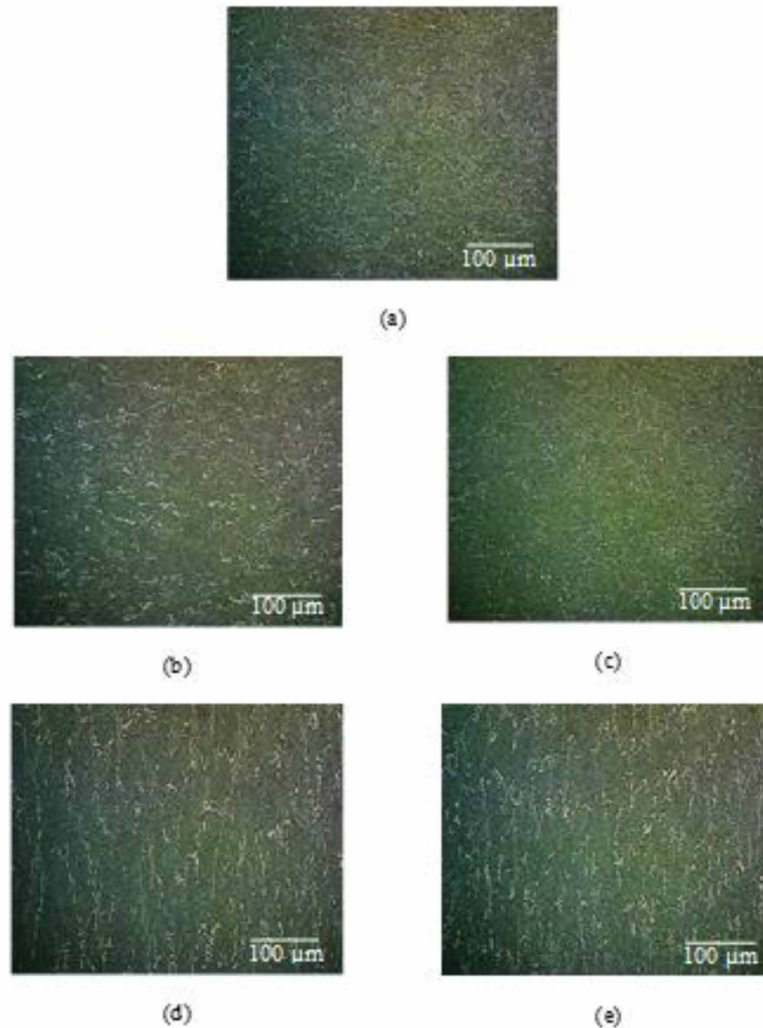
### Microstructure Examination

The microstructure shows grains boundaries of ferrite (white) in a matrix of pearlite (dark) in the as received condition, as shown in Figure 17(a).

A comparison of the microstructure finer grains on the CAAWJ machined surfaces than the AWJ. The AWJ cutting process generates heat in the cutting zone in the range of 45 to 60°C, recorded by the IR thermometer. This was the result of the combined effect of abrasive mesh size of #80 and jet impact angle of 90°. This combination offers abrasives with a high impulse at the cutting zone. As a result, diffusion of temperature to the grain boundaries, and cause restricted to the refinement of grains of the ferrite surrounding the matrix of the pearlite, as shown in Figure 17. In the CAAWJ process, the  $\text{LN}_2$  jet cooling reduces the peak temperature transferred from the top to the bottom cutting region, and helps the insignificant formation of fine grains along the boundaries of the matrix. However, no other change was seen in the microstructure. This was due to the smaller processing time of the target material under the cutting process with AWJ and CAAWJ. In contrast, the microstructure of the abrasive mesh size of #80, and the jet impact angle of 70° under AWJ process were similar to the CAAWJ machined surface, as shown in Figure 17(d)-(e). This result was due to the possibility of minimum temperature through a jet impact angle of 70° by the sufficient and uniform distribution of abrasives involved in the erosive action. This cutting force caused the restriction in the deformation and heat at the cutting zone.

## Performance and Surface Evaluation Characteristics

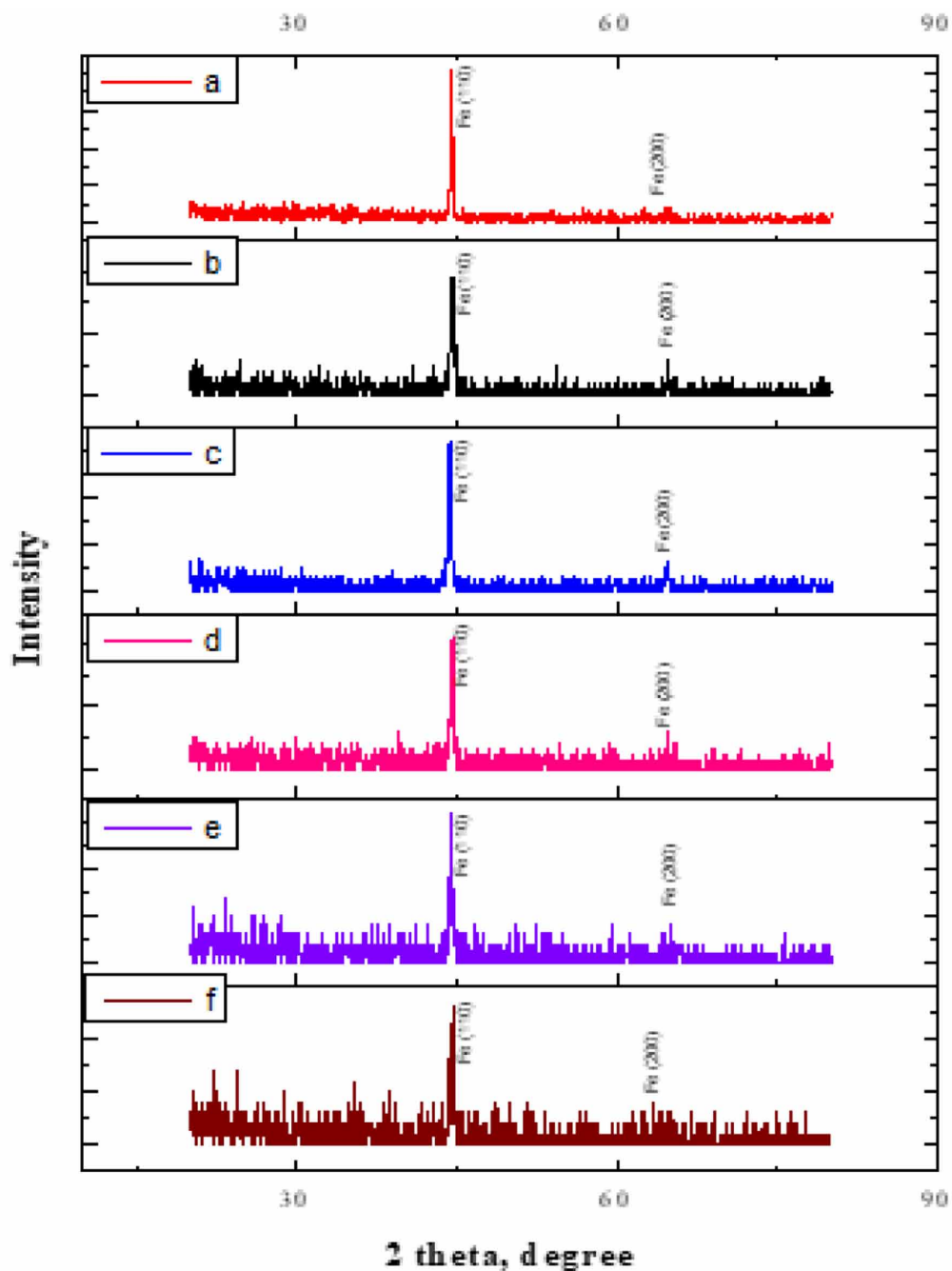
Figure 17. Microstructure of the AWJ and CAAWJ cutting conditions (a) Base material (as received condition) (b) AWJ-P:225 MPa, MS:#80, IA:90° (c) CAAWJ-P:225 MPa, MS:#80, IA:90° (d) AWJ-P:225 MPa, MS:#100, IA:90° (e) CAAWJ-P: 225 MPa, MS:#100, IA:90° (f) AWJ-P:225 MPa, MS:#80, IA:70° (g) CAAWJ-P:225 MPa, MS:#80, IA:70°



## XRD Pattern of the AWJ and CAAWJ Machined Surfaces

Figure 18 shows the XRD pattern of the base material under AWJ and CAAWJ cutting conditions. The kerf wall cut surfaces were subjected to XRD pattern for the analysis of the peak shifting on the cut surfaces with the peak position in the base material. This was confirmed by the presence of the microstructure as shown in Figure 18. The results, confirmed that, XRD pattern out of all cut surfaces maintaining the same peak position with the base material. The reflecting planes in the cut surface such as (110) and (200) specify the elements such as iron. The peaks of the surface reflecting planes follow the standards of XRD also confirming matching of the BCC phase of D2 steel. A rich solid solution of iron as indicated

Figure 18. XRD pattern of the AWJ and CAAWJ cutting conditions (a) base material as received condition, (b) AWJ -P:150 MPa, MS:#80, IA:90°, (c) CAAWJ -P:150 MPa, MS: #80, IA: 90°, (d) AWJ -P:150 MPa, MS: #100, IA: 90° (e) CAAWJ -P: 150 MPa, MS: #100, IA: 90°, (f) AWJ -P: 150 MPa, MS: #80, IA: 70°



in the base material surface, as shown in Figure 18. It also indicated a smaller projection of a few peaks in the XRD profile, confirming the presence of carbon and chromium content. No other components were formed arising out of the lower weight percentage of the elements involved in the D2 steel. The result confirms that AWJ and CAAWJ cutting processes offer an insignificant deformation effect in the surface of the target material; as a result, the peaks of the XRD pattern were not significantly shifted to the other plane and angle. However, it is noticed that the XRD pattern of the jet impact angle of 90° with different abrasive mesh sizes produced lower intensity range which happened as a result of the smaller thermal effect formed in the kerf wall cut surface under AWJ. The higher peak intensity value was due to the roughness of the cut surface being lower under the CAAWJ cutting process. This result also happened in the AWJ process during the employment of jet impact angle of 70°.

The lower ductility of the AISI D2 steel in the cutting process with the presence of a high impulse of the coarse and medium coarse abrasive particles causes a negligible deformation despite the employment of coarse abrasives (#80) with a jet impact angle of 90°. This effect was proved by the “d” spacing value between the hkl planes. With an increase in lattice strain of “d” spacing, there was a modification in the peak shifting position into a lower angle. Their values are listed in Table 4. The results showed LN<sub>2</sub> cooling in the cutting process maintaining the peak position and its intensity.

### Evaluation of Residual Stress in the Machined Surfaces

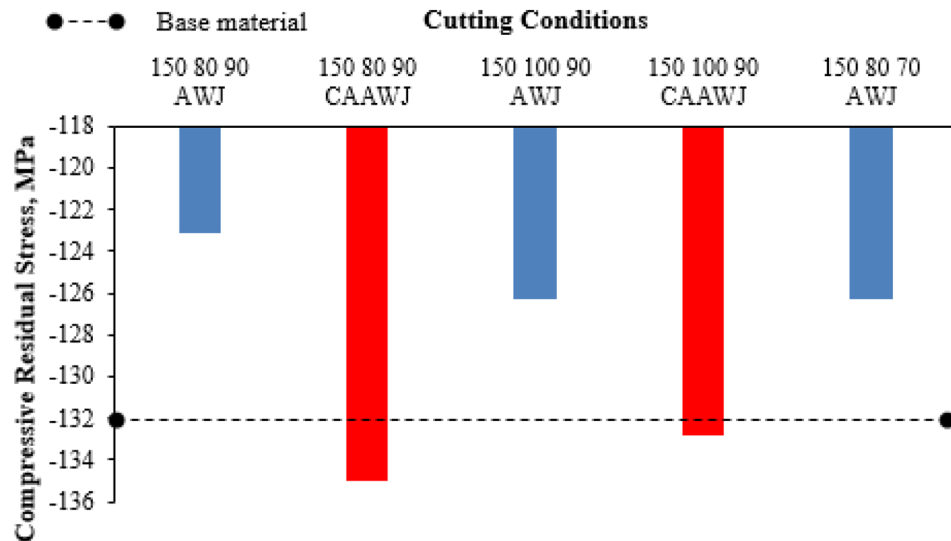
Machined surfaces comprise compressive residual stress under all the cutting conditions, as shown in Figure 19. There is also confirmation of improvement in the fatigue life of the target material by the production of compressive residual stress in the machined surfaces. The magnitude of the AISI D2 Steel compressive residual stress is seen as higher than that of the Aluminium alloy (Yuvaraj & Pradeep Kumar, 2016), due to the occurrence of increase in melting temperature of the work material.

The offer of a small temperature by AWJ machining is well known when compared to the other machining processes. This resulted in the absence or effect of thermal stress of a smaller magnitude in the impact zone and the surface compressive residual stress is induced in the machined surfaces. The results showed a higher residual stress produced by the use of LN<sub>2</sub> in the machining process compared to the process at room temperature. The machined work material maintained the compressive residual stress with the base material (as received condition). Due to a low temperature, an increase in the hardness of the machined surface was found. The result was a high surface compressive residual stress which

*Table 4. XRD pattern and their ‘d’ spacing values for AISI D2 Steel*

Parameter settings	Jet conditions	Peak angles (2θ), deg.	Peak reflecting planes	‘d’ spacing, °A
P:150 MPa, MS:80, IA: 90°	AWJ	44.52	110	2.033
	CAAWJ	44.32	110	2.042
P:150 MPa, MS:100, IA: 90°	AWJ	44.60	110	2.030
	CAAWJ	44.36	110	2.040
P:150 MPa, MS:80, IA: 70°	AWJ	44.60	110	2.030
Base metal	As received	44.44	110	2.036

Figure 19. Variation of compressive residual stress in AWJ and CAAWJ conditions



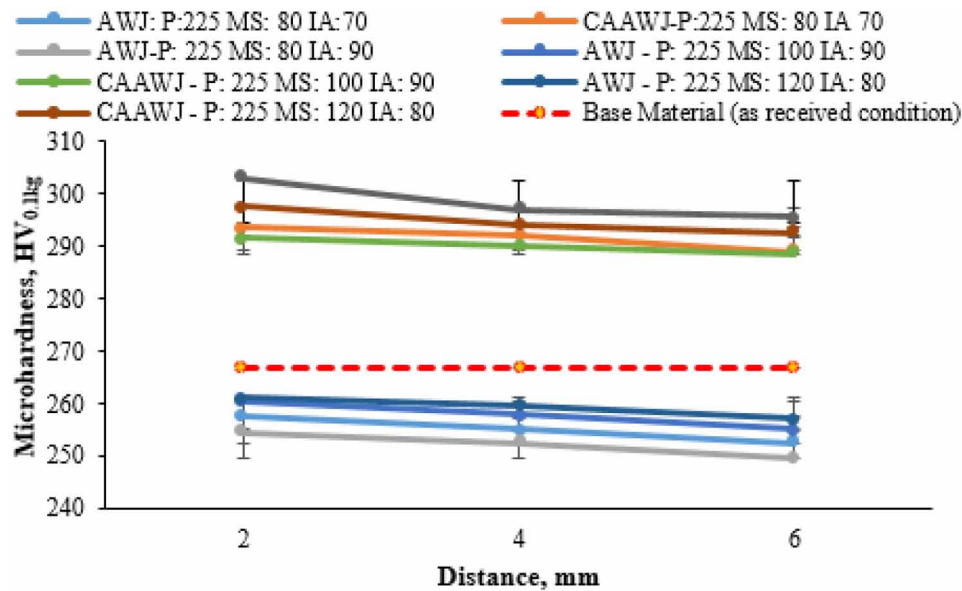
explains the significant reduction in the ductile mode of material removal in the cutting zone, wherein more indentations were produced on the impinged surface through the involvement of coarser grains in mesh size #80 than the mesh size #100. This resulted in the production of surface indentations by the impingement of abrasive particles with a high velocity of the water jet in the cutting process. This is analogous to the development of residual stress by the application of the shot peening process (Arola & Ramulu, 1997). Increase in the compressive residual stress was seen through decrease in an abrasive mesh size or increases the particle size. On increasing the particle size with lower fractured abrasive particles, surface indentation was seen as more in the kerf wall cut surface which in turn, serves to cause an increase in the surface residual stress in the CAAWJ cutting process.

Coarse abrasives in #80 and #100 mesh sizes produce, fracturing and instantaneously losing the kinetic energy of abrasives through a reduction in size and shape of the abrasives. This was followed by a slight indentation of low velocity abrasives yielding a smaller compressive residual stress. This was the result of the ductility of the D2 steel in AWJ. The jet impact angle of 90° with a mesh size of #80 was seen among the cutting conditions causing a decrease in compressive residual stress. This was the significance of the production of temperature at the cutting zone than when the jet impact angle of 70° was employed. This peak temperature allows a slight reduction in the residual stress as observed in AWJ machined surfaces. Due to the assistance of  $LN_2$  in the cutting zone, a reduction in impact zone temperature was found in CAAWJ process.

## Microhardness Evaluation

Figure 20 shows the microhardness of the machined target material surfaces under AWJ and CAAWJ process conditions. CAAWJ cutting kerf wall cut surfaces showed higher hardness under all cutting conditions. In all the cut surfaces, a slight decrease in hardness values was seen with increase in the jet entry distance. This result was due to the thermal diffusivity of the AISI D2 steel. In the bottom cutting

*Figure 20. Microhardness of the AWJ and CAAWJ kerf wall cut surfaces*



region, the ductile mode of cutting and deformation erosion process generated more frictional forces producing a peak temperature in the cutting region, so as to reduce the hardness of the kerf wall cut surface while increasing the penetration depth, despite the hardness variation in the CAAWJ kerf cut surfaces showing a higher level, which could be lower than the aluminium alloy (Yuvaraj & Pradeep Kumar, 2016), as the thermal conductivity of the aluminium alloy was more than that of the AISI D2 steel. The increase in hardness was found in the CAAWJ cutting process could be due to the grain refinement through employment of  $LN_2$  in the machining zone. A higher hardness was found in the following CAAWJ cutting conditions namely higher water jet pressure, coarse abrasive (#80) and jet impact angle of  $90^\circ$ . Owing to the thermal diffusivity of target material, the surface micro hardness values at 6 mm were lower than at 2 mm and 4 mm observed.

Figure 20 also shows insignificant modifications in the hardness of the various AWJ cutting conditions. Nevertheless, a few changes in AWJ cutting conditions were noticed. These arose as a result of the effect of the higher water jet pressure and lower traverse rate with different abrasive mesh sizes under the jet impact angle of  $90^\circ$  was used. At the entry of the jet, parameters produced the peak temperature during their impact with the hard target materials. The details of the mechanism have been described by Ohadi et al. (1992). The production of more friction forces was seen with increase in the depth of jet penetration. This happened as the magnitude of the hardness that showed a decrease on the lower side of the kerf wall cut surface.

## CONCLUSION

In the present chapter, AWJ and CAAWJ processes were conducted on the AISI D2 Steel, as the work-piece and garnet was used as an abrasive under AWJ and CAAWJ machining processes. The major conclusions drawn are given below:



1. Abrasive particle contamination is greatly reduced by 54.54% with the help of the  $\text{LN}_2$  jet in the cutting zone.
2. In the CAAWJ process, the depth of penetration improved by 1.43 - 35.93% over the AWJ cutting process, due to the reduction in particle embedding and changeover erosion mechanism in the cutting zone.
3.  $\text{LN}_2$  jet cooling produced a reduction of about 1.72 - 28.40% over the AWJ in the kerf taper ratio.
4. Projection of surface heights with symmetrical pattern is seen on the CAAWJ machined surfaces, as confirmed by the value of Skewness. Production of extreme peaks with higher levels and valleys with deeper levels are absence in the CAAWJ was confirmed by a kurtosis value.
5. In the CAAWJ process, the inconsequential presence of striations in the bottom region of the cut surface was observed while a jet impact angle of  $90^\circ$  was employed. This result is better than that of the AWJ process.
6. No significant change in the microstructure was observed in the CAAWJ machined D2 steel rather than on the Aluminium alloy, as the thermal diffusivity of the D2 steel is lower than that of the Aluminium alloy.
7. In both the cutting conditions, the orientation of the work material structure was maintained with the base material as confirmed by the XRD peak analysis. This confirmed the presence of only an insignificant amount of deformation effect produced on the cutting zone which helped maintenance of the peaks in the similar position with a slight deviation in the  $2\theta$  value.
8. In the CAAWJ process, the surface compressive residual stress of the machined AISI D2 steel was higher than that of the AWJ cutting process. This happened due to the higher melting point of the work material.
9. Microhardness was increased in the cutting zone under the CAAWJ process through the application of  $\text{LN}_2$ . This increment in hardness was due to the grain size refinement through the control of the peak temperature in the primary impact zone by the assistance of  $\text{LN}_2$  cooling.

## ACKNOWLEDGMENT

N. Yuvaraj acknowledge the CSIR, GoI, New Delhi, for providing financial support under the scheme of CSIR-SRF (Grant file no. 9/468(479)/2014-EMR I).

## REFERENCES

- Aich, U., Bandyopadhyay, A., & Banerjee, S. (2013). A state of art – review on abrasive water jet machining process. *International Review of Mechanical Engineering*, 7(7), 1471–1494.
- Ankush, S., & Lalwani, D. I. (2013). Experimental investigation of process parameters influence on surface roughness in abrasive water jet machining of AISI H13 die steel. In *Proceedings of Conference on Intelligent Robotics, Automation and Manufacturing*. Emerald Group Publishing Limited.
- Arola, D., & Ramulu, M. (1997). Material removal in abrasive waterjet machining of metals: A residual stress analysis. *Wear*, 211(2), 302–310. doi:10.1016/S0043-1648(97)00131-2



- Asif, I., Naeem, U. D., & Ghulam, H. (2011). Optimization of Abrasive Water Jet Cutting of Ductile Materials. *Journal of Wuhan University of Technology*, 26(1), 88–92. doi:10.1007/11595-011-0174-8
- Bach, F.W., Hassel, T., Biskup, C., Hinte, N., & Schenk, A. (2010). In-process generation of water ice particles for cutting and cleaning purposes. *BHR Group 2010 Water Jetting*, 20, 275–283.
- Boud, F., Murray, J. W., Loo, L. F., Clare, A. T., & Kinnell, P. K. (2014). Soluble Abrasives for Waterjet Machining. *Materials and Manufacturing Processes*, 29(11-12), 1346–1352. doi:10.1080/10426914.2014.930949
- Choi, K. K., Nam, W. J., & Lee, Y. S. (2008). Effects of heat treatment on the surface of a die steel STD11 machined by W-EDM. *Journal of Materials Processing Technology*, 201(1-3), 580–584. doi:10.1016/j.jmatprotec.2007.11.156
- Deepak, D., Akash, V., & Anjaiah, D. (2015). Studies on Jet Penetration and Kerf Width at various Operating Pressure in Machining of D2 Heat Treated Steel Using Abrasive Water Jet. *International Journal of Research in Engineering and Technology*, 4(9), 344–347. doi:10.15623/ijret.2015.0409064
- Flynn, T. M. (2005). *Cryogenic Engineering*. Marcel Dekker. New York: Cryogenic Engineering.
- Folkes, J. (2009). Waterjet-An innovative tool for manufacturing. *Journal of Materials Processing Technology*, 209(20), 6181–6189. doi:10.1016/j.jmatprotec.2009.05.025
- Getu, H., Spelt, J. K., & Papini, M. (2008). Cryogenically assisted abrasive jet micromachining of polymers. *Journal of Micromechanics and Microengineering*, 18(11), 1–8. doi:10.1088/0960-1317/18/11/115010
- Getu, H., Spelt, J. K., & Papini, M. (2011). Thermal analysis of cryogenically assisted abrasive jet micro machining of PDMS. *International Journal of Machine Tools & Manufacture*, 61(9), 721–730. doi:10.1016/j.ijmachtools.2011.05.003
- Gradeen, A. G., Spelt, J. K., & Papini, M. (2012). Cryogenic abrasive jet machining of polydimethylsiloxane at different temperatures. *Wear*, 274-275, 335–336. doi:10.1016/j.wear.2011.09.013
- Hlavac, L. M. (2009). Investigation of the Abrasive Water Jet Trajectory Curvature inside the Kerf. *Journal of Materials Processing Technology*, 209(8), 4154–4161. doi:10.1016/j.jmatprotec.2008.10.009
- Hlavac, L. M., Hlavacova, I. M., Geryk, V., & Plancar, S. (2015). Investigation of the taper of kerfs cut in steels by AWJ. *International Journal of Advanced Manufacturing Technology*, 77(9-12), 1811–1818. doi:10.1007/00170-014-6578-9
- Kaynak, Y., Lu, T., & Jawahir, I. S. (2014). Cryogenic machining-induced surface integrity: A review and comparison with dry, mql, and flood-cooled machining. *International Journal of Mining Science and Technology*, 18, 49–198.
- Kim, S. K. U., Lee, D. G., Lee, W., & Song, O. H. S. (2009). Feasibility Study of Cryogenic Cutting Technology by using a Computer Simulation and Manufacture of Main Components for Cryogenic Cutting System. *Journal of the Korean Radioactive Waste Society*, 7(2), 115–125.

- Krolczyk, G. M., Krolczyk, J. B., Maruda, R. W., Legutko, S., & Tomaszewski, M. (2016). Metrological changes in surface morphology of high-strength steels in manufacturing processes. *Measurement*, 88, 176–185. doi:10.1016/j.measurement.2016.03.055
- Kulekci, M. K. (2002). Processes and apparatus developments in industrial waterjet applications. *International Journal of Machine Tools & Manufacture*, 42(12), 1297–1306. doi:10.1016/S0890-6955(02)00069-X
- Muju, M. K., & Pathak, A. K. (1988). Abrasive jet machining of glass at low temperature. *Journal of Mechanical Working Technology*, 17, 325–332. doi:10.1016/0378-3804(88)90034-4
- Ohadi, M. M., Ansari, A. I., & Hashish, M. (1992). Thermal distributions in the workpiece during cutting with an abrasive waterjet. *Journal of Manufacturing Science and Engineering*, 114(1), 67–73. doi:10.1115/1.2899760
- Orbanic, H., & Junkar, M. (2008). Analysis of striation formation mechanism in abrasive water jet cutting. *Wear*, 265(5-6), 821–830. doi:10.1016/j.wear.2008.01.018
- Patel, D., & Tandon, P. (2015). Experimental Investigations of thermally enhanced abrasive water jet machining of hard-to-machine metals. *CIRP Journal of Manufacturing Science and Technology*, 10, 92–101. doi:10.1016/j.cirpj.2015.04.002
- Patel, K. J. (2004). Quantitative evaluation of abrasive contamination in ductile material during abrasive water jet machining and minimizing with a nozzle head oscillation technique. *International Journal of Machine Tools & Manufacture*, 44(10), 1125–1132. doi:10.1016/j.ijmachtools.2003.12.007
- Reitz, W., & Pendray, J. (2001). Cryo processing of materials: A review of current status. *Materials and Manufacturing Processes*, 16(6), 829–840. doi:10.1081/AMP-100108702
- Shokrani, A., Dhokia, V., Munoz-Escalona, P., & Newman, S. T. (2013). State-of-the-art cryogenic machining and processing. *International Journal of Computer Integrated Manufacturing*, 26(7), 616–648. doi:10.1080/0951192X.2012.749531
- Tsunemoto, K., Kazuhiro, K., & Katsuo, S. (2000). Studies of Micro Ice Jet Machining. The Japan Society of Mechanical Engineers, 2, 99-100.
- Uhlář, R., Hlaváč, L., Gembalová, L., Jonšta, P., & Zuchnický, O. (2013). Abrasive Water Jet Cutting of the Steels Samples Cooled by Liquid Nitrogen. *Applied Mechanics and Materials*, 308, 7–12. doi:10.4028/www.scientific.net/AMM.308.7
- Urbanovich, L. I., Kramchenkov, E. M., & Chunosov, Y. N. (1992). Investigation of low temperature gas-abrasive erosion. *Soviet Journal of Friction and Wear*, 13, 80–83.
- Yuvaraj, N., & Pradeep Kumar, M. (2016). Cutting of aluminium alloy with abrasive water jet and cryogenic assisted abrasive water jet: A comparative study of the surface integrity approach. *Wear*, 362-363, 18–32. doi:10.1016/j.wear.2016.05.008
- Yuvaraj, N., & Pradeep Kumar, M. (2017a). Surface integrity studies on abrasive water jet cutting of AISI D2 Steel. *Materials and Manufacturing Processes*, 32(2), 162–170. doi:10.1080/10426914.2016.1221093

Yuvaraj, N., & Pradeep Kumar, M. (2017b). Study and evaluation of abrasive water jet cutting performance on AA5083-H32 aluminum alloy by varying the jet impingement angles with different abrasive mesh sizes. *International Journal of Mining Science and Technology*, 21(3), 385–415.

Zhao, W., & Guo, C. (2014). Topography and microstructure of the cutting surface machined with abrasive waterjet. *International Journal of Advanced Manufacturing Technology*, 73(5-8), 941–947. doi:10.100700170-014-5869-5

## **KEY TERMS AND DEFINITIONS**

**Abrasive Water Jet:** It is a mechanical based cold machining technique. It is mainly used for machining very hard materials. The material removal takes place through a high velocity jet erosion mechanism.

**Cryogenics:** It is a low-temperature substance and is used for improving the material properties in a beneficial manner at low temperature.

**D2 Steel:** Steel is more suitable for cryogenic machining operations as modified and beneficial erosion mechanism attained easily at cryogenic temperature.

**Liquid Nitrogen:** It is a safe refrigerant and is used for safe environmental machining operations. It is colorless, odorless, and non-corrosive.

**Performance Characteristics:** The quantitative responses are the depth of penetration, material removal rate, kerf width, and surface roughness considered as performance characteristics.

**Surface Characteristics:** The qualitative variables are the surface morphology, contamination, topography, micro structure, residual stress, and hardness considered as surface integrity characteristics.

**Surface Integrity:** It influences the functionality of the machined components in various applications. The elements enclosed in the modified machined surface is characterized as integral.

# Chapter 11

## Finite Element Analysis of Tool Wear in Hot Machining Process: Hot Machining

**Asit Kumar Parida**  
*Indian Institute of Technology, India*

### ABSTRACT

*Super alloys have been used widely in all sectors (e.g., automobile, aerospace, biomedical, etc.) for their properties like high hardness, high wear, and corrosion resistance. A central challenge is the significantly higher temperature and pressure on the cutting tool, hence rapid tool wear and bad surface finish. In the present study, a FEM analysis has been developed to calculate the effect of preheating temperature on the surface of the workpiece on tool wear on machining Inconel 718. Usui's tool wear model has been implemented in DEFORM software. In order to validate the results, an experimental investigation has been carried out with same cutting conditions. The evaluated results were also compared with the room temperature machining condition. It was observed that the heating temperature increased the tool life by reducing tool wear, tool temperature compared to room temperature machining condition. The predicted tool wear, tool temperature, and chip morphology have been compared with the experimental results and good correlation was found.*

### INTRODUCTION

The main difficulties in machining hard material like nickel and titanium based alloy is the rapid tool because of low thermal conductivity, strain hardening, and chemical reactivity to almost all tool. The economics of machining operation is mostly influenced by the tool wear (Ezugwu, 2005). As nickel base alloys are difficult to machine, resulting in higher environmental burden. So the best sustainable practices have to be used in machining of nickel alloys as well as in an effort to reduce the carbon footprint and greenhouse gas emission (Pervaiz, 2015). The best way to machine these materials is to heat the workpiece before or during the machining operation. Different researchers worked using different heating sources. The most used heat source is laser source and studied by different researchers for machining of

DOI: 10.4018/978-1-5225-6161-3.ch011

hard and composite materials. Shanmugan et al. (Shanmugam, Chen, Siores, & Brandt, 2002) studied the comparative study of jetting machining over laser machining technology for machining of composite materials. They study the kerf characteristics and surface roughness of two different materials, carbon composite and fibre reinforced plastic using an abrasive water jet, plain water jet, and laser cutting. It was observed that abrasive water jet cutting promises a better cutting compared other. Li et al. (Li, Zheng, Lim, Chu, & Li, 2010) used the laser for machining of the carbon fibre reinforced composite. They found that heat accumulation could be used to increase material removal. Though laser source can be used for machining of hard materials, the set up cost is high. The simple heat source is flame heat source which can be used to heat for machining of hard material. Parida and Maity (A.K. Parida & Maity, 2016; A K Parida & Maity, 2016; Asit Kumar Parida, 2018; Asit Kumar Parida, & Maity, 2017) studied the machining of nickel base alloys using flame heating. They claimed that the heating enhanced the material removal rate, better surface finish, reduces the cutting forces, tool wear and increases the tool life. Maity and Swain (Maity & Swain, 2008) studied the hot machining of high manganese steel using oxy acetylene gas. Tool life increased with heating temperature in their work. Each heating source has some advantage and disadvantages. So the selection of proper heating source is necessary during hot machining. Otherwise, it may damage the surface of the workpiece material (N. Tosun & Ozler, 2004).

Though many analytical models had been used to predict the tool wear, due to some assumption like boundary conditions, simplified tool-workpiece configurations, and geometrical simplification needs to be assigned (Haddag & Nouari, 2013). There are different types of tool wear such as abrasion (Thermo-mechanical), adhesion (BUE, welding), diffusion (due to high temperature) during machining of difficult-to-cut materials. In 1978, Usui et al. (Usui, Shirakashi, & Kitagawa, 1978) first developed the tool wear model to predict the tool wear using finite difference method. They used abrasive wear model to calculate the tool wear. The effect of preheating on cutting force, surface finish and tool wear on machining of EN-24 steel discussed by Thandra and Choudhary (Thandra & Choudhury, 2010). They observed that cutting force and thrust force was decreased in hot machining and surface finish improved compared to room temperature machining. Oliaei and Karpas (Oliaei & Karpas, 2016) discussed the tool wear affect the forces and tool deflection. Dogra et al. (Dogra, Sharma, Sachdeva, & Suri, 2012) reviewed the effect of nose radius, and different cutting edge preparation on tool wear, cutting force, surface integrity, etc.

The benefit of heating on tool life studied by many researchers (Maity & Swain, 2007; Ranganathan, Senthilvelan 2010; Nihat Tosun, 2002) and found that heating significantly reduces the tool wear and increases tool life and material removal rate. Ozel (Özel, 2009) discussed the effect of different micro-geometry of PCBN cutting tool on cutting forces, stresses, tool wear on machining of AISI 4340 using finite element analysis. With the variation of the micro-geometry, the tool wear depth and predicted wear depth rate decreased. Yen et al. (Y. C. Yen, Söhner, Lilly, & Altan, 2004) studied the tool wear of cutting tool with commercial DEFORM software. Usui's wear model was used for adhesive tool and validated with the experimental results. Hunag et al. (Hu & Huang, 2014) studied the performance of ceramic cutting tool in high-speed machining of hard materials. They suggest that fine grain cutting tool may reduce tool wear and validated the numerical data with the experimental result using Archard tool wear model. Ducobu et al. (Ducobu, Arrazola, Rivière-Lorphèvre, & Filippi, 2015) predicted the tool wear of Ti6Al4V using DEFORM software. From the literature, 2D finite element model tool wear can be found in (Attanasio, Ceretti, Giardini, Filice, & Umbrello, 2008; Xie, Schmidt, Schmidt, & Biesinger, 2005) at orthogonal cutting conditions. The primary failure occurs during turning operation are (flank

wear, crater wear, plastic deformation). The effect heating temperature of chip formation and cutting forces on machining of Inconel 718 was reported (A.K. Parida & Maity, 2016a) using finite element analysis. They concluded that a numerical model was in good agreement with the experimental results. In another study (Xing, 2010) analyzed the comparison of numerical model and analytical model in the hot turning of Inconel 718. Flank wear and material removal rate were predicted by (Yadav, Abhishek, & Mahapatra, 2015) in machining of Inconel 718. The effect of rake angle, feed rate on cutting force were studied by (Lungu & Borzan, 2012) using FEM analysis. Hua et al. (Hua & Shivpuri, 2005) analyzed the tool wear model in machining of Ti alloys using cobalt diffusion model. It was observed that the chip contact length decreases with the decrease of cutting velocity whereas, it increases with the increase of temperature and velocity. The wear of coated tool in machining of aluminum was studied (Maheshwera, Paturi, Kumar, & Narala, 2015). Using 2D finite element simulation Kagnaya et al. (Kagnaya, Lambert, Lazard, Boher, & Cutard, 2014) studied the effect of wear on cutting force and temperature in machining of AISI 1045 steel. The effect of tribological behavior of interface of tool and chip in machining of steel on tool wear were analyzed by Haddag et al. (Haddag, Nouari, Barlier, & Dhers, 2014). Mathew et al. (Kuttolamadom, 2012) analyzed the diffusive term which is associated with the wear model in machining. The other wear models like abrasive will disappear when the temperature exceeds some specified limit. Parida and Maity (Asit Kumar Parida & Maity, 2016) studied the effect of nose radius on process parameters and cutting force in hot machining of nickel base alloys. They found that increase in temperature reduced the cutting force and increased the chip tool contact length.

Though many numerical modeling has been implemented in machining to predict some factors of cutting force, residual stress, tool wear, etc., no attention has been paid to modeling and simulation of tool wear in hot machining yet. So, the present study focuses on the prediction of tool wear and tool temperature associated with the heating and room temperature machining conditions. Heat exchange window was used to model the heat source in simulation and its effect on tool temperature, tool wear and cutting force in the simulation process.

## **EXPERIMENTAL ASPECTS**

The machining tests were conducted on a center lathe machine with the spindle speed range from 88 to 1200 rpm. Inconel 718 is a nickel base alloy which is very difficult to machine due to low thermal conductivity, the presence of hard particles in the microstructure and tendency to weld with all cutting tool. This is the reason a cylindrical Inconel 718 round bar has been taken as workpiece material with a diameter of 50 mm, and length 150 mm. The cutting tool is a square uncoated insert, of a WC-Co material (6% cobalt binder phase, cemented tungsten carbide), specified by SNMG1204008-TTS. Flame heating was utilized for heating the workpiece, and  $k$ -type of the thermocouple was used to measure the temperature of the workpiece surface. Tool wear was measured with the help of an optical microscope. The experimental setup and tool microscope is illustrated in Figure 1. The cutting conditions were performed using three values of cutting speeds (40, 60, 100 m/min), and two values of heating temperatures (300°C, 600°C) and keeping feed and depth of cut constant. Nine experimental tests have been carried out with different cutting parameters along with heating temperature, and the cutting parameters are tabulated in Table 1.

Figure 1. Experimental setup for hot machining [a] Optical tool maker microscope [b]

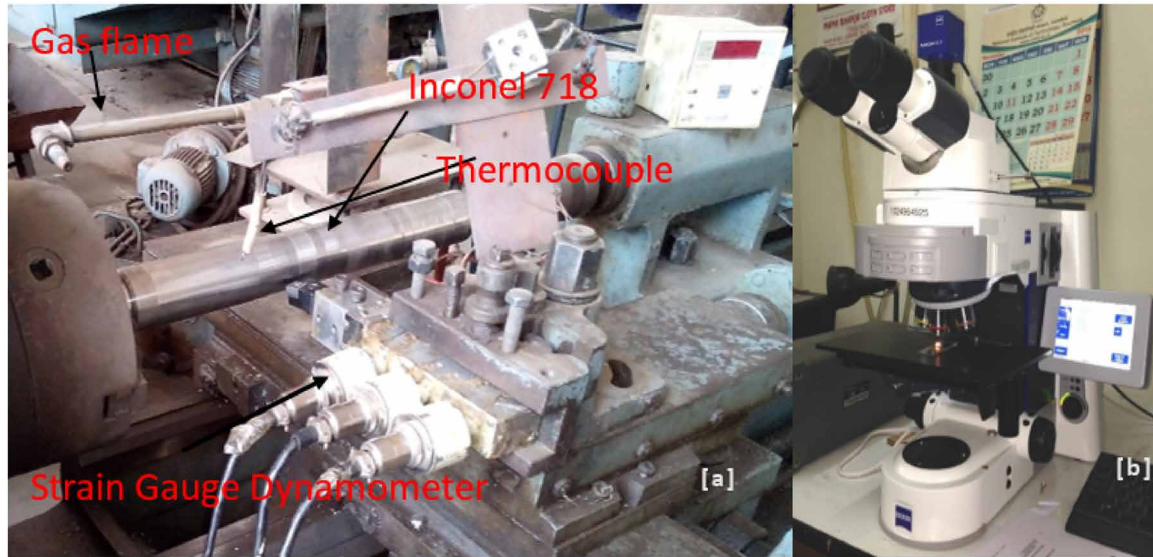


Table 1. Experimental test and cutting conditions

Test ID	1	2	3	4	5	6	7	8	9
Cutting speed[m/min]	40	40	40	60	60	60	100	100	100
Temperature [°C]	30	300	600	30	300	600	30	300	600

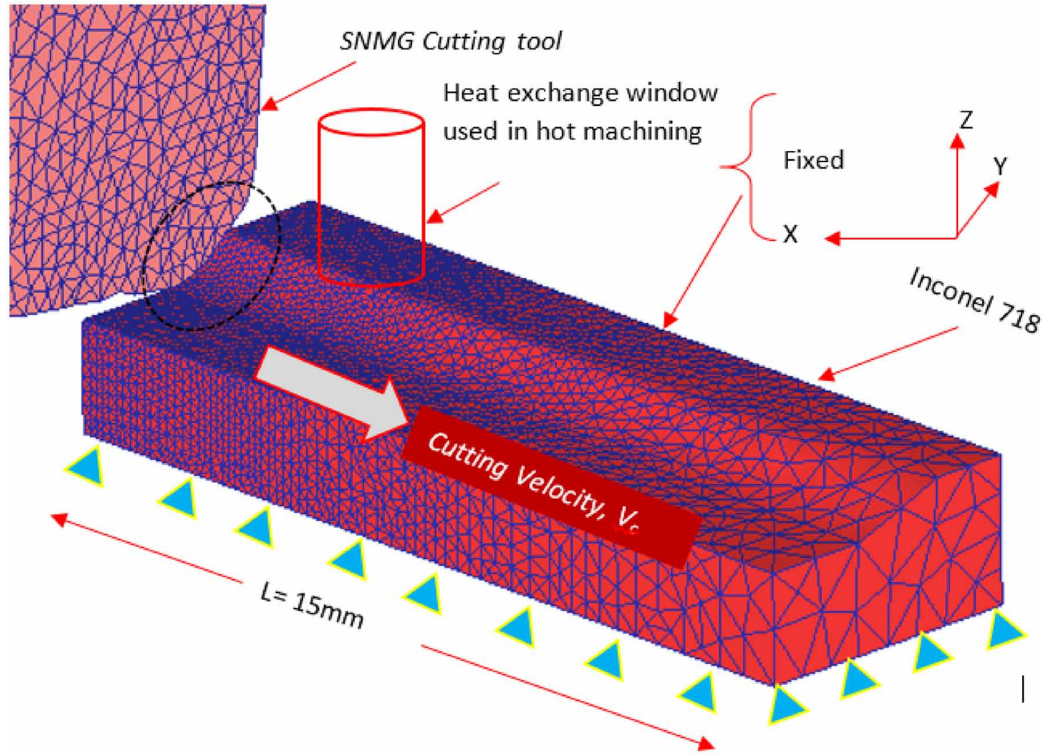
## FINITE ELEMENT MACHINING SIMULATION

A thermo-mechanical finite element model was used, in order to predict the effect of preheating on tool wear with the help of DEFORM software. DEFORM 3D is based on the implicit lagrangian computational routine. Adaptive meshing was used for chip formation. The upper surface of the workpiece is free to deform whereas the bottom surface was fixed. A high-density mesh window has been defined near the cutting area for owing to large gradients of strain, strain rate, and temperature compared to another area.

The workpiece of Inconel 718 is assumed to homogeneous plastic, and Johnson-cook model has been implemented and mesh range model around 30,000 four-node elements. The tool was modelled with 10,000 elements. The material properties of workpiece and tool material were exerted from DEFORM library. There are two types of boundary conditions have been used to represent real cutting conditions. The bottom face of the workpiece is fixed and the tool will move in cutting velocity direction as per mechanical boundary condition, whereas in thermal boundary condition initial temperature configuration is reference room or ambient temperature is imposed to the workpiece.

Johnson-cook constitutive model has been utilized for flow stress of Inconel 718 in hot turning operation as shown in (Eq.1) (Asit Kumar Parida, 2017).

Figure 2. Boundary conditions and schematic representation of the model



$$\sigma = \left( A + B \varepsilon_p^n \right) \left( 1 + C \ln \left( \frac{\dot{\varepsilon}}{\dot{\varepsilon}_0} \right) \right) \left( 1 - \left( \frac{T - T_{room}}{T_{melt} - T_{room}} \right)^m \right) \quad (1)$$

where  $\sigma$  is the equivalent flow stress,  $\varepsilon_p$  is the equivalent plastic strain,  $\dot{\varepsilon}$  and  $\dot{\varepsilon}_0$  are the strain rate and reference plastic strain rate.  $T_{melt}$  and  $T_{room}$  are the melting ( $^{\circ}\text{C}$ ) and room temperature ( $30^{\circ}\text{C}$ ). In the above equation, the parameters  $A$ ,  $B$ ,  $C$ ,  $n$ , and  $m$  are the Johnson-cook constants,  $T_{room}$  is room temperature,  $T_{melt}$  is melting temperature. The Johnson-cook material constant is tabulated in Table 2.

In the present work, shear friction model was utilized to model the friction in the tool-workpiece contact (Eq. 2).

$$\tau = mk \quad (2)$$

where  $m$  is the constant shear friction factor and  $k$  is the shear flow stress on the material at the chip-tool interface (Asit Kumar Parida & Maity, 2017).



*Table 2. Inconel 718 material constants for Johnson-cook model(Uhlmann, Von Der Schulenburg, & Zettier, 2007)*

Material	A(MPa)	B(MPa)	C	n	m	$\dot{\epsilon}_0$ (1/s)
Inconel 718	450	1700	0.017	0.65	1.3	0.001

In hot machining, a heat exchange window is defined to exchange heat between the tool and the workpiece is available in the DEFORM-3D software. This heat exchange window moves on the workpiece. The environment temperature was kept room temperature except for the area of the cylinder, which was defined corresponding heating temperature. The heat exchange from the heat source to the workpiece can be expressed as in (Eq.3).

$$Q = hA(T_{Window} - T_{workpiece}) \quad (3)$$

where  $T_{Workpiece}$  and  $T_{window}$  are the temperature of workpiece and window respectively.  $A$  is the surface area of the cylinder (heat exchange window), and  $h$  is the heat transfer coefficient.

Different tool wear models have been studied in the literature (Lotfi, Jahanbakhsh, & Akhavan Farid, 2016; Y.-C. Yen, Söhner, Lilly, & Altan, 2004; Yue, Liu, Pen, Hu, & Zhao, 2009). In the present work, Usui's tool wear model has been implemented to calculate the tool wear as (Eq.4).

$$w = \int a.p.V.e^{-b/T} dt \quad (4)$$

Where  $V$  is the sliding velocity,  $P$  is the normal pressure,  $T$  is the temperature.  $a$ , and  $b$  are the constant parameter, and these parameters are valid in the range cutting parameter selected in the experiment and might need change for an accurate result.

The measurement of tool wear is in experiment and simulation as shown in Figure 3. The flow chart of tool wear calculation in hot machining is shown in Figure 4.

## RESULTS AND DISCUSSION

The finite element modeling was validated by comparing the numerical tool wears with the experimental ones. The flank wear, temperature at the rake face of the tool, chip thickness were also calculated and compared with experimental results.

### Effect of Preheating Temperature on Tool rake Face Temperature

It was found that the temperature on the rake face of the tool decreases with the increase of heating temperature. At room temperature, the maximum temperature on the rake face of the tool was 385°C,

Figure 3. Measurement of tool wears in the experiment and numerical modeling

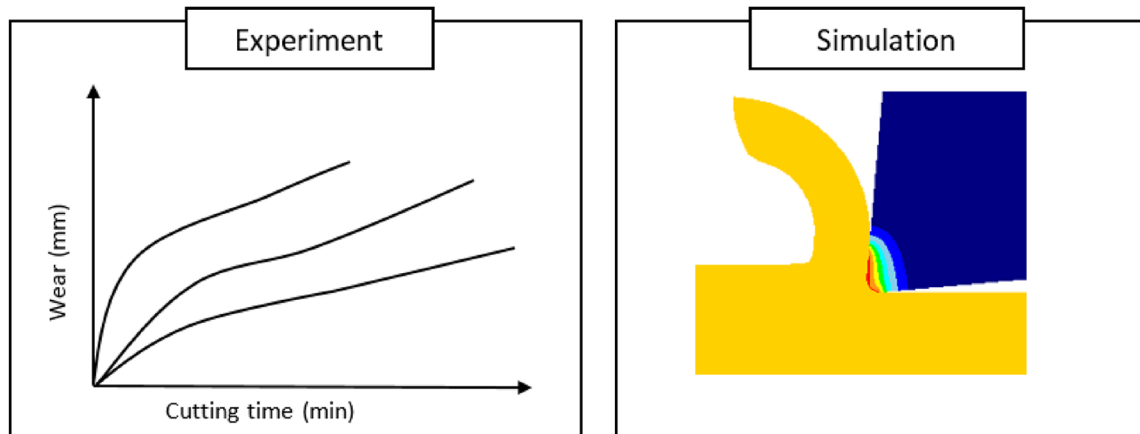
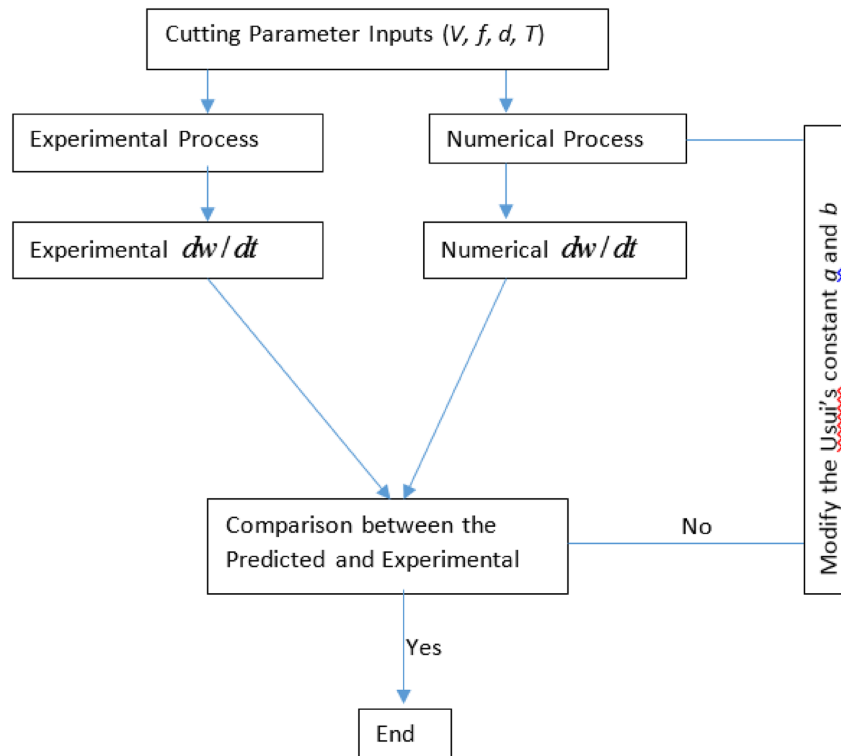
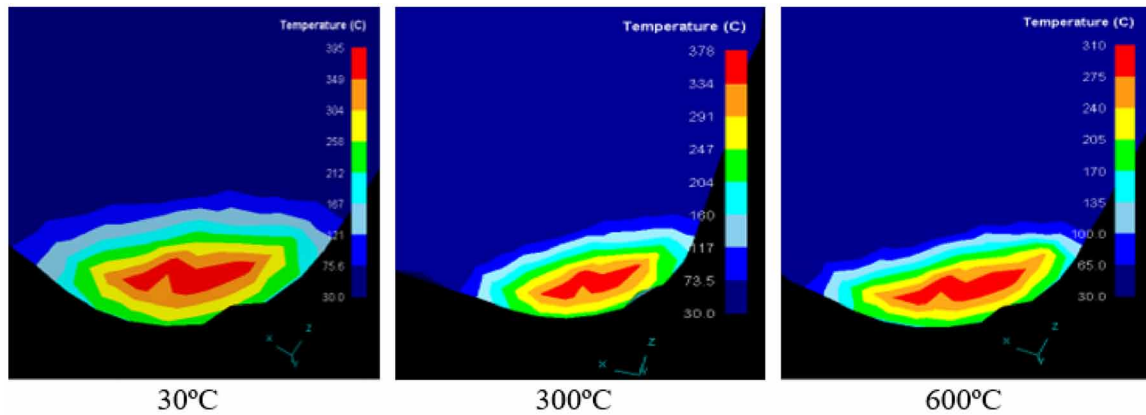


Figure 4. Determination of tool wear model



whereas at 300°C heating it reduced to 387°C and increasing the heating temperature 600°C the rake face temperature 310°C. The process zone temperature increased with the increase of heating temperature which reduces the heat generation due to plastic deformation during machining. Thus temperature distribution on the rake face of the tool decreased with the rise of heating temperature, hence tool wear. The temperature distribution on the rake face of the tool at a different temperature is shown in Figure 5.

*Figure 5. The temperature of the cutting tool at a different heating temperature*

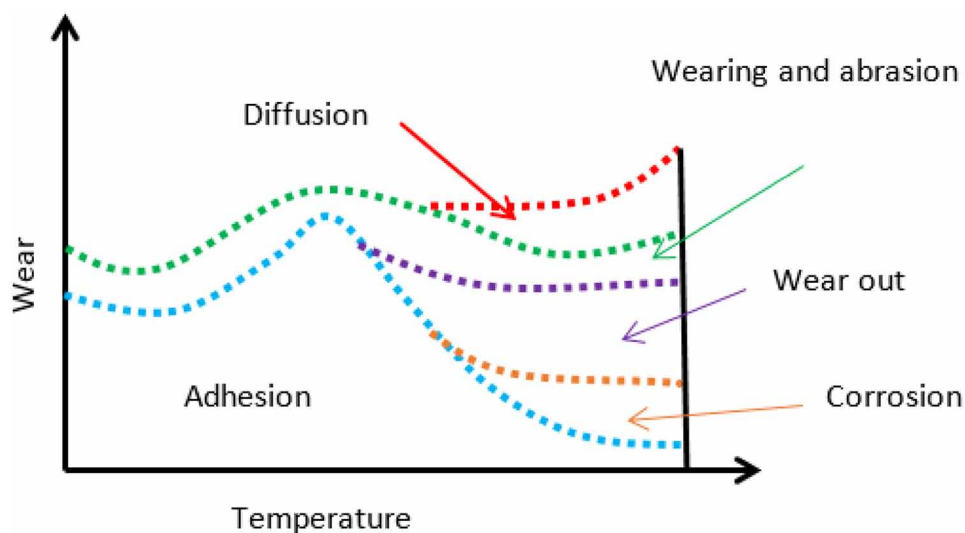


*\*For a more accurate representation see the electronic version.*

### **Effect of Preheating Temperature on Tool Wear and Chip Formation**

Since the numerical cutting time in the finite element modeling is very short, a qualitative prediction of tool wear is sufficient to highlight the localization zones of wears. It is precisely shown that variation of FE prediction and optical microscope observation is a close correspondence. During the contact zones, the temperature and tool wear rate were predicted, which explains the diffusion of the cutting tool material on the rake face. It was observed that at room temperature, abrasion wear more dominant whereas an increase of heating temperature to 600°C diffusion wear is dominant. The effect of temperature on tool wear at a different temperature is shown in Figure 6.

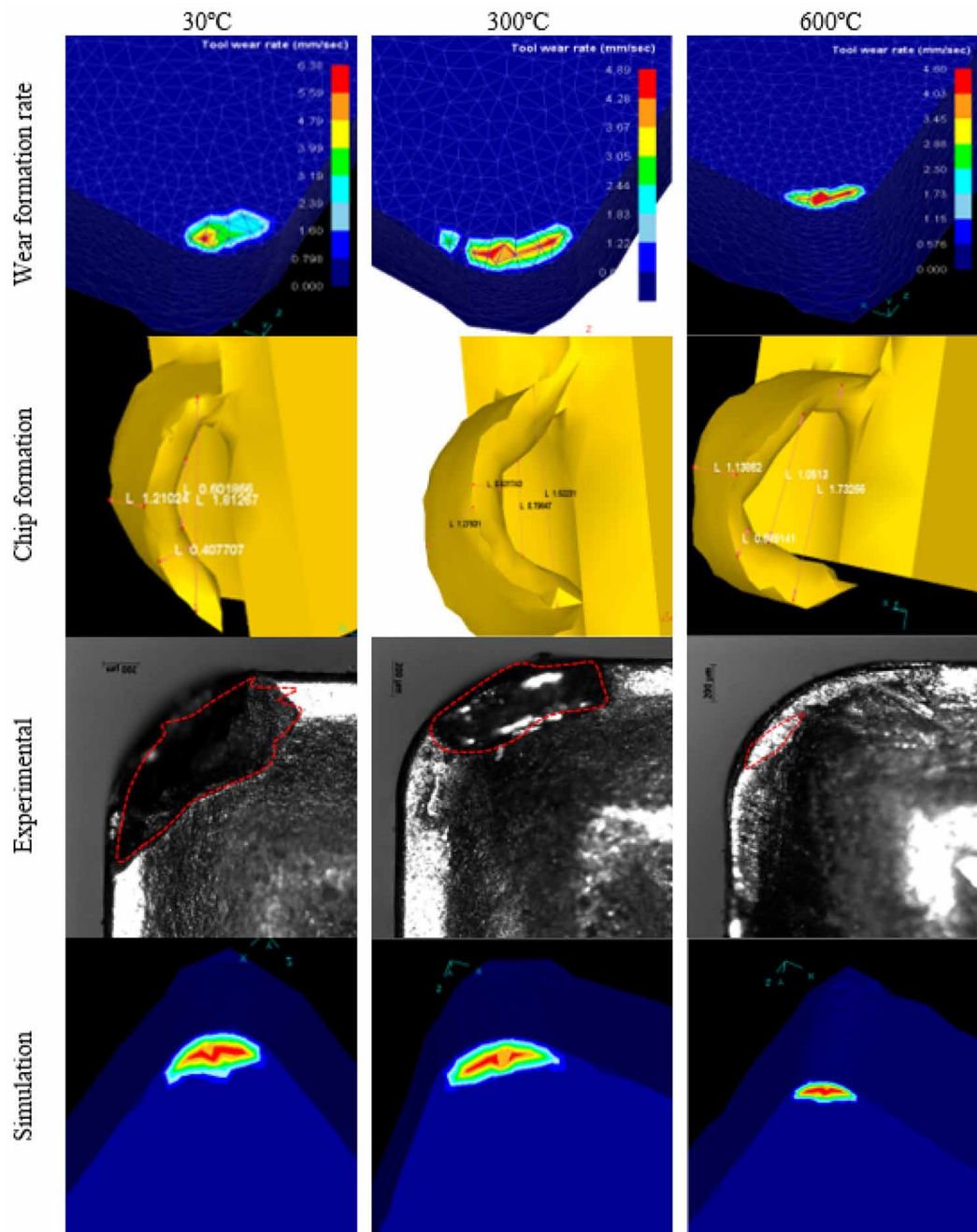
*Figure 6. Tool wear with respect to temperature(Baili, Wagner, Dessein, Sallaberry, & Lallement, 2011)*



*\*For a more accurate representation see the electronic version.*

The tool wear rate decreased with the increase of heating temperature due to the reduction of shear strength of the workpiece and formation of the chip is more continuous compared to room temperature due to ductile nature of workpiece. Tool wear rate, chip formation, and tool wear in experiment and simulation (Figure 7). It was observed that the tool wear formed at room temperature is due friction contact between tool and workpiece. Adhesion wear is the most dominant type of tool wear whereas at

Figure 7. Tool wear formation in experimental and simulation process



\*For a more accurate representation see the electronic version.

heating conditions, not an only workpiece is subjected to heating but also cutting tool affected by heat. So, at heating conditions, some portion of cobalt diffuse from the cutting tool and form wear. This is the type of wear is called diffusion wear and more dominant in high-temperature machining conditions. So, it is necessary to the application of optimum heating condition during thermally enhanced machining condition, in order to avoid this type of wear. From the Figure 7 it is clearly shown that the wear formation at a heating temperature of 600°C is less compared to 30°C room temperature machining condition. The flank wears were measured at different cutting speed in both room and heating conditions, and there was good agreement between the simulation results with the experimental values as shown in Figure 9 [a-c]. Similarly, the tool rake face temperature was compared with the experimental result at different cutting speed, and good correlation was obtained as shown in Figure 10 [a-c].

The chip produced in simulation and experimentally (Figure 10). It was observed that the chip thickness predicted numerically overestimated at room temperature whereas underestimate at 300°C and 600°C heating temperature. The error % variation between the numerical and experiment was 10%, 2% and 10% at 30°C, 300°C, and 600°C respectively as shown in Figure 11. The total comparison of numerical and experimental calculation of temperature, chip thickness, and tool wear is tabulated in Table 3, and corresponding error% is also mentioned.

## CONCLUSION

3D FE model has been applied in hot machining of Inconel 718 using flame heating. The approach is using DEFORM-3D simulation software to calculate tool wear using Usui's based wear model in both room and heating temperature conditions. The heating was done by combination oxygen and liquefied petroleum gas. Experimental work has been done same as simulation input parameters in order to validate the simulation results. From the results, the following point may be drawn.

*Figure 8. Adhesion and diffusion wear formation at room and heating condition at cutting speed of 100 m/min*

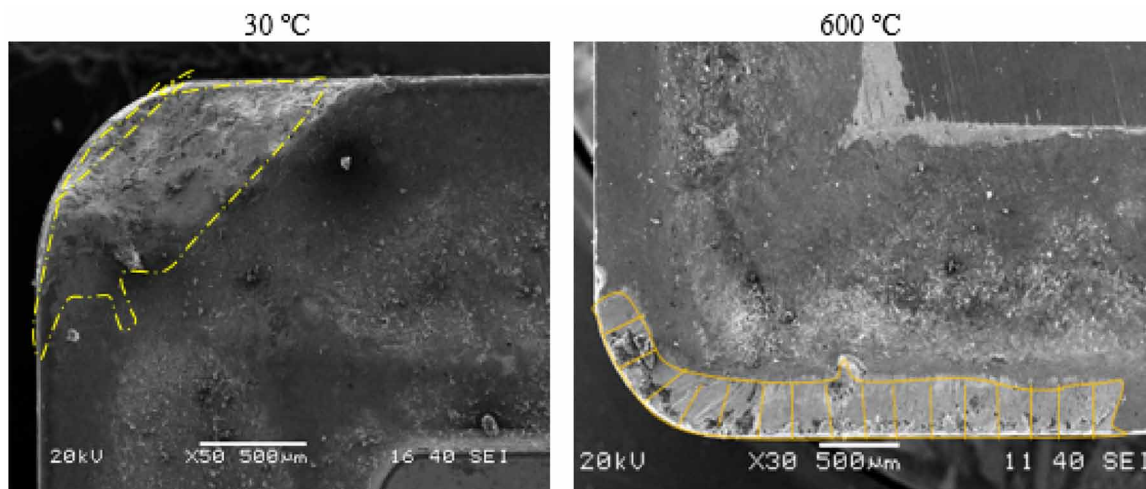


Figure 9. Flank wear vs heating temperature [a]  $V=40$  m/min [b]  $V=60$  m/min [c]  $V=100$  m/min

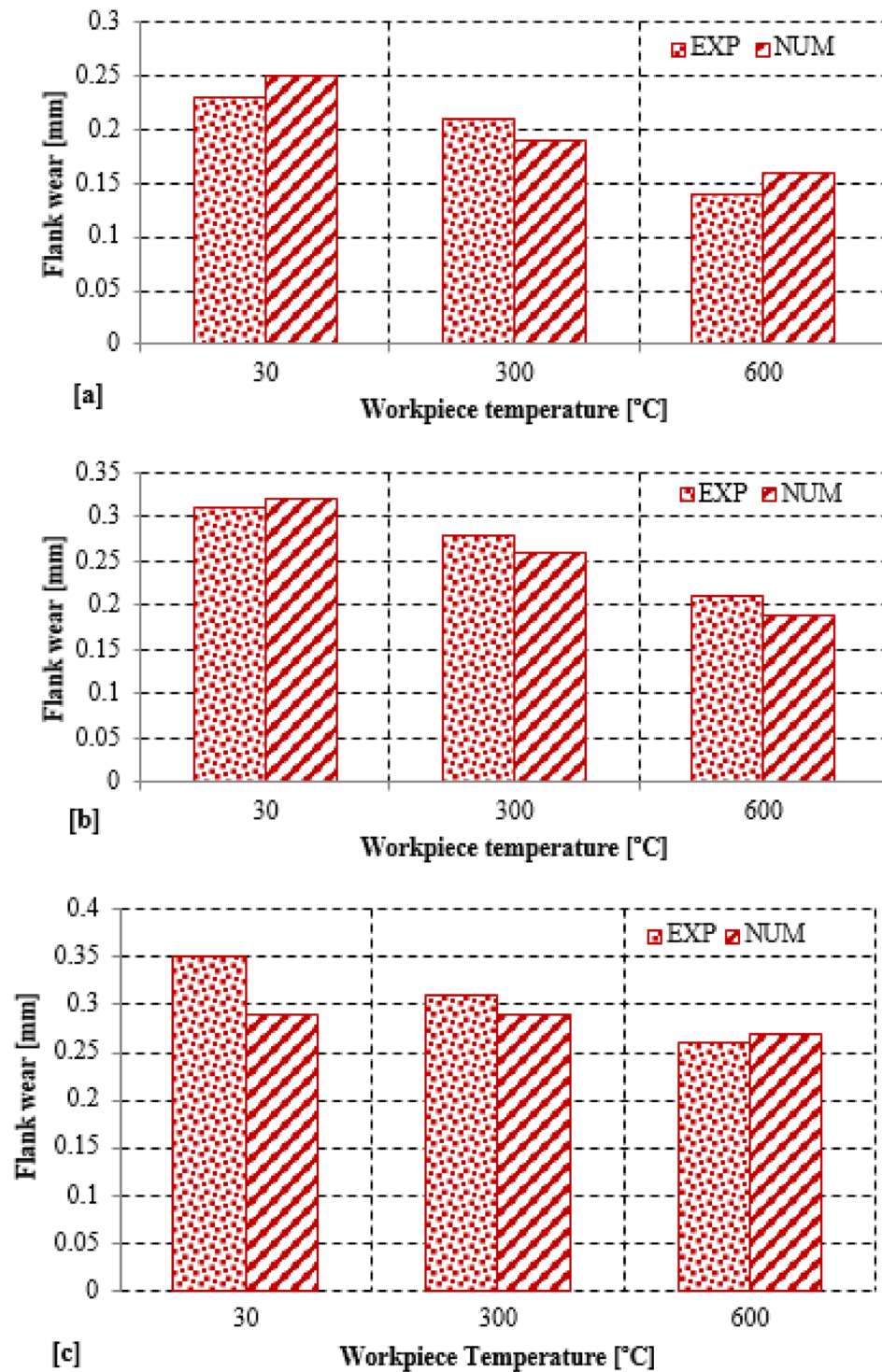




Figure 10. Max Tool temp. vs Heating temp. [a]  $V=40$  m/min [b]  $V=60$  m/min [c]  $V=100$  m/min

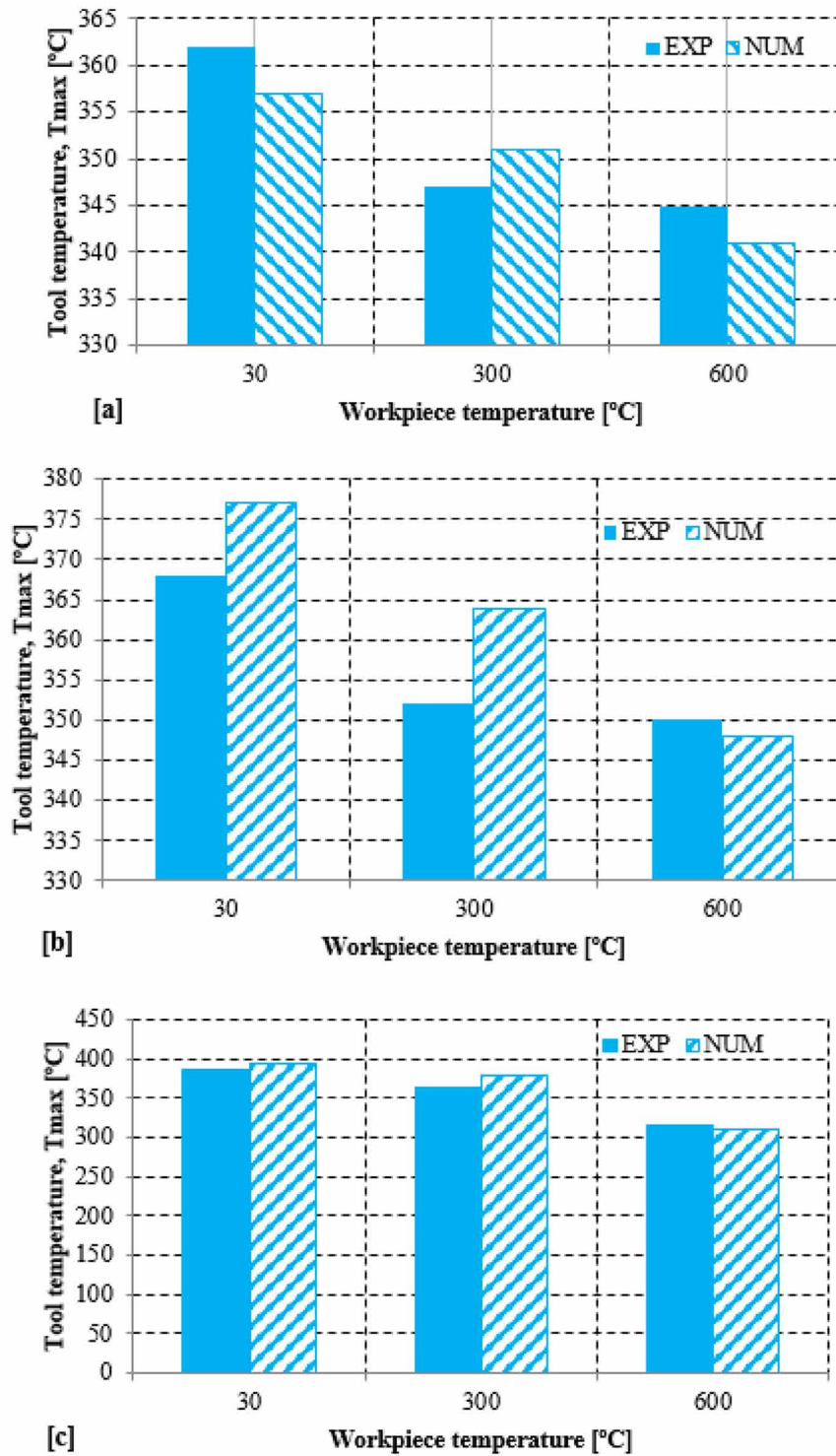


Figure 11. Numerical and Experimental chip thickness

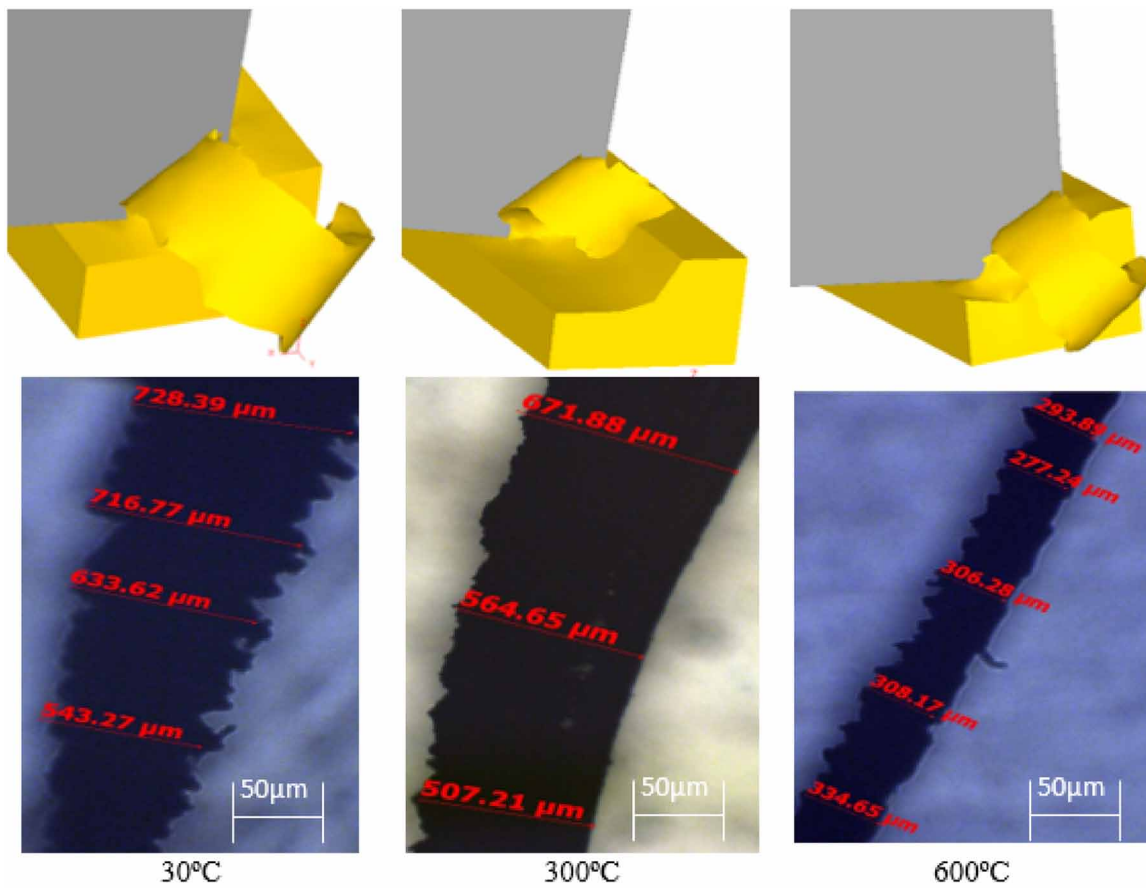
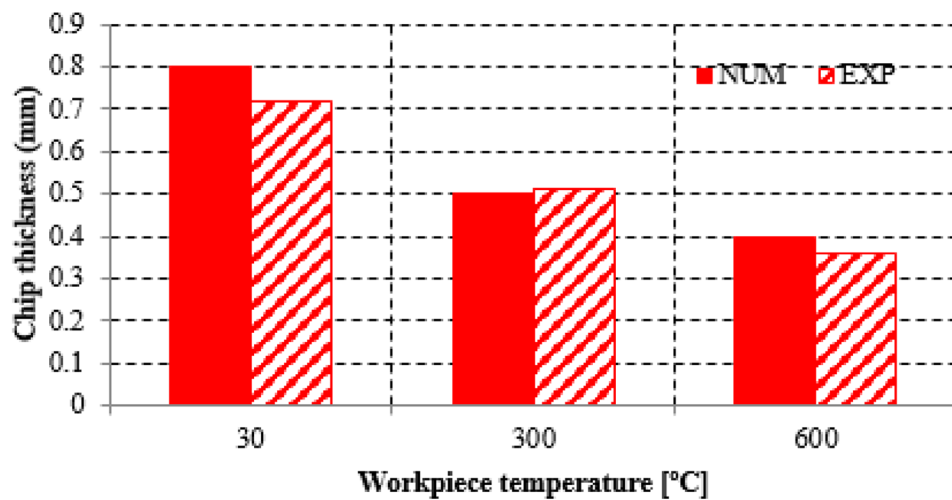


Figure 12. Chip thickness variation at a different heating temperature between numerical and experiment





## Finite Element Analysis of Tool Wear in Hot Machining Process

Table 3. Error % measurement of variables

Test ID	Comparison	Temperature	Chip thickness	Tool wear
1	NUM	357	0.72	0.25
	EXP	362	0.80	0.23
	Err%	-1.42	-11.11	8
2	NUM	351	0.51	0.19
	EXP	347	0.50	0.21
	Err%	1.13	-2	-10.52
3	NUM	341	0.36	0.16
	EXP	345	0.41	0.14
	Err%	-1.17	-13.88	12.5
4	NUM	377	0.67	0.32
	EXP	368	0.65	0.31
	Err%	2.38	29.85	3.125
5	NUM	364	0.49	0.26
	EXP	352	0.53	0.28
	Err%	3.29	-8.16	-7.69
6	NUM	348	0.43	0.19
	EXP	350	0.48	0.21
	Err%	-0.57	-11.62	-10.52
7	NUM	395	0.62	0.29
	EXP	386	0.68	0.35
	Err%	2.27	-9.67	-20.68
8.	NUM	378	0.58	0.29
	EXP	363	0.65	0.31
	Err%	4.02	-12.06	-6.89
9	NUM	310	0.54	0.27
	EXP	314	0.61	0.26
	Err%	-1.29	-12.96	1

The maximum variation (<10%) of tool wear between the experiment and simulation was found at Test ID 2, 3, 6 and 7.

- The tool wear value decreased with the increase of heating temperature from room temperature to 600°C temperature. But it increased with the increase of cutting speed in both room and heating conditions.
- A good agreement between predicated and experimental values was found with maximum error % 20 (EXP-7). This may due to choosing of accurate Usui's constant and accurateness of results is mostly depending upon these two parameters.
- Tool rake face temperature value decreased with the increase of heating temperature compares to room temperature. This is due to the application of heating on the workpiece makes soften the

surface, hence reduce the tool stress and force. With the increase of cutting speed, the tool temperature again decreases because at higher cutting the temperature generator at the process zone is higher which reduce the heat generation due to plastic deformation during machining.

- The chip thickness value decreased with the increased of heating temperature compared to room temperature due to softening of material during heating conditions.

## REFERENCES

- Attanasio, A., Ceretti, E., Giardini, C., Filice, L., & Umbrello, D. (2008). Criterion to evaluate diffusive wear in 3D simulations when turning AISI 1045 steel. *International Journal of Material Forming*, 1(S1), 495–498. doi:10.1007/12289-008-0130-0
- Baili, M., Wagner, V., Dessein, G., Sallaberry, J., & Lallement, D. (2011). An Experimental Investigation of Hot Machining with Induction to Improve Ti-5553 Machinability. *Applied Mechanics and Materials*, 62, 67–76. . doi:10.4028/www.scientific.net/AMM.62.67
- Dogra, M., Sharma, V., Sachdeva, A., & Suri, N. (2012). Tool life and surface integrity issues in continuous and interrupted finish hard turning with coated carbide and CBN tools. *Proceedings of the Institution of Mechanical Engineers. Part B, Journal of Engineering Manufacture*, 226(3), 431–444. doi:10.1177/0954405411418589
- Ducobu, F., Arrazola, P.-J., Rivière-Lorphèvre, E., & Filippi, E. (2015). Finite Element Prediction of the Tool Wear Influence in Ti6Al4V Machining. *Procedia CIRP*, 31, 124–129. doi:10.1016/j.procir.2015.03.056
- Ezugwu, E. O. (2005). Key improvements in the machining of difficult-to-cut aerospace superalloys. *International Journal of Machine Tools & Manufacture*, 45(12–13), 1353–1367. doi:10.1016/j.ijmach-tools.2005.02.003
- Haddag, B., & Nouari, M. (2013). Tool wear and heat transfer analyses in dry machining based on multi-steps numerical modelling and experimental validation. *Wear*, 302(1–2), 1158–1170. doi:10.1016/j.wear.2013.01.028
- Haddag, B., Nouari, M., Barlier, C., & Dhers, J. (2014). Experimental and numerical analyses of the tool wear in rough turning of large dimensions components of nuclear power plants. *Wear*, 312(1–2), 40–50. doi:10.1016/j.wear.2014.02.005
- Hu, H. J., & Huang, W. J. (2014). Tool life models of nano ceramic tool for turning hard steel based on FEM simulation and experiments. *Ceramics International*, 40(7), 8987–8996. doi:10.1016/j.ceramint.2014.01.095
- Hua, J., & Shivpuri, R. (2005). A Cobalt diffusion based model for predicting crater wear of carbide tools in machining titanium alloys. *Journal of Engineering Materials and Technology*, 127(1), 136. doi:10.1115/1.1839192
- Kagnaya, T., Lambert, L., Lazard, M., Boher, C., & Cutard, T. (2014). Investigation and FEA-based simulation of tool wear geometry and metal oxide effect on cutting process variables. *Simulation Modelling Practice and Theory*, 42, 84–97. doi:10.1016/j.simpat.2013.12.009

- Kuttolamadom, M. (2012). *Prediction of the wear & evolution of cutting tools in a carbide / Ti-6Al-4V machining tribosystem by volumetric tool wear*. Academic Press.
- Li, Z. L., Zheng, H. Y., Lim, G. C., Chu, P. L., & Li, L. (2010). Study on UV laser machining quality of carbon fibre reinforced composites. *Composites. Part A, Applied Science and Manufacturing*, 41(10), 1403–1408. doi:10.1016/j.compositesa.2010.05.017
- Lotfi, M., Jahanbakhsh, M., & Akhavan Farid, A. (2016). Wear estimation of ceramic and coated carbide tools in turning of Inconel 625: 3D FE analysis. *Tribology International*, 99, 107–116. doi:10.1016/j.triboint.2016.03.008
- Lungu, N., & Borzan, M. (2012). *Effect of cutting speed and feed rate on tool geometry, temperature and cutting forces in machining Aisi 1045 carbon steel using FEMsimulation*. Academic Press.
- Maheshwera, U., Paturi, R., Kumar, S., & Narala, R. (2015). Finite element analysis and study of tool wear in machining with coated tool. *Imece2013-64342*.
- Maity, K. P., & Swain, P. K. (2008). An experimental investigation of hot-machining to predict tool life. *Journal of Materials Processing Technology*, 198(1–3), 344–349. doi:10.1016/j.jmatprotec.2007.07.018
- Oliaei, S. N. B., & Karpas, Y. (2016). Investigating the influence of built-up edge on forces and surface roughness in micro scale orthogonal machining of titanium alloy Ti6Al4V. *Journal of Materials Processing Technology*, 235, 28–40. doi:10.1016/j.jmatprotec.2016.04.010
- Özel, T. (2009). Computational modelling of 3D turning: Influence of edge micro-geometry on forces, stresses, friction and tool wear in PcBN tooling. *Journal of Materials Processing Technology*, 209(11), 5167–5177. doi:10.1016/j.jmatprotec.2009.03.002
- Parida A. K., (2010). Analytical and numerical modeling of hot machining of Inconel. *American Journal of Mechanical and Materials Engineering*, 71(8), 49–57. 10.11648/j.ajmme.20170104.11
- Parida, A. K. (2017). *Heat assisted machining of nickel base alloys: Experimental and numerical analysis*. PhD Thesis.
- Parida, A. K. (2018). Analysis of chip geometry in hot machining of Inconel 718 Alloy. *Iranian Journal of Science and Technology. Transaction of Mechanical Engineering*. doi:10.100740997-018-0146-0
- Parida, A. K., & Maity, K. (2017). Effect of nose radius on forces, and process parameters in hot machining of Inconel 718 using finite element analysis. *Engineering Science and Technology, an International Journal*, 4–10. 10.1016/j.jestch.2016.10.006
- Parida, A. K., & Maity, K. P. (2016). Finite element method and experimental investigation of hot turning of Inconel 718. *Advanced Engineering Forum*.
- Parida, A. K., & Maity, K. P. (2016). Optimization in hot turning of nickel based alloy using desirability function analysis. *International Journal of Engineering Research in Africa*, 24, 64–70. . doi:10.4028/www.scientific.net/JERA.24.64

- Parida, A. K., & Maity, K. P. (2016). Optimization of multi-responses in hot turning of Inconel 625 alloy using DEA-Taguchi approach. *International Journal of Engineering Research in Africa*, 24, 57–63. . doi:10.4028/www.scientific.net/JERA.24.57
- Pervaiz, S. (2015). *Numerical and experimental investigations of the machinability of Ti6Al4V*. PhD Thesis.
- Ranganathan, S., Senthilvelan, T., & Sriram, G. (2010). Evaluation of machining parameters of hot turning of stainless steel (Type 316) by applying ANN and RSM. *Materials and Manufacturing Processes*, 25(10), 1131–1141. doi:10.1080/10426914.2010.489790
- Shanmugam, D. K., Chen, F. L., Siores, E., & Brandt, M. (2002). Comparative study of jetting machining technologies over laser machining technology for cutting composite materials. *Composite Structures*, 57(1–4), 289–296. doi:10.1016/S0263-8223(02)00096-X
- Thandra, S. K., & Choudhury, S. K. (2010). Effect of cutting parameters on cutting force, surface finish and tool wear in hot machining. *International Journal of Machining and Machinability of Materials*, 7(3/4), 278. doi:10.1504/IJMMM.2010.033070
- Tosun, N. (2002). A study of tool life in hot machining using artificial neural networks and regression analysis method. *Journal of Materials Processing Technology*, 124, 99–104.
- Tosun, N., & Ozler, L. (2004). Optimisation for hot turning operations with multiple performance characteristics. *International Journal of Advanced Manufacturing Technology*, 23(11–12), 777–782. doi:10.100700170-003-1672-4
- Uhlmann, E., Von Der Schulenburg, M. G., & Zettier, R. (2007). Finite element modeling and cutting simulation of inconel 718. *CIRP Annals - Manufacturing Technology*, 56(1), 61–64. 10.1016/j.cirp.2007.05.017
- Usui, E., Shirakashi, T., & Kitagawa, T. (1978). Analytical prediction of three dimensional cutting Process—Part 3: Cutting temperature and crater wear of carbide tool. *Journal of Manufacturing Science and Engineering*, 100(2), 236–243. doi:10.1115/1.3439415
- Xie, L. J., Schmidt, J., Schmidt, C., & Biesinger, F. (2005). 2D FEM estimate of tool wear in turning operation. *Wear*, 258(10), 1479–1490. doi:10.1016/j.wear.2004.11.004
- Yadav, R. K., Abhishek, K., & Mahapatra, S. S. (2015). A simulation approach for estimating flank wear and material removal rate in turning of Inconel 718. *Simulation Modelling Practice and Theory*, 52, 1–14. doi:10.1016/j.simpat.2014.12.004
- Yen, Y.-C., Söhner, J., Lilly, B., & Altan, T. (2004). Estimation of tool wear in orthogonal cutting using the finite element analysis. *Journal of Materials Processing Technology*, 146(1), 82–91. doi:10.1016/S0924-0136(03)00847-1
- Yue, C. X., Liu, X. L., Pen, H. M., Hu, J. S., & Zhao, X. F. (2009). 2D FEM estimate of tool wear in hard cutting operation: Extractive of interrelated parameters and tool wear simulation result. *Advanced Materials Research*, 69–70, 316–321. . doi:10.4028/www.scientific.net/AMR.69-70.316

## Chapter 12

# FEM–ANN Sequential Modelling of Laser Transmission Welding for Prediction of Weld Pool Dimensions

**Bappa Acherjee**  
*Birla Institute of Technology, India*

### ABSTRACT

*In this chapter, a sequential modeling approach has been applied for modeling of laser transmission welding process using finite element method (FEM) and artificial neural network (ANN) technique to predict the weld pool dimensions in a shorter time frame. The scripting language, APDL (ANSYS® Parametric Design Language), is used to develop the three-dimensional FE model. During preprocessing, all the major physical phenomena of laser transmission welding process are incorporated into the model physics. Based on the temperature field predicted by the model, the weld pool dimensions (i.e., weld width and weld penetration depth) are calculated. The weld dimensions predicted by the developed FE model are further used for training a neural network model. It is found from the results of test data sets that the developed ANN model can predict the outputs with significant accuracy and takes less prediction time, which in turn saves time, cost, and the efforts for performing experiments.*

### INTRODUCTION

Plastics are being fastest growing basic materials and the joining techniques of plastics are playing a significant role for manufacturing plastic components in a cost effective way. Plastics can be joined using mechanical fasteners, adhesives or by welding. As the use of plastic components become more widespread, joining techniques play an important role in their processing. Since making the complex plastic components in one piece is not always practical and cost effective, various joining techniques have been developed including plastic adhesive joining, mechanical fastening and welding. The general advantages of welding techniques over other joining techniques are the fast and easy processing, tightness of the joint and high

DOI: 10.4018/978-1-5225-6161-3.ch012

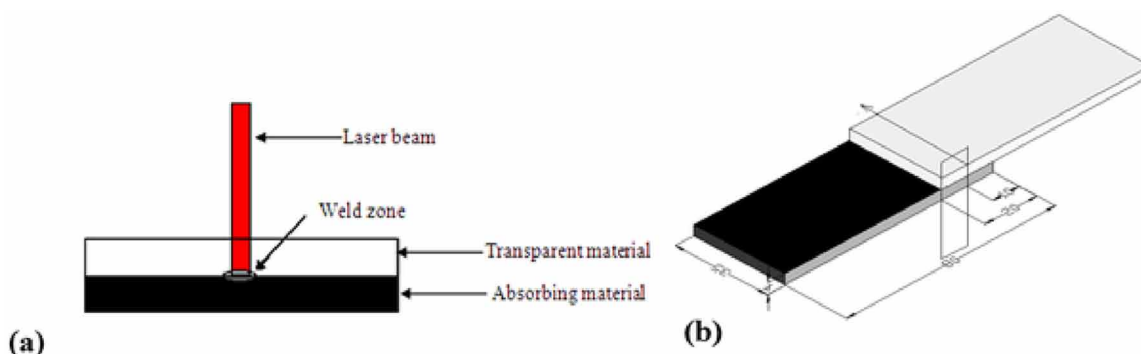
strength. The most widely used plastic welding procedures are heated tool welding, ultrasonic welding and vibration welding. In the case of heated tool welding, residues and contamination on the surface of the heated tool can lead to an undefined strength of the weld seam. Also, the fluff development in the ultrasonic welding is still a problem (Herfurth *et al.*, 1999; Bonten & Tüchert, 2002).

In this context, more favorable presupposition is offered by heating of infra-red radiation, because the heat is transmitted without any contact to the plastic parts. Infra-red radiation can be transmitted by infra-red lamps and also by infra-red lasers. Laser can be used in two general ways: (i) irradiating the surfaces to be joined directly or (ii) passing through one transparent material and directly heating only the second material, precisely at the mating surface. This later process, described as laser transmission welding is providing to be very attractive as clean, precise and flexible process for joining plastic surfaces, even of dissimilar plastics (Baylis, 2002). With this technique melt is only created where it is needed, in the joining area of the both partners, reducing the energy input to a minimum (Hansch *et al.*, 1998). This technique is capable of producing an aesthetically perfect joint with qualitatively sound joint strength. This technique is used to weld thermoplastics and thermoplastic elastomers, as the thermoses can not be remelted.

During laser transmission welding, the laser beam is focused at two overlying thermoplastic plaques, among which the top plastic part is transparent to the laser radiation and the bottom part is to be absorbent of that radiation. The laser energy transmitted through the transparent part is absorbed over a certain depth of the bottom opaque part, and the absorbed laser energy is converted into heat. The heat produced in the bottom part is transferred to the top plastic part; subsequently, interfacial layers of both the plastic parts are melted, which results in a firm joint at weld interface after cooling, as weld seam (Acherjee *et al.*, 2015). Natural thermoplastics have a high transmittance in the wavelength range of 0.8 - 1.1  $\mu\text{m}$ , and thus, the diode lasers, Nd:YAG lasers and fiber lasers are used for the laser transmission welding process, as they are operated at this wavelength range. Figure 1 (a) shows the operational principle of the laser transmission welding process. The isometric view of the sample that is used for the present study is shown in Figure 1. (b).

Different laser types have been used for laser transmission welding of plastics. Since most plastics strongly absorb at 10.6 $\mu\text{m}$ , CO<sub>2</sub> lasers are restricted to thin plastic films joining. By contrast, the Nd:YAG laser and diode laser are well suited for thick part welding due to high transmission of polymers in the near-infrared field. The compact design, modular set-up and high efficiency of diode laser make them convenient for industrial applications.

*Figure 1. (a) Laser transmission welding process, and (b) Scheme of the weld sample used in this study*



With the development of comparatively low cost reliable diode and fiber laser sources at the end of twentieth century, the research on laser transmission welding has seen greater progress through the last two decades of this century, which include: innovation of newer strategies, research on improvement of process qualities to the development of mathematical models, and industrial implementations. Potente, H., *et al.* (1999) analyzed the heating phase in laser transmission welding of nylon 6. For the absorbing part they assumed that the absorbing coefficient is sufficiently high that all of the heat is generated at the interface and is conducted equally into the both parts resulting in a symmetrical temperature distribution. Given the above approximation, they applied an analytical heat transfer model of single sided impulse welding to the laser transmission welding process. The effect and interplay of process influencing parameters and quantities are illustrated by Russek *et al.* (2004) by means of experimental results of systematic investigations as well as the outcome of a thermal process model. The equation of energy conservation is solved for different steps of approximation to indicate the influence of the convective as well as of the diffusive heat flow on the energy density distribution. Mayboudi, *et al.* (2005) developed a two-dimensional heat transfer model of laser transmission welding of unreinforced nylon 6 in T-like joint geometry using the ANSYS® finite element code. The two dimensional transient conduction heat transfer equation is considered to model the heat transfer in laser welding of thermoplastics. It is shown that this two-dimensional heat transfer model is capable of predicting the molten zone depth as well as transient temperature distribution along the weld line. It has also the potential advantage to being able to estimate melt down. The main drawback of such two-dimensional heat transfer model is their inability to predict the temperature distribution in the joint, transverse to the beam travel direction. Huang *et al.* (2006) proposed a two-dimensional heat conduction model of laser transmission welding process, solved with FDM technique. Polypropylene was considered as work materials. It was assumed that 90% of the incident energy was absorbed in a very thin layer of the laser-absorbing part. Temperature distribution was simulated for the same line energy but with different power and speed combinations. Ven and Erdman (2007) developed a two-dimensional finite element model of laser transmission welding of plastics, in which the first dimension is into the material and the second dimension is perpendicular to the path of the laser. This 2-d model for a T-joint geometry used an energy balance method to calculate the temperature at the nodes throughout the materials at specified time steps. Mayboudi *et al.* (2007) developed a three-dimensional FE thermal model of laser transmission welding of unreinforced polyamide 6 (PA6) specimens. The temperature distribution obtained from the model was compared with the thermal imaging observations for a lap joint geometry exposed to a stationary diode laser beam. Mahmood *et al.* (2007) developed a three-dimensional heat transfer FE model for transient heat analysis of laser transmission micro-joining process. The FE code ABAQUS® was used to model and analyze the problem. The spatial and temporal temperature distribution was calculated using a three-dimensional heat conduction equation in a domain, considering only one half of the overlap materials due to symmetry nature of the system. Shaban *et al.* (2007) presented a two-dimensional thermo-mechanical simulation of a laser transmission welding process, employing a FEM code ABAQUS®. A butt-joint geometry made of polycarbonate (PC) was exposed to a diode laser beam. The maximum temperature was obtained inside the laser-absorbing part at a distance of 0.15 mm from the weld interface. Speka *et al.* (2008) used a contact free method such as the infrared thermography for surface temperature measurement on a typical configuration for the laser transmission welding of polymers. The experimental temperature profiles acquired by infrared thermography were also compared with numerical solutions during heating and cooling phase. Coelho *et al.* (2008) developed an analytical model to analyze the influence of beam spot shape in high speed laser lap welding of thermoplastic films. Weld quality and efficiency were compared for beam spots with

circular and elliptical geometry. Ilie *et al.* (2009) investigated the laser beam weldability of ABS plates by combining both experimental and theoretical aspects. In computing the temperature field within the materials and at the interface, the first principle of heat transfer was used taking into account a perfect contact between the two components subjected to welding. The thermal model was employed in a FE code COMSOL®. Taha *et al.* (2009) developed a mathematical model for laser transmission welding of polymer in lap joint geometry. The thermal and physical properties of the polymer were assumed to be constant, thus neglecting the phase change phenomenon. A contact resistance was considered at the weld interface, which in turn depends on contact pressure. Acherjee *et al.* (2012) studied the laser transmission welding through numerical investigation to examine the effect of the carbon black on thermal field and weld contour during welding of polymers. The results obtained have revealed that the carbon black has considerable influence on the temperature field distribution and the formation of the weld pool geometry. Liu *et al.* (2016) presented a thermal contact model of laser transmission welding which is constructed based on volumetric heat source. The evolution of numerical techniques and improvements in high-speed computing has enabled complicated calculations to be performed in relatively short period of time with acceptable accuracy. Theoretical analysis of laser transmission welding process has gained a great interest among the researchers in the recent past, employing both analytical and numerical methods to study various aspects of this joining technique. Numerical results can be used to explain the physics of some complex phenomena in welding and also for process optimization.

In this work, a three-dimension heat transfer finite element model of laser transmission welding is developed by considering a moving volumetric heat source. The model is capable of predicting transient temperature zone in three-dimensional space. The weld dimensions, namely: weld width and weld penetration depth can be measured from this model using the simulated weld zone temperature field. This model is built parametrically and, therefore, the model can predict the outputs for a combination of input parameters. The model outputs are further used to train a neural network which can predict the outputs, i.e., weld pool dimensions as a function of given input parameters in very short time frame.

## **THERMAL MODEL**

The transient temperature field generated during the laser transmission welding is determined based on the mechanism of heat conduction. The following assumptions are made for the calculation of temperature:

1. The laser intensity distribution follows the Gaussian mode.
2. Heat conduction within the specimens and free convection between the surfaces of the specimen and the surrounding air, and the thermal radiation are considered.
3. The heating phenomena due to the phase changes are neglected.

A heat transfer model is developed to calculate the temperature distribution in and around irradiated areas. Commercial multi-physics finite element software ANSYS® is used in all stages of the thermal modeling including pre- and post-processing phases.

The heat generation within the body and the temperature distribution during laser transmission welding at laser irradiated zone is modelled by considering the three-dimensional heat conduction equation as the governing equation,



$$\rho.c \frac{\partial T}{\partial t} = \vec{\nabla} \cdot (k \vec{\nabla} T) + q_v \quad (1)$$

where,  $\rho$  is the density of the material (kg/m<sup>3</sup>),  $c$  is the specific heat (J/kg-K),  $T$  is the temperature (K),  $t$  is the time (s),  $k$  is the thermal conductivity (W/m-K),  $q_v$  is the rate of internal heat generation (W/m<sup>3</sup>), and  $\vec{\nabla}$  is the gradient operator.

A Gaussian volumetric heat generation expression is used to simulate the absorption of laser beam within plastic parts. This expression is also used to calculate the heat generation at irradiated zone with respect to the distance from the beam center. The rate of internal heat generation for a Gaussian laser flux distribution,  $q_v$ , is determined as:

$$q(x, y, z, t) = \begin{cases} 0; & \text{for transparent part} \\ (1 - R_a) K I_a \exp \exp(-K z_a); & \text{for absorbing part} \end{cases} \quad (2)$$

where,  $R_a$  is reflectivity and  $K$  is coefficient of absorption (m<sup>-1</sup>) of the absorbing part,  $z_a$  is the depth (m) within the absorbing part, and  $I_a$  is the laser intensity (W/m<sup>2</sup>) after passing through the transparent material, which can be further expressed as:

$$I_a = \frac{T_t P}{\pi r_0^2} \exp \left( -\frac{r^2}{r_0^2} \right) \quad (3)$$

where,  $T_t$  is the transmissivity of the transparent plastic part,  $P$  is laser power (W),  $r_0$  is the radius of the laser beam (radius of Gauss function curve), and  $r$  is the radial distance of any point on the surface of the material;  $r = \sqrt{(x_s^2 + y_s^2)}$ , where  $x_s$  and  $y_s$  are the Cartesian coordinates of that point.

Convection and radiation boundary conditions are used to realize heat loss from the surfaces of the materials to the surroundings. The temperature dependent convection-radiation combined boundary condition is imposed on external surfaces of the materials as:

$$-k(T) \vec{\nabla} \vec{T} n = h_r (T_s - T_0) \quad (4)$$

where,  $h_r$  is the combined heat transfer coefficient that can be expressed as:

$$h_r = h + \varepsilon \sigma (T_s + T_0) (T_s^2 + T_0^2) \quad (5)$$

The values of  $h_r$  are calculated at different temperatures and stored in a look-up table. Convective heat transfer coefficient,  $h$ , is assumed to be 5 W/m<sup>2</sup>-K (Mayboudi *et al.*, 2005). Emissivity of polycarbonate is taken as 0.95 (Mitchell, 2000). Further details about the FE modeling and implementation of moving heat source are described in Acherjee *et al.* (2012).

## Temperature Field Prediction

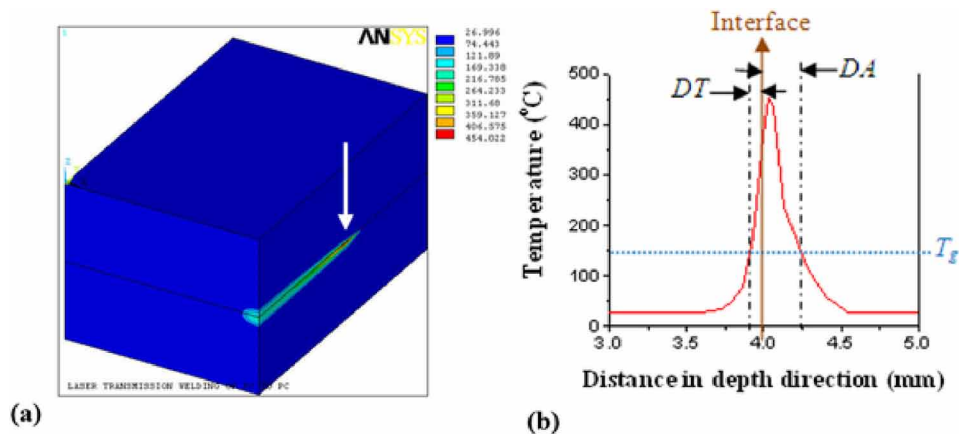
The 3-dimensional finite element model is developed by scripting in ANSYS® Parametric Design Language. Polycarbonate is used as work materials. Temperature dependent material data of polycarbonate are used for thermal modeling. The model size is reduced by utilizing symmetries of geometry and loading, and only one half of the overlapping weld assembly part is considered for modeling (as shown in Figure 1. (b), using selection box). The initial condition, at  $t = 0$  sec, is chosen as  $T_0 = 27^\circ\text{C}$  (300 K), that is the body temperature of the workpiece is equal to ambient temperature.

Figure 2 (a) depicts the distributions of temperature field at weld zone of the polycarbonate to polycarbonate (added 0.15% wt. carbon black to render the bottom part laser absorbing) lap-joint, which is computed by setting the welding parameters at 12 W laser power, 25 mm/s welding speed and 1.5 mm laser beam diameter. It is observed from the figure above that the maximum temperature at laser irradiated zone reaches to  $454^\circ\text{C}$ . The glass transition temperature ( $T_g$ ) of polycarbonates is  $150^\circ\text{C}$ . The region in the temperature contours with temperature more than  $150^\circ\text{C}$ , shows the penetration depths in both the polycarbonate parts from weld interface. The penetration depth can be determined from Figure 2 (b), which plots nodal temperatures with respect to distances along the direction of depth.

Figure 3 (a) presents the distributions of temperature field at weld interface. The maximum temperature of  $379^\circ\text{C}$  is achieved at weld interface. The half width (WW/2) of the weld can be determined from the distance vs. temperature plot as presented in Figure 3 (b).

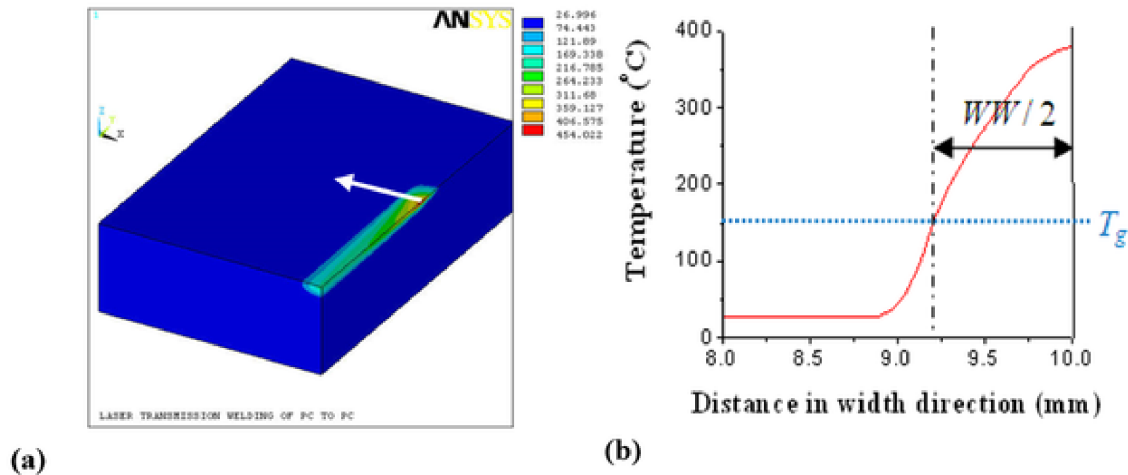
A computer system with 2.66 GHz Core™ 2 Duo processor, 3.0 GB RAM is used to run the code with specified process parameters, which takes around 157 minutes of solution time for thermal analysis (because of higher node density and large number of load steps during solution). The simulation results are validated using the experimental weld dimensions results presented by Russek *et al.* (2004).

Figure 2. (a) Temperature contour on the plane in the direction of depth of the materials, and (b) weld depth penetrations (DT = penetration depth in transparent part, and DA = penetration depth in absorbing part)



\*For a more accurate representation see the electronic version.

Figure 3. (a) Temperature contours at weld interface, and (b) half width of the weld ( $WW/2$  = half of weld width from the centerline of the weld)



\*For a more accurate representation see the electronic version.

## EMPIRICAL MODELING USING ANN

Artificial neural network is a powerful empirical modeling tool that is used to predict the outputs of a process as a function of several input factors within a selected design space. ANN is used here to reduce the prediction time where as FEM is used to minimize the experimental effort. As the solution time for developed FE model is quite high, the ANN model is used to map the design space for quick estimation of weld pool dimensions.

The input factors for the ANN model are laser power ( $P$ ), welding speed ( $S$ ), laser beam spot diameter ( $D$ ) and carbon black content in absorbing plastic ( $B$ ); whereas, the output factors are weld width ( $WW$ ), penetration depth in transparent part ( $DT$ ), and penetration depth in absorbing part ( $DA$ ). Data extracted from FE model solutions are used for training and testing of the network.

Four factors and five levels central composite design is employed for planning of the design matrix. Among 30 data sets, 24 data sets are randomly selected to train the network and remaining 6 data sets are used for testing. Table 1 furnishes the design matrix and the numerically simulated results of the response variables.

The feed-forward neural network with back-propagation algorithm is used to develop the ANN model. The multilayer network architectures are developed using one input layer, one or more hidden layer(s) and one output layer. The input layer has four neurons which represents four input factors, whereas the output layer has three neurons which represent three output factors. The accuracy of the model output depends on several factors, one of which is selection of optimum model architecture (Pal *et al.*, 2008). Thus, the number of hidden layer(s) and the number of neurons in each hidden layer is varied to choose optimum model architecture based on the lowest mean prediction error percentage.

With standard steepest descent, the learning rate is held constant throughout training. The performance of the algorithm is very sensitive to the proper setting of the learning rate. If the learning rate is set too high, the algorithm may oscillate and become unstable. If the learning rate is too small, the algorithm

*Table 1. Design matrix and the numerically simulated results*

Sl. no.	Welding Parameters				Simulated Results		
	<i>P</i>	<i>S</i>	<i>D</i>	<i>B</i>	<i>WW</i>	<i>DT</i>	<i>DA</i>
1	10	15	1.25	0.10	1.29	0.188	0.388
2	14	15	1.25	0.10	1.36	0.285	0.475
3	10	25	1.25	0.10	1.17	0.097	0.294
4	14	25	1.25	0.10	1.28	0.165	0.364
5	10	15	1.75	0.10	1.67	0.134	0.335
6	14	15	1.75	0.10	1.84	0.216	0.419
7	10	25	1.75	0.10	1.47	0.067	0.234
8	14	25	1.75	0.10	1.68	0.111	0.312
9	10	15	1.25	0.20	1.37	0.238	0.352
10	14	15	1.25	0.20	1.47	0.352	0.425
11	10	25	1.25	0.20	1.29	0.141	0.259
12	14	25	1.25	0.20	1.35	0.212	0.325
13	10	15	1.75	0.20	1.82	0.183	0.300
14	14	15	1.75	0.20	1.92	0.275	0.375
15	10	25	1.75	0.20	1.68	0.100	0.207
16	14	25	1.75	0.20	1.84	0.160	0.275
17	8	20	1.50	0.15	1.44	0.098	0.241
18	16	20	1.50	0.15	1.71	0.260	0.389
19	12	10	1.50	0.15	1.76	0.320	0.462
20	12	30	1.50	0.15	1.48	0.095	0.250
21	12	20	1.00	0.15	1.17	0.226	0.374
22	12	20	2.00	0.15	1.92	0.124	0.278
23	12	20	1.50	0.05	1.34	0.090	0.372
24	12	20	1.50	0.25	1.69	0.217	0.300
25	12	20	1.50	0.15	1.59	0.172	0.319
26	12	20	1.50	0.15	1.59	0.172	0.319
27	12	20	1.50	0.15	1.59	0.172	0.319
28	12	20	1.50	0.15	1.59	0.172	0.319
29	12	20	1.50	0.15	1.59	0.172	0.319
30	12	20	1.50	0.15	1.59	0.172	0.319

will take too long to converge. It is not practical to determine the optimal setting for the learning rate before training, and, in fact, the optimal learning rate changes during the training process, as the algorithm moves across the performance surface. The performance of the steepest descent algorithm can be improved if we allow the learning rate to change during the training process. An adaptive learning rate will attempt to keep the learning step size as large as possible while keeping learning stable. First, the initial network output and error are calculated. At each epoch new weights and biases are calculated

using the current learning rate. New outputs and errors are then calculated. As with momentum, if the new error exceeds the old error by more than a predefined ratio  $\text{max\_perf\_inc}$  (typically 1.04), the new weights and biases are discarded. In addition, the learning rate is decreased (typically by multiplying by  $\text{lr\_dec} = 0.7$ ). Otherwise, the new weights, etc., are kept. If the new error is less than the old error, the learning rate is increased (typically by multiplying by  $\text{lr\_inc} = 1.05$ ). This procedure increases the learning rate, but only to the extent that the network can learn without large error increases. Thus, a near-optimal learning rate is obtained for the local terrain (MATLAB Help navigator, 2004).

All the input-output variables are normalized between 0 and 1. Neurons in the input layer do not have transfer function ( $f$ ), while a log-sigmoid transfer function is used in the other layers as the outputs are ranging between 0 and 1. The feed-forward networks are created using the MATLAB® function 'newff'. This command creates the network object and initializes the weights and the biases of the network. During training, the weights and biases of the networks are iteratively adjusted to minimize the performance function mean squared error – the average squared error between the network outputs and the actual outputs. The adaptive learning rate is used for training the networks using MATLAB® function 'traingda'.

The 4-10-4-3 model architecture, as presented in Figure 4, is found to be most suitable for mapping input-output data as this predicts lowest mean prediction error. This network is trained for 1,82,179 iterations and reaches a performance mean squared error of less than 0.0001. Figure 5 shows the performance mean squared error of the neural network model at the end of training. The model takes about 8 minutes to converge to the goal, and hence able to predict the output in very short time, as compared to the developed FE model. The time can further be reduced by setting the goal to a relatively higher value.

Figure 6 presents the comparisons of the results of FE simulation and ANN prediction of weld width, and penetration depths in transparent and absorbing part for test data sets. It is evident from this plot, that the results predicted by the ANN model follow the FE simulation results very closely.

*Figure 4. Back-propagation neural network used for predicting model outputs (4-10-4-3 model architecture)*

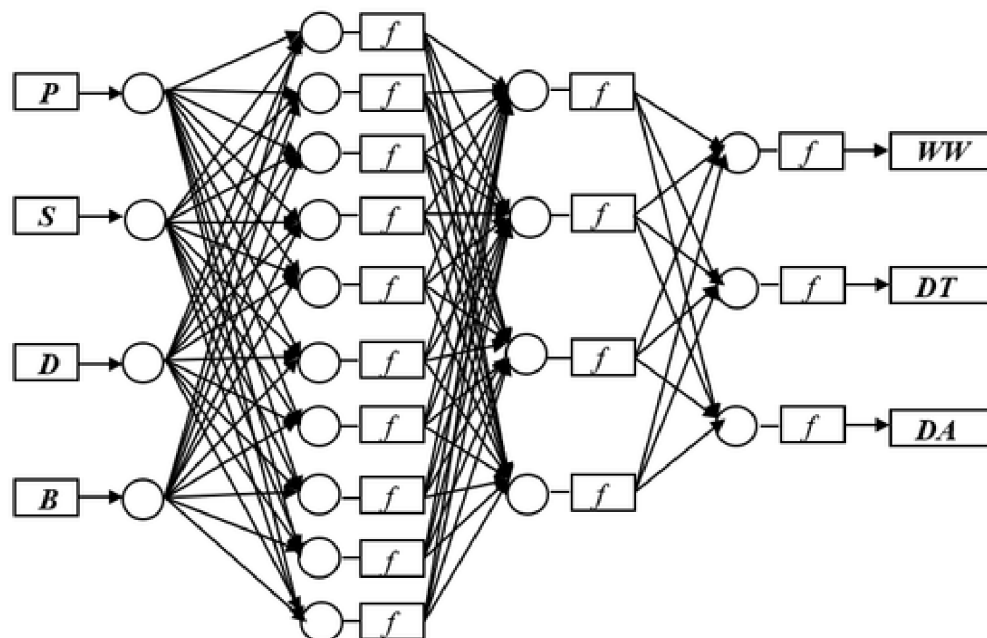


Figure 5. Convergence diagram and mean squared error plot of selected model

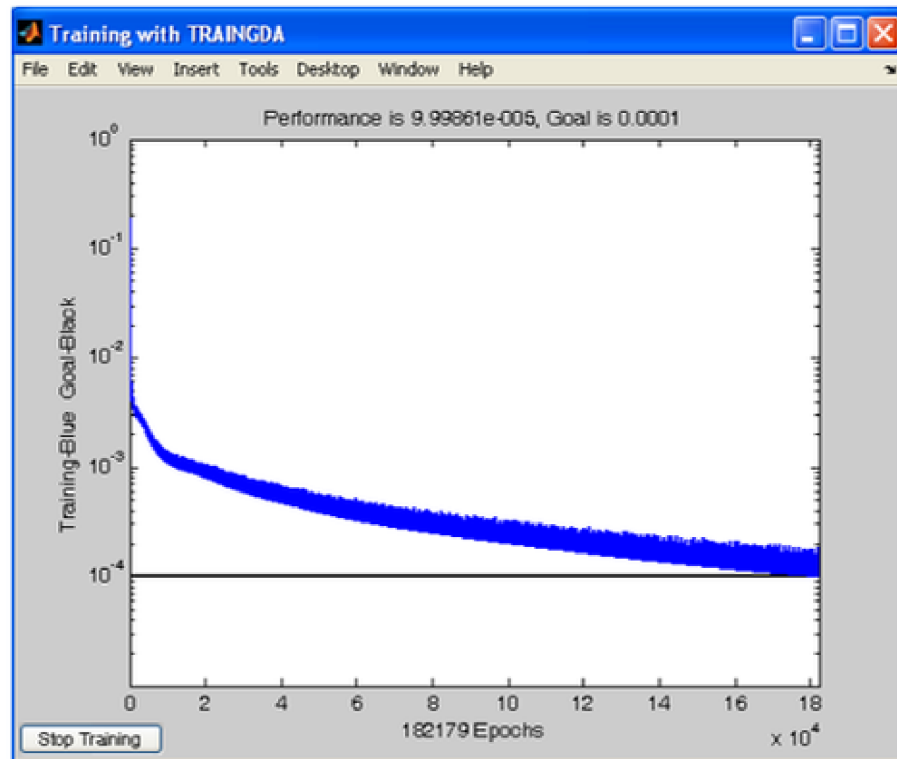


Figure 6. FE simulation results and ANN predictions of weld pool dimensions

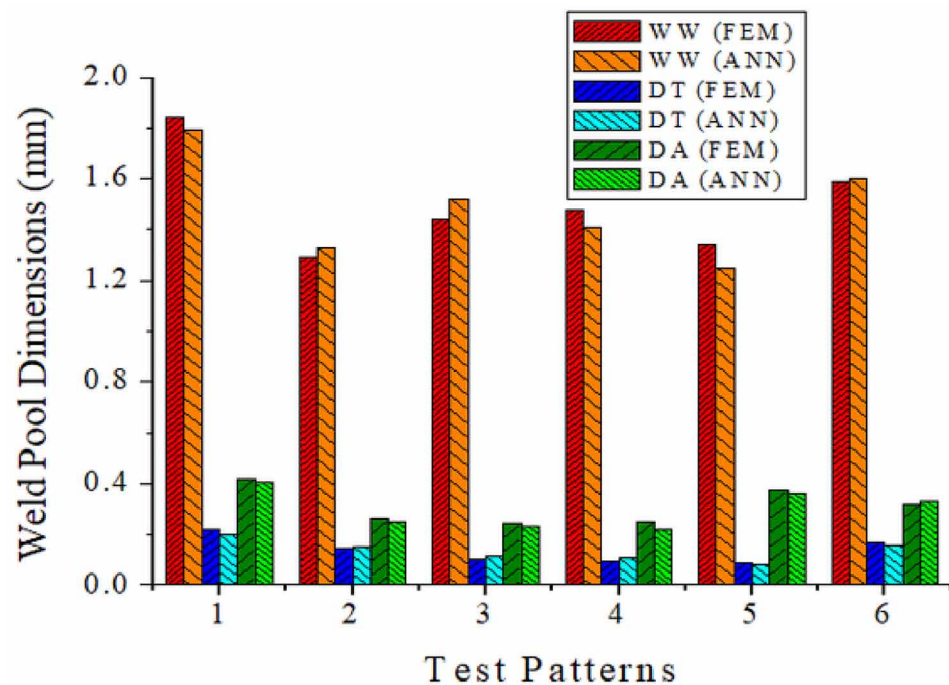
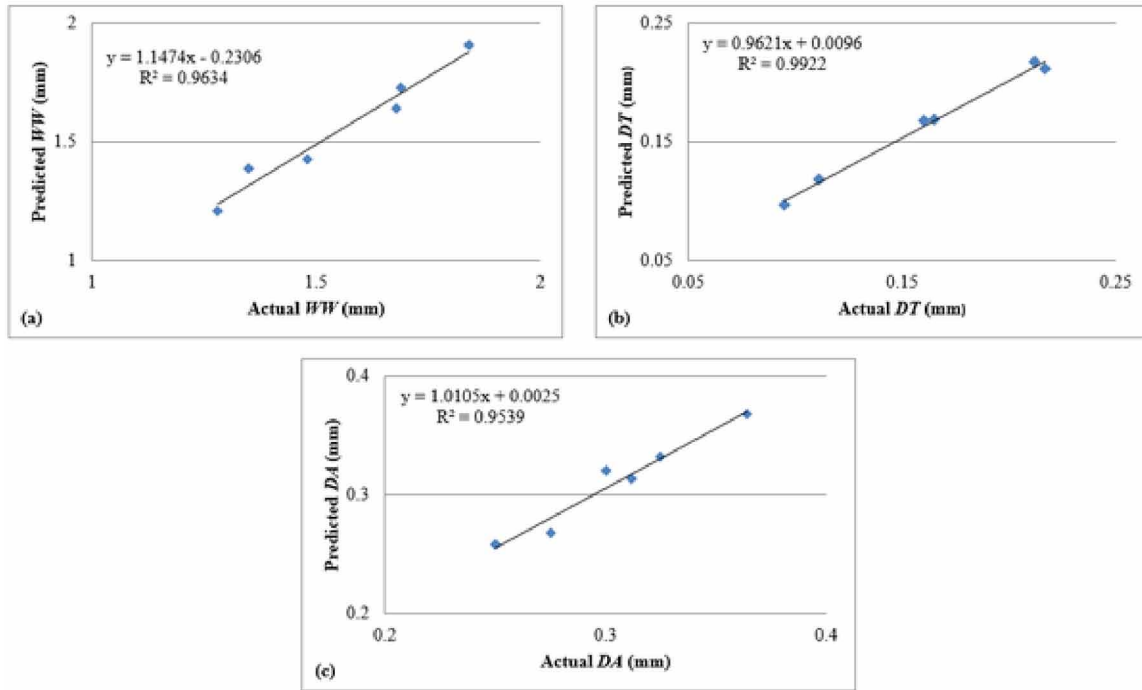


Figure 7. Scatter diagram with best fit of actual data vs. ANN predictions for (a) weld width, (b) penetration depth in transparent part, and (c) penetration depth in absorbing part



Linear regression analysis is also carried out using Microsoft Excel® to determine the coefficient of correlations for the developed ANN model. The coefficient of correlation ( $R^2$ ) is used to quantify the correlation between the results predicted by FE and ANN models. The correlation coefficients of 0.9634, 0.9922 and 0.9539 are obtained for the test patterns while predicting weld width, penetration depths in transparent part and absorbing part, as shown in Figure 7 (a-c), respectively. The  $R^2$  values are found to be close to unity, which indicates the adequacy of the developed model. Therefore, this neural network model can be used for predicting weld pool dimensions during laser transmission welding with significant accuracy.

## CONCLUSION

Following conclusions can be drawn based on the results of this research work:

1. The thermal model of the laser transmission welding process developed using FEM can predict the temperature at weld zone in 3-dimensiaonal space.
2. The weld pool dimensions, namely: weld width, penetration depth in transparent part and in absorbing part are calculated from the temperature data.
3. The results of FE simulations are used to develop an ANN model to establish the empirical relationship between process input parameters and the outputs.

4. The 4-10-4-3 appears as the most appropriate network architecture, which predicts the outputs accurately.
5. The sequential integration of FEM and ANN minimizes the experimental effort and thus saves time and cost of performing experiments.

## REFERENCES

- Acherjee, B., Kuar, A. S., Mitra, S., & Misra, D. (2012). Effect of carbon black on temperature field and weld profile during laser transmission welding of polymers: A FEM study. *Optics & Laser Technology*, 44(3), 514–521. doi:10.1016/j.optlastec.2011.08.008
- Acherjee, B., Kuar, A. S., Mitra, S., & Misra, D. (2015). Laser transmission welding of polycarbonates: Experiments, modeling, and sensitivity analysis. *International Journal of Advanced Manufacturing Technology*, 78(5-8), 853–861. doi:10.1007/00170-014-6693-7
- Baylis, B. (2002). Welding thermoplastic elastomers to polypropylene with a diode laser. *Proceedings of the 21st International Congress on Applications of Lasers & Electro-Optics*, 94.
- Bonten, C., & Tüchert, C. (2002). Welding of plastics-Introduction into heating by radiation. *Journal of Reinforced Plastics and Composites*, 21(8), 699–710. doi:10.1177/073168402128988436
- Coelho, J. M. P., Abreu, M. A., & Rodrigues, F. C. (2008). Modeling the spot shape influence on high-speed transmission lap welding of thermoplastic films. *Optics and Lasers in Engineering*, 46(1), 55–61. doi:10.1016/j.optlaseng.2007.07.001
- Hansch, D., Haff, D., Putz, H., Treusch, H. G., Gillner, A., & Poprawe, R. (1998). Welding of plastics with diode laser. *Proceedings of the 17th International Congress on Applications of Lasers & Electro-Optics*, 131-140.
- Herfurth, H., Ehlers, B., Heinemann, S., & Haensch, D. (1999). New approaches in plastic welding with diode lasers. *Proceedings of the 18th International Congress on Applications of Lasers & Electro-Optics*, 48-56.
- Huang, Y., Yu, A., Watt, D., & Baylis, B. (2006). A numerical study of scanning through-transmission laser welding. *Proceedings of Annual Technical Conference – ANTEC 2006*, 2310-2314.
- Ilie, M., Cicala, E., Grevey, D., Mattei, S., & Stoica, V. (2009). Diode laser welding of ABS: Experiments and process modeling. *Optics & Laser Technology*, 41(5), 608–614. doi:10.1016/j.optlastec.2008.10.005
- Liu, H., Liu, W., Meng, D., & Wang, X. (2016). Simulation and experimental study of laser transmission welding considering the influence of interfacial contact status. *Materials & Design*, 92, 246–260. doi:10.1016/j.matdes.2015.12.049
- Mahmood, T., Mian, A., Amin, M. R., Auner, G., Witte, R., Herfurth, H., & Newaz, G. (2007). Finite element modeling of transmission laser microjoining process. *Journal of Materials Processing Technology*, 186(1-3), 37–44. doi:10.1016/j.jmatprotec.2006.11.225



- Mayboudi, L. S., Birk, A. M., Zak, G., & Bates, P. J. (2005). A 2-D thermal model for laser transmission welding of thermoplastics. *Proceedings of the 24th International Congress on Applications of Lasers & Electro-Optics*, 402-409.
- Mayboudi, L. S., Birk, A. M., Zak, G., & Bates, P. J. (2007). Laser transmission welding of a lap-joint: Thermal imaging observations and Three-dimensional finite element modeling. *Journal of Heat Transfer*, 129(9), 1177–1186. doi:10.1115/1.2740307
- Mitchell, M. (2000). *Design and microfabrication of a molded polycarbonate continuous flow polymerase chain reaction device* (Master thesis). Louisiana State University.
- Pal, S., Pal, S. K., & Samantaray, A. K. (2008). Artificial neural network modeling of weld joint strength prediction of a pulsed metal inert gas welding process using arc signals. *Journal of Materials Processing Technology*, 202(1-3), 464–474. doi:10.1016/j.jmatprotec.2007.09.039
- Potente, H., Korte, J., & Becker, F. (1999). Laser transmission welding of thermoplastics: Analysis of heating phase. *Journal of Reinforced Plastics and Composites*, 18(10), 914–920. doi:10.1177/073168449901801005
- Russek, U. A., Aden, M., Poehler, J., Palmen, A., & Staub, H. (2004). Laser beam welding of thermoplastics parameter influence on weld seam quality - Experiments and Modeling. *Proceedings of the 23rd International Congress on Applications of Lasers & Electro-Optics*.
- Shaban, A., Mahnken, R., Wilke, L., Potente, H., & Ridder, H. (2007). Simulation of rate dependant plasticity for polymers with asymmetric effects. *International Journal of Solids and Structures*, 44(18-19), 6148–6162. doi:10.1016/j.ijsolstr.2007.02.017
- Spekaa, M., Mattei, S., Pilloza, M., & Iliea, M. (2008). The infrared thermography control of the laser welding of amorphous polymers. *NDT & E International*, 41(3), 178–183. doi:10.1016/j.ndteint.2007.10.005
- Taha, Z. A., Roy, G. G., Hajim, K. I., & Mannaa, I. (2009). Mathematical modeling of laser-assisted transmission lap welding of polymers. *Scripta Materialia*, 60(8), 663–666. doi:10.1016/j.scriptamat.2008.12.041
- Van de Ven, J. D., & Erdman, A. G. (2007). Laser transmission welding of thermoplastics — Part I: Temperature and pressure modeling. *Journal of Manufacturing Science and Engineering*, 129(5), 849–858. doi:10.1115/1.2752527

## Compilation of References

Abdulkareem, S., Khan, A., & Zain, Z. M. (2011). Experimental Investigation of Machining Parameters on Surface Roughness in Dry & Wet Wire-Electrical Discharge Machining. *Advanced Materials Research*, 264-265, 831–836. doi:10.4028/www.scientific.net/AMR.264-265.831

Abrate, S., & Walton, D. (1992). Machining of composite materials. Part II: Non-traditional methods. *Composites Manufacturing*, 3(2), 85–94. doi:10.1016/0956-7143(92)90120-J

Acherjee, B., Kuar, A. S., Mitra, S., & Misra, D. (2012). Effect of carbon black on temperature field and weld profile during laser transmission welding of polymers: A FEM study. *Optics & Laser Technology*, 44(3), 514–521. doi:10.1016/j.optlastec.2011.08.008

Acherjee, B., Kuar, A. S., Mitra, S., & Misra, D. (2015). Laser transmission welding of polycarbonates: Experiments, modeling, and sensitivity analysis. *International Journal of Advanced Manufacturing Technology*, 78(5-8), 853–861. doi:10.1007/00170-014-6693-7

Afazov, S. M., Zdebski, D., Ratchev, S. M., Segal, J., & Liu, S. (2013). Effects of micro-milling conditions on the cutting forces and process stability. *Journal of Materials Processing Technology*, 213(5), 671–684. doi:10.1016/j.jmatprotec.2012.12.001

Ahamed, A. R., Asokan, P., & Aravindan, S. (2009). EDM of hybrid Al-SiCp-B<sub>4</sub>Cp and Al-SiC<sub>p</sub>-glass<sub>p</sub> MMCs. *International Journal of Advanced Manufacturing Technology*, 44(5-6), 520–528. doi:10.1007/00170-008-1839-0

Ahmed, L. S., & Kumar, M. P. (2016). Multiresponse optimization of cryogenic drilling on Ti-6Al-4V alloy using topsis method. *Journal of Mechanical Science and Technology*, 30(4), 1835–1841. doi:10.1007/12206-016-0340-1

Aich, U., Bandyopadhyay, A., & Banerjee, S. (2013). A state of art – review on abrasive water jet machining process. *International Review of Mechanical Engineering*, 7(7), 1471–1494.

Akula, S., & Karunakaran, K. P. (2006). Hybrid adaptive layer manufacturing: An Intelligent art of direct metal rapid tooling process. *Robotics and Computer-integrated Manufacturing*, 22(2), 113–123. doi:10.1016/j.rcim.2005.02.006

Albert, M. (1997). *Reaching New Heights with Wire EDM*. Modern Machine Shop.

Allan, E. W., Bocking, C., & Bennett, R. (2001). Electroforming of rapid prototyping mandrels for electro-discharge machining electrodes. *Journal of Materials Processing Technology*, 110(2), 186–196. doi:10.1016/S0924-0136(00)00878-5

Allen, D. M. (2004). Photochemical machining: From ‘manufacturing’s best kept secret’ to a \$6 billion per annum, rapid manufacturing process. *CIRP Annals-Manufacturing Technology*, 53(2), 559–572. doi:10.1016/S0007-8506(07)60029-8

Alting, L., Kimura, F., Hansen, H. N., & Bissacco, G. (2003). Micro Engineering. *CIRP Annals - Manufacturing Technology*, 52(2), 635–657. 10.1016/S0007-8506(07)60208-X

## Compilation of References

- Amin, S. G., Ahmed, M. H. M., & Youssef, H. A. (1993). Optimum design charts of acoustic horns for ultrasonic machining. *Proceedings of the International Conference on AMPT*, 93, 139–147.
- Amorim, F. L., & Weingaertner, W. L. (2007). The behaviour of graphite and copper electrodes on the finish die-sinking electrical discharge machining (EDM) of AISI P20 tool steel. *Journal of the Brazilian Society of Mechanical Sciences and Engineering*, 29(4), 366–371. doi:10.1590/S1678-58782007000400004
- Amorim, F. L., & Weingaertner, W. L. (2014). Die sinking electrical discharge machining of a high strength copper based alloy for injection molds. *Journal of the Brazilian Society of Mechanical Sciences and Engineering*, 26(2), 137–144.
- Anand, K. N. (1996). Development of process technology in wire-cut operation for improving machining quality. *Total Quality Management*, 7(1), 11–28. doi:10.1080/09544129650035016
- Anasane, S. S., & Bhattacharyya, B. (2017). Experimental investigation into micromilling of microgrooves on titanium by electrochemical micromachining. *Journal of Manufacturing Processes*, 28, 285–294. doi:10.1016/j.jmapro.2017.06.016
- Ankush, S., & Lalwani, D. I. (2013). Experimental investigation of process parameters influence on surface roughness in abrasive water jet machining of AISI H13 die steel. In *Proceedings of Conference on Intelligent Robotics, Automation and Manufacturing*. Emerald Group Publishing Limited.
- Aoyama, S. (1999). High-performance Coated Wire Electrodes for High-Speed Cutting & Accurate Machining. *Hitachi Cable Review No.18*.
- Arola, D., & Ramulu, M. (1997). Material removal in abrasive waterjet machining of metals: A residual stress analysis. *Wear*, 211(2), 302–310. doi:10.1016/S0043-1648(97)00131-2
- Arthur, A., & Dickens, P. M. (1995). Rapid prototyping of EDM electrode by stereolithography. *Proceedings of International Symposium for Electromachining (ISEM X1)*, 17-20, 691-699.
- Arthur, A., Dickens, P. M., Cobb, R. C., & Bocking, C. E. (1996). Wear and failure mechanisms for SL EDM electrodes. In *SFFF Symposium*. University of Texas at Austin.
- Arthur, A., & Dickens, P. M. (1998). Measurement of heat distribution in stereolithography electrodes during electro - discharge machining. *International Journal of Production Research*, 36(9), 2451–2461. doi:10.1080/002075498192625
- Arthur, A., Dickens, P. M., & Cobb, R. C. (1996). Using rapid prototyping to produce electrical discharge machining electrodes. *Rapid Prototyping Journal*, 2(1), 4–12. doi:10.1108/13552549610109036
- Asad, A. B. M. A., Masaki, T., Rahman, M., Lim, H. S., & Wong, Y. S. (2007). Tool-based micro-machining. *Journal of Materials Processing Technology*, 192–193, 204–211. doi:10.1016/j.jmatprotec.2007.04.038
- Asif, I., Naeem, U. D., & Ghulam, H. (2011). Optimization of Abrasive Water Jet Cutting of Ductile Materials. *Journal of Wuhan University of Technology*, 26(1), 88–92. doi:10.1007/11595-011-0174-8
- Aspinwall, D.K., Soo, S.L., Berrisford, A.E., & Walder, G. (2008). Work piece surface roughness & integrity after WEDM of Ti-6Al-4V & Inconel 718 using minimum damage generator technology. *CIRP Annals – Manufacturing Technology*, 57, 187–190.
- Aspiwall, D. K., Soo, S. L., Berrisford, A. E., & Walder, G. (2008). Workpiece surface roughness and integrity after WEDM of Ti- 6Al-4V and Inconel 718 using minimum damage generator technology. *CIRP Annals - Manufacturing Technology*, 57(1), 187-190.

- Assarzadeh, S., & Ghoreishi, M. (2013). A dual response surface-desirability approach to process modeling and optimization of  $\text{Al}_2\text{O}_3$  powder-mixed electric discharge machining (PMEDM) parameters. *International Journal of Advanced Manufacturing Technology*, 64(9-12), 1459–1477. doi:10.100700170-012-4115-2
- Atashpaz-Gargari, E., & Lucas, C. (2007b). Imperialist competitive algorithm: an algorithm for optimization inspired by imperialistic competition. In *Evolutionary computation, 2007. CEC 2007. IEEE Congress on* (pp. 4661–4667). IEEE. 10.1109/CEC.2007.4425083
- Atashpaz-Gargari, E., & Lucas, C. (2007a). Designing an optimal PID controller using Colonial Competitive Algorithm. *Proceedings of the First Iranian Joint Congress on Fuzzy and Intelligent Systems*.
- Attanasio, A., Ceretti, E., Giardini, C., Filice, L., & Umbrello, D. (2008). Criterion to evaluate diffusive wear in 3D simulations when turning AISI 1045 steel. *International Journal of Material Forming*, 1(S1), 495–498. 10.100712289-008-0130-0
- Attia, U. M., & Alcock, J. R. (2010). Integration of functionality into polymer-based microfluidic devices produced by high-volume micro-moulding techniques. *International Journal of Advanced Manufacturing Technology*, 48(9–12), 973–991. doi:10.100700170-009-2345-8
- Attia, U. M., Marson, S., & Alcock, J. R. (2009). Micro-injection moulding of polymer microfluidic devices. *Microfluidics and Nanofluidics*, 7(1), 1–28. doi:10.100710404-009-0421-x
- Aurich, J. C., Engmann, J., Schueler, G. M., & Haberland, R. (2009). Micro grinding tool for manufacture of complex structures in brittle materials. *CIRP Annals - Manufacturing Technology*, 58(1), 311–314. 10.1016/j.cirp.2009.03.049
- Bach, F.W., Hassel, T., Biskup, C., Hinte, N., & Schenk, A. (2010). In-process generation of water ice particles for cutting and cleaning purposes. *BHR Group 2010 Water Jetting*, 20, 275–283.
- Baili, M., Wagner, V., Dessein, G., Sallaberry, J., & Lallement, D. (2011). An Experimental Investigation of Hot Machining with Induction to Improve Ti-5553 Machinability. *Applied Mechanics and Materials*, 62, 67–76. . doi:10.4028/www.scientific.net/AMM.62.67
- Bamberg, E., & Rakwal, D. (2008). Experimental investigation of wire electrical discharge machining of gallium-doped germanium. *Journal of Materials Processing Technology*, 197(1-3), 419–427. doi:10.1016/j.jmatprotec.2007.06.038
- Barenji, R. V., Pourasl, H. H., & Khojastehnezhad, V. M. (2016). Electrical discharge machining of the AISI D6 tool steel: Prediction and modelling of the material removal rate and tool wear ratio. *Precision Engineering*, 45, 435–444. doi:10.1016/j.precisioneng.2016.01.012
- Batish, A., Bhattacharya, A., Singla, V. K., & Singh, G. (2012). Study of Material Transfer Mechanism in Die steels using powder mixed Electrical Discharge Machining. *Materials and Manufacturing Processes*, 27(4), 449–456. doi:10.1080/10426914.2011.585498
- Baylis, B. (2002). Welding thermoplastic elastomers to polypropylene with a diode laser. *Proceedings of the 21st International Congress on Applications of Lasers & Electro-Optics*, 94.
- Beltrami, I., & Dauw, D. (1996). A simplified post process for wire cut EDM. *Journal of Materials Processing Technology*, 58(4), 385–389. doi:10.1016/0924-0136(95)02212-0
- Benedict, G. F. (1987). *Electrical discharge machining (EDM)*. In *Non-Traditional Manufacturing Processes* (pp. 231–232). New York: Marcel Dekker, Inc.
- Benedict, G. F. (1987). *Non-traditional manufacturing process*. CRC Press.

## Compilation of References

- Bhattacharya, A., Batish, A., Singh, G., & Singla, V. K. (2012). Optimal parameter settings for rough and finish machining of die-steels in powder-mixed EDM. *International Journal of Advanced Manufacturing Technology*, 61(5-8), 537–548. doi:10.1007/00170-011-3716-5
- Bhattacharyya, B., Munda, J., & Malapati, M. (2004). Advancement in electrochemical micro-machining. *International Journal of Machine Tools & Manufacture*, 44(15), 1577–1589. doi:10.1016/j.ijmachtools.2004.06.006
- Boccadoro, M., & Dauw, D. F. (1995). About application of fuzzy controllers in high-performance die-sinking EDM machines. *Annals CIRP*, 44(1), 147–150. doi:10.1016/S0007-8506(07)62294-X
- Bocking, C.E., Bennett, G.R., Dover, S.J., Arthur, A., Cobb, R.C., & Dickens, P.M. (1997). Electrochemical routes for engineering tool production. *GEC Journal of Technology*, 14(2), 66.
- Bonten, C., & Tüchert, C. (2002). Welding of plastics-Introduction into heating by radiation. *Journal of Reinforced Plastics and Composites*, 21(8), 699–710. doi:10.1177/073168402128988436
- Boopathi, S. (2012). Experimental Comparative Study of Near-Dry Wire-Cut Electrical Discharge Machining (WEDM). *European Journal of Scientific Research*, 75(4), 472–481.
- Boud, F., Murray, J. W., Loo, L. F., Clare, A. T., & Kinnell, P. K. (2014). Soluble Abrasives for Waterjet Machining. *Materials and Manufacturing Processes*, 29(11-12), 1346–1352. doi:10.1080/10426914.2014.930949
- Brinksmeier, E., Riemer, O., & Stern, R. (2001). Machining of Precision Parts and Microstructures. In I. Inasaki (Ed.), *Initiatives of Precision Engineering at the Beginning of a Millennium* (pp. 3–11). Berlin: Springer. doi:10.1007/0-306-47000-4\_1
- Bruyn, H. E., & Pekelharing, A. J. (1982). Has delay time influence on EDM-process? *Annals CIRP*, 31(1), 103–106. doi:10.1016/S0007-8506(07)63277-6
- Bruzzzone, A. A. G., & Reverberi, A. P. (2010). An experimental evaluation of an etching simulation model for photo-chemical machining. *CIRP Annals*, 59(1), 255–258. doi:10.1016/j.cirp.2010.03.070
- Cakir, O. (2006). Copper etching with cupric chloride and regeneration of waste etchant. *Journal of Materials Processing Technology*, 175(1-3), 63-68.
- Çakır, O. (2008). Chemical etching of aluminium. *Journal of Materials Processing Technology*, 199(1-3), 337–340. doi:10.1016/j.jmatprotec.2007.08.012
- Çakır, O., Temel, H., & Kiyak, M. (2005). Chemical etching of Cu-ETP copper. *Journal of Materials Processing Technology*, 162, 275–279. doi:10.1016/j.jmatprotec.2005.02.035
- Capello, E., Polini, W., & Semeraro, Q. (1996). Abrasive water jet cutting of MMC: Analysis of the quality of the generated surfaces. In *ESDA Engineering Systems Design and Analysis Conference: presented at the Third Biennial Joint Conference on Engineering Systems Design and Analysis* (pp. 63-68). Academic Press.
- Caroline, J. E. (2000). Machining of an aluminum/SiC composite using diamond inserts. *Journal of Materials Processing Technology*, 102(1-3), 25–29. doi:10.1016/S0924-0136(00)00425-8
- Çaydas, U., Hasçalık, A., & Ekici, S. (2009). An adaptive neuro-fuzzy inference system (ANFIS) model for wire-EDM. *Expert Systems with Applications*, 36(3), 6135–6139. doi:10.1016/j.eswa.2008.07.019
- Cecil, J., Powell, D., & Vasquez, D. (2007). Assembly and manipulation of micro devices-A state of the art survey. *Robotics and Computer-integrated Manufacturing*, 23(5), 580–588. doi:10.1016/j.rcim.2006.05.010

- Chaudhari, K., Patil, A., Kolekar, M., & Patil, A. (2016). Photochemical machining. *International Journal on Recent and Innovation Trends in Computing and Communication*, 4(4), 132–136.
- Cheng, Y. M., Eubank, P. T., & Gadalla, A. M. (1996). Eubank, P.T. and Gadalla, A.M. Electrical Discharge Machining of ZrB<sub>2</sub>-Based Ceramics. *Materials and Manufacturing Processes*, 11(4), 565–574. doi:10.1080/10426919608947509
- Chen, H. C., Lin, J. C., Yang, Y. K., & Tsai, C. H. (2007). Optimization of wire electrical discharge machining for pure tungsten using a neural network integrated simulated annealing approach. *Expert Systems with Applications*, 37(10), 7147–7153. doi:10.1016/j.eswa.2010.04.020
- Chetty, O. K., & Radhakrishnan, V. (1981). A study on the influence of grain size in electrochemical machining. *International Journal of Machine Tool Design and Research*, 21(1), 57–69. doi:10.1016/0020-7357(81)90014-7
- Choi, K. K., Nam, W. J., & Lee, Y. S. (2008). Effects of heat treatment on the surface of a die steel STD11 machined by W-EDM. *Journal of Materials Processing Technology*, 201(1-3), 580–584. doi:10.1016/j.jmatprotec.2007.11.156
- Choudhary, S. K., & Jadoun, R. S. (2014). Current research development in dry electric discharge machining. *International Journal of Emerging Technology and Advanced Engineering*, 4(8), 832–839.
- Chow, H. M., Yan, B. H., Huang, F. Y., & Hung, J. C. (2000). Study of added powder in kerosene for the micro-slit machining of titanium alloy using electro-discharge machining. *Journal of Materials Processing Technology*, 101(1-3), 95–103. doi:10.1016/S0924-0136(99)00458-6
- Chung, D. K., Kim, B. H., & Chu, C. N. (2007). Micro electrical discharge milling using deionized water as a dielectric fluid. *Journal of Micromechanics and Microengineering*, 17(5), 867–874. doi:10.1088/0960-1317/17/5/004
- Chung, D. K., Shin, H. S., Kim, B. H., Park, M. S., & Chu, C. N. (2009). Shin, H.S. Kim, B.H. Park, M.S. and Chu, C.N. Surface finishing of micro-EDM holes using deionized water. *Journal of Micromechanics and Microengineering*, 19(4), 045025. doi:10.1088/0960-1317/19/4/045025
- Coelho, J. M. P., Abreu, M. A., & Rodrigues, F. C. (2008). Modeling the spot shape influence on high-speed transmission lap welding of thermoplastic films. *Optics and Lasers in Engineering*, 46(1), 55–61. doi:10.1016/j.optlaseng.2007.07.001
- Cogun, C. (1990). A technique & its applications for evaluation of material removal contributions of pulses in electrical discharge machining. *International Journal of Machine Tools & Manufacture*, 30(1), 19–31. doi:10.1016/0890-6955(90)90038-K
- Coughanowr, C. A., Dissaux, B. A., Muller, R. H., & Tobias, C. W. (1986). Electrochemical machining of refractory materials. *Journal of Applied Electrochemistry*, 16(3), 345–356. doi:10.1007/BF01008844
- Czelusniak, T., Amorim, F. L., Lohrengel, A., & Higa, C. F. (2014). Development and application of copper–nickel zirconium diboride as EDM electrodes manufactured by selective laser sintering. *International Journal of Advanced Manufacturing Technology*, 72, 905–917.
- da Silva Neto, J. C., Da Silva, E. M., & Da Silva, M. B. (2006). Intervening variables in electrochemical machining. *Journal of Materials Processing Technology*, 179(1-3), 92–96. doi:10.1016/j.jmatprotec.2006.03.105
- Dahotre, N. B., McCay, T. D., & McCay, M. H. (1989). Laser processing of a SiC/Al-alloy metal matrix composite. *Journal of Applied Physics*, 65(12), 5072–5077. doi:10.1063/1.343183
- Dam, H., Jensen, S., & Quist, P. (1993). Surface characterization of ultrasonic machined ceramics with diamond impregnated sonotrode. *Machining of Advanced Materials*, 125–133.

## Compilation of References

- Dam, H., Quist, P., & Schreiber, M. P. (1995). Productivity, surface quality and tolerances in ultrasonic machining of ceramics. *Journal of Materials Processing Technology*, 51(1-4), 358–368. doi:10.1016/0924-0136(94)01587-Q
- Das, S. S., Tilekar, S. D., Wangikar, S. S., & Patowari, P. K. (2017). Numerical and experimental study of passive fluids mixing in micro-channels of different configurations. *Microsystem Technologies*, 23(12), 5977–5988. doi:10.100700542-017-3482-x
- Das, S., Klotz, M., & Klocke, F. (2003). EDM simulation: Finite element-based calculation of deformation, microstructure and residual stresses. *Journal of Materials Processing Technology*, 142(2), 434–451. doi:10.1016/S0924-0136(03)00624-1
- Datta, S., Bandyopadhyay, A., & Pal, P. K. (2008). Solving multi-criteria optimization problem in submerged arc welding consuming a mixture of fresh flux and fused slag. *International Journal of Advanced Manufacturing Technology*, 35(9-10), 935–942. doi:10.100700170-006-0776-z
- Datta, S., & Mahapatra, S. S. (2010). Modeling, simulation & parametric optimization of Wire-EDM process using response surface methodology coupled with Grey-Taguchi technique. *International Journal of Engineering Science and Technology*, 2(5), 162–183. doi:10.4314/ijest.v2i5.60144
- Dauw, D. F., & Beltrami, I. (1994). High-precision wire-EDM by online wire positioning control. *Annals CIRP*, 43(1), 193–197. doi:10.1016/S0007-8506(07)62194-5
- Dauw, D. F., Sthitoul, H., & Tricarico, C. (1989). Wire analysis & control for precision EDM cutting. *Annals CIRP*, 38(1), 191–194. doi:10.1016/S0007-8506(07)62682-1
- De Silva, A. K. M., Altena, H. S. J., & McGeough, J. A. (2000). Precision ECM by process characteristic modelling. *CIRP Annals-Manufacturing Technology*, 49(1), 151–155. doi:10.1016/S0007-8506(07)62917-5
- Debabrata, M., Pal, S. K., & Partha, S. (2007). Modeling of electrical discharge machining process using back propagation neural network & multi-objective optimization using non-dominating sorting genetic algorithm-II. *Journal of Materials Processing Technology*, 186(1-30), 154-162.
- Deepak, D., Akash, V., & Anjaiah, D. (2015). Studies on Jet Penetration and Kerf Width at various Operating Pressure in Machining of D2 Heat Treated Steel Using Abrasive Water Jet. *International Journal of Research in Engineering and Technology*, 4(9), 344–347. doi:10.15623/ijret.2015.0409064
- Dekeyser, W. L., & Snoeys, R. (1989). Geometric Accuracy of Wire EDM. *Proceedings of Ninth International Symposium for Electro-Machining (ISM-9)*.
- Dekeyser, W., Snoeys, R., & Jennes, M. (1985). A thermal model to investigate wire rupture phenomenon for improving performance in EDM wire cutting. *Journal of Manufacturing Systems*, 4(2), 179–190. doi:10.1016/0278-6125(85)90024-X
- Dekeyser, W., Snoeys, R., & Jennes, M. (1988). Expert system for wire cutting EDM based on pulse classification & thermal modelling. *Robotics and Computer-integrated Manufacturing*, 4(1–2), 219–224. doi:10.1016/0736-5845(88)90080-4
- Dewangan, S., Gangopadhyay, S., & Biswas, C. K. (2015). Study of surface integrity and dimensional accuracy in EDM using Fuzzy TOPSIS and sensitivity analysis. *Measurement*, 63, 364–376. doi:10.1016/j.measurement.2014.11.025
- Di Pietro, P., & Yao, Y. L. (1995). A new technique to characterize and predict laser cut striations. *International Journal of Machine Tools & Manufacture*, 35(7), 993–1002. doi:10.1016/0890-6955(94)00063-P
- Dickens, P. M., & Smith, P. J. (1992). Stereolithography tooling. *Proceedings of the first European conference on RP&M*, 309-317.

- Dimla, D. E., Hopkinson, N., & Rothe, H. (2004). Investigation of complex rapid EDM electrodes for rapid tooling applications. *International Journal of Advance Manufacturing Technology*, 23, 249-255.
- Ding, S., & Jiang, R. (2004). Tool path generation for 4-axis contour EDM rough machining. *International Journal of Machine Tools & Manufacture*, 44(14), 1493–1502. doi:10.1016/j.ijmachtools.2004.05.010
- Ding, X. M., Fuh, J. Y. H., Lee, K. S., Zhang, Y. F., & Nee, A. Y. C. (2000). A computer-aided EDM electrode design system for mold manufacturing. *International Journal of Production Research*, 38(13), 3079–3092. doi:10.1080/00207540050117459
- Ding, Y., Lan, H., Hong, J., & Wu, D. (2004). An integrated manufacturing system for rapid tooling based on rapid prototyping. *Robotics and Computer-integrated Manufacturing*, 20(4), 281–288. doi:10.1016/j.rcim.2003.10.010
- Dogra, M., Sharma, V., Sachdeva, A., & Suri, N. (2012). Tool life and surface integrity issues in continuous and interrupted finish hard turning with coated carbide and CBN tools. *Proceedings of the Institution of Mechanical Engineers. Part B, Journal of Engineering Manufacture*, 226(3), 431–444. doi:10.1177/0954405411418589
- Dubey, A. K., & Yadava, V. (2008). Laser beam machining—a review. *International Journal of Machine Tools & Manufacture*, 48(6), 609–628. doi:10.1016/j.ijmachtools.2007.10.017
- Ducobu, F., Arrazola, P.-J., Rivière-Lorphèvre, E., & Filippi, E. (2015). Finite Element Prediction of the Tool Wear Influence in Ti6Al4V Machining. *Procedia CIRP*, 31, 124–129. doi:10.1016/j.procir.2015.03.056
- Durr, H., Pilz, R., & Eleser, N. S. (1999). Rapid tooling of EDM electrodes by means of selective laser sintering. *Computers in Industry*, 39(1), 35–45. doi:10.1016/S0166-3615(98)00123-7
- Dvivedi, A., & Kumar, P. (2007). Surface quality evaluation in ultrasonic drilling through the Taguchi technique. *International Journal of Advanced Manufacturing Technology*, 34(1-2), 131–140. doi:10.100700170-006-0586-3
- Ebeid, S. J., Hewidy, M. S., El-Taweel, T. A., & Youssef, A. H. (2004). Towards higher accuracy for ECM hybridized with low-frequency vibrations using the response surface methodology. *Journal of Materials Processing Technology*, 149(1-3), 432–438. doi:10.1016/j.jmatprotec.2003.10.046
- Enache, S., & Opran, C. (1993). Dynamic stability of technological machining system in EDM. *Annals CIRP*, 42(1), 209–214. doi:10.1016/S0007-8506(07)62427-5
- Ezugwu, E. O. (2003). Key improvements in the machining of difficult-to-cut aero- space super alloys. *International Journal of Machine Tools and Manufacture*, 45, 1353-1367.
- Ezugwu, E. O. (2005). Key improvements in the machining of difficult-to-cut aerospace superalloys. *International Journal of Machine Tools & Manufacture*, 45(12–13), 1353–1367. doi:10.1016/j.ijmachtools.2005.02.003
- Farrer, J. O. (1948). *Improvements in or relating to cutting, grinding, polishing, cleaning, honing, or the like*. UK Patent (602801).
- Fascio, V., Wuthrich, R., Viquerat, D., & Langen, H. (1999). 3D microstructuring of glass using electrochemical discharge machining (ECDM). In *Micromechatronics and Human Science, 1999. MHS'99. Proceedings of 1999 International Symposium on* (pp. 179-183). IEEE.
- Field, F., Kirchain, R., & Roth, R. (2007). Process cost modeling: Strategic engineering and economic evaluation of Materials technologies. *JOM*, 59(10), 21–32. doi:10.100711837-007-0126-0
- Fixson, S. K. (2005). Product architecture assessment: A tool to link product, process, and supply chain design decisions. *Journal of Operations Management*, 23(3–4), 345–369. doi:10.1016/j.jom.2004.08.006
- Flynn, T. M. (2005). *Cryogenic Engineering*. Marcel Dekker. New York: Cryogenic Engineering.



## Compilation of References

- Folgado, R., Peças, P., & Henriques, E. (2010). Life cycle cost for technology selection: A Case study in the manufacturing of injection moulds. *International Journal of Production Economics*, 128, 368–378. doi:10.1016/j.ijpe.2010.07.036
- Folkes, J. (2009). Waterjet-An innovative tool for manufacturing. *Journal of Materials Processing Technology*, 209(20), 6181–6189. doi:10.1016/j.jmatprotec.2009.05.025
- Fuchs, E. R. H., Field, F. R., Roth, R., & Kirchain, R. E. (2008). Strategic materials selection in the automobile body: Economic opportunities for polymer composite design. *Composites Science and Technology*, 68(9), 1989–2002. doi:10.1016/j.compscitech.2008.01.015
- Furudate, C., & Kunieda, M. (2001). Fundamental study on dry-WEDM. *Journal of Japan Society for Precision Engineering*, 67(7), 1180–1184. doi:10.2493/jjspe.67.1180
- Gamage, J. R., & DeSilva, A. K. M. (2015). Assessment of research needs for sustainability of unconventional machining processes. *Procedia CIRP*, 26, 385–390. doi:10.1016/j.procir.2014.07.096
- Gang, L.I., & Sheng, Z. W. (2007). A special CAD/CAM software for electro-discharge machining of shrouded turbine blisks. *Journal of Shanghai Jiaotong University*, 11(1), 74–78.
- Ganguly, S. (2012). A detailed review of the current research trends in electrical discharge machining (edm). *Proceedings of the National conference on trends and advances in mechanical engineering*, 657–669.
- Gao, Q., Lizarazo-Adarme, J., Paul, B. K., & Haapala, K. R. (2016). An economic and environmental assessment model for microchannel device manufacturing: Part 2–Application. *Journal of Cleaner Production*, 120, 146–156. doi:10.1016/j.jclepro.2015.04.141
- Garbajs, V., & Peklenik, J. (1985). Statistical model for an adaptive control of EDM-process. *Annals CIRP*, 34(1), 499–502. doi:10.1016/S0007-8506(07)61820-4
- Garg, R. K., Singh, K. K., Sachdeva, A., Sharma, V. S., Ojha, K., & Singh, S. (2010). Review of research work in sinking EDM and WEDM on metal matrix composite materials. *International Journal of Advance Manufacturing Technology*, 50, 611–624.
- Garg, R. K., Singh, K. K., Sachdeva, A., Sharma, V. S., Ojha, K., & Singh, S. (2010). Review of research work in sinking EDM and WEDM on metal matrix composite materials. *International Journal of Advanced Manufacturing Technology*, 50(5-8), 611–624. doi:10.1007/00170-010-2534-5
- Gauri, S. K., & Chakraborty, S. (2010). A study on the performance of some multi-response optimisation methods for WEDM processes. *International Journal of Advanced Manufacturing Technology*, 49(1-4), 155–166. doi:10.1007/00170-009-2391-2
- Gauri, S. K., Chakravorty, R., & Chakraborty, S. (2011). Optimization of correlated multiple responses of ultrasonic machining (USM) process. *International Journal of Advanced Manufacturing Technology*, 53(9-12), 1115–1127. doi:10.1007/00170-010-2905-y
- Getu, H., Spelt, J. K., & Papini, M. (2008). Cryogenically assisted abrasive jet micromachining of polymers. *Journal of Micromechanics and Microengineering*, 18(11), 1–8. doi:10.1088/0960-1317/18/11/115010
- Getu, H., Spelt, J. K., & Papini, M. (2011). Thermal analysis of cryogenically assisted abrasive jet micro machining of PDMS. *International Journal of Machine Tools & Manufacture*, 61(9), 721–730. doi:10.1016/j.ijmachtools.2011.05.003
- Ghaderi, M. R., Aghakhani, M., Eslampanah, A., & Ghaderi, K. (2015). The application of imperialist competitive algorithm for optimization of deposition rate in submerged arc welding process using TiO<sub>2</sub> nano particle. *Journal of Mechanical Science and Technology*, 29(1), 357–364. doi:10.1007/12206-014-1242-8

- Ghodsiyeh, D., Golshan, A., Hosseiniyehzad, N., Hashemzadeh, M., & Ghodsiyeh, S. (2012). Optimizing Finishing process in WEDMing of Titanium Alloy (Ti6Al4V) by Zinc Coated Brass Wire based on Response Surface Methodology. *Indian Journal of Science and Technology*, 5(10), 3365–3377.
- Ghodsiyeh, D., Lahiji, M. A., Ghanbari, M., Shirdar, M. R., & Golshan, A. (2012). Optimizing Material Removal Rate (MRR) in WEDMing Titanium alloy (Ti6Al4V) using Taguchi method. *Research Journal of Applied Sciences, Engineering and Technology*, 4(17), 3154–3161.
- Ghodsiyeh, D., Lahiji, M. A., Ghanbari, M., Shirdar, M. R., & Shirdar, M. R. (2012). Optimizing Rough Cut in WEDMing Titanium Alloy (Ti6Al4V) by Brass Wire Using Taguchi Method. *Journal of Basic and Applied Scientific Research*, 2(8), 7488–7496.
- Giboz, J., Copponnex, T., & Mélé, P. (2007). Microinjection molding of thermoplastic polymers: A review. *Journal of Micromechanics and Microengineering*, 17(6), R96–R109. doi:10.1088/0960-1317/17/6/R02
- Gillot, F., Mognol, P., & Furet, B. (2005). Dimensional accuracy studies of copper shells used for electro-discharge machining electrodes made with rapid prototyping and the electroforming process. *Journal of Materials Processing Technology*, 159(1), 33–39. doi:10.1016/j.jmatprotec.2003.11.009
- Gopala Krishna, A., & Prasad, D. V. S. S. V. (2009). Empirical modeling and optimization of wire electrical discharge machining. *International Journal of Advanced Manufacturing Technology*, 43(9-10), 914–925. doi:10.1007/00170-008-1769-x
- Gopalakannan, S., & Senthilvelan, T. (2013). A Parametric Study of Electrical Discharge Machining Process Parameters on Machining of Cast Al/B4C Metal Matrix Nanocomposite. *Proceedings of the Institution of Mechanical Engineers. Part B, Journal of Engineering Manufacture*, 227(7), 993–1004. doi:10.1177/0954405413479505
- Gopalakannan, S., & Senthilvelan, T. (2013). Application of response surface method on machining of Al - SiC nanocomposites. *Measurement*, 46(8), 2705–2715. doi:10.1016/j.measurement.2013.04.036
- Gopalakannan, S., & Senthilvelan, T. (2013). EDM of cast Al/SiC metal matrix nano composites by applying response surface method. *International Journal of Advanced Manufacturing Technology*, 67(1), 485–493. doi:10.1007/00170-012-4499-z
- Gowthaman, S., Balamurugan, K., Kumar, P. M., Ali, S. K. A., Kumar, K. L. M., & Ram Gopal, N. V. (2018). Electrical Discharge Machining studies on Monel- Super Alloy. *Procedia Manufacturing*, 20, 386–391. doi:10.1016/j.promfg.2018.02.056
- Gradeen, A. G., Spelt, J. K., & Papini, M. (2012). Cryogenic abrasive jet machining of polydimethylsiloxane at different temperatures. *Wear*, 274-275, 335–336. doi:10.1016/j.wear.2011.09.013
- Griffiths, C. A., Dimov, S. S., Brousseau, E. B., & Hoyle, R. T. (2007). The effects of tool surface quality in micro-injection moulding. *Journal of Materials Processing Technology*, 189(1–3), 418–427. doi:10.1016/j.jmatprotec.2007.02.022
- Gu, L., Le, L., Zhao, W., & Rajurkar, K. P. (2012). Electrical discharge machining of Ti6Al4V with bundled electrode. *International Journal of Machine Tools & Manufacture*, 53(1), 100–106. doi:10.1016/j.ijmachtools.2011.10.002
- Guo, E. (2014). Surface integrity evolution from main cut to finish trim cut in W-EDM of shape memory alloy. *Procedia CIRP*, 13, 137–142. doi:10.1016/j.procir.2014.04.024
- Habib, S. S. (2009). Study of the parameters in electrical discharge machining through response surface methodology approach. *Applied Mathematical Modelling*, 33(12), 4397–4407. doi:10.1016/j.apm.2009.03.021

## Compilation of References

- Haddag, B., & Nouari, M. (2013). Tool wear and heat transfer analyses in dry machining based on multi-steps numerical modelling and experimental validation. *Wear*, 302(1–2), 1158–1170. doi:10.1016/j.wear.2013.01.028
- Haddag, B., Nouari, M., Barlier, C., & Dhers, J. (2014). Experimental and numerical analyses of the tool wear in rough turning of large dimensions components of nuclear power plants. *Wear*, 312(1–2), 40–50. doi:10.1016/j.wear.2014.02.005
- Hamatani, G., & Ramulu, M. (1990). Machinability of high temperature composites by abrasive waterjet. *Journal of Engineering Materials and Technology*, 112(4), 381–386. doi:10.1115/1.2903346
- Hamid, S., & Ramezanali, M. (2017). A comparative investigation on temperature distribution in electric discharge machining process through analytical, numerical and experimental methods. *International Journal of Machine Tools & Manufacture*, 114, 35–53. doi:10.1016/j.ijmachtools.2016.12.005
- Hanaoka, D., Fukuzawa, Y., Ramirez, C., Minrazo, P., Osend, M. J., & Belmonte, M. (2013). EDM machining of ceramic/carbon nanostructure composites. *Procedia CIRP*, 6, 95–100. doi:10.1016/j.procir.2013.03.033
- Han, F., Chen, L., Yu, D., & Zhou, X. (2007). Basic study on pulse generator for micro-EDM. *International Journal of Advanced Manufacturing Technology*, 33(5), 474–479. doi:10.1007/00170-006-0483-9
- Han, F., Jiang, J., & Yu, D. (2007a). Influence of discharge current on machined surfaces by thermo-analysis in finish cut of WEDM. *International Journal of Machine Tools & Manufacture*, 47(7–8), 1187–1196. doi:10.1016/j.ijmachtools.2006.08.024
- Han, F., Jiang, J., & Yu, D. (2007b). Influence of machining parameters on surface roughness in finish cut of WEDM. *International Journal of Advanced Manufacturing Technology*, 34(5–6), 538–546. doi:10.1007/00170-006-0629-9
- Han, F., Zhang, J., & Soichiro, I. (2007). Corner error simulation of rough cutting in wire EDM. *Precision Engineering*, 31(4), 331–336. doi:10.1016/j.precisioneng.2007.01.005
- Hansch, D., Haff, D., Putz, H., Treusch, H. G., Gillner, A., & Poprawe, R. (1998). Welding of plastics with diode laser. *Proceedings of the 17th International Congress on Applications of Lasers & Electro-Optics*, 131–140.
- Harcuba, P. (2012). Surface treatment by electric discharge machining of Ti-6Al-4V alloy for potential application in orthopaedics. *Journal of the Mechanical Behavior of Biomedical Materials*, 7, 96–105. doi:10.1016/j.jmbbm.2011.07.001 PMID:22340689
- Hascaly, A., & Caydas, U. (2004). Experimental study of wire electrical discharge machining of AISI D5 tool Steel. *Journal of Materials Processing Technology*, 148(3), 362–367. doi:10.1016/j.jmatprotec.2004.02.048
- Hashish, M. (1995). Waterjet machining of advanced composites. *Material and Manufacturing Process*, 10(6), 1129–1152. doi:10.1080/10426919508935098
- Hassan, M. A., Mehat, N. S., Sharif, S., Daud, R., Tomadi, S. H., & Reza, M. S. (2009). Study of Surface Integrity of AISI 4140 Steel in Wire Electrical Discharge Machining. *Proceedings of International Multi Conference of Engineers & Computer Scientists, II*, 1–6.
- Heckele, M., & Schomburg, W. K. (2004). Review on micro molding of thermoplastic polymers. *Journal of Micromechanics and Microengineering*, 14(3), R1–R14. doi:10.1088/0960-1317/14/3/R01
- Herfurth, H., Ehlers, B., Heinemann, S., & Haensch, D. (1999). New approaches in plastic welding with diode lasers. *Proceedings of the 18th International Congress on Applications of Lasers & Electro-Optics*, 48–56.

- Hewidy, M. S., El-Taweel, T. A., & El-Safty, M. F. (2005). Modelling machining parameters of wire electrical discharge machining of Inconel 601 using RSM. *Journal of Materials Processing Technology*, 169(2), 328–336. doi:10.1016/j.jmatprotec.2005.04.078
- Hihara, L. H., & Panquites, I. V. P. (2000). *U.S. Patent No. 6,110,351*. Washington, DC: U.S. Patent and Trademark Office.
- Hlavac, L. M. (2009). Investigation of the Abrasive Water Jet Trajectory Curvature inside the Kerf. *Journal of Materials Processing Technology*, 209(8), 4154–4161. doi:10.1016/j.jmatprotec.2008.10.009
- Hlavac, L. M., Hlavacova, I. M., Geryk, V., & Plancar, S. (2015). Investigation of the taper of kerfs cut in steels by AWJ. *International Journal of Advanced Manufacturing Technology*, 77(9-12), 1811–1818. doi:10.1007/00170-014-6578-9
- Ho, K. H., & Newman, S. T. (2003). State of the art electrical discharge machining (EDM). *International Journal of Machine Tools & Manufacture*, 43(13), 1287–1300. doi:10.1016/S0890-6955(03)00162-7
- Ho, K. H., Newman, S. T., Rahimifard, S., & Allen, R. D. (2004). State of art in wire electrical discharge machining (WEDM). *International Journal of Machine Tools & Manufacture*, 44(12-13), 1247–1259. doi:10.1016/j.ijmachtools.2004.04.017
- Hong, L., Vilar, R. M., & Youming, W. (1997). Laser beam processing of a SiC particulate reinforced 6061 aluminium metal matrix composite. *Journal of Materials Science*, 32(20), 5545–5550. doi:10.1023/A:1018668322943
- Hsue, W. J., Liao, Y. S., & Lu, S. S. (1999). Fundamental geometry analysis of wire electrical discharge machining in corner cutting. *International Journal of Machine Tools & Manufacture*, 39(4), 651–667. doi:10.1016/S0890-6955(98)00046-7
- Hua, J., & Shivpuri, R. (2005). A Cobalt diffusion based model for predicting crater wear of carbide tools in machining titanium alloys. *Journal of Engineering Materials and Technology*, 127(1), 136. doi:10.1115/1.1839192
- Huang, J. T., & Liao, Y. S. (1997). A Study of Finish Cutting Operation Number & Machining Parameters Setting in Wire Electrical Discharge Machining. *Proceedings of International Conference on Precision Machining (ICPE'97)*.
- Huang, J. T., & Liao, Y. S. (2000). A wire-EDM maintenance & fault-diagnosis expert system integrated with an artificial neural network. *International Journal of Production Research*, 38(5), 1071–1082. doi:10.1080/002075400189022
- Huang, J. T., & Liao, Y. S. (2003). Optimization of machining parameters of Wire-EDM based on Grey relational & statistical analyses. *International Journal of Production Research*, 41(8), 1707–1720. doi:10.1080/1352816031000074973
- Huang, J. T., Liao, Y. S., & Hsue, W. J. (1999). Dedurationination of finish-cutting operation number & machining parameters setting in wire electrical discharge machining. *Journal of Materials Processing Technology*, 87(1-3), 69–81. doi:10.1016/S0924-0136(98)00334-3
- Huang, Y. H., Zhao, G. G., Zhang, Z. R., & Yau, C. Y. (1986). The identification & its means of servo feed adaptive control system in WEDM. *Annals CIRP*, 35(1), 121–123. doi:10.1016/S0007-8506(07)61852-6
- Huang, Y., Yu, A., Watt, D., & Baylis, B. (2006). A numerical study of scanning through-transmission laser welding. *Proceedings of Annual Technical Conference – ANTEC 2006*, 2310-2314.
- Hu, C., & Baker, T. N. (1997). A new aluminium silicon carbide formed in laser processing. *Journal of Materials Science*, 32(19), 5047–5051. doi:10.1023/A:1018653030270
- Hu, H. J., & Huang, W. J. (2014). Tool life models of nano ceramic tool for turning hard steel based on FEM simulation and experiments. *Ceramics International*, 40(7), 8987–8996. doi:10.1016/j.ceramint.2014.01.095
- Ilie, M., Cicala, E., Grevey, D., Mattei, S., & Stoica, V. (2009). Diode laser welding of ABS: Experiments and process modeling. *Optics & Laser Technology*, 41(5), 608–614. doi:10.1016/j.optlastec.2008.10.005

## Compilation of References

- Izwan, N. S. L. B., Feng, Z., Patel, J. B., & Hung, W. N. (2016). Prediction of Material Removal Rate in Die-sinking Electrical Discharge Machining. *Procedia Manufacturing*, 5, 658–668. doi:10.1016/j.promfg.2016.08.054
- Jadoun, R. S., Kumar, P., & Mishra, B. K. (2009). Taguchi's optimization of process parameters for production accuracy in ultrasonic drilling of engineering ceramics. *Production Engineering*, 3(3), 243–253. doi:10.1007/11740-009-0164-2
- Jain, V.K. (2005). *Advanced Machining Processes*. Allied Publishers Pvt. Limited.
- Jameson, E. C. (2001). Description & development of electrical discharge machining (EDM). *Electrical Discharge Machining, Society of Manufacturing Engineers*, 2001, 16.
- Jayakumar, N., Yu, Z., & Kamlakar, R. P. (2004). Tool wear compensation and path generation in micro and macro EDM. *Transactions of NAMRI/SME*, 32, 1-8.
- Jennes, M., Dekeyser, W., & Snoeys, R. (1984). Comparison of various approaches to model thermal load on EDM-wire electrode. *Annals CIRP*, 33(1), 93–98. doi:10.1016/S0007-8506(07)61387-0
- Jeswani, M. L. (1981). Effects of the addition of graphite powder to kerosene used as dielectric fluid in electrical discharge machining. *Wear*, 70(2), 133–139. doi:10.1016/0043-1648(81)90148-4
- Jeyapaul, R., Shahabudeen, P., & Krishnaiah, K. (2006). Simultaneous optimization of multi-response problems in Taguchi method using genetic algorithm. *International Journal of Advanced Manufacturing Technology*, 3(9-10), 870–878. doi:10.1007/00170-005-0095-9
- Jha, B., Ram, K., & Rao, M. (2011). An overview of technology and research in electrode design and manufacturing in sinking electrical discharge machining. *Journal of Engineering Science and Technology Review*, 4(2), 118-130.
- Johnson, M. D., & Kirchain, R. E. (2009). Quantifying the effects of product family decisions on material selection: A process-based costing approach. *International Journal of Production Economics*, 120(2), 653–668. doi:10.1016/j.ijpe.2009.04.014
- Kagawa, Y., Utsunomiya, S., & Kogo, Y. (1989). Laser cutting of CVD-SiC fibre/A6061 composite. *Journal of Materials Science Letters*, 8(6), 681–683. doi:10.1007/BF01730441
- Kagnaya, T., Lambert, L., Lazard, M., Boher, C., & Cutard, T. (2014). Investigation and FEA-based simulation of tool wear geometry and metal oxide effect on cutting process variables. *Simulation Modelling Practice and Theory*, 42, 84–97. doi:10.1016/j.simpat.2013.12.009
- Kainth, G. S., Nandy, A., & Singh, K. (1979). On the mechanics of material removal in ultrasonic machining. *International Journal of Machine Tool Design and Research*, 19(1), 33–41. doi:10.1016/0020-7357(79)90019-2
- Kalaiselvan, K., Muruganand, N., & Siva, P. (2011). Production and characterization of AA6061-B<sub>4</sub>C stir cast composite. *Materials & Design*, 32(7), 4004–4009. doi:10.1016/j.matdes.2011.03.018
- Kanlayasiri, K., & Boonmung, S. (2007a). An investigation on effects of wire-EDM machining parameters on surface roughness of newly developed DC53 die steel. *Journal of Materials Processing Technology*, 187-188, 26–29. doi:10.1016/j.jmatprotec.2006.11.220
- Kanlayasiri, K., & Boonmung, S. (2007b). Effects of wire- EDM machining variables on surface roughness of newly developed DC 53 die steel: Design of experiments & regression model. *Journal of Materials Processing Technology*, 192–193, 459–464. doi:10.1016/j.jmatprotec.2007.04.085

- Kansala, H. K., Singh, S., & Kumar, P. (2008). Numerical simulation of Powder Mixed Electric Discharge Machining (PMEDM) using finite element method. *Mathematical and Computer Modelling*, 47(11-12), 1217–1237. doi:10.1016/j.mcm.2007.05.016
- Kansal, H. K., Singh, S., & Kumar, P. (2005). Parametric optimization of powder mixed electrical discharge machining by response surface methodology. *Journal of Materials Processing Technology*, 169(3), 427–436. doi:10.1016/j.jmatprotec.2005.03.028
- Kansal, H. K., Singh, S., & Kumar, P. (2006). Performance parameters optimization (multi-characteristics) of powder mixed electric discharge machining (PMEDM) through Taguchi's method and utility concept. *Indian Journal of Engineering and Materials Sciences*, 13, 209–216.
- Kansal, H. K., Singh, S., & Kumar, P. (2007). Effect of Silicon powder mixed EDM on machining rate of AISI D2 die steel. *Journal of Manufacturing Processes*, 9(1), 13–22. doi:10.1016/S1526-6125(07)70104-4
- Kao, Y. C., Tsao, S. S., & Hsu, Y. (2010). Optimization of the EDM parameters on machining Ti-6Al-4V with multiple quality characteristics. *International Journal of Advanced Manufacturing Technology*, 47(1-4), 395–402. doi:10.1007/00170-009-2208-3
- Kapoor, J., Singh, S., & Khamba, J. S. (2010). Recent developments in wire electrodes for high performance WEDM. *Proceedings of the world congress on engineering*, 2, 1065-1068.
- Karimi, N., Zandieh, M., & Najafi, A. A. (2011). Group scheduling in flexible flow shops: A hybridised approach of imperialist competitive algorithm and electromagnetic-like mechanism. *International Journal of Production Research*, 49(16), 4965–4977. doi:10.1080/00207543.2010.481644
- Karthikeyan, R., Lakshmi Narayanan, P. R., & Naagarazan, R. S. (1999). Mathematical modeling for electric discharge machining of aluminum–silicon carbide particulate composites. *Journal of Materials Processing Technology*, 87(1-3), 59–63. doi:10.1016/S0924-0136(98)00332-X
- Kaynak, Y., Lu, T., & Jawahir, I. S. (2014). Cryogenic machining-induced surface integrity: A review and comparison with dry, mql, and flood-cooled machining. *International Journal of Mining Science and Technology*, 18, 49–198.
- Kechagias, J. (2008). EDM electrodes manufacture using rapid tooling: A review. *Journal of Materials Science*, 43, 2522–2535. doi:10.1007/10853-008-2453-0
- Kern, R. (2007). Techtips. *EDM Today Magazine*, Kinoshita, N., Fukui, M., & Gamo, G. (1982). Control of wire-EDM preventing electrode from breaking, *Annals. CIRP*, 31(1), 111–114.
- Khairy, A. B. E. (1990). Assessment of some dynamic parameters for the ultrasonic machining process. *Wear*, 137(2), 187–198. doi:10.1016/0043-1648(90)90135-W
- Khan, A., & Maity, K. (2017). Application of MCDM-based TOPSIS method for the selection of optimal process parameter in turning of pure titanium. *Benchmarking: An International Journal*, 24(7), 2009–2021. doi:10.1108/BIJ-01-2016-0004
- Kim, J. (1999). Making sense of emergence. *Philosophical Studies*, 95(1), 3–36. doi:10.1023/A:1004563122154
- Kim, S. K. U., Lee, D. G., Lee, W., & Song, O. H. S. (2009). Feasibility Study of Cryogenic Cutting Technology by using a Computer Simulation and Manufacture of Main Components for Cryogenic Cutting System. *Journal of the Korean Radioactive Waste Society*, 7(2), 115–125.
- Kinoshita, N., Fukui, M., Shichida, H., Gamo, G., & Sata, T. (1976). Study on E.D.M. with wire electrode; gap phenomena. *Annals CIRP*, 25, 141–145.

## Compilation of References

- Kinsohita, N., Fukui, M., & Kimura, Y. (1984). Study on Wire-EDM: In process measurement of mechanical behaviour of electrode-wire. *Annals. CIRP*, 33(1), 89–92. doi:10.1016/S0007-8506(07)61386-9
- Kiyak, M., & Cakır, O. (2007). Examination of machining parameters on surface roughness in EDM of tool steel. *Journal of Materials Processing Technology*, 191(1-3), 141–144. doi:10.1016/j.jmatprotec.2007.03.008
- Komaraiah, M., Manan, M. A., Reddy, P. N., & Victor, S. (1988). Investigation of surface roughness and accuracy in ultrasonic machining. *Precision Engineering*, 10(2), 59–65. doi:10.1016/0141-6359(88)90001-3
- Komaraiah, M., & Reddy, P. N. (1993a). A study on the influence of workpiece properties in ultrasonic machining. *International Journal of Machine Tools & Manufacture*, 33(3), 495–505. doi:10.1016/0890-6955(93)90055-Y
- Komaraiah, M., & Reddy, P. N. (1993b). Relative performance of tool materials in ultrasonic machining. *Wear*, 161(1-2), 1–10. doi:10.1016/0043-1648(93)90446-S
- Konda, R., Rajurkar, K. P., Bishu, R. R., Guha, A., & Parson, M. (1999). Design of experiments to study & optimize process performance. *International Journal of Quality & Reliability Management*, 16(1), 56–71. doi:10.1108/02656719910226914
- Konig, W., Aachen, T. H., & Lindenlauf, P. (1978). Surface generation in electrochemical machining. *Annals of the CIRP*, 27(1), 97–100.
- Korean Patent No. 10-1985-0009194
- Kovacevic, R., Hashish, M., Mohan, R., Ramulu, M., Kim, T. J., & Geskin, E. S. (1997). State of the art of research and development in abrasive waterjet machining. *Journal of Manufacturing Science and Engineering*, 119(4B), 776–785. doi:10.1115/1.2836824
- Kozak, J. (1998). Mathematical models for computer simulation of electrochemical machining processes. *Journal of Materials Processing Technology*, 76(1-3), 170–175. doi:10.1016/S0924-0136(97)00333-6
- Kozak, J., Rajurkar, K. P., & Wang, S. Z. (1994). Material removal in WEDM of PCD blanks. *Journal of Engineering for Industry*, 116(3), 363–369. doi:10.1115/1.2901953
- Krolczyk, G. M., Krolczyk, J. B., Maruda, R. W., Legutko, S., & Tomaszewski, M. (2016). Metrological changes in surface morphology of high-strength steels in manufacturing processes. *Measurement*, 88, 176–185. doi:10.1016/j.measurement.2016.03.055
- Kulekci, M. K. (2002). Processes and apparatus developments in industrial waterjet applications. *International Journal of Machine Tools & Manufacture*, 42(12), 1297–1306. doi:10.1016/S0890-6955(02)00069-X
- Kumar, R., Sahani, O.P., & Vashista, M. (2014). Effect of EDM process parameters on tool wear. *Journal of Basic and Applied Engineering Research*, 1(2), 53–56.
- Kumar, A. (2012). Modelling of Micro Wire Electro Discharge Machining (WEDM). In *Aerospace Material*. NIT Rourkela.
- Kumar, A., Kumar, V., & Kumar, J. (2012). Prediction of surface roughness in wire electric discharge machining (WEDM) process base on response surface methodology. *IACSIT International Journal of Engineering and Technology*, 2(4), 708–719.
- Kumar, J., & Khamba, J. S. (2009). An investigation into the effect of work material properties, tool geometry and abrasive properties on performance indices of ultrasonic machining. *International Journal of Machining and Machinability of Materials*, 5(2-3), 347–366. doi:10.1504/IJMMM.2009.023399
- Kumar, J., & Khamba, J. S. (2010). Modeling the material removal rate in ultrasonic machining of titanium using dimensional analysis. *International Journal of Advanced Manufacturing Technology*, 48(1-4), 103–119. doi:10.1007/00170-009-2287-1

- Kumar, J., Khamba, J. S., & Mohapatra, S. K. (2008). An investigation into the machining characteristics of titanium using ultrasonic machining. *International Journal of Machining and Machinability of Materials*, 3(1-2), 143–161. doi:10.1504/IJMMM.2008.017631
- Kung, K. Y., & Chiang, K. T. (2008). Modeling & Analysis of Machinability Evaluation in Wire Electrical Discharge Machining (WEDM) Process of Aluminum Oxide-Based Ceramic. *Materials and Manufacturing Processes*, 23(3), 241–250. doi:10.1080/10426910701860616
- Kunieda, M., Kojima, H., & Kinoshita, N. (1990). On-line detection of EDM spark location by multiple connection of branched electric wires. *Annals. CIRP*, 39(1), 171–174. doi:10.1016/S0007-8506(07)61028-2
- Kuppan, P., Rajadurai, A., & Narayanan, S. (2008). Influence of EDM process parameters in deep hole drilling of Inconel 718. *International Journal of Advance Manufacturing Technology*, 38, 74-84.
- Kuriakose, S., Mohan, K., & Shunmugam, M. S. (2003). Data mining applied to wire-EDM process. *Journal of Materials Processing Technology*, 142(1), 182–189. doi:10.1016/S0924-0136(03)00596-X
- Kuriakose, S., & Shunmugam, M. S. (2004). Characteristics of wire-electro discharge machined Ti6Al4V surface. *Materials Letters*, 58(17-18), 2231–2237. doi:10.1016/j.matlet.2004.01.037
- Kuriakose, S., & Shunmugam, M. S. (2005). Multi-objective optimization of wire electro discharge machining process by Non-Dominated Sorting Genetic Algorithm. *Journal of Materials Processing Technology*, 170(1-2), 133–141. doi:10.1016/j.jmatprotec.2005.04.105
- Kuruville, N., & Ravindra, H. V. (2011). Parametric Influence & Optimization of Wire EDM of Hot Die Steel. *Machining Science & Technology. International Journal (Toronto, Ont.)*, 15(1), 47–75.
- Kuttalamadom, M. (2012). *Prediction of the wear & evolution of cutting tools in a carbide / Ti-6Al-4V machining tribo-system by volumetric tool wear*. Academic Press.
- Lau, W. S., Yue, T. M., & Wang, M. (1994). Ultrasonic-aided laser drilling of aluminium-based metal matrix composites. *CIRP Annals-Manufacturing Technology*, 43(1), 177–180. doi:10.1016/S0007-8506(07)62190-8
- Lavwers, B., Kruth, J. P., Liu, W., Eeraerts, W., Schacht, B., & Bleys, P. (2004). Investigation of MRR mechanism in EDM of composite ceramic material. *Journal of Materials Processing Technology*, 149(1-3), 347–352. doi:10.1016/j.jmatprotec.2004.02.013
- Lee, H. T., & Tai, T. Y. (2003). Relationship between EDM parameters and surface crack formation. *Journal of Materials Processing Technology*, 142(3), 676–683. doi:10.1016/S0924-0136(03)00688-5
- Lee, J. G., & Won, T. (2007). Three-dimensional numerical simulation for anisotropic wet chemical etching process. *Molecular Simulation*, 33(7), 593–597. doi:10.1080/08927020601067508
- Lee, S. H., & Li, X. P. (2007). Study of the effect of machining parameters on the machining characteristics in electrical discharge machining of tungsten carbide. *Journal of Materials Processing Technology*, 115(3), 344–358. doi:10.1016/S0924-0136(01)00992-X
- Lee, T. C., & Chan, C. W. (1997). Mechanism of the ultrasonic machining of ceramic composites. *Journal of Materials Processing Technology*, 71(2), 195–201. doi:10.1016/S0924-0136(97)00068-X
- Liao, Y. S., Chu, Y. Y., & Yan, M. T. (1997). Study of wire breaking process & monitoring of WEDM. *International Journal of Machine Tools & Manufacture*, 37(4), 555–567. doi:10.1016/S0890-6955(95)00049-6



## Compilation of References

- Liao, Y. S., Huang, J. T., & Chen, Y. H. (2004). A study to achieve a fine surface finish in Wire-EDM. *Journal of Materials Processing Technology*, 149(1-3), 165–171. doi:10.1016/j.jmatprotec.2003.10.034
- Liao, Y. S., & Woo, J. C. (1997). The effects of machining settings on behaviour of pulse trains in WEDM process. *Journal of Materials Processing Technology*, 71(3), 433–439. doi:10.1016/S0924-0136(97)82076-6
- Liao, Y. S., & Woo, J. C. (1998). A New Fuzzy Control System for Adaptive Control of WEDM Process. *Proceedings of Twelfth International Symposium for Electro-Machining (ISEM-12)*.
- Liao, Y. S., & Woo, J. C. (2000). Design of a fuzzy control system for adaptive control of WEDM process. *International Journal of Machine Tools & Manufacture*, 40(15), 2293–2307. doi:10.1016/S0890-6955(00)00036-5
- Li, L. (2001). EDM performance of TiC/CU based sintered electrode. *Materials & Design*, 22, 669–678. doi:10.1016/S0261-3069(01)00010-3
- Li, L., Wong, Y. S., Fuh, J. Y. H., & Lu, L. (2001). Effect of TiC in copper Tungsten electrodes on EDM performance. *Journal of Materials Processing Technology*, 113(1-3), 563–567. doi:10.1016/S0924-0136(01)00622-7
- Lin, C. T., Chung, I. F., & Huang, S. Y. (2001). Improvement of machining accuracy by fuzzy logic at corner parts of wire-EDM. *Fuzzy Sets and Systems*, 122(3), 499–511. doi:10.1016/S0165-0114(00)00034-8
- Lindroos, V. K., & Talvitie, M. J. (1995). Recent advances in metal matrix composites. *Journal of Materials Processing Technology*, 53(1-2), 273–284. doi:10.1016/0924-0136(95)01985-N
- Lin, J. L., Wang, K. S., Yan, B. H., & Tarng, Y. S. (2000). Optimization of electrical discharge machining process based on Taguchi method with fuzzy logics. *Journal of Materials Processing Technology*, 102(1-3), 48–55. doi:10.1016/S0924-0136(00)00438-6
- Liou, A. C., & Chen, R. H. (2006). Injection molding of polymer micro- and sub-micron structures with high-aspect ratios. *International Journal of Advanced Manufacturing Technology*, 28(11–12), 1097–1103. doi:10.1007/00170-004-2455-2
- Liu, H., Liu, W., Meng, D., & Wang, X. (2016). Simulation and experimental study of laser transmission welding considering the influence of interfacial contact status. *Materials & Design*, 92, 246–260. doi:10.1016/j.matdes.2015.12.049
- Liu, J. W., Wu, Y.-Z., & Yue, T.-M. (2015). High Speed Abrasive Electrical Discharge Machining of Particulate Reinforced Metal Matrix Composites. *International Journal of Precision Engineering and Manufacturing*, 16(7), 1399–1404. doi:10.1007/12541-015-0184-0
- Liu, J. W., Yue, T. M., & Guo, Z. N. (2013). Grinding-aided electrochemical discharge machining of particulate reinforced metal matrix composites. *International Journal of Advanced Manufacturing Technology*, 68(9-12), 2349–2357. doi:10.1007/00170-013-4846-8
- Liu, L., Zhuang, Z., Liu, F., & Zhu, M. (2013). Additive manufacturing of steel-bronze bimetal by shaped metal deposition: Interface characteristics and tensile properties. *International Journal of Advanced Manufacturing Technology*, 69(9), 2131–2137. doi:10.1007/00170-013-5191-7
- Liu, Q., Zhang, Q., Zhu, G., Wang, K., Zhang, J., & Dong, C. (2016). Effect of electrode size on the performances of Micro EDM. *Materials and Manufacturing Processes*, 31(4), 391–396. doi:10.1080/10426914.2015.1059448
- Liu, X., Kang, X., Zhao, W., & Liang, W. (2013). Electrode feeding path searching for 5-axis EDM of integral shrouded blisks. *Procedia CIRP*, 6, 107–111. doi:10.1016/j.procir.2013.03.041

- Li, Z. L., Zheng, H. Y., Lim, G. C., Chu, P. L., & Li, L. (2010). Study on UV laser machining quality of carbon fibre reinforced composites. *Composites. Part A, Applied Science and Manufacturing*, 41(10), 1403–1408. doi:10.1016/j.compositesa.2010.05.017
- Lok, Y. K., & Lee, T. C. (1999). Processing of advanced ceramics using the Wire-Cut EDM process. *Journal of Materials Processing Technology*, 63(1-3), 839–843. doi:10.1016/S0924-0136(96)02735-5
- Lonardo, P. M., & Bruzzone, A. A. (1999). Effect of flushing and electrode material on die sinking EDM. *Annals of the CIRP*, 48(1), 123–126. doi:10.1016/S0007-8506(07)63146-1
- Lopez J.G., Verleysen P., & Degrieck, J. (2012). Effect of fatigue damage on static & dynamic tensile behavior of electro-discharge machined Ti-6Al-4V. *Journal of Fatigue & Fracture & Engineering Materials & Structures*, 35(12), 1120-1132.
- Lotfi, M., Jahanbakhsh, M., & Akhavan Farid, A. (2016). Wear estimation of ceramic and coated carbide tools in turning of Inconel 625: 3D FE analysis. *Tribology International*, 99, 107–116. doi:10.1016/j.triboint.2016.03.008
- Luciano, A. M., Fred, L. A., & Walter, L. W. (2014). Automated system for the measurement of spark current and electric voltage in wire EDM performance. *Journal of Brazilian Society of Science and Engineering*.
- Lungu, N., & Borzan, M. (2012). *Effect of cutting speed and feed rate on tool geometry, temperature and cutting forces in machining Aisi 1045 carbon steel using FEMsimulation*. Academic Press.
- Luo, Y.F. (1999). Rupture failure & mechanical strength of electrode wire used in wire EDM. *J. Mater. Process. Technology*, 94(2–3), 208–215.
- Lu, Y., Wang, T., Wang, C., & Wang, C. (2012). Empirical Modeling of High-speed WEDM Finishing in Gas. *Advanced Materials Research*, 486, 503–508. doi:10.4028/www.scientific.net/AMR.486.503
- Mahajan, K. R., Knoppers, G. E., Oosterling, J. A. J., & Lutervelt, C. A. (2004). Knowledge based design of EDM electrodes for mould cavities pre-machined by high-speed milling. *Journal of Materials Processing Technology*, 149(1-3), 71–76. doi:10.1016/j.jmatprotec.2004.02.007
- Mahapatra, S. S., & Patnaik, A. (2006). Optimization of wire electrical discharge machining (WEDM) process parameters using Taguchi method. *International Journal of Advance Manufacturing Technology*, 34, 911-925.
- Mahapatra, S. S., & Patnaik, A. (2006). Optimization of Wire Electrical Discharge Machining (WEDM) process parameters using genetic algorithm. *Indian Journal of Engineering and Materials Sciences*, 13, 494–502.
- Mahapatra, S. S., & Patnaik, A. (2006a). Optimization of wire electrical discharge machining (WEDM) process parameters using Taguchi method. *International Journal of Advanced Manufacturing Technology*, 34(9-10), 911–925. doi:10.1007/00170-006-0672-6
- Mahapatra, S. S., & Patnaik, A. (2006b). Parametric Optimization of Wire Electrical Discharge Machining (WEDM) Process using Taguchi Method. *Journal of Brazilian Society of Mechanical Sciences & Engineering*, 8(4), 422–429. doi:10.1590/S1678-58782006000400006
- Mahendran, S., Devarajan, R., Nagarajan, T., & Majdi, A. (2010). A Review of Micro-EDM. *Proceeding of international multi conference of engineers and computer scientist*, 2, 981-986.
- Maheshwera, U., Paturi, R., Kumar, S., & Narala, R. (2015). Finite element analysis and study of tool wear in machining with coated tool. *Imece2013-64342*.

## Compilation of References

- Mahmood, T., Mian, A., Amin, M. R., Auner, G., Witte, R., Herfurth, H., & Newaz, G. (2007). Finite element modeling of transmission laser microjoining process. *Journal of Materials Processing Technology*, 186(1-3), 37–44. doi:10.1016/j.jmatprotec.2006.11.225
- Maity, K. P., & Swain, P. K. (2008). An experimental investigation of hot-machining to predict tool life. *Journal of Materials Processing Technology*, 198(1–3), 344–349. doi:10.1016/j.jmatprotec.2007.07.018
- Majeed, M. A., Vijayaraghavan, L., Malhotra, S. K., & Krishnamoorthy, R. (2008). AE monitoring of ultrasonic machining of Al<sub>2</sub>O<sub>3</sub>/LaPO<sub>4</sub> composites. *Journal of Materials Processing Technology*, 207(1-3), 321–329. doi:10.1016/j.jmatprotec.2008.06.039
- Marafona, J., & Wykes, C. (2000). A new method of optimising material removal rate using EDM with copper–tungsten electrodes. *International Journal of Machine Tools & Manufacture*, 40(2), 153–164. doi:10.1016/S0890-6955(99)00062-0
- Markov, A. I. (1966). *Ultrasonic machining of intractable materials*. London: Iliffe Books Ltd.
- Masuzawa, T. (2000). State of the Art of Micromachining. *CIRP Annals - Manufacturing Technology*, 49(2), 473–488. 10.1016/S0007-8506(07)63451-9
- Masuzawa, T., Cui, X., & Taniguchi, N. (1992). Improved jet flushing for EDM. *CIRP Annals - Manufacturing Technology*, 41(1), 239–242.
- Matin, R., Shabgard, M. R., & Barzegar, R. (2015). Effect of electrode shape configuration on tool steel (DIN1.2379) in Electrical Discharge Machining (EDM). *National Conference on Economics, Management and Accounting*.
- Mayboudi, L. S., Birk, A. M., Zak, G., & Bates, P. J. (2005). A 2-D thermal model for laser transmission welding of thermoplastics. *Proceedings of the 24th International Congress on Applications of Lasers & Electro-Optics*, 402–409.
- Mayboudi, L. S., Birk, A. M., Zak, G., & Bates, P. J. (2007). Laser transmission welding of a lap-joint: Thermal imaging observations and Three-dimensional finite element modeling. *Journal of Heat Transfer*, 129(9), 1177–1186. doi:10.1115/1.2740307
- Meena, V. K., & Nagahanumaiah. (2006). Optimization of EDM machining parameters using DMLS electrode. *Rapid Prototyping Journal*, 12(4), 222–228. doi:10.1108/13552540610682732
- Misal, N. D., & Sadaiah, M. (2013). Comparison of Design of Experiments and Gray Rational Analysis of Photochemical Machining. *International Journal of Innovations in Engineering and Technology*, 3, 121–126.
- Misal, N. D., & Sadaiah, M. (2017). Investigation on Surface Roughness of Inconel 718 in Photochemical Machining. *Advances in Materials Science and Engineering*.
- Misal, N. D., Saraf, A. R., & Sadaiah, M. (2017). Experimental investigation of surface topography in photochemical machining of Inconel 718. *Materials and Manufacturing Processes*, 32(15), 1756–1763. doi:10.1080/10426914.2017.1317786
- Mitchell, M. (2000). *Design and microfabrication of a molded polycarbonate continuous flow polymerase chain reaction device* (Master thesis). Louisiana State University.
- Mizugaki, Y. (1996). Contouring electrical discharge machining with on-machine measuring and dressing of a cylindrical graphite electrode. *Proceedings of the IEEE IECON, 22nd International conference on industrial electronics, control, and instrumentation*, 1514–1517. 10.1109/IECON.1996.570608
- Mohammadi, A., Tehrani, A. F., & Abdullah, A. (2013). Introducing a new technique in wire electric discharge turning & evaluating ultrasonic vibration on MRR. *Procedia CIRP*, 6, 583–588. doi:10.1016/j.procir.2013.03.005

- Mohapatra, K., & Sahoo, S. (2018). A multi objective optimization of gear cutting in WEDM of Inconel 718 using TOPSIS method. *Decision Science Letters*, 7(2), 157–170. doi:10.5267/j.dsl.2017.6.002
- Mohri, N., Yamada, H., Furutani, K., Narikiyo, T., & Magara, T. (1998). System identification of wire electrical discharge machining. *Ann. CIRP*, 47(1), 173–176. doi:10.1016/S0007-8506(07)62811-X
- Montgomery, D. C. (2009). *Design & Analysis of Experiments* (7th ed.). John Wiley & Sons (Asia) Pte Ltd.
- Moses, M. D., & Jahan, M. P. (2015). Micro-EDM machinability of difficult-to-cut Ti-6Al-4V against soft brass. *International Journal of Advance Manufacturing Technology*, 81(5), 1345–1361.
- Mozafari, H., Abdi, B., & Ayob, A. (2012). Optimization of adhesive-bonded fiber glass strip using imperialist competitive algorithm. *Procedia Technology*, 1, 194–198. doi:10.1016/j.protcy.2012.02.036
- Mudigonda, S., & Patil, D. H. (2015, June). Some investigations on surface texturing on monel 400 using photochemical machining. In *ASME 2015 International Manufacturing Science and Engineering Conference* (pp. V001T02A045–V001T02A045). American Society of Mechanical Engineers. 10.1115/MSEC2015-9294
- Muju, M. K., & Pathak, A. K. (1988). Abrasive jet machining of glass at low temperature. *Journal of Mechanical Working Technology*, 17, 325–332. doi:10.1016/0378-3804(88)90034-4
- Mukherjee, R., Chakraborty, S., & Samanta, S. (2012). Selection of wire electrical discharge machining process parameters using non-traditional optimization algorithms. *Applied Soft Computing*, 12(8), 2506–2516. doi:10.1016/j.asoc.2012.03.053
- Müller, F., & Monaghan, J. (2000). Non-conventional machining of particle reinforced metal matrix composite. *International Journal of Machine Tools & Manufacture*, 40(9), 1351–1366. doi:10.1016/S0890-6955(99)00121-2
- Munz, M., Risto, M., & Haas, R. (2013). Specifics of flushing in electrical discharge drilling. *Procedia CIRP*, 6, 83–88. doi:10.1016/j.procir.2013.03.024
- Narender Singh, P., Raghukandan, K., Rathinasabapathi, M., & Pai, B. C. (2004). Electric discharge machining of Al–10%SiCP as-cast metal matrix composites. *Journal of Materials Processing Technology*, 155–156, 1653–1657. doi:10.1016/j.jmatprotec.2004.04.321
- Nishikawa, M., & Kunieda, M. (2009). Prediction of wire-EDMed surface shape by in-process measurement of wire electrode behavior. *Journal of Japan Society for Precision Engineering*, 75(9), 1078–1082. doi:10.2493/jjspe.75.1078
- Noordin, M. Y., Venkatesh, V. C., Sharif, S., Elting, S., & Abdullah, A. (2004). Application of response surface methodology in describing performance of coated carbide tools when turning AISI 1045 steel. *Journal of Materials Processing Technology*, 145(1), 46–58. doi:10.1016/S0924-0136(03)00861-6
- Obara, H., Iwata, Y., & Ohsumi, T. (1995). An Attempt to Detect Wire Temperature Distribution During Wire EDM. *Proceedings of Eleventh International symposium for Electro-Machining (ISEM-11)*.
- Ohadi, M. M., Ansari, A. I., & Hashish, M. (1992). Thermal distributions in the workpiece during cutting with an abrasive waterjet. *Journal of Manufacturing Science and Engineering*, 114(1), 67–73. doi:10.1115/1.2899760
- Oliaei, S. N. B., & Karpat, Y. (2016). Investigating the influence of built-up edge on forces and surface roughness in micro scale orthogonal machining of titanium alloy Ti6Al4V. *Journal of Materials Processing Technology*, 235, 28–40. doi:10.1016/j.jmatprotec.2016.04.010
- Orbanic, H., & Junkar, M. (2008). Analysis of striation formation mechanism in abrasive water jet cutting. *Wear*, 265(5–6), 821–830. doi:10.1016/j.wear.2008.01.018

## Compilation of References

- Osman, H. M., & Abdel-Rahman, M. (1993). Integrity of surfaces produced by electrochemical machining. *Journal of Materials Processing Technology*, 37(1-4), 667–677. doi:10.1016/0924-0136(93)90126-Q
- Ouyang, P. R., Tjiptoprodjo, R. C., Zhang, W. J., & Yang, G. S. (2008). Micro-motion devices technology: The state of arts review. *International Journal of Advanced Manufacturing Technology*, 38(5–6), 463–478. doi:10.1007/00170-007-1109-6
- Özel, T. (2009). Computational modelling of 3D turning: Influence of edge micro-geometry on forces, stresses, friction and tool wear in PcBN tooling. *Journal of Materials Processing Technology*, 209(11), 5167–5177. doi:10.1016/j.jmatprotec.2009.03.002
- Pal, S., Pal, S. K., & Samantaray, A. K. (2008). Artificial neural network modeling of weld joint strength prediction of a pulsed metal inert gas welding process using arc signals. *Journal of Materials Processing Technology*, 202(1-3), 464–474. doi:10.1016/j.jmatprotec.2007.09.039
- Pandit, S. M., & Wittig, W. H. (1984). A data-dependent systems approach to optimal microcomputer control illustrated by EDM. *Journal of Engineering for Industry*, 106(2), 137–142. doi:10.1115/1.3185924
- Parashar V., Rehman, A., Bhagoria, J.L.(2012). Performance Measurement & Data Analysis of Material Removal Rate for Wire Cut Electro Discharge Machining Process. *Applied Mechanics & Materials*, 110-116, 1683-1690.
- Parashar, V., Rehman, A., Bhagoria, J. L., & Puri, Y. M. (2010). Kerfs width analysis for wire cut electro discharge machining of SS 304L using design of experiments. *Indian Journal of Science and Technology*, 3(4), 369–373.
- Parida A. K., (2010). Analytical and numerical modeling of hot machining of Inconel. *American Journal of Mechanical and Materials Engineering*, 71(8), 49–57. 10.11648/j.ajmme.20170104.11
- Parida, A. K. (2017). *Heat assisted machining of nickel base alloys: Experimental and numerical analysis*. PhD Thesis.
- Parida, A. K., & Maity, K. (2017). Effect of nose radius on forces, and process parameters in hot machining of Inconel 718 using finite element analysis. *Engineering Science and Technology, an International Journal*, 4–10. 10.1016/j.jestch.2016.10.006
- Parida, A. K., & Maity, K. P. (2016). Finite element method and experimental investigation of hot turning of Inconel 718. *Advanced Engineering Forum*.
- Parida, A. K. (2018). Analysis of chip geometry in hot machining of Inconel 718 Alloy. *Iranian Journal of Science and Technology. Transaction of Mechanical Engineering*. doi:10.1007/40997-018-0146-0
- Parida, A. K., & Maity, K. P. (2016). Optimization in hot turning of nickel based alloy using desirability function analysis. *International Journal of Engineering Research in Africa*, 24, 64–70. . doi:10.4028/www.scientific.net/JERA.24.64
- Parida, A. K., & Maity, K. P. (2016). Optimization of multi-responses in hot turning of Inconel 625 alloy using DEA-Taguchi approach. *International Journal of Engineering Research in Africa*, 24, 57–63. . doi:10.4028/www.scientific.net/JERA.24.57
- Patel, K. M., Pulak, M., Pandey, & Venkateswara Rao, P. (2009). Determination of an optimum parametric combination using a surface roughness prediction model for EDM of  $\text{Al}_2\text{O}_3/\text{SiCw}/\text{TiC}$  ceramic composite. *Journal of Materials and Manufacturing Process*, 24, 675-682.
- Patel, D., & Tandon, P. (2015). Experimental Investigations of thermally enhanced abrasive water jet machining of hard-to-machine metals. *CIRP Journal of Manufacturing Science and Technology*, 10, 92–101. doi:10.1016/j.cirpj.2015.04.002

- Patel, K. J. (2004). Quantitative evaluation of abrasive contamination in ductile material during abrasive water jet machining and minimizing with a nozzle head oscillation technique. *International Journal of Machine Tools & Manufacture*, 44(10), 1125–1132. doi:10.1016/j.ijmachtools.2003.12.007
- Patil, D. H., & Mudigonda, S. (2016). The effect of the rolling direction, temperature, and etching time on the photochemical machining of monel 400 microchannels. *Advances in Materials Science and Engineering*.
- Patil, D. H., & Mudigonda, S. (2017). Investigation on effect of grain orientation in photochemical machining of Monel 400. *Materials and Manufacturing Processes*, 32(16), 1831–1837. doi:10.1080/10426914.2017.1291953
- Peças, P., Henriques, E., & Ribeiro, I. (2010). Integrated approach to product and process design based on life cycle engineering. In *Handbook of Research on Trends in Product Design and Development: Technological and Organizational Perspectives*. Academic Press. doi:10.4018/978-1-61520-617-9.ch021
- Pecas, P., & Henriques, E. (2003). Influence of silicon powder-mixed dielectric on conventional electrical discharge machining. *International Journal of Machine Tools & Manufacture*, 43(14), 1465–1471. doi:10.1016/S0890-6955(03)00169-X
- Peças, P., Ribeiro, I., Folgado, R., & Henriques, E. (2009). A Life Cycle Engineering model for technology selection: A case study on plastic injection moulds for low production volumes. *Journal of Cleaner Production*, 17(9), 846–856. doi:10.1016/j.jclepro.2009.01.001
- Peças, P., Ribeiro, I., Silva, A., & Henriques, E. (2013). Comprehensive approach for informed life cycle-based materials selection. *Materials & Design*, 43. doi:10.1016/j.matdes.2012.06.064
- Peronczyk, J. (2011). Selected problems of electrical discharge machining (edm) of metal composite materials applied in manufacturing of mechanical vehicles. *Journal of KONES Power Train and Transport*, 18(1), 429–442.
- Pervaiz, S. (2015). *Numerical and experimental investigations of the machinability of Ti6Al4V*. PhD Thesis.
- Pham, D. T., Dimov, S. S., Bigot, S., Ivanov, A., & Popov, K. (2004). Micro-EDM - Recent developments and research issues. *Journal of Materials Processing Technology*, 149, 50–57. doi:10.1016/j.jmatprotec.2004.02.008
- Pham, D. T., Dimov, S. S., & Petkov, P. V. (2007). Laser milling of ceramic components. *International Journal of Machine Tools & Manufacture*, 47(3-4), 618–626. doi:10.1016/j.ijmachtools.2006.05.002
- Ponappa, K., Aravindan, S., Rao, P. V., Ramkumar, J., & Gupta, M. (2010). The effect of process parameters on machining of magnesium nano alumina composites through EDM. *International Journal of Advance Manufacturing Technology*, 46, 1035–1042.
- Poro's, D., & Zaborski, S. (2009). Semi-empirical model of efficiency of wire electrical discharge machining of hard-to-machine materials. *Journal of Materials Processing Technology*, 209(3), 1247–1253. doi:10.1016/j.jmatprotec.2008.03.046
- Potente, H., Korte, J., & Becker, F. (1999). Laser transmission welding of thermoplastics: Analysis of heating phase. *Journal of Reinforced Plastics and Composites*, 18(10), 914–920. doi:10.1177/073168449901801005
- Pradhan, M. K., Das, R., & Biswas, C. K. (2009). Comparisons of neural network models on surface roughness in electrical discharge machining. *Proceedings of the Institution of Mechanical Engineers. Part B, Journal of Engineering Manufacture*, 223(7), 801–808. doi:10.1243/09544054JEM1367
- Pramanik, A., Islam, M. N., Basak, A., & Littlefair, G. (2013). Machining and tool wear mechanisms during machining titanium alloys. *Advanced Materials Research*, 651, 338–343. doi:10.4028/www.scientific.net/AMR.651.338

## Compilation of References

- Pramanik, A., Neo, K. S., Rahman, M., Li, X. P., Sawa, M., & Maeda, Y. (2009). Ultraprecision turning of electroless nickel: Effects of crystal orientation and origin of diamond tools. *International Journal of Advanced Manufacturing Technology*, 43(7-8), 681–689. doi:10.1007/00170-008-1748-2
- Pramanik, A., Zhang, L. C., & Arsecularatne, J. A. (2006). Prediction of cutting forces in machining of metal matrix composites. *International Journal of Machine Tools & Manufacture*, 46(14), 1795–1803. doi:10.1016/j.ijmachtools.2005.11.012
- Pramanik, A., Zhang, L. C., & Arsecularatne, J. A. (2007). An FEM investigation into the behavior of metal matrix composites: Tool–particle interaction during orthogonal cutting. *International Journal of Machine Tools & Manufacture*, 47(10), 1497–1506. doi:10.1016/j.ijmachtools.2006.12.004
- Praneetpong, C., Fakuzawa, Y., Nagasawa, S., & Yamashita, K. (2010). Effect of Edm Combined Ultrasonic Vibration on machining properties of Si<sub>3</sub>N<sub>4</sub>. *Materials Transactions*, 51(11), 2113–2120. doi:10.2320/matertrans.M2010194
- Prasad, A. V. S. R., Ramji, K., & Datta, G.L. (2014). An experimental study of wire EDM on Ti-6Al-4V alloy. *Procedia Materials Science*, 5, 2567-2576.
- Puri, A. B., & Bhattacharyya, B. (2003). An analysis & optimization of geometrical inaccuracy due to wire lag phenomenon in WEDM. *International Journal of Machine Tools & Manufacture*, 43(2), 151–159. doi:10.1016/S0890-6955(02)00158-X
- Puri, A. B., & Bhattacharyya, B. (2005). Modeling & analysis of white layer depth in a wire-cut EDM process through response surface methodology. *International Journal of Advanced Manufacturing Technology*, 25(67), 301–307. doi:10.1007/00170-003-2045-8
- Rahman, M. M., Md. Khan, A. R., Kadirgama, K., Noor, M. M., & Baskar, R. A. (2010). Modeling of material removal on machining of Ti-6Al-4V through EDM copper tungsten electrode and positive polarity. *International Journal of Mechanical and Materials Engineering*, 3, 135–140.
- Rajurkar, K. P. (1994). Non-traditional Manufacturing Processes. In *Handbook of Design, Manufacturing and Automation*. Wiley.
- Rajurkar, K. P., & Hewidy, M. S. (1988). Effect of grain size on ECM performance. *Journal of Mechanical Working Technology*, 17, 315-324.
- Rajurkar, K. P., Sundaram, M. M., & Malshe, A. P. (2013). Review of electrochemical and electro discharge machining. *Procedia CIRP*, 6, 13–26. doi:10.1016/j.procir.2013.03.002
- Rajurkar, K. P., & Wang, W. M. (1993). Thermal modeling & on-line monitoring of wire-EDM. *Journal of Materials Processing Technology*, 38(1-2), 417–430. doi:10.1016/0924-0136(93)90214-Q
- Rajurkar, K. P., & Wang, W. M. (1997). Improvement of EDM performance with advanced monitoring & control systems. *Journal of Manufacturing Science and Engineering*, 119(4B), 770–775. doi:10.1115/1.2836823
- Rajurkar, K. P., Wang, W. M., & Lindsay, R. P. (1990). Real-time stochastic model & control of EDM. *Annals CIRP*, 39(1), 187–190. doi:10.1016/S0007-8506(07)61032-4
- Rajurkar, K. P., Wang, W. M., & Lindsay, R. P. (1991). On-line monitor & control for wire breakage in WEDM. *Annals CIRP*, 40(1), 219–222. doi:10.1016/S0007-8506(07)61972-6
- Rajurkar, K. P., Wang, W. M., & McGeough, J. A. (1994). WEDM identification & adaptive control for variable-height components. *Annals CIRP*, 43(1), 199–202. doi:10.1016/S0007-8506(07)62195-7
- Rajurkar, K. P., Wang, W. M., & Zhao, W. S. (1997). WEDM-adaptive control with a multiple input model for identification of work-piece height. *Annals CIRP*, 46(1), 147–150. doi:10.1016/S0007-8506(07)60795-1

- Ramakrishnan, R., & Karunamoorthy, L. (2006). Multi response optimization of wire EDM operations using robust design of experiments. *International Journal of Advanced Manufacturing Technology*, 29(1-2), 105–112. doi:10.1007/00170-004-2496-6
- Ramulu, M., & Arola, D. (1993). Water jet and abrasive water jet cutting of unidirectional graphite/epoxy composite. *Composites*, 24(4), 299–308. doi:10.1016/0010-4361(93)90040-F
- Ranganathan, S., Senthilvelan, T., & Sriram, G. (2010). Evaluation of machining parameters of hot turning of stainless steel (Type 316) by applying ANN and RSM. *Materials and Manufacturing Processes*, 25(10), 1131–1141. doi:10.1080/10426914.2010.489790
- Rao, P. S., Ramji, K., & Satyanarayana, B. (2011). Effect of WEDM Conditions on Surface Roughness: A Parapmetric Optimization Using Taguchi Method. *International Journal of Advanced Engineering Sciences & Technologies*, 6, 41–48.
- Rao, R. V., & Kalyankar, V. D. (2013). Parameter optimization of modern machining processes using teaching--learning-based optimization algorithm. *Engineering Applications of Artificial Intelligence*, 26(1), 524–531. doi:10.1016/j.engappai.2012.06.007
- Rao, R. V., Pawar, P. J., & Davim, J. P. (2010). Parameter optimization of ultrasonic machining process using nontraditional optimization algorithms. *Materials and Manufacturing Processes*, 25(10), 1120–1130. doi:10.1080/10426914.2010.489788
- Rathod, V., Doloi, B., & Bhattacharyya, B. (2014). Experimental investigations into machining accuracy and surface roughness of microgrooves fabricated by electrochemical micromachining. *Proceedings of the Institution of Mechanical Engineers. Part B, Journal of Engineering Manufacture*, 229(10), 1781–1802. doi:10.1177/0954405414539486
- Reitz, W., & Pendray, J. (2001). Cryo processing of materials: A review of current status. *Materials and Manufacturing Processes*, 16(6), 829–840. doi:10.1081/AMP-100108702
- Reza, M. S., Azmir, M. A., Tomadi, S. H., Hassan, M. A., & Daud, R. (2010). Effects of polarity parameter on machining of tool steel workpiece using electrical discharge machining. *National conference in mechanical engineering research and postgraduate students*, 621–626.
- Ribeiro, I., Kaufmann, J., Schmidt, A., Peças, P., Henriques, E., & Götze, U. (2016). Fostering selection of sustainable manufacturing technologies - A case study involving product design, supply chain and life cycle performance. *Journal of Cleaner Production*, 112, 3306–3319. doi:10.1016/j.jclepro.2015.10.043
- Ribeiro, I., Peças, P., & Henriques, E. (2013). Incorporating tool design into a comprehensive life cycle cost framework using the case of injection molding. *Journal of Cleaner Production*, 53, 297–309. doi:10.1016/j.jclepro.2013.04.025
- Ribeiro, I., Peças, P., Silva, A., & Henriques, E. (2008). Life cycle engineering methodology applied to material selection, a fender case study. *Journal of Cleaner Production*, 16(17), 1887–1899. doi:10.1016/j.jclepro.2008.01.002
- Russek, U. A., Aden, M., Poehler, J., Palmen, A., & Staub, H. (2004). Laser beam welding of thermoplastics parameter influence on weld seam quality - Experiments and Modeling. *Proceedings of the 23rd International Congress on Applications of Lasers & Electro-Optics*.
- Sadeghpour-Motlagh, M., Mokhtari-Zonouzi, K., Aghajani, H., & Kakroudi, M. G. (2014). Effects of etching time and NaOH concentration on the production of alumina nanowires using porous anodic alumina template. *Journal of Materials Engineering and Performance*, 23(6), 2007–2014. doi:10.1007/11665-014-1011-y



## Compilation of References

- Sahli, M., Millot, C., Roques-Carmes, C., Khan Malek, C., Barriere, T., & Gelin, J. C. (2009). Quality assessment of polymer replication by hot embossing and micro-injection moulding processes using scanning mechanical microscopy. *Journal of Materials Processing Technology*, 209(18–19), 5851–5861. doi:10.1016/j.jmatprotec.2009.06.011
- Sahu, A. K., Mahapatra, S. S., & Chatterjee, S. (2017). Optimization of electro-discharge coating process using harmony search. In *International Conference on Materials, Manufacturing and Modelling (ICMMM)*. VIT University.
- Sahu, A. K., Chatterjee, S., Nayak, P. K., & Mahapatra, S. S. (2018, March). Study on effect of tool electrodes on surface finish during electrical discharge machining of Nitinol. *IOP Conference Series. Materials Science and Engineering*, 338(1), 012033. doi:10.1088/1757-899X/338/1/012033
- Sahu, A. K., Mohanty, P. P., & Sahoo, S. K. (2017). *Electro discharge machining of Ti-alloy (Ti6Al4V) and 316L Stainless Steel and Optimization of process parameters by Grey relational analysis (GRA) method*. In *Advances in 3D Printing & Additive Manufacturing Technologies* (pp. 65–78). Singapore: Springer.
- Sahu, J., Mohanty, C. P., & Mahapatra, S. S. (2013). A DEA Approach for Optimization of Multiple Responses in Electrical Discharge Machining of AISI D2 Steel. *Procedia Engineering*, 51, 585–591. doi:10.1016/j.proeng.2013.01.083
- Sait, A. N., Aravindan, S., & Haq, A. N. (2009). Optimisation of machining parameters of glass-fibre-reinforced plastic (GFRP) pipes by desirability function analysis using Taguchi technique. *International Journal of Advanced Manufacturing Technology*, 43(5-6), 581–589. doi:10.1007/00170-008-1731-y
- Sanchez-Salmeron, A. J., Lopez-Tarazon, R., Guzman-Diana, R., & Ricolfe-Viala, C. (2005). Recent development in micro-handling systems for micro-manufacturing. *Journal of Materials Processing Technology*, 167(2-3), 499–507. doi:10.1016/j.jmatprotec.2005.06.027
- Saraf, A. R., & Sadaiah, M. (2013). Application of artificial intelligence for the prediction of undercut in photochemical machining. *International Journal of Mechatronics and Manufacturing Systems*, 6(2), 183–194. doi:10.1504/IJMMS.2013.053829
- Saraf, A. R., & Sadaiah, M. (2017). Magnetic field-assisted photochemical machining (MFAPCM) of SS316L. *Materials and Manufacturing Processes*, 32(3), 327–332. doi:10.1080/10426914.2016.1198014
- Saraf, A. R., & Sadaiah, M. (2017). Photochemical machining of a novel cardiovascular stent. *Materials and Manufacturing Processes*, 32(15), 1740–1746. doi:10.1080/10426914.2016.1198025
- Sarkar, S., Mitra, S., & Bhattacharyya, B. (2005). Parametric analysis & optimization of wire electrical discharge machining of  $\gamma$ -titanium aluminide alloy. *Journal of Materials Processing Technology*, 159(3), 286–294. doi:10.1016/j.jmatprotec.2004.10.009
- Sarkar, S., Sekh, M., Mitra, S., & Bhattacharyya, B. (2008). Modeling & optimization of wire electrical discharge machining of  $\gamma$ -TiAl in trim cutting operation. *Journal of Materials Processing Technology*, 205(1-3), 376–387. doi:10.1016/j.jmatprotec.2007.11.194
- Satishkumar, D., Kanthababu, M., Vajjiravelu, V., Anburaj, R., Thirumalai Sundarajan, N., & Arul, H. (2011). Investigation of wire electrical discharge machining characteristics of Al6063/SiCp composites. *International Journal of Advanced Manufacturing Technology*, 56(9-12), 975–986. doi:10.1007/00170-011-3242-5
- Satyanarayana, A., & Reddy, B. G. K. (1984). Design of velocity transformers for ultrasonic machining. *Electrical India*, 24(14), 11–20.
- Savrun, E., & Taya, M. (1988). Surface characterization of SiC whisker/2124 aluminium and Al<sub>2</sub>O<sub>3</sub> composites machined by abrasive water jet. *Journal of Materials Science*, 23(4), 1453–1458. doi:10.1007/BF01154616

- Scott, D., Boyina, S., & Rajurkar, K. P. (1991). Analysis & optimization of parameter alloy in wire electrical discharge machining. *International Journal of Production Research*, 29(11), 2189–2207. doi:10.1080/00207549108948078
- Sen, M., & Shan, H. S. (2005). Analysis of hole quality characteristics in the electro jet drilling process. *International Journal of Machine Tools & Manufacture*, 45(15), 1706–1716. doi:10.1016/j.ijmachtools.2005.03.005
- Senthilkumar, C., Ganesan, G., & Karthikeyan, R. (2009). Study of electrochemical machining characteristics of Al/SiC p composites. *International Journal of Advanced Manufacturing Technology*, 43(3-4), 256–263. doi:10.100700170-008-1704-1
- Senthilkumar, V., & Uday Omprakash, B. (2011). Effect of titanium carbide particles addition in the aluminum composite on EDM process parameters. *Journal of Manufacturing Processes*, 13(1), 60–66. doi:10.1016/j.jmapro.2010.10.005
- Senthil, P., Vinodh, S., & Singh, A. K. (2014). Parametric optimisation of EDM on Al-Cu/TiB<sub>2</sub> in-situ metal matrix composites using TOPSIS method. *International Journal of Machining and Machinability of Materials*, 16(1), 80–94. doi:10.1504/IJMMM.2014.063922
- Shaban, A., Mahnken, R., Wilke, L., Potente, H., & Ridder, H. (2007). Simulation of rate dependant plasticity for polymers with asymmetric effects. *International Journal of Solids and Structures*, 44(18-19), 6148–6162. doi:10.1016/j.ijsolstr.2007.02.017
- Shabgard, M., Ahmadi, R., Seyedzavvar, M., & Samad, N. B. O. (2013). Mathematical and Numerical modeling of the Effect of Input-parameters on the Flushing Efficiency of Plasma Channel in EDM process. *International Journal of Machine Tools & Manufacture*, 65, 79–87. doi:10.1016/j.ijmachtools.2012.10.004
- Shah, A. A., Hasan, F., Hameed, A., & Ahmed, S. (2008). Biological degradation of plastics: A comprehensive review. *Biotechnology Advances*, 26(3), 246–265. doi:10.1016/j.biotechadv.2007.12.005 PMID:18337047
- Shah, A., Mufti, A. N., Rakwal, D., & Bamberg, E. (2011). Material Removal Rate, Kerf, & Surface Roughness of Tungsten Carbide Machined with Wire Electrical Discharge Machining. *Journal of Materials Engineering and Performance*, 20(1), 71–76. doi:10.100711665-010-9644-y
- Shanmugam, D. K., Chen, F. L., Siores, E., & Brandt, M. (2002). Comparative study of jetting machining technologies over laser machining technology for cutting composite materials. *Composite Structures*, 57(1-4), 289–296. doi:10.1016/S0263-8223(02)00096-X
- Shoda, K., Kaneko, Y., Nishimura, H., Kunieda, M., & Fan, M. X. (1992). Adaptive Control of WEDM with On-line Detection of Spark Locations. *Proceeding of Tenth International Symposium for Electro-Machining(ISEM-10)*.
- Shokrani, A., Dhokia, V., Munoz-Escalona, P., & Newman, S. T. (2013). State-of-the-art cryogenic machining and processing. *International Journal of Computer Integrated Manufacturing*, 26(7), 616–648. doi:10.1080/0951192X.2012.749531
- Shorowordi, K. M., Haseeb, A., & Celis, J. P. (2006). Tribo-surface characteristic B<sub>4</sub>C and Al-SiC composites worn under different contact pressures. *Wear*, 261(5-6), 634–641. doi:10.1016/j.wear.2006.01.023
- Sidhu, S. S., Batish, A., & Kumar, S. (2013). Fabrication and electrical discharge machining of metal-matrix composites: A review. *Journal of Reinforced Plastics and Composites*, 32(17), 1310–1320. doi:10.1177/0731684413489366
- Singaravel, B., & Selvaraj, T. (2016). Application of desirability function analysis and utility concept for selection of optimum cutting parameters in turning operation. *Journal of Advanced Manufacturing Systems*, 15(01), 1–11. doi:10.1142/S0219686716500013
- Singh, H., & Singh, A. (2013). Effect of pulse on/pulse off on machining of steel using cryogenic treated copper electrode. *International Journal of Engineering Research and Development*, 5(12), 29-34.

## Compilation of References

- Singh, B., Singh, P., Tejpal, G., & Singh, G. (2012). An experimental study of surface roughness of H-11 in EDM process using copper tool electrode. *International Journal of Advances in Engineering and Technology*, 3(4), 30–33.
- Singh, H., & Garg, R. (2009). Effects of process parameters on material removal rate in WEDM. *Journal of Achievements in Materials & Manufacturing Engineering*, 32, 70–74.
- Singh, H., & Singh, A. (2012). Effect of pulse on / pulse off time on machining of AISI D3 die steel using copper and brass electrode in EDM. *Journal of Engineering and Science*, 1(9), 19–22.
- Singh, J., & Gill, S. S. (2009). Fuzzy modeling and simulation of ultrasonic drilling of porcelain ceramic with hollow stainless steel tools. *Materials and Manufacturing Processes*, 24(4), 468–475. doi:10.1080/10426910802714407
- Singh, N. P., Raghukandan, K., & Pai, B. C. (2004). Optimization by Grey relational analysis of EDM parameters on machining Al–10% SiCP composites. *Journal of Materials Processing Technology*, 155–156.
- Singh, P. (2010). Some experimental investigation on aluminum powder mixed EDM on machining performance of hastelloy steel. *International Journal of Advances in Engineering and Technology*, 1(2), 28–45.
- Singh, R., & Khamba, J. S. (2007). Taguchi technique for modeling material removal rate in ultrasonic machining of titanium. *Materials Science and Engineering A*, 460, 365–369. doi:10.1016/j.msea.2007.01.093
- Singh, R., & Khamba, J. S. (2008). Mathematical modelling of surface roughness in ultrasonic machining of titanium using Buckingham-II approach: A review. *International Journal of Abrasive Technology*, 2(1), 3–24. doi:10.1504/IJAT.2009.021635
- Singh, S., & Bhardwaj, A. (2011). Review to EDM by Using Water and Powder-Mixed Dielectric Fluid. *Journal of Minerals & Materials Characterization & Engineering*, 10(2), 199–230. doi:10.4236/jmmce.2011.102014
- Sinha, S. K. (2010). Effects of Wire Lag in Wire Electrical Discharge Machining. *International Journal of Engineering Science and Technology*, 2(11), 6622–6625.
- Skrabalaka, G. (2013). Optimization of dry EDM milling process. *Procedia CIRP*, 6, 332–337. doi:10.1016/j.procir.2013.03.027
- Snoeys, R., Dauw, D. F., & Kruth, J. P. (1983). Survey of EDM adaptive control in electro discharge machining. *Journal of Manufacturing Systems*, 2(2), 147–164. doi:10.1016/S0278-6125(83)80028-4
- Snoeys, R., Dekeyser, W., & Tricarico, C. (1998). Knowledge-based system for wire EDM. *Annals CIRP*, 37(1), 197–202. doi:10.1016/S0007-8506(07)61617-5
- Sohani, M. S., Gaitonde, V. N., Siddeswarappa, B., & Deshpande, A. S. (2009). Investigations into the effect of tool shapes with size factor consideration in sink electrical discharge machining (EDM) process. *International Journal of Advance Manufacturing Technology*, 45, 1131–1145.
- Sorkhel, S. K., & Bhattacharyya, B. (1994). Parametric control for optimal quality of the workpiece surface in ECM. *Journal of Materials Processing Technology*, 40(3-4), 271–286. doi:10.1016/0924-0136(94)90455-3
- Spedding, T. A., & Wang, Z. Q. (1997a). Study on modeling of wire EDM process. *Journal of Materials Processing Technology*, 69(1-3), 18–28. doi:10.1016/S0924-0136(96)00033-7
- Spedding, T. A., & Wang, Z. Q. (1997b). Parametric optimization & surface characterization of wire electrical discharge machining process. *Precision Engineering*, 20(1), 5–15. doi:10.1016/S0141-6359(97)00003-2
- Spekaa, M., Mattei, S., Pilloza, M., & Iliea, M. (2008). The infrared thermography control of the laser welding of amorphous polymers. *NDT & E International*, 41(3), 178–183. doi:10.1016/j.ndteint.2007.10.005

- Stucker, B. E., Bradley, W.L., Eubank, P.T., Norasetthekul, S., & Bozkurt, B. (1997). Zirconium Diboride/Copper EDM electrodes from selective laser sintering. *Proceedings of the solid free form fabrication symposium*, 257-265.
- Stucker, B. E., Bradley, W. L., Norasetthekul, S., & Eubank, P. T. (1995). The production of electrical discharge machining electrodes using SLS: Preliminary results. *Proceedings of the solid free form fabrication symposium*, 278-286.
- Sultan, T., Kumar, A., & Gupta, R. D. (2014). Material removal rate, electrode wear rate, and surface roughness evaluation in die sinking EDM with hollow tool through response surface methodology. *Journal of Manufacturing Engineering*, 259, 1–16.
- Suresh Kumar, S., Uthayakumar, M., Thirumalai Kumaran, S., & Parameswaran, P. (2014). Electrical Discharge Machining of Al (6351)–SiC–B<sub>4</sub>C Hybrid Composite. *Materials and Manufacturing Processes*, 29(11-12), 1395–1400. doi:10.1080/10426914.2014.952024
- Suresh Kumar, S., Uthayakumar, M., Thirumalai Kumaran, S., Parameswaran, P., & Mohandas, E. (2014). Electrical Discharge Machining of Al (6351)-5% SiC-10% B<sub>4</sub>C hybrid composite: A Grey Relational approach. *Modelling and Simulation in Engineering*, 2014, 7. doi:10.1155/2014/426718
- Swain, A.K., Ray, S., & Mandal, N.K., (2012). Study on Kerf Width in Wire-EDM based on Taguchi Method. *Applied Mechanics & Materials*, 110-116, 1808-1816.
- Taha, M. A. (2001). Practicalization of cast metal matrix composites. *Materials & Design*, 22(6), 431–441. doi:10.1016/S0261-3069(00)00077-7
- Taha, Z. A., Roy, G. G., Hajim, K. I., & Mannaa, I. (2009). Mathematical modeling of laser-assisted transmission lap welding of polymers. *Scripta Materialia*, 60(8), 663–666. doi:10.1016/j.scriptamat.2008.12.041
- Tanabe, R., Ito, Y., Mohri, N., & Masuzawa, T. (2011). *Development of peeling tool for micro-EDM* (Vol. 60). CIRP Annals - Manufacturing Technology.
- Tang, Y., Hong, J., Zhou, H., & Lu, B. (2005). A new technique for the fabrication of graphite EDM electrodes. *Journal of Materials Processing Technology*, 166(2), 199–204. doi:10.1016/j.jmatprotec.2004.08.019
- Tanimura, T., Heuvelman, C. J., & Vennstra, P. C. (1977). The properties of servo gap sensor with wire spark-erosion machining. *Annals CIRP*, 26(1), 59–63.
- Tao, J., Shih, A. J., & Ni, J. (2008). Experimental study of the dry and near dry electrical discharge milling processes. *Journal of Manufacturing Science and Engineering*, 130(1), 1–9. doi:10.1115/1.2784276
- Tarng, Y. S., Ma, S. C., & Chung, L. K. (1995). Dedurationination of optimal cutting parameters in wire electrical discharge machining. *International Journal of Machine Tools & Manufacture*, 35(12), 1693–170. doi:10.1016/0890-6955(95)00019-T
- Tay, F., & Haider, E. (2001). The potential of plating techniques in the development of rapid EDM tooling. *International Journal of Advance Manufacturing Technology*, 18, 892-896.
- Teicher, U., Müller, S., Münzner, J., & Nestler, A. (2013). Micro-EDM of carbon fibre-reinforced plastics. *Procedia CIRP*, 6, 320–325. doi:10.1016/j.procir.2013.03.092
- Thandra, S. K., & Choudhury, S. K. (2010). Effect of cutting parameters on cutting force, surface finish and tool wear in hot machining. *International Journal of Machining and Machinability of Materials*, 7(3/4), 278. doi:10.1504/IJMMM.2010.033070

## Compilation of References

- Thirumalai Kumaran, S., & Uthayakumar, M. (2014). Investigation on the machining studies of AA6351-SiC-B<sub>4</sub>C hybrid metal matrix composites. *International Journal of Machining and Machinability of Materials*, 15(3/4), 174–185. doi:10.1504/IJMMM.2014.060548
- Torres, A., Luis, C. J., & Puertas, I. (2015). Analysis of the influence of EDM parameters on surface finish, material removal rate, and electrode wear of an INCONEL 600 alloy. *The International Journal of Advance Manufacturing Technology*, 80(1), 123–140.
- Torres, A., Puertas, I., & Luis, C. J. (2015). Modelling of surface finish, electrode wear and material removal rate in electrical discharge machining of hard-to-machine alloys. *Precision Engineering*, 40, 33–45. doi:10.1016/j.precisioneng.2014.10.001
- Tosun, N. (2002). A study of tool life in hot machining using artificial neural networks and regression analysis method. *Journal of Materials Processing Technology*, 124, 99–104.
- Tosun, N., Cogunb, C., & Tosun, G. (2004). A study on kerf & material removal rate in wire electrical discharge machining based on Taguchi method. *Journal of Materials Processing Technology*, 152(3), 316–322. doi:10.1016/j.jmatprotec.2004.04.373
- Tosun, N., & Cogun, C. (2003). An investigation on wire wear in WEDM. *Journal of Materials Processing Technology*, 134(3), 273–278. doi:10.1016/S0924-0136(02)01045-2
- Tosun, N., Cogun, C., & Inan, A. (2003). The Effect of Cutting Parameters on Workpiece Surface Roughness in Wire EDM. *Machining Science & Technology. International Journal (Toronto, Ont.)*, 7(2), 209–219.
- Tosun, N., & Ozler, L. (2004). Optimisation for hot turning operations with multiple performance characteristics. *International Journal of Advanced Manufacturing Technology*, 23(11–12), 777–782. doi:10.1007/00170-003-1672-4
- Tracht, K., Weikert, F., & Hanke, T. (2012). Suitability of the ISO 10303-207 standard for product modeling of line linked micro parts. In *Procedia CIRP* (Vol. 3, pp. 358–363). Academic Press. doi:10.1016/j.procir.2012.07.062
- Tripathy, S., & Tripathy, D. K. (2016). Multi-attribute optimization of machining process parameters in powder mixed electro-discharge machining using TOPSIS and grey relational analysis. *Engineering Science and Technology, an International Journal*, 19(1), 62–70.
- Tripathy, S., & Tripathy, D. K. (2017). Grey Relational Analysis and its application on surface properties during EDM and Powder Mixed EDM. *Journal of Engineering Science and Technology*, 12(9), 2374–2392.
- Tripathy, S., & Tripathy, D. K. (2017). Multi-response optimization of machining process parameters for powder mixed electro-discharge machining using grey relational analysis and topsis. *Machining Science and Technology*, 21(3), 362–384. doi:10.1080/10910344.2017.1283957
- Tripathy, S., & Tripathy, D. K. (2017). Surface Characterization and Multi-response optimization of EDM process parameters using powder mixed dielectric. *Materials Today: Proceedings*, 4(2), 2058–2067. doi:10.1016/j.matpr.2017.02.051
- Tsai, Y. Y., Masuzawa, T., & Fujino, M. (2001). Investigations on electrode wear in micro EDM. *International symposium for electromachining XIII*, 2, 719–726.
- Tsai, H. C., Yan, B. H., & Huang, F. Y. (2003). EDM performance of Cr/Cu-based composite electrodes. *International Journal of Machine Tools & Manufacture*, 43(3), 245–252. doi:10.1016/S0890-6955(02)00238-9
- Tsunemoto, K., Kazuhiro, K., & Katsuo, S. (2000). Studies of Micro Ice Jet Machining. *The Japan Society of Mechanical Engineers*, 2, 99–100.

- Uhlář, R., Hlaváč, L., Gembalová, L., Jonšta, P., & Zuchnický, O. (2013). Abrasive Water Jet Cutting of the Steels Samples Cooled by Liquid Nitrogen. *Applied Mechanics and Materials*, 308, 7–12. doi:10.4028/www.scientific.net/AMM.308.7
- Uhlmann, E., Von Der Schulenburg, M. G., & Zettier, R. (2007). Finite element modeling and cutting simulation of inconel 718. *CIRP Annals - Manufacturing Technology*, 56(1), 61–64. 10.1016/j.cirp.2007.05.017
- Urbanovich, L. I., Kramchenkov, E. M., & Chunosov, Y. N. (1992). Investigation of low temperature gas-abrasive erosion. *Soviet Journal of Friction and Wear*, 13, 80–83.
- US Patent No. 14,927-1979
- US Patent No. 1896613-1933
- US Patent No. 20070295695 US Patent No. 4,686,153-87
- US Patent No. 4,968,867-90
- US Patent No. 4,998,552-91
- US Patent No. 4287404-1981
- US patent No. 4935594-90
- US Patent No. 5,762,726-98
- US Patent No. 5,945,010-97
- US Patent No. 5196665-90
- US Patent No. 6875943-2005
- Usui, E., Shirakashi, T., & Kitagawa, T. (1978). Analytical prediction of three dimensional cutting Process—Part 3: Cutting temperature and crater wear of carbide tool. *Journal of Manufacturing Science and Engineering*, 100(2), 236–243. doi:10.1115/1.3439415
- Valentincic, J., Brissaud, D., & Junkar, M. (2007). A novel approach to DFM in toolmaking: A case study. *International Journal of Computer Integrated Manufacturing*, 20(1), 28–38. doi:10.1080/09511920600667333
- Vamsi, K. P., Surendra, B. B., Madar, V. P., & Swapna, M. (2010). Optimizing Surface Finish in WEDM Using Taguchi Parameter Design Method. *Journal of the Brazilian Society of Mechanical Sciences and Engineering*, 32(2), 107–113.
- Van de Ven, J. D., & Erdman, A. G. (2007). Laser transmission welding of thermoplastics — Part I: Temperature and pressure modeling. *Journal of Manufacturing Science and Engineering*, 129(5), 849–858. doi:10.1115/1.2752527
- Velten, T., Schuck, H., Haberer, W., & Bauerfeld, F. (2010). Investigations on reel-to-reel hot embossing. *International Journal of Advanced Manufacturing Technology*, 47(1–4), 73–80. doi:10.100700170-009-1975-1
- Venkata Rao, R., Pawar, P. J., & Davim, J. P. (2009). Optimisation of process parameters of mechanical type advanced machining processes using a simulated annealing algorithm. *International Journal of Materials & Product Technology*, 37(1-2), 83–101.
- Verdian, M. M. (2017). *Comprehensive Materials Finishing*. Comprehensive Materials Finishing. doi:10.1016/B978-0-12-803581-8.09200-6
- Wagh, D. V., & Dolas, D. R. (2016). Multi Response Optimization of Process Parameters in PCM of Inconel 600 Using Desirability Function Approach of RSM. *International Journal of Engine Research*, 5(2), 127–130.

## Compilation of References

- Wagh, D. V., Dolas, D. R., & Dhagate, M. D. (2014). Experimental investigation of photochemical machining on Inconel 600 using ferric chloride. *International Journal of Engineering Research & Technology*, 4(2), 289–293.
- Wang, C. C., Chowm, H. M., Yang, L. D., & Te Lu, C. (2009). Recast layer removal after electrical discharge machining via Taguchi analysis: A feasibility study. *Journal of Materials Processing Technology*, 209(8), 4134–4140. doi:10.1016/j.jmatprotec.2008.10.012
- Wang, C. C., & Yan, B. H. (2000). Blind-hole drilling of  $\text{Al}_2\text{O}_3/6061\text{Al}$  composite using rotary electro-discharge machining. *Journal of Materials Processing Technology*, 102(1-3), 90–102. doi:10.1016/S0924-0136(99)00423-9
- Wangikar, S. S., Patowari, P. K., & Misra, R. D. (2016, December). Parametric Optimization for Photochemical Machining of Copper Using Grey Relational Method. In *Techno-Societal 2016, International Conference on Advanced Technologies for Societal Applications* (pp. 933-943). Springer.
- Wangikar, S. S., Patowari, P. K., & Misra, R. D. (n.d.). Numerical and experimental investigations on the performance of a serpentine microchannel with semicircular obstacles. *Microsystem Technologies*, 1-14.
- Wangikar, S.S., Patowari, P.K., & Misra, R.D. (2018). Parametric Optimization for Photochemical Machining of Copper using Overall Evaluation Criteria. *Materials Today Proceedings*. doi:10.1016/j.matpr.2017.12.046 (accepted for publication)
- Wangikar, S. S., Patowari, P. K., & Misra, R. D. (2017). Effect of process parameters and optimization for photochemical machining of brass and German silver. *Materials and Manufacturing Processes*, 32(15), 1747–1755. doi:10.1080/10426914.2016.1244848
- Wang, J., & Ravani, B. (2003). Computer aided contouring operation for travelling wire electric discharge machining (EDM). *Computer Aided Design*, 35(10), 925–934. doi:10.1016/S0010-4485(02)00207-5
- Wang, T., & Kunieda, M. (2004). Dry WEDM for Finish Cut. *Key Engineering Materials*, 259-260, 562–566. doi:10.4028/www.scientific.net/KEM.259-260.562
- Wang, T., Lu, Y. M., Hao, S. S., Xie, S. Q., Xu, X. C., & Wang, Y. (2009). Dry WEDM in Improving HS-WEDMed Surface Quality. *Key Engineering Materials*, 392-394, 624–628. doi:10.4028/www.scientific.net/KEM.392-394.624
- Wang, T., Xie, S. Q., Xu, X. C., Chen, Q., Lu, X. C., & Zhou, S. H. (2012). Application of Uniform Design in Experiments of WEDM in Gas. *Advanced Materials Research*, 426, 11–14. doi:10.4028/www.scientific.net/AMR.426.11
- Wang, T., Zhang, X., & Zhao, X. (2006). Study on Finishing Cut with Dry WEDM. *Materials Science Forum*, 532-533, 273–276. doi:10.4028/www.scientific.net/MSF.532-533.273
- Wang, T., Zhang, X., & Zhao, X. (2008). Study on Dry WEDMed Surface Quality of Mould Steel. *Key Engineering Materials*, 375-376, 416–420. doi:10.4028/www.scientific.net/KEM.375-376.416
- Watanabe, H., Sato, T., Suzuki, I., & Kinoshita, N. (1990). WEDM monitoring with a statistical pulse-classification method, *Annals. CIRP*, 39(1), 175–178. doi:10.1016/S0007-8506(07)61029-4
- Wei, C., Zhao, L., Hu, D., & Ni, J. (2013). Electrical discharge machining of ceramic matrix composites with ceramic fiber reinforcements. *International Journal of Advanced Manufacturing Technology*, 64(1), 187–194. doi:10.1007/00170-012-3995-5
- Wong, Y. S., Rahman, M., Lim, H. S., Han, H., & Ravi, N. (2003). Investigation of micro-EDM material removal characteristics using single RC pulse discharges. *Journal of Materials Processing Technology*, 140(1-3), 303–307. doi:10.1016/S0924-0136(03)00771-4

- Worgull, M. (2009). Hot embossing: theory and technology of microreplication. *Annals of Physics*, 54. 10.1016/B978-0-8155-1579-1.50001-X
- Wu, B., Wu, X., Lei, J., Xu, B., Ruan, S., & Zhong, J. (2017). Study on machining 3D micro mould cavities using reciprocating micro ECM with queued foil microelectrodes. *Journal of Materials Processing Technology*, 241, 120–128. doi:10.1016/j.jmatprotec.2016.11.011
- Wu, K. L., Yan, B. H., Huang, F. Y., & Chen, S. C. (2005). Improvement of surface finish on SKD steel using electro-discharge machining with aluminum and surfactant added dielectric. *International Journal of Machine Tools & Manufacture*, 45(10), 1195–1201. doi:10.1016/j.ijmachtools.2004.12.005
- Wüthrich, R., & Fascio, V. (2005). Machining of non-conducting materials using electrochemical discharge phenomenon—an overview. *International Journal of Machine Tools & Manufacture*, 45(9), 1095–1108. doi:10.1016/j.ijmachtools.2004.11.011
- Xiaopeng, L., Yonghong, L., & Renjie, J. (2012). A new method for electrical discharge machining of non-conductive engineering ceramics. *Proceedings of 2<sup>nd</sup> International conference on electronic and mechanical engineering and information technology*, 1266-1269.
- Xie, L. J., Schmidt, J., Schmidt, C., & Biesinger, F. (2005). 2D FEM estimate of tool wear in turning operation. *Wear*, 258(10), 1479–1490. doi:10.1016/j.wear.2004.11.004
- Xu, C. S. (2012). Working Principle & Performance of Wire Electrical Discharge Machining. *Advanced Materials Research*, 507, 180–183. doi:10.4028/www.scientific.net/AMR.507.180
- Yadav, R. K., Abhishek, K., & Mahapatra, S. S. (2015). A simulation approach for estimating flank wear and material removal rate in turning of Inconel 718. *Simulation Modelling Practice and Theory*, 52, 1–14. doi:10.1016/j.simpat.2014.12.004
- Yadav, R. P., & Teli, S. N. (2014). A Review of issues in photochemical machining. *International Journal of Modern Engineering Research*, 4(7), 49–53.
- Yan, B. H., & Wang, C. C. (1999). The machining characteristics of Al<sub>2</sub>O<sub>3</sub>/6061Al composite using rotary electro-discharge machining with a tube electrode. *Journal of Materials Processing Technology*, 95(1-3), 222–231. doi:10.1016/S0924-0136(99)00322-2
- Yang, B., & Leu, M. C. (1999). Integration of rapid prototyping and electroforming for tooling application. *Annals of the CIRP*, 48(1), 119–123. doi:10.1016/S0007-8506(07)63145-X
- Yan, M. T., & Huang, P. H. (2004). Accuracy improvement of wire-EDM by real-time wire tension control. *International Journal of Machine Tools & Manufacture*, 44(7-8), 807–814. doi:10.1016/j.ijmachtools.2004.01.019
- Yan, M. T., & Laio, Y. S. (1998). Adaptive control of WEDM process using fuzzy control strategy. *Journal of Manufacturing Systems*, 17(4), 263–274. doi:10.1016/S0278-6125(98)80074-5
- Yan, M. T., & Liao, Y. S. (1995). Adaptive Control of WEDM Process Using Fuzzy Control Strategy. *Proceedings of Eleventh International Symposium for Electro-Machining (ISEM-11)*.
- Yan, M. T., & Liao, Y. S. (1996). A self-learning fuzzy controller for wire rupture prevention in WEDM. *International Journal of Advanced Manufacturing Technology*, 11(4), 267–275. doi:10.1007/BF01351284
- Yan, M. T., & Liao, Y. S. (1996). Monitoring & self-learning fuzzy control for wire rupture prevention in wire electrical discharge machining. *International Journal of Machine Tools & Manufacture*, 36(3), 339–353. doi:10.1016/0890-6955(95)00050-X



## Compilation of References

- Yan, M. T., Liao, Y. S., & Chang, C. C. (2001). On-line estimation of work-piece height using neural networks & hierarchical adaptive control of WEDM. *International Journal of Advanced Manufacturing Technology*, 18(12), 884–891. doi:10.1007/PL00003956
- Yan, M. T., Li, H. P., & Liang, J. F. (1999). The application of fuzzy control strategy in servo feed control of wire electrical discharge machining. *International Journal of Advanced Manufacturing Technology*, 15(11), 780–784. doi:10.1007/001700050131
- Yarlagadda, P. K. D. V., Christodoulou, P., & Subramanian, V. S. (1999). Feasibility studies on the production of electro-discharge machining electrodes with rapid prototyping and the electroforming process. *Journal of Materials Processing Technology*, 89-90, 231–237. doi:10.1016/S0924-0136(99)00072-2
- Yazdipour, A., & Ghaderi, M. R. (2014). Optimization of weld bead geometry in gtaw of cp titanium using imperialist competitive algorithm. *International Journal of Advanced Manufacturing Technology*, 72(5-8), 619–625. doi:10.1007/00170-014-5682-1
- Yen, Y.-C., Söhner, J., Lilly, B., & Altan, T. (2004). Estimation of tool wear in orthogonal cutting using the finite element analysis. *Journal of Materials Processing Technology*, 146(1), 82–91. doi:10.1016/S0924-0136(03)00847-1
- Younis, A.M., Gouda, M., Mahmoud, F., & Abd Allah, A.S. (2015). Effect of electrode material on electrical discharge machining of tool steel surface. *Ain Shams Engineering Journal*, 6(3), 977-986.
- Yuangang, W., Fuling, Z., & Jin, W. (2009). Wear-resist Electrodes for Micro-EDM. *Chinese Journal of Aeronautics*, 22(3), 339–342. doi:10.1016/S1000-9361(08)60108-9
- Yuan, J., Liu, C. L., Liu, X., Wang, K., & Yu, T. (2009). Incorporating prior model into Gaussian processes regression for WEDM process modeling. *Expert Systems with Applications*, 36(4), 8084–8092. doi:10.1016/j.eswa.2008.10.048
- Yue, C. X., Liu, X. L., Pen, H. M., Hu, J. S., & Zhao, X. F. (2009). 2D FEM estimate of tool wear in hard cutting operation: Extractive of interrelated parameters and tool wear simulation result. *Advanced Materials Research*, 69–70, 316–321. . doi:10.4028/www.scientific.net/AMR.69-70.316
- Yue, T. M., & Lau, W. S. (1996). Pulsed Nd: YAG laser cutting of Al/Li/SiC metal matrix composites. *Materials and Manufacturing Processes*, 11(1), 17–29. doi:10.1080/10426919608947458
- Yunxiao, H., Zhidong, L., Zhongli, C., Linglei, K., & Mingbo, Q. (2018). Mechanism study of the combined process of electrical discharge machining ablation and electrochemical machining in aerosol dielectric. *Journal of Materials Processing Technology*, 254, 221–222. doi:10.1016/j.jmatprotec.2017.11.025
- Yu, P. H., Lin, Y.-X., Lee, H.-K., Mai, C.-C., & Yan, B.-H. (2011). Improvement of wire electrical discharge machining efficiency in machining polycrystalline silicon with auxiliary-pulse voltage supply. *International Journal of Advanced Manufacturing Technology*, 57(9-12), 991–1001. doi:10.1007/00170-011-3350-2
- Yu, P.-H., Lee, H.-K., Lin, Y.-X., Qin, S.-J., Yan, B.-H., & Huang, F.-Y. (2011). Machining Characteristics of Polycrystalline Silicon by Wire Electrical Discharge Machining. *Materials and Manufacturing Processes*, 26(12), 1443–1450. doi:10.1080/10426914.2010.544808
- Yuvaraj, N., & Pradeep Kumar, M. (2016). Cutting of aluminium alloy with abrasive water jet and cryogenic assisted abrasive water jet: A comparative study of the surface integrity approach. *Wear*, 362-363, 18–32. doi:10.1016/j.wear.2016.05.008
- Yuvaraj, N., & Pradeep Kumar, M. (2017a). Surface integrity studies on abrasive water jet cutting of AISI D2 Steel. *Materials and Manufacturing Processes*, 32(2), 162–170. doi:10.1080/10426914.2016.1221093

- Yuvaraj, N., & Pradeep Kumar, M. (2017b). Study and evaluation of abrasive water jet cutting performance on AA5083-H32 aluminum alloy by varying the jet impingement angles with different abrasive mesh sizes. *International Journal of Mining Science and Technology*, 21(3), 385–415.
- Zhang, G., Guo, Y., & Wang, L. (2016). Experimental study on the machining of inclined holes for thermal barrier-coated nickel super alloys by EDM. *Journal of Materials Engineering and Performance*, 25(10), 4574–4580. doi:10.1007/11665-016-2287-x
- Zhang, J., & Meng, Y. (2012). A study of surface texturing of carbon steel by photochemical machining. *Journal of Materials Processing Technology*, 212(10), 2133–2140. doi:10.1016/j.jmatprotec.2012.05.018
- Zhang, L. (2011). A Survey on Electrode Materials for Electrical Discharge Machining, Advances in Materials Manufacturing Science and Technology XIV. *Materials Science Forum*, 495, 697–698.
- Zhang, Q. H., Du, R., Zhang, J. H., & Zhang, Q. (2006). An investigation of ultrasonic-assisted electrical discharge machining in gas. *International Journal of Machine Tools & Manufacture*, 46(12-13), 1582–1588. doi:10.1016/j.ijmachtools.2005.09.023
- Zhang, X. Y., Wang, D., & Li, X. J. (2012). Comparison study for finished accuracy of WEDM process. *Advanced Materials Research*, 479-481, 476–480. doi:10.4028/www.scientific.net/AMR.479-481.476
- Zhang, Y. M., Chen, Y., Li, P., & Male, A. T. (2003). Weld deposition-based rapid prototyping: A preliminary study. *Journal of Materials Processing Technology*, 135(2), 347–357. doi:10.1016/S0924-0136(02)00867-1
- Zhao, J., Li, Y., Zhang, J., Yu, C., & Zhang, Y. (2003). Analysis of the wear characteristics of an EDM electrode made by selective laser sintering. *Journal of Materials Processing Technology*, 138(1-3), 475–478. doi:10.1016/S0924-0136(03)00122-5
- Zhao, J., Yang, M. K. G., & Yuan, X. M. (2010). Performance of bunched-electrode in EDM. *Key Engineering Materials*, 447-448, 282–286. doi:10.4028/www.scientific.net/KEM.447-448.282
- Zhao, W., & Guo, C. (2014). Topography and microstructure of the cutting surface machined with abrasive waterjet. *International Journal of Advanced Manufacturing Technology*, 73(5-8), 941–947. doi:10.1007/00170-014-5869-5

## About the Contributors

**Kaushik Kumar**, B.Tech (Mechanical Engineering, REC [Now NIT], Warangal), MBA (Marketing, IGNOU) and Ph.D (Engineering, Jadavpur University), is presently an Associate Professor in the Department of Mechanical Engineering, Birla Institute of Technology, Mesra, Ranchi, India. He has 14 years of Teaching & Research and over 11 years of industrial experience in a manufacturing unit of Global repute. His areas of teaching and research interest are Quality Management Systems, Optimization, Non-conventional machining, CAD / CAM, Rapid Prototyping and Composites. He has 9 Patents, 15 Book, 6 Edited Book 35 Book Chapters, 120 international Journal publications, 18 International and 8 National Conference publications to his credit. He is on the editorial board and review panel of 7 International and 1 National Journals of repute. He has been felicitated with many awards and honours.

**Nisha Kumari** (B.Tech, Mechanical Engineering, ITER SOA University, Bhubaneswar), M.E. (Design of Mechanical Equipment, BIT Mesra). Her areas of interests are Biomechanics, Manufacturing, Composites, Product and Process Design and Automation. She has 4 International Journal publications and 1 National Conference publication to her credit. She is a recipient of Academic Awards.

\* \* \*

**Bappa Acherjee** is presently working as an Assistant Professor in the Department of Production Engineering at BIT Mesra, Ranchi, India. He received his Ph.D. in Engineering from Jadavpur University, India in 2012, in the field of laser beam welding. His research interest includes laser material processing, welding and application of finite element method in manufacturing processes. He is the author of over 60 peer-reviewed publications including journal papers, conference papers and book chapters. He has delivered a number of invited talks and tutorials, and reviewed several journal and conference papers. His biography appeared in 'Marquis Who's Who in the World' 2011 (28th Edition), 2018 (35th Edition) and '2017 Albert Nelson Marquis Lifetime Achievement Award'. Dr. Acherjee is a member of ASME and a life member of IIPE.

**Sumit Bhowmik** is an Assistant Professor in Department of Mechanical Engineering, National Institute of Technology Silchar, Assam. He received his B. E. in Mechanical Engineering from Tripura Engineering College (Tripura University), India, Master in Mechanical Engineering and PhD from Jadavpur University, Kolkata. He has over 15 years of teaching and research experience. He has more than 25 international journals and international Conference publications to his credit. His areas of interests are Fracture Mechanics, Materials properties, Composites, and Optimization, etc.

**J. Paulo Davim** received the Ph.D. degree in Mechanical Engineering in 1997, the M.Sc. degree in Mechanical Engineering (materials and manufacturing processes) in 1991, the Mechanical Engineering degree (5 years) in 1986, from the University of Porto (FEUP), the Aggregate title (Full Habilitation) from the University of Coimbra in 2005 and the D.Sc. from London Metropolitan University in 2013. He is Eur Ing by FEANI-Brussels and Senior Chartered Engineer by the Portuguese Institution of Engineers with an MBA and Specialist title in Engineering and Industrial Management. Currently, he is Professor at the Department of Mechanical Engineering of the University of Aveiro, Portugal. He has more than 30 years of teaching and research experience in Manufacturing, Materials, Mechanical and Industrial Engineering, with special emphasis in Machining & Tribology. He has also interest in Management, Engineering Education and Higher Education for Sustainability. He has guided large numbers of postdoc, Ph.D. and masters students as well as coordinated & participated in several research projects. He has received several scientific awards. He has worked as evaluator of projects for international research agencies as well as examiner of Ph.D. thesis for many universities. He is the Editor in Chief of several international journals, Guest Editor of journals, books Editor, book Series Editor and Scientific Advisory for many international journals and conferences. Presently, he is an Editorial Board member of 25 international journals and acts as reviewer for more than 80 prestigious Web of Science journals. In addition, he has also published as editor (and co-editor) more than 100 books and as author (and co-author) more than 10 books, 80 book chapters and 400 articles in journals and conferences (more than 200 articles in journals indexed in Web of Science core collection/h-index 45+/6000+ citations and SCOPUS/h-index 52+/8000+ citations).

**Rahul Dev Misra** received his B.E. in Mechanical Engineering from Jorhat Engineering College under Dibrugarh University in 1991, M.Tech. in Energy Studies from Indian Institute of Technology Delhi in 1996, and Ph. D. in Thermal Engineering from Indian Institute of Technology Roorkee in 2004. He has joined as faculty in Mechanical Engineering in the National Institute of Technology Silchar in 1992. He has served NIT Silchar as Lecturer from 1992 to 2003, as Assistant /Associate Professor from 2004 to 2009, and as Professor from 2010 till date. He is a professional member of the Indian Society for Technical Education and The Engineering Society For Advancing Mobility Land Sea Air and Space (SAEINDIA).

**Azhar Equbal** is a research Scholar in the Department of Manufacturing Engineering at National Institute of Foundry and Forge Technology (NIFFT) Hatia, Ranchi, Jharkhand. He has got more than 20 papers published in journals of international repute including Elsevier, Inderscience and MDPI. He also has got a chapter published in IRPH Publication House, New Delhi. His area of interest are Non-Conventional Manufacturing processes with special relevance to Electrical Discharge Machining (EDM), Coating of Plastic materials and use of Soft Computing approaches for optimisation of manufacturing processes.

**Md. Asif Equbal** is an Assistant Professor in the Department of Mechanical Engineering at Cambridge Institute of Technology, Ranchi, India. He has more than Seven years of experience in teaching and research. His current area of research includes rapid prototyping, non traditional machining, multi-criteria decision making and supply chain management. He has published more than 10 research articles in referred journals.

### **About the Contributors**

**Md. Israr Equbal** is an Assistant Professor in the department of Mechanical engineering at Aurora's technological and research Institute. He has done his doctorate with Forging as his specialization. He is author of more than 25 research papers in journals of international repute. His research areas include Forging of metals, thermomechanical simulation of materials and optimization of manufacturing processes.

**Nadeem Faisal**, B.Tech (Mechanical Engineering, ITM University, Gwalior, India), M.E. Pursuing (Design of Mechanical Equipment, Birla Institute of Technology, Mesra, India). He has over 1 year of Industrial experience. His areas of interests are Optimization, Material Science, Product and Process Design, CAD/CAM/CAE and Rapid Prototyping. He has 2 books, 4 Book Chapters, 2 SCI Indexed international publication to his credit.

**Elsa Maria Pires Henriques** has a doctorate degree in Mechanical Engineering and is associated professor at Instituto Superior Tecnico in the University of Lisbon. She is responsible for the "Engineering Design and Advance Manufacturing (LTI/EDAM)" post-graduation. During the last fifteen years she has participated and/or coordinated several national and European R&D projects in collaboration with different industrial sectors, from tooling to automotive and aeronautics, mainly related to manufacturing, life cycle based decisions and management of complex design processes. She has a large number of scientific and technical publications in national and international conferences and journals. She was a national delegate in the 7th Framework Programme of the EU.

**Pradeep Kumar M.** is an Associate Professor in the Department of Mechanical Engineering at Anna University Chennai, India. He completed his PhD in Mechanical Engineering and ME in Manufacturing Engineering at the Anna University, Chennai. He has guided 12 PhD and eight are pursuing PhD under his guidance. He also guided several ME projects in advanced manufacturing processes. He has published more than 60 research articles in reputed international and national journals. He also published more papers in various international and national conferences. His research interests are cryogenic machining, application of FEM in machining, micromachining and unconventional machining processes.

**Uthayakumar M.** was born in Cumbum Theni Dist, India. He has obtained Bachelor of Engineering in Mechanical Engineering from PSNA College of Engineering & Technology, Dindigul and Masters in Production Engineering from Thiagarajar College of Engineering (Autonomous), Madurai. He did his research on bimetallic piston machining studies in the Department of Production Engineering, National Institute of Technology Tiruchirappalli. The work was supported by India Pistons Ltd Chennai. He was awarded as young scientist by Tamil Nadu state council for Science and Technology and undergone the post doctoral fellowship on Tribology in the Department of Mechanical Engineering, Indian Institute of Technology, New Delhi. He has published currently 80 papers in the referred international journals. Eight of his research scholars have completed their Ph.D and currently 6 members are pursuing. He has developed Advanced Machining and Measurement lab funded under DST-FIST program. He is the Principal Investigator for research projects from BRNS-Department of Atomic Energy and Ministry of Environment and Forest, Government of India. He has visited Cracow University of Technology, Poland and Yeungnam University, Korea as visiting professor. He has organized the second International conference on Advanced Manufacturing and Automation (INCAMA 2013) successfully and produced special issues in reputed journals. Currently he is working as Director (International Relations) of Kalasalingam

University. He is a member in the professional societies namely ISTE, SAE, ISNT and IEI. He is actively taking part in SAE activities and holding the position of Senior Faculty Advisor of SAEINDIA KLU club and at present he is in the Management committee of SAEINDIA Southern section Madurai Division.

**Siba Mahapatra** is a Professor in the Department of Mechanical Engineering, National Institute of Technology Rourkela, India. He has more than twenty years of experience in teaching and research. His current area of research includes Multi-criteria Decision-Making, Quality Engineering, Assembly Line Balancing, Group Technology, Neural Networks, and Non-traditional Optimization and Simulation. He has published more than one hundred twenty papers in peer-reviewed international journals. He has written few books related to his research work. He is currently dealing with few sponsored projects.

**Nitin D. Misal** is Principal of SVERI's College of Engineering (Polytechnic) Pandharpur. He received his B.E. in Production Engineering from K.B.P. College of Engineering, Satara under Shivaji University, Kolhapur in 1994, M. Tech. in Manufacturing Engineering from Dr. B.A.T.U. Lonere in 2007, and Ph. D. from Dr. B.A.T.U. Lonere in 2017. He served as Production Manager in Abhijat Equipments Pvt. Ltd., Satara from 1994 to 1998. He worked as Factory Incharge for Sawant Industries, Andheri, Mumbai from 1998 to 2001. He has joined as faculty in Mechanical Engineering Department in the SVERI's College of Engineering, Pandharpur in 2001. His area of specialization is Micro-manufacturing and machine tool building. His work focuses on photochemical machining, vertical axis wind turbines, atomization in rural industries, etc. He has published 20 papers in reputed international journals and conference proceedings, one book, two book chapters in Springer, and filed one patent. He was member of the professional body ASME and he is a life member of the Indian Society for Technical Education (ISTE) and Institution of Engineers India (IEI).

**Yuvaraj Natarajan** is currently working as Assistant Professor (Research) in the Department of Mechanical Engineering, Vel Tech Rangarajan Dr. Sagunthala R&D Institute of Science and Technology, Chennai, India. He completed his Ph.D. in the Department of Mechanical Engineering at CEG campus, Anna University, Chennai. He received his B.Tech. degree in Automobile Technology from University College of Engineering – BIT campus, Trichy and M.E degree in Manufacturing Systems Management at CEG campus, Anna University, India. His research interests are machining science, cryogenics, surface integrity and optimization techniques. And also he is a recipient of CSIR-SRF and best young researcher awards for his research work.

**Asit Parida** currently works as a Postdoctoral fellow in the Mechanical Engineering Department at Indian Institute of Technology, Delhi.

**Promod Kumar Patowari** obtained B.Tech. in Mechanical Engineering from North Eastern Regional Institute of Science and Technology (NERIST), Itanagar in 1994, M.Prod.E. in Production Engineering from Jadavpur University, Kolkata in 1999, and Ph.D. from Indian Institute of Technology (IIT) Kharagpur in 2008. He has joined as a faculty member in the Department of Mechanical Engineering of National Institute of Technology (NIT) Silchar in 1995 and presently serves as Associate Professor. He is the life member of professional bodies like Indian Society for Technical Education (ISTE) and Institute of Smart Structures and Systems (ISSS).

### **About the Contributors**

**Paulo Peças** has a graduation (1991) and a doctorate (2004) in Mechanical Engineering at Instituto Superior Técnico (Universidade de Lisboa). Since 1998, he is an assistant professor at Instituto Superior Técnico in the Manufacturing Technologies and Industrial Management scientific area, being responsible for programmes in Production Management and Industrial Management. During the last ten years has participated and integrated coordination teams of R&DT projects in collaboration with the industry, at both national and European levels. The research activity has focused the development of models to support decision-making, comparative analysis and best-practices implementation in the scope of Life Cycle Engineering and lean & agile manufacturing. These models foster the build-up and implementation of solutions for productivity and competitiveness increasing in several industrial sectors. He has published and edited scientific books, published 22 research papers in International Journals and 6 chapters in scientific books, 60 publications in International Conferences Proceedings and 23 dissemination articles in national magazines.

**Pedro Dias Pereira** received his MS in Mechanical Engineering from the University of Instituto Superior Técnico in 2012. In 2013 he was hired as research in the mechanical department of Instituto Superior Técnico.

**B. C. Routara** is working as Professor in School of Mechanical Engineering, KIIT deemed to be University, Bhubaneswar since 2009. He obtained his PhD degree in Production Engineering from Jadavpur University, Kolkata, India. He completed his Bachelor's degree from OUAT, Odisha and post graduate degree from Bengal Engineering College, Howrah India. He has 24 years of teaching experience and 10 years of research experience. He has published 43 technical papers in international journals as well as 40 international conference proceedings. His areas of interest include simulation and modelling of advanced manufacturing process, hard machining, composite materials.

**Thirumalai Kumaran S.** completed his Doctoral work in the area of Tribology and Machining Studies of Metal Matrix Composites. His areas of interest include characterization and study of surface morphology in composite materials.

**Anshuman Kumar Sahu** is currently pursuing his PhD in the Department of Mechanical Engineering, National Institute of Technology, Rourkela, Odisha, India. He is currently working on non-conventional machining, rapid tooling and rapid manufacturing.

**M. P. Satpathy** is an Assistant professor in School of Mechanical Engineering, KIIT Deemed to be University, Bhubaneswar. He obtained his PhD degree in production engineering from National Institute of Technology Rourkela, India. He received his Bachelor's degree from BPUT, Odisha and post graduate degree from KIIT University, Odisha, India. He has 4 years of teaching experience and has published 15 technical papers in international journals as well as 20 international conference proceedings. His areas of interest include simulation and modelling of advanced manufacturing process, welding technology, metal forming process and advanced machining process.

**Anoop Kumar Sood** is actively engage in research area pertaining to additive manufacturing and he has more than 35 publications in this area in peer reviewed reputed journals.

**Deba Kumar Tripathy** is Professor Emeritus, IIT Kharagpur. He had an illustrious career of more than 40 years with several accomplishments in Teaching, Research in the area of Production Engineering and Polymer Engineering, heading of large Academic Institutions with tremendous success marked by various National and International Award, fellowship, patent and publications.

**Sasmeeta Tripathy** is working as an Associate Professor Mechanical Engineering at Siksha 'O' Anusandhan (Deemed to be University). She has completed Ph.D. in Production Engineering and has a teaching experience of 11 years. She has one state and one national award to her credit.

**Sandeep Sitaram Wangikar** is an Asst. Professor in Department of Mechanical Engineering at SVERI's College of Engineering, Pandharpur. He received his B.E. in Production Engineering from SVERI's College of Engineering, Pandharpur under Shivaji University, Kolhapur in 2005, M.E. in Design Engineering from Solapur University in 2012, and pursuing Ph. D. at National Institute of Technology Silchar. He served as Production Engineer in Nuclear group in Special Products Division at Walchandnagar Industries Limited, Walchandnagar from 2005 to 2010. He has joined as faculty in Mechanical Engineering Department in the SVERI's College of Engineering, Pandharpur in 2010. His area of specialization is Manufacturing and Microfluidics. His work focuses on photochemical machining, vertical axis wind turbines, experimental and computational analysis of microchannels, etc. He has published 15 papers in reputed international journals and conference proceedings and one book chapter in Springer. He was member of the professional body ASME and also acted as a Faculty Adviser for SAE India Collegiate Club. He is a life member of the Indian Society for Technical Education (ISTE) and Institution of Engineers India (IEI).

**Divya Zindani** (BE, Mechanical Engineering, Rajasthan Technical University, Kota), M.E. (Design of Mechanical Equipment, BIT Mesra), presently pursuing PhD (National Institute of Technology, Silchar). He has over 2 years of Industrial experience. His areas of interests are Optimization, Product and Process Design, CAD/CAM/CAE, Rapid prototyping and Material Selection. He has 1 Patent, 2 Books, 4 Edited books 14 Book Chapters, 2 SCI journals, 7 Scopus Indexed international journal and 4 International Conference publications to his credit.



# Index

## A

abrasive water jet 175-176, 178, 183, 202-207, 231, 233  
 AISI D2 steel 83, 202, 204-206, 208-209, 214-215, 217-218, 220, 225-227  
 ANN 249, 255, 257-259  
 average height of the profile (Rz) 83, 85, 91-92, 95-96, 105-106, 108  
 average roughness (Ra) 83, 85, 91-93, 105-106, 108

## B

B4C 109, 111, 114-115, 117-118, 120, 166  
 brass 35, 38, 45, 110, 126, 128-130, 165, 188, 190-191, 197, 199

## C

COH 153, 157, 160, 166, 169, 171  
 complex shapes 125-126, 141, 176, 180, 188, 198  
 composite 37-38, 45-46, 85, 109-112, 115, 118-120, 131-132, 175, 183, 233, 255  
 concentration 34, 36, 38, 40, 55, 59, 62, 70-71, 77-78, 131, 139, 153, 156, 166-169, 180-181, 183, 190, 195-197, 199  
 cryogenics 204-205, 219, 231

## D

D2 steel 83, 202-206, 208-210, 214-215, 217-218, 220-221, 223, 225-227, 231  
 DEFORM 232-233, 235  
 desirability function 82-85, 91, 95, 105-106  
 dielectric 33-38, 40, 45, 56-57, 61-62, 68, 70-72, 77-79, 83, 90, 110, 114, 126, 128, 130, 132-136  
 dimensional accuracy 40, 42-44, 84, 134, 167, 176

## E

EDM 33-46, 55-57, 59, 70-71, 82-85, 89-92, 95, 100, 103-105, 108-113, 120, 125-127, 129-132, 135-140, 142, 154, 176, 182, 184, 189  
 electrical discharge 33-35, 37, 44, 55, 83-84, 89-90, 105, 109-111, 113, 125-126, 128-140, 182, 189  
 electrical discharge machining 33-35, 37, 44, 55, 83-84, 89-90, 105, 109-111, 125-126, 128-139, 182, 189  
 Electrochemical spark 176, 182  
 electrode 34-46, 55, 59-61, 70, 82-85, 89-90, 92, 94-95, 100, 103, 105, 109-110, 112-116, 119, 125-132, 134, 136, 139  
 electrode wear ratio 55, 59-60, 70, 84, 109-110, 112-115  
 electro-discharge machining (EDM) 83, 108, 176  
 etching time 190, 195-197, 199  
 excessive heating 182-183

## F

FEM 132, 232, 234, 249, 251, 255

## G

GRA 55-56, 65, 84

## H

HOS 153, 157, 159, 166-169, 171  
 hot machining 232-235, 237, 241

## I

ICA 153, 155-157, 161, 163, 170-171  
 Inconel 718 40, 84, 188, 190-191, 198-199, 232, 234-235, 241

**K**

kerf width 84, 133-135, 177, 207, 231

**L**

laser transmission welding 249-252, 259

liquid nitrogen 204, 206, 231

**M**

machined surface 34-35, 38, 61, 70-72, 78, 83, 85, 92, 94, 104, 106, 109, 113, 117, 119-120, 175, 177, 179, 181, 184, 203, 209, 212, 214, 217, 219, 222, 225, 231

material removal rate 36-41, 44-45, 55, 59-60, 68, 71, 84, 110, 113-114, 117, 130-133, 141, 153-155, 159, 175-176, 180-181, 183, 190-191, 194-199, 231, 233-234

matrix composites 37, 42, 110, 153, 175-176

maximum height of the profile (Rt) 83, 85, 91-92, 94-95, 105-106, 108

metal matrix 37, 42, 109-110, 175-176

metal matrix composite 109-110, 175

micro-electro discharge 3, 10

micro-engineering 1-13, 17, 20-23, 25, 27

micro-hardness 37, 55-56, 59, 61, 72-73

micro-hot embossing 2, 4, 9-13, 16-17, 19-27

micro-injection molding 1-2, 4, 9-11, 17, 19-22, 25-27

modeling 5-8, 13, 56, 110, 137-138, 153, 170, 234, 237-239, 249, 252-255

MRR 39-41, 43, 45-46, 55-56, 59-61, 66, 68-70, 73, 77, 79, 84, 110, 131-134, 136, 139, 153, 155-157, 159, 167-169, 171, 190, 196

**N**

Near Dry Wire Cut 130

non-traditional machining 55, 125, 175-176, 184

**O**

orthogonal array 56, 62, 67, 82, 85, 90, 105, 113, 137, 156, 166

**P**

performance 1-8, 10, 15, 35-36, 38, 40, 42-46, 56, 59, 63, 65-67, 72, 74, 79, 83-85, 99, 101, 104, 109-111, 115, 118, 128, 133, 142, 153-154, 158, 170-171, 176, 180-182, 189, 191-192, 194-195,

199, 202-205, 207-208, 231, 233, 255-257  
performance characteristics 56, 59, 63, 65, 67, 72, 74, 109, 111, 153-154, 158, 202, 231  
photochemical machining 188-191, 194, 197-199  
PMEDM 55-56, 58-59, 132  
Powder Mixed WEDM 132  
powder-injection molding 1-2  
power consumption 109-113, 118  
power supply 33-36, 44-45, 126  
process-based cost 1-2, 4-5, 8, 27  
Process-Based Cost Models 4, 27

**R**

recast layer thickness 55-56, 59, 61, 71, 136

RSM 136-137

**S**

Selective laser sintering 41, 82-83, 108

selective laser sintering (SLS) 41, 82-83, 108

sensitivity analysis 4, 6, 8, 18-19, 23-24, 27, 84

SiC 40, 69-70, 72, 79, 84, 109, 111, 115, 118, 120, 177-180

Sparking gap 134

SR 40, 55-56, 59, 61, 66, 70-71, 73, 78-79, 109, 116-117, 134, 139, 156, 159

surface characteristics 56, 83-85, 91-92, 95, 100, 103, 205, 231

surface finish 36, 38, 40-42, 44, 46, 82-85, 91, 105, 110, 117, 120, 127, 129-130, 134, 159, 168, 175-179, 181-184, 188, 190, 195-196, 203, 219, 221, 232-233

surface integrity 136, 202-205, 231, 233

surface roughness 36, 40-42, 55, 59, 61, 70-71, 82-84, 91-92, 106, 109-113, 117-118, 120, 130-134, 136, 156, 159, 169, 178-179, 181-183, 190-191, 194-199, 204, 231, 233

**T**

Taguchi 41, 56, 61-62, 65, 67, 79, 82, 84-85, 90, 105, 137-138, 153-154, 156-157, 166, 171

Taguchi philosophy 153-154, 156, 171

technology selection 2, 8, 19, 27

temperature 10-12, 34, 37, 43-44, 70-71, 83-85, 104, 110-111, 126, 128, 130, 132, 139, 164, 178, 183, 188, 190, 195-199, 202-205, 207, 210, 212, 216, 219, 222, 225-227, 231-242, 244, 249, 251-255

thermal coefficient 110

tool 3-6, 8-15, 17-19, 23, 25, 27, 33-46, 55-56, 58-61,

## ***Index***

68, 70-71, 74, 79, 82-85, 89-90, 92, 94-95, 100, 103-106, 110, 113-114, 127, 132, 137, 154-156, 158-159, 164-165, 167, 171-172, 175-176, 180-182, 191-192, 203, 205, 207, 232-235, 237-241, 243, 250, 255

tool temperature 232, 234

tool wear 36-44, 55, 59-60, 68, 70-71, 84, 110, 113-114, 156, 159, 176, 232-235, 237-241

tool wear rate 36-41, 55, 59-60, 70-71, 84, 110, 113-114, 156, 159, 239-240

TOPSIS 56, 82, 84-85, 87, 91, 99-100, 104-106, 153-154, 156-157, 160, 169, 171

## **U**

USM 153-160, 164, 166-167, 169-172

## **V**

VIKOR 82-85, 88, 91, 101, 103-106

## **W**

weld penetration depth 249, 252

weld width 249, 252, 255, 257, 259

wire 35-36, 38, 44, 56, 84, 125-142, 154

wire breakage 128, 131, 138-140

wire EDM 35-36, 44, 56, 126-127, 130-131, 135-137, 142

wire lag 135, 139-140

WIRE MATERIALS 128

wire vibration 139-140

wire wear ratio 135